

**SEISMIC RETROFIT OF NON-DUCTILE REINFORCED  
CONCRETE COLUMNS USING RECTANGULAR  
STEEL JACKETS**

by

**RIYAD SAID ABOUTAHA, B.E., M.Sc.**

**DISSERTATION**

Presented to the Faculty of the Graduate School of

The University of Texas at Austin

in Partial Fulfillment

of the Requirements

for the Degree of

**DOCTOR OF PHILOSOPHY**

**THE UNIVERSITY OF TEXAS AT AUSTIN**

December 1994

**Copyright**

**by**

**Riyad Said Aboutaha**

**1994**

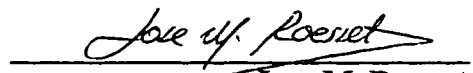
**SEISMIC RETROFIT OF NON-DUCTILE REINFORCED  
CONCRETE COLUMNS USING RECTANGULAR  
STEEL JACKETS**

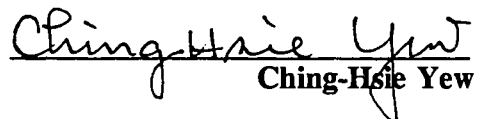
**APPROVED BY  
DISSERTATION COMMITTEE**

  
Michael D. Engelhardt

  
James O. Jirsa

  
Michael E. Kreger

  
Jose M. Roesset

  
Ching-Hsie Yew

*TO MY FAMILY*



## ACKNOWLEDGMENTS

The author gratefully acknowledge the financial support provided by The National Science Foundation (Grant No. BCS-9016828). Thanks are also extended to Hilti Inc. for donating the adhesive anchor bolts and some fine construction tools used in this research.

The author would like to express his deepest thanks to Dr. Michael D. Engelhardt for his guidance, constructive criticism, continuous support and encouragement throughout this research. It was a pleasure to work with him. Thanks are extended to Dr. James O. Jirsa and Dr. Michael E. Kreger for their valuable suggestions and comments during this study.

Thanks are extended to Dr. Jose' M. Roesset and Dr. Ching Hsie Yew for serving on the supervising committee. The Author also would like to thank Mr. Loring A. Wyllie and Dr. Thomas A. Sabol for providing many useful suggestions and comments during the course of this project.

This research was conducted at Ferguson Structural Engineering Laboratory of The University of Texas at Austin. The experimental phase of this study could not have been accomplished so rapidly without the assistance of the undergraduate research assistants: Mohamad Najah, Emad Ahmad, Jim Doran, Tim Able and Kamram Azad. I appreciate their help as well as the assistance of the staff and the students (too many to name them all) at the laboratory.

Sincere thanks to Dr. Ned H. Burns and his wife Martha for their kindness, encouragement, generosity and wisdom. Special thanks to Dr. Dan Wheat for his assistance and support when I needed him most.

The author is indebted to his family in Beirut, Lebanon, whose understanding, patience and encouragement gave him a lot of strength when he needed it most. Thank you for your love and support.

Riyad S. Aboutaha  
Austin, Texas  
December 1994

**SEISMIC RETROFIT OF NON-DUCTILE REINFORCED  
CONCRETE COLUMNS USING RECTANGULAR  
STEEL JACKETS**

Publication No. \_\_\_\_\_

Riyad Said Aboutaha, Ph.D.

The University of Texas at Austin, 1994

Supervisor: Michael D. Engelhardt

Many existing buildings in the United States designed and constructed according to old standards are inadequate to withstand major earthquakes. A major class of existing structures identified as posing major seismic hazards are non-ductile reinforced concrete frames. Accordingly, significant research has been devoted to develop different techniques to enhance the seismic resistance of these structures.

This experimental research investigated the use of rectangular steel jackets for seismic retrofit of non-ductile reinforced concrete frame columns. Large scale columns were tested to examine the effectiveness of various types of steel jackets for improving the ductility and strength of columns with inadequate shear strength or with an inadequate lap splice in the longitudinal reinforcement.

Response of columns before and after being strengthened with steel jackets were examined. Several types of steel jackets were investigated, including rectangular solid steel jackets with and without adhesive anchor bolts. The addition of adhesive anchor bolts stiffens the steel jacket, and is essential for retrofitting wide columns with inadequate lap splices. Field welded as well as field bolted steel jackets were examined. Bolted steel jackets offer the advantage of eliminating field welding.

Many of the retrofit schemes are shown to provide dramatic improvements in the behavior of non-ductile reinforced concrete columns under large cyclic inelastic loadings. Design guidelines for the use of rectangular steel jackets as a seismic retrofit for non-ductile reinforced concrete columns were developed and presented.

# LIST OF CONTENTS

<b>CHAPTER 1 - INTRODUCTION</b> .....	1
1.1    GENERAL .....	1
1.2    BACKGROUND .....	2
1.2.1    General .....	2
1.2.2    Forces and Deformations in R/C Columns Caused by Earthquakes .....	3
1.2.3    Common Deficiencies in Non-Ductile R/C Frames .....	5
1.2.3.1    Inadequate Lap Splice .....	7
1.2.3.2    Inadequate Shear Strength .....	10
1.2.3.3    Embedment of Beam Positive Reinforcement .....	12
1.2.3.4    Beam-Column Joint Transverse Reinforcement .....	14
1.2.4    Summary of the ACI Code Provisions for R/C Buildings .....	14
1.2.4.1    General .....	14
1.2.4.2    Column Lap Splice .....	15
1.2.4.3    Transverse Reinforcements .....	17
1.2.4.4    Embedment of Beam Positive Reinforcement .....	18
1.2.4.5    Beam-Column Joint Shear Reinforcement .....	18
1.3    OBJECTIVES .....	19
1.4    SCOPE .....	19
1.4.1    General .....	19
1.4.2    Retrofit of Columns with Inadequate Lap Splice .....	20
1.4.3    Retrofit of Columns with Inadequate Shear Strength .....	20
 <b>CHAPTER 2 - SEISMIC RETROFIT OF R/C FRAMES-REVIEW OF                     LITERATURE</b> .....	 23
2.1    INTRODUCTION .....	23
2.2    SEISMIC RETROFIT - BACKGROUND AND REVIEW OF LITERATURE .....	24
2.2.1    General .....	24

2.2.2	Jacketing of Columns with Inadequate Lap Splice	27
2.2.2.1	Splice Retrofit Using Steel Jackets	27
2.2.2.2	Splice Retrofit Using Fiber Wrap	29
2.2.3	Jacketing of Columns with Inadequate Shear Strength	29
2.2.3.1	Shear Retrofit Using Steel Jackets	29
2.2.3.2	Shear Retrofit Using Concrete Jackets.	32
2.2.3.3	Shear Retrofit Using Fiber Wrap	33
2.2.4	Column Retrofit by the Use of Rectangular Steel Jackets	33
2.3	SUMMARY	34
<b>CHAPTER 3 - EXPERIMENTAL PROGRAM-GENERAL</b>		<b>66</b>
3.1	INTRODUCTION	66
3.2	SPECIMENS DETAILS	68
3.2.1	Basic Flexural Columns (With Inadequate Lap Splice)	68
3.2.2	Basic Shear Columns (With Inadequate Shear Strength)	71
3.2.3	Retrofitted Flexural Columns	73
3.2.3.1	Rectangular Solid Steel Jacket with Adhesive Anchor Bolts	73
3.2.3.2	Steel Collars	76
3.2.3.3	Rectangular Steel Jackets with Through Bolts	76
3.2.3.4	Welded Lap Splice	78
3.2.4	Retrofitted Shear Columns	78
3.2.4.1	Rectangular Solid Steel Jackets - (Welded & Bolted)	80
3.2.4.2	Steel Collars	80
3.2.4.3	Partial Steel Jackets	81
3.3	MATERIALS	83
3.3.1	Concrete	83
3.3.2	Steel	83
3.3.2.1	Deformed Reinforcing Bars	83
3.3.2.2	Steel Plates	83
3.3.3	Non-Shrink Grout	86
3.4	TEST SETUP	86

3.5	LOADING PROGRAM .....	88
3.6	INSTRUMENTATION .....	88
3.6.1	Load Cell and Pressure Transducers .....	88
3.6.2	Linear Transducers .....	90
3.6.3	Linear Potentiometers .....	90
3.6.4	Strain Gages .....	92
3.7	DATA ACQUISITION .....	92
<b>CHAPTER 4 - EXPERIMENTAL PROGRAM-FLEXURAL COLUMNS</b>		
<b>( With Inadequate Lap Splices ) .....</b>		
		<b>93</b>
4.1	INTRODUCTION .....	93
4.2	FLEXURAL COLUMN FC1 ( BASIC-UR ) .....	94
4.3	FLEXURAL COLUMN FC2 ( PRE-EQ-S ) .....	96
4.4	FLEXURAL COLUMN FC3 ( POST-EQ-R ) .....	97
4.5	FLEXURAL COLUMN FC4 ( BASIC-UR ) .....	99
4.6	FLEXURAL COLUMN FC5 ( BASIC-UR ) .....	100
4.7	FLEXURAL COLUMN FC6 ( POST-EQ-R ) .....	101
4.8	FLEXURAL COLUMN FC7 ( POST-EQ-R ) .....	103
4.9	FLEXURAL COLUMN FC8 ( PRE-EQ-S ) .....	104
4.10	FLEXURAL COLUMN FC9 ( PRE-EQ-S ) .....	105
4.11	FLEXURAL COLUMN FC10 ( POST-EQ-R ) .....	107
4.12	FLEXURAL COLUMN FC11 ( PRE-EQ-S ) .....	108
4.13	FLEXURAL COLUMN FC12 ( PRE-EQ-S ) .....	110
4.14	FLEXURAL COLUMN FC13 ( POST-EQ-R ) .....	112
4.15	FLEXURAL COLUMN FC14 ( BASIC-UR ) .....	115
4.16	FLEXURAL COLUMN FC15 ( BASIC-UR ) .....	116
4.17	FLEXURAL COLUMN FC16 ( PRE-EQ-S ) .....	117
4.18	FLEXURAL COLUMN FC17 ( PRE-EQ-S ) .....	119
4.19	SUMMARY .....	121

**CHAPTER 5 - EXPERIMENTAL PROGRAM - SHEAR COLUMNS  
(With Inadequate Shear Strength) . . . . . 166**

5.1 INTRODUCTION . . . . . 166

5.2 SHEAR COLUMN SC1 ( BASIC-UR ) . . . . . 167

5.3 SHEAR COLUMN SC2 ( PRE-EQ-S ) . . . . . 168

5.4 SHEAR COLUMN SC3 ( BASIC-UR ) . . . . . 170

5.5 SHEAR COLUMN SC4 ( BASIC-UR ) . . . . . 171

5.6 SHEAR COLUMN SC5 ( PRE-EQ-S ) . . . . . 173

5.7 SHEAR COLUMN SC6 ( PRE-EQ-S ) . . . . . 174

5.8 SHEAR COLUMN SC7 ( PRE-EQ-S ) . . . . . 177

5.9 SHEAR COLUMN SC8 ( PRE-EQ-S ) . . . . . 179

5.10 SHEAR COLUMN SC9 ( BASIC-UR ) . . . . . 181

5.11 SHEAR COLUMN SC10 ( PRE-EQ-S ) . . . . . 182

5.12 SHEAR COLUMN SC11 ( PRE-EQ-S ) . . . . . 184

5.13 SUMMARY . . . . . 186

**CHAPTER 6 - ADDITIONAL EXPERIMENTAL DATA - FLEXURAL  
COLUMNS ( With Inadequate Lap Splices ) . . . . 220**

6.1 INTRODUCTION . . . . . 220

6.2 ENVELOPES OF THE CYCLIC RESPONSE . . . . . 220

6.3 LATERAL STIFFNESS OF COLUMNS . . . . . 226

6.4 ENERGY DISSIPATION . . . . . 228

6.5 STRAIN GAGE DATA . . . . . 230

6.5.1 Strains in the Longitudinal Reinforcing Bars . . . . . 230

6.5.2 Strains in the Transverse Reinforcement . . . . . 231

6.5.3 Strains in the Through Rods . . . . . 233

6.5.4 Strains in the Steel Jackets . . . . . 234

6.6 MOMENT - CURVATURE AND LOAD - ROTATION DIAGRAMS . 236



6.7	SUMMARY .....	237
<b>CHAPTER 7 - ADDITIONAL EXPERIMENTAL DATA - SHEAR COLUMNS</b>		
<b>( With Inadequate Shear Strength ) .....</b>		
<b>283</b>		
7.1	INTRODUCTION .....	283
7.2	ENVELOPES OF THE CYCLIC RESPONSE .....	284
7.3	LATERAL STIFFNESS OF COLUMNS .....	285
7.4	ENERGY DISSIPATION .....	286
7.5	STRAIN GAGE DATA .....	287
7.5.1	Strains in the Transverse Reinforcement .....	287
7.5.2	Strains in the Steel Jackets .....	289
7.6	MOMENT - CURVATURE DIAGRAMS .....	290
7.7	SUMMARY .....	290
<b>CHAPTER 8 - EVALUATION AND DESIGN OF STEEL JACKETED</b>		
<b>COLUMNS .....</b>		
<b>312</b>		
8.1	INTRODUCTION .....	312
8.2	SHORTEST REPAIRABLE LAP SPLICE .....	312
8.3	SHEAR FRICTION MECHANISM OF LAP SPLICES .....	314
8.4	DESIGN OF STEEL JACKETS WITHOUT ANCHOR BOLTS .....	318
8.5	DESIGN OF STEEL JACKETS WITH ANCHOR BOLTS .....	321
8.6	ULTIMATE FLEXURAL CAPACITY .....	324
8.7	HEIGHT OF THE STEEL JACKET .....	327
8.8	CONCRETE COMPRESSIVE STRENGTH .....	328
8.9	NON-SHRINK GROUT .....	329
8.10	ADHESIVE ANCHOR BOLTS .....	329

8.11	BEHAVIOR OF JACKETED COLUMNS FAILING IN SHEAR	331
8.12	SHEAR ANALYSIS OF STEEL JACKETS	332
8.13	INFLUENCE OF AXIAL LOAD	334
8.14	SUMMARY	335
<b>CHAPTER 9 - SUMMARY AND CONCLUSION</b>		<b>349</b>
9.1	SUMMARY	349
9.2	CONCLUSIONS	350
9.2.1	Pre-Earthquake Strengthening of Flexural Columns	350
9.2.2	Post-Earthquake Repair of Flexural Columns	351
9.2.3	Strengthening of Shear Columns	352
9.3	RECOMMENDED FUTURE RESEARCH	353
<b>APPENDIX A - CONSTRUCTION OF BASIC COLUMNS</b>		<b>354</b>
<b>APPENDIX B - INSTALLATION OF ANCHOR BOLTS</b>		<b>357</b>
<b>APPENDIX C - DESIGN OF RETROFITTED FLEXURAL COLUMN</b>		<b>359</b>
<b>APPENDIX D - NOTATIONS</b>		<b>365</b>
<b>BIBLIOGRAPHY</b>		<b>368</b>
<b>VITA</b>		<b>374</b>

# **CHAPTER 1**

## **INTRODUCTION**

### **1.1 GENERAL**

Many existing reinforced concrete frame buildings designed according to older codes lack adequate seismic resistance. These buildings were typically designed primarily for gravity loads, and were often inadequately detailed to resist earthquake forces in zones of high seismicity. As a consequence, considerable research has been devoted towards evaluating the seismic behavior of non-ductile reinforced concrete frames, and examining the performance of different retrofit techniques to improve the seismic behavior of these structures.

The seismic retrofit of non-ductile reinforced concrete building frames depends on many factors, including the types of structural deficiencies, available stiffness, strength and ductility of the frame, importance of the structure, site conditions, characteristics of expected earthquakes and the desired level of upgrading. Possible strengthening systems include steel or reinforced concrete jacketing, the addition of infill panels or shear walls, the addition of steel bracing and the use of base isolation.

Older reinforced concrete building columns can be particularly vulnerable structural elements. Collapse of a column or of a group of columns is usually associated with at least partial collapse of the structure. Two major deficiencies in non-ductile reinforced concrete columns are inadequate lap splice in the longitudinal reinforcement and inadequate shear

strength. Both of these deficiencies can significantly reduce the strength and ductility of a column.

This study is directed towards strengthening and repair of rectangular non-ductile reinforced concrete columns by the use of rectangular steel jackets. Compared to concrete jacketing, steel jacketing may offer advantages of reduced labor, cost and disruption to existing facilities. For some buildings, the addition of steel bracing may not be adequate to prevent shear failure of some columns. Steel jacketing may be considered a possible solution for such columns.

Collapse of the Cypress viaduct during the Loma Prieta earthquake of October 17, 1989 [1] led to a major seismic upgrade of bridge columns in California. In a research study sponsored by the California Department of Transportation, Chai et al [2] investigated seismic retrofitting of bridge columns by the use of steel jackets. Test results for circular and oval jackets indicated that steel jacketing provides an effective means of enhancing the performance of columns with an inadequate lap splice or with inadequate shear strength. However, the use of circular or oval steel jackets for strengthening building columns may be undesirable since they occupy a larger space compared to a rectangular steel jacket. Rectangular steel jackets may fit better with partition walls and other non-structural elements.

## **1.2 BACKGROUND**

### **1.2.1 General**

Past earthquakes, including the 1971 San Fernando earthquake[4] and the 1989 Loma Prieta earthquake[1] caused severe damage to older existing structures. Lessons learned from previous earthquakes led to major changes

in design codes for new structures. On the other hand, considerable research has been conducted on retrofit techniques to enhance the seismic resistance of existing structures. In order to prevent loss to human life and property, work is underway to strengthen older existing structures and bridges in regions of high seismicity. Seismic retrofit of an existing structure may be needed to enhance the seismic performance of the structure in future seismic events, or to repair a damaged structure that has experienced an earthquake, i.e. pre-earthquake strengthening and post-earthquake repair. To develop an effective retrofit technique it is very important to identify the deficiencies and the types of failure mechanisms to be prevented. This chapter reviews the forces and deformations caused by earthquakes and the typical deficiencies in non-ductile reinforced concrete frames, and in columns in particular.

### **1.2.2 Forces and Deformations in R/C Columns Caused by Earthquakes**

An elevation of a three story frame is shown in Figure 1.1(a). Under typical gravity loads, building columns see very small lateral deformations as shown in Figure 1.1(b), resulting in small shear forces and bending moments. However, under lateral loads, columns see large lateral deformations associated with much higher shear forces and bending moments as shown in Figure 1.1 (c-e). Reinforced concrete building columns must be adequately designed to resist these high shear forces through the use of a sufficiently large cross-section combined with an adequate amount of well detailed transverse reinforcement. Columns in older frames designed primarily for gravity load may lack adequate shear strength. Such columns may see rapid degradation in lateral strength and stiffness, and possible loss of gravity load capacity in a severe earthquake.

In addition to large shear forces, large bending moments develop at the column's ends during an earthquake. Adequate flexural capacity must be

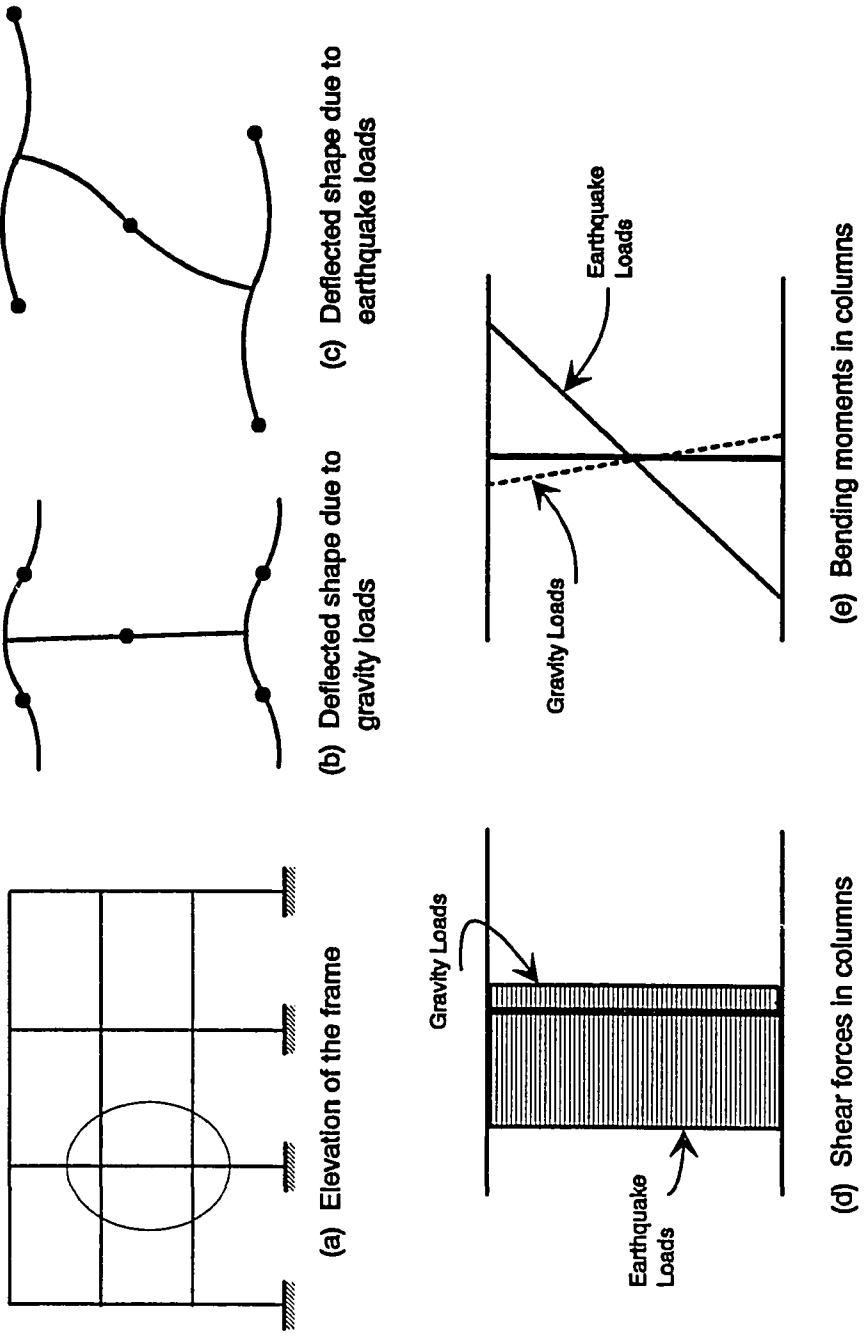


Figure 1.1 Forces and Deformations caused by Gravity and Earthquake loads

provided at the column ends to resist these large moments. If the development of plastic hinges is anticipated at the column ends, adequate flexural ductility must also be provided. Continuity in longitudinal reinforcement at the column ends is preferred in order to fully develop the flexural capacity and ductility of the column cross-section.

If the longitudinal bars have to be spliced, the splice should be well proportioned to transfer large cyclic inelastic forces. A sufficient amount of well detailed transverse reinforcement is also needed to confine any lap splice in that region, confine the column concrete core and prevent outward buckling of the longitudinal bars.

### **1.2.3 Common Deficiencies in Non-Ductile R/C Frames**

Older non-ductile reinforced concrete frames were often designed and detailed primarily to resist gravity loads. These frames may lack the lateral strength and ductility to survive an earthquake without the risk of severe damage or collapse. In order to develop an effective strengthening system for these frames, the deficiencies should be well understood. This section presents typical deficiencies in non-ductile reinforced concrete frames constructed in the 1950's and 60's. The design of these buildings were based on the provisions of the ACI 318-56 [5] and ACI 318-63 [6] building codes.

An elevation view of a portion of a non-ductile reinforced concrete frame between two floors is shown in Figure 1.2. This figure illustrates common deficiencies that may limit lateral strength and ductility.

1. Column has inadequate flexural strength and ductility due to short and lightly confined lap splice located in the potential plastic hinge regions.

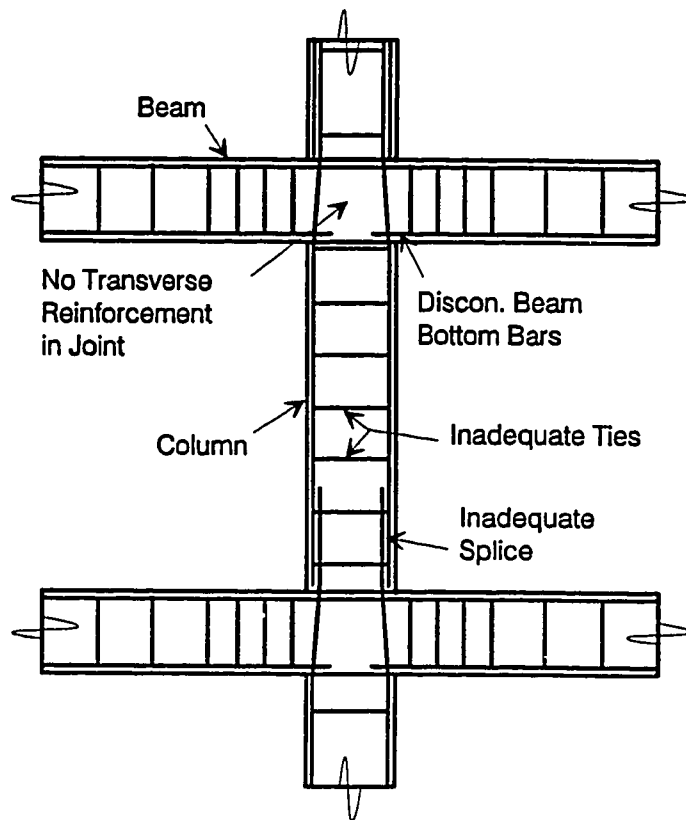


Figure 1.2 Elevation View of a Non-Ductile R/C Frame Between Two Floors

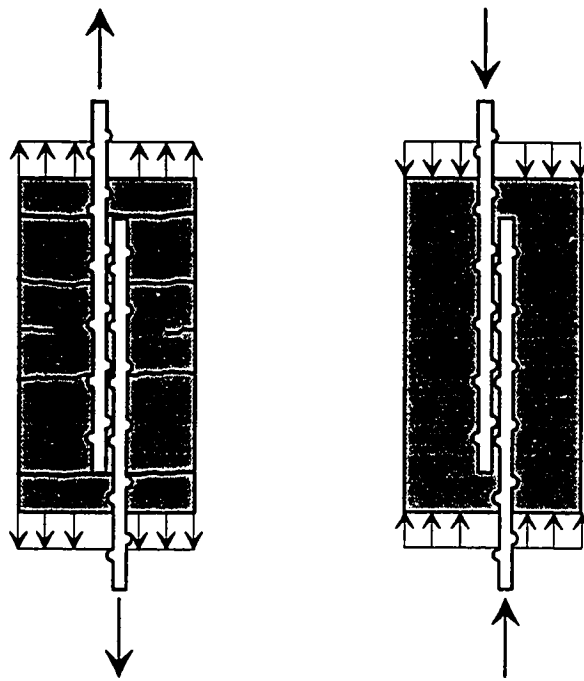


2. Column has inadequate shear strength and ductility due to insufficient and poorly detailed transverse reinforcement.
3. Beam has inadequate positive flexural strength and ductility due to discontinuity of the beam bottom longitudinal reinforcement.
4. Beam-column joint has inadequate shear strength due to lack of shear transverse reinforcement.

Sections 1.2.3.1 through 1.2.3.4 present discussions of these typical deficiencies. Sections 1.2.4.1 through 1.2.4.4 present a brief summary of the American Concrete Institute - ACI 318 design code provisions related to these details from the 1951 edition through the current code edition.

#### **1.2.3.1 Inadequate Lap Splice**

For practical reasons, reinforcing bars in reinforced concrete members often need to be spliced. This is usually done by overlapping parallel bars. Tension and compression lap splices are shown in Figure 1.3. In a lapped tensile splice the tensile force is transferred from one bar to the other through the concrete surrounding the two bars. Force transmission depends on bond between the bars and the surrounding concrete. The transfer of this force at a lap splice causes radial pressure on the concrete, which may result in a splitting crack along the plane of bars. The splitting cracks usually initiate at the end of the spliced bar that is closer to the concrete surface. Transverse cracks generally also develop along a lapped tensile splice. The major transverse cracks occur at the end of the spliced bars, due to the sudden reduction in the amount of steel bars in that region. In the presence of moment gradient the first major crack occurs at the higher moment end. The performance of a lapped tensile splice can be improved by the presence of well detailed transverse reinforcement in the splice region. Ties in the



(a) Tension Lap Splice

(b) Compression Lap Splice

**Figure 1.3 Reinforcement Bar Lap Splice Under Tensile and Compressive Forces**

splice region do not prevent the formation of splitting cracks, but delay the opening of the splitting cracks and hence improve splice capacity.

In a lapped compression splice, force in one bar is transferred to the other bar by bond between the bars and uncracked concrete surrounding the bars. The uncracked concrete allows the use of compression lap splices shorter than tension lap splices. In older existing buildings, column bar lap splices were generally designed as compression lap splices. For ease of construction, column bars were usually spliced just above the floor level in the potential plastic hinge region as shown in Figure 1.2. During an earthquake, these column lap splices may see large tensile forces. This, and the fact that all the column bars are spliced at one location in the potential plastic hinge region, may result in an early splice failure during an earthquake.

Because the lapped splice causes radial stresses which result in a tensile stress field around the spliced bars, concrete tensile strength and concrete cover thickness greatly influence the behavior of lapped splices. When the tensile stresses exceed the concrete tensile strength, a tensile splitting crack will form along the lapped bars. If adequate cover is provided and longitudinal bars are properly spaced, then bond failure may occur without a general splitting failure along the plane of bars. Under large inelastic loading, concrete strength and cover thickness play a less important role in confining the splice and the benefit of adequate confinement by transverse reinforcement increases. However, the benefit of cross ties at lap splices in older existing buildings may be limited since the cross ties are typically of insufficient amount, widely spaced and poorly detailed. For ease of installation, cross ties in existing buildings were provided with 90 degree hooks. These hooks tend to open when the concrete cover spalls off, reducing cross tie effectiveness to confine the splice. As a result column lap splices in

existing buildings are vulnerable during earthquakes. Concrete to steel bond strength and the behavior of reinforced concrete lap splices have been investigated by many researchers [27,28,29,30,31].

### **1.2.3.2 Inadequate Shear Strength**

Short columns with inadequate shear strength experience brittle shear failure under large cyclic shear force, which results in rapid strength and stiffness degradation. Shear dominates the behavior of columns with small span to depth ratios. Such columns exist in structural frames either as a part of the original design or as the result of partial restraint of a taller column by structural or non-structural elements over a portion of its height. The latter is called a captive column. Figure 1.4 shows a captive column partially restrained by a non-structural masonry wall. The partial restraint of a captive column restricts the lateral deformation of the column and results in large shear forces.

Under the actions of earthquake forces, large cyclic shear forces develop in short/captive columns over their entire length. With each shear reversal diagonal cracks cross each other at approximately 90 degrees. Shear transfer along diagonal cracks depends on, along with other factors, the level of strains developed in the transverse reinforcement. Yielding of transverse reinforcement may result in significant degradation of shear transfer. However, this is not the case when strain in the transverse reinforcement remains in the elastic range. For older existing buildings, reinforced concrete columns are lightly reinforced with transverse reinforcement. Consequently, the strains in ties may reach levels well beyond yield, which results in early strength and stiffness degradation of the column.



Figure 1.4 Shear Failure of a Captive Column in a School Building, Tokachi-oki Earthquake, Japan, 1968, Ref.[32].

Shear inadequacy can be in the form of ties of insufficient amount and wide spacing. Also, ties were typically anchored into the concrete cover with 90 degree hooks which tend to open when the cover spalls off under large inelastic cyclic shear loading. Such transverse reinforcement does not provide enough confinement for the concrete core nor is it adequate to resist the high shear forces developed in short columns. Besides resisting a portion of the shear forces, transverse reinforcement confines the concrete compression zone, allowing larger strains to be reached before failure. The effectiveness of transverse reinforcement on confining concrete has been investigated by many researchers [7,8,9,10,11,12].

### **1.2.3.3 Embedment of Beam Positive Reinforcement**

Under gravity loading, negative moments develop in beams at the face of columns, causing tension at the top of the beam and compression at the bottom. Since gravity loads controlled the design of older buildings, beam longitudinal reinforcement at the face of columns was designed to resist negative moment. However, large earthquake motions will cause moment reversals at the beam ends. Beams in older existing buildings may not be able to resist positive moment at the face of columns since beam bottom reinforcement is typically embedded just 6 inches into the beam-column joint. This very short embedment length is insufficient to develop the yielding capacity of the steel bars at the face of the column.

The pull-out of the beam bottom reinforcement at the face of the joint may limit the lateral resistance and energy absorption of a frame structure. Pessiki et al [13] conducted a series of tests on full scale beam-column interior joints to investigate the behavior of lightly reinforced concrete columns and beam-column joint details. The test results showed that

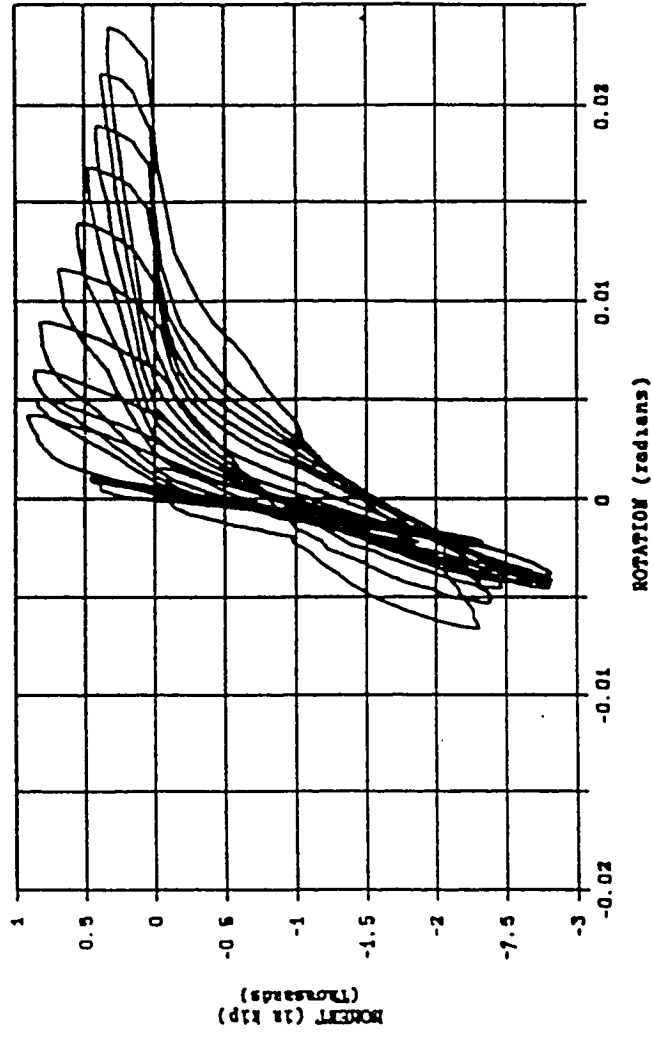


Figure 1.5 Typical Moment-Rotation Relationship for a R/C Beam-Column Subassemblage with Short Embedments of Beam Bottom Reinforcement, Ref. [13].

anchorage failure of beam positive reinforcement caused significant strength and stiffness degradation of the beam-column subassemblage specimens. Figure 1.5 shows a typical moment-rotation relationship for a specimen with short embedded bottom beam reinforcement.

#### **1.2.3.4 Beam-Column Joint Transverse Reinforcement**

The design of beam-column joints received little attention in the 1950's and 60's relative to the design of frame members. As a result, joints in older reinforced concrete frames may lack adequate shear resistance, which may limit the lateral resistance of frames, if not causing a complete collapse of the structure[14]. Under lateral loads, large shear forces develop in the beam-column joints. Such high shear forces in the joints may require a large amount of transverse reinforcement. Older frames were typically provided with little or no joint transverse reinforcement.

#### **1.2.4 Summary of the ACI Code Provisions for R/C Buildings**

##### **1.2.4.1 General**

Sections 1.2.4.2 through 1.2.4.5 present a summary of the provisions of the ACI 318 building codes since 1951. The summary will be limited to the issues related to deficiencies in non-ductile reinforced concrete frames. It includes summaries of the requirements related to column lap splices, shear transverse reinforcement, embedment of beam positive reinforcement into the beam-column joint, and beam-column joint shear reinforcement.



#### 1.2.4.2 Column Lap Splice

Table 1.1 Summarizes the required lap splice length in columns according to the provisions of the ACI 318-51 through ACI 318-89 codes. The requirements for the length of the column lap splice in non-seismic zones have not been changed since 1951. Beginning with the 1963 code, column lap splices are presented as compression splices with minimum length of 12 inches. Whereas, beginning with the 1971 code, special provisions are presented for seismic zones, and longer lap splices are required in regions of high seismicity. Although the ACI 318-1977 code does not prohibit splicing column bars at the column ends, the potential hinge region, the commentary of the ACI 318-1977 (A.6.8) indicates that the mid-length region of the column is a preferred region for splicing column bars. Beginning with the 1983 code, lap splices are permitted only within the center half of the member length and should be proportioned as tension splices. This provision prohibits the use of lap splices in the column's potential plastic hinge regions.

In summary, lap splices in the 1951, 1956 and 1963 ACI code editions were relatively short and were permitted at the column ends. In the 1971 and 1977 editions, lap splices in seismic zones were longer than required by previous codes, but were still permitted at the column ends. The 1983 and 1989 code provisions required column lap splices to be proportioned as tension splices with better confinement by transverse reinforcement. The required lap splice lengths are longer than required by any previous ACI code. Other major change in the 1983 and 1989 editions is prohibiting lap splices at the column ends.

Table 1.1 Column Lap Splice According to the ACI Code Provisions												
$F_y$ (ksi)	$f'_c$ (psi)	1951	1956	1963	1971 <sup>1</sup>	1971 <sup>2</sup> App (A)	1977 <sup>1</sup>	1977 <sup>2</sup> App (A)	1983 <sup>1</sup>	1983 <sup>3</sup> App (A)	1989 <sup>1</sup>	1989 <sup>4</sup> Ch.21
40	≥3000	20 $d_b$	20 $d_b$	20 $d_b$	20 $d_b$	30 $d_b$	20 $d_b$	30 $d_b$	20 $d_b$		20 $d_b$	
	<3000	27 $d_b$	27 $d_b$	27 $d_b$	27 $d_b$	30 $d_b$	27 $d_b$	30 $d_b$	27 $d_b$	39 $d_b$	27 $d_b$	30 $d_b$
50	≥3000	20 $d_b$	20 $d_b$	20 $d_b$	25 $d_b$	30 $d_b$	25 $d_b$	30 $d_b$	25 $d_b$		25 $d_b$	
	<3000	27 $d_b$	27 $d_b$	27 $d_b$	33 $d_b$	33 $d_b$	33 $d_b$	33 $d_b$	33 $d_b$	49 $d_b$	33 $d_b$	38 $d_b$
60	≥3000	24 $d_b$	24 $d_b$	24 $d_b$	30 $d_b$	30 $d_b$	30 $d_b$	30 $d_b$	30 $d_b$		30 $d_b$	
	<3000	32 $d_b$	32 $d_b$	32 $d_b$	40 $d_b$	40 $d_b$	40 $d_b$	40 $d_b$	40 $d_b$	59 $d_b$	40 $d_b$	45 $d_b$
Min. $L_s$		No Min.	≥ 12"	≥ 12"	≥ 12"	≥ 16"	≥ 12"	≥ 16"	≥ 12"	≥ 12"	≥ 12"	≥ 12"

1. Values may be reduced by 17% for confinement by "minimum ties".
2. Appendix "A" of the ACI code, "Special Provisions For Seismic Design".
3. Appendix "A" of the ACI code, Class "C" Lap Splice calculated for  $f'_c=3000$  psi.
4. Chapter 21 of the ACI code, Class "B" Lap Splice calculated for  $f'_c=3000$  psi.

### 1.2.4.3 Transverse Reinforcement

Column ties as small as #2 (0.25 inch) bars were allowed in the older ACI codes. In the 1971 code, the minimum bar diameter was associated with the diameter of the longitudinal bars. All nonprestressed bars were required to be enclosed by ties of at least #3 in size for longitudinal bars #10 or smaller, and at least #4 in size for #11, #14 and #18 longitudinal bars. Minimum bar diameters for transverse reinforcement have not changed since 1971.

The ACI code provisions for spacing between ties in non-seismic zones have remained the same throughout all the ACI code editions since 1951. The spacing is required to be the least of 16 column bar diameters, 48 tie diameters or the smaller dimension of the column. In the 1971 code, the maximum spacing between ties was limited to 4.0 inches in seismic zones. In the 1983 and 1989 editions, tie spacing was limited to the smaller of one quarter of the minimum column dimension or 4.0 inches.

Codes prior to 1963 required the restraint of every column bar by a 90 degree corner of a tie. In the 1963 edition, this code provision was relaxed. A tie was required at every corner and alternate bar if the spacing between longitudinal bars was not greater than 6.0 inches. Such tie was required to have an included angle of not more than 135 degrees. This particular ACI 1963 code provision has remained almost the same throughout the 1989 ACI code, even in seismic zones.

#### **1.2.4.4 Embedment of Beam Positive Reinforcement**

In non-seismic zones the embedment of beam positive reinforcement basically remained the same throughout all the editions of the ACI 318 code. At least one third of the positive moment reinforcement in simple span members and one-fourth the positive moment reinforcement in continuous members are required to be extended into the support. In beams, this extension is required to be at least 6.0 inches.

In the 1971 code, special provisions for seismic zones were first introduced. For members that are part of a primary lateral load resisting system, the fraction of the positive reinforcement extended into the support is required to be embedded to develop the yield strength of the bar in tension at the face of the column. Starting with the 1983 edition, lap splices of the reinforcement within the joint or within a distance of twice the member depth from the face of the joint have been prohibited because such splices are not considered reliable under inelastic cyclic loading. This provision is an attempt to avoid bond failure and ensure the development of the nominal flexural capacity of the beam at the face of the joint under cyclic inelastic loading.

#### **1.2.4.5 Beam-Column Joint Shear Reinforcement**

The provisions of the ACI 318 codes prior to 1971 did not require any transverse reinforcement in the beam-column joint. Beginning with the 1971 code, beam-column joints are required to be designed for shear equal to the maximum shear in the connection, taking into account the column shear and the shears developed from the yield forces in the beam reinforcement. Since the development of inelastic rotations at the face of the joint is associated with strains in the beam reinforcement well in excess of the yield strain, the

ACI 318-89 code provisions require the joint to develop a shear strength based on 1.25 the yield strength of the beam longitudinal reinforcement.

### **1.3 OBJECTIVES**

The objective of this study is to examine the effectiveness of thin rectangular steel jackets for seismic strengthening and repair of non-ductile reinforced concrete columns. An additional objective is to develop design guidelines for the use of rectangular steel jackets as a seismic retrofit technique.

In one phase of the research program, columns with an inadequate lap splice in the longitudinal reinforcement were tested before and after being strengthened with steel jackets. Pre-earthquake strengthening and post-earthquake repair of columns using steel jackets were examined. In another phase, columns with inadequate shear strength were tested in both the weak and the strong directions of the column cross section. Columns were also tested before and after being strengthened with thin rectangular steel jackets.

### **1.4 SCOPE**

#### **1.4.1 General**

The behavior of non-ductile reinforced concrete columns before and after being retrofitted with steel jackets was experimentally evaluated. Test specimens represented typical building columns designed and constructed in the 1950's and 60's in the United States. Large scale columns were tested under static reversed cyclic loading. All specimens were tested without axial load.

#### **1.4.2 Retrofit of Columns with Inadequate Lap Splice**

Seventeen large scale columns with an inadequate lap splice in the longitudinal reinforcement at the base of the column were tested in this phase. Details of column reinforcement were based on provisions of the ACI 318-56 [5] and ACI 318-63 [6] building codes. Five columns were tested as basic unretrofitted specimens. Since the column width is an important factor for strengthening columns with an inadequate lap splice, the test specimens were of three different widths. The column splice was provided on the longer side of the column cross section. Seven columns were strengthened with different steel jackets before testing. Solid steel jackets with and without adhesive anchor bolts were investigated for pre-earthquake strengthening of columns. Five damaged columns were repaired before testing. Solid steel jackets with and without adhesive anchor bolts or through-bolts were investigated for post-earthquake repair of columns. Figure 1.6 shows a column with an inadequate lap splice strengthened by the use of a rectangular solid steel jacket and anchor bolts.

#### **1.4.3 Retrofit of Columns with Inadequate Shear Strength**

Eleven large scale columns were tested in this phase. Four columns were tested as basic unretrofitted specimens. The remaining seven columns were tested after being strengthened with steel jackets. Full and partial steel jackets were investigated, as well as, welded and bolted steel jackets. Eight columns were loaded in the weak direction and three in the strong direction to examine the effectiveness of rectangular steel jackets in strengthening columns with inadequate shear strength in both major directions. Figure 1.7 shows a column with inadequate shear strength retrofitted by the use of a rectangular steel jacket.

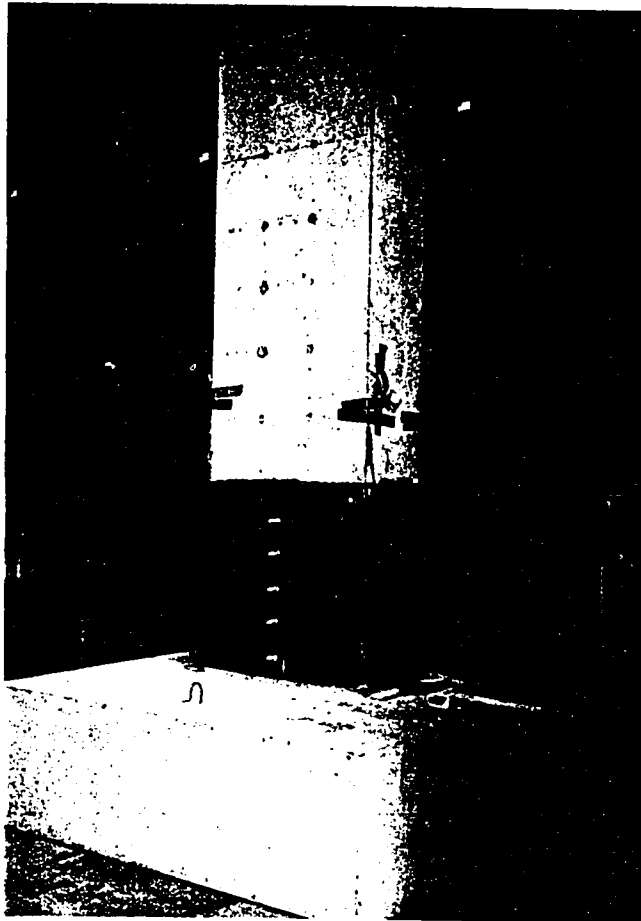


Figure 1.6 Column with Inadequate Lap Splice Strengthened by Rectangular Steel Jacket and Anchor Bolts.



Figure 1.7 Column with Inadequate Shear Strength Retrofitted by Rectangular Steel Jacket.



## **CHAPTER 2**

### **SEISMIC RETROFIT OF R/C FRAMES -REVIEW OF LITERATURE**

#### **2.1 INTRODUCTION**

Selection of an effective seismic retrofit system for a particular reinforced concrete frame building is dependent on many factors, including the structural deficiencies in the frame, its period, available strength, stiffness and ductility, soil conditions, characteristics of expected earthquakes, importance of the structure and the required level of upgrading. Access to the structure during strengthening operations can also be an important factor. In general, strengthening the peripheral frames of a structure is often preferred, since it minimizes disturbance to the occupants of the building. However, preserving the aesthetics of existing elevations of some buildings may limit the use of an external strengthening system. Further, external strengthening systems are not always the most structurally effective retrofit choice.

In the absence of current codes for seismic retrofit of older buildings, most of the seismic strengthening of the existing buildings depends on the engineer's judgements. In general, the strengthening process starts with the owner's requirement, then evaluation of the existing structure and finally selection and design of an adequate retrofitting technique for that particular structure.

In 1984, the Federal Highway Administration released a report including guidelines for seismic retrofitting of highway bridges[15]. In 1989,

the Federal Emergency Management Agency (FEMA) released a document containing recommendations on different techniques for seismic retrofit of existing buildings [16]. These documents provide some guidance for engineers involved in seismic retrofitting. However, many of the recommended techniques and retrofitting details reported in these documents have not been proven by experimental research. This chapter highlights some significant past research results on seismic retrofit techniques for non-ductile reinforced concrete frames. A detailed discussion is also provided on past research of jacketing techniques for retrofitting columns with an inadequate lap splice or with inadequate shear strength.

## **2.2 SEISMIC RETROFIT - BACKGROUND AND REVIEW OF LITERATURE**

### **2.2.1 General**

Several techniques have been developed to improve the seismic resistance of non-ductile reinforced concrete frames. These techniques include addition of infill walls, addition of steel bracing and jacketing of frame members.

Gaynor [17] experimentally investigated the use of concrete infill walls to improve the lateral strength of non-ductile reinforced concrete frames. A one bay, single story frame was tested under cyclic lateral loading. Epoxy grouted dowels were installed into the columns and beams across the interface between the shotcrete infill wall and the concrete frame. The frame columns act as boundary elements for the infill wall. Having short lap splices, the frame columns failed in tension, limiting the lateral capacity of the strengthened frame. Jimenez [18] investigated the use of an eccentric reinforced concrete infill wall on a frame similar to that tested by Gaynor.

The frame columns were jacketed with reinforced concrete to confine the lap splice. The infill wall and the column's jackets were cast in place monolithically. The eccentric wall placement avoided the problem usually associated with filling the gap between the top of the cast-in-place infill wall and the bottom of the floor beam. Figures 2.1 through 2.3 show the details and response of the specimens examined by Gaynor and Jimenez. Compared to the concentric infill wall, the eccentric infill wall showed higher strength, and developed the flexural capacity of the system. The lap splices in the latter system performed well and the reinforcing bars developed yield. The Gaynor and Jimenez studies showed the importance of strengthening column splices even for frames strengthened by the addition of infill walls.

Alcocer and Jirsa [19] investigated the use of concrete jacketing to improve the performance of a reinforced concrete frame connection. Figures 2.4 and 2.5 show the details of the test specimen. Tests were conducted on large scale beam-column subassemblages. The repaired specimen was strengthened by jacketing both the columns and the beams, including the beam-column joint. The amount of added reinforcement in the column and the beam concrete jackets was chosen to achieve ductile response. The specimens were tested under bi-directional cyclic loading. Figure 2.6 shows the hysteretic response of the basic unretrofitted and the strengthened specimens in the north-south direction. Test results showed that concrete jacketing could considerably increase the strength and stiffness of the retrofitted specimens.

Estrada [20] tested a 3/4 scale model of an exterior beam-column joint of an existing building strengthened by the addition of steel elements. Figures 2.7 and 2.8 show the details of the test specimen. The embedment of the beam bottom reinforcement was inadequate to develop the yielding capacity of the bottom bars at the face of the column. Steel plates were

attached with anchor bolts to the bottom of the beams at the beam-column joint to improve the positive flexural capacity of the beams. Brackets were welded to the plates at the column face. The two brackets on the opposite faces of the column were connected with a large threaded rod passing through the column located just below the soffit of the beam. The columns did not have adequate transverse reinforcement. The columns were strengthened with fabricated steel channels attached with threaded rods to the front and back faces of the columns. Partial encasement of the columns with steel, rather than total encasement, was used to avoid removing the glass curtain walls in the real building. The specimen was tested under cyclic loading. The overall performance of the specimen was excellent. Figure 2.9 shows the hysteretic response of the specimen.

Pincheira [21] conducted analytical studies on the use of post-tensioned steel bracing as a seismic retrofit for non-ductile reinforced concrete frames. Low and medium rise buildings detailed according to older codes in the United States were investigated on soft and firm soils. The study showed that the lateral resistance of unstrengthened buildings was limited by the failure of lap splices in the existing columns. The same study revealed that shear failure of some columns in a strengthened medium rise building on firm soils could not be prevented by the addition of bracing. Bouadi et al [22] analytically investigated the use of eccentrically braced frames for seismic retrofit of non-ductile concrete building frames. The study also showed that the addition of steel bracing, by itself, may not be adequate to prevent shear failure of columns.

Based on the above cited research, strengthening of columns may be needed even with the use of some other strengthening system such as the addition of infill walls or the addition of steel bracing systems. Column strengthening could be done by jacketing the column to enhance flexural

strength and ductility due to a short lap splice or to improve shear strength and ductility due to lack of adequate shear reinforcement.

Jacketing of reinforced concrete columns consists of encasing existing columns with reinforced concrete (cast-in-place or shotcrete), or steel elements. Figure 2.10 shows details of typical column jackets. To avoid excessive increase in flexural capacity, which may impose higher shear forces on the member or on the joints, the jacket is often terminated before the joint. Column jacketing may be the sole strengthening measure for a frame, or it may be combined with other measures such as infill walls or bracing, as noted above.

## **2.2.2 Jacketing of Columns With An Inadequate Lap Splice**

### **2.2.2.1 Splice Retrofit Using Steel Jackets**

After the 1989 Loma Prieta earthquake, considerable progress has been made by the California Department of Transportation (CALTRANS) in implementing retrofit measures to upgrade the seismic resistance of bridges in California. One of the major deficiencies in older bridge columns is inadequate flexural strength and ductility. Chai et al [2] conducted a series of tests on four- 0.4 scale test specimens representing rectangular bridge columns designed in the mid 1960's. Figures 2.11 and 2.12 show the details of the test columns. Column bars were all spliced at the base of the column. Splice length was 15 inches, equivalent to 20 bar diameters. The specimens were cantilever type fixed at the bottom and free at the top. All specimens were tested under reversed cyclic load at the tip and a compressive axial load equivalent to  $0.1 A_g f_c'$ . The retrofitted columns were strengthened with three different types of steel jackets. All steel jackets were 48 inches high. The jackets were terminated slightly short of the adjoining footing to ensure that

only confinement was provided to the column, rather than an increase in size of the critical section. One retrofitted column was strengthened with an elliptical steel jacket made of 3/16 inch thick steel plates. The other two retrofitted columns were strengthened with 3/16 inch thick rectangular steel jackets and different types of stiffeners.

Figures 2.13 and 2.14 show the hysteretic response of the tested specimens. The elliptical retrofit showed stable response up to 3.75 % drift ratio (Column height = 144 inches). The steel channel retrofit showed an acceptable response up to 2.75 % drift ratio. However, both retrofits may be unacceptable for retrofit of building columns since both occupy large space and may not fit well with partition walls. The stiffened rectangular steel jacket (Figure 2.8d) showed rather poor response compared to the other two jackets.

Valluvan [23] investigated the use of corner steel angles and straps for strengthening of 12"x12" square columns with an inadequate lap splice. Figures 2.15 through 2.17 show the details of the specimens. The average concrete strength was 3500 psi. Specimens were subjected to repeated cycles of axial load reversals. Two retrofitted specimens were strengthened with four 36 inch long 2"x2"x1/4"- A36 steel angles, and 12"x1"x1/4" steel straps at every 6 inches. The quarter inch gap between the concrete column and the steel elements was filled with dry-pack cementitious grout. The unstrengthened column showed an early splice failure by splitting tensile failure at a load equivalent to 70 % of the tensile yield capacity of the column. However, the response of the two strengthened specimens was satisfactory. Both specimens developed the yield capacity of the steel bars in tension. No cracking was observed on the strengthened specimens in the splice region until the final stage of loading.

### **2.2.2.2 Splice Retrofit Using Fiber Wrap**

Priestley [34] investigated the use of fiberglass/epoxy composite wraps for strengthening of circular columns with an inadequate lap splice. Cantilever type columns were tested under constant axial load of 400 kips, and reversed cyclic lateral load. The test column was 12 feet high and 24 inches in diameter. It was reinforced with 26 # 6 grade 40 longitudinal deformed bars. Transversely, the specimen was reinforced with #2 hoops at every 5 inches. The lap splice length was 20 bar diameters. The fiber wrap jacket was 4 feet high. It was extended over the bottom end of the column in the lap splice region. The test results indicated that the high strength fiber retrofit technique could improve the behavior of circular columns with an inadequate lap splice, and increase both lateral strength and ductility.

It is important to note that the fiber wrap has a modulus of elasticity of 3000 to 3500 ksi, approximately one tenth of steel's modulus of elasticity. This and the fact that the fiber wrap jacket has a small thickness suggests that rectangular fiber wrap jackets may not be suitable for strengthening wide rectangular/square columns with an inadequate lap splice.

### **2.2.3 Jacketing of Columns With Inadequate Shear Strength**

#### **2.2.3.1 Shear Retrofit Using Steel Jackets**

Unjoh and Kawashima [24] investigated the use of 1.0 mm (0.04") thick steel jackets for strengthening bridge piers with short development length in the longitudinal bars. Figure 2.18 shows the details of the four columns tested in this series. All specimens were 500x500 mm (20"x20") square columns. Every column was reinforced with 46-10mm (46 # 3) deformed longitudinal bars. Half of the longitudinal bars were terminated at 900 mm from the top of the base. The columns were transversely reinforced by 6mm (#2) round bars every

250mm (10"). The yield strength of the longitudinal bars was  $3000 \text{ kg/cm}^2$  ( $F_y=42.7 \text{ ksi}$ ) and the yield strength of the ties was  $2400 \text{ kg/cm}^2$  ( $F_y=34 \text{ ksi}$ ). Column R-12 was tested as a basic unretrofitted specimen. Columns R-9 and R-10 were strengthened with 1.0mm thick steel jacket of length equal to the total depth of the column cross section. For column R-9, the 12 mm (1/2") gap between the concrete column and the steel jacket was filled with concrete mortar. However, the 3 mm (0.12") gap in column R-10 was injected with epoxy resin. Column R-11 was similar to column R-10 but the length of the steel jacket was 1.5 the total depth of the column cross section. Figure 2.19 shows the cracking patterns and failure modes. The basic column R-12 showed the development of a hinge at the bar cut-off section, and a shear failure at the same location. However, the strengthened columns developed the flexural capacity of the column. With the longer steel jacket, shear cracks were completely eliminated near the bar cut-off section.

Termination of half the longitudinal bars close to the base of the column caused shifting of the hinge region from the base of the column to the bar cut-off location. It is important to notice here that the shear failure concentrated at the bar cut-off location. Although the columns were subjected to constant shear force along the full height, no serious shear cracks were observed at any other locations, even on the retrofitted columns. Deterioration of the concrete in the hinge region under cyclic loading severely weakened that section. This and the fact that the column was lightly reinforced by ties resulted in shear failure at the bar cut-off location. This suggests why just a 1.0mm (0.04") thick steel jacket was able to solve this particular problem. Relative to its flexural capacity, the original column did not have a very serious shear strength problem.

Yoshimura et al [3] conducted a study on the use of welded steel plates for seismic retrofit of short columns with inadequate shear strength. A total of nine 7"x7" specimens were tested. Three columns were tested as basic



unretrofitted columns with different amounts of longitudinal and transverse reinforcement. The shear span to depth ratio was 1.0. Three columns were strengthened with 6 mm (1/4") thick steel plates. The steel plates were fabricated in two L-shaped panels in plan. After installation around the column the panels were welded at two opposite corners. The 5 mm (0.2") gap between the concrete column and the steel plates was injected with epoxy-based polymer cement. The three basic columns were repaired after testing with similar steel jackets. Figures 2.20 and 2.21 show the details of the specimens. All the specimens were tested under a constant axial load equivalent to  $0.1 A_g f_c'$  and reversed cyclic lateral load. Test results demonstrated that, if a short column is strengthened by welded steel plates, then brittle shear failure can be prevented, and the column can develop its ultimate flexural capacity. It was shown that similar steel jackets can be used for repair of damaged short columns which have failed in shear. Figures 2.22 and 2.23 show the hysteretic response of all the columns.

Chai et al [2] investigated the use of cylindrical steel jackets for seismic shear strengthening of circular columns with inadequate shear strength. Six 24 inch diameter columns were tested under constant axial load equivalent to  $0.1 A_g f_c'$  and reversed cyclic lateral load. Three columns were tested as basic unretrofitted columns with different amounts of steel reinforcement. Figure 2.24 shows the details of a basic unretrofitted column and a retrofitted column with a cylindrical steel jacket. The retrofitted columns were strengthened with 3/16" thick cylindrical steel jackets. The "as built" circular shear column exhibited relatively stable response up to a drift ratio of just less than 1.0 %. Afterwards, the column failed in a brittle shear manner. The hysteretic response of the retrofitted columns showed a large increase in ductility and energy absorption. Figure 2.15 shows the hysteretic response of a basic unretrofitted column reinforced with 2.5 % grade 40 steel and a similar retrofitted column.

### 2.2.3.2 Shear Retrofit Using Concrete Jackets

Bett et al [25] conducted an experimental study on the behavior of repaired and strengthened reinforced concrete short columns using concrete jackets. The test specimens had a 12 inch square cross section reinforced with eight #6 longitudinal bars, #2 ties spaced at 8 inches, and 1.0 inch cover. One of the specimens was tested, repaired by jacketing and then retested. The remaining two specimens were strengthened by jacketing prior to testing. Figure 2.26 shows the details of the test specimens. All specimens were tested under reversed cyclic lateral load and constant axial load. Strengthening was done by encasing the original column with a shotcrete jacket reinforced with closely spaced transverse ties. Specimens were first roughened by light sand-blasting. The jacket reinforcement cages were tied and placed in position, then the columns were shotcreted and float finished. The repaired column was done in a similar way, but after removal of the loose concrete cover. Figure 2.27 shows the envelope of the hysteretic response of the specimens. Testing of the basic unstrengthened column showed shear dominated failure with considerable loss of stiffness at displacements in excess of 1.0 % drift. Both the strengthened and repaired columns performed better than the original column. They were laterally stiffer and stronger than the original unstrengthened column.

Sugano [26] reported results of an experimental investigation on seismic shear strengthening of short reinforced concrete columns using welded wire fabric wrapping and mortar. The test specimen had a 250x250 mm (10"x10") cross section. The shear span to depth ratio was 1.0. The specimens were tested under reversed cyclic lateral load and constant axial stress of  $26.3 \text{ kg/cm}^2$  (375 psi). Figures 2.28 and 2.29 show the details and the response of the test specimens. Compared to the basic unretrofitted column, the strengthened column showed a considerable increase in strength and stiffness with reasonable ductility.

### **2.2.3.3 Shear Retrofit Using Fiber Wrap**

Priestley [35] investigated the use of fiberglass/epoxy composite wraps for strengthening of circular columns with inadequate shear strength. Eight foot high, 24 inch diameter columns were tested under a comparatively low constant axial load of 133 kips and reversed cyclic lateral load. The shear span to depth ratio was 2.0. The column was reinforced with 26 # 6 grade 60 longitudinal deformed bars. Transversely, the column was reinforced with #2 hoops at every 5 inches. The fiber wrap jacket was extended over the full height of the column. The test results indicated that fiber wrap jackets could improve shear strength and ductility of circular reinforced concrete columns with inadequate shear strength.

### **2.2.4 Column Retrofit by the Use of Rectangular Steel Jackets**

As presented in the previous sections, several retrofit schemes have been investigated for strengthening of non-ductile reinforced concrete frames. For columns with inadequate lap splices, no previous research has successfully developed rectangular steel jackets for strengthening of columns. In this study, the use of rectangular steel jackets was successfully investigated for strengthening of non-ductile reinforced concrete columns with inadequate lap splices.

Rectangular steel jackets can provide adequate confinement for columns with inadequate lap splices, however, they have poor out-of plane flexural stiffness, which may result in an insufficient confinement of wide columns, as shown in Figure 2.30(a). Adhesive anchor bolts could be used to enhance the stiffness of rectangular steel jackets. Figure 2.30(b-d) shows columns strengthened with steel jackets and anchor bolts. Wide washers help distribute the anchor bolt force over wider zone, which can result in an additional increase in the steel jacket stiffness. In this study, rectangular steel jackets with

and without adhesive anchor bolts were investigated for strengthening of columns with inadequate lap splices.

Rectangular steel jackets can be used for strengthening of columns with inadequate shear strength. The sides of the steel jacket parallel to the direction of loading contribute to the shear resistance of retrofitted columns, but unlike the transverse reinforcement, they may reach a critical dilation strain before the development of the yield strain of the steel jacket. Figure 2.30(e-f) shows columns retrofitted with rectangular and partial steel jackets for shear seismic retrofit. The latter offers the advantage of strengthening columns with limited accessibility to its all four sides. In this study, rectangular steel jackets were investigated for strengthening columns with inadequate shear strength loaded either in the weak direction or the strong direction. Also, the effectiveness of isolated steel collars and partial steel jackets were examined.

### **2.3 SUMMARY**

Some significant past research results on seismic retrofit techniques for non-ductile reinforced concrete frames were presented. A detailed discussion is also provided on past research of jacketing techniques for retrofitting columns with an inadequate lap splice or with inadequate shear strength. Some of the previous research showed that addition of steel bracing, by itself, may not be adequate to prevent shear failure of columns. This indicates that in some cases columns need to be strengthened even if a different global seismic retrofit system was selected. Results of some previous research indicated that rectangular steel jackets were not adequate as a seismic retrofit for columns with inadequate lap splices. Also the effectiveness of rectangular steel jackets as a seismic retrofit for columns with inadequate shear strength was questioned. Rectangular steel jackets are the most suitable steel jackets for seismic strengthening of non-ductile reinforced concrete building columns. Compared to circular or elliptical steel jackets, rectangular steel jackets fit well with the

partition walls and occupy considerably less space for retrofitting square and rectangular columns.

In the study reported here, the use of rectangular steel jackets for seismic strengthening and repair of columns with inadequate lap splices and columns with inadequate shear strength was investigated. Design guidelines for the use of rectangular steel jackets as a seismic retrofit technique are also presented.

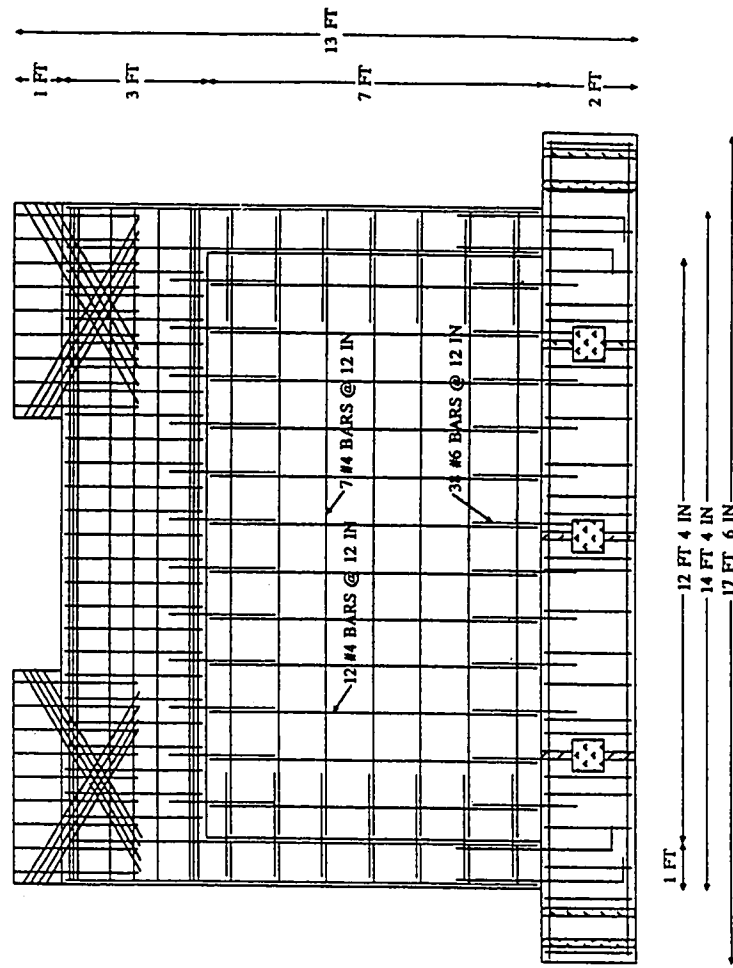


Figure 2.1 Seismic Strengthening by the Addition of Infill Walls,  
 Details of Concentric Infill Wall, Gaynor, Ref. [17].

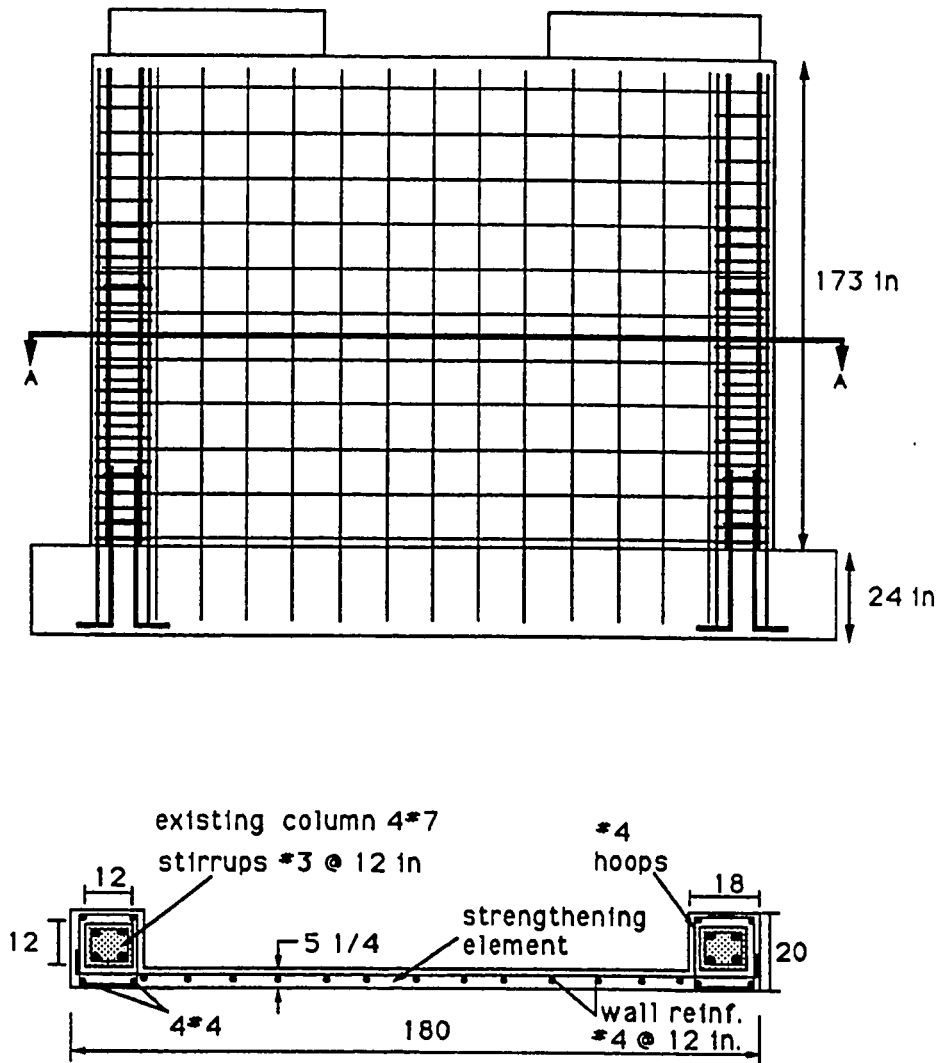


Figure 2.2 Seismic Strengthening by the Addition of Infill Walls,  
Details of Eccentric Infill Wall, Jimenez, Ref. [18].

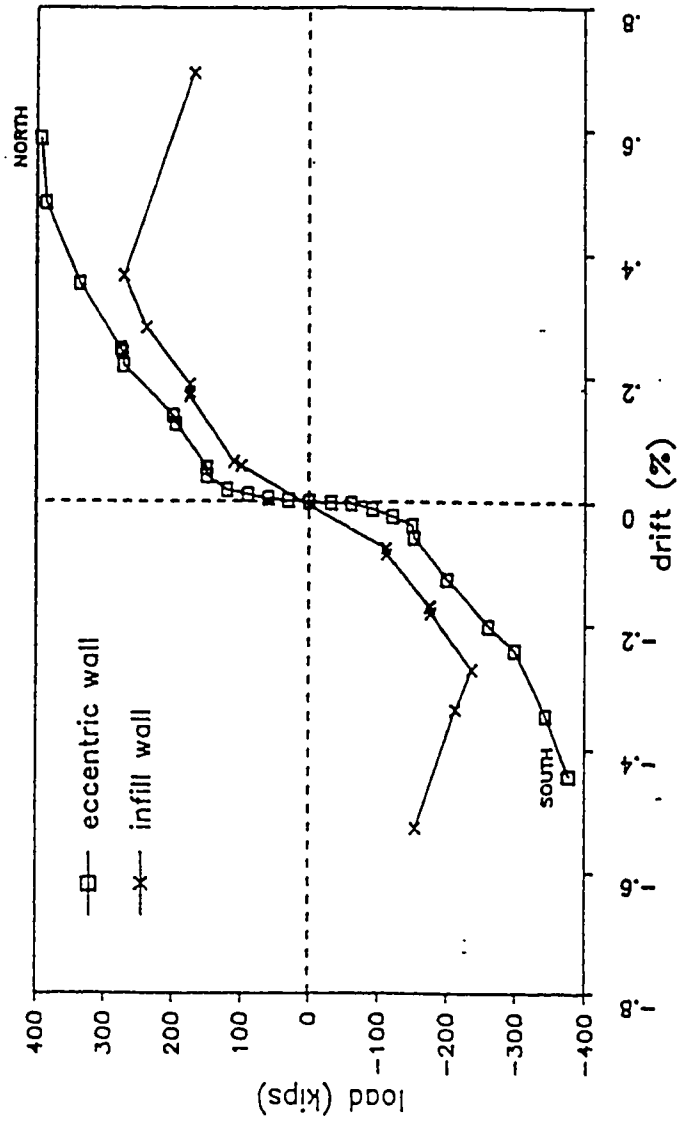


Figure 2.3 Seismic Strengthening by the Addition of Infill Walls, Envelopes of Cyclic Response of Infill Walls, Refs. [17,18].



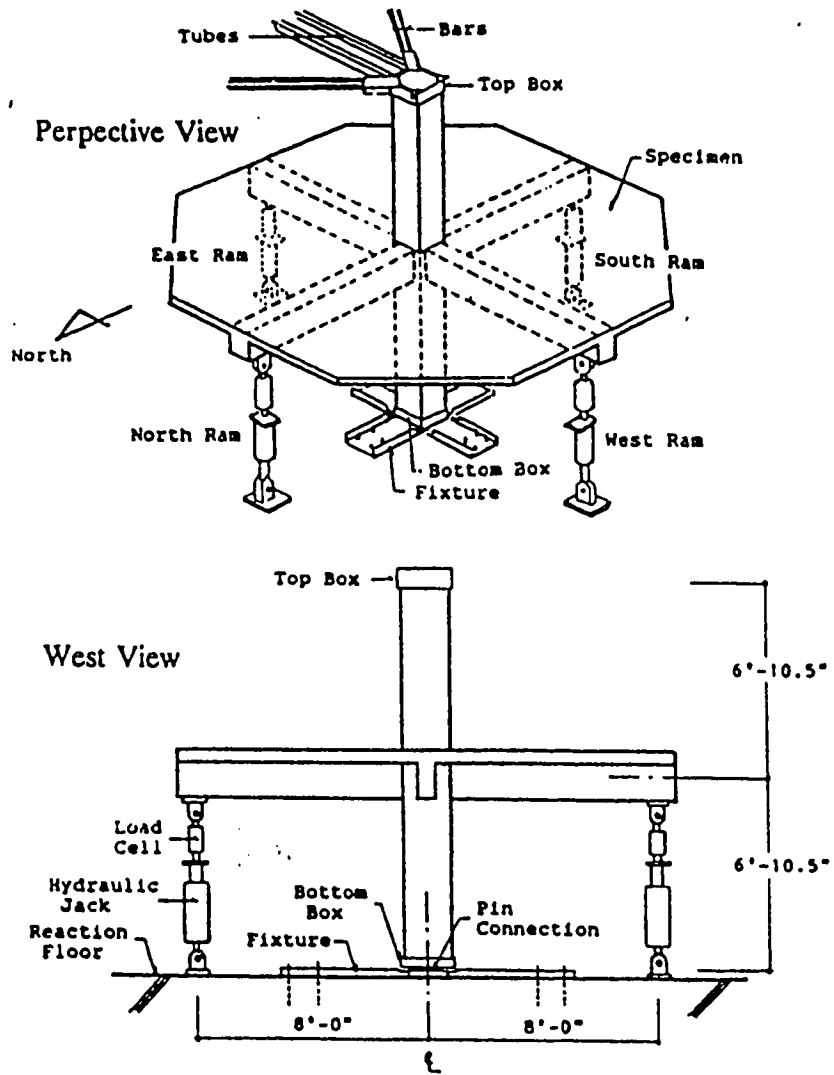


Figure 2.4 Strengthening by the Use of Concrete Jackets, Test Setup, Ref.[19].

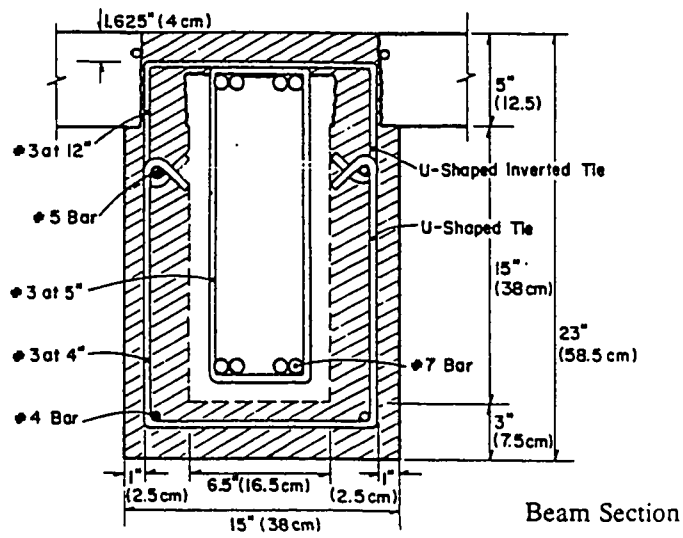
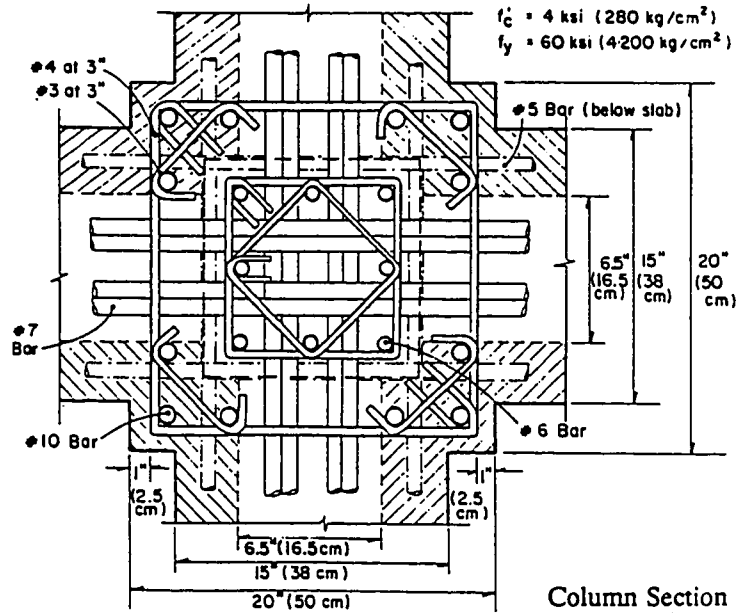
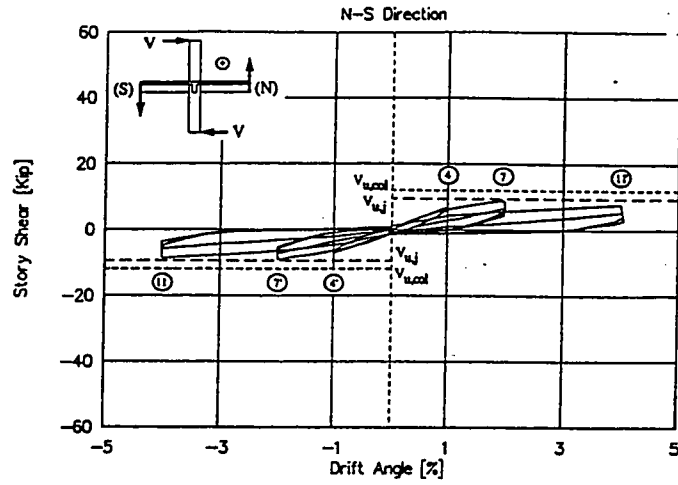
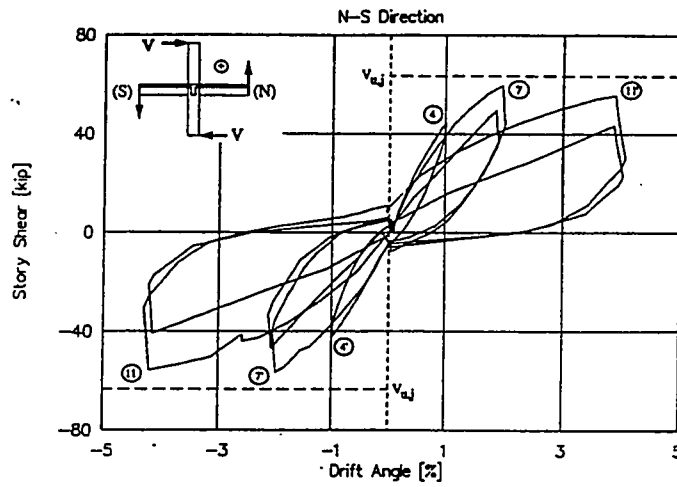


Figure 2.5 Strengthening by the Use of Concrete Jackets, Details of the Strengthened Specimen, Ref.[19].



(a) Hysteretic Response of the Unstrengthened Specimen



(b) Hysteretic Response of the Strengthened Specimen

Figure 2.6 Response of Beam-Column Subassemblages Retrofitted by the use of Concrete Jackets, Ref. [19].

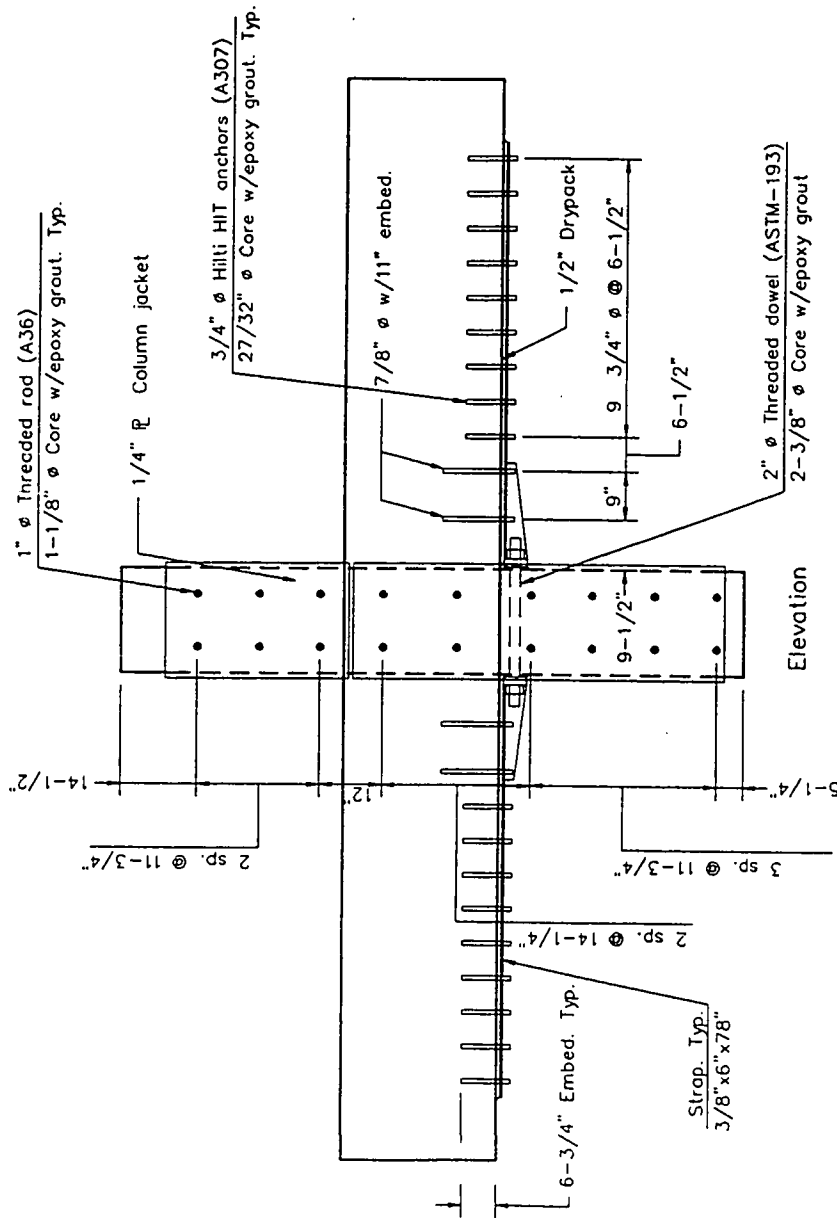


Figure 2.7 Strengthening by the Addition of Steel Plates, Details of the Strengthened Specimen, Ref. [20].

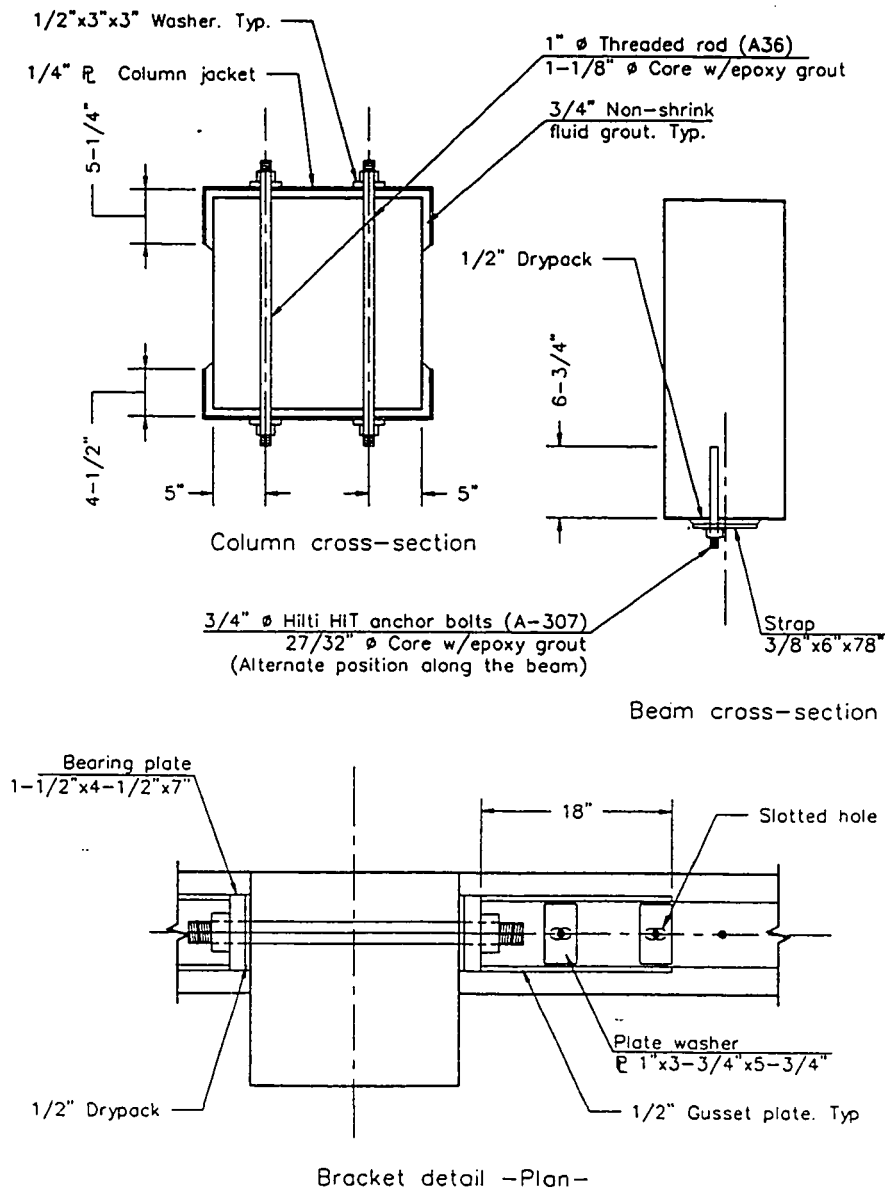


Figure 2.8 Strengthening by the Addition of Steel Plates, Sections Through Strengthened Column and Beam Ref. [20].

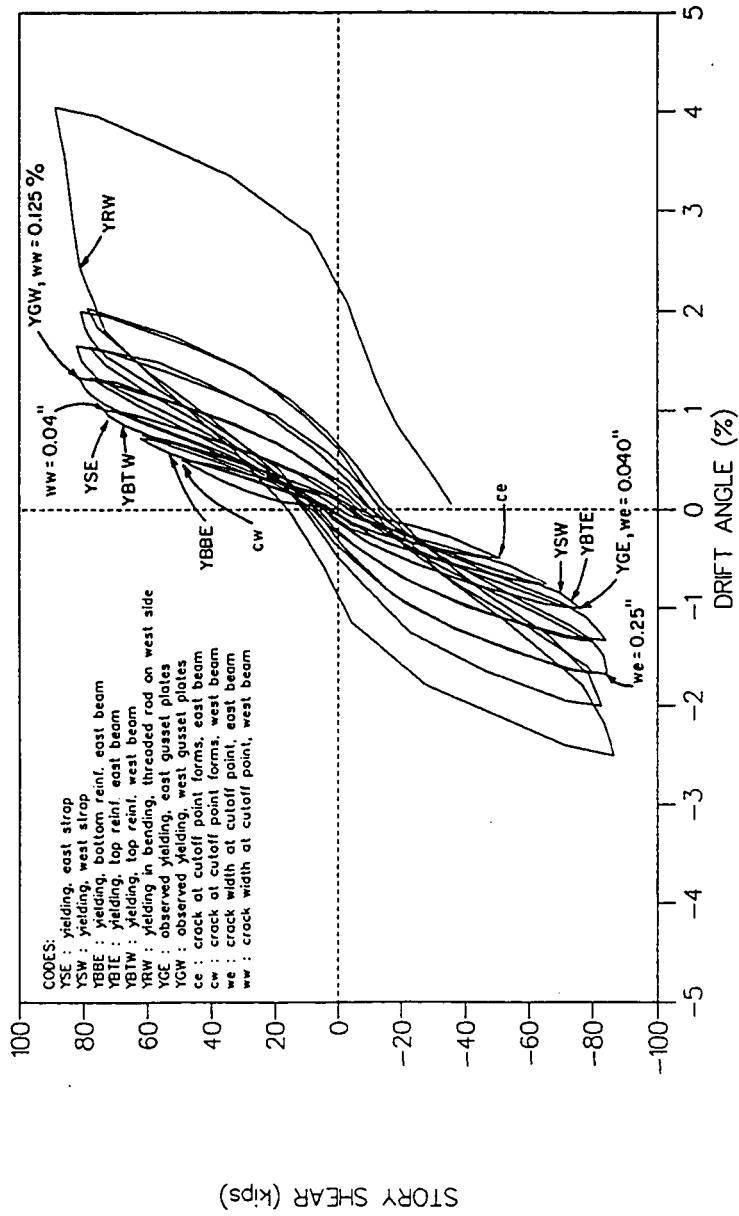


Figure 2.9 Response of the Specimen Tested by Estrada, Ref. [20].

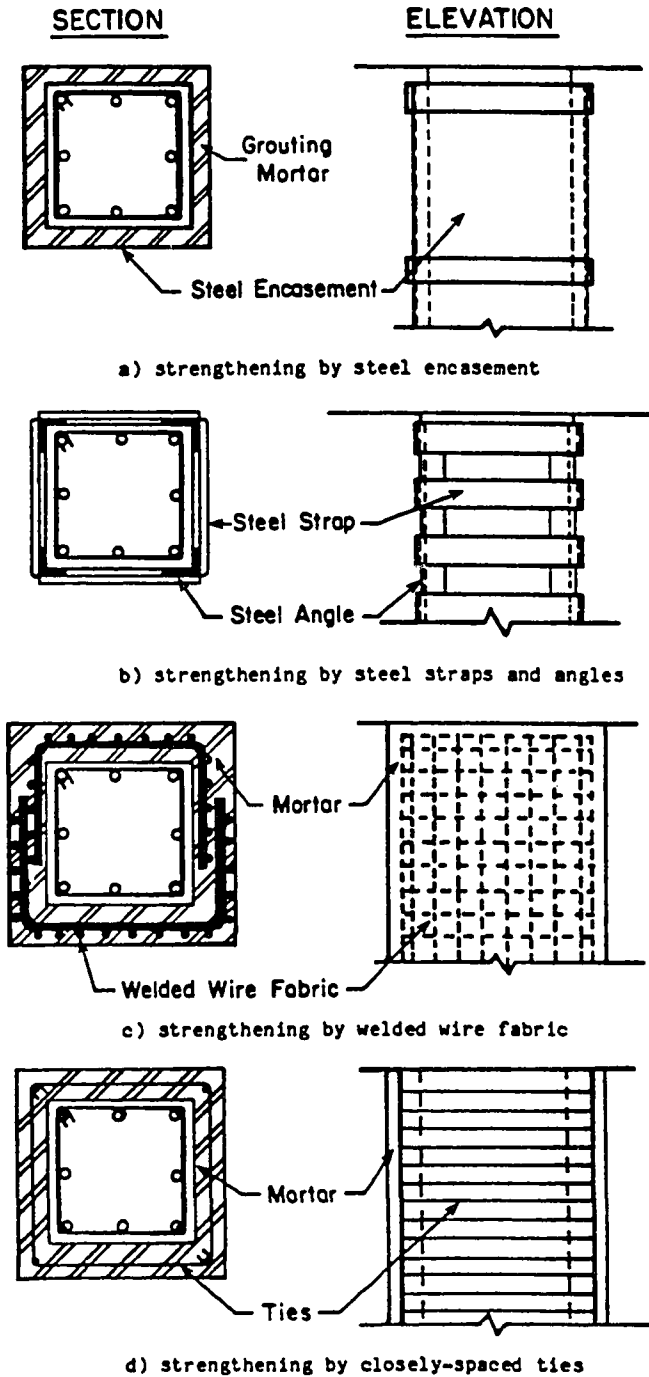
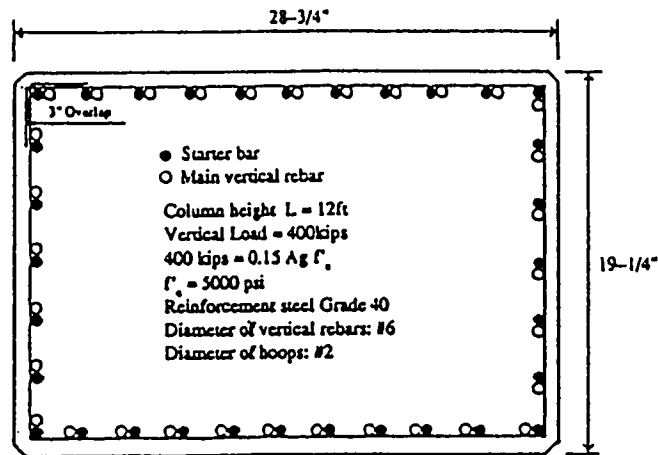
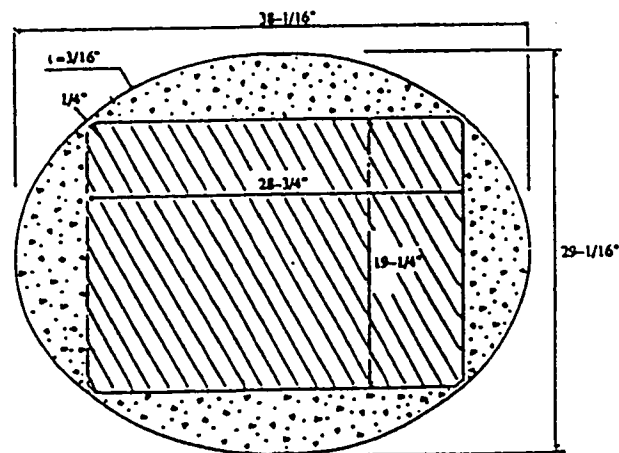


Figure 2.10 Column Jacketing Techniques, Ref. [26].



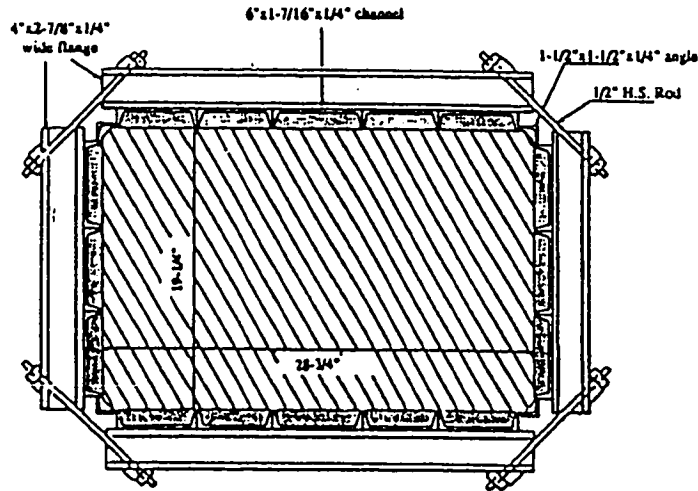
(a) Column 1 - 'As-Built'



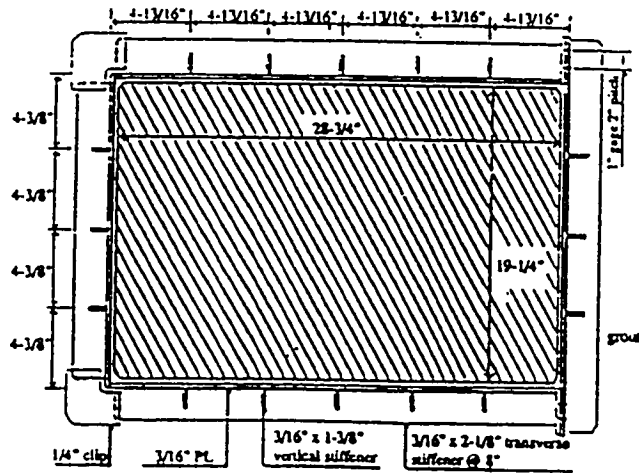
(b) Column 2 - Elliptical Retrofit

Figure 2.11 Strengthening of Columns with Inadequate Lap Splices, Ref.[2].



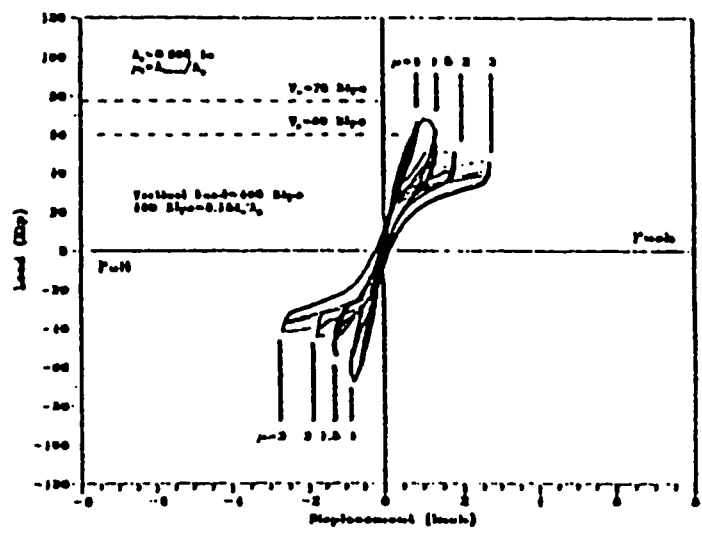


(c) Column 3 - 'Built-up' Steel Channels

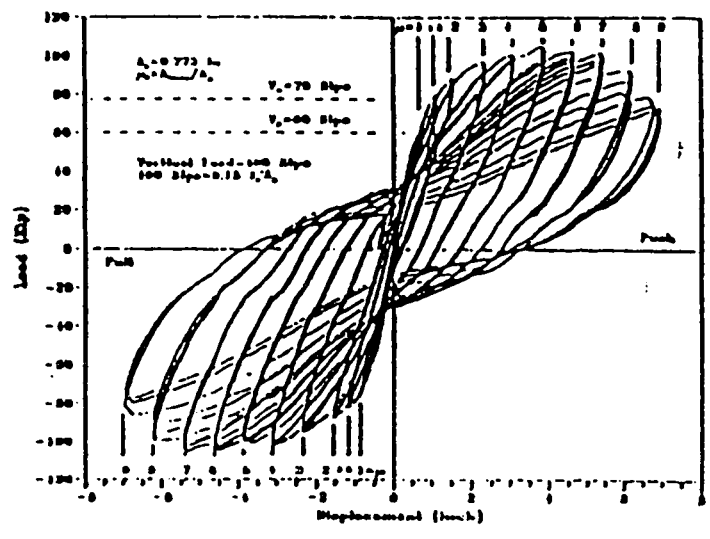


(d) Column 4 - Stiffened Rectangular Jacket

Figure 2.12 Strengthening of Columns with Inadequate Lap Splices, Ref.[2].

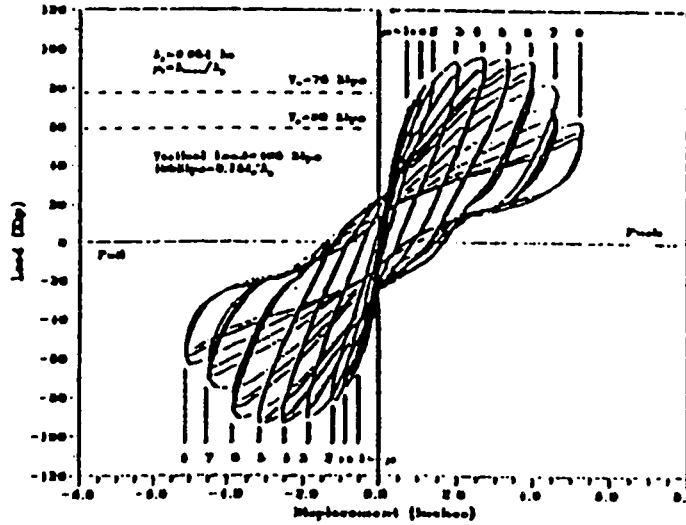


(a) Column 1 - 'As-Built'

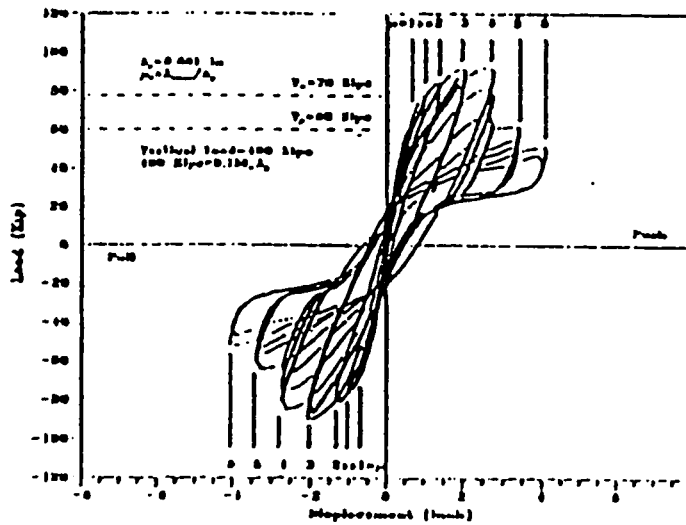


(b) Column 2 - Elliptical Retrofit

Figure 2.13 Response of Strengthened Columns with Inadequate Lap Splices, Ref.[2].



(c) Column 3 - 'Built-up' Steel Channels



(d) Column 4 - Stiffened Rectangular Jacket

Figure 2.14 Response of Strengthened Columns with Inadequate Lap Splices, Ref.[2].

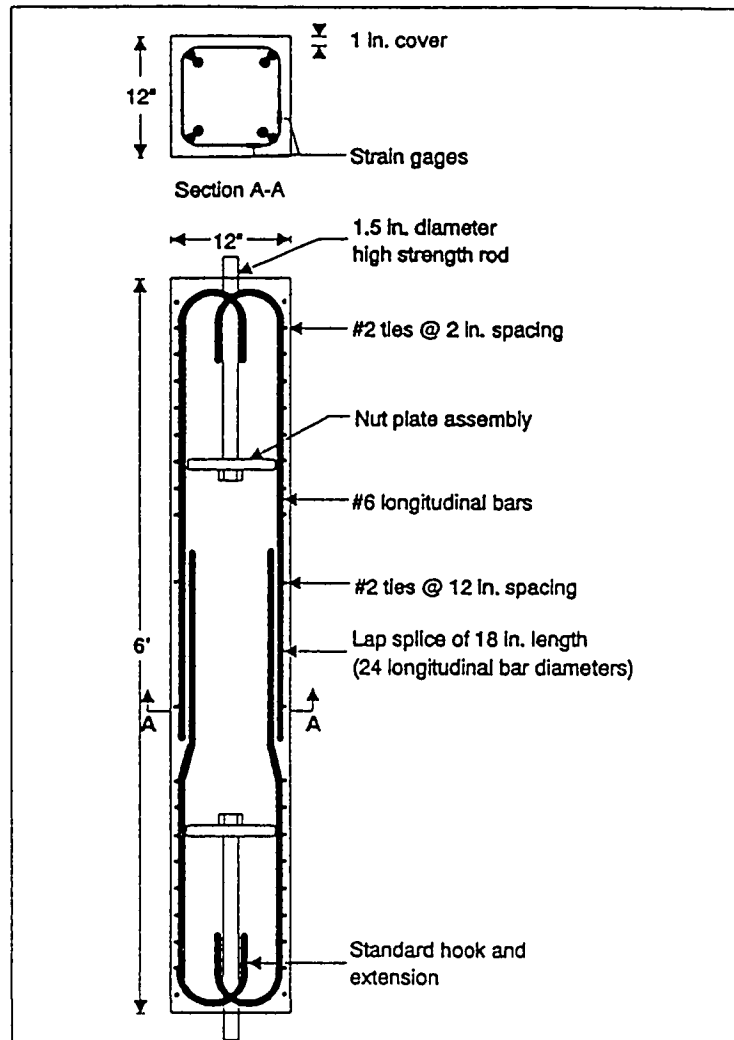


Figure 2.15 Strengthening of Columns With Inadequate Lap Splices, Reinforcement Details of the basic Column, Ref.[23].

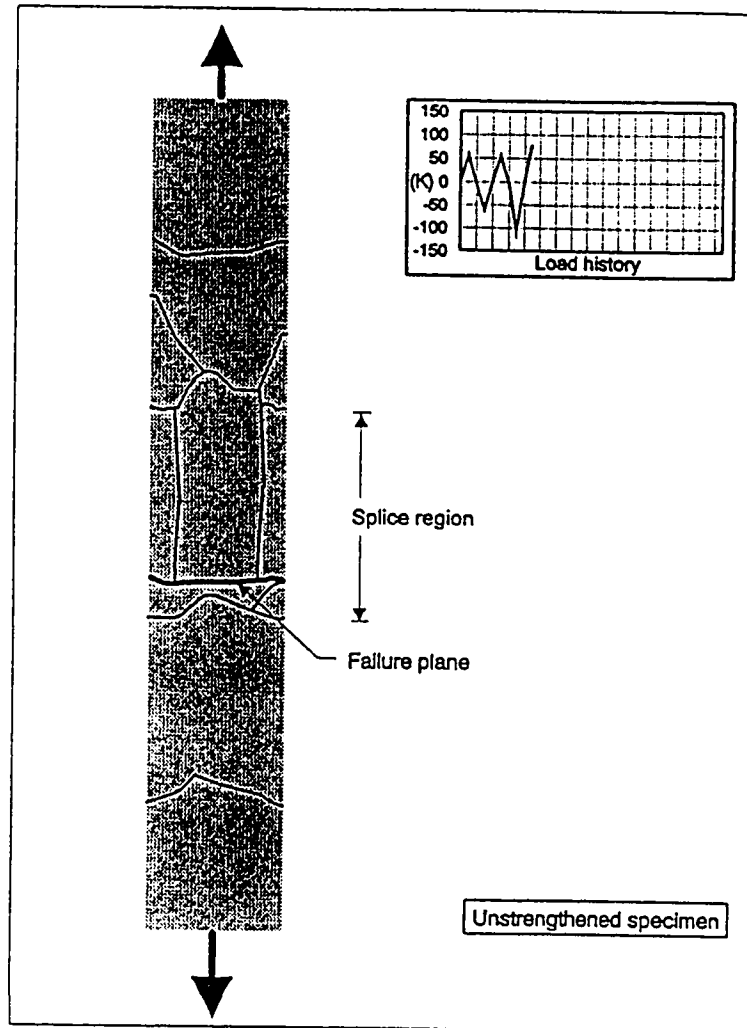


Figure 2.16 Strengthening of Columns With Inadequate Lap Splices, Crack Pattern in the Basic Unretrofitted Column, Ref.[23].

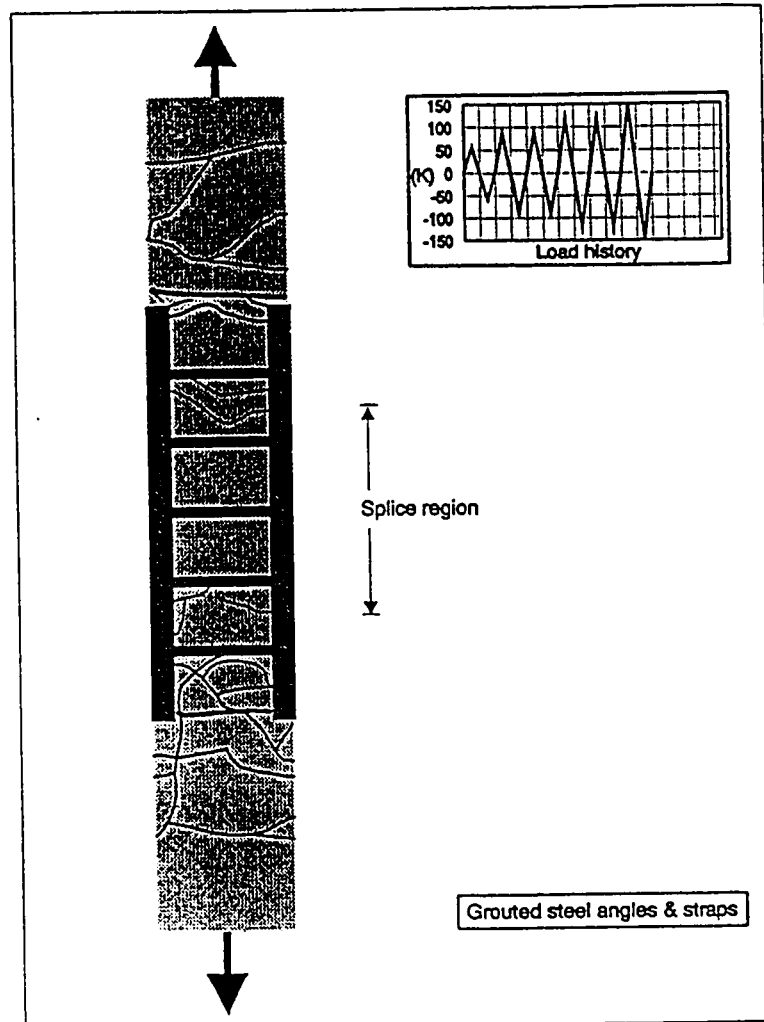


Figure 2.17 Strengthening of Columns With Inadequate Lap Splices, Crack Pattern in the Retrofitted Column, Ref.[23].

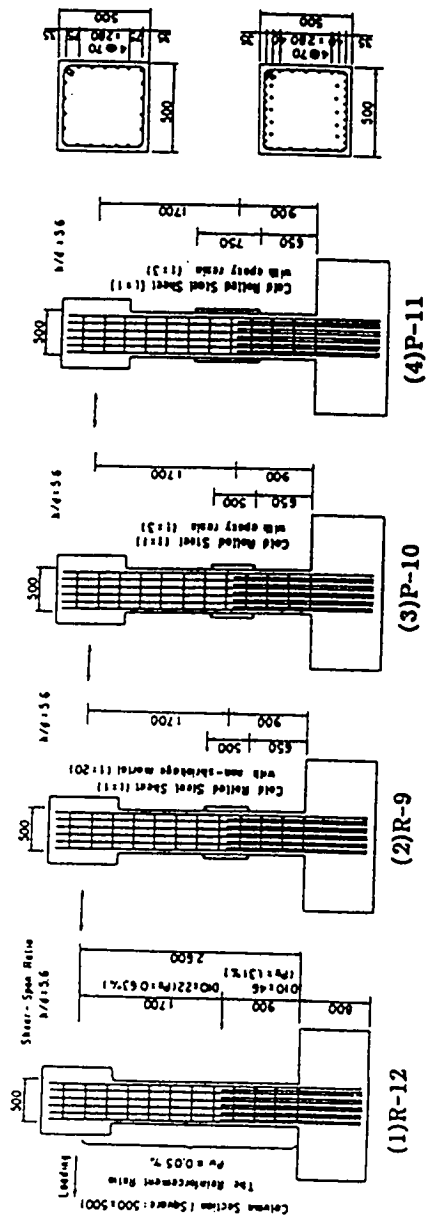


Figure 2.18 Shear Strengthening of Square Columns by the Use of Steel Jackets, Details of the test Columns, Ref. [24].

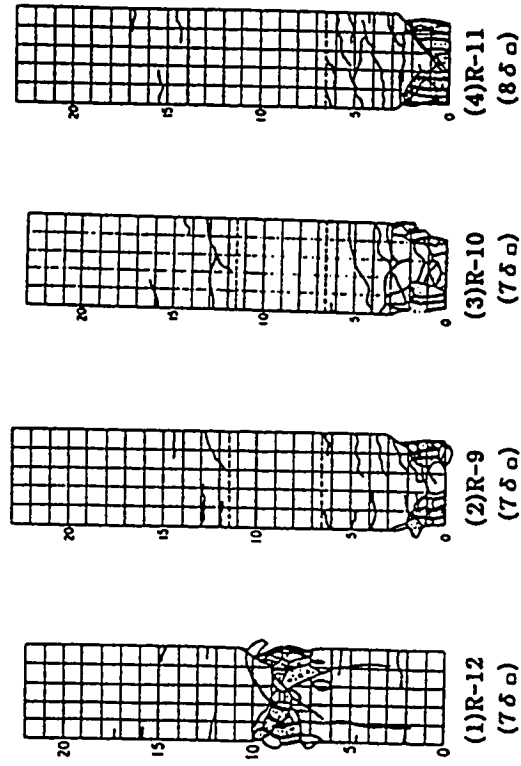


Figure 2.19 Shear Strengthening of Square Columns by the Use of Steel Jackets, Crack Pattern of the test Columns, Ref. [24].



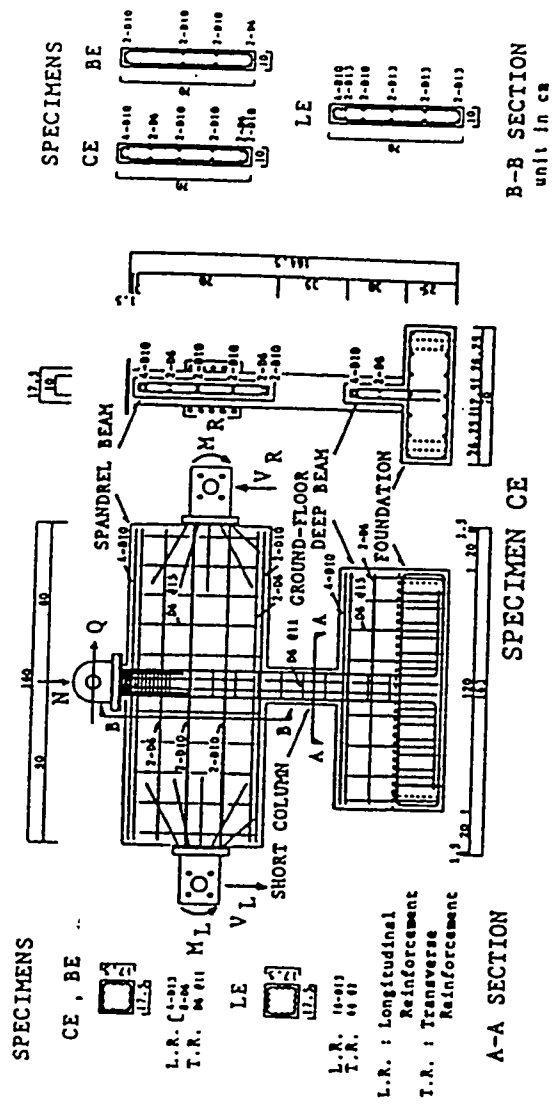
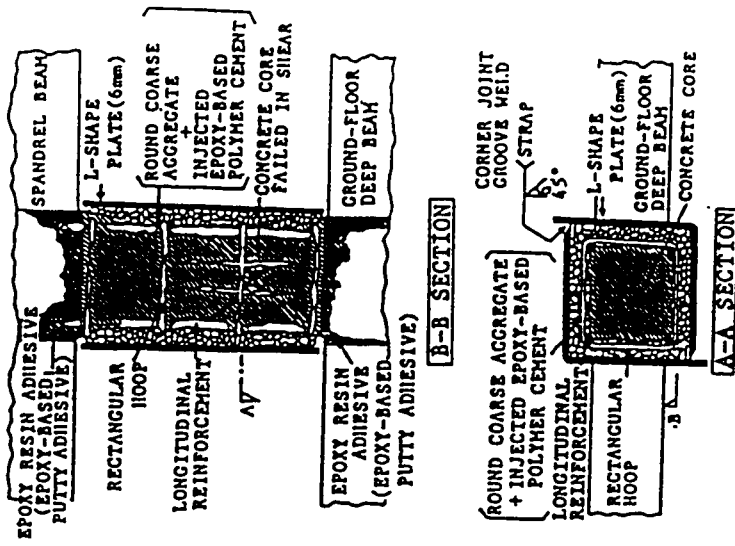
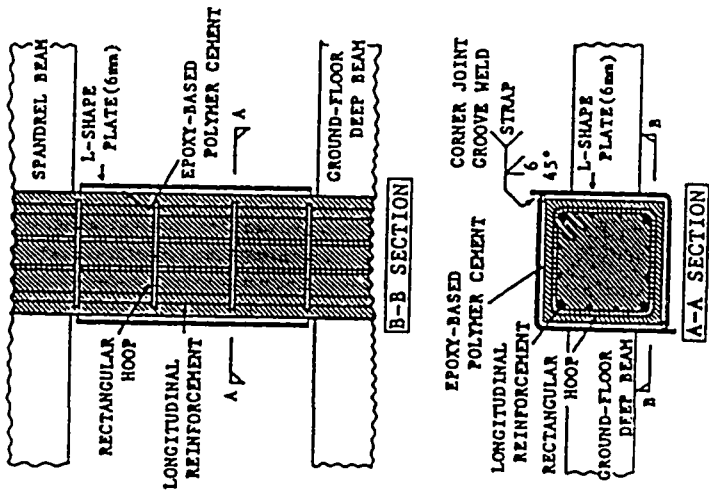


Figure 2.20 Shear Strengthening and Repair of Short Square Columns by the Use of Steel Jackets, Details of the Basic Test Specimen, Ref. [3].

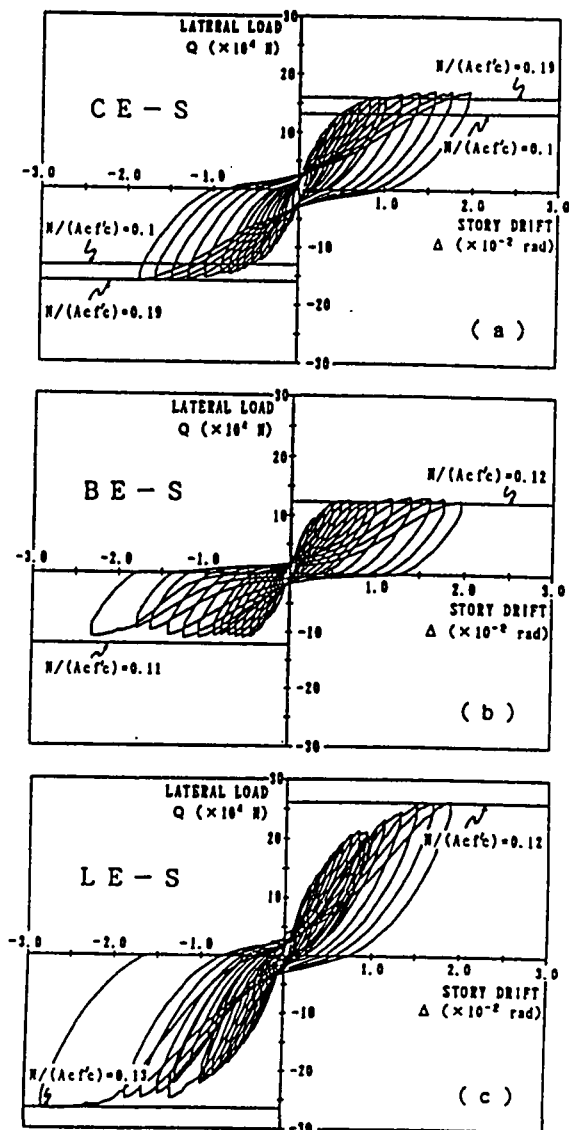


(a) Strengthened Short Column.



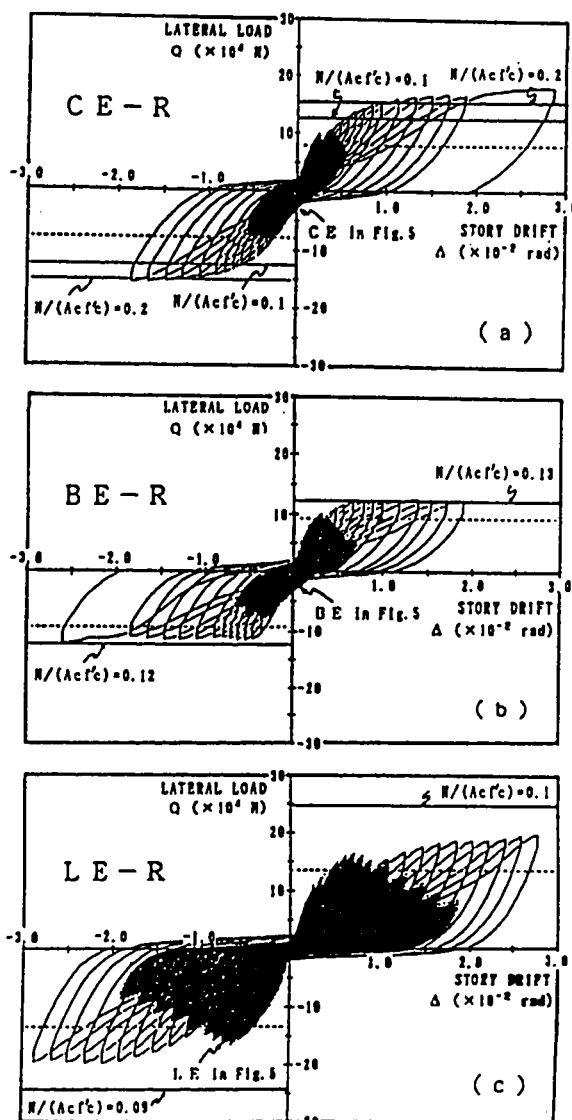
(b) Repaired Short Column.

Figure 2.21 Shear Strengthening and Repair of Short Square Columns by the Use of Steel Jackets, Details of the Strengthened and Repaired Columns, Ref. [3].



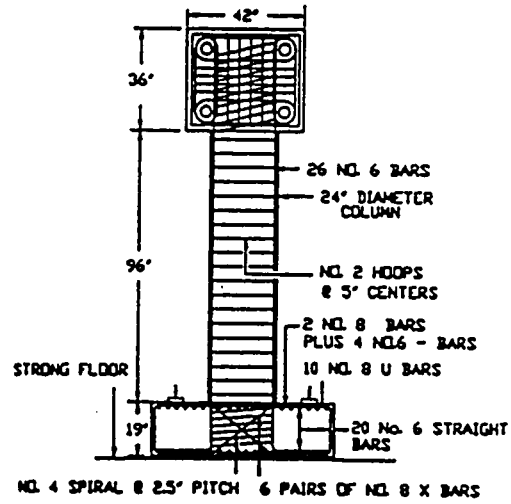
## Strengthened Columns

Figure 2.22 Response of Columns with Inadequate Shear Strength Retrofitted by the Use of Steel Jackets, Ref.[3].

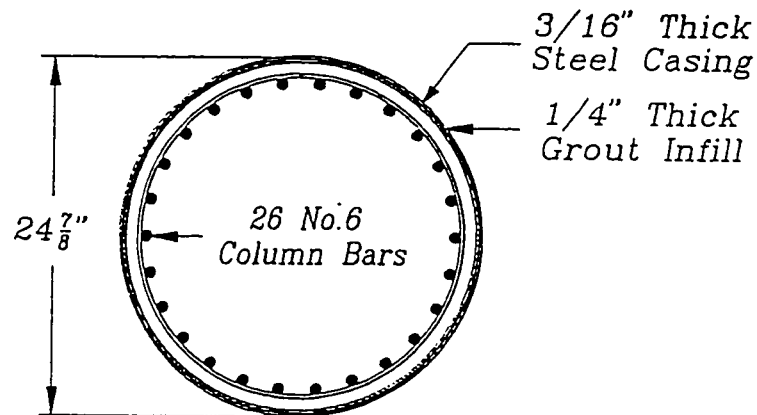


### Unretrofitted and Repaired Columns

Figure 2.23 Response of Columns with Inadequate Shear Strength Repaired by the Use of Steel Jackets, Ref.[3].

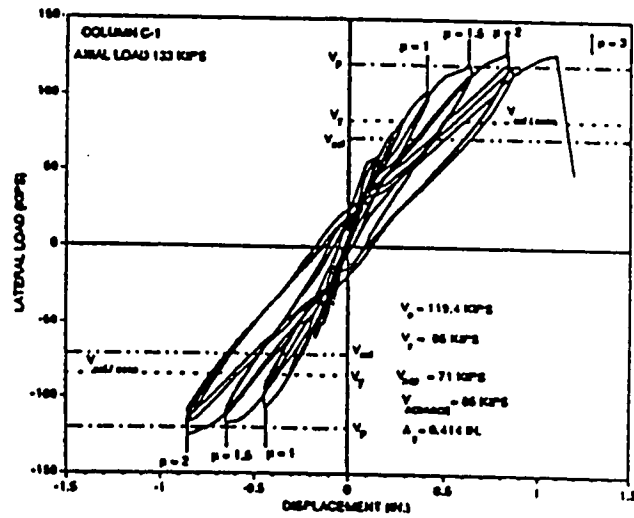


(a) Details of Circular Shear Column

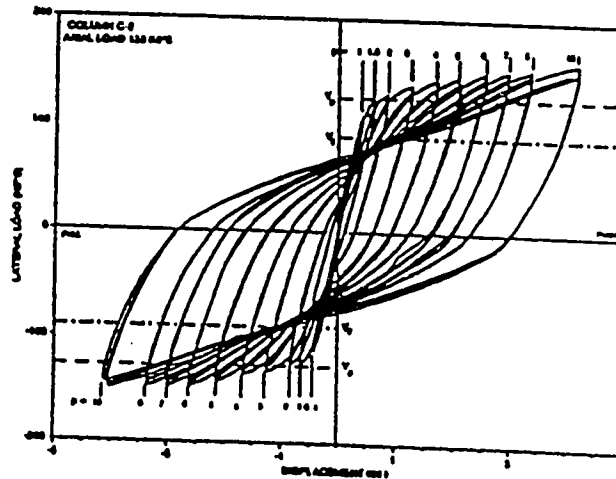


(b) Cross-Section of Retrofitted Circular Column

Figure 2.24 Details of Columns with Inadequate Shear Strength Retrofitted by the Use of Cylindrical Steel Jackets, Ref.[2].

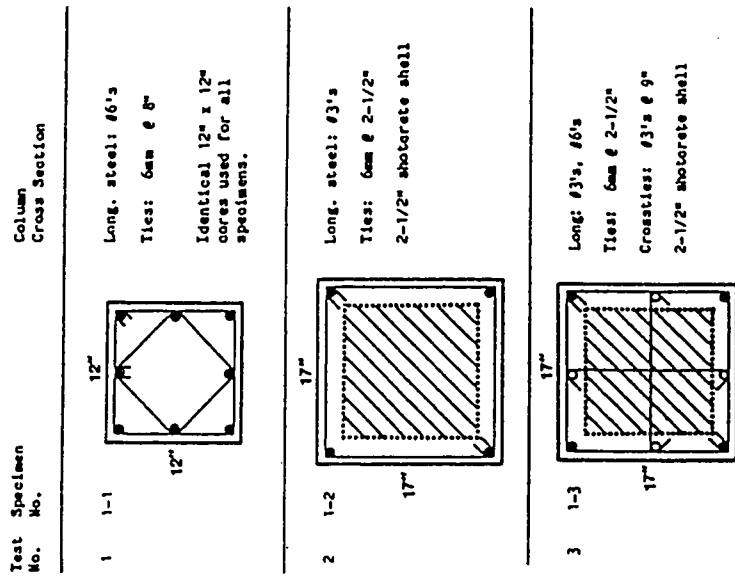


(a) Response of the Unretrofitted Column

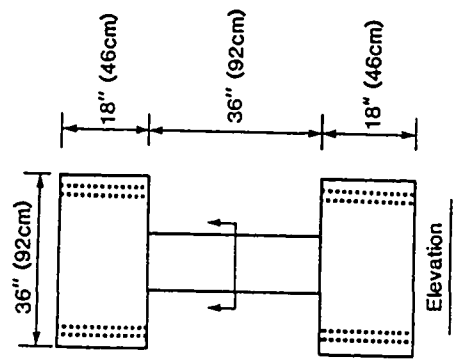


(b) Response of the Retrofitted Column

Figure 2.25 Response of Columns with Inadequate Shear Strength Retrofitted by the Use of Cylindrical Steel Jackets, Ref.[2].

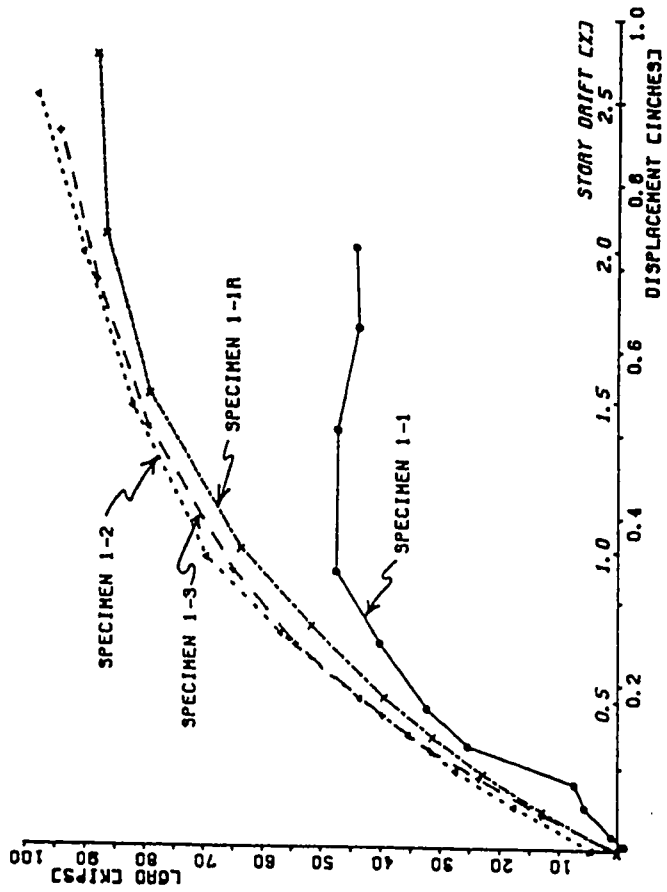


(b) Cross-Section Details of Columns



(a) Details of Basic Column

Figure 2.26 Seismic Shear Strengthening of Columns by the Use of Concrete Jackets, Ref.[25].



Envelope the of Cyclic Response (Push Direction only )

Figure 2.27 Seismic Shear Strengthening of Columns by the Use of Concrete Jackets, Ref.[25].



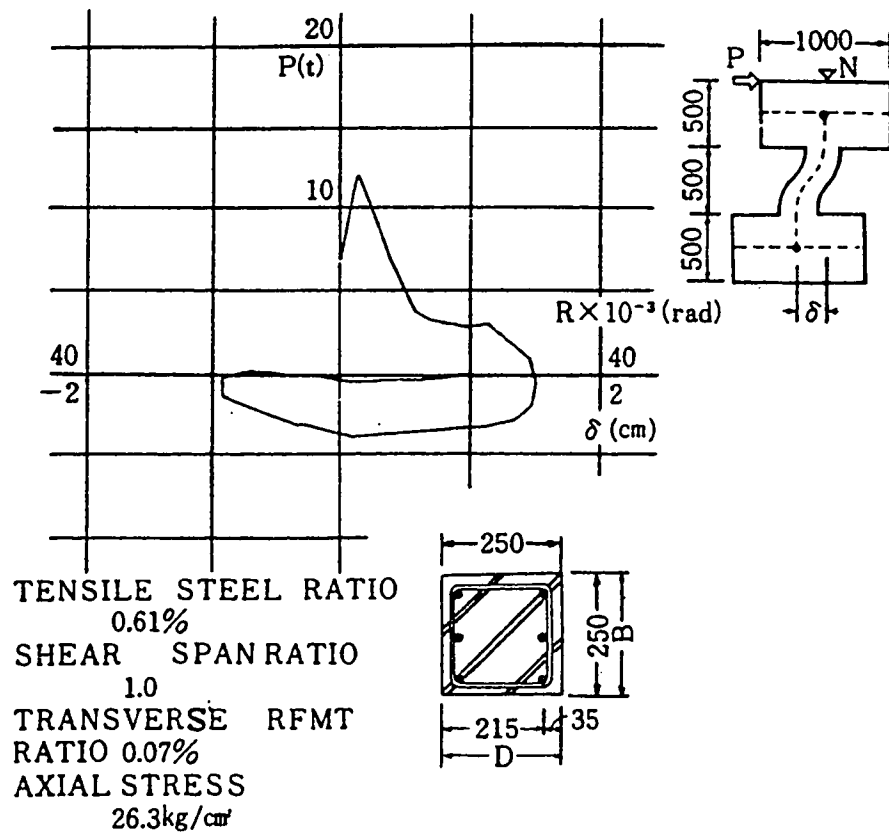


Figure 2.28 Shear Strengthening of Columns by the Use of Concrete Jackets, Details & Response of the Unretrofitted Column, Ref.[26].

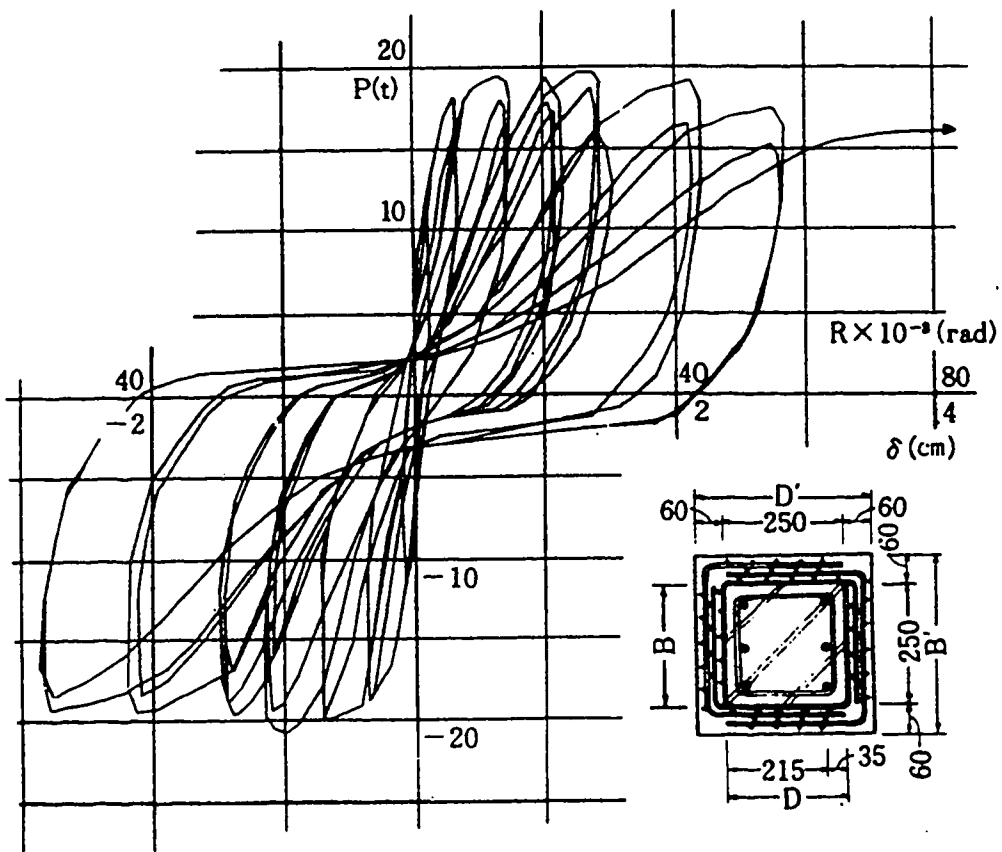


Figure 2.29 Shear Strengthening of Columns by the Use of Concrete Jackets, Details & Response of the Retrofitted Column, Ref.[26].

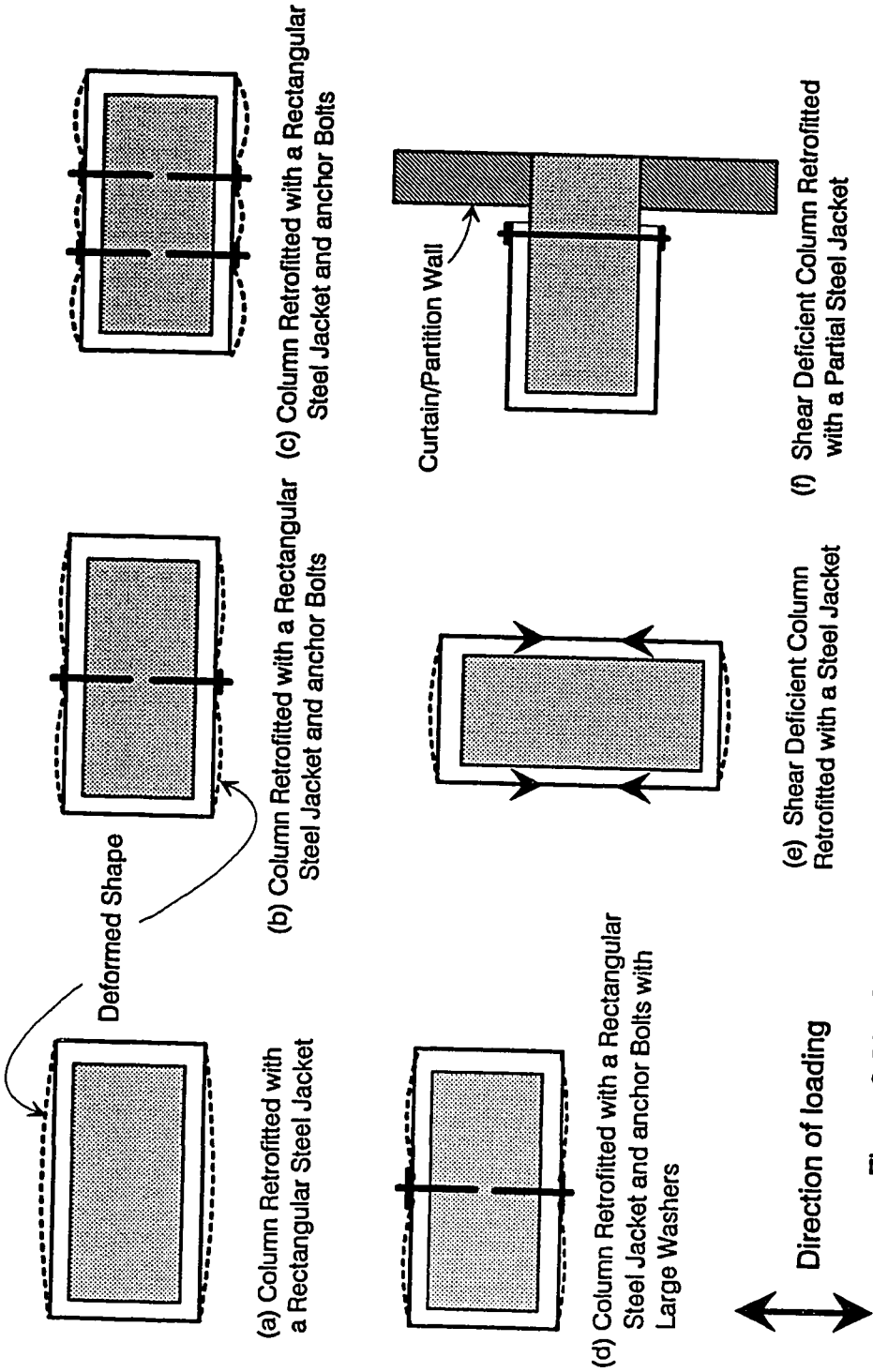


Figure 2.30 Column Strengthening by the use of Rectangular steel jackets

## **CHAPTER 3**

### **EXPERIMENTAL PROGRAM- GENERAL**

#### **3.1 INTRODUCTION**

In this study the use of rectangular steel jackets as a seismic retrofit technique for non-ductile reinforced concrete columns was examined. Large scale columns with inadequate lap splices in the longitudinal reinforcement and columns with inadequate shear strength were experimentally investigated. Columns were detailed according to the provisions of the ACI 318-56 and ACI 318-63 codes. This Chapter presents part of the experimental program including specimens details, test setup and instrumentation.

Twenty-eight large scale reinforced concrete columns were constructed and tested before and after being retrofitted with steel jackets. Appendix "A" presents the construction sequence of four columns. In one phase of this experimental program, seventeen columns were tested to examine the effectiveness of steel jackets in seismic retrofit of columns with an inadequate lap splice in the longitudinal bars. In this report, these specimens are referred to as "Flexural Column". Pre-earthquake strengthening and post-earthquake repair of the flexural columns were investigated. Table 3.1 summarizes the experimental program in this phase. Section 3.2.1 presents the details of the basic unretrofitted flexural columns. The details of the retrofitted flexural columns are presented in section 3.2.3. The behavior of individual specimens with inadequate lap splice is presented in Chapter 4.

Table 3.1 Summary of the Flexural Columns

Col. #	Type	Size (W"xD")	Cross ties	X-Sec. Type	Retrofit Type	Ref. Column	Damaged Column	Concrete $f_c$ (psi)	Footing
FC1	Basic	36"x18"	EB	B	N/A	N/A	N/A	4700	F1
FC2	S	36"x18"	EB	B	LSI/AB	FC1	N/A	4900	F2
FC3	R	36"x18"	EB	B	Collars	FC1	FC2	4900	F2
FC4	Basic	36"x18"	EOB	A	N/A	N/A	N/A	2850	F1
FC5	Basic	36"x18"	EB	B	N/A	N/A	N/A	2980	F2
FC6	R	36"x18"	EOB	A	LSI/AB	FC4	FC4	2850	F1
FC7	R	36"x18"	EB	B	Welded	FC5	FC5	2980	F2
FC8	S	36"x18"	EOB	A	Collars	FC4	N/A	2595	F5
FC9	S	36"x18"	EOB	A	LSI/AB	FC4	N/A	2905	F6
FC10	R	36"x18"	EOB	A	SSI/AB	FC4	FC8	2595	F5
FC11	S	36"x18"	EOB	A	SSI/AB	FC4	N/A	2850	F6
FC12	S	36"x18"	EOB	A	LSI/AB	FC4	N/A	3265	F5
FC13	R	36"x18"	EOB	A	LSI/TB	FC4	FC12	3265	F5
FC14	Basic	27"x18"	EOB	C	N/A	N/A	N/A	4165	F1
FC15	Basic	18"x18"	NO	D	N/A	N/A	N/A	4165	F6
FC16	S	27"x18"	EOB	C	LSI/AB	FC14	N/A	2565	F1
FC17	S	18"x18"	NO	D	LSI/AB	FC15	N/A	2635	F6

R= Repaired, S= Strengthened, EB= Cross tie at Every Bar, EOB= Cross tie at Every Other Bar.

LSI = Long Steel Jacket, SSI= Short Steel Jacket, AB= Anchor Bolts, TB= Through Bolts.

1. See Figure 3.1.

2. Damaged columns that were repaired after testing.

3. Uniaxial Compressive Strength of 6x12" cylinder at the day of Testing.

4. Columns having the same footing number were built and tested using the same footing.

In a second phase of this experimental program, eleven columns with inadequate shear strength were tested before or after being strengthened with different steel jackets. In this report, these specimens are referred to as "Shear Columns". Columns were loaded either in the weak or the strong direction. Table 3.2 summarizes the experimental program in this series. All columns in this series were 18" x 36" in cross section. No post-earthquake repair was examined in this series, just pre-earthquake strengthening. The details of the basic unretrofitted shear columns are presented in section 3.2.2. The details of the retrofitted shear columns are presented in section 3.2.4. The behavior of each individual specimen with inadequate shear strength is presented in Chapter 5.

## **3.2 SPECIMEN DETAILS**

### **3.2.1 Basic Flexural Columns (With Inadequate Lap Splice)**

The test specimen was a cantilever type column, representing half a column in a real building frame. Cyclic lateral load was applied at the tip of the column. Figure 3.1 shows the details of the basic flexural columns. Footings were 80" x 80" in plan and 24" thick. Every footing was reinforced with a top and bottom mesh of 14#6 grade 60 deformed bars in both directions. Flexural columns were all 9.0 feet high from the top of the footing to the point of load application, to ensure flexure dominated behavior. All columns were loaded in the weak direction. Longitudinal bars/splices were located on the longer side of the column cross section, to examine the effectiveness of the steel jackets in confining lap splices on large size/wide columns. Longitudinal bars were all spliced at the base of the column as shown in Figure 3.1(e). The lap splice length was 24 bar diameters. Flexural columns were transversely reinforced with #3@16" grade 40 deformed bars.

Table 3.2 Summary of the Shear Columns							
Col. #	Type	Cross Ties	X-Sec. <sup>1</sup> Type	Retrofit Type	Direction of loading	Concrete <sup>2</sup> $f_c$ (psi)	Footings <sup>3</sup>
SC1	Basic	EB	B	N/A	Weak	5040	F3
SC2	Strengthened	EB	B	Collar	Weak	5040	F4
SC3	Basic	EOB	A	N/A	Weak	3170	F3
SC4	Basic	EB	B	N/A	Weak	3170	F4
SC5	Strengthened	EOB	A	Collar	Weak	2240	F3
SC6	Strengthened	EOB	A	W-SJ	Weak	2255	F4
SC7	Strengthened	EOB	A	B-SJ	Weak	2940	F7
SC8	Strengthened	EOB	A	U-PSJ	Weak	2785	F8
SC9	Basic	EOB	C	N/A	Strong	2325	F3
SC10	Strengthened	EOB	C	W-SJ	Strong	2390	F7
SC11	Strengthened	EOB	C	C-PSJ	Strong	2360	F8

EB = Cross tie at Every Bar, EOB = Cross tie at Every Other Bar.

W,SJ = Welded Steel Jacket, B,SJ = Bolted Steel Jacket, U-PSJ = U-shape Partial Steel Jacket, C-PSJ = 2C-shape Partial Steel Jacket.

1. See Figure 3.2.

2. Uniaxial Compressive Strength of 6x12" cylinder at the day of Testing.

3. Columns having the same footing number were built and tested using the same footing.

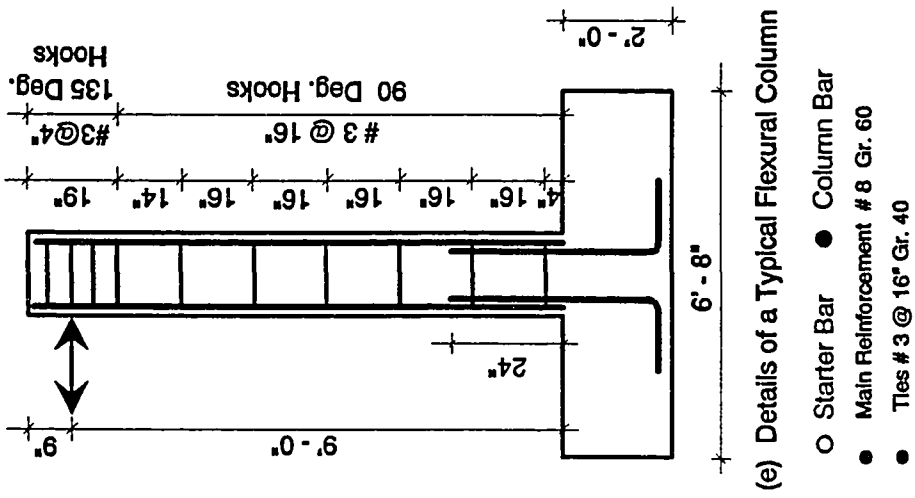
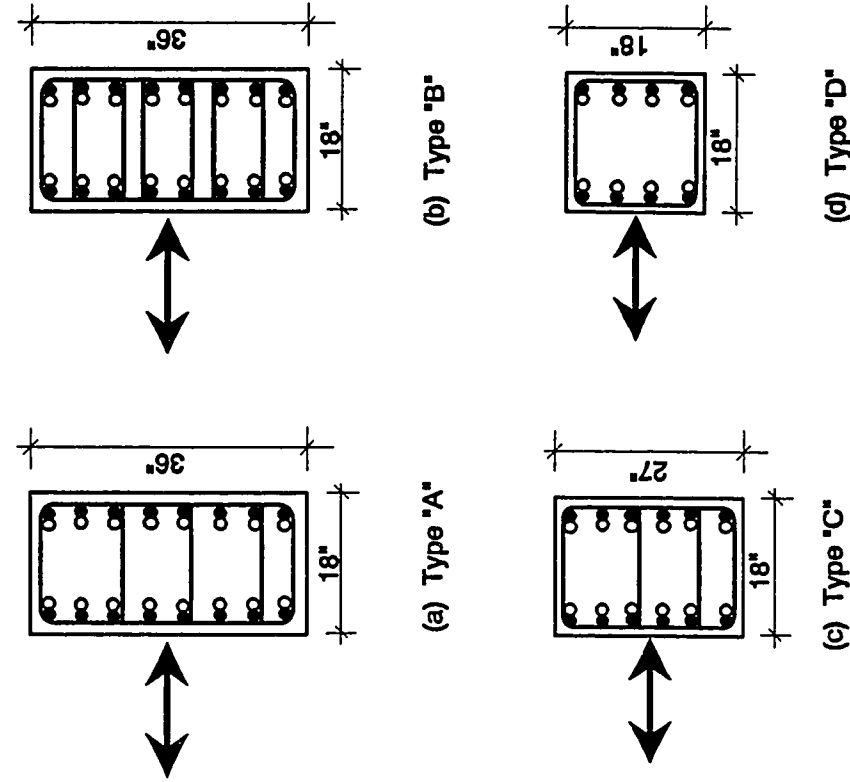


Figure 3.1 Details of the Basic Flexural Columns



Cross ties were provided with 90 degree hooks, as typically found in older buildings. A concrete cover of 1-1/2 inches was provided for all column ties.

Flexural specimens were of four different types. Type "A" columns were 18"x36" and reinforced with 16#8 longitudinal grade 60 deformed bars. They were designed according to the ACI 318-63 code provisions, which allowed the use of cross ties at every other bar if the spacing between the longitudinal bars was less than 6.0 inches. Thus, type "A" columns were transversely reinforced with #3 @ 16" grade 40 deformed cross ties at every other longitudinal bar as shown in Figure 3.1(a). Type "B" columns were designed according to the ACI 318-56 code provisions. The details of type "B" columns were similar to those of type "A" columns, but a cross tie was provided at every longitudinal bar, as shown in Figure 3.1(b). Type "C" columns were 18"x27" and reinforced with 12#8 grade 60 longitudinal deformed bars. Cross ties were #3 @ 16" grade 40 and were provided at every other longitudinal bar, as shown in Figure 3.1(c). The type "D" specimen was an 18"x18" square column, reinforced with 8#8 longitudinal deformed bars. Transversely, the type "D" column was reinforced with only one #3 peripheral tie every 16 inches. Figure 3.1(d) shows the cross section details of column type "D".

### **3.2.2 Basic Shear Columns (With Inadequate Shear Strength)**

Figure 3.2 shows the details of the basic shear columns. Shear columns were built on footings similar to those used for the flexural columns. All shear columns were 4.0 feet high from the top of the footing to the point of load application, to ensure shear dominated behavior. Eight columns were loaded in the weak direction, having a shear span to depth ratio of 2.67. Three columns were loaded in the strong direction, having a shear span to depth ratio of 1.33. All columns were reinforced with 16#8 grade 60

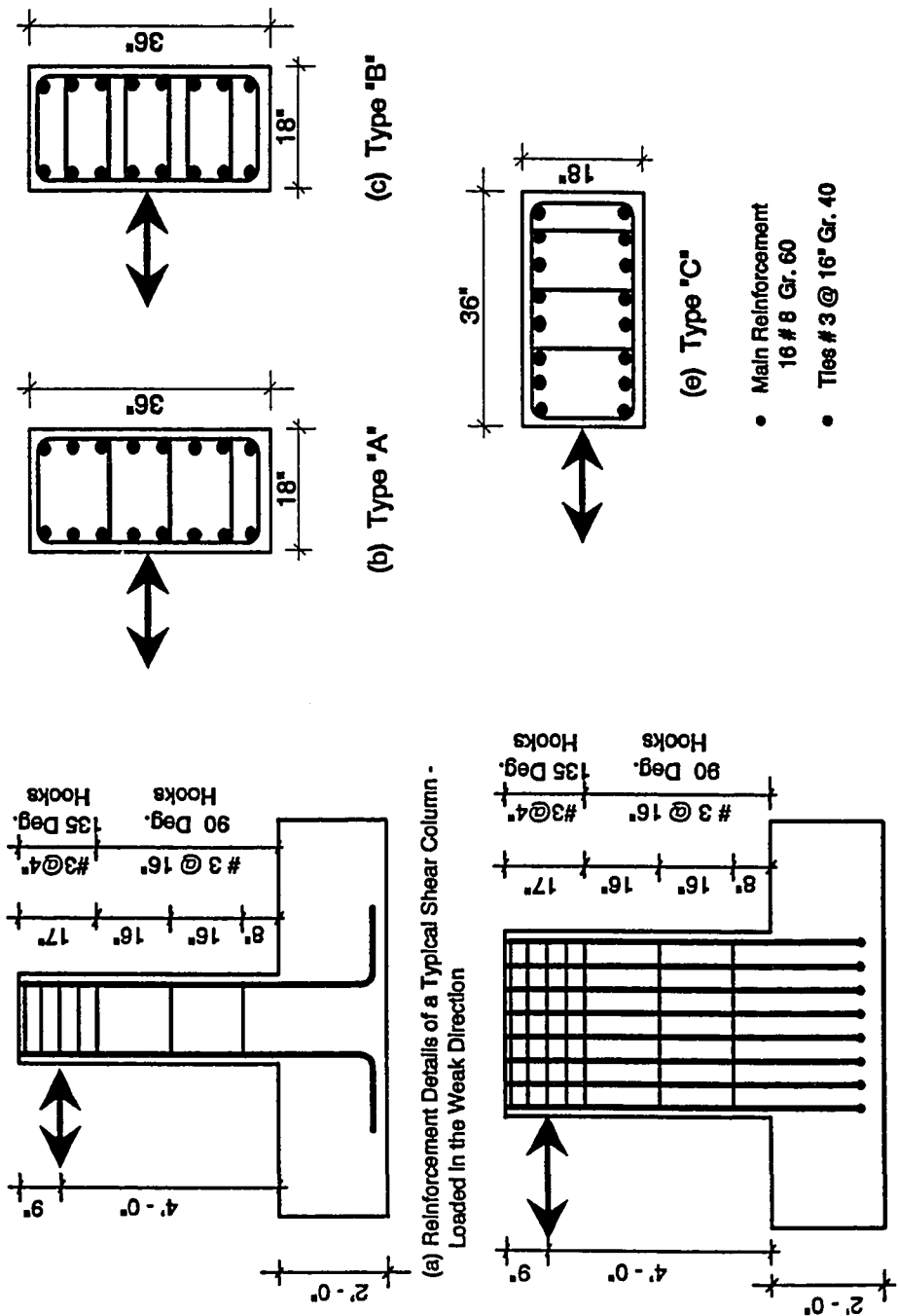


Figure 3.2 Details of the Basic Shear Columns

longitudinal deformed bars. Bars were not spliced, but continuous throughout the column and into the footing, as shown in Figure 3.2(a) & (d). Types "A" & "C" were transversely reinforced with cross ties at every other longitudinal bar. However, type "B" columns were transversely reinforced with cross ties at every longitudinal bar. Type "A" & "B" columns were loaded in the weak direction, while type "C" columns were loaded in the strong direction.

### **3.2.3 Retrofitted Flexural Columns**

Retrofitted columns were strengthened or repaired by the use of rectangular steel jackets, except specimen FC7, where the lap splice was welded. Steel jackets were provided in the splice region at the base of the column. The specific details of each steel jacket are presented in chapter 4. Section 3.2.3.1 presents the general details of rectangular solid steel jackets with and without adhesive anchor bolts. Section 3.2.3.2 presents the general details of steel collars used for strengthening columns with an inadequate splice. The general details of steel jackets with through bolts used for repair of damaged columns with an inadequate splice are presented in section 3.2.3.3. The details of a welded splice for repair of a damaged column are presented in section 3.2.3.4.

#### **3.2.3.1 Rectangular Solid Steel Jacket with Adhesive Anchor Bolts**

Columns retrofitted using rectangular solid steel jackets were of three different widths, 36", 27" and 18". The height of the rectangular solid steel jacket was either 1.5 or 1.2 times the length of the lap splice. The steel jacket was terminated 1.5 inches above the column base to prevent any possible bearing of the steel jacket against the footing. Such bearing may considerably increase the column's required shear strength, or may damage the jacket. For

the 36 inch wide columns, the confinement provided by the steel jacket may be reduced because the steel plate has poor out-of-plane flexural stiffness. Such a steel jacket was tested with and without adhesive anchor bolts. Figure 3.3(b) shows a column strengthened by the use of a rectangular steel jacket and adhesive anchor bolts.

Adhesive anchor bolts stiffen the steel jacket and potentially improve the performance of the strengthened column. All adhesive anchor bolts were 1.0 inch in diameter and 12 inches long. They were embedded eight inches into the concrete column. Appendix "B" shows the details and the installation procedure for anchor bolts used in this research.

Figure 3.3 shows the details of a typical steel jacket. The steel jacket was made of 1/4 inch thick A36 steel plates. The corners of the jacket were 2"x2"x1/4" steel angles. The steel plates were welded to the angles by 1/4 inch fillet welds. The steel jacket was fabricated in two L-shaped panels in plan. Holes were then drilled into the jacket for placement of the anchor bolts. The hole diameter was 1 5/8 inches. Holes were made oversize for ease of anchor bolt installation. A 4"x4"x1/2" plate washer was used with each anchor bolt to distribute the bolt force over a larger area and confine a larger zone at the splice plane. One inch thick steel spacers were welded on the inside face of the steel jacket to maintain the 1.0 inch gap between the concrete column and the steel jacket during assembly, and before grouting.

No special surface preparation was performed for the column concrete surface before the installation of the steel jacket. After being assembled around the column, the two free opposite corners of the L-panels were then welded. The final inside dimensions of the steel jacket were 2 inches larger than the dimensions of the concrete column. The one inch gap between the

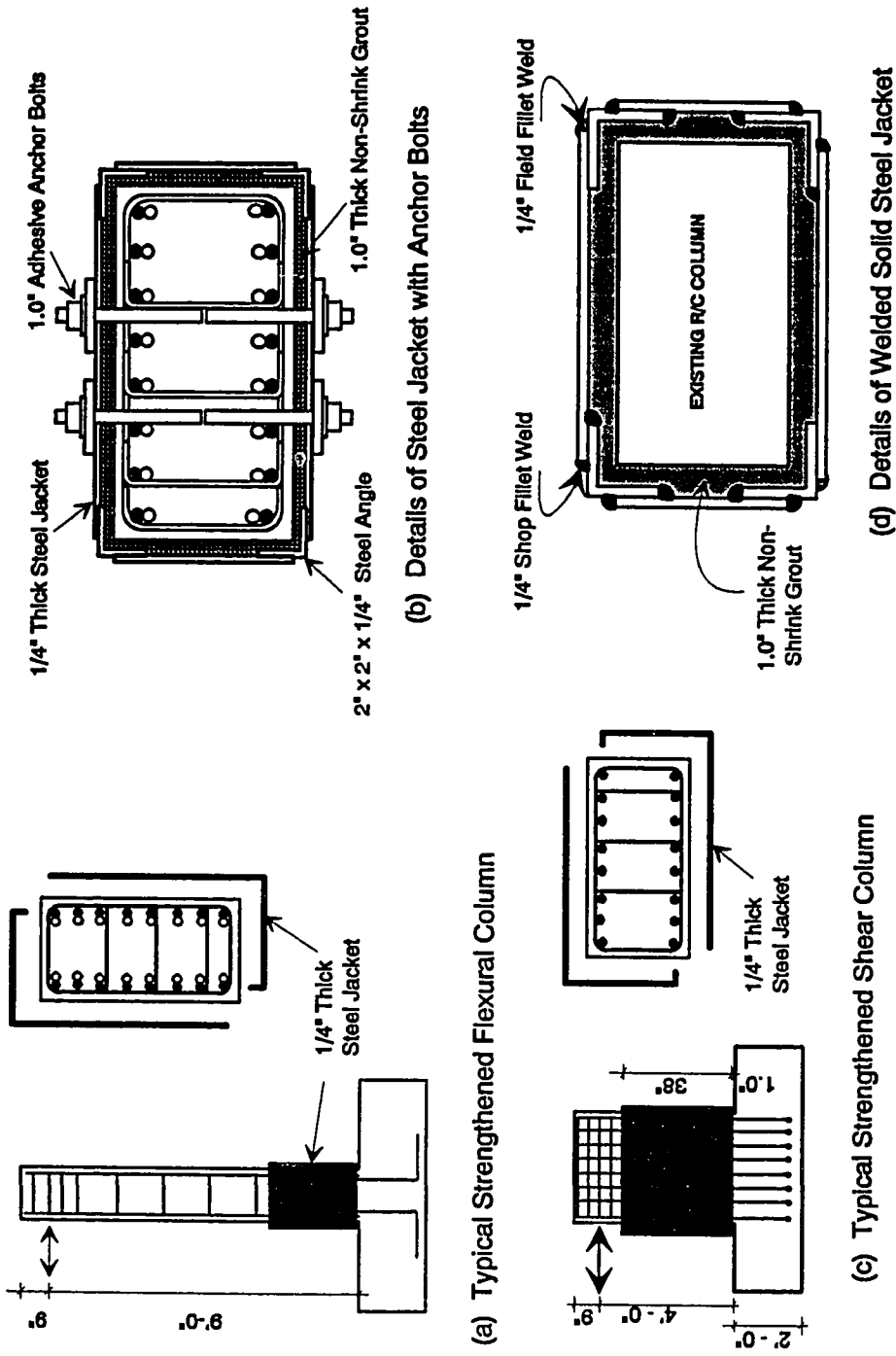


Figure 3.3 Details of Columns Strengthened with Steel Jackets

concrete column and the steel jacket was filled with commercial premixed non-shrink cementitious grout.

### **3.2.3.2 Steel Collars**

Figure 3.4 shows the details of a steel collar jacket used for strengthening columns with an inadequate lap splice. A feature of this system is that it does not require any field welding, which may be advantageous in some applications. The steel collars were made of C4x7.25 A36 steel channels. Each collar was made of four channels connected with two 1/2 inch A325 bolts at each corner. The ends of each channel were cut at 45 degrees. A 1/2 inch steel plate was welded at the channel ends for connection with the 1/2 inch bolts. A 3/4 inch gap was maintained between the concrete column and the steel collar. The gap was later filled with commercial premixed non-shrink cementitious grout. The steel collars were investigated with and without anchor bolts.

### **3.2.3.3 Rectangular Steel Jackets with Through Bolts**

Figure 3.5 shows the details of a steel jacket with through bolts. This particular steel jacket was used for repair of damaged columns with an inadequate lap splice. The details and assembly procedure of the steel jacket are similar to the steel jacket with anchor bolts. Before installation of the steel jacket, all the loose concrete cover on the damaged specimen was removed. The concrete was chipped off at least one inch behind the interior spliced bar. This allowed spliced bars to be embedded into new concrete/grout, which may have contributed to the improved splice behavior and kept the cold construction joint away from the potential splitting crack plane. The minimum thickness of the non-shrink grout was 6.0 inches. After the grout had gained enough strength, holes were drilled into the concrete

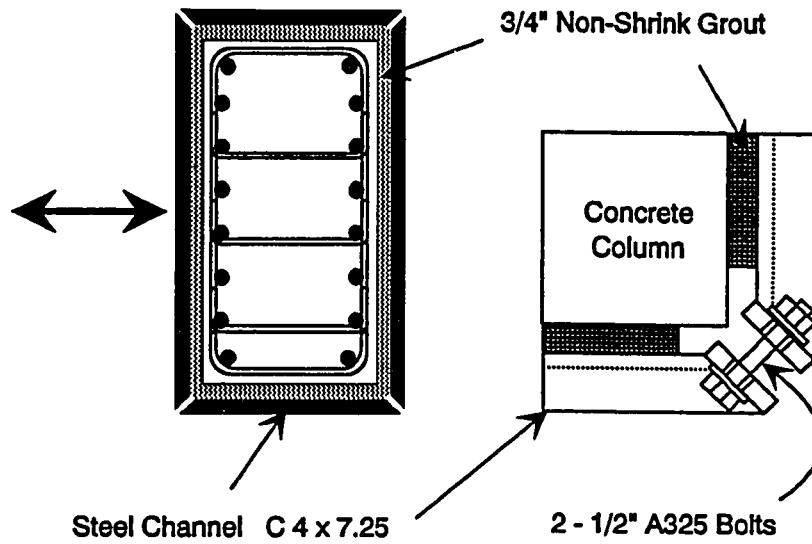


Figure 3.4 Shear Strengthening by the use of Steel Collars

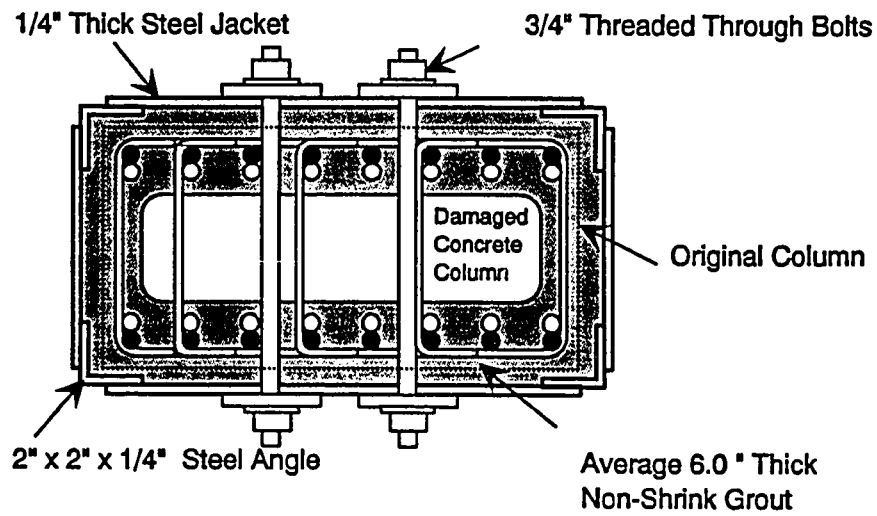


Figure 3.5 Details of Steel Jacket with Through Bolts

column. Each hole was drilled from opposite faces of the column. The diameter of the hole was 1-1/8 inch in diameter. The threaded rod was 3/4 inch in diameter. The through threaded rods were not bonded to the concrete column.

#### **3.2.3.4 Welded Lap Splice**

This technique was used for repair of a severely damaged column with an inadequate lap splice. Figure 3.6 shows the details of the welded lap splice. Weld design was according to the American Welding Society Standard AWS D1.4-79 [33]. A double-flare-V-groove weld was used for all lap splices, unless the splice was accessible from only one side. In such a case welding was performed on one side of the spliced bars using a single-flare-V-groove weld, but the weld length was doubled. An axial tensile test of a welded lap splice, welded by double-flare-V-groove weld, showed that such a welded splice could develop at least 90% of the ultimate tensile strength of the bar.

#### **3.2.4 Retrofitted Shear Columns**

The columns with inadequate shear strength were retrofitted using several different types of steel jackets. In addition to solid steel jackets and steel collars, partial steel jackets were investigated for cases with limited access to all four sides of a column. Section 3.2.4.1 presents the details of rectangular steel jackets used for strengthening columns loaded in either the weak or the strong direction. The details of steel collars used for strengthening columns with inadequate shear strength are presented in section 3.2.4.2. The details of the partial steel jackets are presented in section 3.2.4.3.



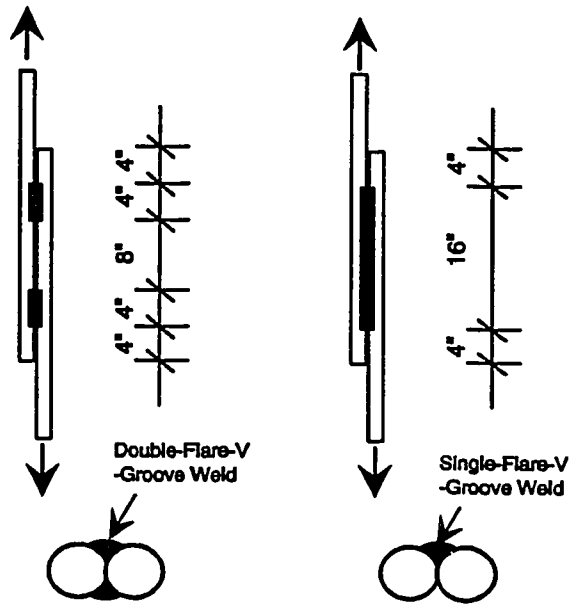


Figure 3.6 Details of Welded Lap Splices

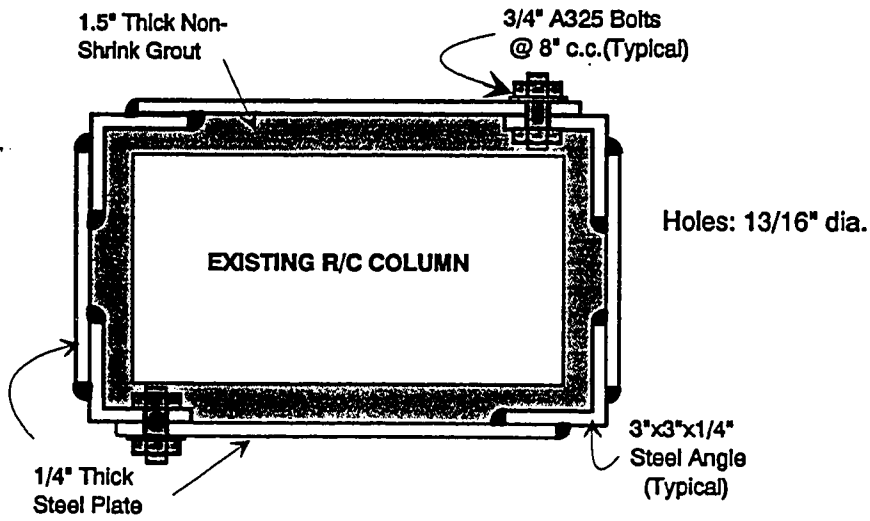


Figure 3.7 Details of a Bolted Solid Steel Jacket

#### **3.2.4.1 Rectangular Solid Steel Jackets - ( Welded & Bolted )**

The steel jacket covered the full height of the column, and was terminated 1.0 inch above the base of the column. Other details of the steel jackets used for strengthening columns with inadequate shear strength (Figure 3.3) were very similar to those used for strengthening columns with an inadequate lap splice. However, for the shear columns, no anchor bolts or through bolts were used with the full rectangular steel jackets. Since welding may not be permitted inside some existing structures, to avoid fire hazards or welding fumes, a bolted rectangular steel jacket was investigated in this series. Figure 3.7 shows the details of a bolted steel jacket. The steel jacket was fabricated in two L-shaped panels. The corners of the bolted steel jacket were 3"x3"x1/4" steel angles. The free ends of the L-panels were drilled for the installation of 3/4 inch A325 bolts. The nuts were welded to the inside of the steel jacket. After being placed around the column, the two L-panels were bolted using 3/4 inch bolts. The connection was treated as slip critical. The bolts were fully tensioned to the values given in the AISC Specifications, using turn of the nut technique. The inside dimensions of the steel jacket were 3.0 inches larger than the dimensions of the concrete column. This left a gap of 1.5 inches between the column and the steel jacket. A larger gap was used for the bolted jacket than the welded jacket to facilitate assembly.

#### **3.2.4.2 Steel Collars**

The details of the steel collars used for strengthening of columns with inadequate shear strength are very similar to those used for strengthening columns with an inadequate lap splice (See section 3.2.3.2). No anchor bolts

or through bolts were used with the steel collars for strengthening columns with inadequate shear strength.

#### **3.2.4.3 Partial Steel Jackets**

Two types of partial steel jackets were examined. Figure 3.8 shows the details of the 2/3 U-shape partial steel jacket. This steel jacket was examined for strengthening columns with inadequate shear strength loaded in the weak direction. It offers the advantage of strengthening columns with limited accessibility to its four sides. This represents a situation where a curtain/partition wall is framing into the outer 1/3 of the column cross section. The jacket was along the full height of the column, and was fabricated in one U-shaped panel. Five 1-1/8 inch holes were drilled into the column every 8 inches for the use of 3/4 inch threaded rods. The matching holes in the steel jacket were 1-5/8 inches in diameter. The threaded rods were greased and covered with plastic tape to prevent bond between the rods and the concrete column. The one inch gap between the column and the steel jacket was filled with commercial premixed non-shrink cementitious grout.

Figure 3.9 shows the details of the C-shaped partial steel jacket. This steel jacket was examined for strengthening columns with inadequate shear strength loaded in the strong direction. It offers the advantage of strengthening columns with limited accessibility to two its four sides. This represents a situation where a partition wall is framing into the middle 1/3 of the column cross section. The jacket was along the full height of the column, and was attached to the column by sixteen 1.0 inch diameter adhesive anchor bolts. Holes were drilled into the concrete column, and the steel jacket, separately. After the jacket was erected around the column, adhesive anchor bolts were then placed 8.0 inches into the concrete column.

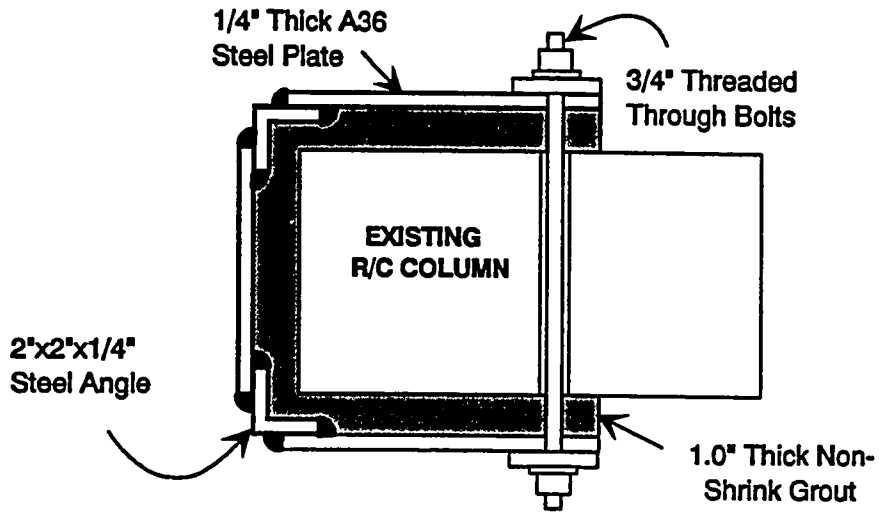


Figure 3.8 Details of 2/3 U-Shaped Partial Steel Jacket

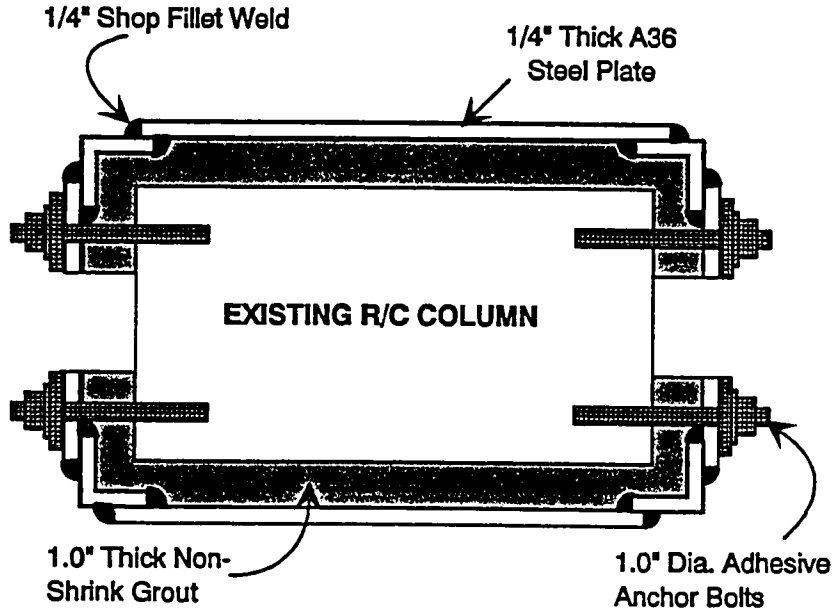


Figure 3.9 Details of C-Shaped Partial Steel Jacket

The one inch gap between the column and the steel jacket was filled with commercial premixed non-shrink cementitious grout.

### **3.3 MATERIAL**

#### **3.3.1 Concrete**

The concrete properties for the different test columns are summarized in Tables 3.3 and 3.4. Ready-Mix concrete was used for all columns. It was mixed and delivered by a local concrete supplier.

#### **3.3.2 Steel**

##### **3.3.2.1 Deformed Reinforcing Bars**

Grade 60 deformed reinforcing bars were used for all longitudinal bars in both the flexural and shear columns. Grade 40 deformed reinforcing bars were used for all column transverse reinforcement ties. These grades of steel for longitudinal and transverse reinforcement were chosen to represent 1950's and 1960's construction. Table 3.5 summarizes the properties of the steel reinforcing bars used in this research. Note that the actual yield strength of the Grade 40 bars was nearly 60 ksi.

##### **3.3.2.2 Steel Plates**

The steel jackets were made of 1/4 inch thick A36 steel plates. Table 3.5 shows the specified and actual tensile strengths. Note that the actual yield strength of the A36 plates was 50 ksi.

Table 3.3 Concrete and Grout Properties for the Flexural Columns							
Col. #	Concrete <sup>1</sup> fc' (psi)	Concrete fc' (psi)	Type of Aggregate	Max. Size of Aggregate	W/C Ratio	Type of Grout	Grout <sup>2</sup> fc' (psi)
FC1	4700	4500	Rock	3/4"	0.35	N/A	N/A
FC2	4900	4500	Rock	3/4"	0.35	Sika	7490
FC3	4900	4500	Rock	3/4"	0.35	Sika	5045
FC4	2850	3170	Rock	3/4"	0.385	N/A	N/A
FC5	2980	3170	Rock	3/4"	0.385	N/A	N/A
FC6	2850	3170	Rock	3/4"	0.385	Sika	6745
FC7	2980	3170	Rock	3/4"	0.385	Sika	6745
FC8	2595	2800	Rock	3/4"	0.36	Euclid	6335
FC9	2905	3075	Rock	3/4"	0.32	Euclid	5220
FC10	2595	2800	Rock	3/4"	0.36	Euclid	7195
FC11	2850	2725	Lime	3/4"	0.19	Euclid	6045
FC12	3265	3225	Rock	3/4"	0.34	Euclid	6260
FC13	3265	3225	Rock	3/4"	0.34	Euclid	5910
FC14	4165	4165	Rock	3/4"	0.475	N/A	N/A
FC15	4165	4165	Rock	3/4"	0.475	N/A	N/A
FC16	2565	2600	Rock	3/4"	0.237	Euclid	5605
FC17	2635	2600	Rock	3/4"	0.237	Euclid	7445

1. Uniaxial Compressive Strength of 6x12" cylinder at the day of Testing.
2. Uniaxial Compressive Strength of 2" cube at the day of Testing.

Table 3.4 Concrete and Grout Properties for the Shear Columns										
Col. #	Concrete <sup>1</sup> fc (psi)	Concrete fc' (psi)	Type of Aggregate	Max. Size of Aggregate	W/C Ratio	Type of Grout	Grout <sup>2</sup> fc (psi)			
SC1	5040	4500	Rock	3/4"	0.35	N/A	N/A			
SC2	5040	4500	Rock	3/4"	0.35	Sika	6860			
SC3	3170	3170	Rock	3/4"	0.385	N/A	N/A			
SC4	3170	3170	Rock	3/4"	0.385	N/A	N/A			
SC5	2240	2150	Lime	3/4"	0.388	Sika	6745			
SC6	2255	2150	Lime	3/4"	0.388	Sika	5910			
SC7	2940	3075	Rock	3/4"	0.32	Euclid	5220			
SC8	2785	2800	Rock	3/4"	0.36	Euclid	4300			
SC9	2325	2245	Lime	3/4"	0.29	N/A	N/A			
SC10	2390	2245	Lime	3/4"	0.29	Euclid	6540			
SC11	2360	2530	Rock	3/4"	0.414	Euclid	5615			

1. Uniaxial Compressive Strength of 6x12" cylinder at the day of Testing.

3. Uniaxial Compressive Strength of 2" cube<sup>2</sup> at the day of Testing.

### 3.3.3 Non-Shrink Grout

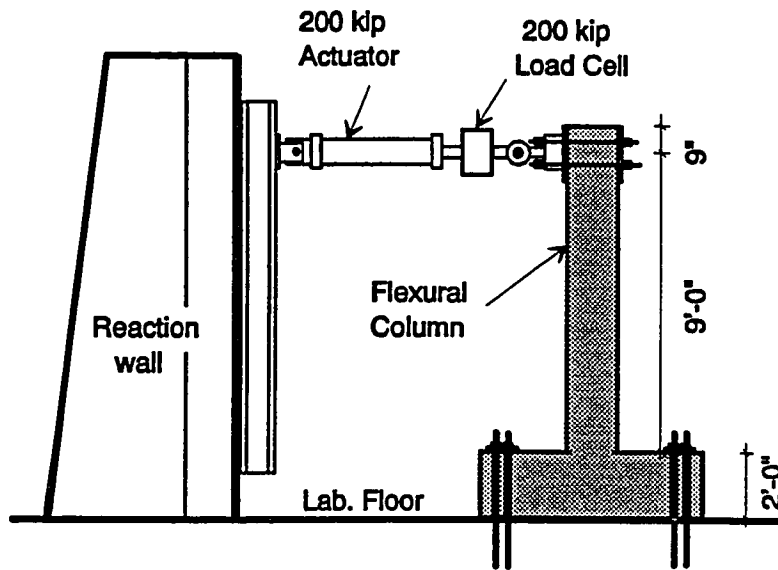
Two different types of non-shrink grout were used in this research. They are commercially known as, "Sika Grout 212" and "Euclid N-S". Both are non-corrosive, non-shrink cementitious grouts. They are supplied in 50 lb pre-mixed bags, ready to use after the addition of water. The average water/grout ratio was 0.15.

Table 3.5 Summary of the Steel Properties			
Type of Steel	Specified Yield Strength	Actual Properties	
	Fy ( ksi )	Fy ( ksi )	Fu ( ksi )
Longitudinal Bars # 8, Gr.60	60	63	100
Ties #3, Gr.40	40	58	91
1/4" A36 Plates	36	50	64

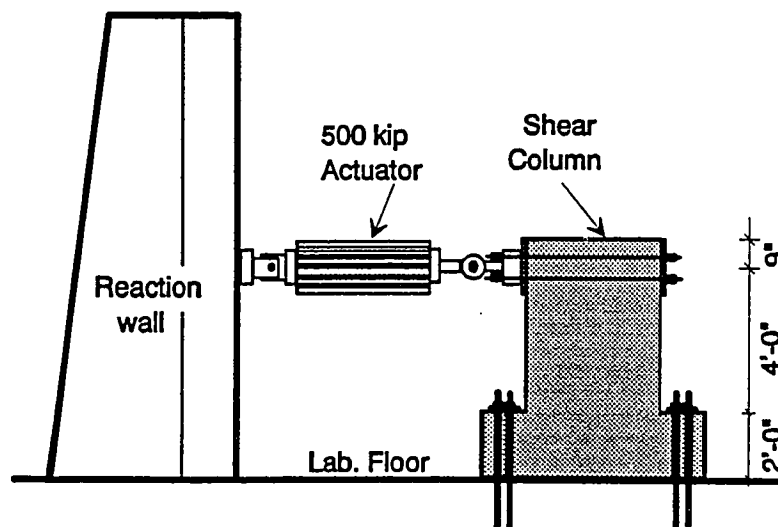
### 3.4 TEST SETUP

Figure 3.10 shows the test setup for the flexural and the shear columns. The test column was framed into a large footing to provide a fixed end. The footing was prestressed to the laboratory floor using 1-1/4 inch threaded rods. A lateral load was applied at the tip of the column using either a 200 kip or a 500 kip actuator. A 200 kip load cell, or pressure transducers were used to monitor the lateral force. This test setup provided





(a) Flexural Column Test Setup



(b) Shear Column Test Setup

Figure 3.10 TEST SETUP

for linear moment and constant shear along the full height of the column. This represents the same kind of forces experienced by building columns during earthquakes.

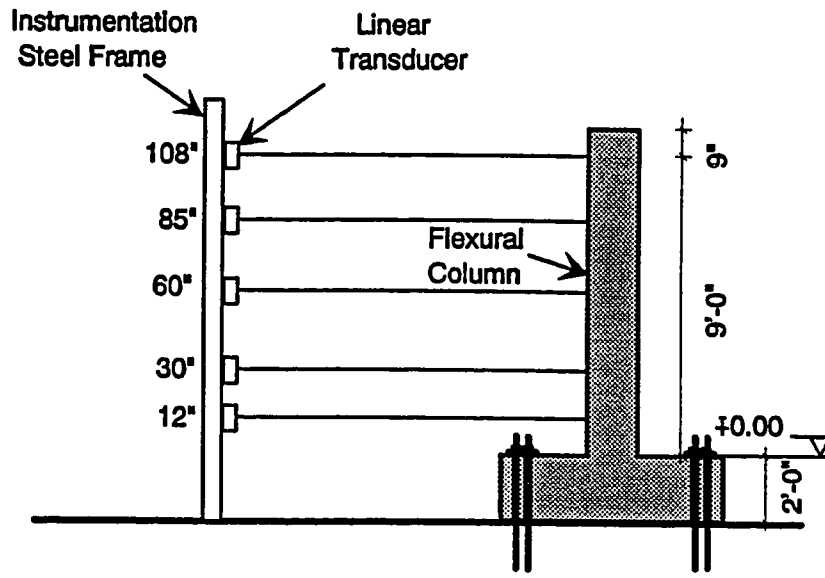
### **3.5 LOADING PROGRAM**

No axial load was applied on any of the test columns. For the flexural columns, the lateral load was increased in 5 kip increments until significant inelastic displacement was observed. Lateral displacements were then increased in increments corresponding to 0.5% drift ratios. The columns were laterally loaded two complete cycles at every load/drift ratio level. The loading sequence for the shear columns was similar, except the load increment was 10 kips instead of 5 kips. Columns FC1, FC2, SC1 and SC2 were loaded an additional two, 20 kip complete cycles after yielding of the longitudinal bars.

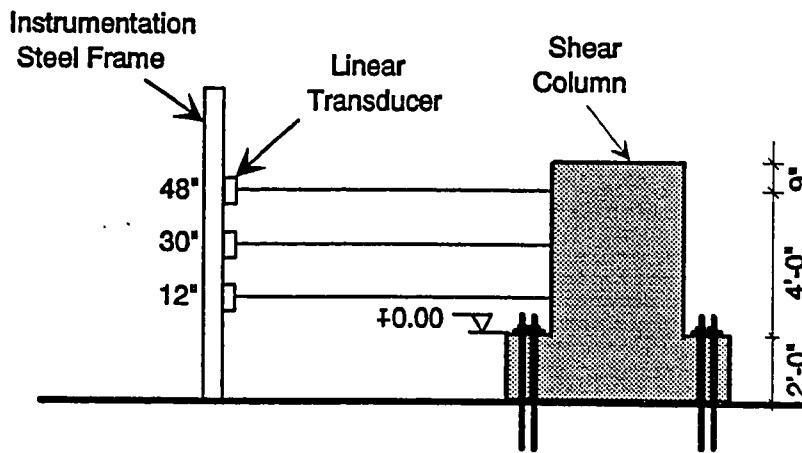
### **3.6 INSTRUMENTATION**

#### **3.6.1 Load Cell and Pressure transducers**

A 200 kip load cell was used to measure the lateral loads applied at the tip of the column with the 200 kip actuator. The load cell was mounted in series with the hydraulic actuator. For specimens having lateral strength higher than 200 kips, load was applied with a 500 kip actuator and pressure transducers were used to monitor the lateral load. Pressure transducers were mounted on the pressure hoses connected to the 500 kip actuator.



(a) Flexural Column, Layout of Linear Transducers



(b) Shear Column, Layout of Linear Transducers

Figure 3.11 Layout of Linear Transducers

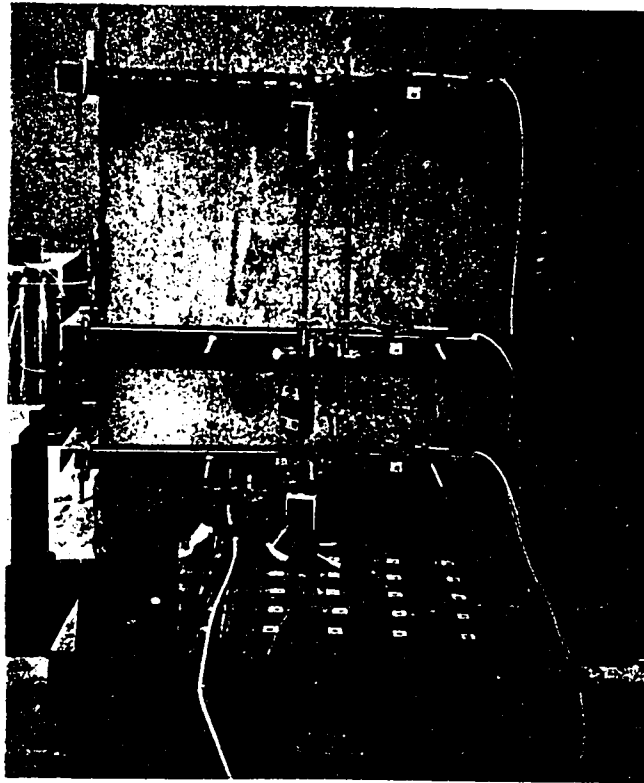
### 3.6.2 Linear Displacement Transducers

For the flexural column, ten linear displacement transducers were used to monitor the lateral displacements of the column. Lateral displacements were measured at five different levels along the height of the flexural column. For the shear columns six linear transducers were utilized to monitor lateral displacements at three different levels. Figure 3.11 shows the locations of the linear transducers. Linear transducers were mounted on a reference steel frame, and were of 5.0 inch stroke or 15 inch stroke with accuracy of 1/1000 of an inch.

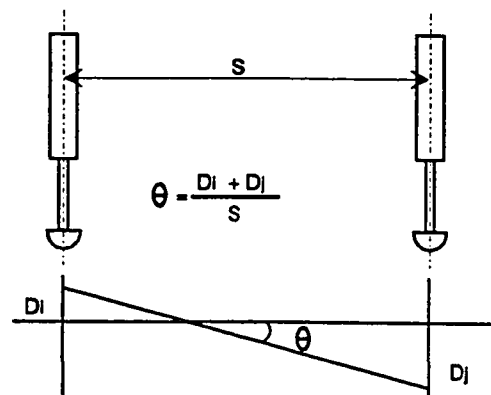
### 3.6.3 Linear Potentiometers

Linear potentiometers were used to measure the rotation of the flexural column at three different locations. They were of 2.0 inch stroke with an accuracy of 1/1000 of an inch. Figure 3.12(a) shows the locations of the linear potentiometers on the flexural column. The rotation values were computed from the measured relative vertical displacements at the linear potentiometers and the horizontal spacing between the linear potentiometers on the opposite faces of the column. The linear potentiometers were mounted on aluminum channels which were bolted to threaded rods embedded into the concrete column. Figure 3.12(b) shows how the rotation was computed from the measured displacement changes relative to a reference value.

Linear potentiometers were also used to monitor any possible rotation and displacement of the footing. These values were very small compared to the displacements of the column. The column displacements reported in the



(a) Rotation Instrumentation



(b) Computation of Rotation

Figure 3.12 Linear Potentiometers for the computation of Rotations

following chapters have been corrected for the small measured footing movements.

#### **3.6.4 Strain Gages**

The strains in selected reinforcing bars and in portions of the steel jackets were measured using electrical strain gages. The locations of the strain gages are shown in Chapters 6 and 7.

### **3.7 DATA ACQUISITION**

The instrumentation devices were connected to a high-speed scanner, which was controlled by a microcomputer. At each load increment the instrumentation channels were read and saved. The software used allowed conversion of test data to engineering units during the test. In addition, the load and deflection of the tip of the column was monitored during each test using an X-Y recorder.

## **CHAPTER 4**

### **EXPERIMENTAL PROGRAM - FLEXURAL COLUMNS**

#### **( With Inadequate Lap Splices )**

#### **4.1 INTRODUCTION**

The overall performance of the flexural columns (with inadequate lap splices), including the lateral load versus drift ratio response is presented in this Chapter. The drift ratio is defined as the tip displacement divided by the column height, expressed as a percentage. The performance of each flexural column during testing is presented and discussed. Details of the columns are shown without the footing reinforcement for clarity.

A total of seventeen flexural columns were tested in this phase. Test columns are presented in series as they were tested. For clarity they are designated as follows :

1. Basic Unretrofitted Column ( BASIC-UR );
2. Pre-Earthquake Strengthened Column ( PRE-EQ-S );
3. Post-Earthquake Repaired Column ( POST-EQ-R ).

Flexural columns were tested under reversed cyclic lateral loading. No axial load was applied to any of the columns. This is considered a more severe test for columns with an inadequate lap splice, since axial compressive load reduces the tensile force transferred by the splice. The main variables studied in the flexural column tests are :

1. Height of the steel jacket;
2. Pattern and number of adhesive anchor bolts ;
3. Width of the concrete column;
4. Different types of steel jackets.

Detailed presentation of the additional experimental data is presented and discussed in chapter 6. This additional data includes measured strains on the longitudinal reinforcing bars, on the steel jacket, and on the through bolts, as well as measured rotations in the hinge region. Chapter 6 also presents a complete discussion and comparison of the flexural columns. Sections 4.2 through 4.18 present the details and performance of the flexural columns FC1 through FC17 during testing, respectively.

#### **4.2 FLEXURAL COLUMN FC1 ( BASIC -UR )**

Column FC1 is a basic unretrofitted type "B" flexural column (Figure 3.1). It was reinforced with a cross tie at every longitudinal bar. Column FC1 was designed according to the ACI 318-56 code provisions. Figure 4.1(a) shows the details of column FC1. The splice length was 24 times the longitudinal bar diameter. The splice was located at the bottom of the column. Figure 4.2(a) shows column FC1 in the test setup.

During the test, the first flexural cracks developed on the tension face of the column at the bottom of the splice, during the 10 kip cycle. These cracks formed at the column/footing interface. Also, at a load of 10 kips, other flexural cracks developed in and beyond the splice region. It was observed that the cracks inside the splice region were shorter and narrower than the cracks outside the splice region. Figure 4.2(b) shows the crack pattern in the splice



region at the end of the test, on the south side of the column. For column FC1, the marked numbers on the column represent the cycle number, however, for all other columns they represent the lateral load or the drift ratio. New flexural cracks formed over the height of the column as the load was increased to 20 kips. During the 30 kip cycles, new flexural cracks formed inside the splice region, along with minor extension of the existing flexural cracks. Increased loading to 35 kips caused vertical splitting cracks along the bottom half of the splice. The longitudinal starter bars yielded during the cycle to 40 kips. At the same load, minor diagonal extension of the flexural cracks was observed.

The vertical splitting cracks extended over almost the bottom 3/4 of the splice height during the cycles to 50 kips. This lateral load is equivalent to the yielding flexural capacity of the column. Beyond the two cycles to 50 kips, gradual loss of stiffness was observed. Yielding of the column bars just above the top of the splice was observed at 1.5% drift ratio. Vertical splitting cracks extended along the full length of the splice during the cycles to 1.5% drift ratio. As the displacement was increased to 2.0% drift ratio the first layer of transverse reinforcement above the footing yielded. Vertical cracks along the spliced corner bars on the east and west sides of the column formed at 2.0% drift ratio. Also, flexural shear cracks formed inside the splice at 2.0% drift ratio, which indicated the influence of shear.

Figure 4.1(b) shows the hysteretic response of column FC1. The response of the column shows stable hysteretic loops up to 1.5% drift ratio. However, beyond 2.0% drift ratio the column showed dramatic loss in strength and stiffness. Splice failure after yielding of the main longitudinal bars, and the gradual rather than sudden extension of the vertical splitting cracks may be

attributed to the relatively higher concrete compressive strength than the target compressive strength. Column FC1 serves as a basic unretrofitted reference specimen for column FC2 and FC3.

### 4.3 FLEXURAL COLUMN FC2 ( PRE-EQ-S )

Column FC2 is a strengthened type "B" flexural column. It was strengthened with a 1/4 inch thick A36 steel jacket. Figure 4.3(a) shows the details of column FC2. Since the cross section of the concrete column was symmetrical about its weak axis, two different strengthening patterns were used on either side of the column. The west side was strengthened with a "plain" steel jacket. However, on the east side, the steel jacket was stiffened with one vertical line of five adhesive anchor bolts. The bolts were provided at mid-width of the column. Figure 4.4(a) shows a photograph of column FC2.

During the test, the first flexural cracks formed at the column/footing interface during the cycles to 10 kips. Several new flexural cracks developed above the steel jacket as the load was increased to 30 kips. Also, at the same load, cracks formed between the grout and the concrete column at the top of the steel jacket. These cracks did not open, but rather remained very narrow. Increased loading to 45 kips caused development of vertical splitting cracks at the bottom of the splice, visible on the 1.5 inch unjacketed portion at the column base. The vertical crack at the splice did not appear to affect the performance of the column. First yielding of the main reinforcement bars was observed at the same 45 kip load. This load is equivalent to the theoretical flexural capacity of the column. During the cycles to 50 kips flexural cracks extended diagonally forming flexural shear cracks, reflecting the influence of

shear. The 50 kip load is equivalent to  $1.25\sqrt{f_c}$  bd. Figure 4.4(b) shows the crack pattern after the completion of the test and removal of the steel jacket.

Column FC2 showed an elastic response up to a lateral load of 50 kips. Increased loading above 50 kips produced large inelastic deformations. Figure 4.3(b) shows the hysteretic response of column FC2. The column was loaded in 0.5% drift ratio increments up to 4.5% drift ratio. In the inelastic range the column showed gradual minor stiffness degradation. However, it did not show any loss of strength until the end of the test. Compared to the basic unretrofitted column FC1, column FC2 showed higher strength and much higher ductility. Both the side with anchor bolts and the side without anchor bolts showed similar responses. The need for anchor bolts was not clear in this test. It is believed that the high concrete strength contributed to the satisfactory observed response.

The maximum measured strains on the steel jacket were approximately 35% of the actual yield strain of the steel jacket. More detailed discussion on the strains in the column is presented in chapter 6. After completion of the test, the steel jacket and non-shrink grout were removed. No cracks on the concrete column in the splice region were observed by the unaided eye. But, the column was unloaded at that point. The same column was repaired with steel collars and anchor bolts, and then retested as presented in the next section.

#### 4.4 FLEXURAL COLUMN FC3 ( POST-EQ-R )

Column FC3 is a repaired type "B" flexural column. Although column

FC2 was subjected to a 4.5% drift ratio, it showed no sign of distress in the splice region. The only major cracks were outside the splice region, immediately above and below the steel jacket. The same column was repaired with two steel collars as shown in Figure 4.5(a). Since no cracks were observed on the column in the splice region after the column FC2 test, the concrete cover was not removed before the installation of the steel collars for test FC3.

Column FC3 had poor initial stiffness due to the presence of old cracks over the height of the column. It was loaded in 0.5% drift ratio increments up to the maximum stroke of the actuator. Figure 4.5(b) shows the hysteretic response of column FC3. The first new flexural cracks formed immediately above the splice at 1.0% drift ratio. As the load was increased to 2.0% drift ratio, the flexural cracks extended diagonally. The first vertical splitting crack at the splice was observed at 35 kips during the push cycle to 2.5% drift ratio. The lateral strength in the push direction was a little bit higher than in the pull direction, likely due to the presence of the anchor bolts on the east side only. The splice splitting crack extended along the full height of the splice at 3.0% drift ratio. The column was loaded up to the maximum stroke of the actuator. The steel collars were clearly not as effective as the steel jacket. The level of stress in the steel collars was very low during the test.

The poor stiffness of column FC3 may be due to two reasons:-

1. The cracks in the concrete column were inherited from the previous test. These cracks opened up at an early stage of loading.
2. Not removing the old concrete cover. Although no major splitting cracks were observed at the splice, this did not mean that the concrete in the vicinity of the spliced bars was not distressed and

experienced micro-cracking due to the severe cyclic loading.

It is believed that repairing of the existing column cracks by epoxy injection and replacement of the concrete cover might have enhanced the stiffness of column FC3. In general, the performance of column FC3 was unsatisfactory. Figure 4.6 shows column FC3 during the test.

#### **4.5 FLEXURAL COLUMN FC4 ( BASIC-UR )**

Column FC4 is a basic unretrofitted type "A" flexural column. It was reinforced with a cross tie at every other longitudinal bar. Column FC4 was designed according to the ACI 318-63 code provisions. Figure 4.7(a) shows the details of column FC4. The splice length was 24 bar diameters. The concrete uniaxial compressive strength at the day of testing was 2850 psi, significantly lower than the previous columns.

During the test, the first flexural cracks formed at the column/footing interface, at a load of 10 kips. Increased loading to 15 kips caused the formation of flexural cracks just above the top of the spliced bars. Several new flexural cracks developed above the splice at higher levels and inside the splice region during the cycles to 20 kips. As the load was increased to 30 kips, vertical splitting cracks formed at the bottom of the spliced bars. During the cycles to 35 kips, the vertical splitting cracks extended over the bottom half of the splice. Also at the same load, some flexural cracks extended deeper into the column section. Increased loading to 40 kips caused splice failure at both the east and the west sides of the column. Figure 4.8 shows the crack pattern on column FC4. The splice failure was associated with vertical splitting cracks along the full height of the splice. Other vertical cracks were observed on the east and west

sides of the column, due to bond failure between the steel reinforcement bars and the concrete in the splice region.

Strain readings showed that the strain in the main longitudinal reinforcement bars was just below yielding. The splice failure thereafter occurred before the development of the flexural yielding capacity of the column. Figure 4.7(b) shows the hysteretic response of column FC4. It is quite evident that column FC4 showed virtually no ductility and very limited energy dissipation. As column FC4 showed a non-ductile, brittle splice failure, it was chosen as a reference specimen for the remaining type "A" flexural columns of the same size.

#### **4.6 FLEXURAL COLUMN FC5 ( BASIC - UR )**

Column FC5 is a basic unretrofitted type "B" flexural column. It was transversely reinforced with a cross tie at every longitudinal bar. Figure 4.9(a) shows the details of column FC5. The splice length was 24 bar diameters. The concrete uniaxial compressive strength at the day of testing was 2980 psi.

Figure 4.9(b) shows the hysteretic response of column FC5. Column FC5 had a higher amount of transverse reinforcement and slightly higher concrete strength than column FC4. However, column FC5 showed lower initial stiffness compared to column FC4. This is due to some bond deterioration between the splice starter bars and the concrete footing. The same footing and starter bars were used for the column FC2 test, which experienced a very severe test.

The first flexural cracks formed at the column/footing interface, at a load

of 10 kips. Increased loading to 20 kips caused the development of several flexural cracks over the bottom 2/3 of the column height. These flexural cracks formed inside the splice region too. As the load was increased to 25 kips, vertical splitting cracks formed at the bottom of the splice. These cracks developed over the bottom 1/3 of the splice length. During the 30 kip cycles the flexural cracks extended deeper into the column cross section.

The vertical splitting cracks extended to almost half the height of the splice as the load was increased to 35 kips. Splice failure occurred when the vertical splitting cracks extended over the full length of the lap splice, at a load of 40 kips. Also, at the same load the flexural cracks extended diagonally, reflecting the influence of shear. Figure 4.10 shows the crack pattern on column FC5. Testing was continued up to 4.0% drift ratio at 0.5% increments, where the column showed considerable strength and stiffness degradation. As mentioned in the previous section, since column FC4 showed a more dramatic splice failure, it was chosen as a basic reference unretrofitted specimen for the flexural columns with the same size.

#### **4.7 FLEXURAL COLUMN FC6 ( POST-EQ-R )**

Column FC6 is a repaired type "A" flexural column. The basic unretrofitted column FC4 was repaired, and then designated FC6. It was repaired by the use of a rectangular steel jacket and anchor bolts. Figure 4.11(a) shows the details of column FC6. After the completion of the column FC4 test, the concrete cover over the bottom three feet was removed. This included the two foot long splice region and an additional one foot above the splice. The column reinforcement bars were exposed. However, the splice starter bars were

left unexposed. The concrete core appeared to be in relatively good condition so no further concrete was removed or chipped off behind the plane of the spliced bars. The details of the steel jacket are similar to the column FC2 steel jacket. The average thickness of the non-shrink grout was 3.0 inches.

Figure 4.11(b) shows the hysteretic response of column FC6. The observed poor initial stiffness was likely due to the existing cracks in the concrete column above the steel jacket, which was inherited from the previous test. The first flexural cracks formed at the column/footing interface at a load of 10 kips. Increased loading to 15 kips caused the opening of most of the old flexural cracks in the concrete column above the steel jacket. Large inelastic deformations were observed at loads higher than 40 kips. At displacements above 2.5% drift ratio, the column showed significant strength and stiffness degradation. At 4.0% drift ratio the column showed more than 60% loss of strength. Figure 4.12 shows column FC6 during and after the test. The response of the east and west side of column FC6 were almost identical. The presence of anchor bolts on the east side did not enhance the response of that side over the west side.

After completion of the test, the steel jacket was removed and the cracks on the non-shrink grout were marked. Figure 4.13 shows the crack pattern on the non-shrink grout. Notice the formation of a hinge at the bottom of the north end, and concentration of cracks at the bar splice locations. The overall performance of the column was not considered satisfactory due to the limited ductility and low energy dissipation.

Test results of column FC6 indicate that:



1. The use of anchor bolts may not improve the performance of the steel jacket for post-earthquake repair of wide columns with inadequate lap splice, possibly because they are embedded into cracked concrete.
2. Removing the old loose concrete cover of the damaged column may not be enough. It may be beneficial to remove more concrete in order to move the new cold construction joint away from the potential splitting crack plane at the center of the spliced bars.

Removing the portion of the concrete core in the vicinity of the spliced bars results in replacing all the concrete surrounding the spliced bars by new concrete. However, removing concrete that is intact with the column concrete core may be undesirable. Since the core may be needed to carry gravity loads during the repair operation. Therefore, another repaired column was tested without further chipping of the concrete core. Column FC10 was repaired by addition of a steel jacket after the removal of only the loose concrete cover. Additional bolts were utilized in order to achieve a better performance by the repaired column FC10 than that of column FC6. Section 4.11 presents the details and the response of column FC10.

#### **4.8 FLEXURAL COLUMN FC7 ( POST-EQ-R )**

Column FC7 is a repaired type "B" flexural column. The basic unretrofitted column FC5 was repaired and then designated FC7 and then retested. It was repaired by welding the spliced bars. Double and single -flare-V-groove welds were used as described in section 3.2.3.4. All the loose concrete was removed over the bottom 32 inches of the column. After welding the

spliced bars, the removed concrete was replaced by non-shrink grout. The original dimensions of the column were maintained after repair. Figure 4.14(a) shows the details of column FC7.

The first flexural cracks formed at the two cold construction joints, at the column/footing interface and at the top of the non-shrink grout. These cracks formed at a load of 10 kips. The old flexural cracks in the column above the bottom 32 inches opened up during the cycle to 15 kips. At the same load new flexural cracks developed just above the splice, and also inside the splice. Several new flexural cracks formed at loads of 20 kips and 30 kips. However, during the 30 kip cycles the cracks were steeper. Increased loading to 40 kips caused yielding of the longitudinal bars, and extension of the flexural cracks deeper into the column cross section. During the cycle to 60 kips most of the flexural cracks extended diagonally. These diagonal cracks were very steep. At loads above 60 kips the column showed large inelastic deformations. The test was continued up to 4.0% drift ratio. The column did not show any sign of strength degradation. However, very minor stiffness degradation was observed at large inelastic displacements. Figure 4.14(b) shows the hysteretic response of column FC7. The response showed a typical pinching in the hysteretic loops of reinforced concrete members under cyclic loading, but the overall performance of column FC7 was considered satisfactory. Figure 4.15 shows column FC7 by the end of the test.

#### **4.9 FLEXURAL COLUMN FC8 ( PRE-EQ-S )**

Column FC8 is a strengthened type "A" flexural column. It was retrofitted with three steel collars as shown in Figure 4.16(a). The collars were spaced at

8 inches over the height of the splice, with the first collar at 6 inches from the top of the footing. Adhesive anchor bolts were provided only on the east side.

During the test, the first flexural cracks formed at the column/footing interface at a load of 15 kips. During the 20 kip cycles, flexural cracks developed above the splice. New flexural cracks above the splice formed at the 25 kip and 30 kip cycles. The first vertical splitting crack in the splice region was observed at a load of 35 kips. Figure 4.17 shows column FC8 during and after the test. Increased loading to 40 kips caused the formation of vertical splitting cracks over the full length of the splice. This was the same failure load as for the basic unretrofitted column FC4. This indicated that the steel collars were ineffective in confining the column lap splice. After the two 40 kip cycles, the column showed large inelastic deformations. Figure 4.16(b) shows the hysteretic response of column FC8. After the formation of vertical splitting cracks over the length of the splice, the column showed dramatic loss in strength and stiffness.

The main longitudinal bars remained elastic with maximum observed strains just below the yielding strain. Figure 4.18 shows the splice region during and after the test. The cracks that formed behind the steel collars were marked after the test. The overall performance of column FC8 was considered unsatisfactory.

#### **4.10 FLEXURAL COLUMN FC9 ( PRE-EQ-S )**

Column FC9 is a strengthened type "A" flexural column. It was retrofitted with a rectangular steel jacket. Figure 4.19(a) shows the details of column FC9. The steel jacket was similar to that of column FC2. The east side of the steel

jacket was stiffened with one vertical line of five anchor bolts spaced at 6 inches. No anchor bolts were provided on the west side. The concrete uniaxial compressive strength at the day of testing was 2905 psi.

During the test, the first flexural cracks formed at the column/footing interface, at a load of 15 kips. During the cycle to 20 kips flexural cracks formed just above the steel jacket. Increased loading to 25 kips caused the development of several new flexural cracks over the middle one-third of the column, above the steel jacket. Flexural cracks extended diagonally as the load was increased to 40 kips. The longitudinal bars yielded during the 40 kip cycles. These strains reached levels well beyond the yielding strain as the load was increased to 50 kips. At the same load, the strains on the steel jacket measured close to the bottom of the splice reached almost one-quarter the actual yield strain of the steel jacket.

Beyond the 50 kip cycles the column showed un-symmetrical response. Figure 4.19(b) shows the hysteretic response of column FC9. In the push direction, the splice on the east tension side was retrofitted with a steel jacket and anchor bolts. However, in the pull direction, the west tension side was retrofitted with only a steel jacket and no anchor bolts. Increased push loading caused some gradual stiffness degradation, but did not affect the strength of the column until large drift ratios. The east side with anchor bolts maintained its lateral strength to more than 3.0% drift ratio. Although degradation of strength was observed beyond 3.2% drift ratio, it was at a low rate.

On the west side, without anchor bolts, the column showed more rapid strength and stiffness degradation beyond 1.5% drift ratio. It showed much

lower ductility than the east side. Beyond 3.0% drift ratio the column showed poor stiffness due to slip of the spliced bars under frequent cyclic loading. The response of this column clearly showed the advantage of using anchor bolts with the steel jacket. Figure 4.20 shows column FC9 before and after the test.

It was observed during the test that the steel jacket lost its effectiveness in confining the spliced bars when the strains in the steel jacket reached levels between 650 - 750 micro strains. This is discussed in detail in chapter 6. Compared to the basic unretrofitted column FC4, the east side of column FC9, with anchor bolts, exhibited higher strength much higher ductility and energy dissipation. Although the results of this column were considered very encouraging, two more specimens of the same column size were tested to examine two major variables. These variables are the height for the steel jacket and the number of anchor bolts. The other two columns FC11 and FC12 are presented in sections 4.12 and 4.13, respectively.

#### **4.11 FLEXURAL COLUMN FC10 ( POST-EQ-R )**

Column FC10 is a repaired type "A" flexural column. After the completion of the column FC8 test, the column was repaired by the use of a short steel jacket and was then designated as column FC10. The height of the steel jacket was 27 inches, 7.5 inches shorter than the previous steel jackets. Splitting cracks developed between the spliced bars during the FC8 test. The concrete cover was first removed and the column main reinforcement bars were exposed, as shown in Figure 4.22(a). The column concrete core was in relatively good condition, so, no further concrete was removed or chipped off behind the plane of the spliced bars. Figure 4.21(a) shows the details of column FC10.

During the test of column FC10, the old existing flexural cracks on the concrete column opened up at a load of 15 kips. This resulted in an initial stiffness lower than that of column FC8. Figure 4.21(b) shows the hysteretic response of column FC10. At a load of 25 kips, vertical splitting cracks were observed below the steel jacket at the bar splice locations. Increased loading to 35 kips caused yielding of the corner longitudinal bars. The column showed essentially elastic response until the cycles to 40 kips. As the load was increased to 50 kips, the column showed some inelastic deformations. At the same load, strains in the periphery tie reached half the actual yielding strain. Afterwards, the column showed loss of stiffness until the cycles to 2.5% drift ratio. At displacements above 2.5% drift ratio stiffness degradation was associated with strength degradation. The test was stopped at 3.5% drift ratio, where the drop in strength reached almost 50%. Figure 4.22(b) shows column FC10 during the test.

Test results of column FC10 was reasonably acceptable. However, one more column in this series was repaired and tested. The last repaired column named FC13 was retrofitted by the use of a steel jacket and through bolts. Section 4.14 presents the details and performance of column FC13.

#### **4.12 FLEXURAL COLUMN FC11 ( PRE-EQ-S )**

Column FC11 is a strengthened type "A" flexural column. It was strengthened by the use of a short steel jacket. The height of the steel jacket was 27 inches. Figure 4.23(a) shows the details of column FC11. The steel jacket was stiffened with eight anchor bolts on the east side. The bolts were distributed on two vertical lines of four anchor bolts each. On the west side, the steel jacket

was stiffened with six anchor bolts, distributed on two vertical lines of three anchor bolts each.

The first flexural cracks formed at the column/footing interface at a load of 15 kips. As the load was increased to 20 kips, several new flexural cracks developed over the middle one-third of the column, above the steel jacket. During increased loading to 30 kips, the flexural cracks extended deeper into the column cross section. Also, new flexural cracks developed at the same 30 kip load. Increased loading to 50 kips caused yielding of the longitudinal bars. The flexural cracks, in the center one-third of the column, extended diagonally during the 50 kip cycles. As the load was increased to 60 kips the column showed some inelastic deformations. Figure 4.23(b) shows the hysteretic response of column FC11.

Large inelastic deformations were observed at loads above 60 kips. A 63 kip lateral load was reached at a 2.5% drift ratio. At this drift ratio, the strains in the steel jacket close to the bottom of the splice were about 500 micro-strains, which were almost 30% of the actual yield strain of the steel jacket. Lateral loading beyond 2.5% drift ratio was associated with significant loss of strength and stiffness. Figure 4.24(a) shows column FC11 during the test. After the completion of the test, the steel jacket was removed and the non-shrink grout was investigated. It was revealed that the grout was severely cracked, particularly near the spliced bars. Figure 4.24(b) shows column FC11 after the removal of the steel jacket. The figure shows several cracks at the bar splice locations. The cracks formed over the full height of the lap splice.

The response of column FC11 indicated that using additional bolts within

the splice region increased the lateral strength of the column, but did not ensure large ductility, which may be needed for some older buildings during major earthquakes. Compared to the basic unretrofitted column FC4, column FC11 showed higher strength and energy dissipation. However, column FC11 did not exhibit high ductility. The overall performance of column FC11 is considered acceptable, although the use of a longer steel jacket might have improved the ductility, as for column FC9.

#### **4.13 FLEXURAL COLUMN FC12 ( PRE-EQ-S )**

Column FC12 is a strengthened type "A" flexural column. It was strengthened with a long steel jacket and anchor bolts. The height of the steel jacket was 34.5 inches, the same as the height of column FC9's steel jacket. The east side of the steel jacket was stiffened with two vertical lines of three anchor bolts each. The west side was stiffened with two vertical lines of two anchor bolts each. Figure 4.26 shows the east and the west elevations of column FC12. In plan, the anchor bolts were arranged in such a way that they divided the column width into three 12 inch segments, as shown in Figure 4.25(a).

The first flexural cracks formed at the column/footing interface at a load of 15 kips. As the load was increased to 20 kips, flexural cracks developed just above the steel jacket. Several new flexural cracks formed on the column above the steel jacket during the 30 kip cycles. Increased loading to 50 kips caused the yielding of the main longitudinal bars. The first vertical splitting crack at the splice was observed during the 60 kip cycles. Also at the same load, the column showed large inelastic deformations. Figure 4.27 shows column FC12 during the test. Starting from the 2.0% drift ratio, the displacement was increased in 0.5%



drift ratio increments.

As the column was loaded to 2.5% drift ratio the concrete in the compression zones showed some sign of distress and minor crushing of the outer fibers below the steel jacket. At the same 2.5% drift ratio the cross ties yielded. Up to 4.0% drift ratio both the east and the west sides of column FC12 showed similar responses. However, the east side with six anchor bolts showed higher strength in the push direction than the west side with four anchor bolts in the pull direction. The difference, however, was not significant.

Figure 4.25(b) shows the hysteretic response of column FC12. After the completion of the two 4.0% drift ratio cycles, the column was loaded two complete cycles to the maximum stroke of the actuator. In the push direction the column was loaded up to only 4.0% drift ratio. Just minor stiffness degradation was observed in that direction. In the pull direction the column was loaded up to 5.5% drift ratio. Strength and stiffness degradation was observed beyond 4.5% drift ratio in the pull direction. Also, at 4.5% drift ratio the strains in the steel jacket were about 750 micro strain, approximately 60% of the theoretical yield strain. Compared to the basic unretrofitted column FC4, column FC12 exhibited 50% higher strength and very large displacement ductility. The hysteretic response of column FC12 showed very stable hysteretic loops and high energy dissipation.

Investigation of the concrete surface after the removal of the steel jacket revealed that concrete flexural cracks were very evident at the bottom of the column. Also, it was observed that the north side showed very narrow and short vertical cracks. However, the south side showed a narrower and shorter crack.

It is important to notice here that the peripheral tie was continuous at the south end, while it was ended with two 90 degree hooks at the north end. Figure 4.28 shows the crack pattern on the concrete surface at the north and south ends. These cracks did not have a major influence on the performance of the column.

Test results of this column indicate that a rectangular steel jacket with anchor bolts can considerably improve the seismic performance of wide rectangular columns with an inadequate lap splice. Also, it suggests that anchoring the steel jacket at its upper and lower ends to the concrete column by anchor bolts ensures some sort of composite action between the steel jacket and the concrete column. This sort of composite action improves the confinement of the splice by the steel jacket. However, the height of the steel jacket should be at least 1.5 times the length of the lap splice. This would allow the installation of the upper anchor bolts at least 6.0 inches above the top of the splice where major flexural cracks might form. Although the west side was provided with four anchor bolts, it was unlike column FC9 ( with five anchor bolts ), the stiffness degradation of column FC12 was at a very low rate.

#### **4.14 FLEXURAL COLUMN FC13 ( POST-EQ-R )**

Column FC13 is a repaired type "A" flexural column. After the completion of the column FC12 test, the steel jacket was dismantled and the concrete cover was removed. The repair of this column was performed differently from the repair of columns FC6 and FC10. Although the concrete core was intact, the concrete was chipped off to at least one inch behind the splice starter bars. Chipping the concrete one inch behind the splice bar offers the advantage of embedding both spliced bars into new concrete, in this case

new non-shrink grout. Also, it offers the advantage of moving the cold construction joint between the concrete and the non-shrink grout away from the potential splitting crack plane, at the center of the splice. Figure 4.30 shows the splice region of column FC13. Notice that the concrete core is severely cracked.

Since the concrete core was already cracked and all the spliced bars were exposed, through bolts were used instead of anchor bolts. Figure 4.29(a) shows the details of column FC13. The threaded bolts allow external confinement of the splice. Anchoring the bolts does not depend on the condition of the damaged concrete core, as it does with the adhesive anchors.

Since the column FC12 was loaded to very large displacements, the concrete column was severely cracked. During the column FC13 test, all the old existing flexural cracks above the steel jacket opened up at a load of 10 kips. Increased loading to 30 kips caused the formation of vertical splitting cracks at the corner bars on the east and the west sides. These cracks were observed below the steel jacket. The cracks did not open as the load was increased. The longitudinal corner bars yielded during the cycle to 45 kips. As the load was increased to 55 kips, new flexural cracks formed immediately above the steel jacket. Column FC13 showed elastic response up to 60 kip load.

Figure 4.29(b) shows the hysteretic response of column FC13. Column FC13 showed poor initial stiffness due to the presence of the old flexural cracks in the upper 2/3 of the column. These cracks were left unrepaired, and opened up at an early stage of loading. In the pull direction the column was loaded up to 4.0% drift ratio. In the push direction the column was loaded up to 5.0% drift ratio. A major shear crack developed in the middle one-third of the column

during the push to 5.0% drift ratio. This shear crack did not open, since column FC13 was not loaded beyond 5.0% drift ratio. The overall performance of column FC13 was excellent. The maximum lateral capacity was maintained up to 5.0% drift ratio. At large displacements stiffness degradation was observed at a very low rate. Figure 4.31 shows column FC13 before and after being repaired.

Strain gages were attached to the threaded rods before they were installed to monitor the initial forces in the rods. The initial forces in the threaded rods were as follows:-

1. The upper rods  $F = 4.20$  kips/rod
2. The middle rods  $F = 5.57$  kips/rod
3. The bottom rods  $F = 5.27$  kips/rod.

The threaded rods showed different force increase for different levels. The upper rods showed the smallest force increase during the test. However, the bottom rods showed the highest force increase. This is presented in detail in chapter 6. It is important to mention here that most of the strain readings measured on the steel jacket near the bottom of the spliced bars showed maximum strains of about 750 micro strain, equivalent to 60 % of the theoretical yield strain.

Column FC12 test suggested that using anchor bolts just at the top and the bottom of the steel jacket would be adequate to ensure good confinement by the steel jacket in confining the lap splice. So, after the completion of the column FC13 test, the middle threaded rods were removed and the test was

resumed. The column was designated FC13A. Figure 4.32(a) shows the details of column FC13A. Since the column FC13 had already been tested to the full stroke of the actuator, column FC13A was loaded 10 full cycles to the maximum stroke of the actuator.

Figure 4.32(b) shows the hysteretic response of column FC13A. In the pull direction, the column was loaded up to 4.0% drift ratio. On this side the column showed very small strength and stiffness degradation. In the push direction, the column was loaded up to 5.0% drift ratio. On this side the column showed some strength and stiffness degradation, due to the presence of the major shear crack in that direction inherited from the previous test. However, the drop in strength and stiffness was at a low rate. Test results of this column suggests that through bolts provided at the top and the bottom of the steel jacket are adequate for post-earthquake repair of columns with inadequate lap splice using rectangular steel jackets.

#### **4.15 FLEXURAL COLUMN FC14 ( BASIC-UR- 27"x18" )**

The previous flexural columns FC1 through FC13 had cross sections of 36"x18". Two major variables studied the height of the steel jacket and the required number of adhesive anchor bolts for retrofit of 36 inch wide columns. In the remaining four flexural columns, 27 inch and 18 inch wide columns were examined. The height of the steel jacket was kept 1.5 times the length of the splice. For the strengthened columns, the east side of the steel jacket was provided with one vertical line of two anchor bolts and the west side was left without anchor bolts.

The flexural column FC14 is a basic unretrofitted 27"x18" type "C" flexural column. Figure 4.33(a) shows the details of column FC14. During the test, the first flexural cracks formed at the column/footing interface, at a load of 10 kips. As the load was increased to 15 kips, two flexural cracks formed above the splice. Several new flexural cracks formed over the bottom 2/3 of the column height, including the splice region. Figure 4.34(a) shows the south side of column FC14 during the push cycle to 20 kips. The first vertical splitting cracks were observed during the cycles to 25 kips. These cracks were short and narrow. At the same load several flexural cracks extended deeper into the column cross section. During the two 30 kip cycles, the vertical splitting cracks extended upward, but did not cause any loss in strength nor in stiffness. Also, the cross ties yielded at the same 30 kip load. While the load was being increased to 35 kips, the splice failed as the load reached just 30 kips. Figure 4.34(b) shows the splice region at failure. The splice failure was very dramatic, and occurred before the development of flexural yielding. It was associated with very rapid loss in strength and stiffness. Figure 4.33(b) shows the hysteretic response of column FC14. Column FC14 exhibited non-ductile response and very low energy dissipation.

#### **4.16 FLEXURAL COLUMN FC15 ( BASIC-UR- 18"x18" )**

Column FC15 is a basic unretrofitted 18"x18" type "D" square flexural column. It was transversely reinforced with a #3 periphery tie at every 16 inches and no cross ties. Figure 4.35(a) shows the details of column FC15.

The first flexural cracks formed at the column/footing interface, at a load of 10 kips. During the same 10 kip cycle two pairs of flexural cracks formed at

the mid-height of the splice and above the top of the splice. As the load was increased to 15 kips, flexural cracks extended deeper into the column cross section. Vertical splitting cracks formed at the bottom of the splice during the same cycles to 15 kips. Also, several new flexural cracks formed in the middle third of the column height. The vertical splitting cracks extended upward to almost the mid-height of the splice, but did not affect the response of the column. Figure 4.36(a) shows column FC15 during the cycle to 20 kips.

Increased loading to 25 kips caused dramatic splice failure. Vertical splitting cracks formed over the full height of the splice. Figure 4.37 shows the north and south elevations of column FC15 at the splice region. The splice failure occurred at 1.25% drift ratio. At higher displacements the column showed considerable loss of strength and stiffness. Figure 4.35(b) shows the hysteretic response of column FC15. None of the longitudinal bars yielded during the test. The splice failure occurred before the development of the yield capacity of the column. Column FC15 exhibited non-ductile response and very low energy dissipation.

#### **4.17 FLEXURAL COLUMN FC16 ( PRE-EQ-S )**

Column FC16 is a strengthened type "C" flexural column. It was retrofitted by the use of a steel jacket and anchor bolts. On the east side, the steel jacket was stiffened by one vertical line of two anchor bolts. However, the west side was left without anchor bolts. Figure 4.38(a) shows the details of column FC16.

The first two flexural cracks formed at the column/footing interface

during the cycle to 10 kips. Also, two other flexural cracks formed above the steel jacket at a load of 10 kips. During the cycles to 15 kips and 20 kips several new flexural cracks developed in the middle third of the column height. These cracks extended deeper into the column cross section during the cycles to 25 kips and 30 kips. Figure 4.39(a) shows column FC16 during the 25 kip cycle. The first two vertical splitting cracks at the splice were observed just below the steel jacket at a load of 30 kips. The longitudinal bars yielded as the load was increased to 35 kips. During the push loadings, where the steel jacket was provided with anchor bolts on the east tension side, the column developed the yield capacity and maintained the maximum load up to 2.8% drift ratio. At 3.3% drift ratio strength and stiffness degradation were observed on that side. It is important to mention here that the strains in the steel jacket near the bottom of the splice were about 650 micro-strains. Strength and stiffness degradation on the east side were very gradual.

Figure 4.38(b) shows the hysteretic response of column FC16. During the pull loadings, where the steel jacket was not provided with anchor bolts on the west tension side, the column developed the yield capacity and maintained the maximum load up to 1.9% drift ratio. At 2.45% drift ratio the column showed loss in strength and stiffness. Also, at the same load, the measured strains on the steel jacket near the bottom of the splice were about 650 micro-strains. At 3.0% drift ratio, separation between the concrete column and the steel jacket was observed. This separation was observed at the top of the steel jacket, on the west side. However, no separation was observed on the east side, where the steel jacket was provided with two adhesive anchor bolts. The steel jacket on the east side maintained compatible deformations with the concrete column which apparently resulted in more effective confinement of the lap splice by the steel



jacket and the anchor bolts. Figure 4.40 shows the top of the steel jacket on the east and west sides at 3.0% drift ratio.

The concrete uniaxial compressive strength at the day of testing was 2565 psi, which was less than 62% of the concrete strength of the basic unretrofitted column FC14. However, column FC16 exhibited much higher ductility and energy dissipation. Also, it is important to mention here that according to older codes the required lap splice length in columns is 32 bar diameters for concrete strength below 3000 psi (see Table 1.1), while the lap splice length in column FC16 was just 24 bar diameters.

After completion of the FC16 column test, the steel jacket and the non-shrink grout were removed. Investigation of the concrete surface in the splice region revealed several cracks along the splice, and general distress of the concrete column at the bottom of the splice. Figure 4.41 shows the concrete column at the splice region after the removal of the steel jacket and the non-shrink grout.

#### **4.18 FLEXURAL COLUMN FC17 ( PRE-EQ-S )**

Column FC17 is a strengthened type "D" square flexural column. It was strengthened by the use of a steel jacket and anchor bolts. On the east side, the steel jacket was retrofitted by one vertical line of two anchor bolts. However, the west side was left without anchor bolts. Figure 4.42(a) shows the details of column FC17. Unlike all other strengthened columns, column FC17 was provided with four additional 3"x3"x1/4" steel angles at the jacket corners. These angles were welded to the steel jacket after the casting and setting of the non-

shrink grout. Figure 4.43(b) shows views of the corner detail of the steel jacket.

The first two flexural cracks on column FC17 formed at a load of 10 kips. As the load was increased to 15 kips several new flexural cracks formed over the middle third of the column height and right above the steel jacket. Increased loading to 20 kips caused the formation of vertical splitting cracks at the bottom of the splice. These cracks were observed just below the steel jacket. Most of the flexural cracks extended deeper into the column cross section as the load was increased to 30 kips. Some of these cracks extended diagonally forming flexure shear cracks. After the completion of the two 30 kip cycles, the column showed large inelastic deformations associated with yielding of the main longitudinal bars.

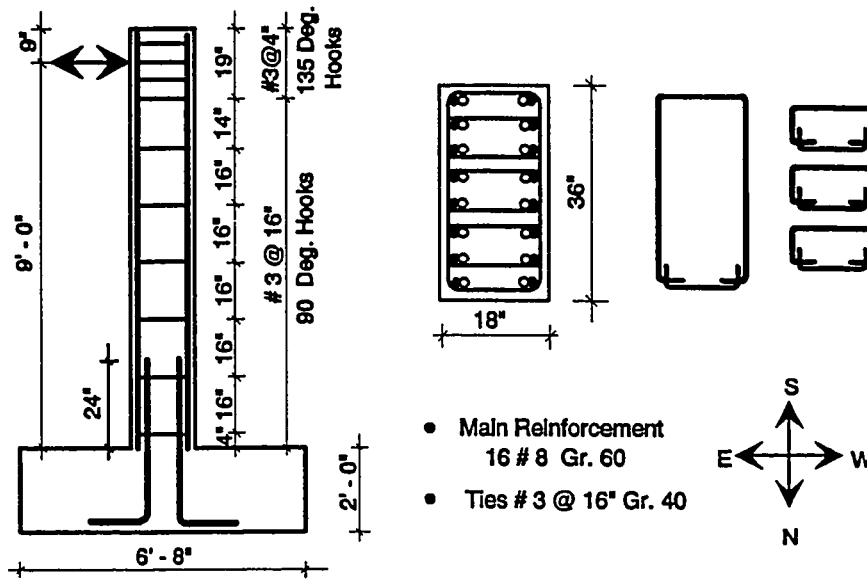
Column FC17 showed minor stiffness degradation with increasing loads. However, it did not show any major strength degradation. At 2.5% drift ratio the concrete in the compression zones deteriorated at the face of the column, just below the bottom of the steel jacket. The concrete deterioration might have caused the 2 to 3 kip drop in strength with increased loading above 2.5% drift ratio. Figure 4.42(b) shows the hysteretic response of column FC17. The response of column FC17 showed wide hysteretic loops, which were not exhibited by any other retrofitted column. Welding of the four extra corner angles to the steel jacket after the setting of the non-shrink grout may have caused some residual tensile stresses in the steel jacket. These residual tensile stresses developed active confinement of the lap splice by the steel jacket.

After completion of the column FC17 test, the steel jacket and the non-shrink grout were removed. The concrete column in the splice region was then

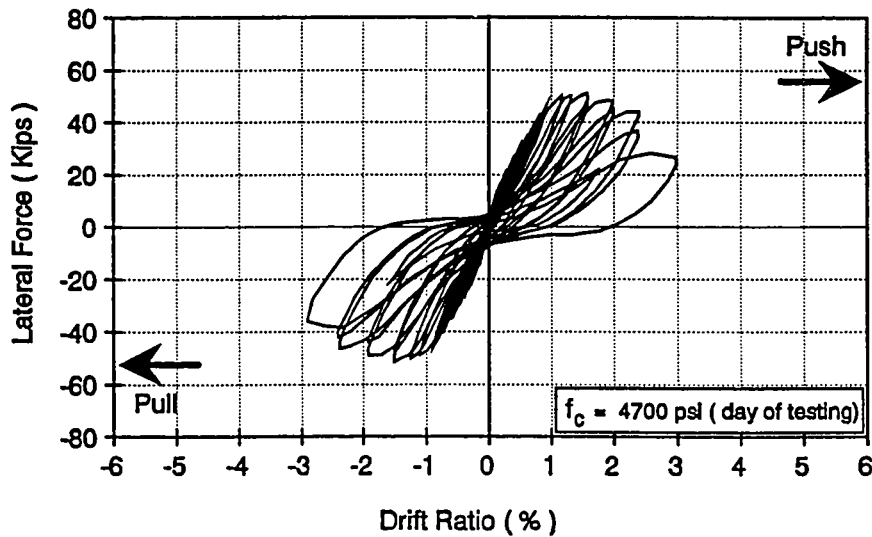
inspected. Close investigation of the concrete column surface in the splice region revealed very minor damage at the bottom of the splice. Figure 4.44 shows the splice region of column FC17 before and after the removal of the steel jacket. It is important to mention here that the concrete strength at the day of testing was 2635 psi, which was less than 64% of the concrete strength of the basic unretrofitted column FC15. However, the performance of column FC17 was by far better than the performance of the basic unretrofitted column FC15. Column FC17 exhibited very stable hysteretic response, wide hysteretic loops, large ductility and high energy dissipation.

#### **4.19 SUMMARY**

The performance of seventeen basic unretrofitted and retrofitted flexural columns with an inadequate lap splice in the longitudinal bars was presented. The effectiveness of rectangular steel jackets in seismic retrofit of 36", 27" and 18" wide columns was investigated. The response of several of the basic unretrofitted columns showed very dramatic splice failure. However, for pre-earthquake strengthening, similar columns retrofitted with 1/4 inch thick rectangular steel jackets of adequate height and with an adequate number of anchor bolts showed considerable increase in strength and ductility. Also, for post-earthquake repair, damaged columns retrofitted with similar rectangular steel jackets and through bolts showed similar improvements. Chapter 6 presents detailed discussion and comparison of the experimental data of the flexural columns.

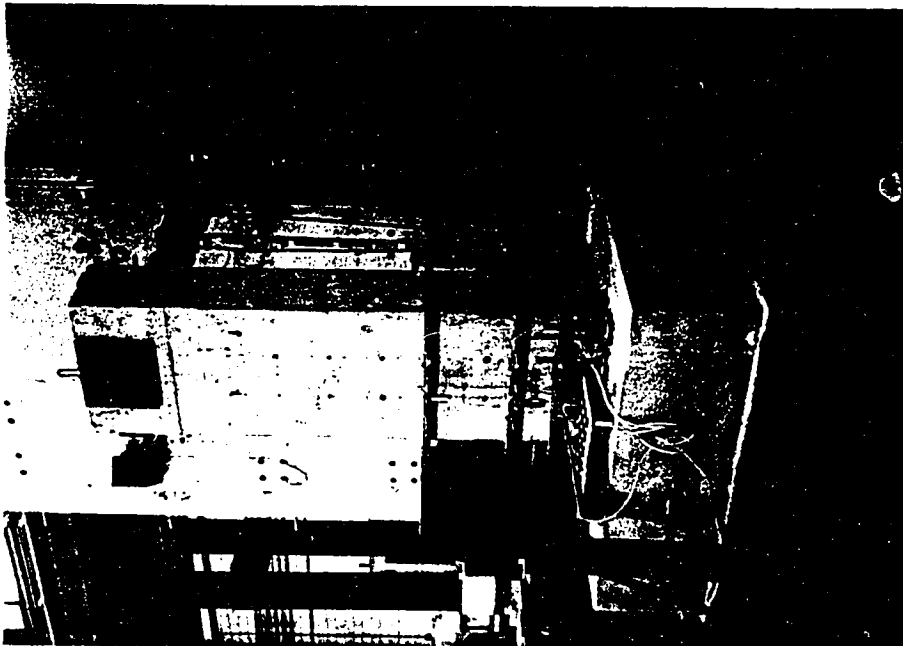


(a) Details of Column FC1

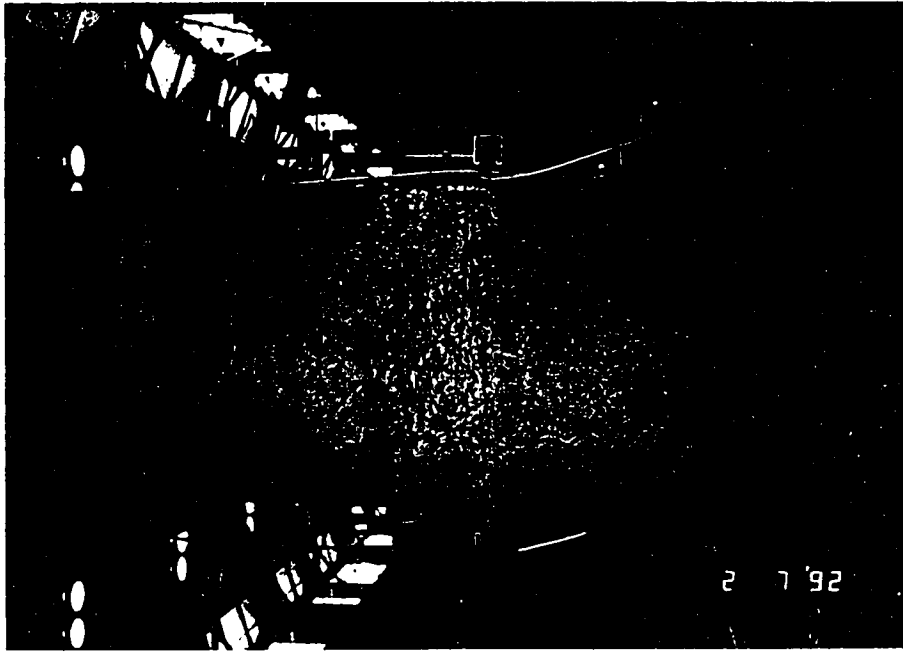


(b) Hysteretic Response

Figure 4.1 Basic Unretrofitted Flexural Column FC1

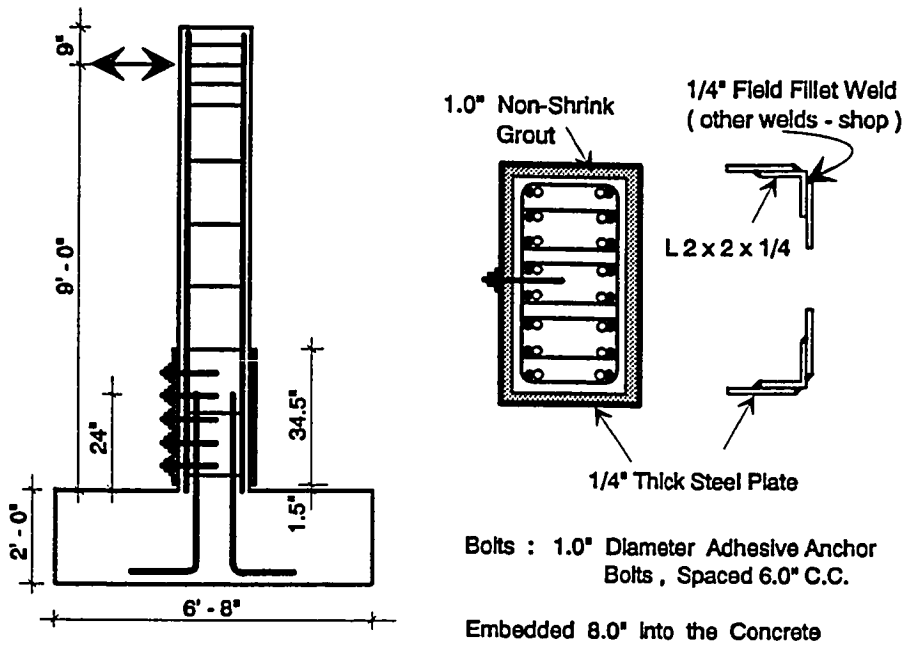


(a) Column FC1 in the test setup

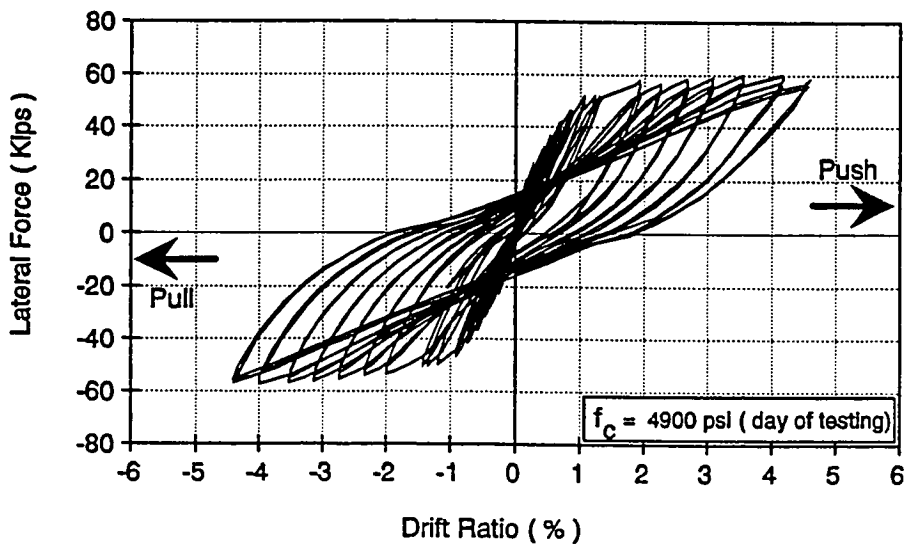


(b) Crack pattern at the splice, south side (at end of test)

Figure 4.2 Basic Unretrofitted Flexural Column FC1

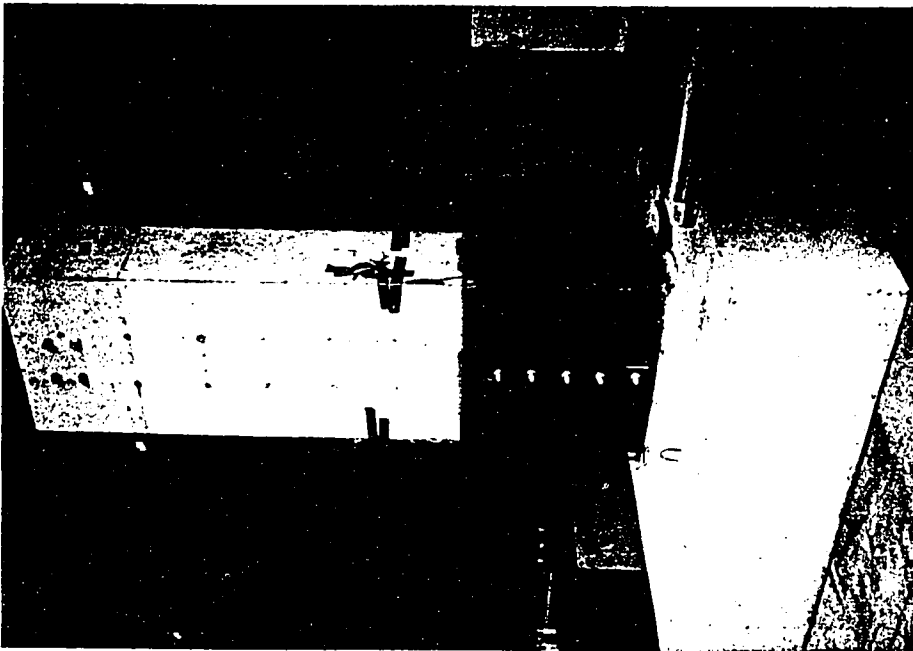


(a) Details of Column FC2

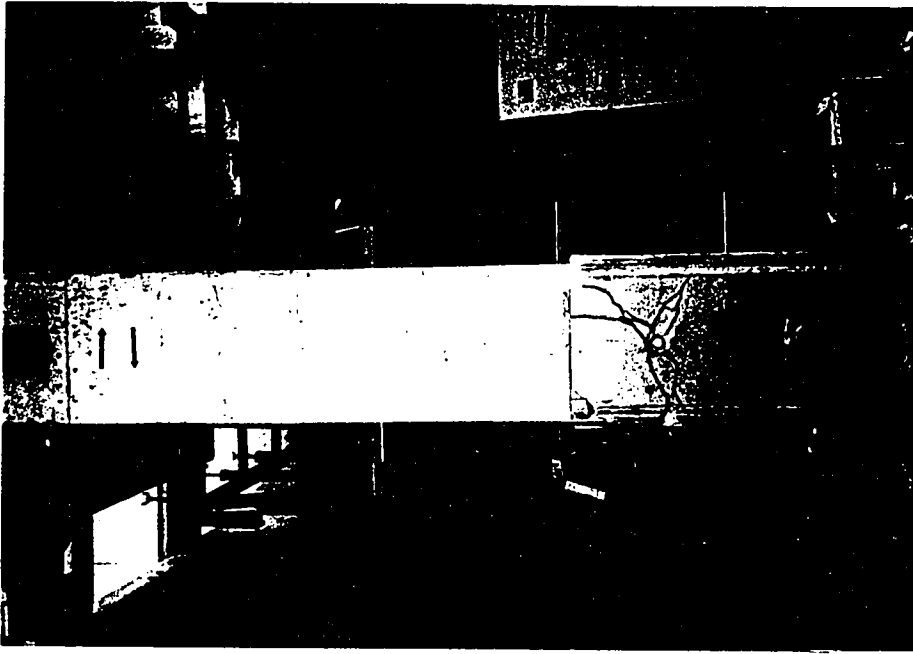


(b) Hysteretic Response

Figure 4.3 Strengthened Flexural Column FC2

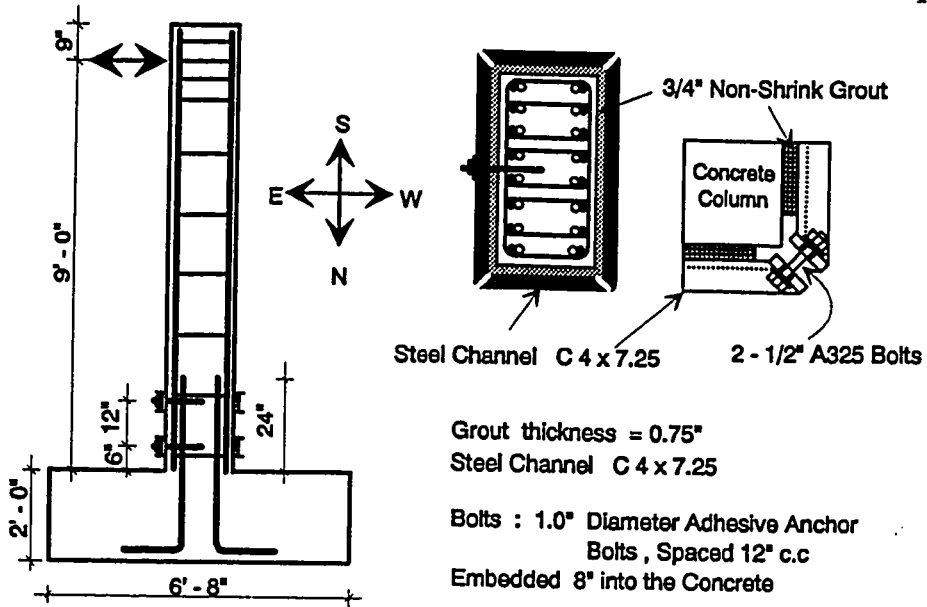


(a) Column FC2 before the test

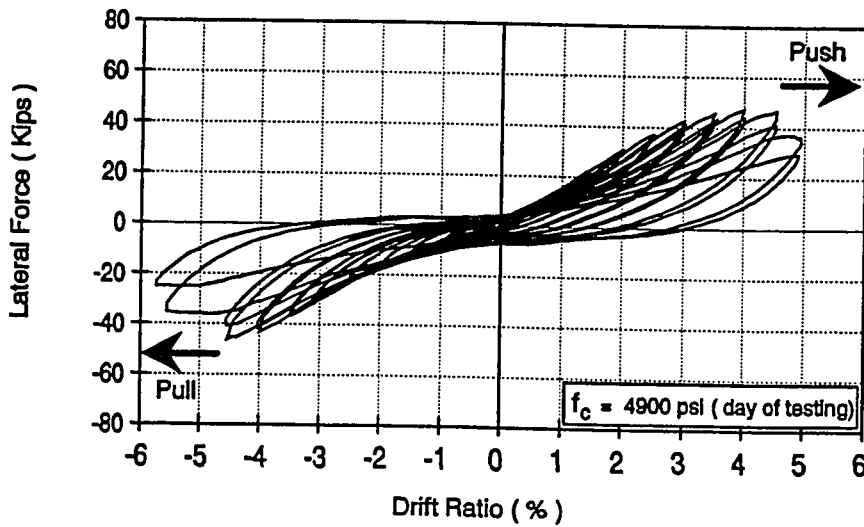


(b) Crack pattern , north side

Figure 4.4 Strengthened Flexural Column FC2



(a) Details of Column FC3



(b) Hysteretic Response

Figure 4.5 Repaired Flexural Column FC3



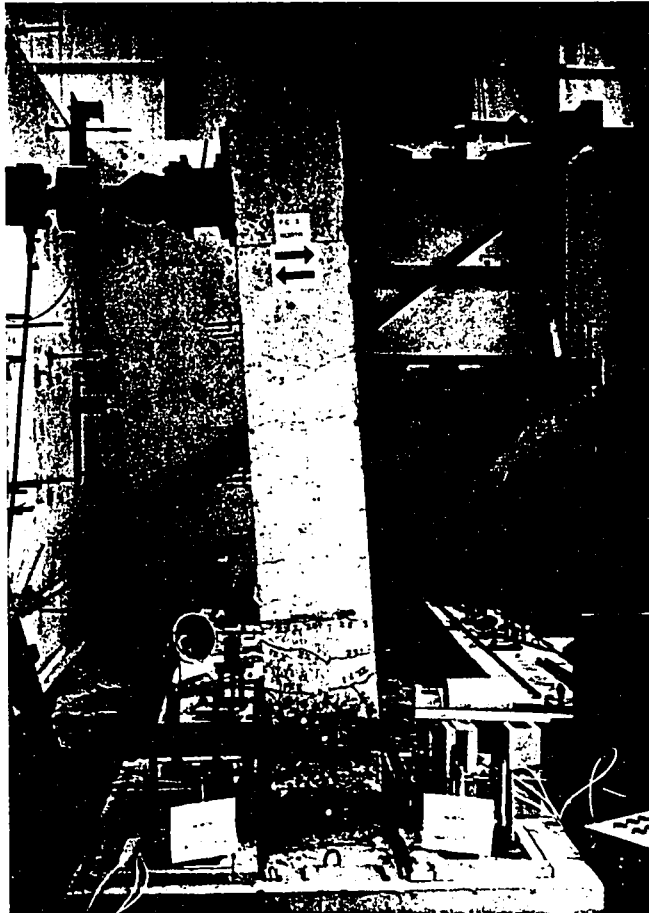
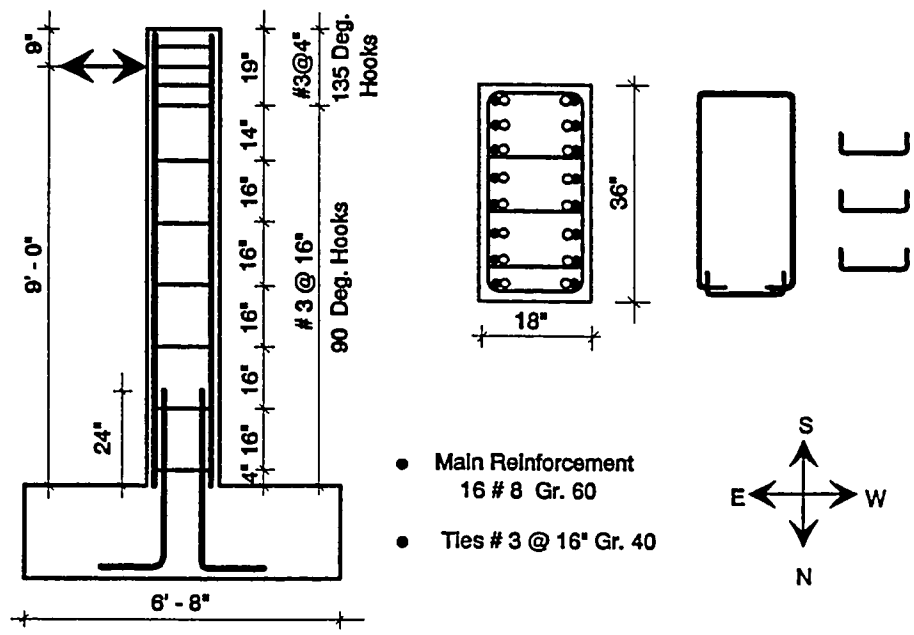
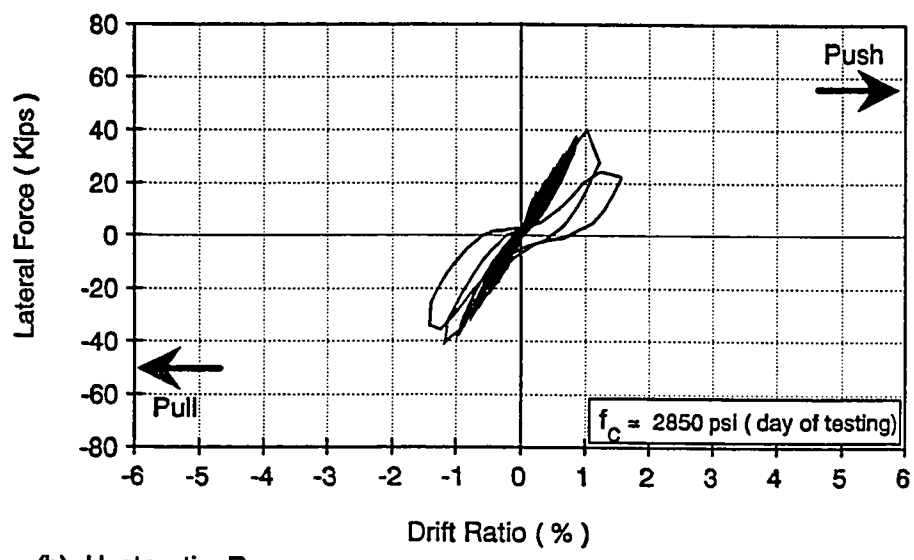


Figure 4.6 Repaired Flexural Column FC3

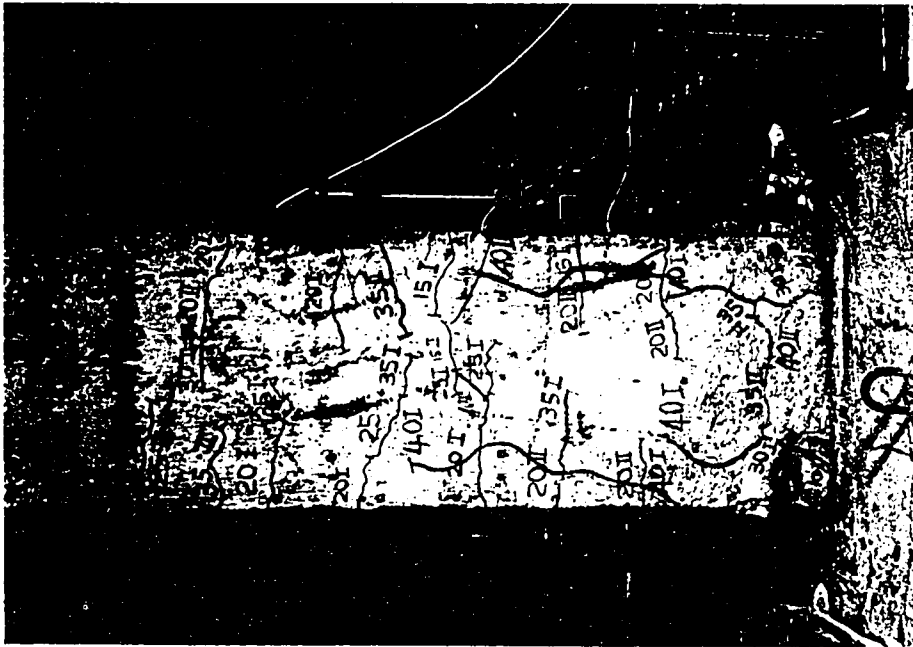


(a) Details of Column FC4



(b) Hysteretic Response

Figure 4.7 Basic Unretrofitted Flexural Column FC4

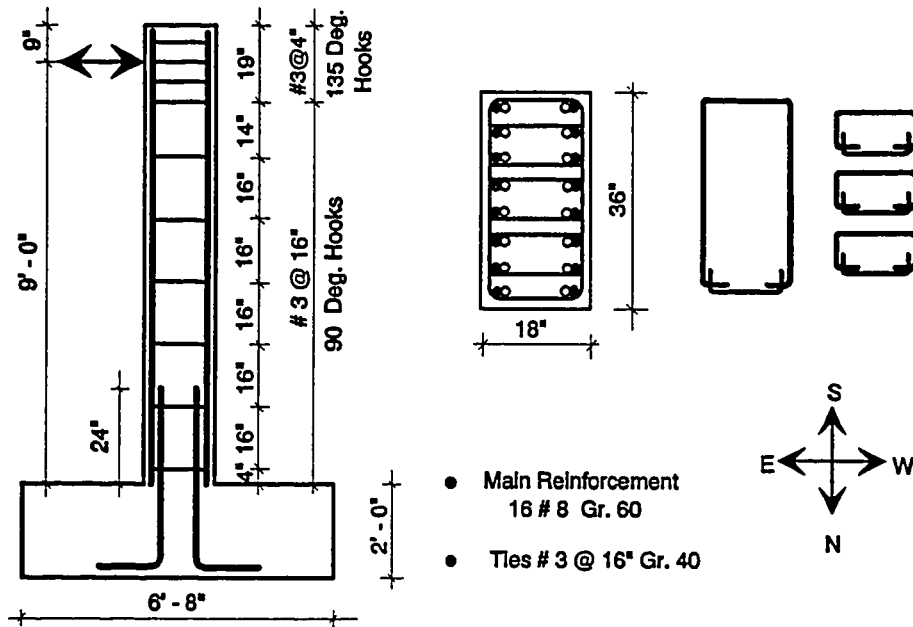


(a) Crack pattern at the splice, north side

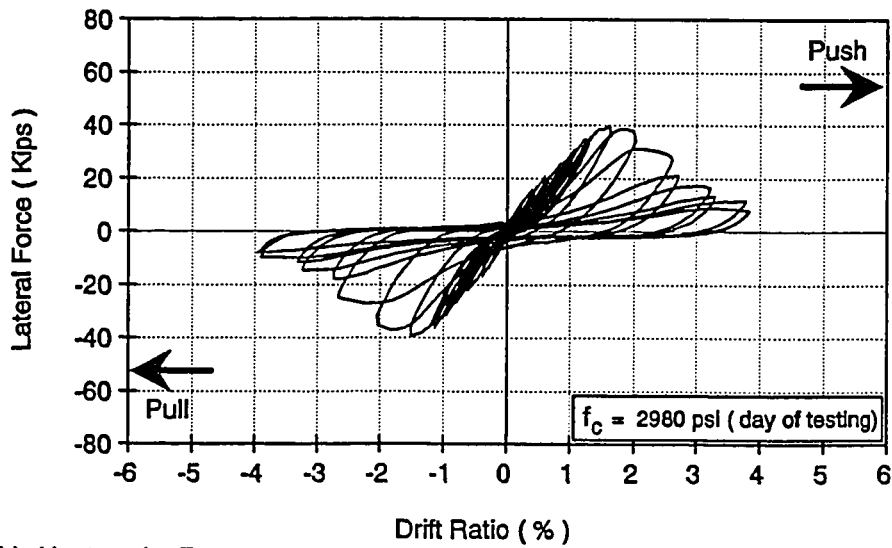


(b) Crack pattern at the splice, south side

Figure 4.8 Basic Unretrofitted Flexural Column FC4



(a) Details of Column FC5

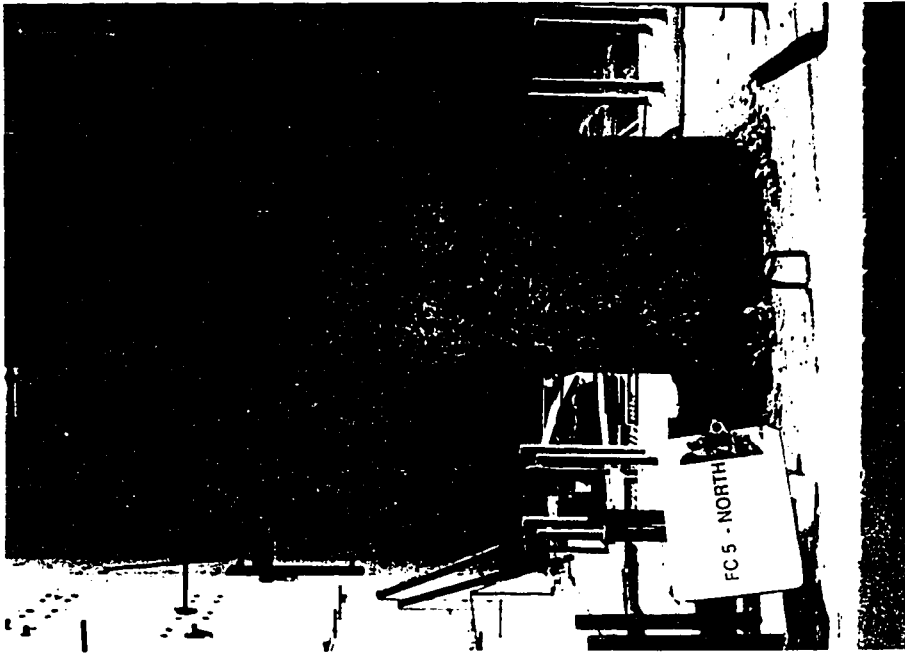


(b) Hysteretic Response

Figure 4.9 Basic Unretrofitted Flexural Column FC5

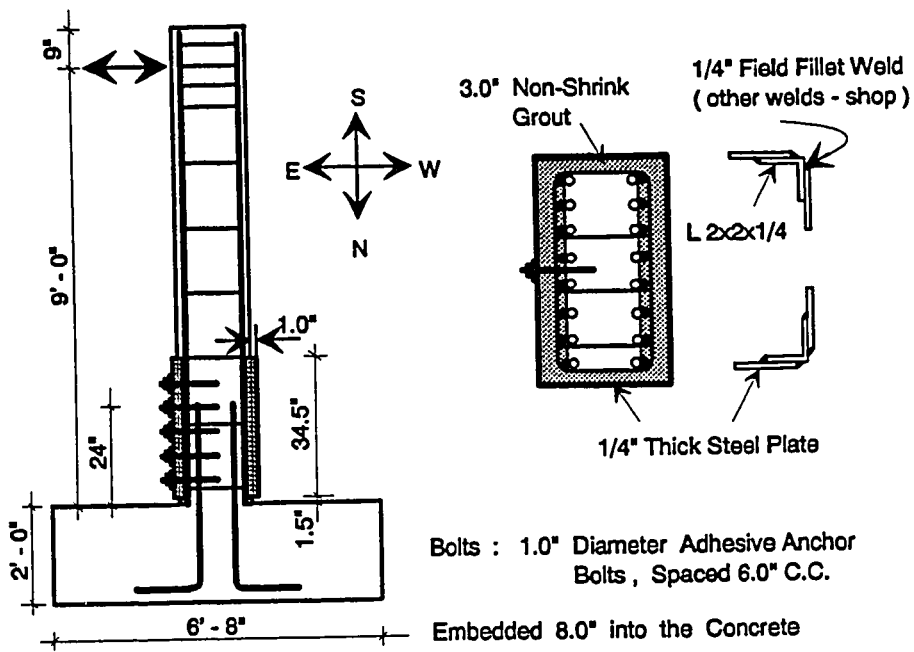


(a) Column FC5 at the end of the test

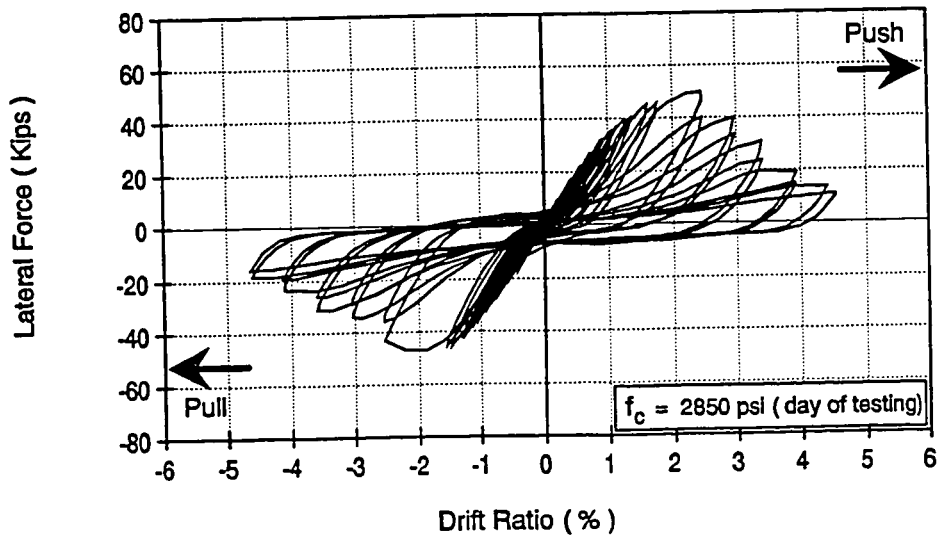


(b) Crack pattern at the splice, north side

Figure 4.10 Basic Unretrofitted Flexural Column FC5

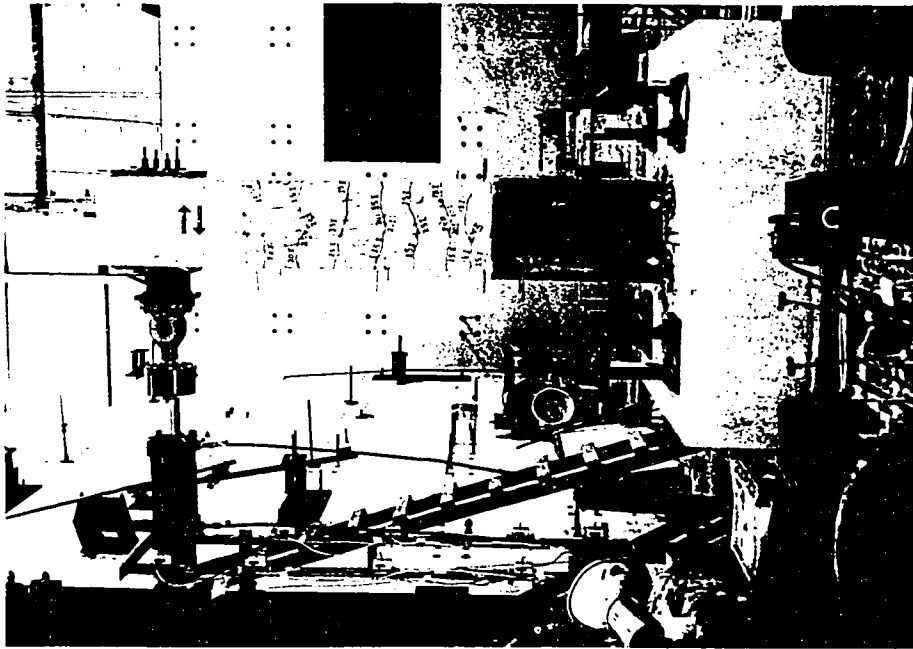


(a) Details of Column FC6

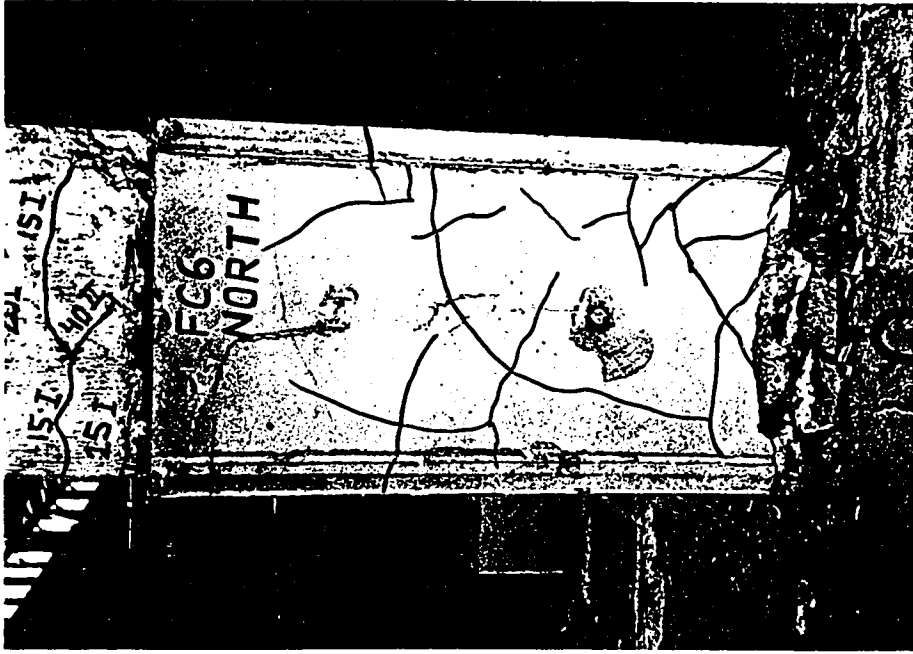


(b) Hysteretic Response

Figure 4.11 Repaired Flexural Column FC6



(a) Column FC6 during the test



(b) Crack pattern at the splice, north side

Figure 4.12 Repaired Flexural Column FC6



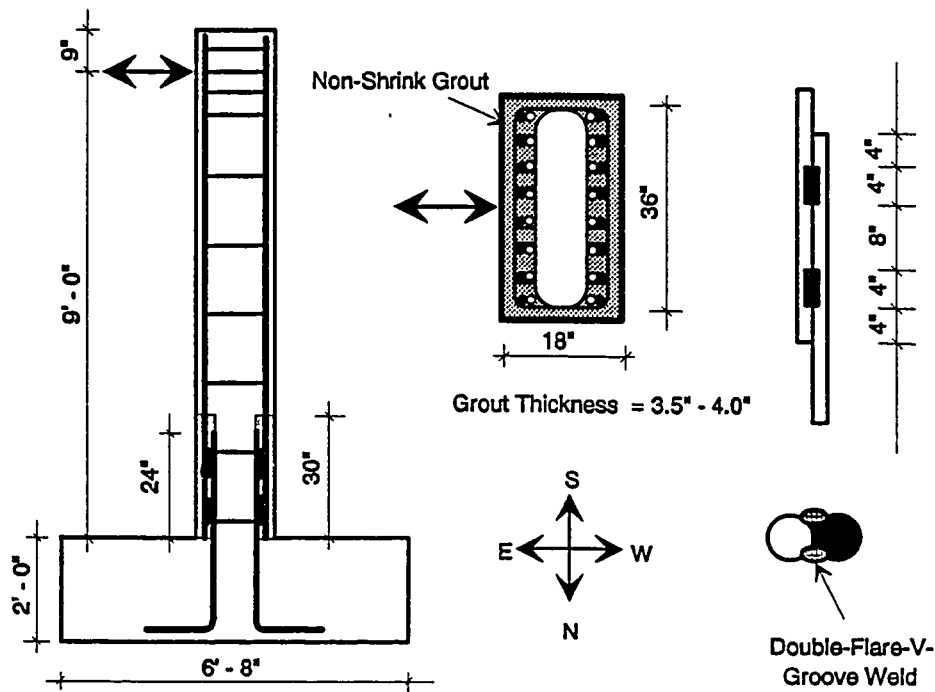
(a) Crack pattern on non-shrink grout, N-E side



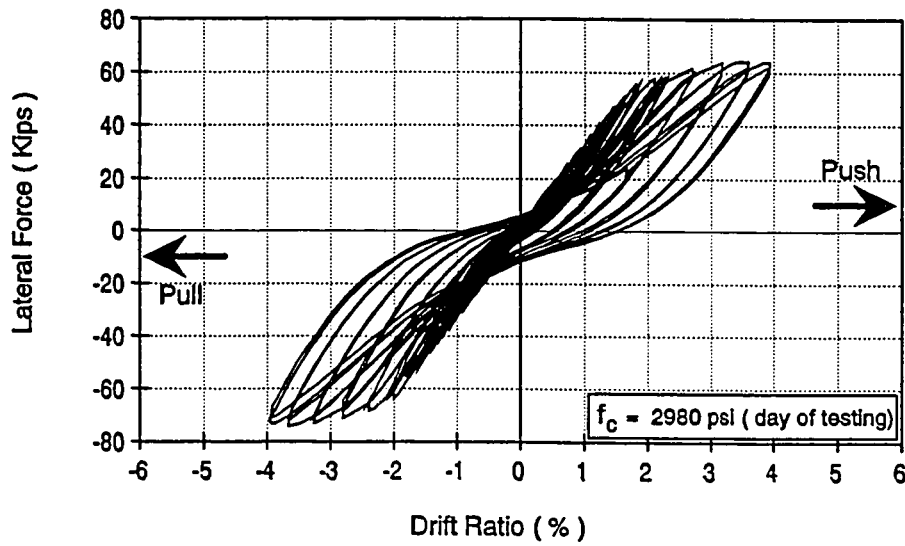
(b) Crack pattern on non-shrink grout, N-W side

Figure 4.13 Repaired Flexural Column FC6



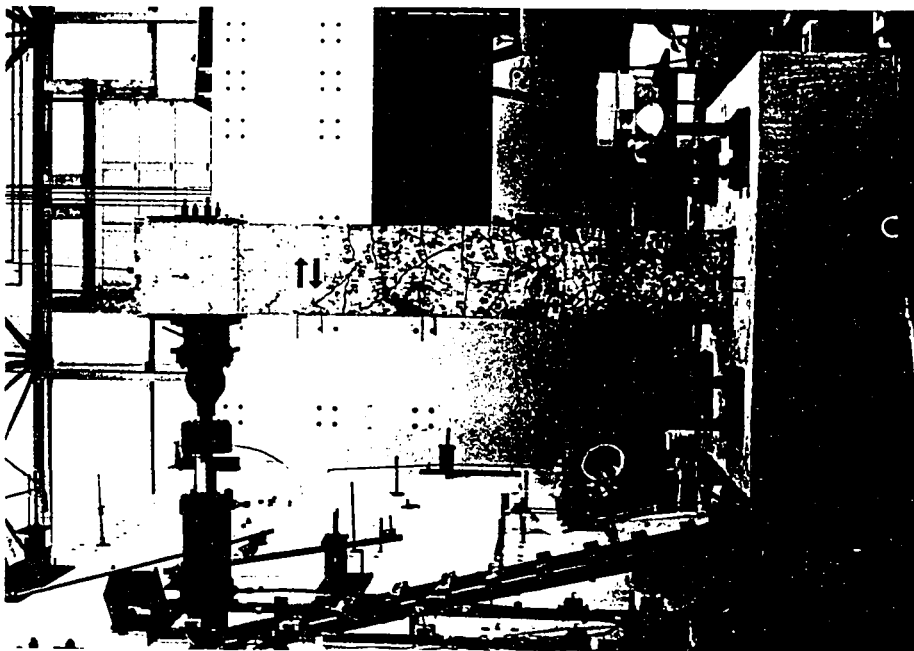


(a) Details of Column FC7

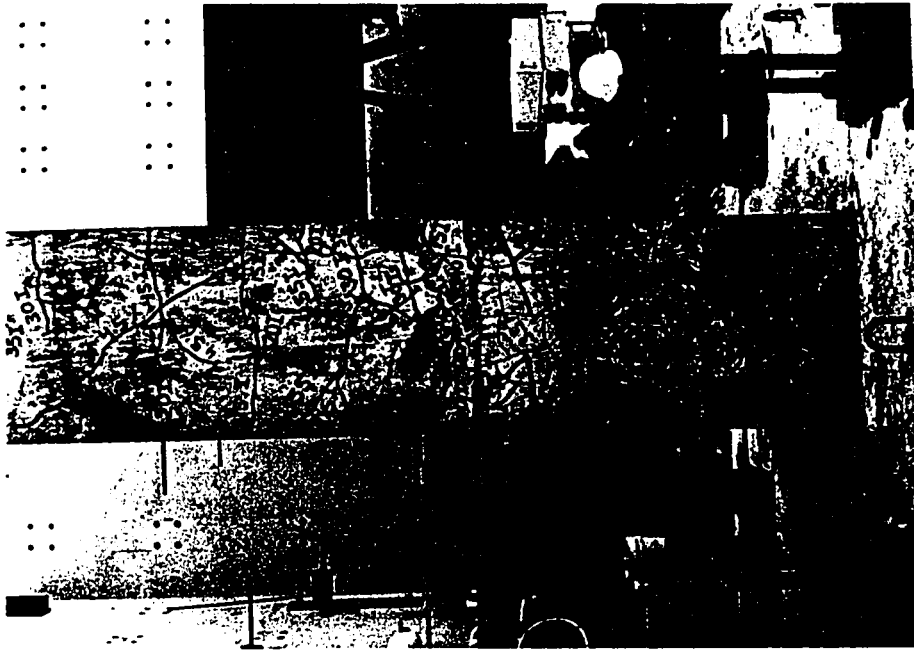


(b) Hysteretic Response

Figure 4.14 Repaired Flexural Column FC7

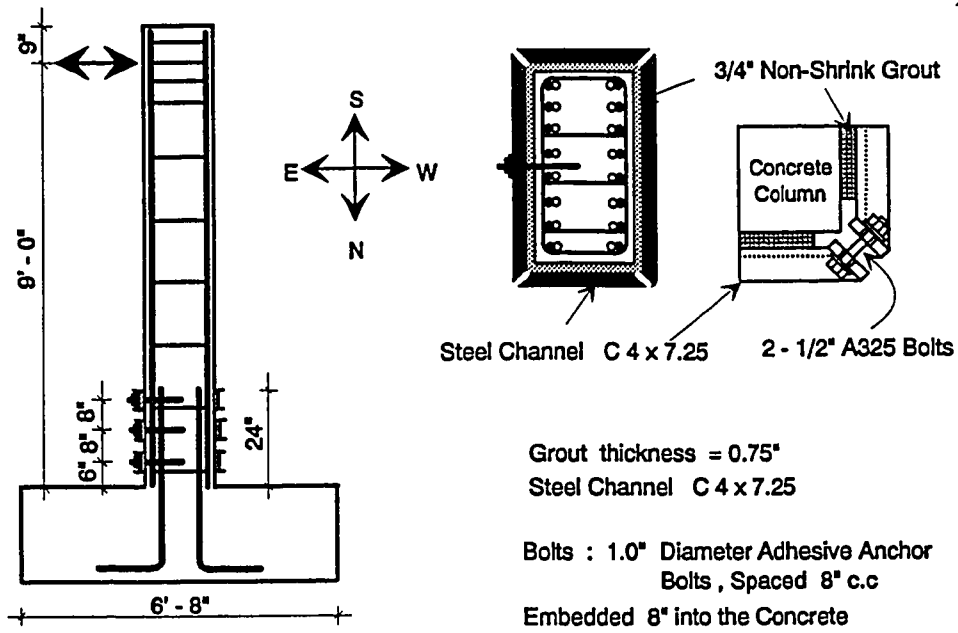


(a) Column FC7 at the end of the test

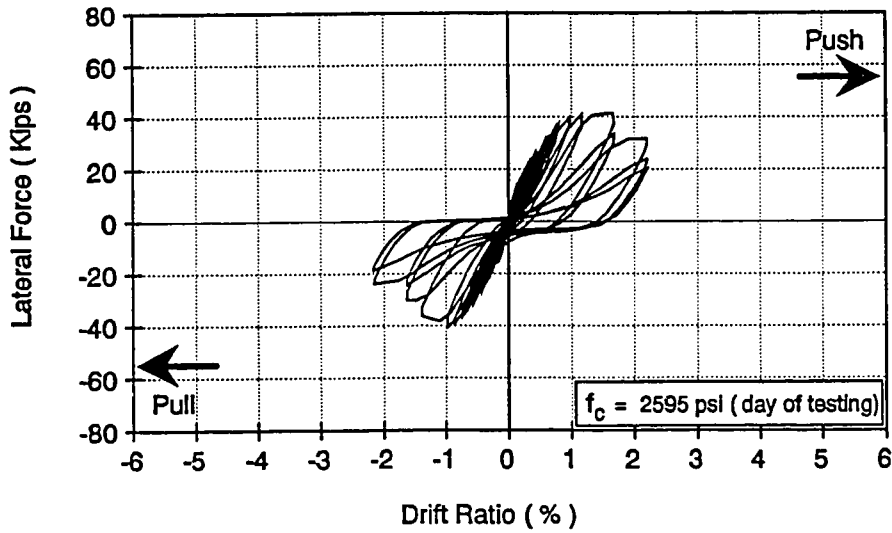


(b) Crack pattern at the splice, north side

Figure 4.15 Repaired Flexural Column FC7

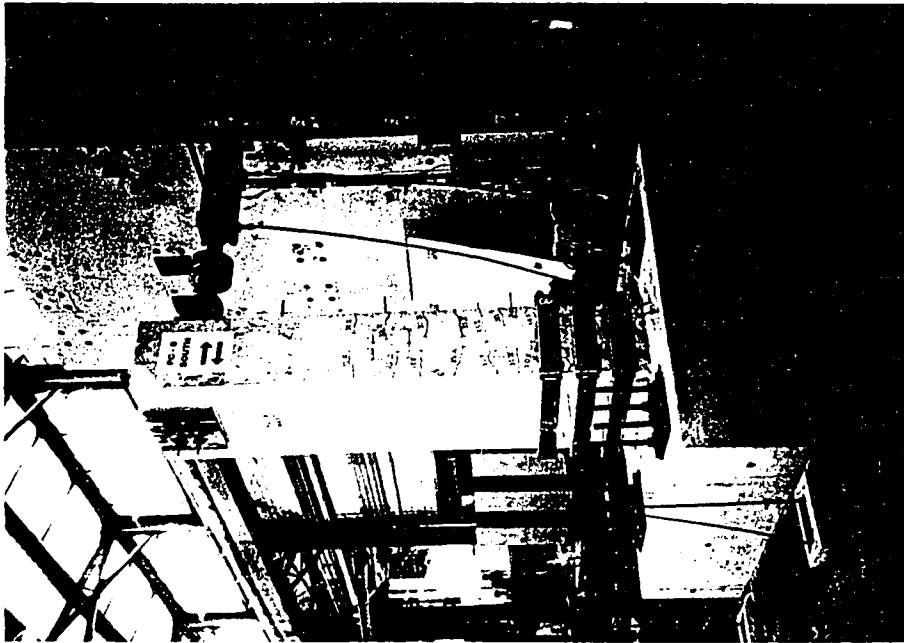


(a) Details of Column FC8



(b) Hysteretic Response

Figure 4.16 Strengthened Flexural Column FC8

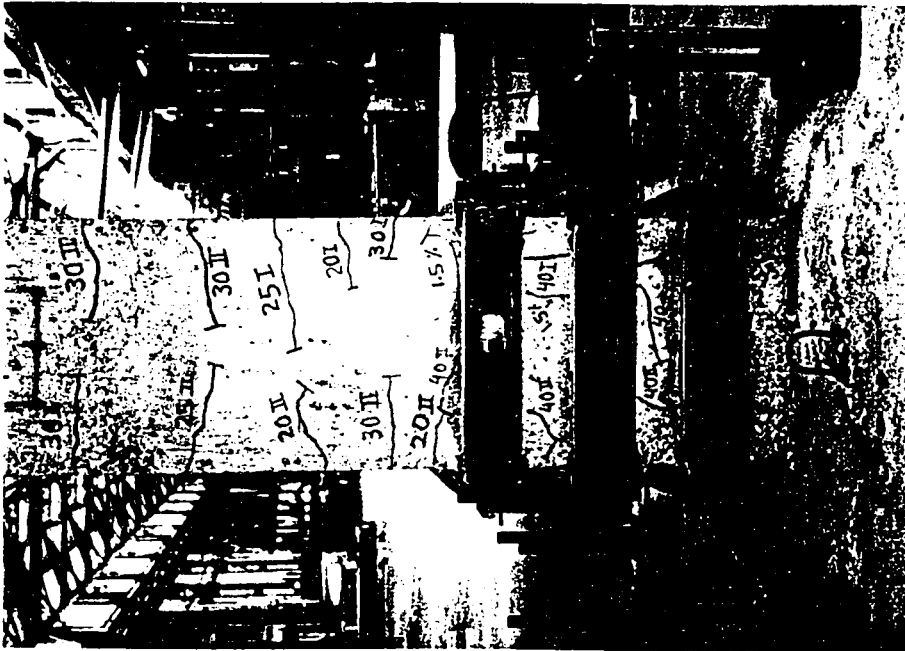


(a) Column FC8 at the end of the test

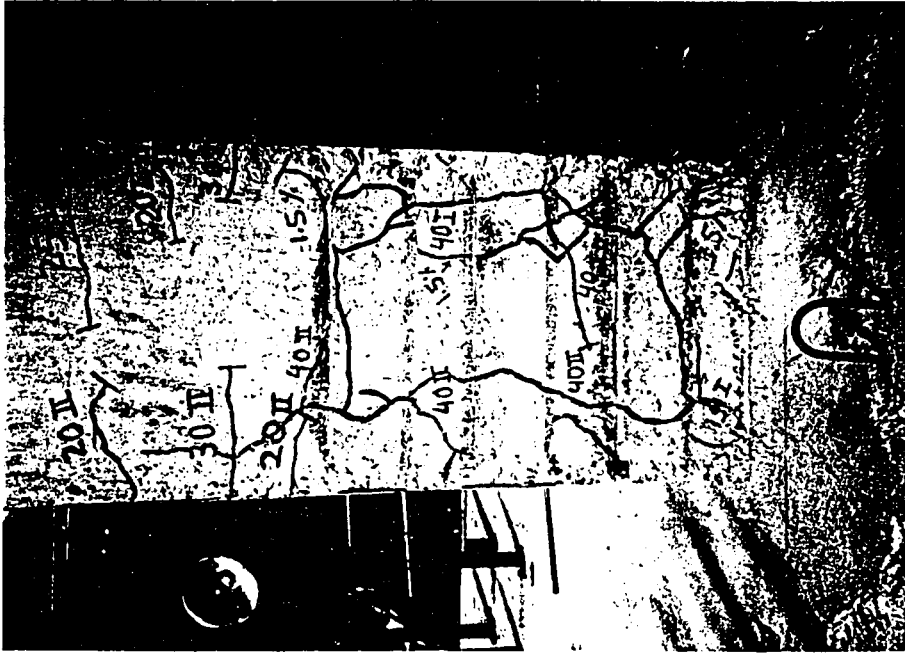


(b) Column FC8 after the removal of the steel collars

Figure 4.17 Strengthened Flexural Column FC8

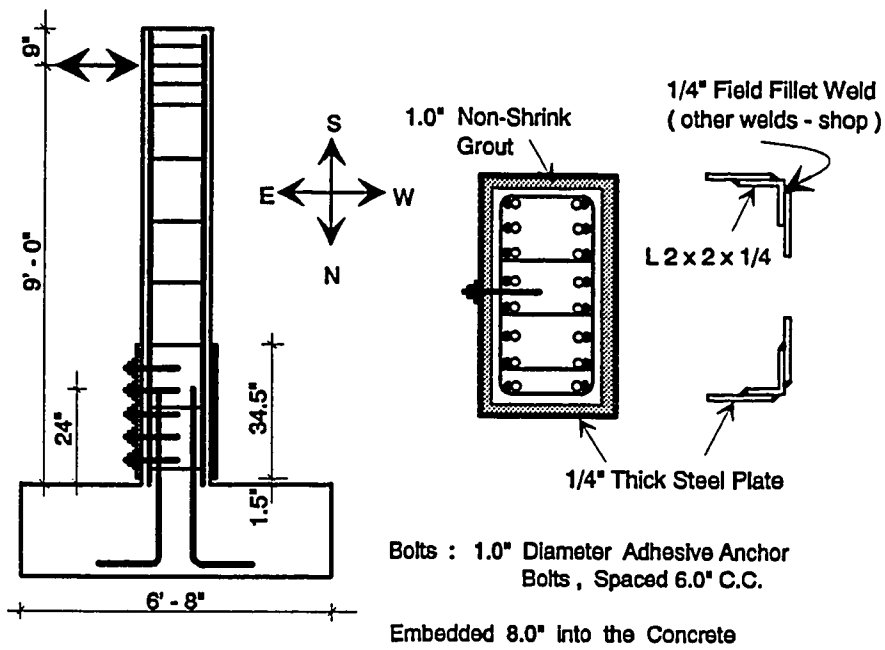


(a) Splice region during the test, south side

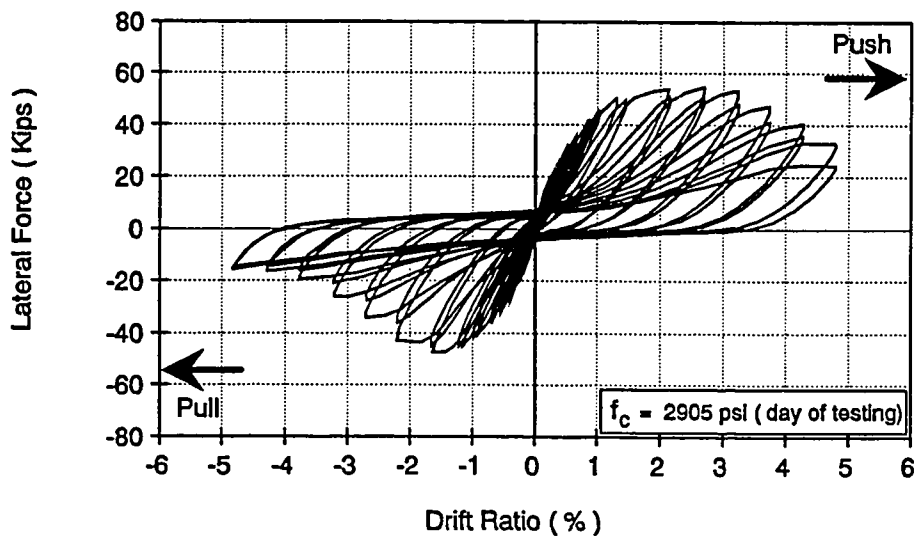


(b) Splice region after the test, south side

Figure 4.18 Strengthened Flexural Column FC8

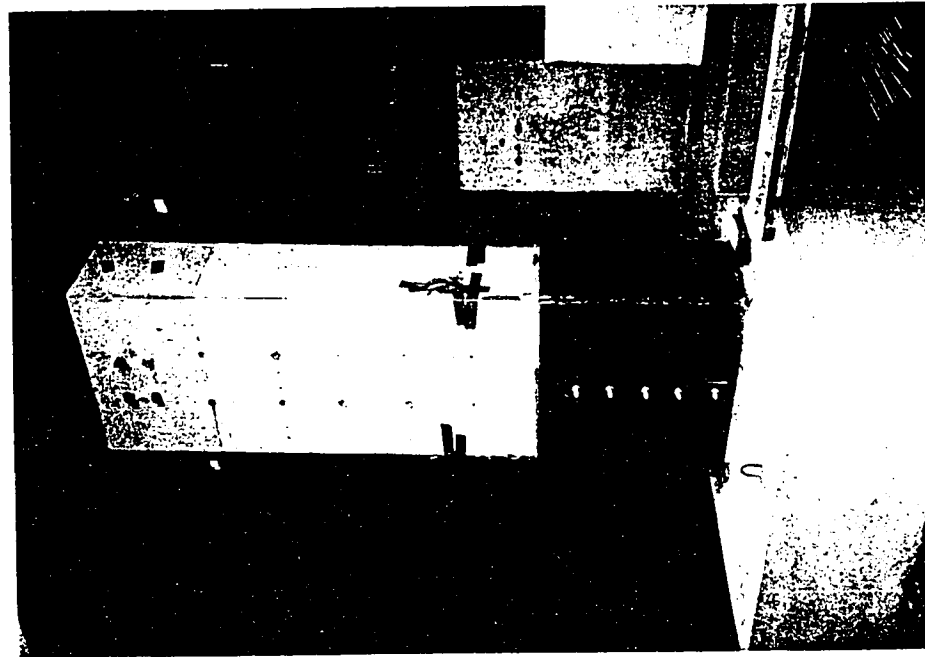


(a) Details of Column FC9

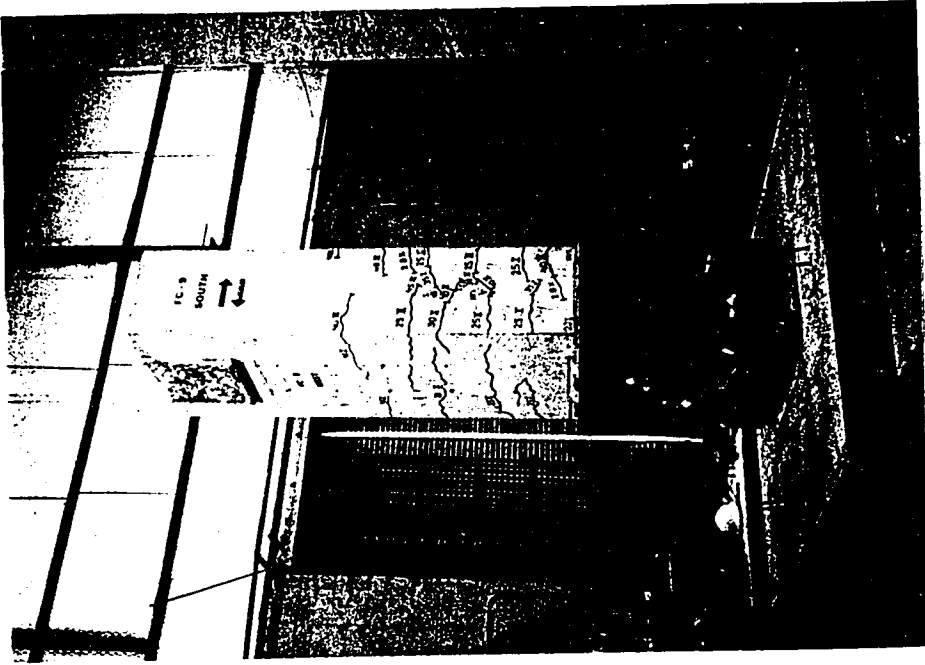


(b) Hysteretic Response

Figure 4.19 Strengthened Flexural Column FC9

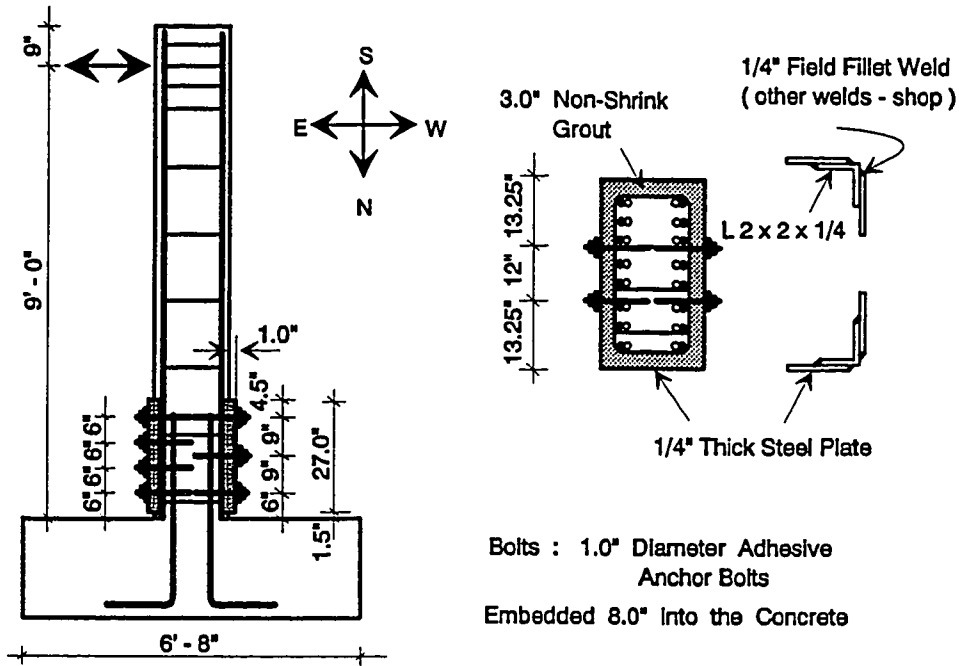


(a) Column FC9 before the test, N-E side

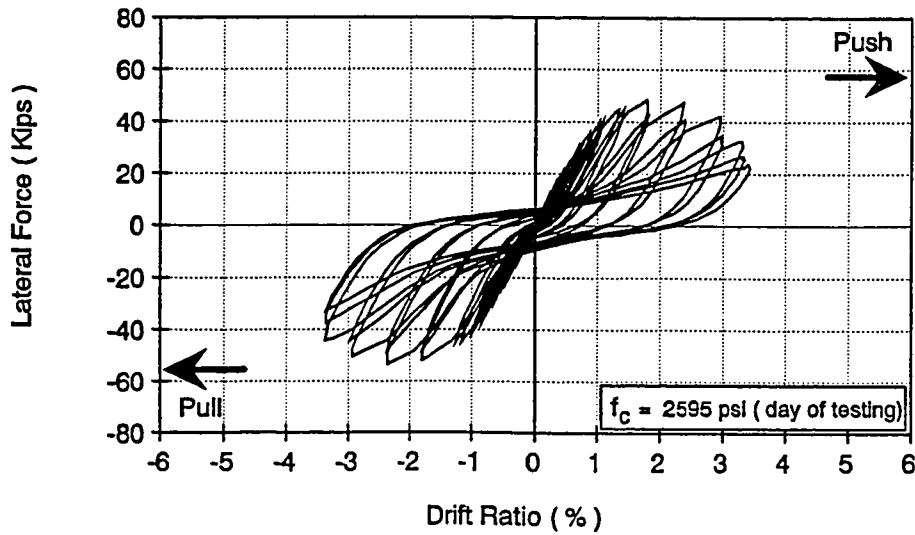


(b) Column FC9 after the test, S-W side

Figure 4.20 Strengthened Flexural Column FC9



(a) Details of Column FC10



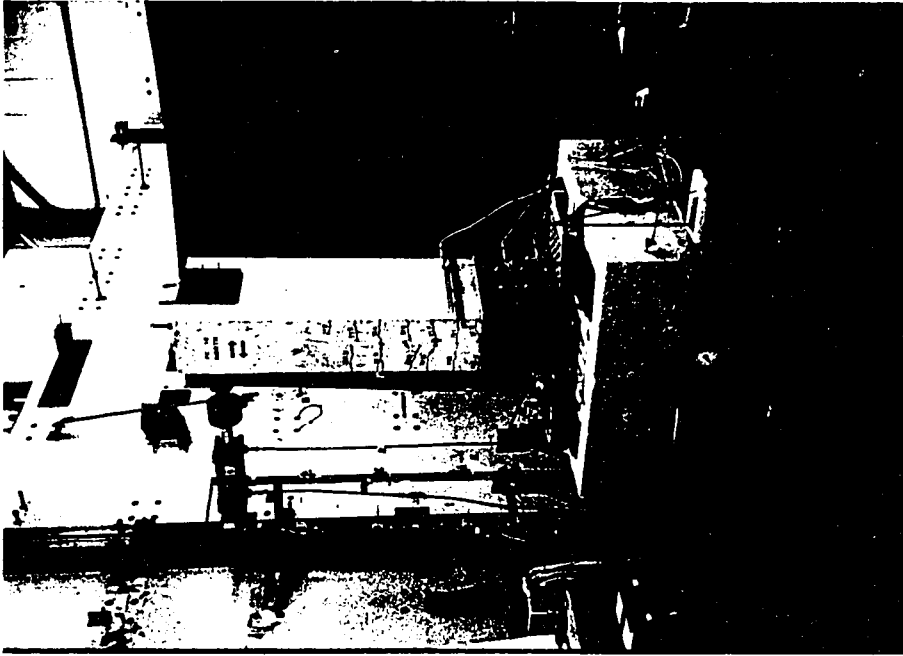
(b) Hysteretic Response

Figure 4.21 Repaired Flexural Column FC10



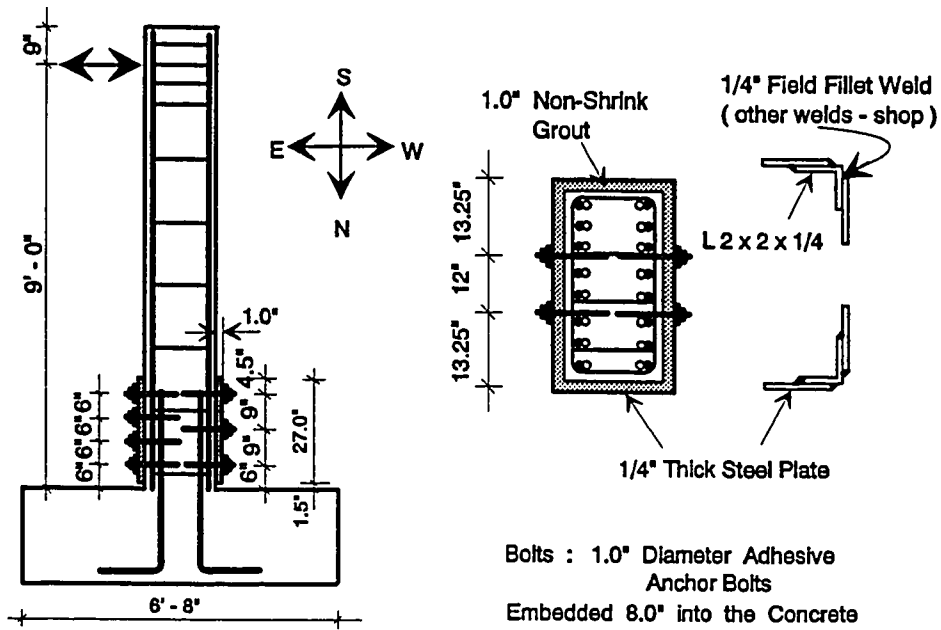


(a) Column FC10 before the test

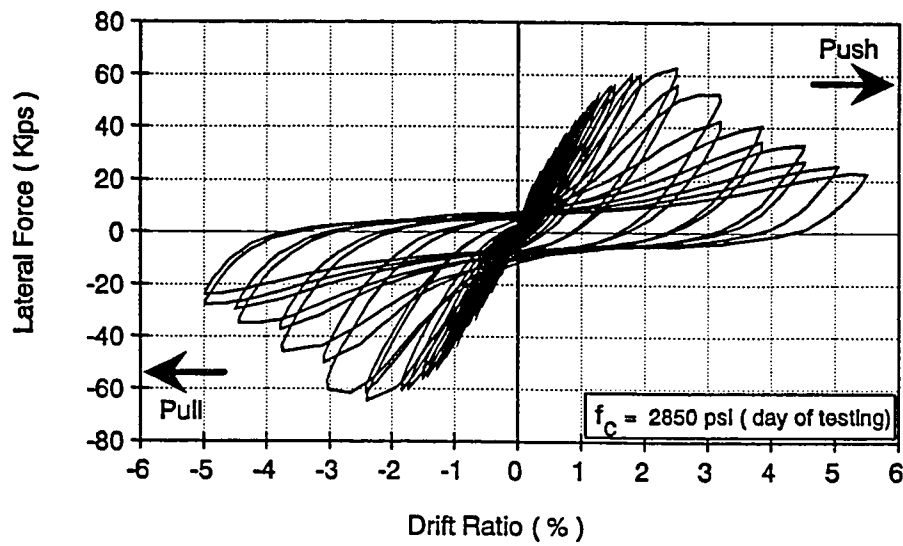


(b) Column FC10 during the test

Figure 4.22 Repaired Flexural Column FC10

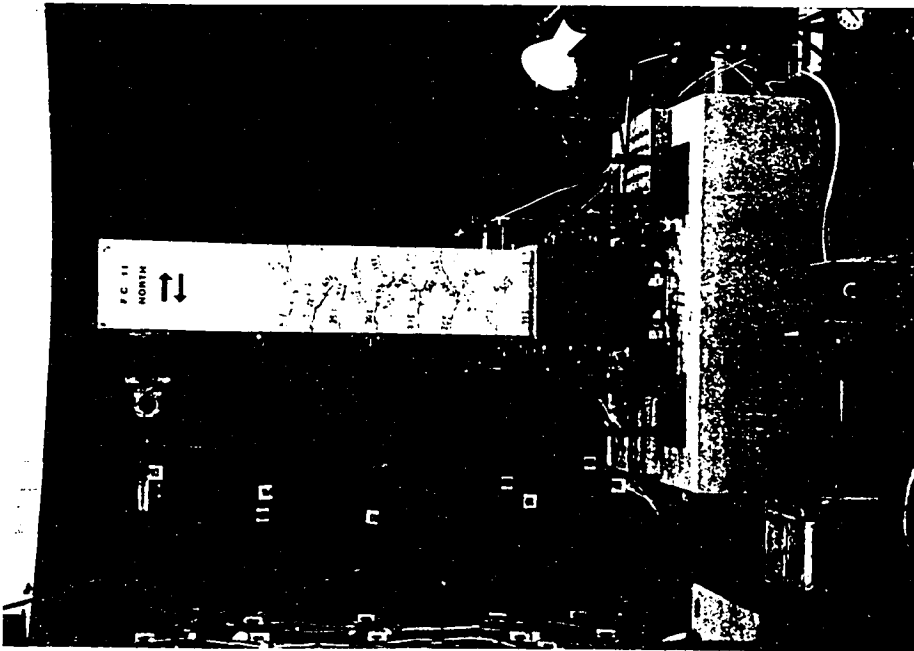


(a) Details of Column FC11

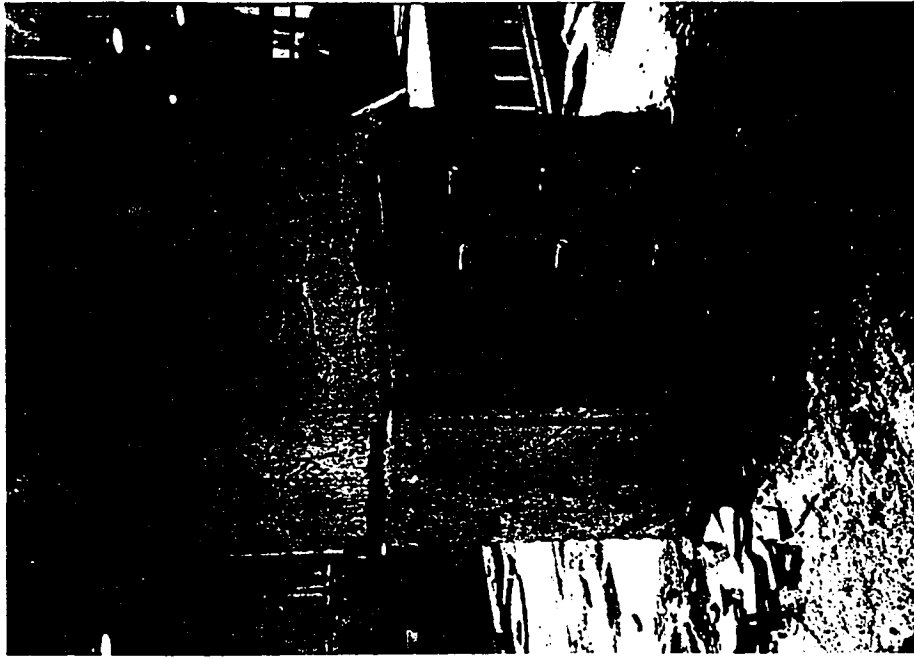


(b) Hysteretic Response

Figure 4.23 Strengthened Flexural Column FC11

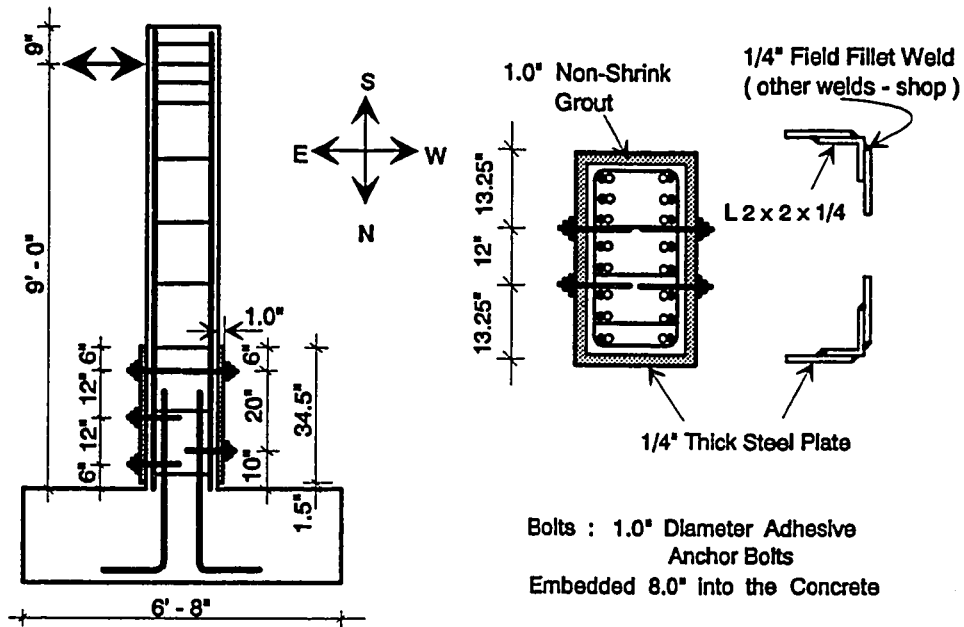


(a) Column FC11 during the test

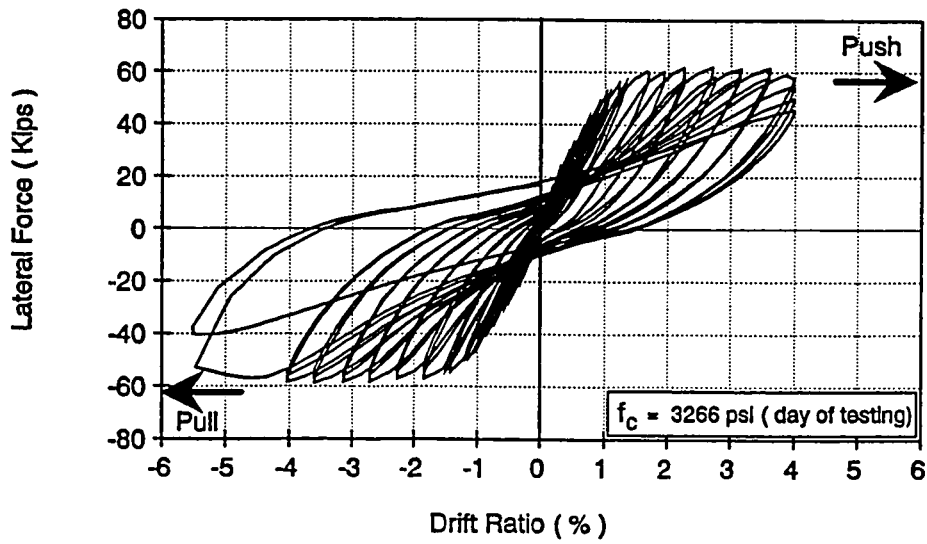


(b) Crack pattern on non-shrink grout, N-W side

Figure 4.24 Strengthened Flexural Column FC11

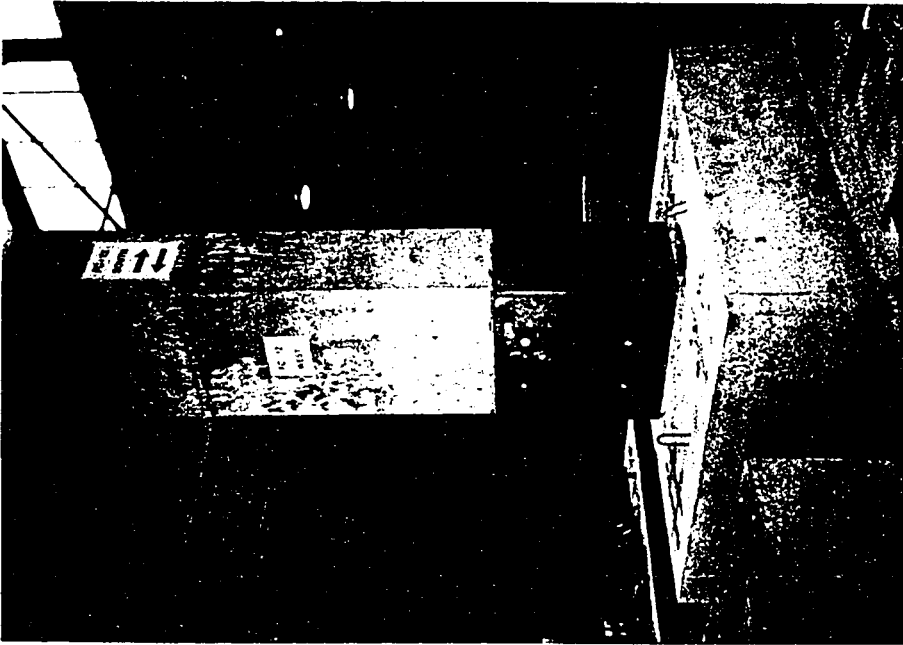


(a) Details of Column FC12

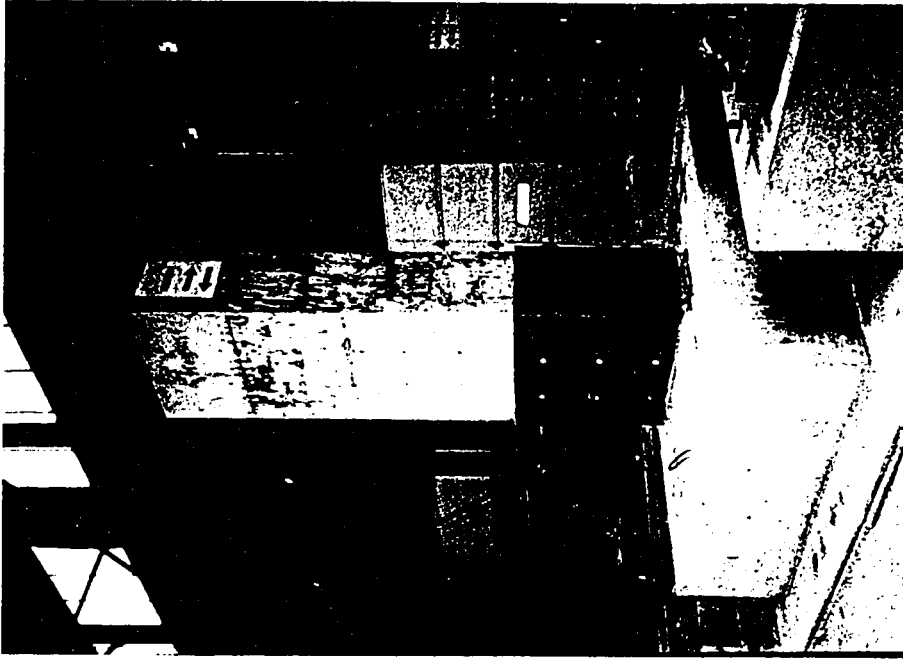


(b) Hysteretic Response

Figure 4.25 Strengthened Flexural Column FC12

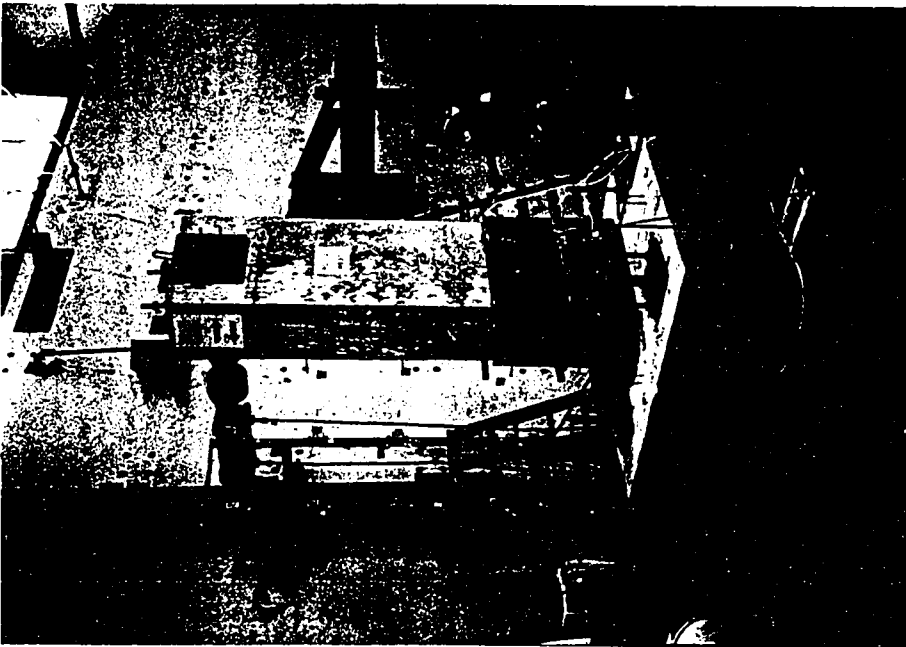


(a) Column FC12, S-W elevation

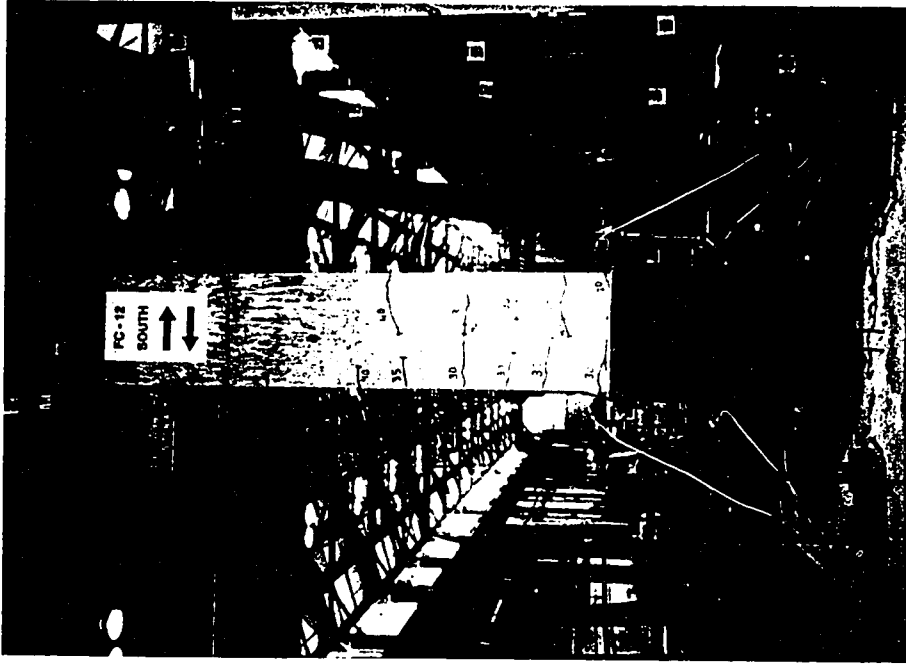


(b) Column FC12, N-E elevation

Figure 4.26 Strengthened Flexural Column FC12

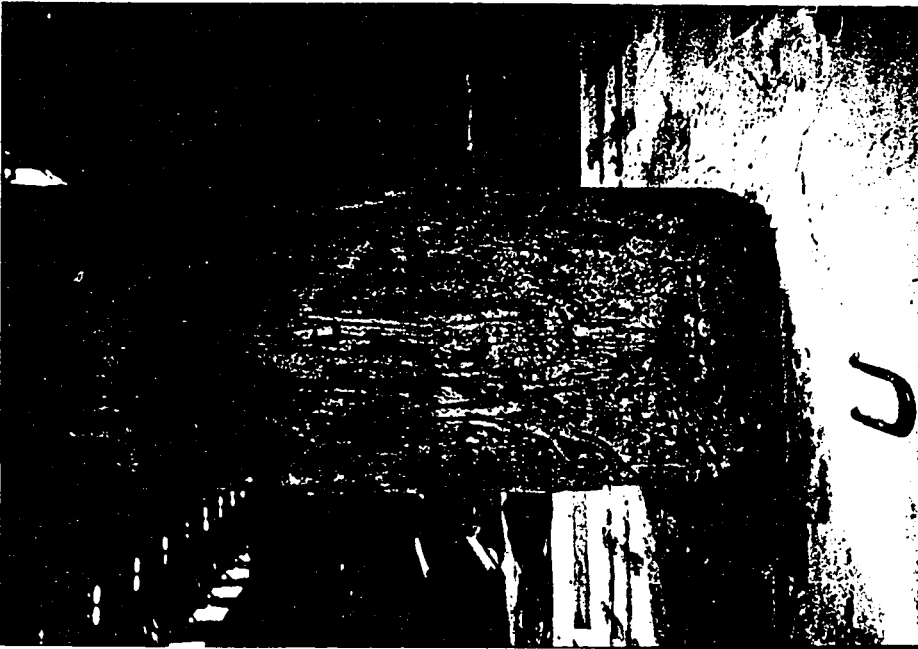


(a) Column FC12 under the test setup

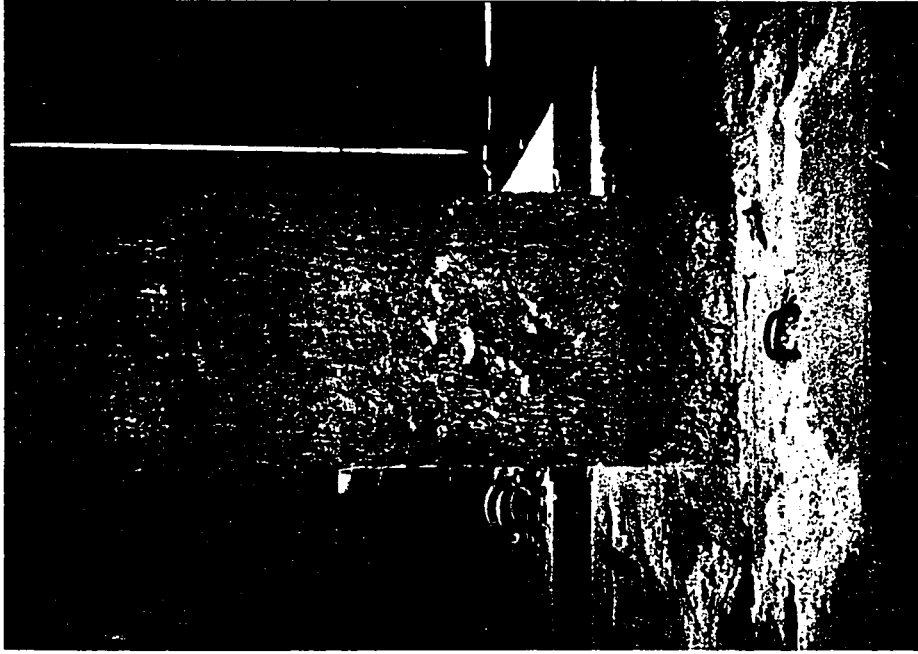


(b) Column FC12 during the test

Figure 4.27 Strengthened Flexural Column FC12

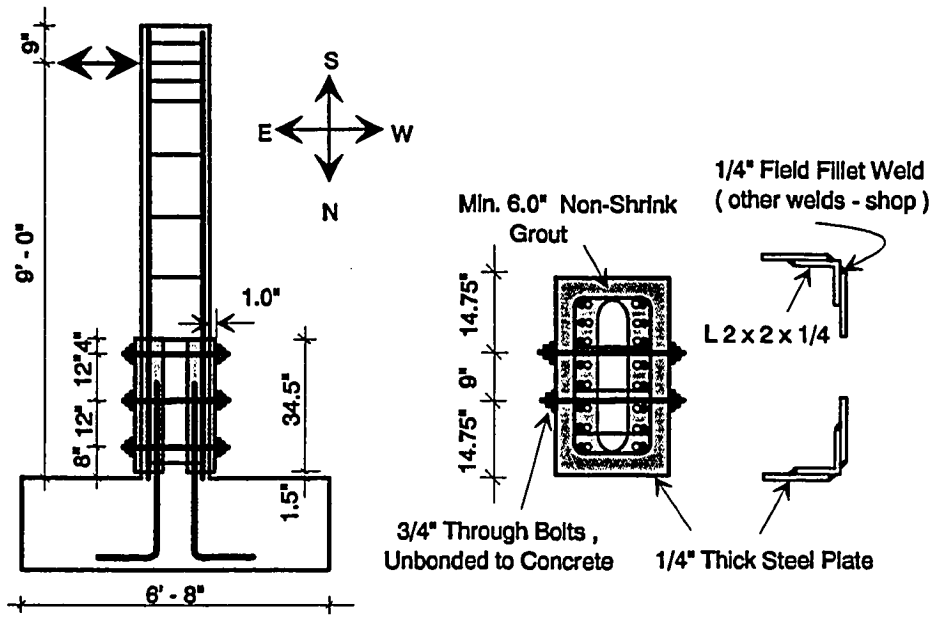


(a) Crack pattern at splice, north side

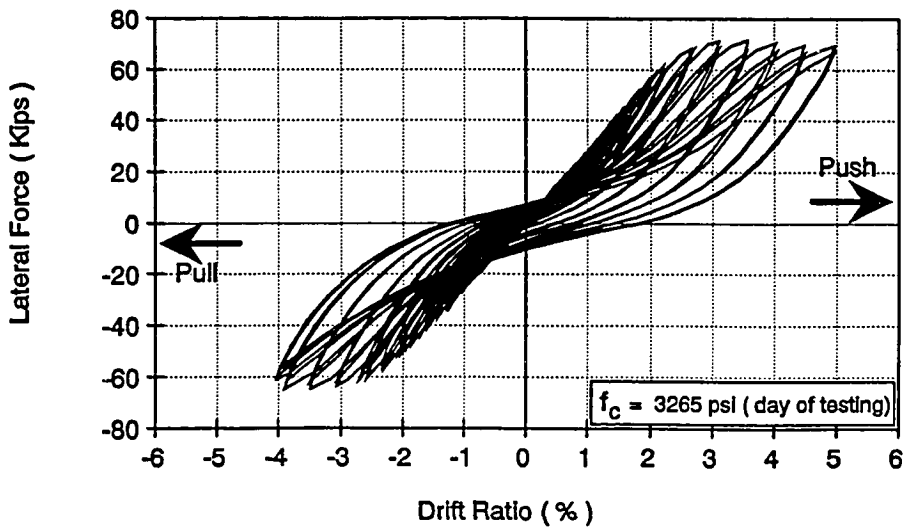


(b) Crack pattern at splice, south side

Figure 4.28 Strengthened Flexural Column FC12



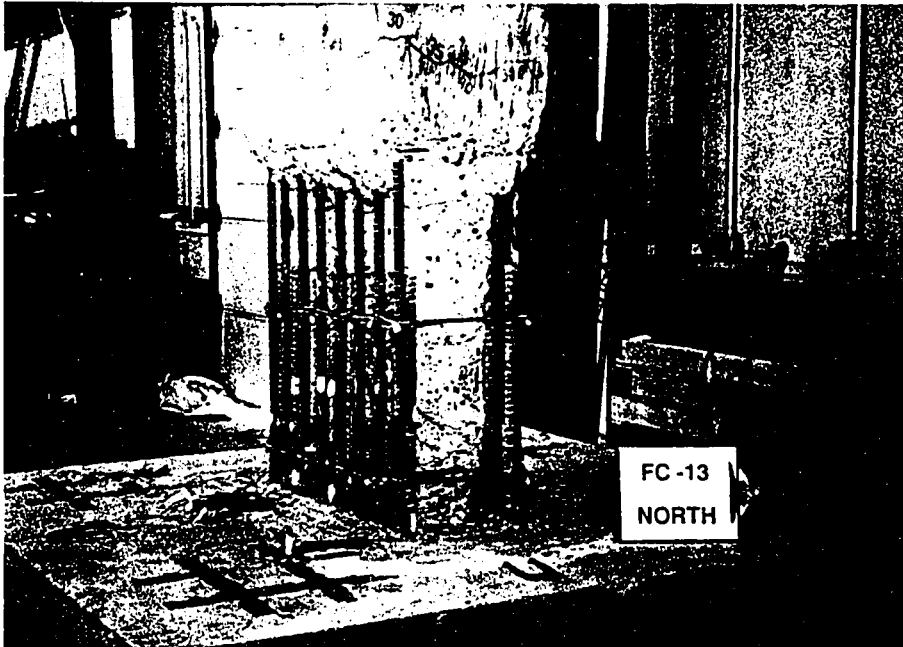
(a) Details of Column FC13



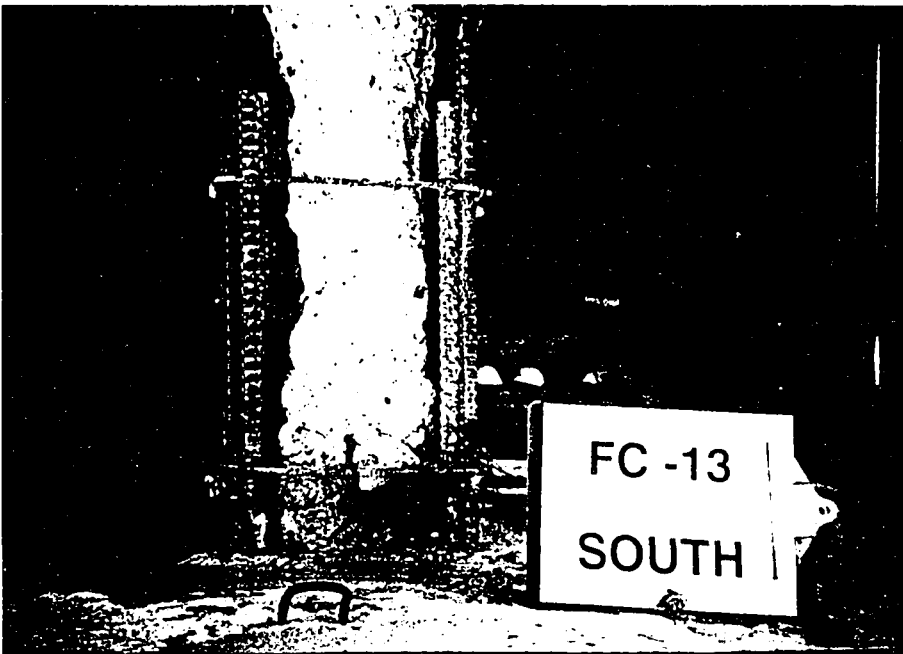
(b) Hysteretic Response

Figure 4.29 Repaired Flexural Column FC13



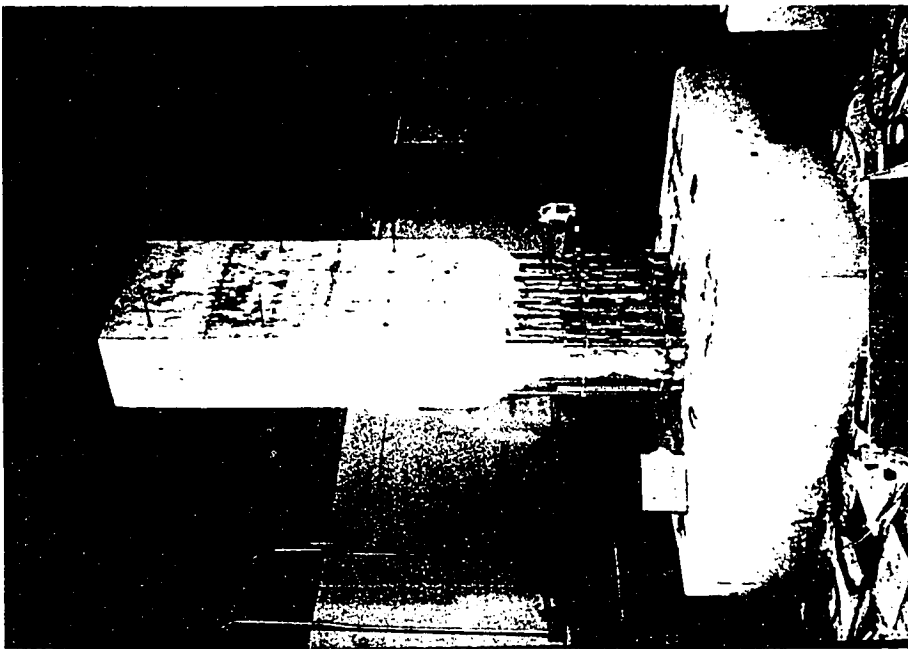


(a) Splice region after the removal of loose concrete

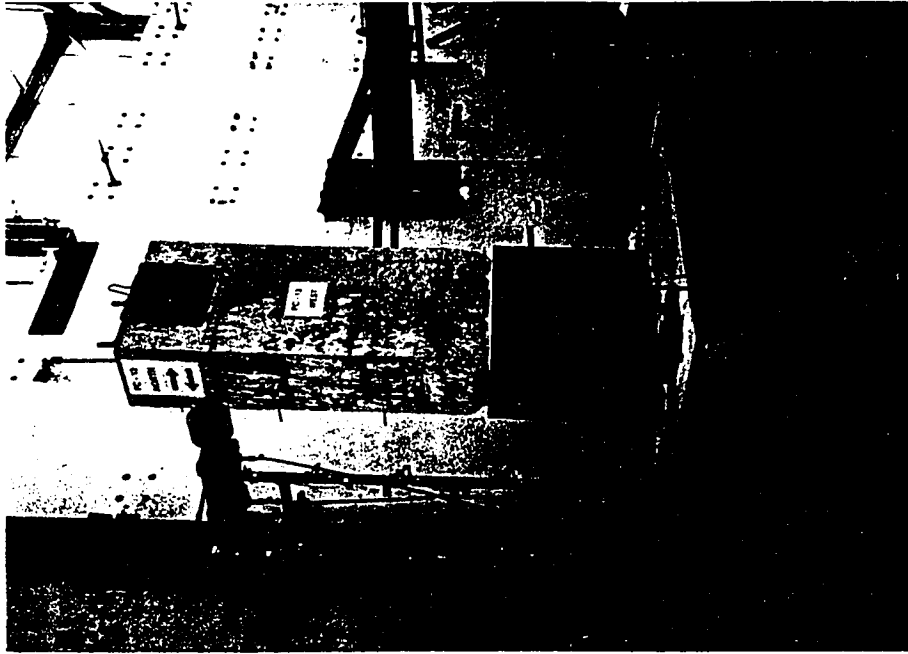


(b) Splice region after chipping off behind starter splice bars

Figure 4.30 Repaired Flexural Column FC13

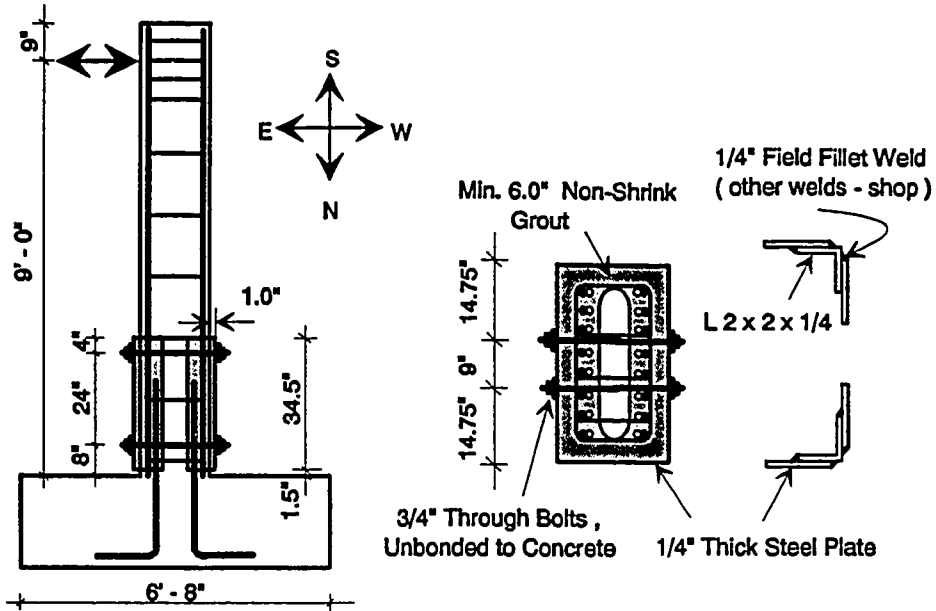


(a) Before the installation of the steel jacket

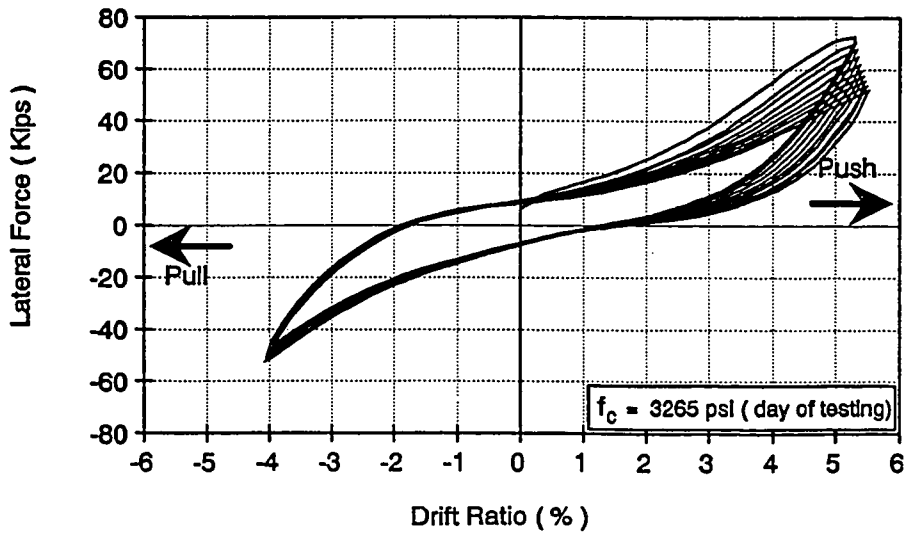


(b) Column FC13 under the test setup

Figure 4.31 Repaired Flexural Column FC13

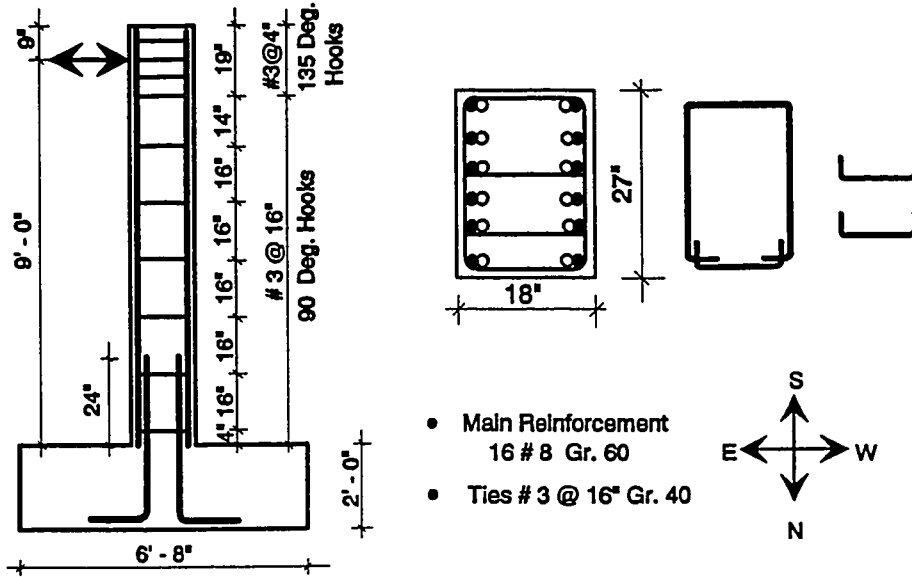


(a) Details of Column FC13A

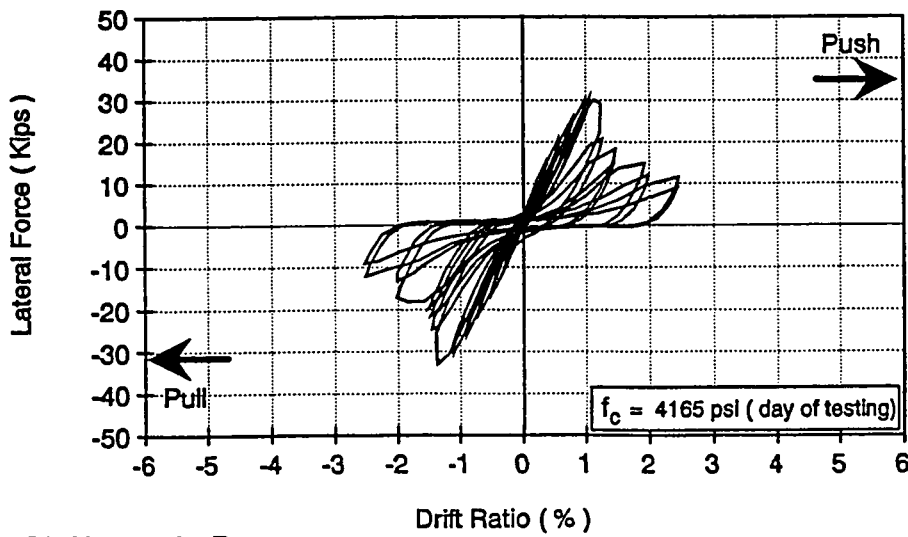


(b) Hysteretic Response

Figure 4.32 Repaired Column Flexural FC13A

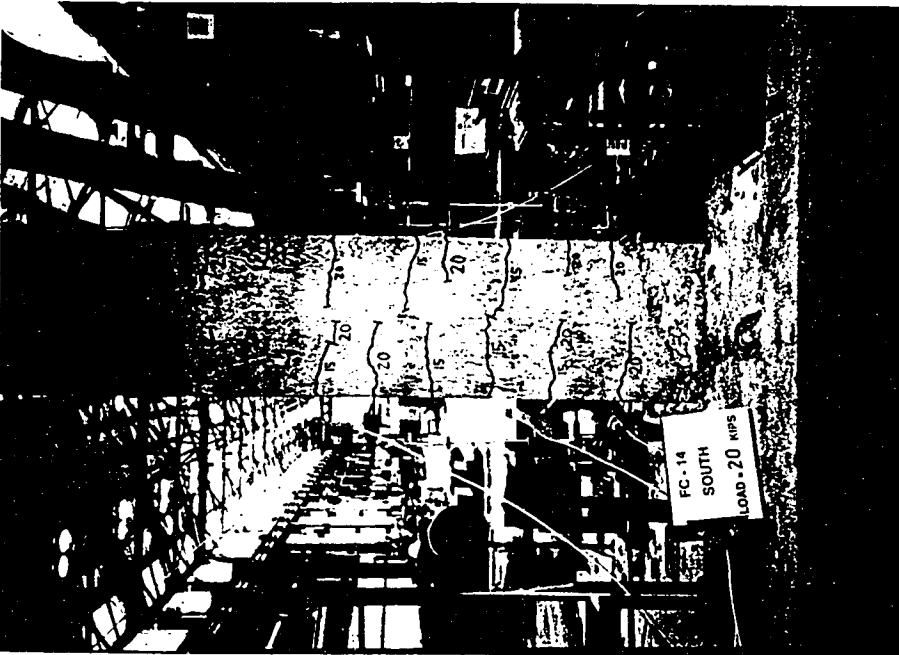


(a) Details of Column FC14

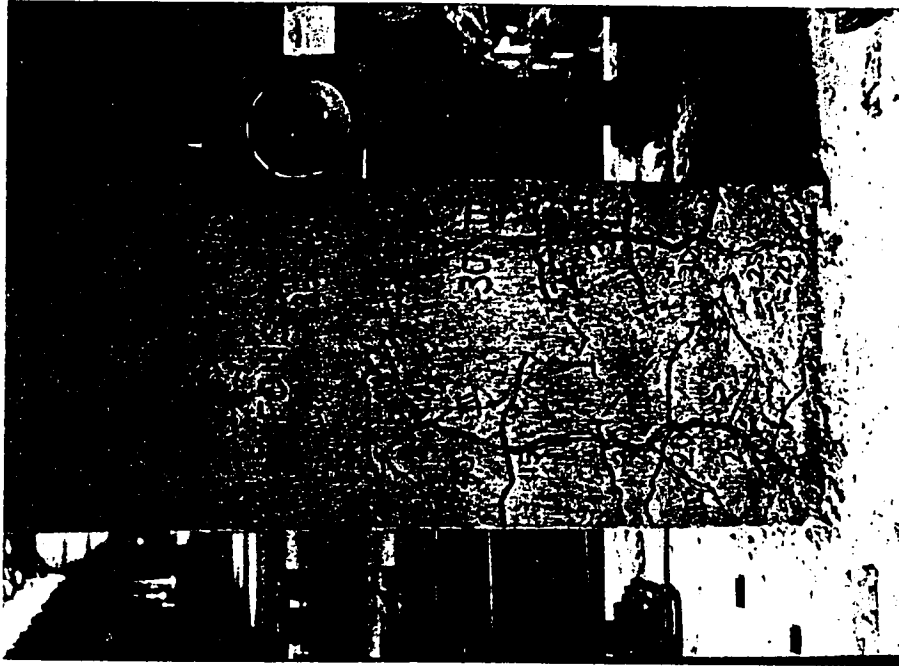


(b) Hysteretic Response

Figure 4.33 Basic Unretrofitted Flexural Column FC14

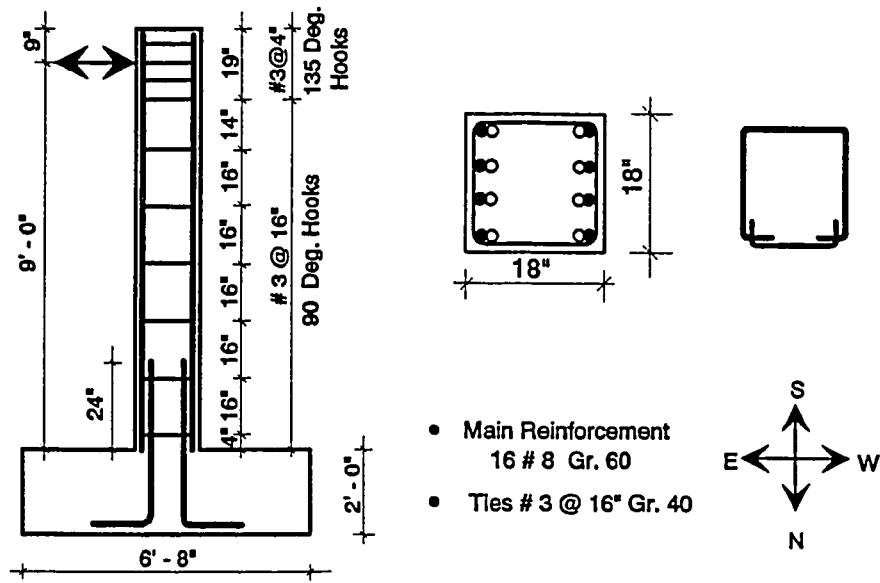


(a) During the push cycle to 20 kips

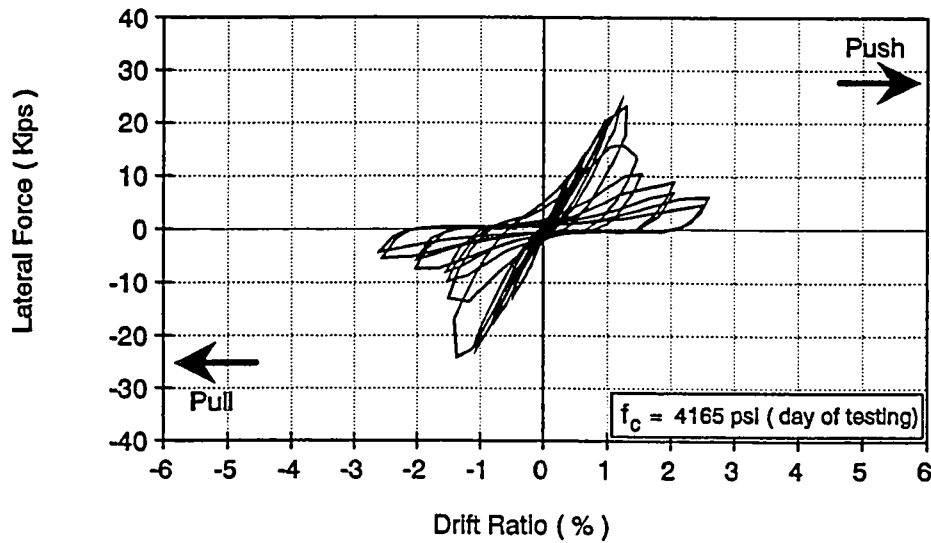


(b) Crack pattern at splice, south side

Figure 4.34 Basic Flexural Column FC14

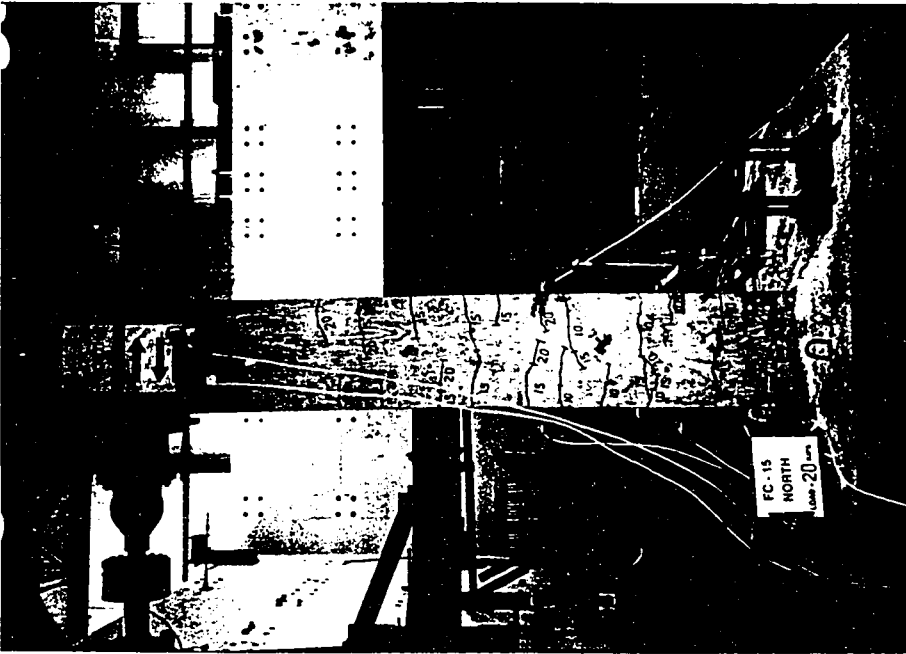


(a) Details of Column FC15

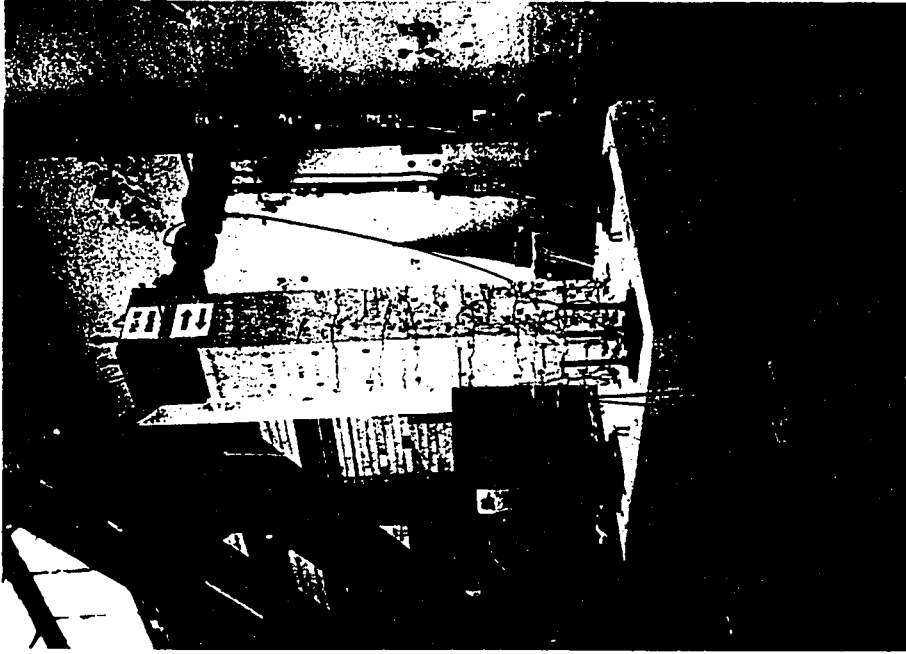


(b) Hysteretic Response

Figure 4.35 Basic Unretrofitted Flexural Column FC15

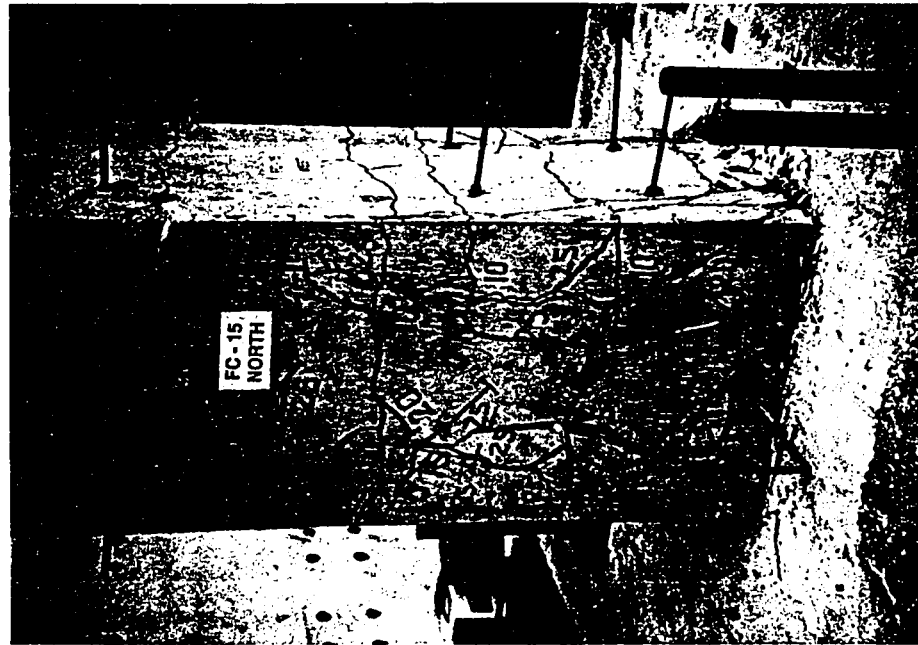


(a) During the cycle to 20 kips

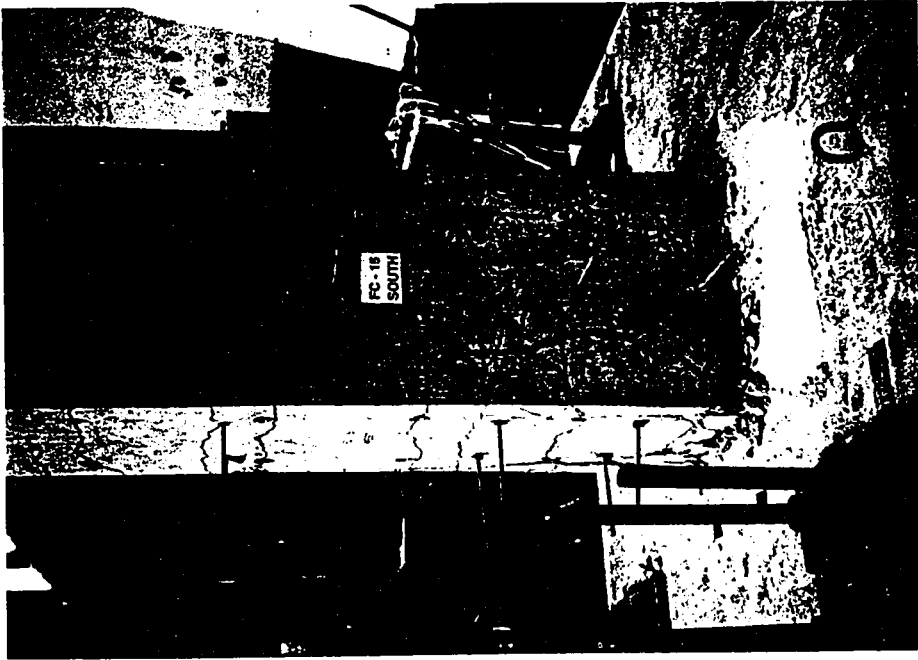


(b) Column FC-15 at the end of the test

Figure 4.36 Basic Flexural Column FC15



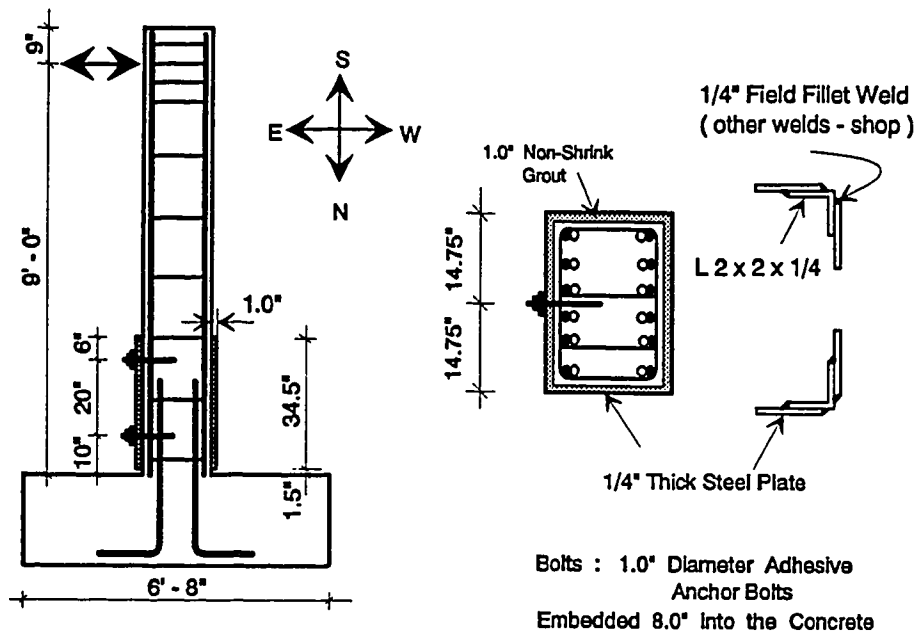
(a) Crack pattern at splice, N-W side



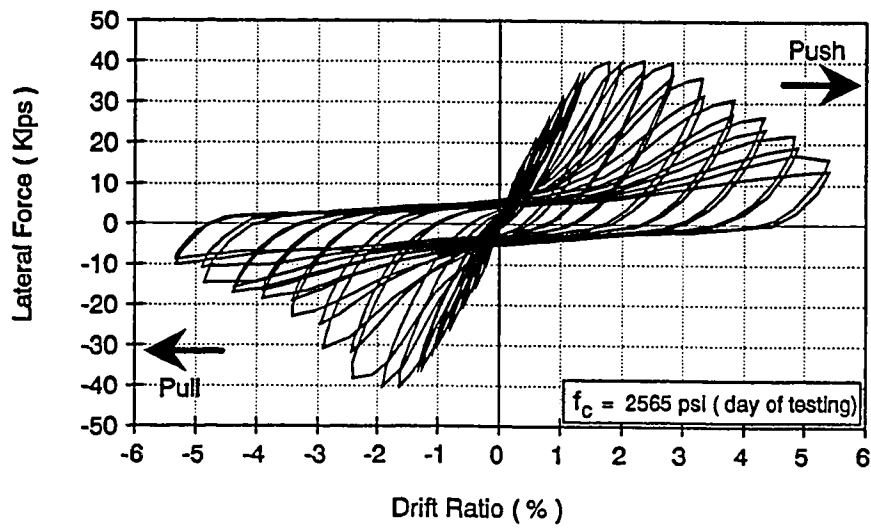
(b) Crack pattern at splice, S-W side

Figure 4.37 Basic Flexural Column FC15



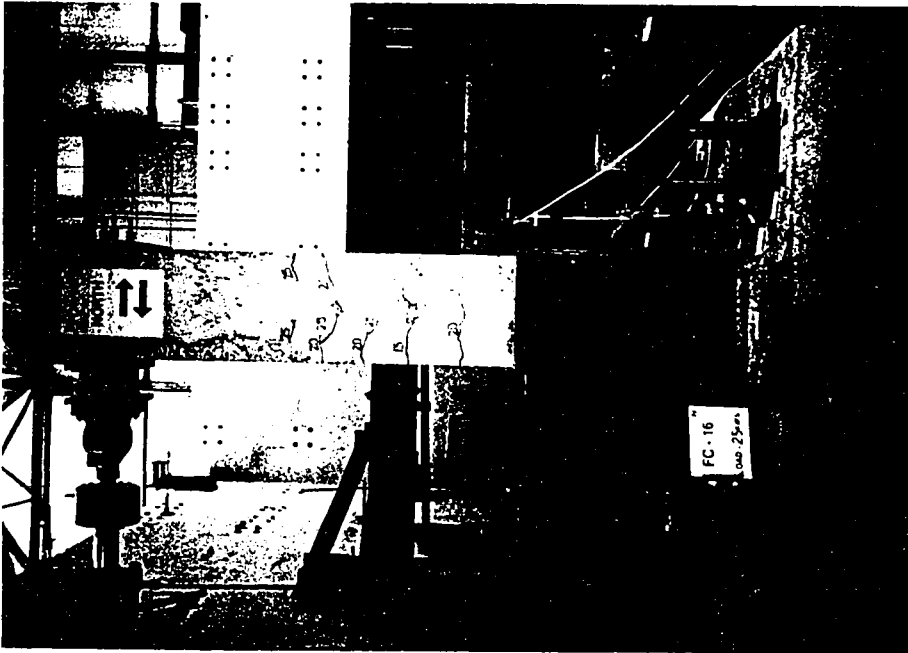


(a) Details of Column FC16

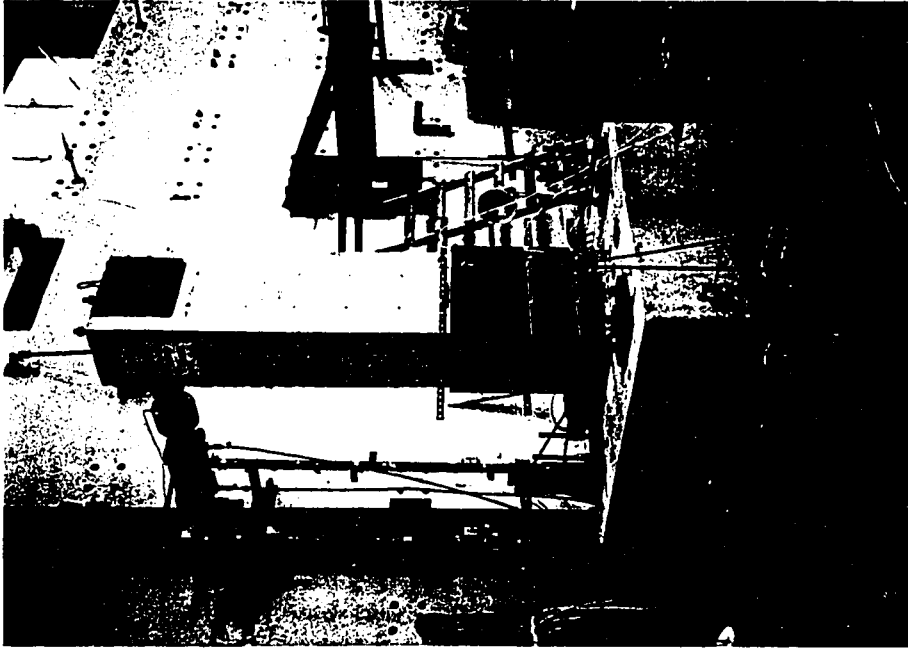


(b) Hysteretic Response

Figure 4.38 Strengthened Flexural Column FC16

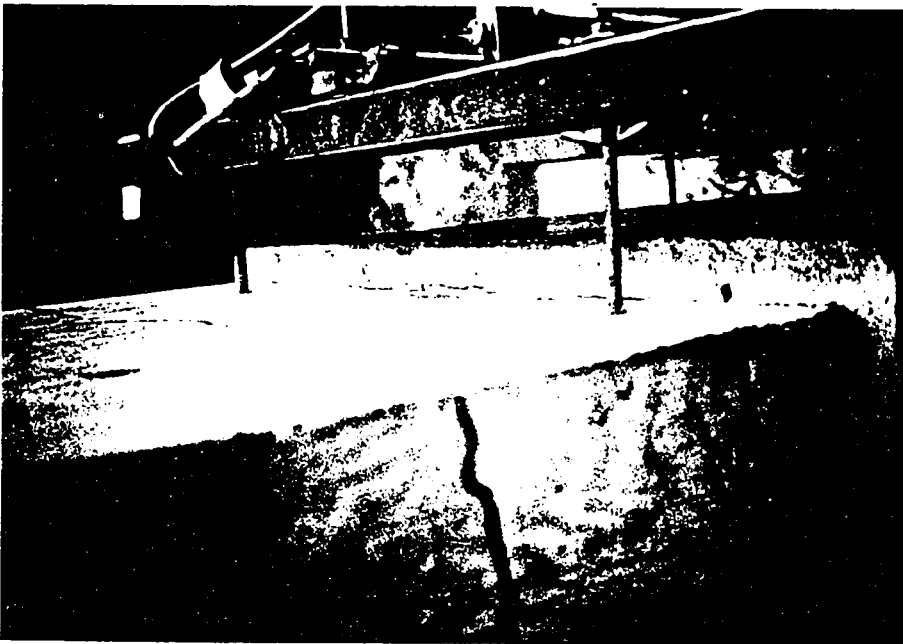


(a) During the cycle to 25 kips

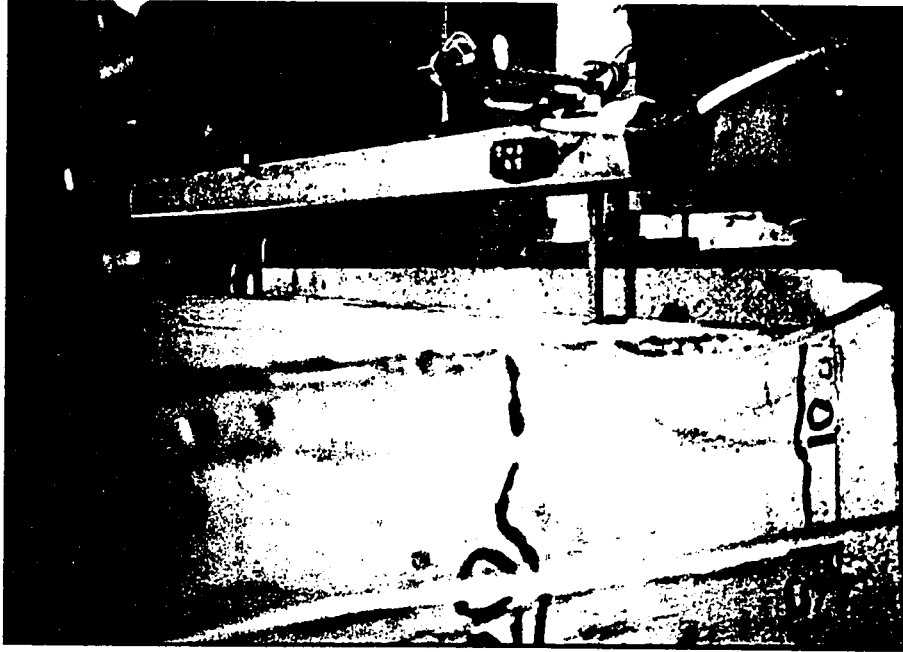


(b) Column FC16 during the test

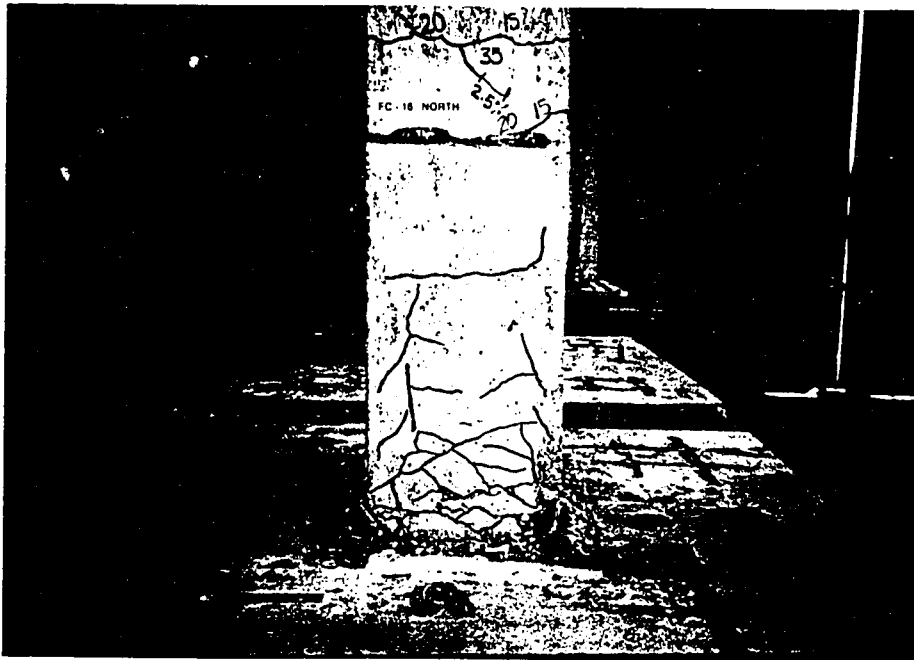
Figure 4.39 Strengthened Flexural Column FC16



(a) West side without anchor bolts



(b) East side with anchor bolts

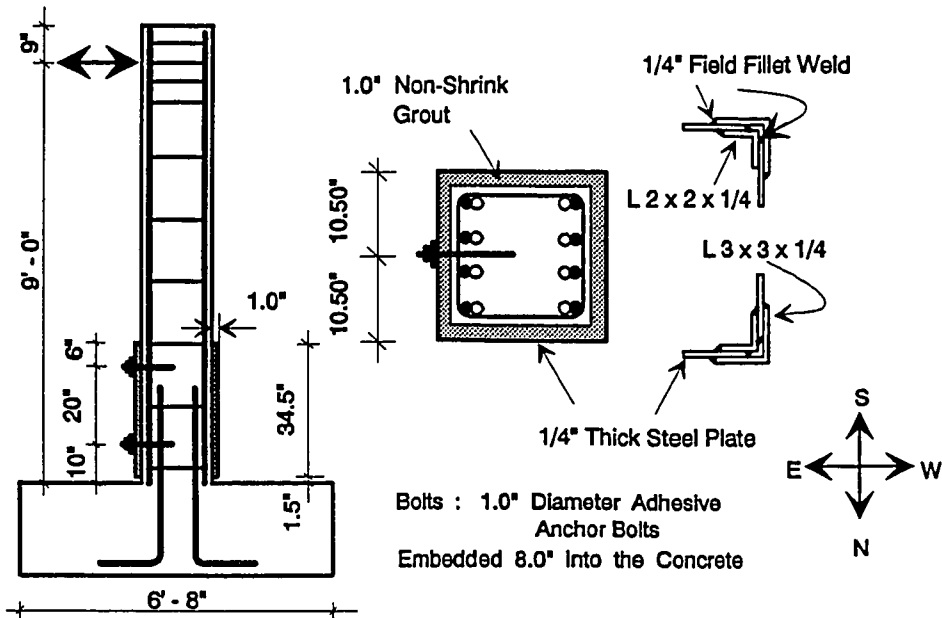


(a) Crack pattern at the splice, north side

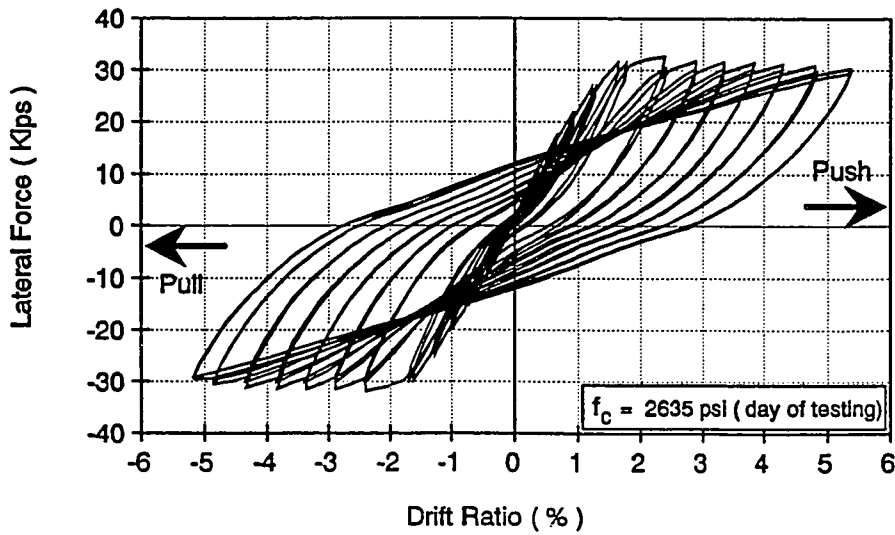


(b) Crack pattern at the splice, S-E side

Figure 4.41 Strengthened Flexural Column FC16

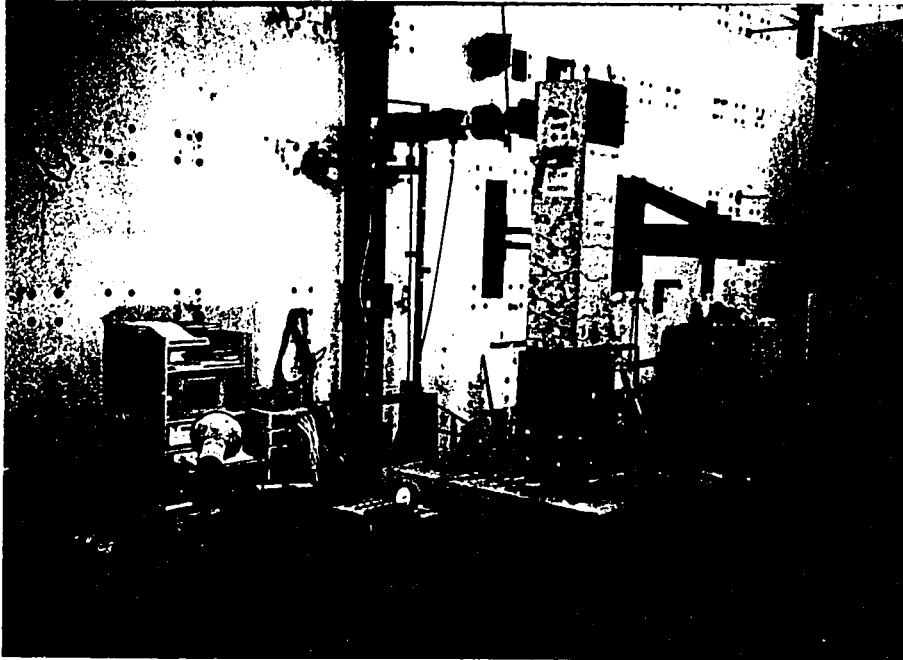


(a) Details of Column FC17



(b) Hysteretic Response

Figure 4.42 Strengthened Flexural Column FC17

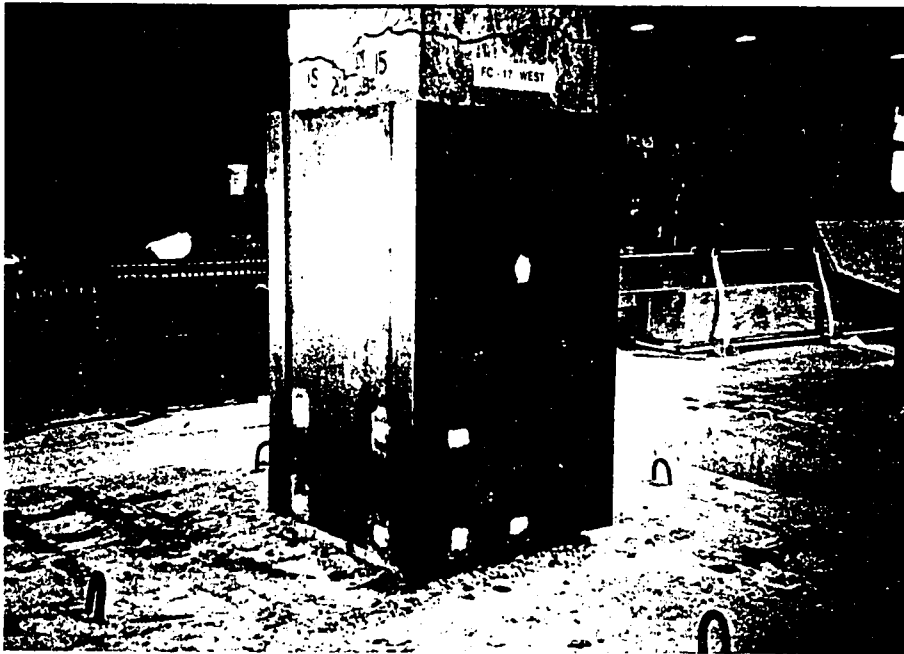


(a) Column FC17 in the test setup



(b) Corner view of the steel jacket

Figure 4.43 Strengthened Flexural Column FC17



(a) Before the removal of the steel jacket, N-W side



(b) After the removal of the steel jacket, S-W side

Figure 4.44 Strengthened Flexural Column FC17, Splice region

## **CHAPTER 5**

### **EXPERIMENTAL PROGRAM - SHEAR COLUMNS ( With Inadequate Shear Strength )**

#### **5.1 INTRODUCTION**

This chapter presents the overall performance of the shear columns (with inadequate shear strength). The response of each shear column during the test is presented and discussed. The details of the columns are shown without the footing reinforcement for clarity.

A total of eleven shear columns were tested in this phase. Results of the column tests are presented in series in the order in which they were tested. For clarity they are designated as follows :

1. Basic Unretrofitted Column ( BASIC-UR );
2. Pre-Earthquake Strengthened Column ( PRE-EQ-S )

All shear columns were 36"x18" in cross section. Columns SC1 through SC8 were tested in the weak direction. Columns SC9, SC10 and SC11 were tested in the strong direction. Shear columns were loaded under reversed cyclic lateral load. No axial load was applied to any of the columns. The influence of the axial load is discussed in detail in chapter 7. The main variables studied in the shear column tests are :-



1. Direction of loading: weak/strong;
2. Different Shear span / depth ratios;
3. Different types of steel jackets;
4. Partial steel jackets.

Chapter 7 presents complete discussion and comparison of the shear columns, along with additional experimental data which include measured strains on the longitudinal bars and on the steel jackets, as well as measured rotations. Sections 5.2 through 5.12 present the performance of columns SC1 through SC11 during testing, respectively.

## 5.2 SHEAR COLUMN SC1 ( BASIC-UR )

Column SC1 is a basic unretrofitted type "B" shear column. It was loaded in the weak direction. Column SC1 was transversely reinforced with #3 deformed bars at every 16 inches. A cross tie was provided at every longitudinal bar. Figure 5.1(a) shows the details of column SC1. The shear span to depth ratio is 2.67. The target and actual concrete compressive strength were 3000 psi and 5040 psi.

During the test the first two flexural cracks formed at a load of 40 kips. They were located at eleven inches above the top of the footing. As the load was increased to 50 kips, several new flexural cracks developed over the bottom 2/3 of the column height. Flexural cracks extended diagonally during the cycles to 80 kips ( which corresponds to  $2 \sqrt{f_c} bd$ ). During the 120 kip ( $3 \sqrt{f_c} bd$ ) cycles the main longitudinal and the transverse reinforcement yielded. At the 120 kip load, major shear cracks formed over the full height of the column.

Inelastic deformations were first observed at a load of 130 kips ( $3.25 \sqrt{f_c} bd$ ). After the two cycles to 130 kips, the displacement was increased in 0.5% drift ratio increments. At 2.25% drift ratio, the major diagonal cracks opened widely. At displacements larger than 2.25% drift ratio, the column showed considerable strength and stiffness degradation. During the second cycle to 2.25% drift ratio, the column showed more than 35% loss in strength. Figure 5.1(b) shows the hysteretic response of column SC1. The performance of column SC1 was satisfactory. It maintained its peak load to 2.2% drift ratio. Concrete compressive strength higher than the target compressive strength is attributed to the development of the flexural capacity before the development of the shear capacity. Figure 5.2 shows column SC1 before the test.

Section 5.4 presents the details and response of a similar shear column (Column SC3), but transversely reinforced with a cross tie at every other bar and much lower concrete compressive strength. Column SC3 serves as the basic reference column for the strengthened type "A" shear columns loaded in the weak direction. Column SC1 serves as a basic unretrofitted column for the strengthened column SC2.

### 5.3 SHEAR COLUMN SC2 ( PRE-EQ-S )

Column SC2 is a strengthened type "B" shear column. It was strengthened by the use of two steel collars. Figure 5.3(a) shows the details of column SC2. The steel collars were installed at mid-distance between the layers of the transverse reinforcement.

The first flexural cracks were observed at the column/footing interface, at a load of 30 kips. As the load was increased to 40 kips, four flexural cracks formed above and below the bottom collar. Also, cracks were observed between the concrete column and the non-shrink grout at a load of 40 kips. Several new flexural cracks developed during the cycles to 70 kips. Flexural cracks extended diagonally as the load was increased to 80 kips ( $2 \sqrt{f_c} bd$ ), reflecting the influence of shear. As the load was increased to 100 kips ( $2.5 \sqrt{f_c} bd$ ), major diagonal cracks formed between the collars. These diagonal cracks caused severe damage in the bottom 16 inches of the column. Increased loading to 130 kips ( $3.25 \sqrt{f_c} bd$ ) caused the formation of major diagonal cracks crossing the collars. The cracks above and below the collars were lined up, which indicated that the cracks formed even behind the collars. The first yielding of the longitudinal bars was observed during the cycle to 120 kips ( $3 \sqrt{f_c} bd$ ). However, the yielding of the transverse reinforcement was observed at a load of 130 kips. During the 130 kip cycles the column showed some inelastic deformations. Increased loading to 2.5% drift ratio caused major distress of the compression zones at the base of the column and permanent bending deformations on the long side of the steel collars. Also at 2.5% drift ratio, major diagonal cracks extended over the full height of the column.

Figure 5.3(b) shows the hysteretic response of column SC2. After the 3.25% drift ratio cycles, the column showed considerable strength and stiffness degradation, as well as major physical degradation over the bottom 16 inches of the column. Figure 5.4 shows column SC2 after the test. The performance of

column SC2 was better than that of column SC1. It showed a more stable hysteretic response and larger energy dissipation, but it cannot be considered a significant improvement over the response of column SC1.

#### 5.4 SHEAR COLUMN SC3 ( BASIC-UR )

Column SC3 is a basic unretrofitted type "A" shear column. It was transversely reinforced with a cross tie at every other longitudinal bar. Figure 5.5(a) shows the details of column SC3. The concrete strength of column SC3, at the day of testing, was 3170 psi.

The first flexural cracks formed at the column/footing interface, at a load of 20 kips. As the load was increased to 30 kips, flexural cracks formed on the column. Increased loading to 40 kips ( $1.25 \sqrt{f_c} bd$ ) caused the development of several flexural cracks over the bottom half of the column. The column showed almost pure flexural cracks up to a load of 60 kips ( $1.9 \sqrt{f_c} bd$ ). During the cycle to 70 kips ( $2.2 \sqrt{f_c} bd$ ), most of the flexural cracks extended diagonally, reflecting the influence of shear. Figure 5.6 shows the crack pattern at 60 and 70 kips lateral loads.

Increased loading to 80 kips ( $2.53 \sqrt{f_c} bd$ ) caused the development of major diagonal shear cracks over 70% of the column height. During the 90 kip ( $2.8 \sqrt{f_c} bd$ ) cycle the major diagonal shear cracks extended over the full height of the column. The major cracks penetrated the concrete compression zones at

the base of the column, reducing the depth of the compression zone to the thickness of the concrete cover. Also, the cross ties yielded as the load was increased to 90 kips. Figure 5.7 shows the crack pattern at 80 and 90 kips lateral loads.

During the cycles to loads above 90 kips the column showed large inelastic deformations. Column SC3 showed dramatic loss in strength and stiffness at displacements larger than 2.0% drift ratio. Also at the same load, the major diagonal cracks opened very widely. This was accompanied by physical degradation of the concrete compression zones. Afterwards, the column lost its lateral strength due to major diagonal shear failure mechanism followed by concrete compression shear failure. Figure 5.8 shows the crack pattern at 2.0% and 2.5% drift ratios. Column SC3 did not develop its flexural capacity, and the strains in the longitudinal bars did not exceed  $\frac{3}{4}$  the yielding strains. Figure 5.5(b) shows the hysteretic response of column SC3. Column SC3 showed some ductility, but it was not flexural ductility that is usually seen after the development of the flexural yielding strength. The ductility exhibited by column SC3 was due to the yielding of the transverse reinforcement crossing the major diagonal crack. Column SC3 serves as a basic unretrofitted reference shear column for all retrofitted type "A" shear columns loaded in the weak direction.

## **5.5 SHEAR COLUMN SC4 ( BASIC-UR )**

Column SC4 is a basic unretrofitted type "B" shear column. It was transversely reinforced with a cross tie at every longitudinal bar. Figure 5.9(a) shows the details of column SC4.

The first flexural cracks were observed at the column/footing interface, at a load of 20 kips. As the load was increased to 40 kips, several new flexural cracks developed on the column. All cracks were flexural cracks until the end of the 60 kip ( $1.9 \sqrt{f_c} bd$ ) cycles. During the cycles to 70 kips ( $2.2 \sqrt{f_c} bd$ ), flexural cracks extended diagonally, reflecting the influence of shear. At a load of 80 kips ( $2.53 \sqrt{f_c} bd$ ), the flexural shear cracks extended deeper into the concrete cross section, reducing the depth of the concrete compression zones. Figure 5.10 shows the crack pattern during the 70 and 80 kip cycles.

Increased loading to 90 kips ( $2.8 \sqrt{f_c} bd$ ) caused the development of major shear cracks over the middle 60 % of the column height. These cracks crossed the middle layer of the transverse reinforcement, but did not cause the yielding of the ties until the load was increased to 110 kips ( $3.47 \sqrt{f_c} bd$ ). Afterwards, the major diagonal cracks extended over the full height of the column. The longitudinal reinforcement yielded during the cycles to 120 kips ( $3.8 \sqrt{f_c} bd$ ). During the cycle to 130 kips ( $4.1 \sqrt{f_c} bd$ ) the column showed large inelastic deformations. A maximum load of only 124 kips was reached at 1.75% drift ratio. Figure 5.11 shows the crack pattern during the 90 kips and 2.0% drift ratio cycles. At displacements higher than 2.0% drift ratio, the column showed considerable loss in strength and stiffness. Figure 5.9(b) shows the hysteretic response of column SC4.

Compared to the shear column SC3, column SC4 showed higher lateral strength and a lower rate of stiffness degradation. This is attributed to a higher

amount of transverse reinforcement in column SC4. Thus, column SC3 was used as a basic unretrofitted reference shear column for all the remaining strengthened shear columns loaded in the weak direction.

## 5.6 SHEAR COLUMN SC5 ( PRE-EQ-S )

Column SC5 is a strengthened type "A" shear column. It was strengthened with three steel collars. The collars were spaced at 13.0 inches along the height of the column. The first bottom collar was located at 7.0 inches from the top of the footing. Figure 5.12(a) shows the details of column SC5. This system offers the advantage of eliminating field welding.

The first two flexural cracks formed at the column/footing interface, at a load of 30 kips. As the load was increased to 50 kips ( $1.9 \sqrt{f_c} bd$ ), four flexural cracks developed between the collars. These flexural cracks extended diagonally during the cycles to 70 kips ( $2.63 \sqrt{f_c} bd$ ). Figure 5.13 shows column SC5 during the 80 kip ( $3 \sqrt{f_c} bd$ ) cycles. Increased loading to 90 kips ( $3.38 \sqrt{f_c} bd$ ) caused the formation of major diagonal cracks between the collars. These cracks extended over the full height of the column during the 100 kip ( $3.76 \sqrt{f_c} bd$ ) cycles. The inelastic deformations were observed during the 110 kip cycles. Figure 5.14 shows the crack pattern at the 100 kip and 110 kip ( $4.13 \sqrt{f_c} bd$ ) cycles.

A maximum observed strength of 120 kips ( $4.5 \sqrt{f_c} bd$ ) was reached as the column approached 2.0% drift ratio. Figure 5.12(b) shows the hysteretic response of column SC5. Afterwards, column SC5 showed loss of strength and stiffness with increasing displacements. Physical degradation was evident at displacements above 3.0% drift ratio. Also, the steel collar at 7 inches elevation showed inelastic deformation beyond 3.0% drift ratio. Although the column developed its flexural yielding capacity, it did not show high ductility. In general, the performance of column SC5 was not considered satisfactory, Although its performance was significantly improved compared to the reference column SC3.

It is believed that the performance of column SC5 might have been improved by providing the steel collars with intermediate bolts, passing through the column. The use of such bolts, however, adds to the cost of the jacketing system. Consequently, a bolted solid steel jacket was examined instead, as presented in section 5.8.

## **5.7 SHEAR COLUMN SC6 ( PRE-EQ-S )**

Column SC6 is a strengthened type "A" shear column.. It was strengthened with a welded solid steel jacket, made of 1/4 inch thick steel plates. Figure 5.15(a) shows the details of column SC6. The steel jacket was terminated one inch above the top of the footing to prevent any possible bearing against the footing. Such bearing might develop higher shear forces on the column associated with the development of higher flexural capacity and may damage the jacket. The details of fabrication and assembly of the steel jacket was presented in sections 3.2.3.1 and 3.2.4.1. It is important to mention here that



the concrete compressive strength of column SC6 is just 2/3 of that of the basic unretrofitted shear column SC3. The south side of the steel jacket was painted with whitewash to detect any possible localized yielding of the steel jacket. Figure 5.16(a) shows column SC6 under the test setup.

The first two flexural cracks formed at the column/footing interface, at a load of 20 kips. The initial response of the column was essentially elastic up to the 140 kip ( $5.24 \sqrt{f_c} bd$ ) cycles. However, the first observed crack above the steel jacket was at a load of 130 kips. Figure 5.15(b) shows the hysteretic response of column SC6. In the push direction, the column maintained the maximum strength up to 5.0% drift ratio. In the pull direction, however, the strength dropped down during the cycles beyond 4.0% drift ratio, apparently due to bond-shear failure at the top of the column. Although the column transverse reinforcement at the top of the column was symmetrical, bond-shear failure occurred on the west side only. The cross ties at the top of the column were slightly larger than required, they touched the longitudinal bars on the east side, but did not quite touch the longitudinal bars on the west side. Figure 5.17 shows the details of the transverse reinforcement at the top 17 inches of the column. Additional #3 grade 40 steel pins were added to all the remaining columns, SC7 through SC11, to avoid any possible bond-shear failure at the top of the column.

The corner longitudinal bars yielded during the cycle to 90 kips ( $3.37 \sqrt{f_c} bd$ ). However, the intermediate longitudinal bars yielded during the cycle to 130 kips. It appears that the corner bars are well confined by the corners of the steel jacket, they yielded at an earlier stage. The maximum measured strain

on the steel jacket was just below 300 micro-strains, approximately 1/6 of the actual yielding strain of the steel jacket.

The non-shrink grout remained in good condition during the test. The first crack between the grout and the concrete column was observed at the top of the steel jacket at a load of 60 kips ( $2.25 \sqrt{f_c} bd$ ). After the completion of the test the steel jacket was removed and the concrete column was inspected. Investigation of the concrete column revealed the following:-

1. Major bond failure between the main longitudinal bars and the surrounding concrete over the bottom 2/3 of the column height.
2. Severe deterioration of the concrete compression zones. However, these zones maintained integrity since they were well confined between the column concrete core on one side and the grout and the steel jacket on the other side. Figure 5.16(b) shows a closeup of the concrete compression zone on the west side.
3. Steep diagonal shear cracks were observed on the north and south sides. These cracks were narrow, and did not open up because they were restrained by the steel jacket, during the test and the column was unloaded after the test. Figure 5.18 shows the crack pattern on the north and south sides of column SC6.

The overall response of column SC6 was excellent. The response showed stable hysteretic loops with much larger energy dissipation and displacement ductility than the basic column SC3. Although its concrete strength was just 2/3 of that of the basic column SC3, it showed almost twice the lateral strength and

was able to maintain it to large displacements.

The results of column SC6 indicate that a rectangular solid steel jacket was a very effective passive retrofitting system. It considerably improved the strength and ductility of columns with inadequate shear strength. However, the concrete column must deform and perhaps develop cracking in order the steel jacket to provide confinement.

#### **5.8 SHEAR COLUMN SC7 ( PRE-EQ-S )**

As presented in sections 3.2.3.1 and 3.2.4.1, the welded steel jacket was fabricated in two L-shaped panels in plan. After being assembled around the column, the two opposite free ends were welded together. However, welding might not be permitted at some existing facilities. The next section presents shear strengthening by the use of a bolted steel jacket, where the two opposite free ends of the L-panels are bolted instead of being welded.

Column SC7 is a strengthened type "A" shear column. It was retrofitted with a bolted steel jacket. Section 3.2.4.1 presents the details of the bolted steel jacket. The steel jacket was fabricated and assembled in a similar way as the welded steel jacket, but the opposite free ends of the two L-panels were bolted after they were assembled around the concrete column. Figure 5.19(a) shows the details of column SC7.

The first flexural cracks were observed at the column/footing interface, at a load of 40 kips. The column performance was essentially elastic up to a

load of 120 kips ( $3.93 \sqrt{f_c} bd$ ). During the cycle to 100 kips ( $3.28 \sqrt{f_c} bd$ ), the corner longitudinal bars yielded. The intermediate bars yielded during the cycle to 130 kips ( $4.26 \sqrt{f_c} bd$ ). Inelastic deformations were first observed at a load of 130 kips. Beyond the 130 kips cycles, the column showed minor stiffness degradation, but loss of strength. Figure 5.20 shows column SC7 before and during the test. The first crack above the steel jacket was observed during the cycle to 3.0% drift ratio. The crack was steep, which indicated the influence of shear. It is believed that the crack was an extension of a major shear crack developed earlier behind the steel jacket. The concrete compression zones showed minor distress during the same cycles to 3.0% drift ratio.

The test was continued up to 6.0% drift ratio. The cross ties showed strains higher than the actual yielding strain of the #3 bars. This strain level was reached at 6.0% drift ratio. At the same load, the maximum strain measured on the steel jacket was 700 micro strains, 40% of the actual yielding strain of the steel jacket. The grout maintained its integrity during the test. Just two fine cracks formed in the grout on the north and south sides, during the cycles to 90 kips ( $2.95 \sqrt{f_c} bd$ ).

After the completion of the test the steel jacket was dismantled and the concrete column was inspected. Figure 5.21 shows column SC7 after the test. Investigation of the concrete column revealed the presence of steep diagonal shear cracks. These cracks were concentrated between the layers of transverse reinforcement. No major diagonal shear crack was observed extending over the full height of the column. The concrete compression zones were severely

deteriorated. However, the column did not show any sign of strength deterioration. This is attributed to the confinement of the concrete compression zones by the column concrete core on one side and the grout and the steel jacket on the other side. Figure 5.19(b) shows the hysteretic response of column SC7. The performance of column SC7 was excellent. It exhibited very stable hysteretic loops, with very large displacement ductility and energy dissipation.

### 5.9 SHEAR COLUMN SC8 ( PRE-EQ-S )

Column SC8 is a strengthened type "A" shear column. It was strengthened by utilizing a partial steel jacket that confines only 2/3 of the column cross section. This is intended to represent a situation where a curtain/partition wall is framing into the outer 1/3 of the column cross section. The entire steel jacket was fabricated as a single U-shaped panel. Section 3.2.4.3 presents the details of U-shaped partial steel jackets. Figure 5.22(a) shows the details of column SC8. Five 3/4 inch through bolts were used across the concrete column at the free end of the steel jacket. Anchor bolts would likely be ineffective in this case, since they would behave as non-continuous ties.

The first flexural cracks were observed at the column/footing interface, at a load of 30 kips. During the cycle to 40 kips, the first two flexural cracks formed on the south unconfined side of the column. They were located at about 10 inches from the bottom of the column. These cracks extended deeper into the column cross section as the load was increased to 50 kips ( $1.68 \sqrt{f_c} bd$ ). New flexural cracks formed at approximately the mid-height of the column as the load was increased to 60 kips ( $2 \sqrt{f_c} bd$ ). During the cycle to 70 kips ( $2.36$

$\sqrt{f_c}$  bd), the flexural cracks extended diagonally forming flexural shear cracks.

Figure 5.23 shows column SC8 during the 80 kips ( $2.7 \sqrt{f_c}$  bd) and 3.5% drift ratio cycles. These cracks extended diagonally deeper into the concrete section, reducing the depth of the compression zone, as the load was increased to 80 kips. The diagonal cracks extended over the full height of the column during the cycles to 90 kips ( $3 \sqrt{f_c}$  bd). At the same load, the corner reinforcement bars at the north side yielded. However, the intermediate bars yielded at a load of 110 kips ( $3.7 \sqrt{f_c}$  bd). Increased loading to 2.5% drift ratio caused the diagonal cracks to open very widely. Until this load no cracks were observed on the north side .

The first crack formed on the confined north side was observed above the steel jacket during the cycle to 3.0% drift ratio. The crack was a diagonal shear crack, and it extended from behind the steel jacket towards the top of the column. Since the steel jacket confined 2/3 of the column section, the north and south sides showed quite different levels of physical damage. Figure 5.24 shows the north and the south sides of column SC8 after the test. Due to the lack of symmetry of the retrofitted column section, the column developed torsional shear stresses that caused severe physical damage on the south unconfined side of the column. During the 2.0% drift ratio cycles, the cross ties yielded. However, the strains measured on the steel jacket were well below yielding, in the range between 150 and 200 micro strains.

The actual physical degradation occurred at very large displacements,

which are not usually expected in buildings during earthquakes. Although column SC8 experienced severe physical damage on the south side, it maintained its peak lateral load to almost 7.0% drift ratio. Figure 5.22(b) shows the hysteretic response of column SC8. The response of column SC8 showed high energy dissipation and large ductility. Figure 5.25 shows column SC8 before and after the removal of the steel jacket by the end of the test. The influence of torsion is very evident from the crack pattern on the column. The difference in the level of damage on the north and the south sides is also evident.

#### 5.10 SHEAR COLUMN SC9 ( BASIC-UR )

Columns SC9, SC10 and SC11 were loaded in the strong direction. The shear span to depth ratio was 1.33. Column SC9 was a basic unretrofitted type "C" shear column. Figure 5.26(a) shows the details of column SC9. The peripheral tie was the only transverse reinforcement resisting shear forces.

The first crack was observed at the column/footing interface, at a load of 30 kips. As the load was increased to 40 kips, flexural cracks formed on the column. New flexural cracks developed during the 50 kip and the 60 kip ( $2\sqrt{f_c}$  bd) cycles. The flexural cracks extended diagonally as the load was increased to 70 kips ( $2.4\sqrt{f_c}$  bd). All the flexural-shear cracks extended during the cycles to 80 kips ( $2.74\sqrt{f_c}$  bd). Several diagonal shear cracks and flexural shear cracks formed over the full height of the column during the cycles to 90 kips ( $3.1\sqrt{f_c}$  bd) and 100 kips ( $3.4\sqrt{f_c}$  bd). Figure 5.27 shows column SC9

during the test. Increased loading to 110 kips ( $3.77 \sqrt{f_c} bd$ ) caused the development of major diagonal cracks over the height of the column. These diagonal cracks did not have any observable effect on the load displacement response of the column at that load. As the load was increased to 130 kips ( $4.45 \sqrt{f_c} bd$ ), the transverse reinforcement yielded. Also, several diagonal cracks penetrated the concrete compression zones at the bottom of the column. Increased loading beyond 130 kips caused concrete compression shear failure at the bottom of the column.

Figure 5.26(b) shows the hysteretic response of column SC9. Column SC9 showed a very dramatic loss of strength and stiffness during the cycles beyond 130 kips push and 140 kips ( $4.8 \sqrt{f_c} bd$ ) pull. The response of column SC9 showed very limited energy dissipation and displacement ductility. Figure 5.28 shows column SC9 before and at the end of the test.

### 5.11 SHEAR COLUMN SC10 ( PRE-EQ-S )

Column SC10 is a strengthened type "C" shear column. It was retrofitted with a welded solid steel jacket. Column SC10 was loaded in the strong direction. Figure 5.29(a) shows the details of column SC11.

The first two flexural cracks were observed at the column/footing interface, at a load of 50 kips. Increased loading to 110 kips ( $3.72 \sqrt{f_c} bd$ ) caused the development of major shear cracks behind the steel jacket. Portions



of the cracks could be seen on the column just above the top of the steel jacket. At a load of 100 kips ( $3.38 \sqrt{f_c} bd$ ) the main longitudinal bars yielded, immediately followed by the development of major diagonal shear cracks. New diagonal shear cracks formed just above the steel jacket at a load of 200 kips ( $6.76 \sqrt{f_c} bd$ ). Inelastic deformations were first observed during the cycles to 260 kips ( $8.8 \sqrt{f_c} bd$ ). Figure 5.29(b) shows the hysteretic response of column SC10.

In the pull direction the column was loaded to 3.0% drift ratio, the maximum stroke of the actuator in that direction. However, in the push direction the column was loaded until it developed its flexural capacity at 4.0% drift ratio. During the last cycle the column was loaded to the maximum stroke of the actuator in the push and pull directions. The flexural capacity was developed by fracturing one of the main longitudinal bars on the east side, close to the column/footing interface. At the peak load the strains in the transverse reinforcement reached 1500 micro strain, more than 75% of the actual yielding strain. At the same load the maximum measured strain on the steel jacket was 450 micro strain, 26% of the actual yielding strain of the steel jacket.

Figures 5.30 shows column SC10 during and after the test. After the completion of the test the steel jacket was removed and the column concrete surface was inspected. Investigation of the concrete column revealed severe damage of the concrete compression zones, bond failure between the main bars and the surrounding concrete over the bottom 2/3 of the column height, and steep diagonal shear cracks over the full height of the column. The shear cracks

were narrow since they were restrained by the steel jacket during the test and the column was unloaded after the test. The overall performance of column SC10 was excellent. Compared to the basic unretrofitted column SC9, it showed much higher strength, displacement ductility and energy dissipation.

### 5.12 SHEAR COLUMN SC11 ( PRE-EQ-S )

Column SC11 is a strengthened type "C" shear column. It was strengthened by the use of two C-shaped steel panels. Figure 5.31(a) shows the details of column SC11. The C-panels were attached to the concrete column by 1.0 inch diameter adhesive anchor bolts. Section 3.2.4.3 discusses the installation of partial steel jackets.

During the test, the first cracks formed at the column/footing interface, at a load of 40 kips. During the cycles to 100 kips ( $3.4 \sqrt{f_c} bd$ ), diagonal shear cracks formed just above the top of the steel jacket. These cracks did not affect the performance of the column at that load. The response of column SC11 was essentially elastic up to the 150 kip ( $5.1 \sqrt{f_c} bd$ ) cycles. Flexural cracks formed on the east and the west sides of column SC11 at a load of 150 kips. Also, at the same load, minor deterioration of the concrete surrounding the upper and lower anchor bolts was observed. Figure 5.31(b) shows the hysteretic response of column SC11. Increased loading to 160 kips ( $5.44 \sqrt{f_c} bd$ ) caused some inelastic deformations. Sudden anchorage failure at the anchor bolts was observed as the load was increased to 170 kips ( $5.78 \sqrt{f_c} bd$ ). Figure 5.32 shows

column SC11 at the end of the test. Splitting of the concrete surrounding the anchor bolts over the height of the column caused outward movement of the steel jacket. Consequently column SC11 lost most of its lateral capacity and stiffness since the steel jacket lost its lateral load carrying capacity after the bolt anchorage failure. The maximum measured strain on the steel jacket was about 225 micro-strains, during the cycle to 170 kips. At the same load the strains in the transverse reinforcement were well beyond the actual yielding strain.

Figure 5.33 shows column SC11 at the end of the test. After the test, the steel jacket was removed. Investigation of the concrete surface revealed the following:-

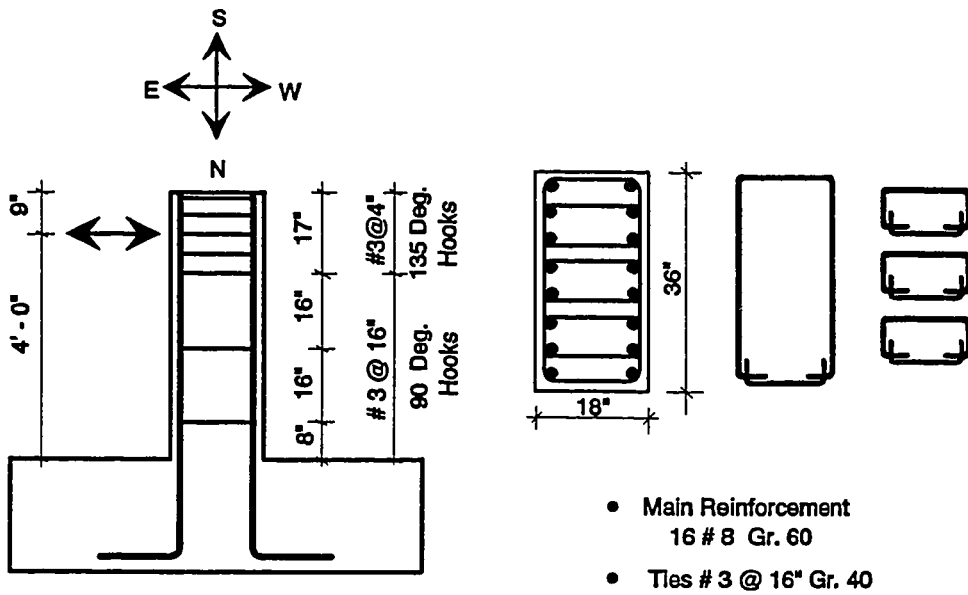
1. Vertical splitting cracks formed over the full height of the column in the vicinity of the anchor bolts.
2. On the east and west sides, the splitting cracks formed in the plane of the anchor bolts.
3. On the north and the south sides, the splitting cracks formed in planes passing through the ends of the anchor bolts.
4. Severe diagonal shear cracks formed over the height of the column.
5. The concrete compression zones were deteriorated.

The performance of column SC11 indicates that the use of partial steel jackets with anchor bolts did prevent sudden shear failure nor improve displacement ductility. It is believed that connecting the ends of the two C-panels to each other by the use of through bolts might have improved the performance of column SC11.

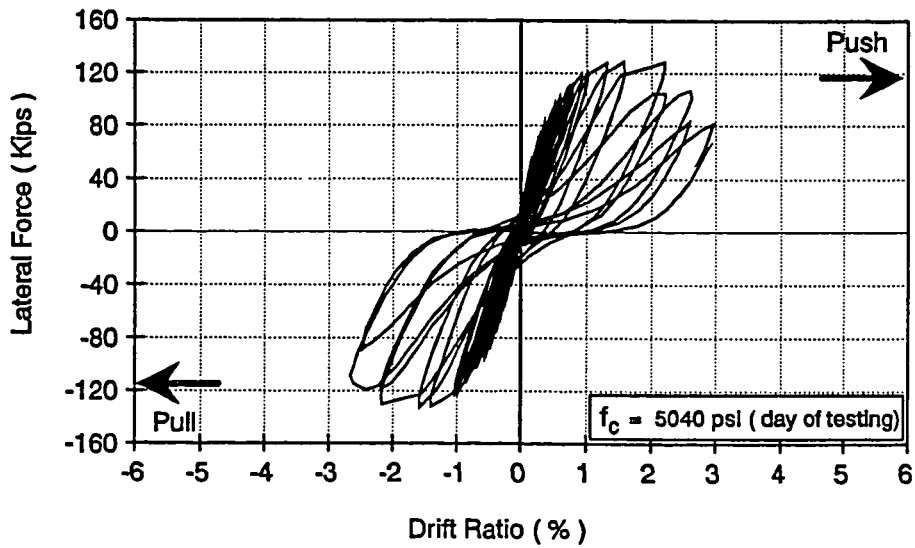
### 5.13 SUMMARY

The performance of eleven shear columns with inadequate shear strength was presented. The effectiveness of 1/4 inch thick rectangular steel jackets in seismic shear strengthening of reinforced concrete columns with inadequate shear strength was investigated. Retrofitted columns were loaded in the weak direction or in the strong direction. Partial steel jackets for strengthening columns with limited accessibility to all sides due to the presence of curtain/partition walls were also investigated.

The response of the basic unretrofitted columns showed dramatic shear failure. However, the performance of the columns retrofitted with solid steel jackets was excellent. They exhibited much higher strength, displacement ductility and energy dissipation than the unretrofitted columns. Chapter 7 presents detailed discussion and comparison of the experimental data for the various shear columns.



(a) Details of Column SC1

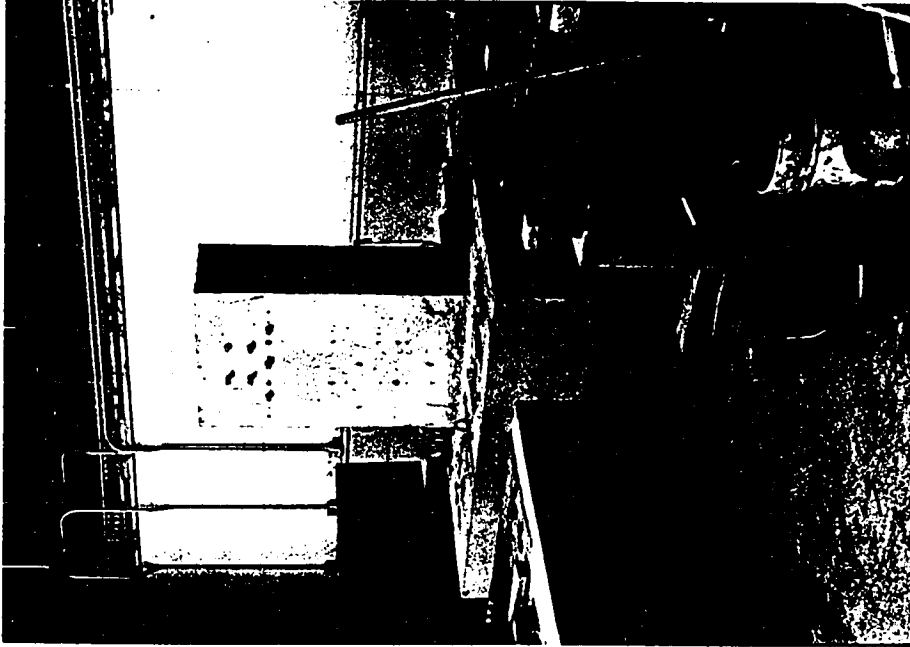


(b) Hysteretic Response

Figure 5.1 Basic Unretrofitted Shear Column SC1

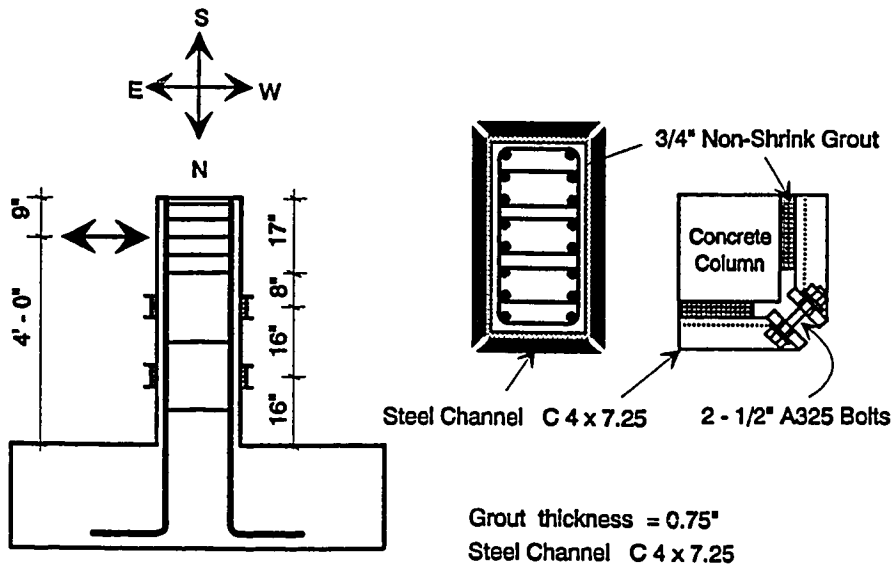


(a) Column Reinforcement

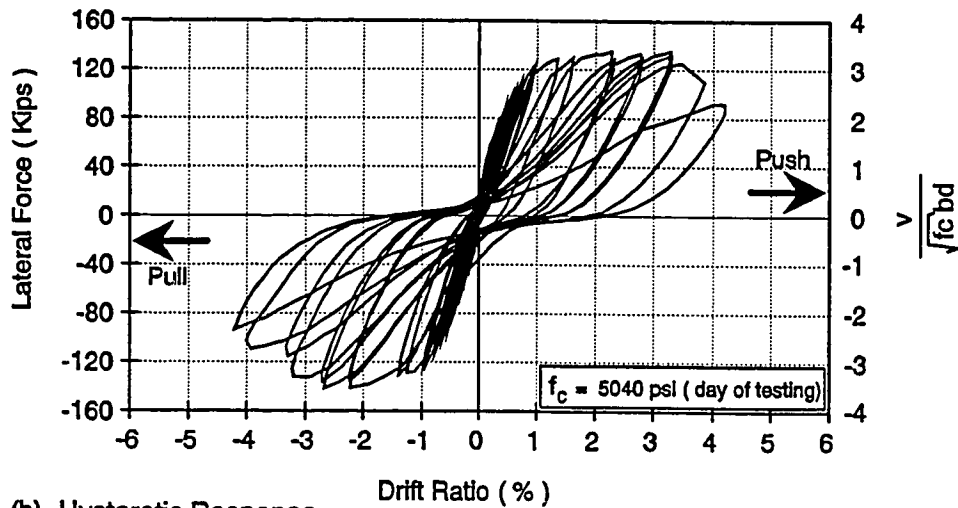


(b) After placing concrete

Figure 5.2 Basic Unretrofitted Shear Column SC1

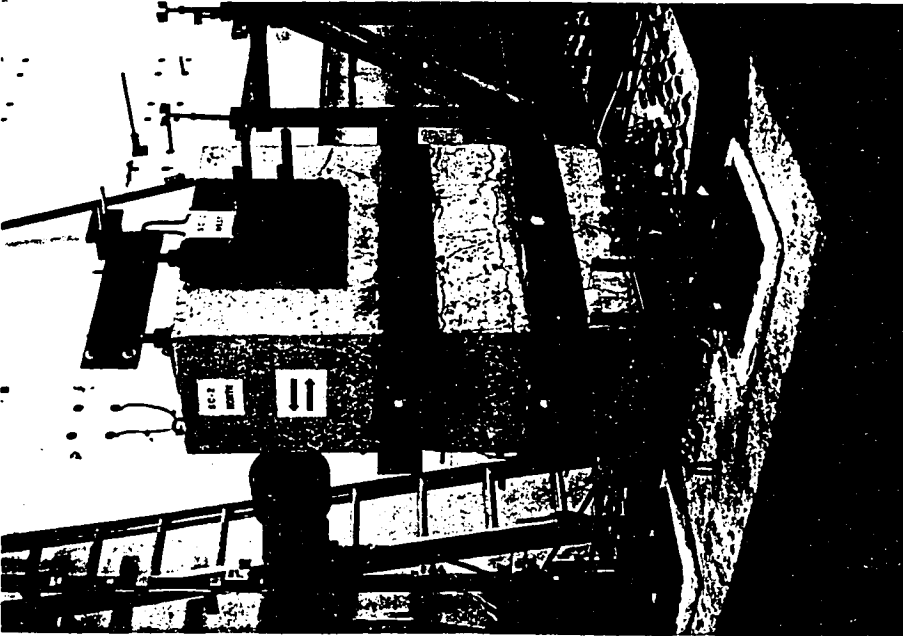


(a) Details of Column SC2

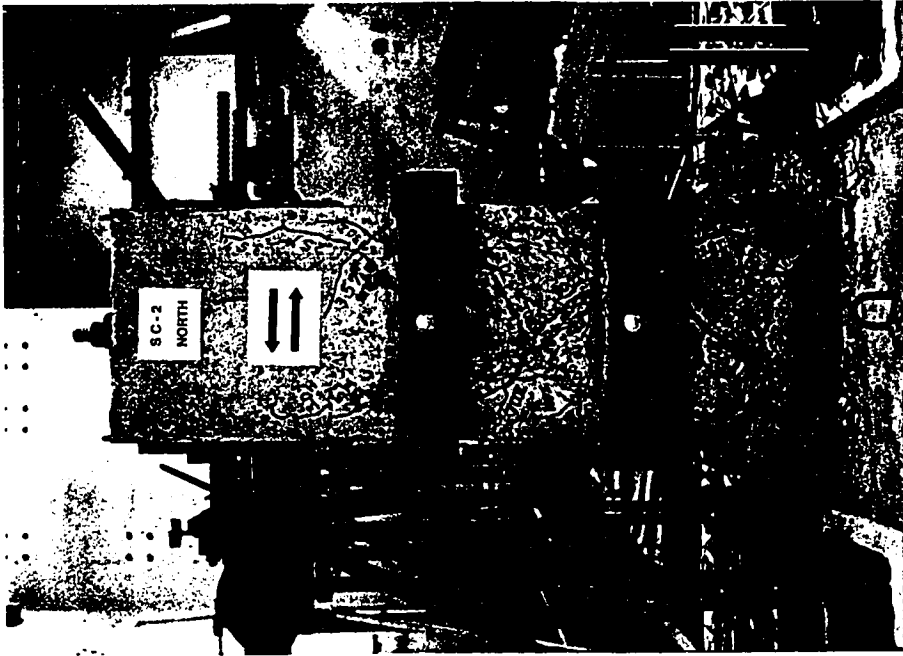


(b) Hysteretic Response

Figure 5.3 Strengthened Shear Column SC2



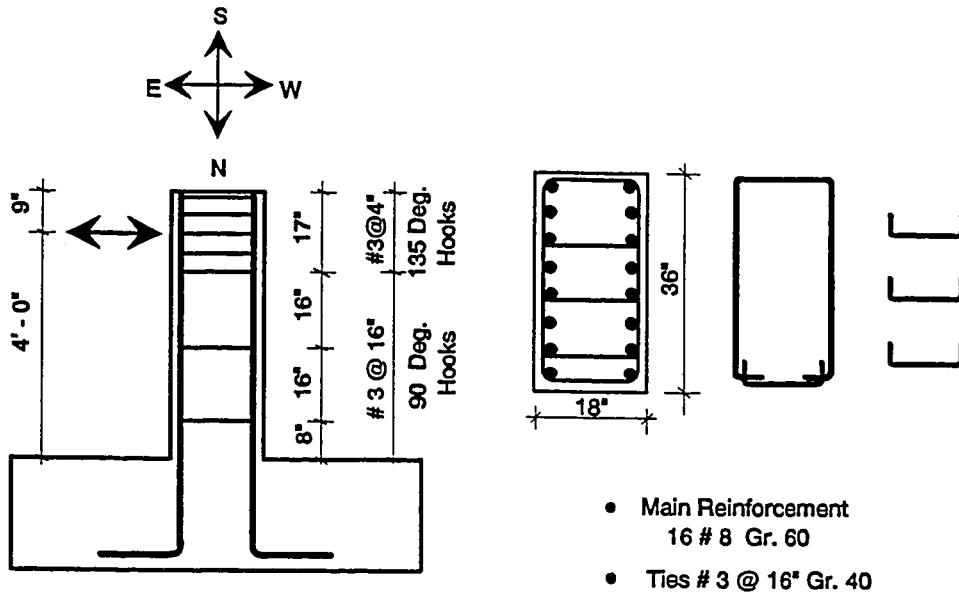
(a) After the test, N-W view



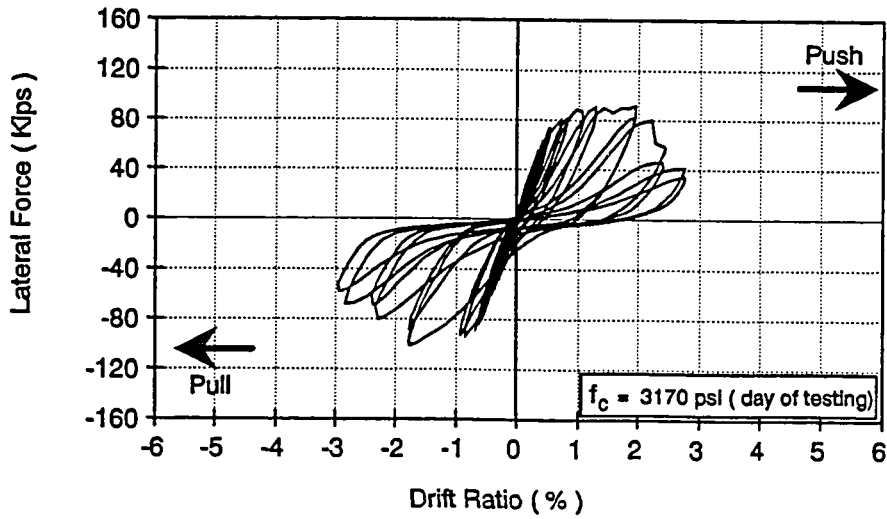
(b) After the test, north side

Figure 5.4 Strengthened Shear Column SC2





(a) Details of Column SC3

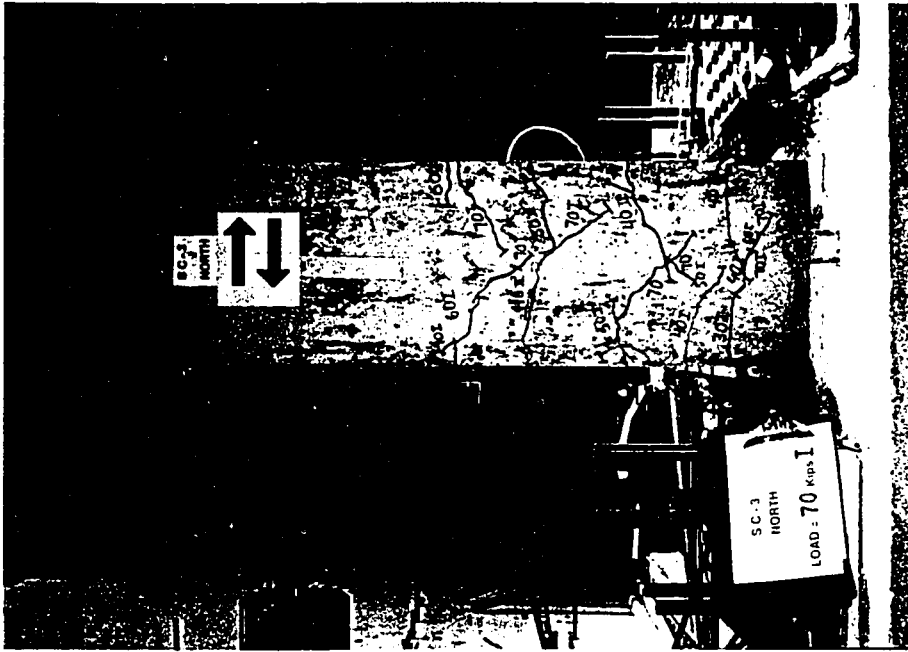


(b) Hysteretic Response

Figure 5.5 Basic Unretrofitted Shear Column SC3

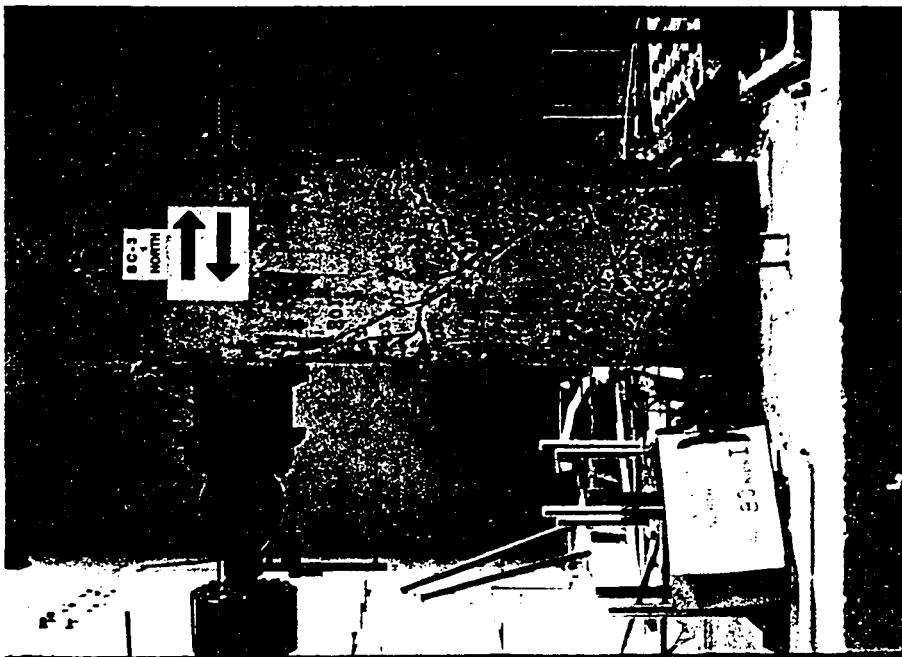


(a) Crack pattern during the cycle to 60 kips

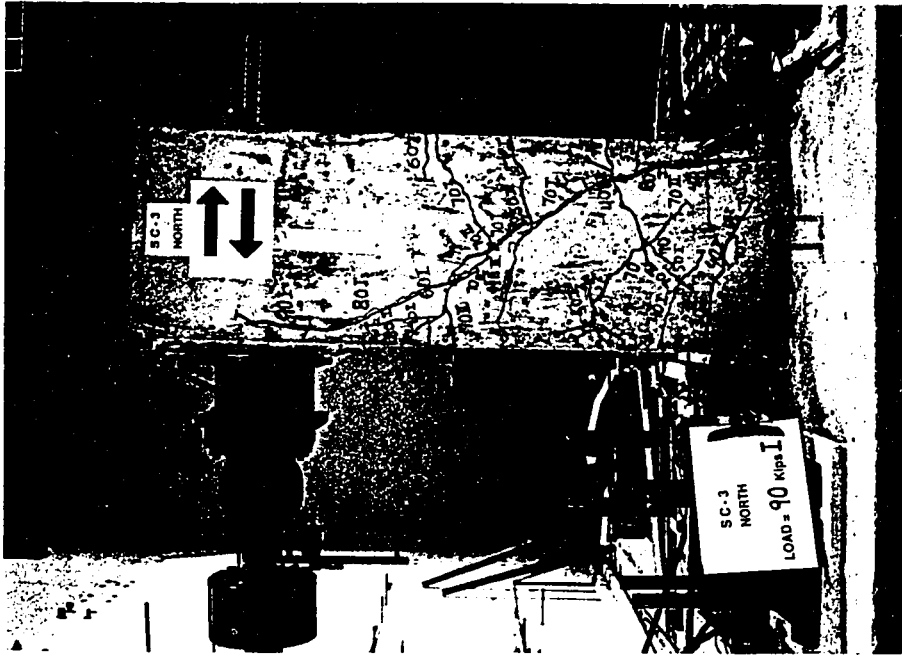


(b) Crack pattern during the cycle to 70 kips

Figure 5.6 Basic Unretrofitted Shear Column SC3

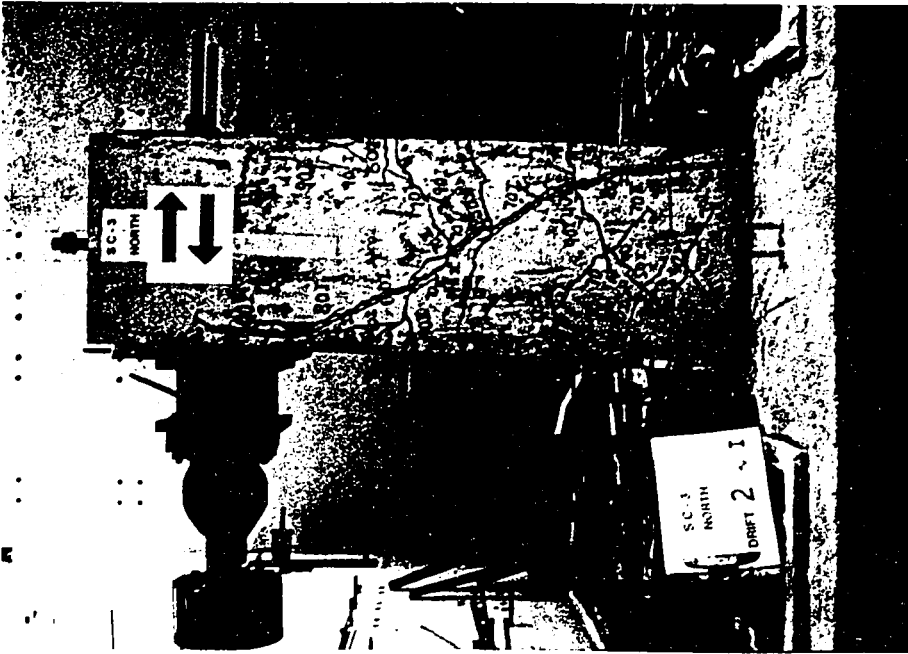


(a) Crack pattern during the cycle to 80 kips

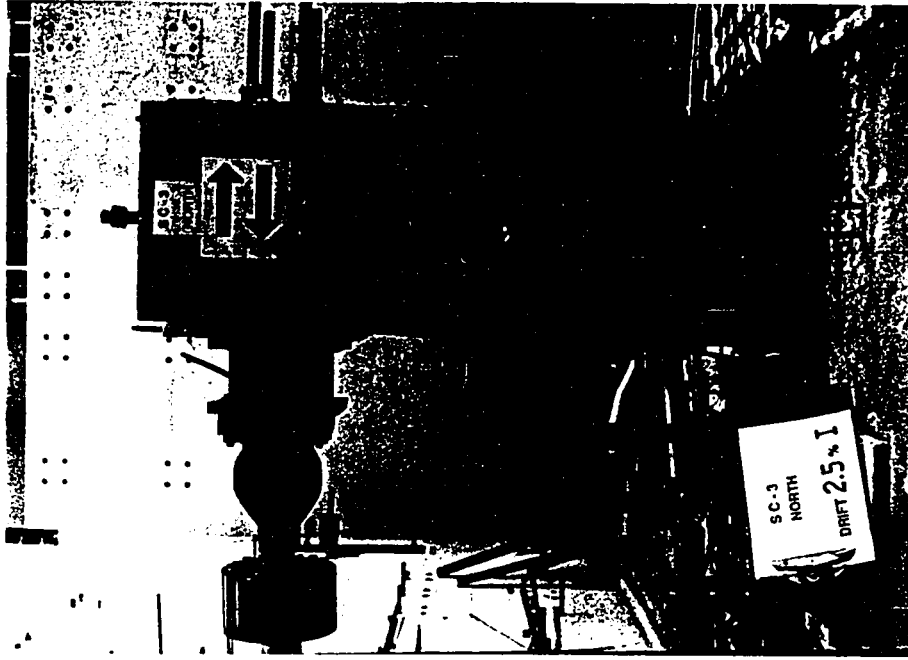


(b) Crack pattern during the cycle to 90 kips

Figure 5.7 Basic Unretrofitted Shear Column SC3

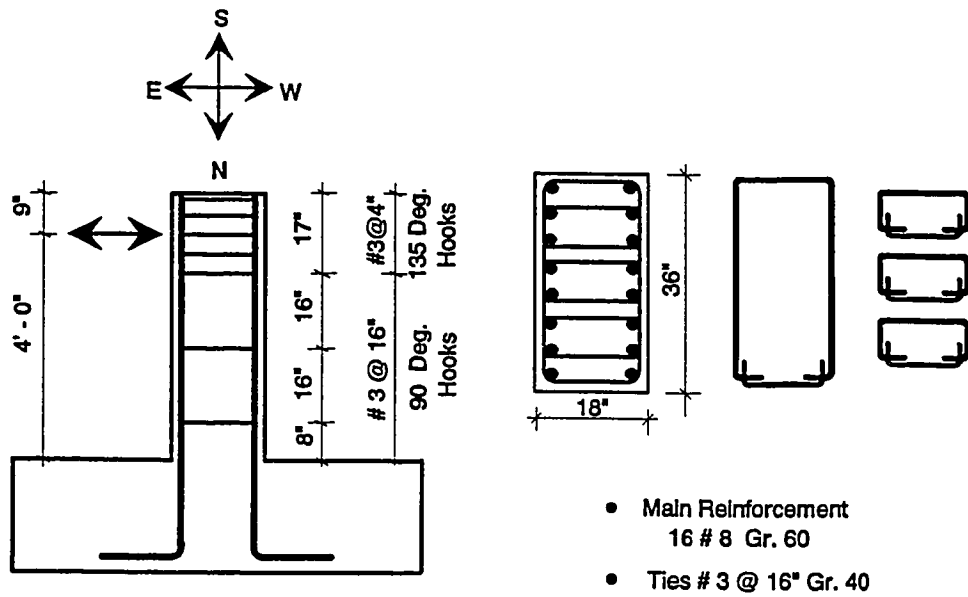


(a) Crack pattern during the cycle to 2.0% drift ratio

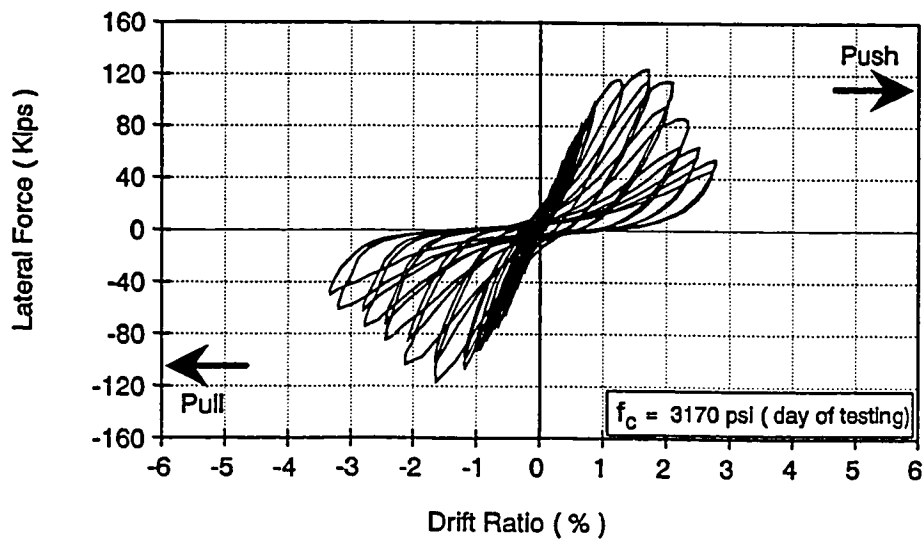


(b) Crack pattern during the cycle to 2.5% drift ratio

Figure 5.8 Basic Unretrofitted Shear Column SC3

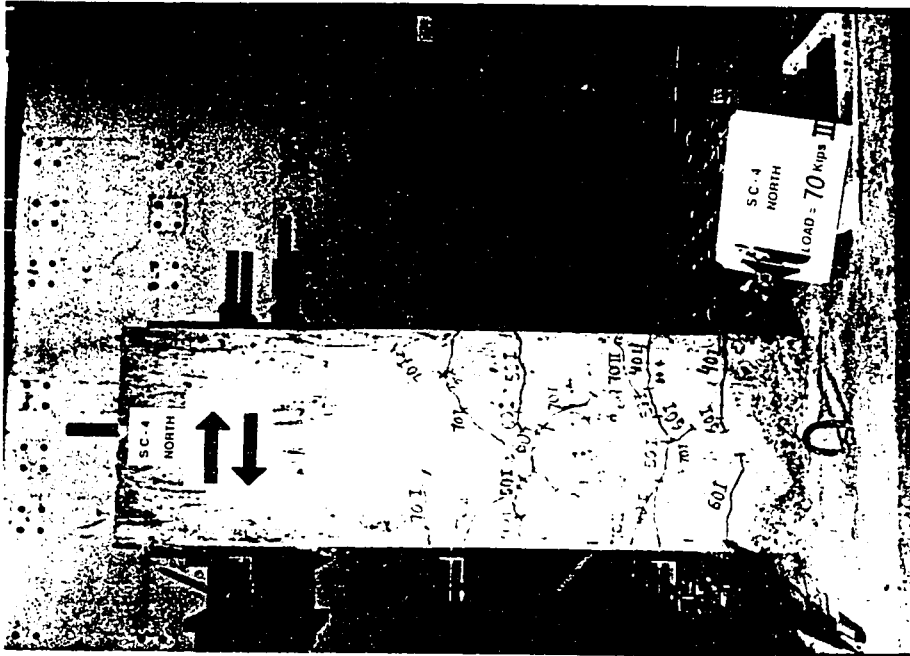


(a) Details of Column SC4

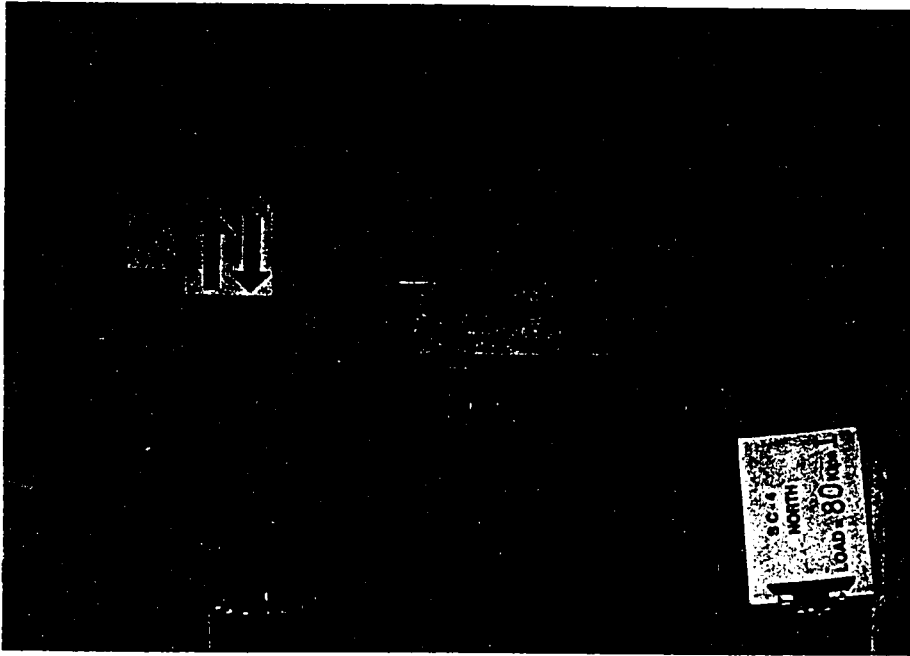


(b) Hysteretic Response

Figure 5.9 Basic Unretrofitted Shear Column SC4

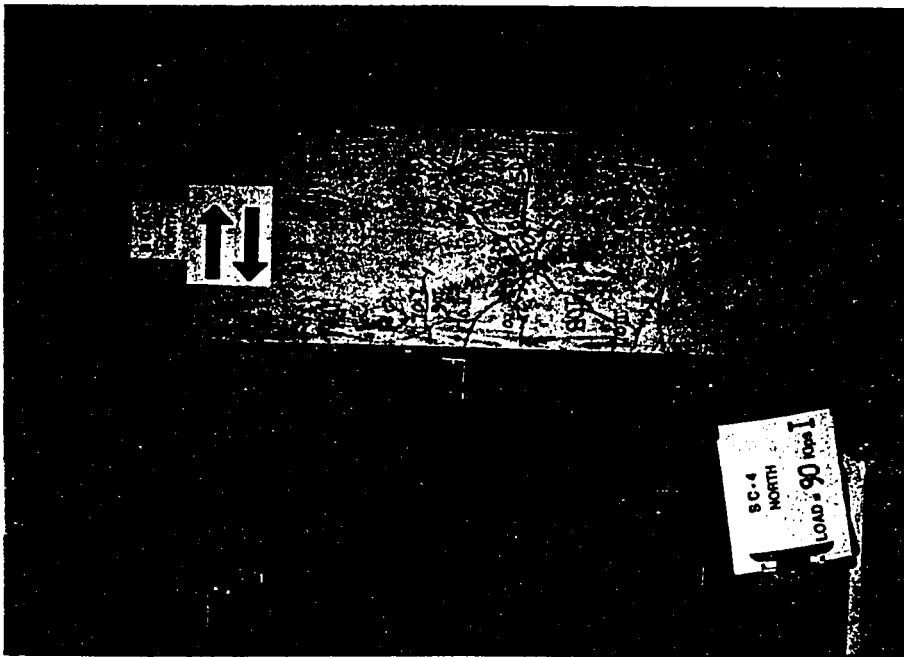


(a) Crack pattern during the cycle to 70 kips

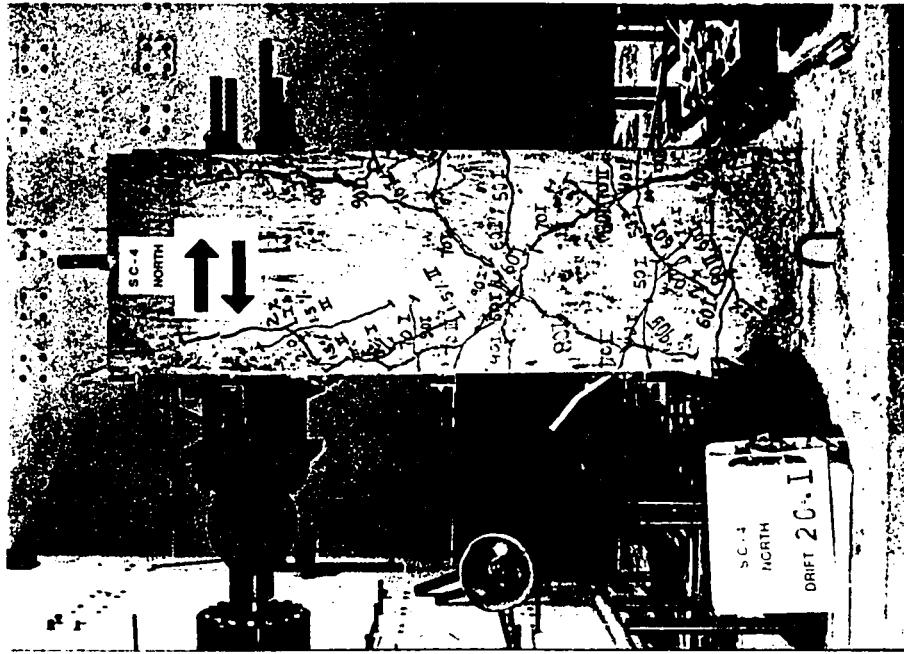


(b) Crack pattern during the cycle to 80 kips

Figure 5.10 Basic Unretrofitted Shear Column SC4

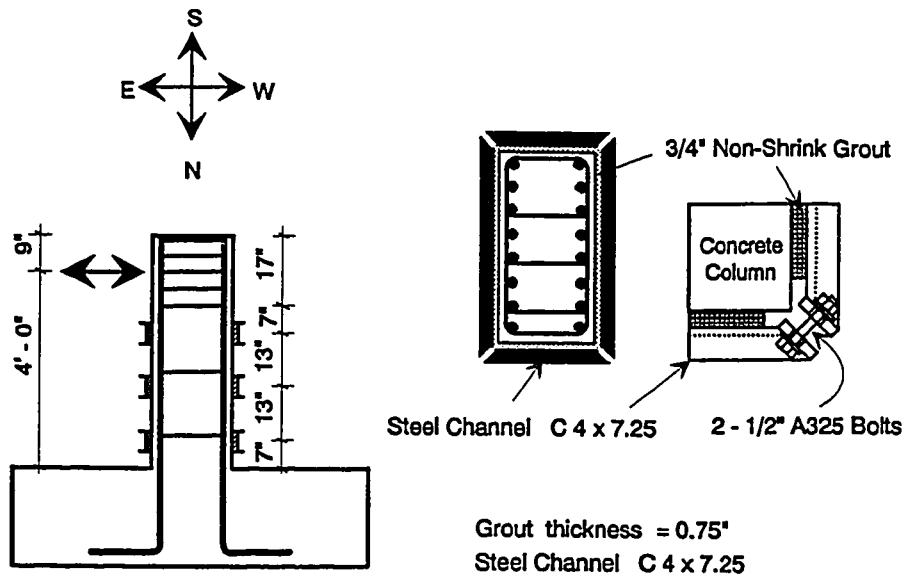


(a) Crack pattern during the cycle to 90 kips

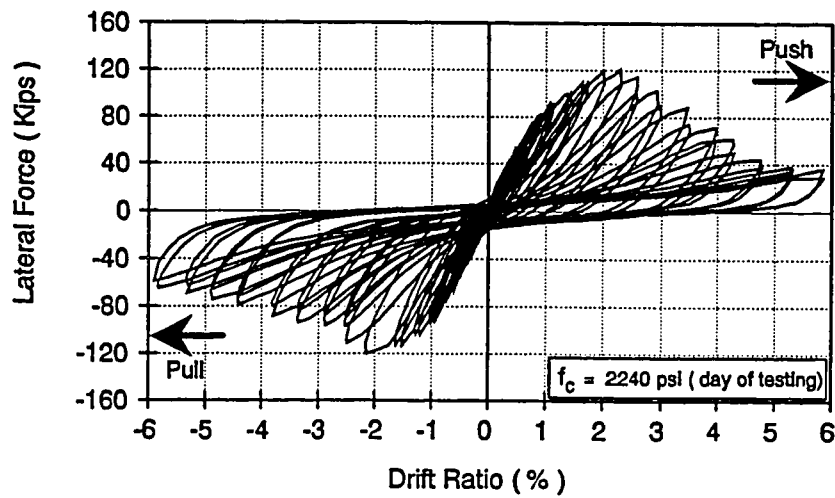


(b) Crack pattern during the cycle to 2.0% drift ratio

Figure 5.11 Basic Unretrofitted Shear Column SC4



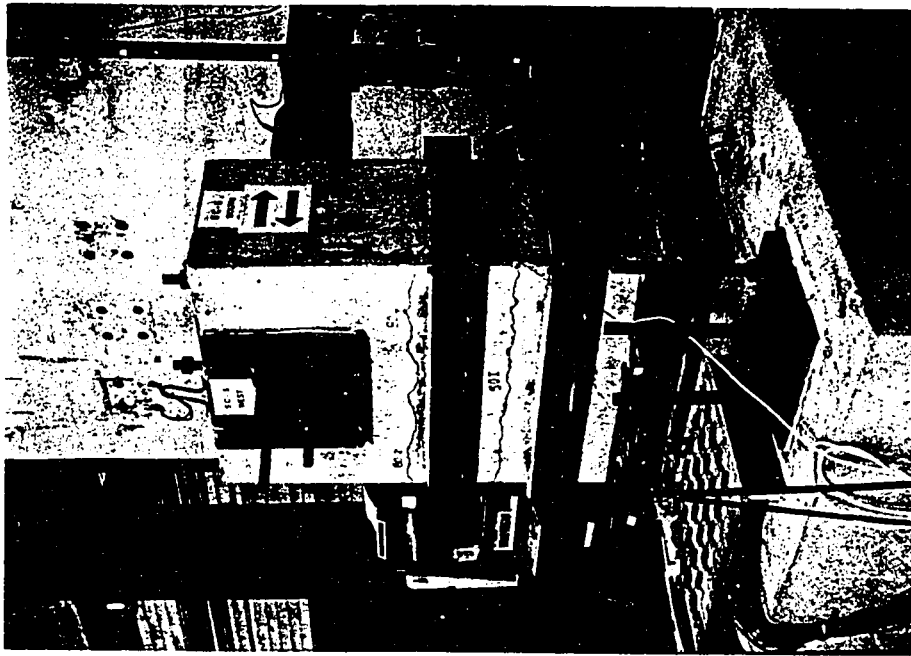
(a) Details of Column SC2



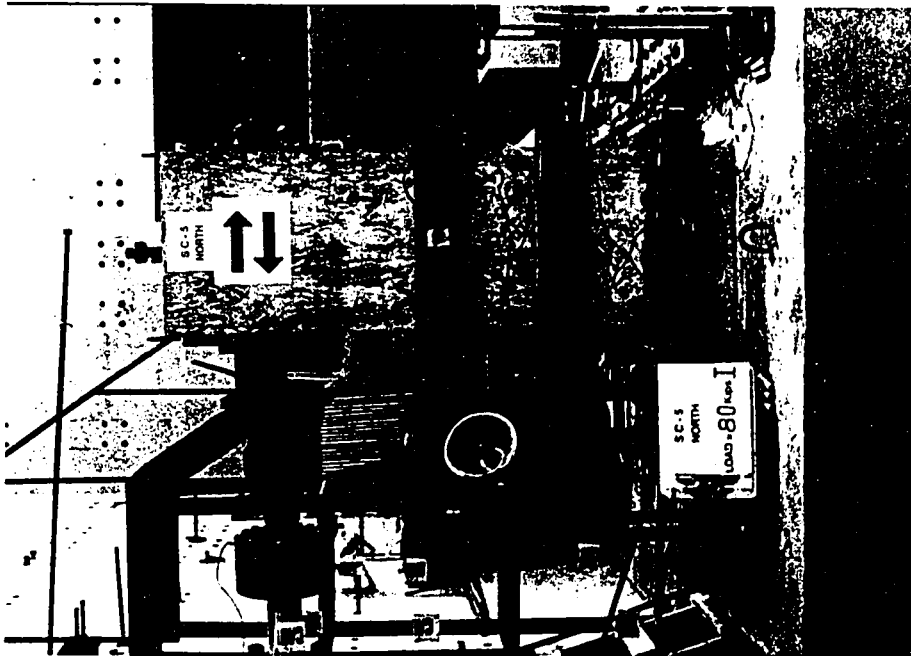
(b) Hysteretic Response

Figure 5.12 Strengthened Shear Column SC5



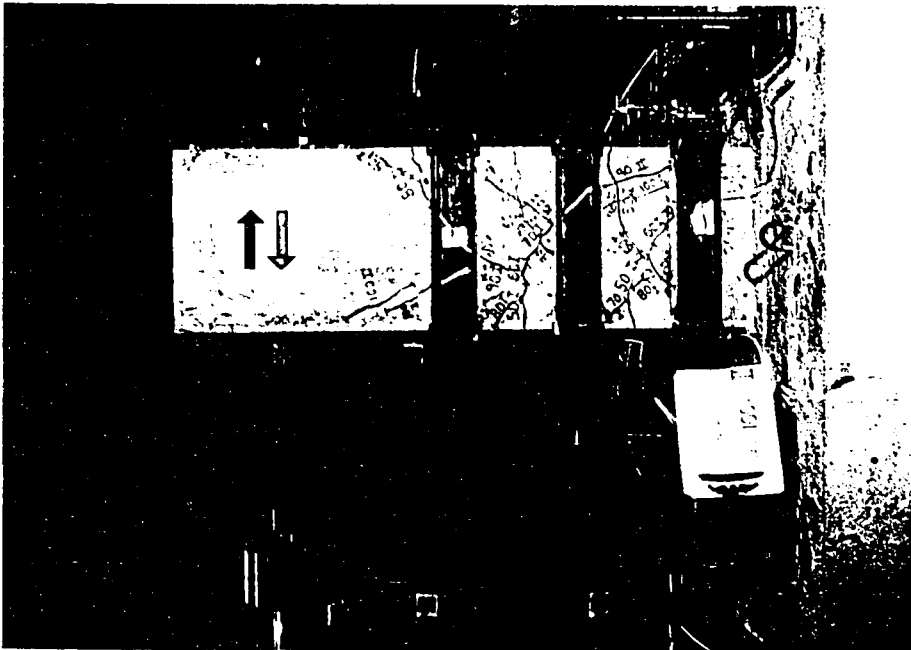


(a) Crack pattern during the cycle to 80 kip, S-W view

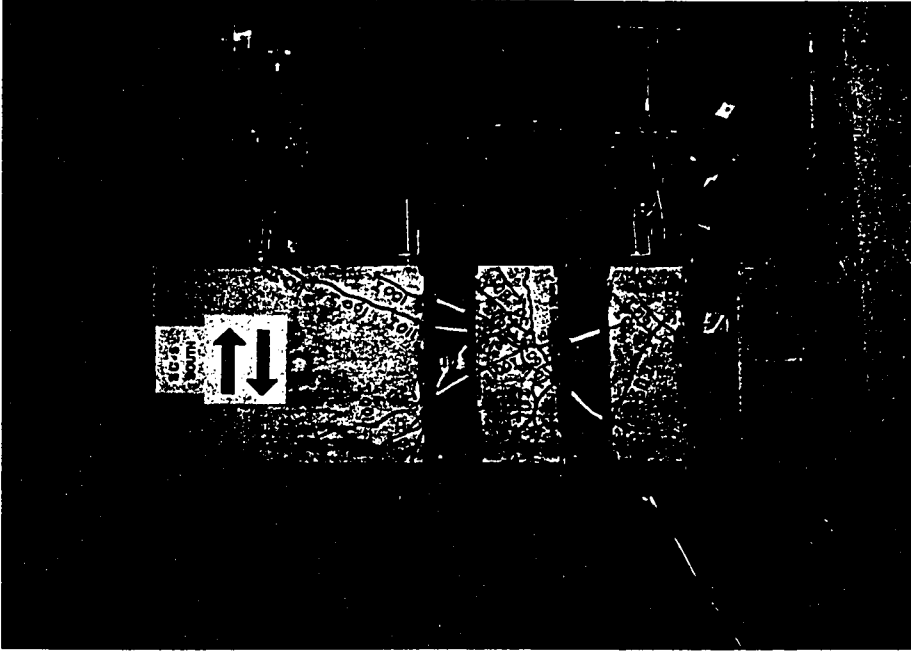


(b) Crack pattern during the cycle to 80 kips, north side

Figure 5.13 Strengthened Shear Column SC5

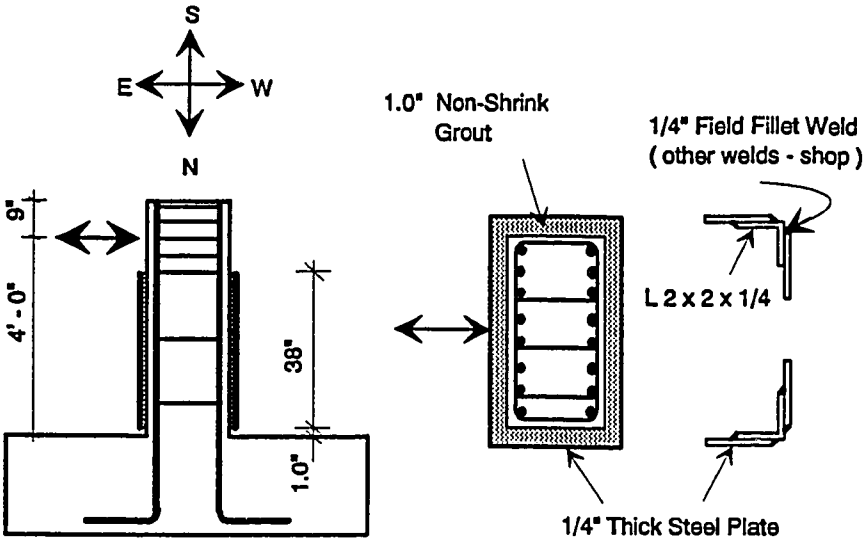


(a) Crack pattern during the cycle to 100 kips, north side

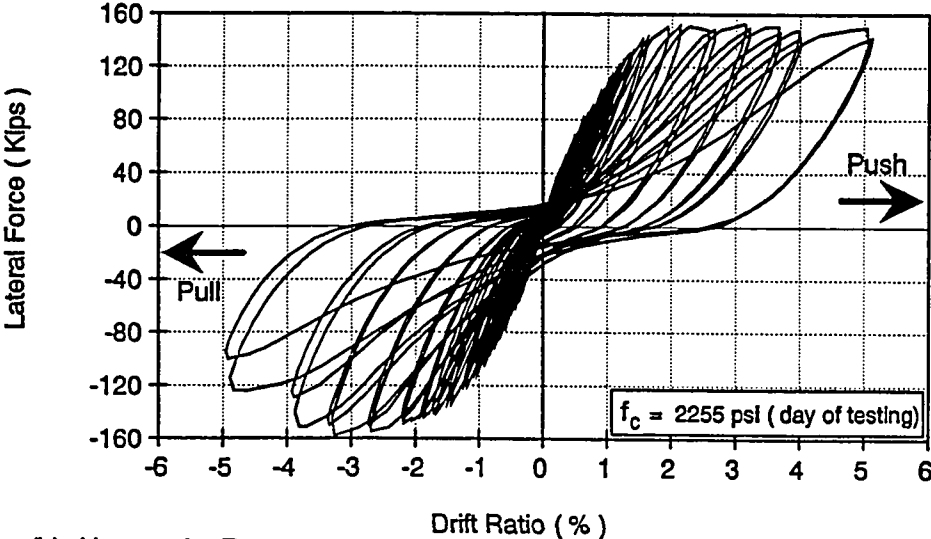


(b) Crack pattern during the cycle to 110 kips, south side

Figure 5.14 Strengthened Shear Column SC5

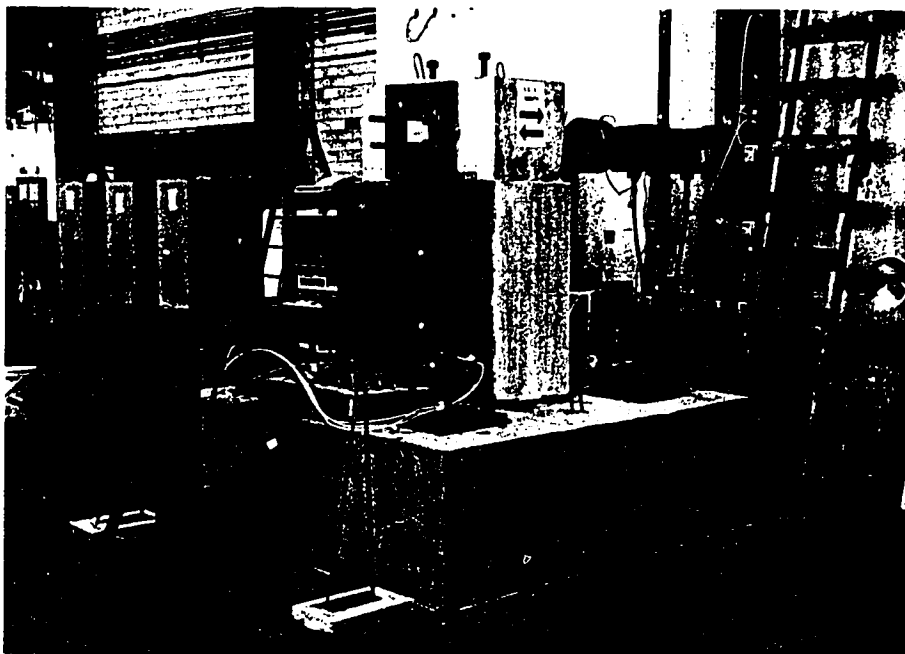


(a) Details of Column SC6



(b) Hysteretic Response

Figure 5.15 Strengthened Shear Column SC6

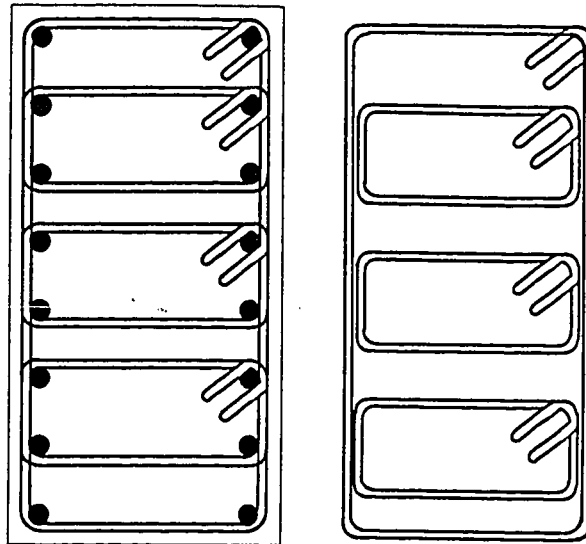


(a) Column SC6 under the test setup

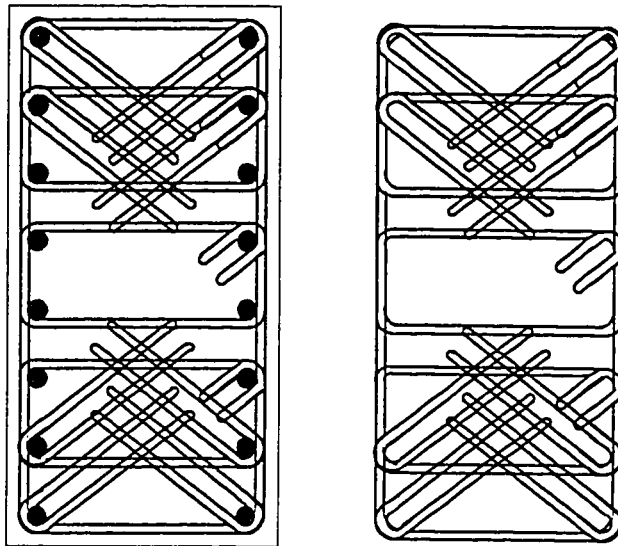


(b) The concrete compression zone on the west side

Figure 5.16 Strengthened Shear Column SC6

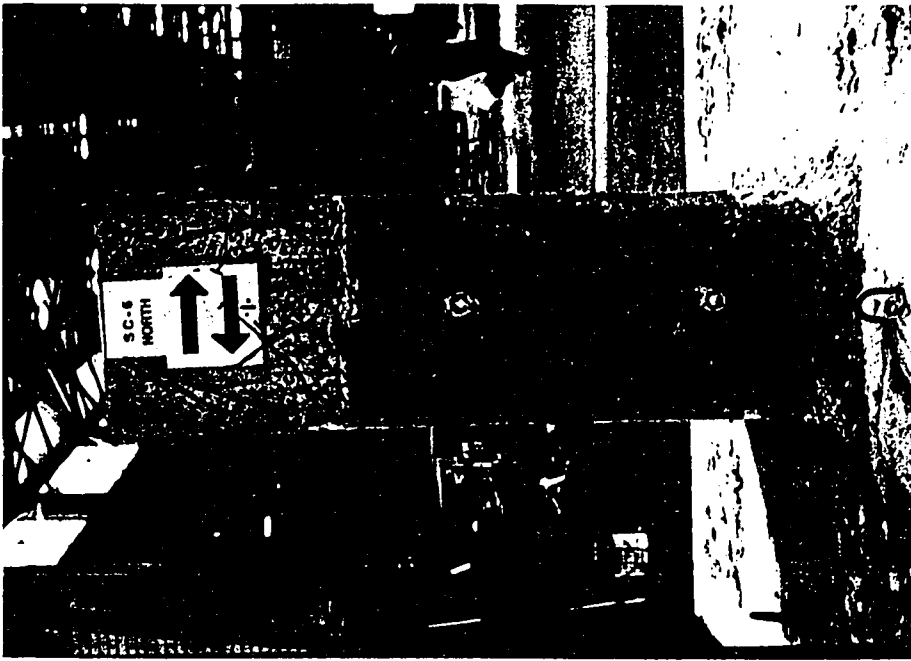


(a) Columns SC1 through SC6

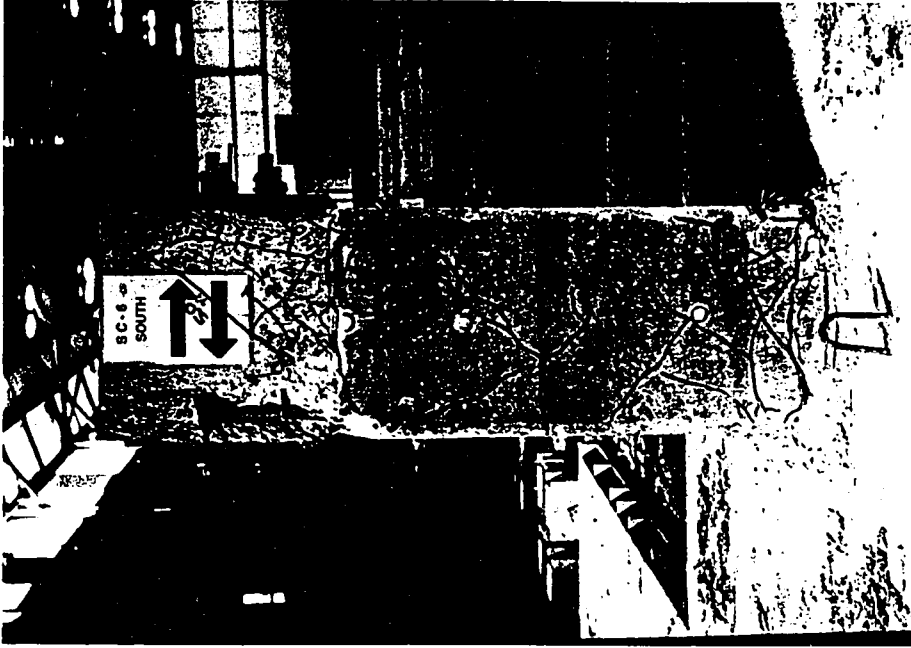


(b) Columns SC7 through SC11

Figure 5.17 Details of the transverse reinforcement at the top 17 inches.

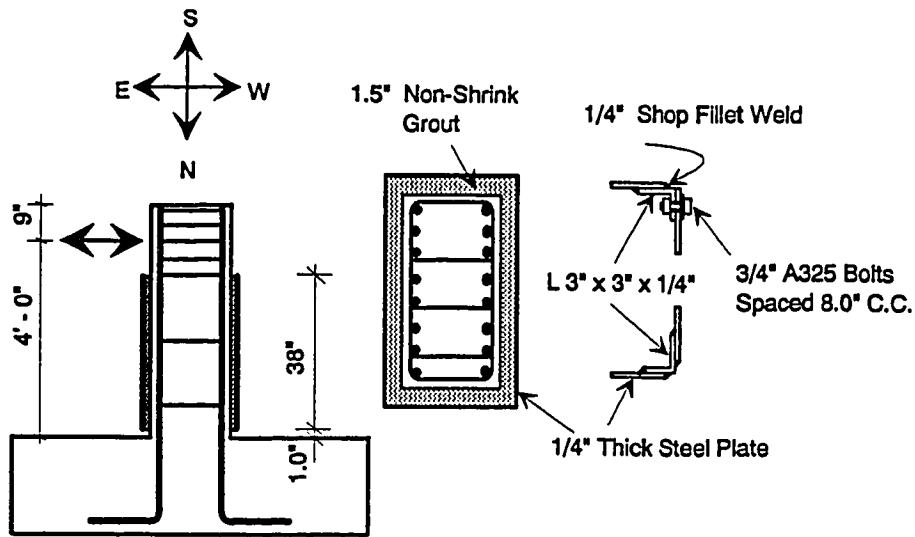


(a) Crack pattern on the north side

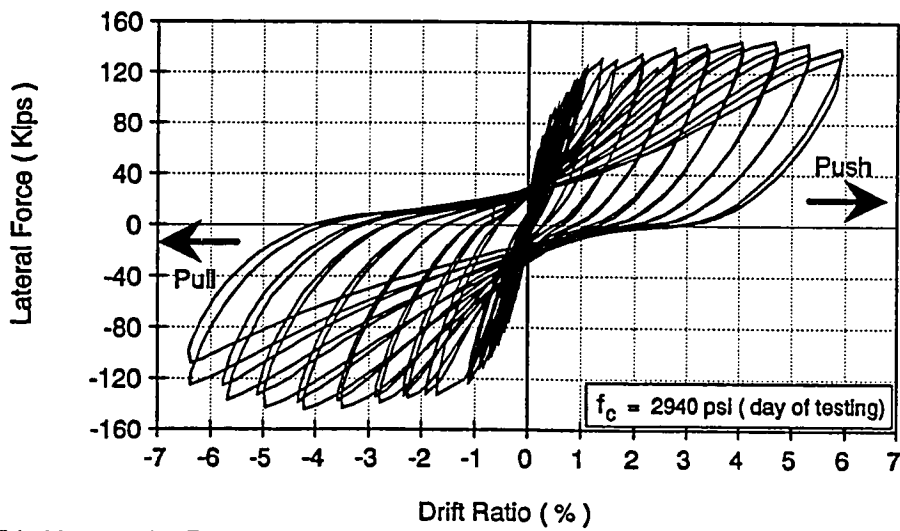


(b) Crack pattern on the south side

Figure 5.18 Strengthened Shear Column SC6

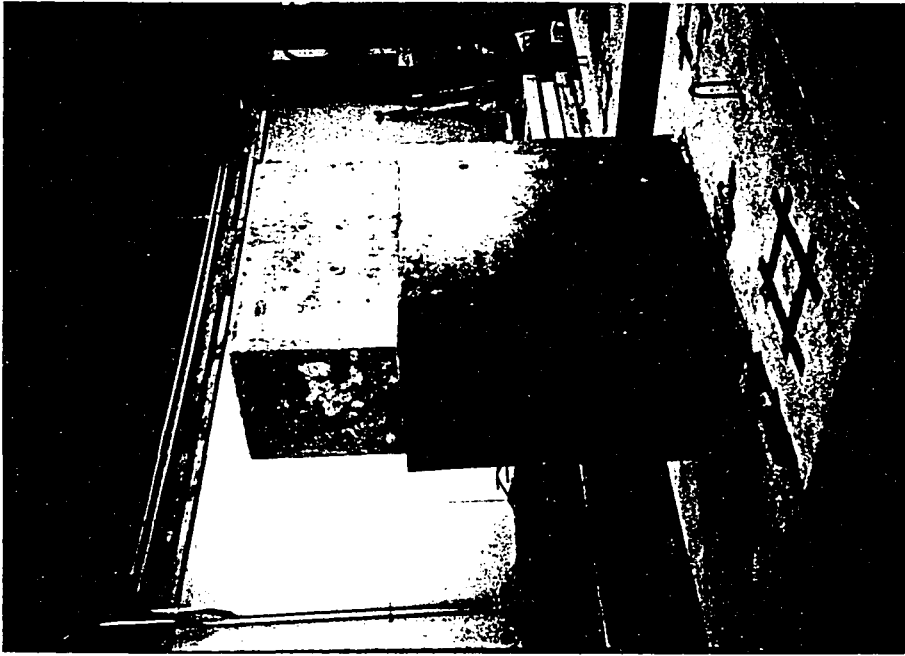


(a) Details of Column SC7

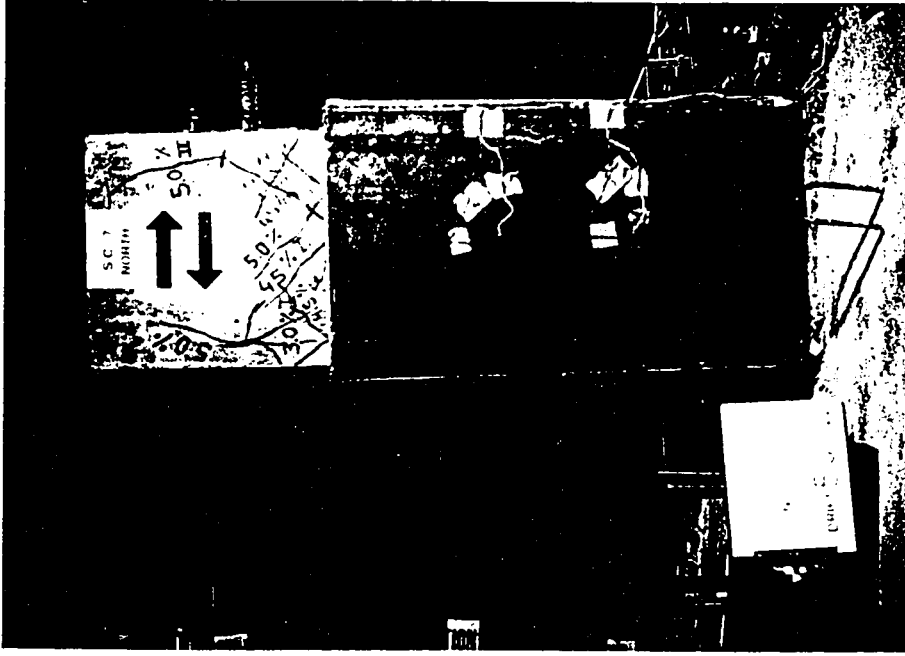


(b) Hysteretic Response

Figure 5.19 Strengthened Shear Column SC7



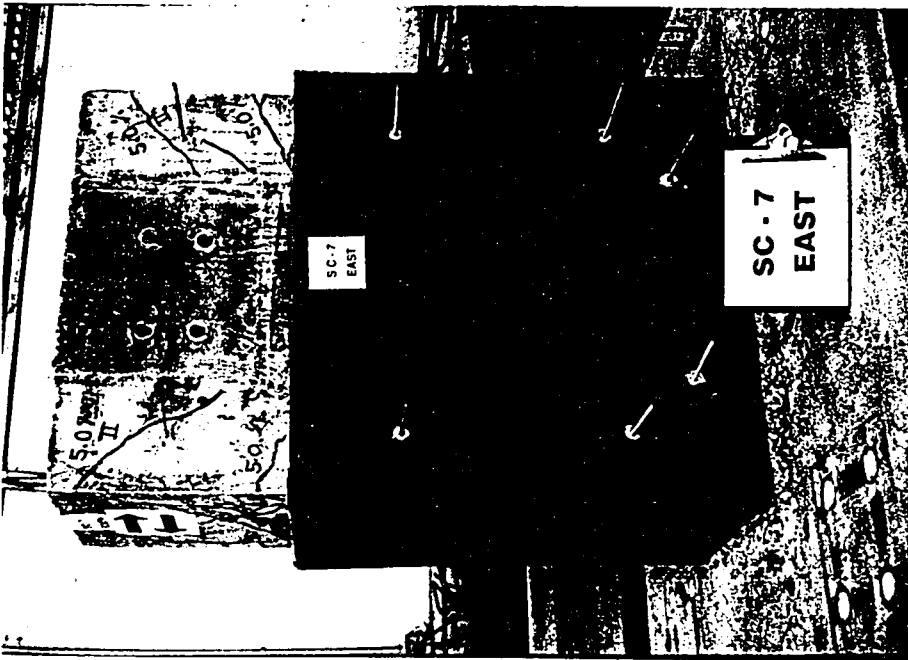
(a) Column SC7 before the test



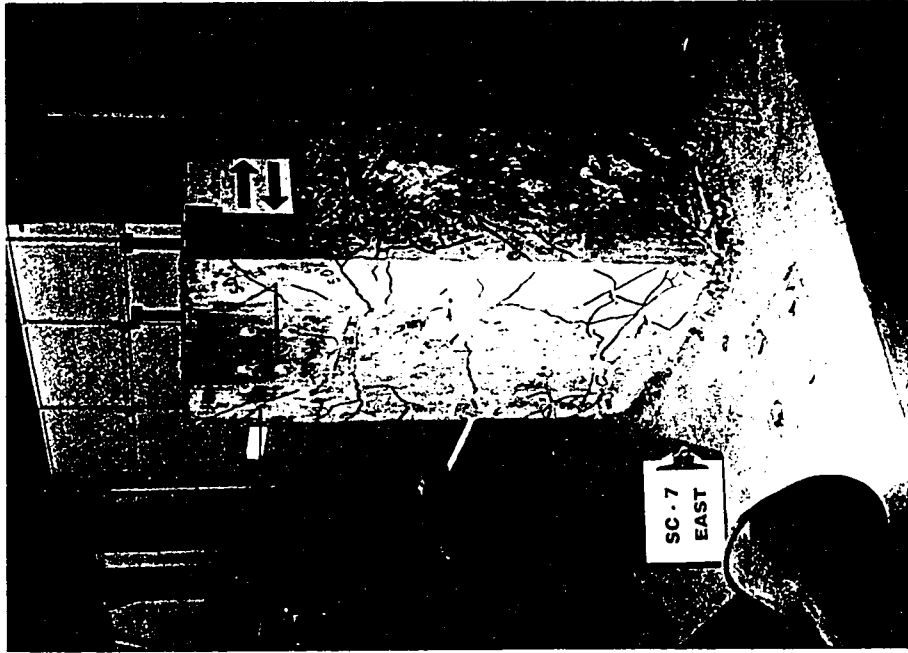
(b) Column SC7 during the test

Figure 5.20 Strengthened Shear Column SC7



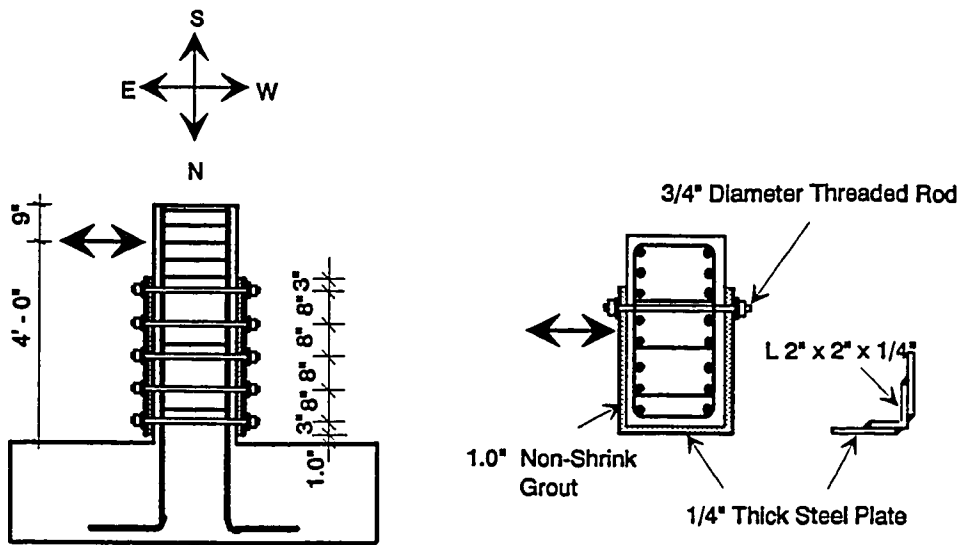


(a) Before the removal of the steel jacket

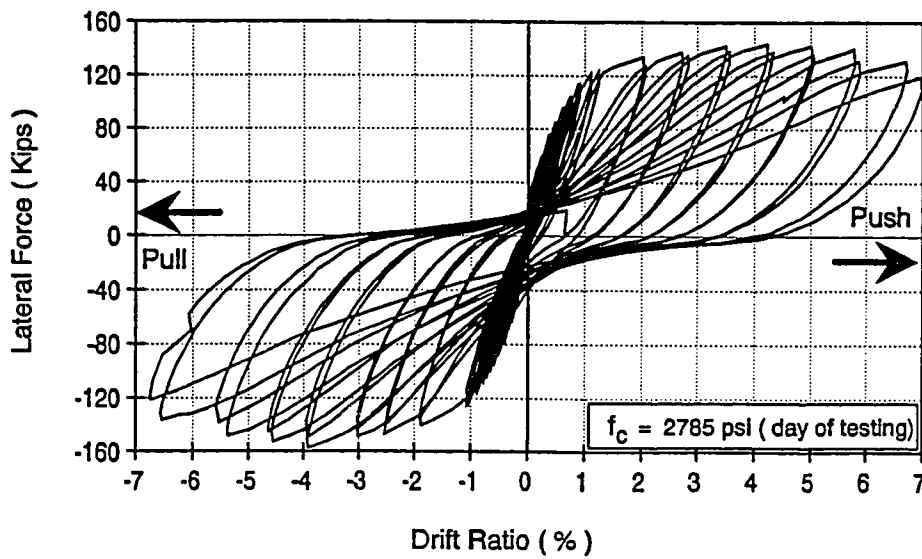


(b) Crack pattern, N-E view

Figure 5.21 Strengthened Shear Column SC7, after the test

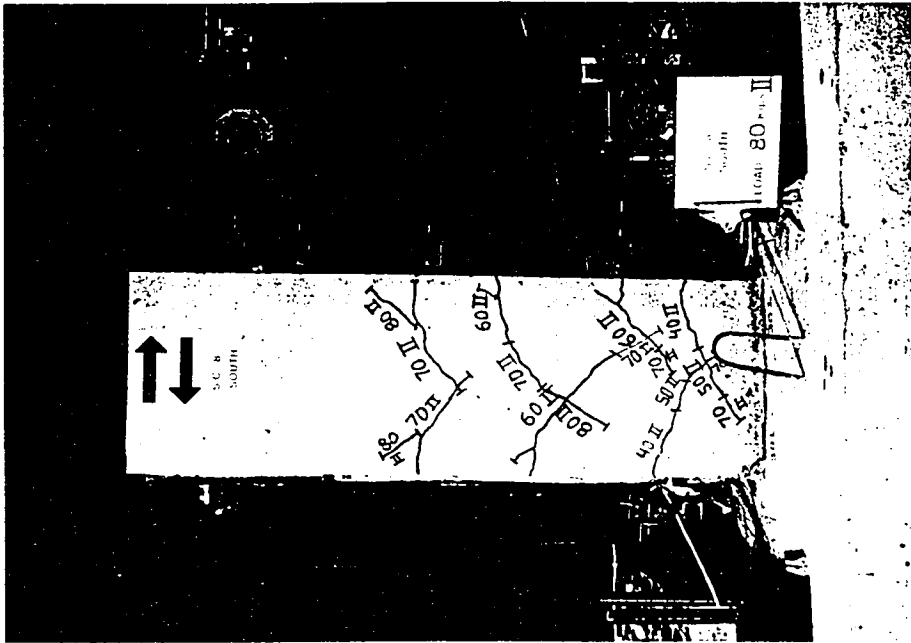


(a) Details of Column SC8

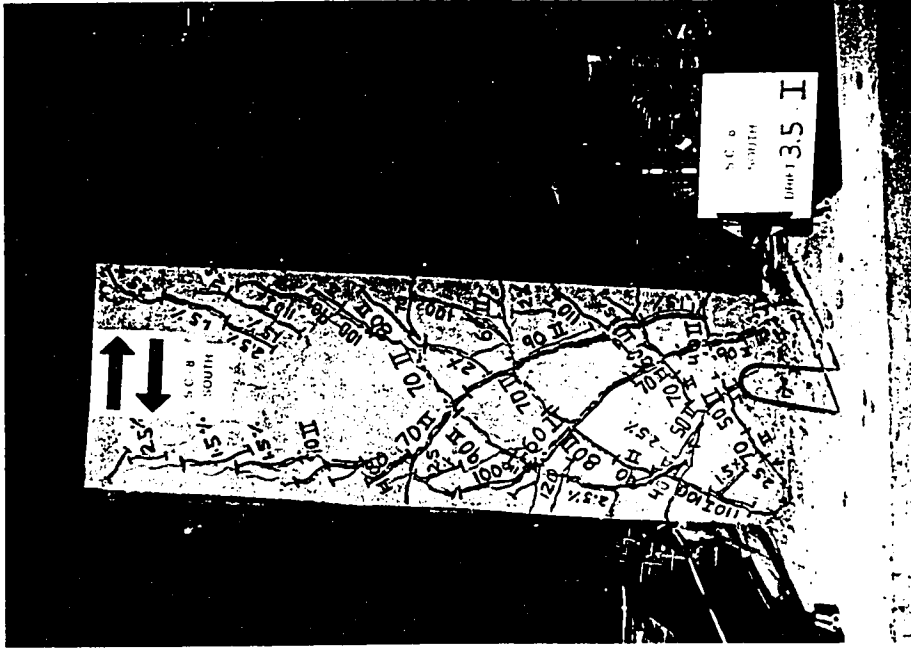


(b) Hysteretic Response

Figure 5.22 Strengthened Shear Column SC8

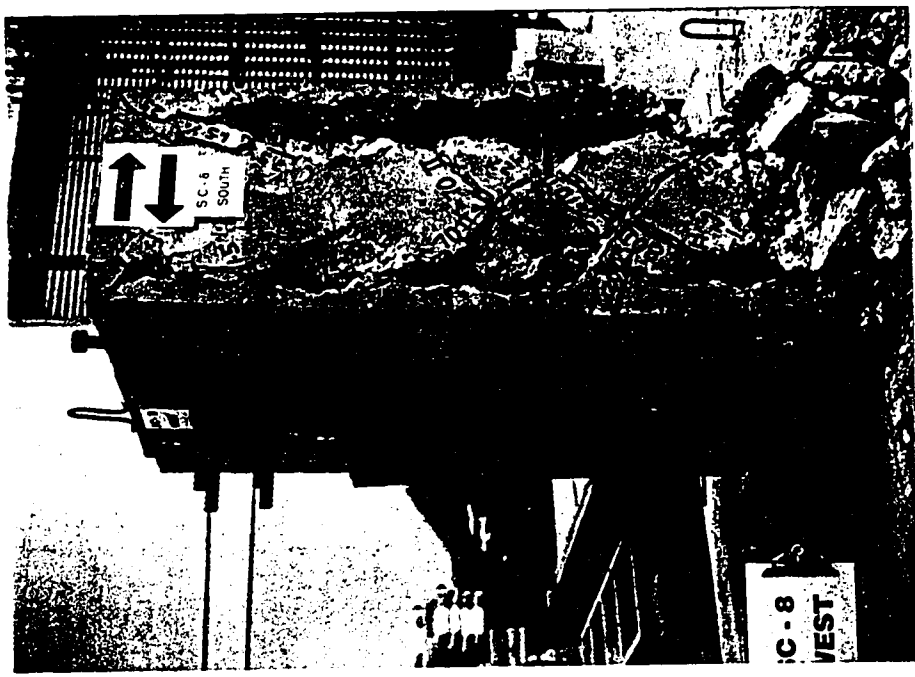


(a) Crack pattern during the cycle to 80 kips

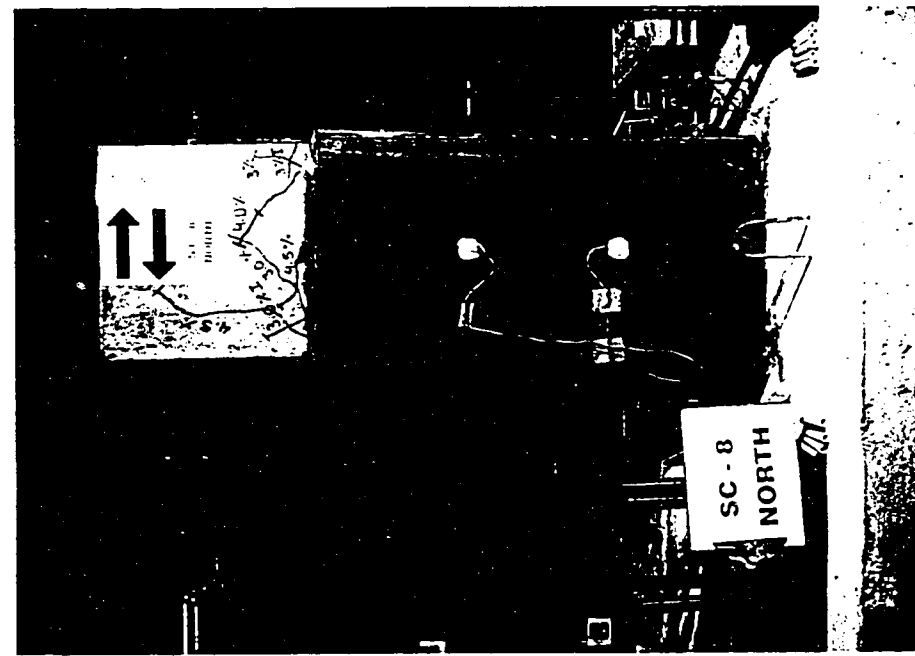


(b) Crack pattern during the cycle to 3.5% drift ratio

Figure 5.23 Strengthened Shear Column SC8



(b) South side



(a) North side

Figure 5.24 Strengthened Shear Column SC8, after the test

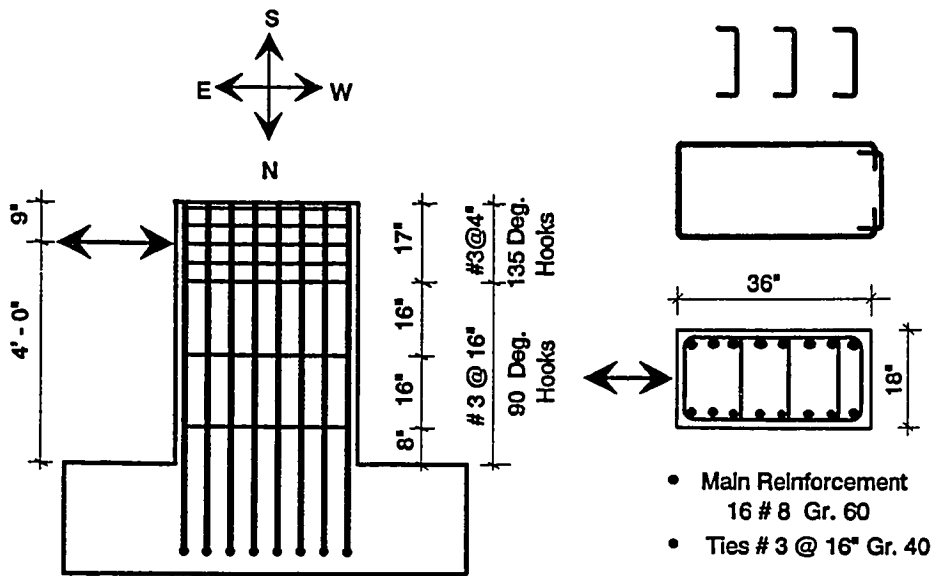


(a) Before the removal of the steel jacket

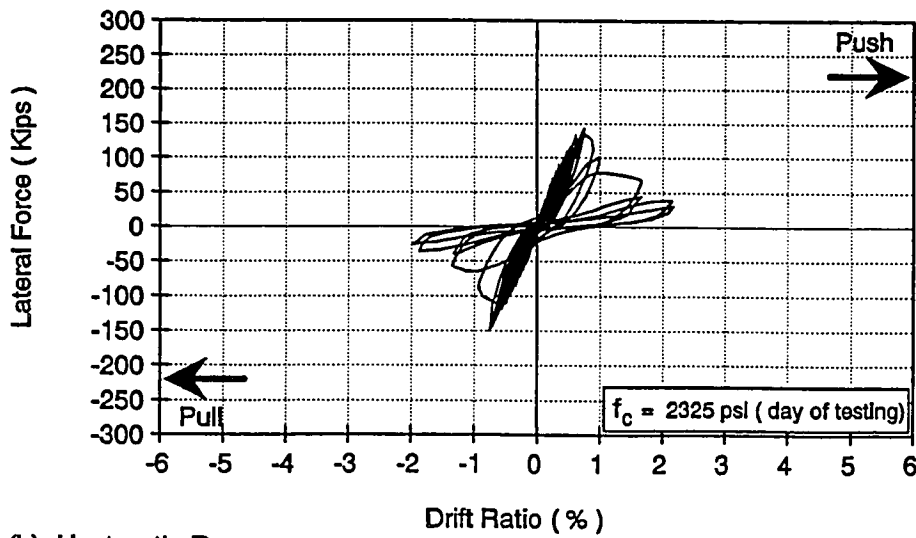


(b) Crack pattern after the removal of the steel jacket

Figure 5.25 Strengthened Shear Column SC8, after the test, east side

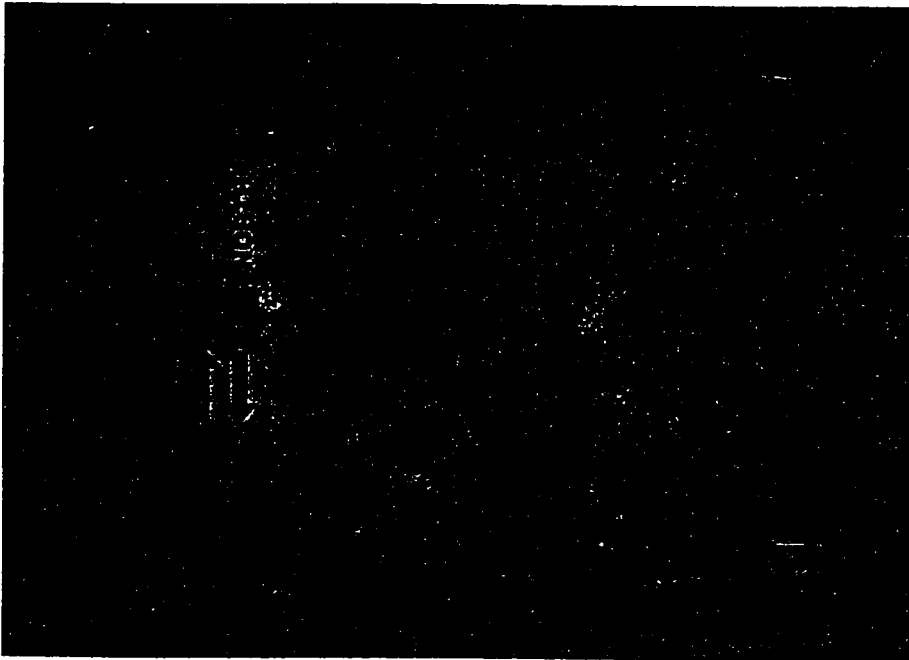


(a) Details of Column SC9

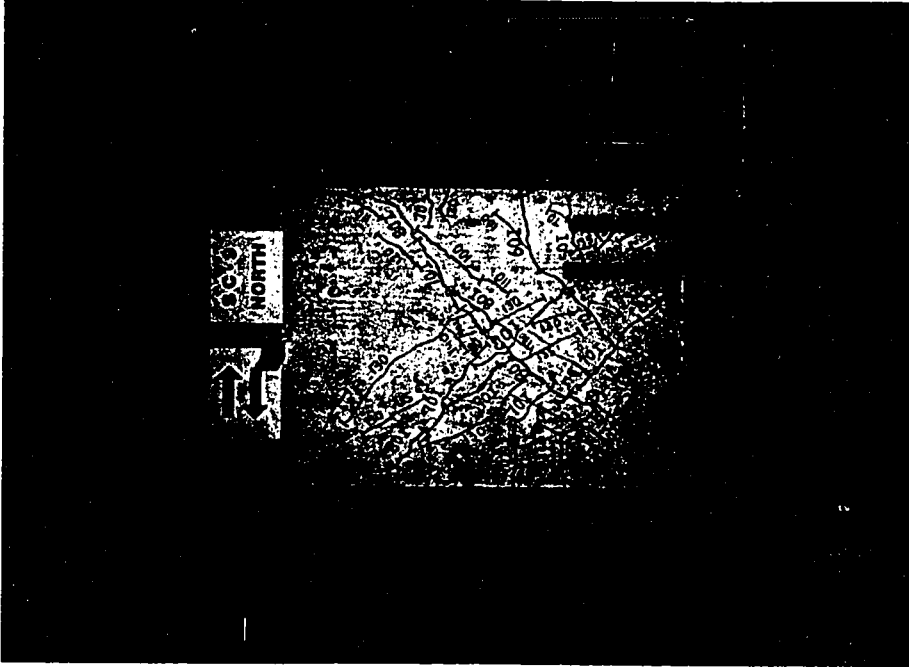


(b) Hysteretic Response

Figure 5.26 Basic Unretrofitted Shear Column SC9

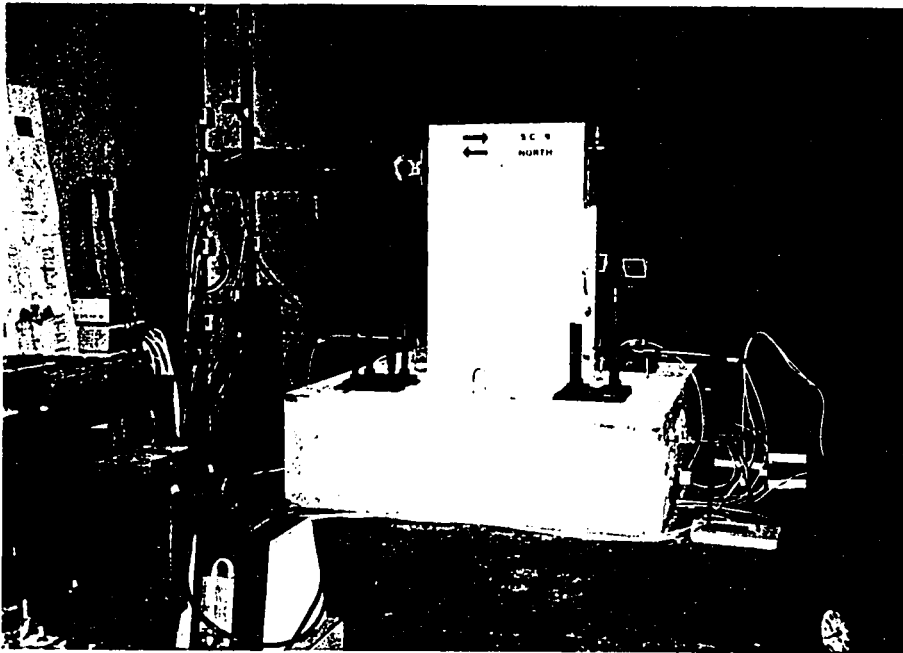


(a) Crack pattern during the cycle to 80 kips

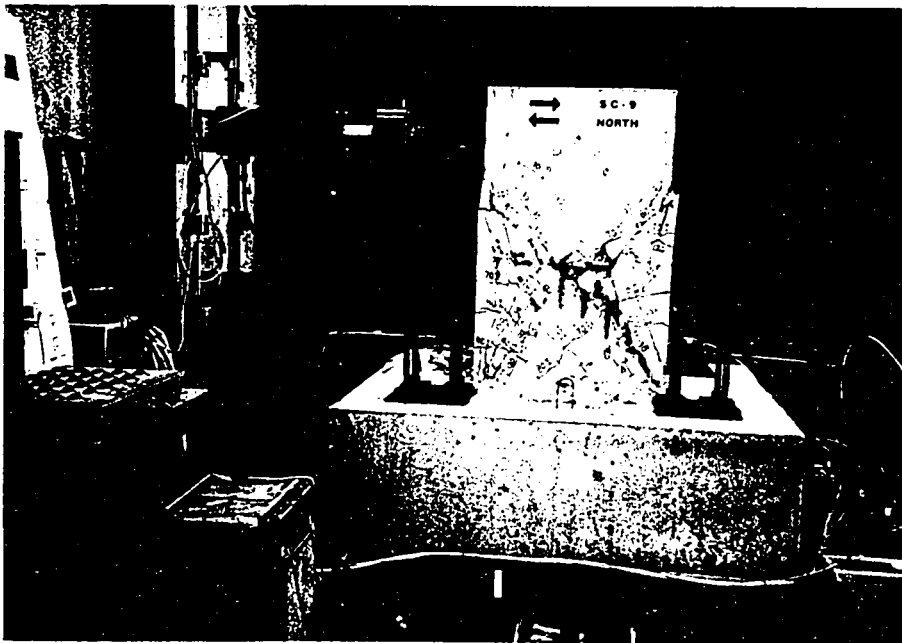


(b) Crack pattern during the cycle to 140 kips

Figure 5.27 Basic Unretrofitted Shear Column SC9



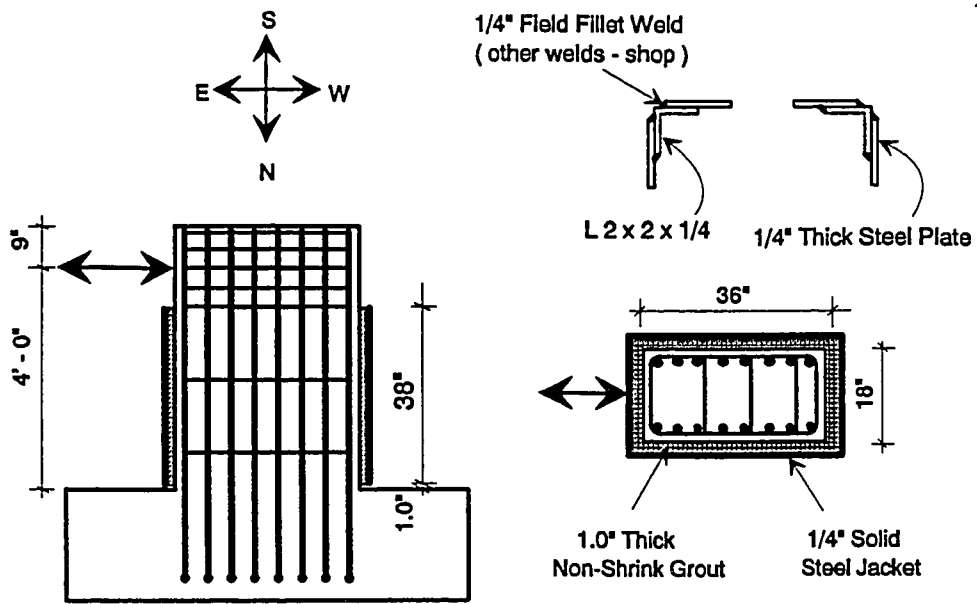
(a) Column SC9 under the test setup



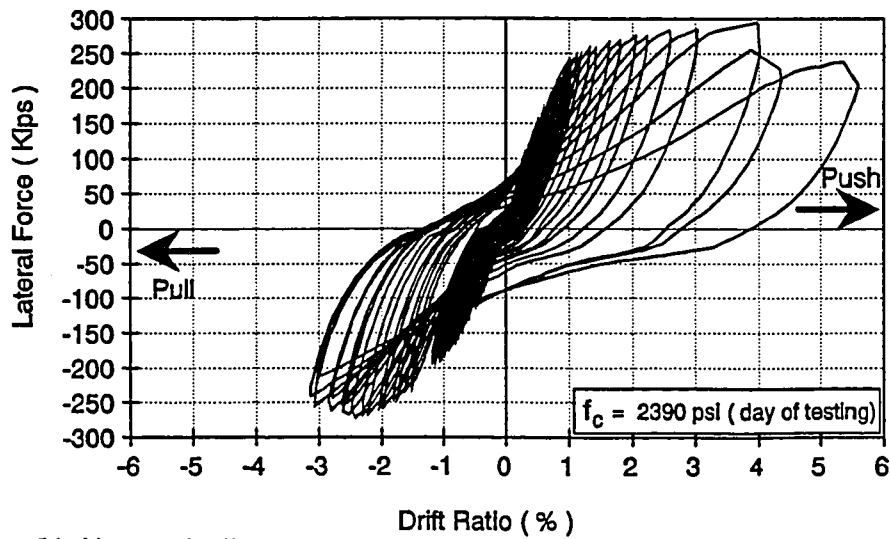
(b) Column SC9 at the end of the test

Figure 5.28 Basic Unretrofitted Shear Column SC9



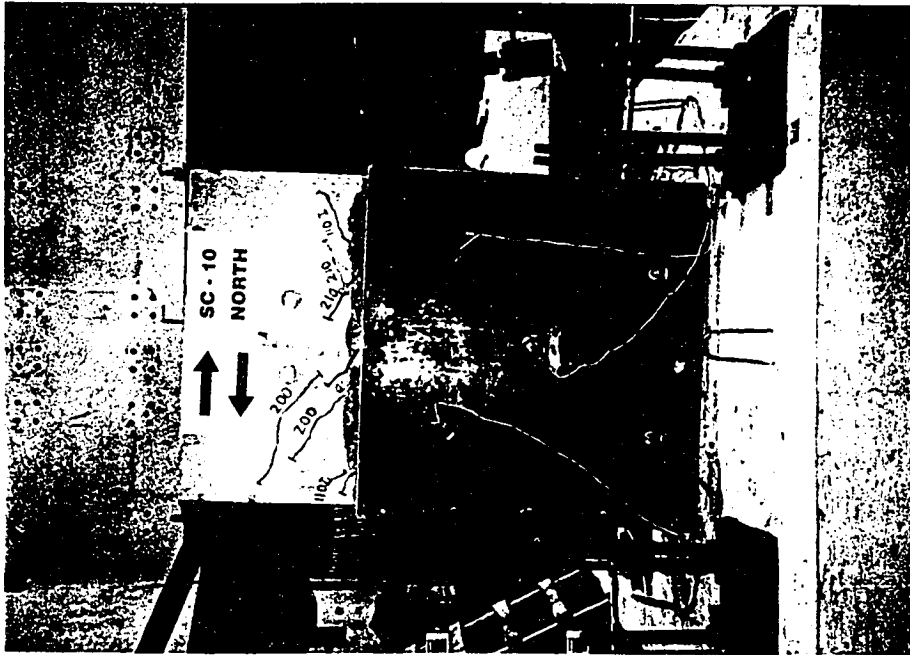


(a) Details of Column SC10

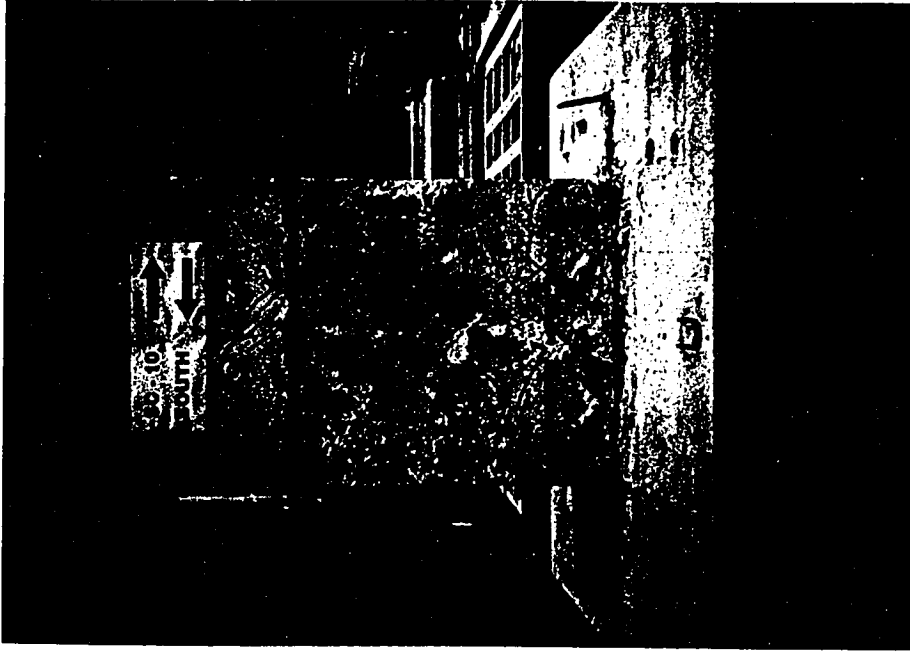


(b) Hysteretic Response

Figure 5.29 Strengthened Shear Column SC10

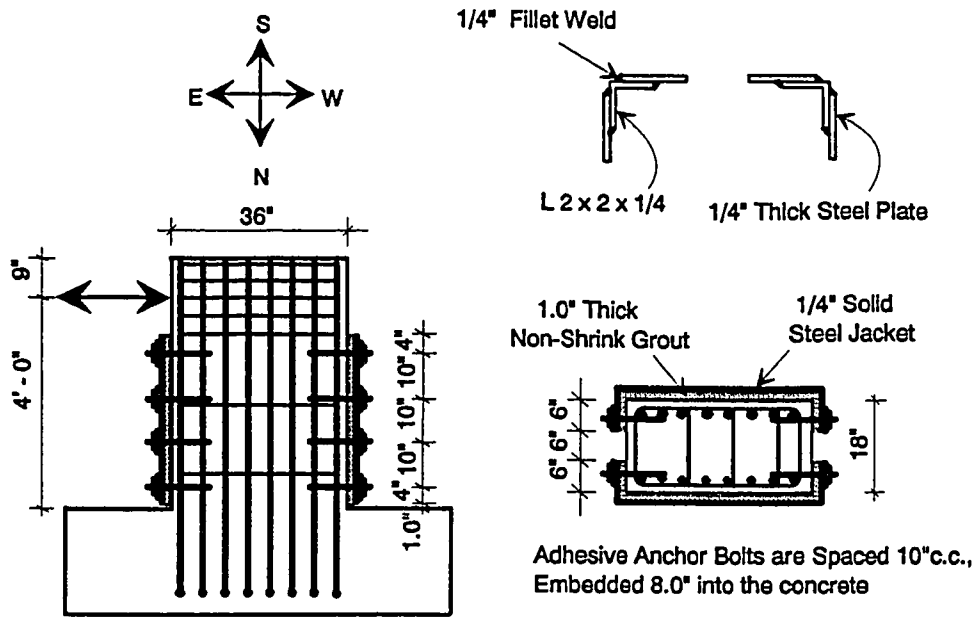


(a) Column SC10 during the test

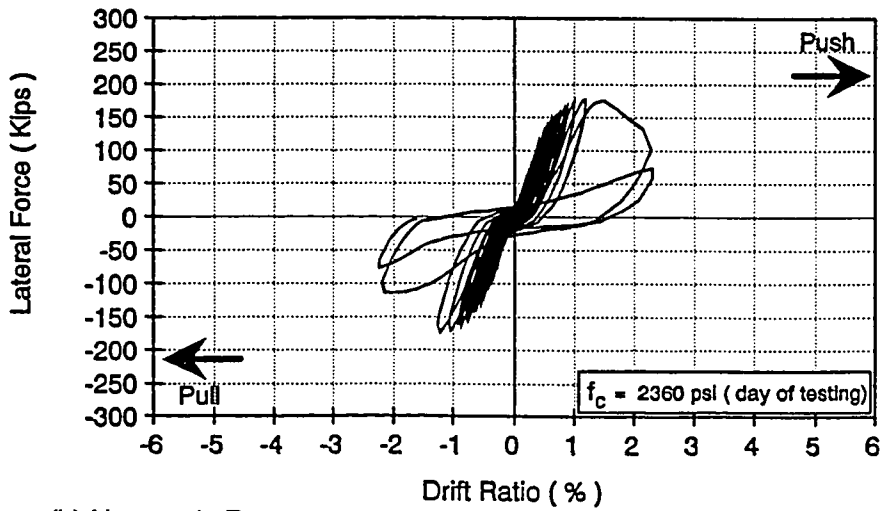


(b) Crack pattern after the removal of the steel jacket

Figure 5.30 Strengthened Shear Column SC10

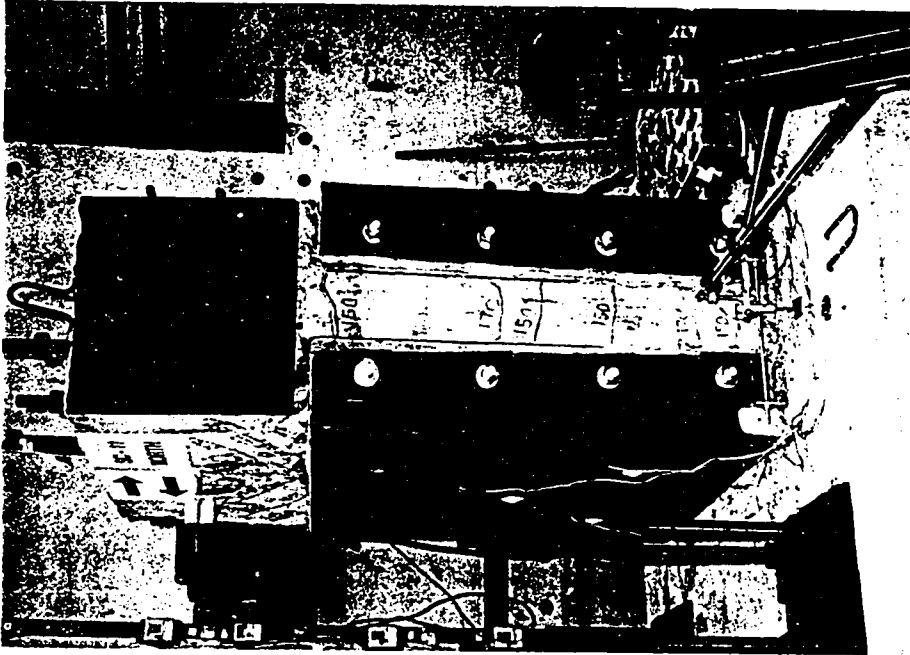


(a) Details of Column SC11

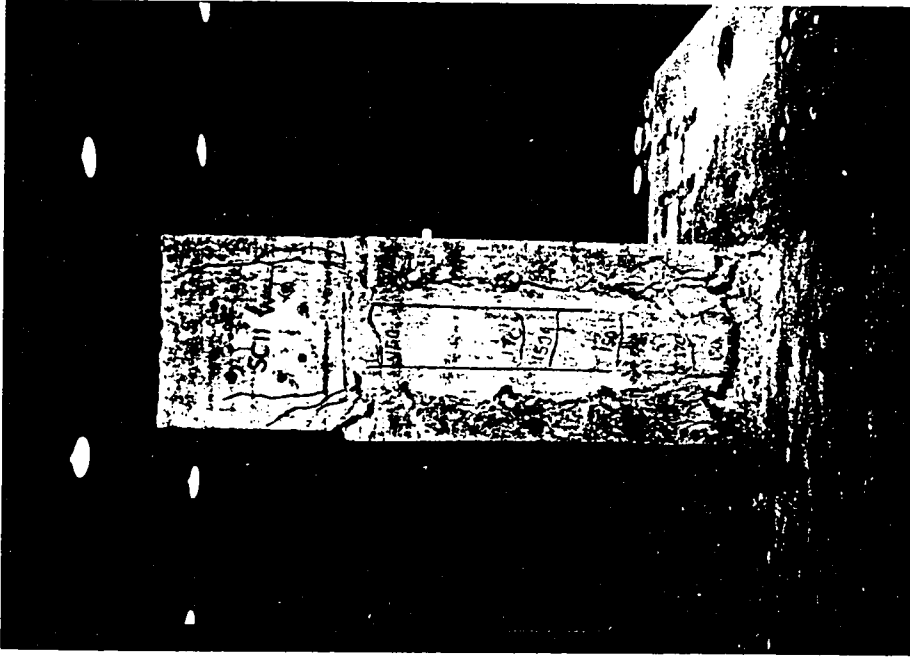


(b) Hysteretic Response

Figure 5.31 Strengthened Shear Column SC11

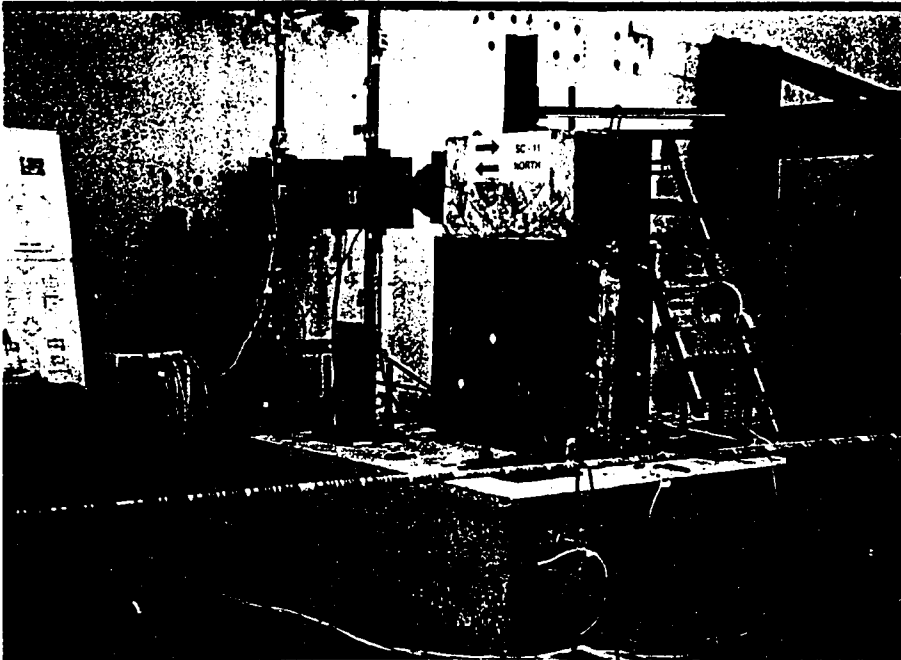


(a) Column SC11 at the end of the test

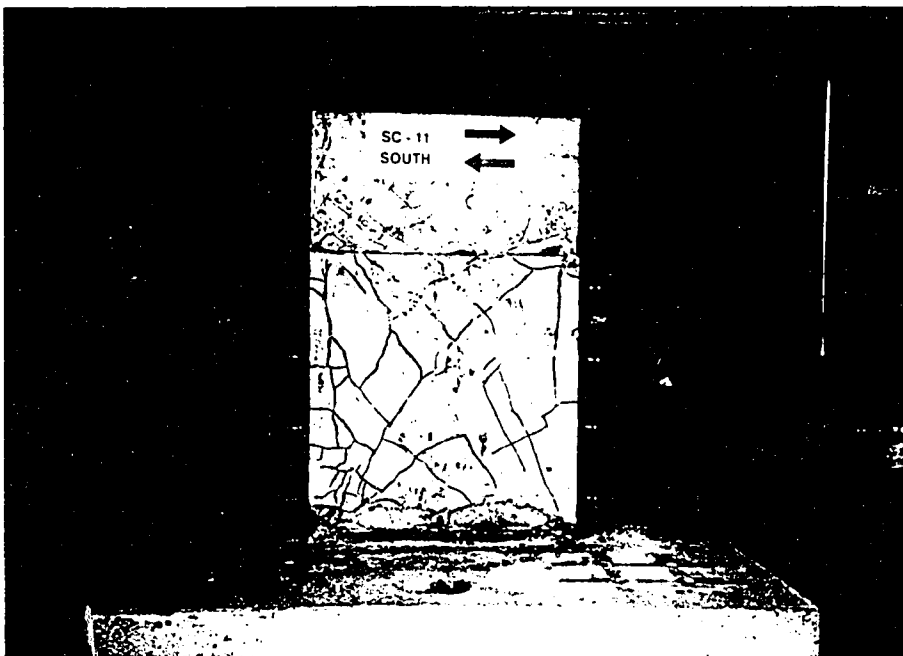


(b) Crack pattern after the removal of the steel jacket

Figure 5.32 Strengthened Shear Column SC11



(a) Column SC11 at the end of the test



(b) Crack pattern after the removal of the steel jacket

Figure 5.33 Strengthened Shear Column SC11

## **CHAPTER 6**

### **ADDITIONAL EXPERIMENTAL DATA - FLEXURAL COLUMNS ( With Inadequate Lap Splices )**

#### **6.1 INTRODUCTION**

This chapter presents comparison and further discussion of the flexural columns. Selected strain gage data measured on the reinforcing bars and on the steel jackets are also presented. Envelopes of load versus drift ratio, energy dissipation, column stiffness and column rotation are described. The effectiveness of steel jackets with anchor bolts and through rods is evaluated. The influence of different variables is discussed. These variables include:-

- height of the steel jacket,
- number and pattern of adhesive anchor bolts,
- width of column

Further discussion and analysis of the test results are also provided in Chapter 8.

#### **6.2 ENVELOPES OF THE CYCLIC RESPONSE**

In this section the envelopes of the cyclic response of the flexural

columns with inadequate lap splices is presented. The envelopes of the load-drift curves are plotted in the first quadrant for easier comparison.

Figure 6.1 shows the envelopes of the cyclic response of the flexural columns FC1 and FC2. Notice that the envelopes of the east and west sides of column FC2 are plotted on the same side. Figure 6.1 shows that both sides of column FC2 developed higher strength and stiffness than the basic unretrofitted column FC1. While column FC1 showed strength degradation at drift ratios higher than 1.65 %, both sides of column FC2 maintained their lateral strength to over 4.0 % drift ratio.

On the east side of column FC2, the steel jacket was stiffened with one vertical line of five adhesive anchor bolts. The presence of these bolts provided for a small increase in the lateral strength of column FC2 on the east side over the west side ( without anchor bolts ). On such 36 inch wide columns, a 1/4 inch thick steel jacket has poor out-of-plane flexural stiffness. Adhesive anchor bolts stiffen the steel jacket and help confine the splice. Columns FC1 and FC2 had relatively high concrete strength. The concrete compressive strength at the day of testing for columns FC1 and FC2 were 4700 and 4900 psi, respectively. This high concrete strength resulted in a relatively strong splice. Consequently, the anchor bolts produced only modest improvements. Improvements in column performance resulting from the anchor bolts are more dramatic for specimens with lower strength concrete, as discussed below.

Figure 6.2 shows the envelopes of the cyclic response of columns FC4,

FC9 and FC12. The main variables in this series are the number and pattern of the adhesive anchor bolts. Concrete strength for these columns varied between 2850 and 3265 psi. The basic unretrofitted column FC4 exhibited low strength and ductility. The splice failure occurred just before the development of the nominal yielding flexural capacity. However, the retrofitted columns FC9 and FC12 showed significantly higher strength and ductility.

The response of columns FC9 and FC12 clearly show the effectiveness of the use of anchor bolts with the steel jacket for strengthening wide columns with inadequate lap splices. In a retrofitted column, the corner spliced bars receive good confinement by the corner of the steel jacket. The intermediate spliced bars along the width of the column do not get similar confinement due to the poor out-of-plane flexural stiffness of the steel jackets. The use of anchor bolts for wide columns ensures the confinement of the intermediate spliced bars.

The results for column FC12 reveal that a good distribution of anchor bolts over the sides of the steel jacket can result in higher strength and better ductility. On the west side of column FC12, the steel jacket was stiffened with only four anchor bolts. This side, however, exhibited better performance than the east side of column FC9 which was stiffened with five anchor bolts. This is attributed to the better distribution of the adhesive anchor bolts and a slightly higher concrete strength.

Figure 6.3 illustrates the deformation of the steel jacket with and



without anchor bolts as observed during the tests. During the tests, it was observed that the anchor bolts forced the steel jacket to deform with the concrete column and helped confine the splice region.

Figure 6.4 shows the response envelopes of columns FC4, FC11 and FC12. The main variables in this series are the height of the steel jacket and the number of the adhesive anchor bolts. The height of the steel jackets on columns FC11 and FC12 were equivalent to 1.2 and 1.5 times the splice length, respectively. On the east side of column FC11, the steel jacket was stiffened with a total of eight anchor bolts. On the west side of column FC12, the steel jacket was stiffened with only four adhesive anchor bolts. As can be seen from Figure 6.4, column FC11 showed slightly higher lateral strength than FC12. However, column FC12 exhibited much better ductility. The presence of more anchor bolts improved the confinement of the intermediate bars and consequently, allowed the development of almost equal strains in the longitudinal bars in the splice region. However, the presence of more anchor bolts did not ensure good column ductility. On the other hand, increasing the height of the steel jacket by approximately 12 inches above the top of the spliced bars considerably improved the ductility of the column. Extending the steel jacket above the top of the splice allowed fastening the top of the steel jacket to the concrete column above the location of a potential major flexural crack, right above the top of the splice.

Figure 6.5 shows the envelopes of the cyclic response of columns FC14 and FC16. The main variable in this series was the anchor bolts. Specimens FC14 and FC16 were each 27 inch wide columns. The concrete strength of

columns FC14 and FC16 were 4165 and 2565 psi, respectively. Although the concrete strength of column FC16 was less than  $2/3$  of that of column FC14, it showed higher strength and ductility because of the presence of the steel jacket. The east side of column FC16, which was strengthened with a steel jacket and anchor bolts, exhibited more stable response than the west side which was strengthened with only a plain steel jacket.

Figure 6.6 shows the envelopes of the cyclic response of column FC15 and FC17. Specimens FC15 and FC17 were 18 inch wide columns. The steel jacket of column FC17 was different from all other steel jackets. It was provided with four additional corner angles. These angles were welded to the steel jacket after casting and hardening of the non-shrink grout as described in section 4.18. The concrete strength of column FC15 and FC17 at the day of testing were 4165 and 2635 psi, respectively. Compared to the response of the basic unretrofitted column FC15, both sides of column FC17 exhibited much higher strength and ductility. The west side of column FC17, without anchor bolts, performed as good as the east side with anchor bolts. For such 18 inch wide columns with an inadequate lap splices, plain steel jackets appear capable of improving their seismic resistance without anchor bolts.

Figures 6.7 and 6.8 show the envelopes of the cyclic response of the basic unretrofitted and repaired columns. The repaired columns represent post-earthquake repair of columns with an inadequate lap splices. Columns FC4, FC6, FC10 and FC13 were transversely reinforced with a cross tie at every other longitudinal bar. Columns FC5 and FC7 were transversely reinforced with a cross tie at every longitudinal bar.

Adhesive anchor bolts with steel jackets were very effective for pre-earthquake strengthening of columns with inadequate lap splices. However, the use of anchor bolts with steel jackets were not as effective for post-earthquake repair of columns with inadequate lap splices, as seen in Figure 6.7. The severe deterioration of the concrete column's core considerably reduces anchorage strength and stiffness of the adhesive anchor bolts. However, columns repaired by the use of steel jackets with through threaded rods exhibited very satisfactory performance.

The results of the post-earthquake repaired columns, show that the initial stiffness of the repaired columns was lower than that of the basic unretrofitted column FC4. This low initial stiffness is due to the presence of several cracks outside the splice region over theunjacketed height of the column. These cracks open up under small loads and contribute to the observed poor initial stiffness. On the other hand, it is important to notice here that the basic unretrofitted column FC4 was an initially undamaged column; it had no cracks prior to testing.

The results of the repaired columns indicate that if it is desirable to control drift of a damaged structure, it is important to jacket the columns over their full height, although the columns may have only inadequate lap splices at their ends. Jacketing the column over its full height will likely improve stiffness and reduce drifts.

### 6.3 LATERALSTIFFNESS OF COLUMNS

Stiffness degradation of reinforced concrete members is attributed to spalling of concrete cover, bond deterioration between steel bars and concrete, decrease of the modulus of elasticity of the cracked concrete, and alternate opening and closing of residual cracks.

In this section, comparison of the lateral stiffnesses of columns with inadequate lap splices is presented. The lateral stiffness versus the drift ratio plots are discussed. Most of the retrofitted columns were strengthened with un-symmetrical steel jackets. Thus, the secant stiffness of the specimens was evaluated, to minimize the influence of one side of the specimen on the other. The secant stiffness is the slope of a line from the origin to a point on the load-deformation plot.

Figure 6.9 through 6.15 show the lateral stiffness of the basic and the strengthened columns with inadequate lap splices. The variations in actual concrete strengths and the resulting variations in the actual modulus of elasticity of concrete was not accounted for in the plots. Concrete strength of the test columns is presented in Table 3.3. Lateral stiffness plots show sharp decreases in the column stiffness with increasing drift ratio. Also, these plots show that the rate of loss in stiffness is lower for columns retrofitted with steel jackets and anchor bolts than those retrofitted with plain steel jackets (without anchor bolts).

Although column FC11 had a shorter steel jacket than column FC12,

it showed higher stiffness than column FC12 at drift ratios below 3.0 %. This is likely due to the higher number of anchor bolts used on the column FC11 steel jacket.

Figure 6.12 shows the lateral stiffness versus drift ratio plots for columns FC14 and FC16. Due to higher concrete strength, column FC14 exhibited higher initial stiffness than column FC16. Column FC14 experienced a 50 % sudden drop in stiffness after the failure of the splice at 1.2 % drift ratio. While, column FC16 did not experience any sudden drop in stiffness. The side of FC16 with anchor bolts showed stiffness degradation at a lower rate than the side without anchor bolts.

Figure 6.13 shows the lateral stiffness versus drift ratio for columns FC15 and FC17. Although column FC15 had higher concrete strength, the initial stiffness of column FC15 was lower than the initial stiffness of the east side of column FC17, probably due to the presence of the adhesive anchor bolts and the residual tensile stresses in column FC17's steel jacket. These residual stresses produced by welding additional angles at the jacket corners after grouting, likely caused active lateral confinement of the concrete column in the splice region.

In general, it was observed that, compared with the basic unretrofitted columns, the retrofitted columns with steel jackets exhibited a lower rate of stiffness degradation. Further, the use of anchor bolts reduced the rate of stiffness degradation of the jacketed columns.

Figures 6.14 and 6.15 show the envelopes of the lateral stiffness versus drift ratio for the basic unretrofitted and the repaired columns with inadequate lap splices. The plots reveal that the repaired columns had initial stiffness lower than that of the basic unretrofitted columns. After testing, column FC12 was repaired and tested as column FC13. Only the splice region of column FC12 was repaired. The flexural cracks on the concrete column outside the splice region were left unrepaired. These cracks opened up under very small lateral loads and contributed to the observed poor initial stiffness. Column FC7, repaired by welding the splice, showed similar poor initial stiffness. Both repaired columns FC13 and FC7 exhibited a much lower rate of stiffness degradation compared to the basic unretrofitted columns FC4 and FC5, respectively.

#### **6.4 ENERGY DISSIPATION**

In order to survive major earthquakes, structures should be capable of absorbing and dissipating energy greater than that input to the structure by the earthquake. In this section the cumulative energy dissipated by the test columns is presented and discussed. The dissipated energy presented is considered approximate because frictional losses in the test system are ignored. The energy dissipated during the tests was computed as the area within the hysteretic loops from the lateral load-displacement. Energy values were computed for each half of a test column, since different retrofits were used on opposite sides of many of the columns. The reported energy values can therefore be interpreted as half of the total energy dissipation capacity of a column, if the same retrofit were used on both sides.

Figures 6.16 through 6.22 show the envelopes of the cumulative energy dissipated by the basic unretrofitted, strengthened and repaired flexural columns with inadequate lap splices. The cumulative energy dissipation plots reveal that columns retrofitted with steel jackets are capable of dissipating large amounts of energy as compared to the basic unretrofitted columns.

Columns strengthened with steel jackets and anchor bolts showed higher energy dissipation than columns strengthened with plain steel jackets, as shown in Figures 6.16 through 6.20. However, the increase in the energy dissipation due to the use of anchor bolts becomes insignificant when the concrete strength of the column is high (Column FC2) and/or the steel jacket has high tensile residual stresses in the transverse direction (Column FC17). It is also observed that columns strengthened with longer steel jackets and fewer anchor bolts dissipated more energy than columns that were strengthened with shorter steel jackets and a larger number of anchor bolts. Compared with the strengthened columns, the repaired columns exhibited lower energy dissipation, as shown in Figures 6.17, 6.21 and 6.22.

The total energy dissipated by each test column was computed for either push or pull direction of loading separately, and is shown in Figures 6.23 through 6.25. The maximum drift ratio to which the column was loaded is shown in parentheses on the plots. Observations from these plots are similar to those discussed above.

## 6.5 STRAIN GAGE DATA

In this section, selected strain gage data, helpful in understanding the behavior of the unretrofitted and the retrofitted columns is presented. Strain gages were installed on selected longitudinal reinforcing bars, transverse reinforcement, through rods and steel jackets. The properties of the steel reinforcement and the steel jacket plates are presented in Table 3.5. The strain gage data is presented as the lateral load applied on the specimen versus the strain in the steel bars/jackets.

A large number of strain gages were used. However, only selected results are presented which represent typical strain gage data and which are most useful in understanding the behavior of the test specimens.

### 6.5.1 Strains in the Longitudinal Reinforcing Bars

Figures 6.27 through 6.31 show plots of the strain gage data measured on the main longitudinal reinforcing bars for the basic unretrofitted column FC4, the strengthened columns FC9, FC11 and FC12, and the repaired column FC13. Figure 6.26 shows the locations of the strain gages. For the basic unretrofitted column FC4, the maximum strain at the peak load was just below the actual yielding strain of the reinforcing bars. The peak load was limited by the inadequate lap splice, which failed before the development of the yielding flexural capacity of the column. For the strengthened and repaired columns, the maximum strain measured on the longitudinal bars was well above the yielding strain of the bars. As revealed by the plots in Figures



6.28 and 6.31, all the retrofitted columns developed the yielding flexural capacity of the column section, but at different drift ratios.

### 6.5.2 Strains in the Transverse Reinforcement

The strains in the transverse reinforcement were measured at the mid-length of the cross-ties at/or near the spliced bar location. The spacing between the layers of the transverse reinforcement was 16 inches. The first two layers were at 4 inches and 20 inches from the face of the footing. For the basic unretrofitted column FC4, the strains in the cross ties were measured at the first two layers. The transverse reinforcement was #3 grade 40 deformed bars. However, the actual yield strength was 58 ksi.

Figure 6.32 shows the locations of reported strain gages. For column FC4, strain gages SG6 and SG7 were installed on the mid-length of the cross ties located at 4 inches and 20 inches from the bottom of the splice. Figure 6.33 and 6.34 show the recorded strains by strain gages SG6 and SG7, respectively. The plots revealed that the strains in the strain gage SG6 are almost twice those of strain gage SG7. This is due to the arrangement of the spliced bars. The column main longitudinal bars were the outside spliced bars. They were terminated at the bottom of the column. If the splice were to form a mechanism, the column bars near the bottom of the splice would tend to move outward more than near the top of the splice. This helps explain the observed high strains in the strain gage SG6 relative to SG7.

Column FC9 was strengthened by the use of a long rectangular steel

jacket. The steel jacket on the east side of column FC9 was provided with one vertical line of five anchor bolts located at the mid-width of the column. Strain gage SG8 was installed at the mid-length of a cross tie located at 4 inches from the bottom of the splice. Figure 6.35 shows the measured strains of the strain gage SG8. The plot reveals that the cross tie exhibited higher strains when the splice without anchor bolts is in tension. This indicates that the presence of anchor bolts reduces the required confinement by the transverse reinforcement to develop the yielding flexural capacity of the column.

Column FC12 was strengthened by the use of a long steel jacket and anchor bolts. Strain gage SG9 was installed on a cross tie near a pair of spliced bars located at 4 inches from the bottom of the splice. Figure 6.36 shows strain gage SG9's measured strains. The plot shows high strains by the cross tie before any splice failure. This indicates that the presence of the steel jacket prevents anchorage failure of the cross tie.

Column FC13 was repaired by the use of steel jacket and through rods. Strain gage SG10 was installed on a cross tie near a pair of spliced bars located at 4 inches from the bottom of the splice. Figure 6.37 shows strain gage SG10's measured strains. Both columns FC12 and FC13 developed their yielding flexural capacity and maintained it to large drift ratios. The maximum strains measured by the strain gage SG9 was near 25000 micro-strain. However, the maximum strains recorded by strain gage SG10 was below 2200 micro-strain. The splice region of column FC12 was passively confined by the transverse reinforcement and the steel jacket with anchor

bolts. The splice region of column FC13 was passively confined by transverse reinforcement and actively confined by the steel jacket and through threaded rods.

### 6.5.3 Strains in the Through Rods

Column FC13 was repaired by the use of a steel jacket and two vertical lines of three through rods each. The rods were 3/4 inch in diameter. They were unbonded to the concrete column. The threaded through rods were inserted into pre-drilled holes in the column, and tightened manually by a wrench. Strain gages were installed on three through rods at three different levels: 8", 20" and 32" above the bottom of the splice. The top, middle and bottom through rods had an initial prestress equivalent to strains of 330, 437 and 413 micro-strain, respectively. This corresponds to approximate preloads of 3.3 kips, 4.3 kips and 4.1 kips, respectively.

Figures 6.38 through 6.40 show the strains in the strain gages SG11, SG12 and SG13. The plots reveal that the bottom through rod showed the highest stress increase, while the top rod showed the lowest stress increase. This indicates that the bottom of the splice causes an outward pressure on the steel jacket higher than the top of the splice. Note that the maximum strains in the through rods were all well below the actual yield strain of the rods.

#### 6.5.4 Strains in the Steel Jackets

Strain gages were installed on the steel jackets of the retrofitted columns as shown in Figure 6.41. Strain gages SG14 through SG25 were installed on the steel jacket at 4 inches from the bottom of the column, except strain gages SG22 and SG24, where they were installed at 12" from the bottom of the column (the mid-height of the splice). The strain gages were all in the plane of the splices.

Figures 6.42 and 6.43 show the measured strains in column FC2's steel jacket. The concrete strength of column FC2 at the day of testing was 4900 psi. This relatively high concrete strength contributed considerably to the good performance of column FC2. The plots in Figures 6.42 and 6.43 reveal that the east side (with anchor bolts) showed slightly lower strains than the west side (without anchor bolts). The difference in strains was likely due to the presence of the adhesive anchor bolts on the east side. The difference was insignificant due to the high concrete strength. It is also observed that the levels of strains on either side of the steel jacket were unequal. This suggests that the type of deformations at the bottom of the steel jacket are not pure transverse axial tensile strains, but rather, are influenced by some shear forces transferred by the steel jacket.

Figures 6.44 and 6.45 show the plots of the measured strains on column FC9's steel jacket. Column FC9 had concrete strength of 2905 psi at the day of testing. Figures 6.44 and 6.45 reveal that both sides of the steel jacket, with and without anchor bolts, showed almost the same maximum

strain. However, the east side ( with anchor bolts ) of column FC9 maintained its peak lateral capacity to over 3.0 % drift ratio, while the west side ( without anchor bolts ) exhibited loss in strength at drift ratios above 1.6 %. It is also observed that the maximum measured strain on the west side occurred at 2.7 % drift ratio. At higher displacements the strain gage SG17 showed lower strains. This may be due to deterioration of the concrete in the vicinity of the spliced bars in the splice region, and consequently bond deterioration between the spliced bars and the surrounding concrete. The east side strain gage SG16 showed similar performance except the maximum strain was reached at 3.2 % drift ratio. It is observed that the lateral strength of column FC9 started degrading at 750 micro-strain and 650 micro-strain on the east and west side, respectively.

Figure 6.46 and 6.47 show plots of measured strains on column FC12's steel jacket. The east and the west sides of column FC12's steel jacket were stiffened with eight and six adhesive anchor bolts, respectively. The west side of column FC12 was loaded to larger displacements than the east side. The maximum measured strain was, on the west side, just below 950 micro-strain. However, the drop in the lateral strength on the west side of column FC12 was observed at strains near 770 micro-strain.

Figures 6.48 and 6.49 show the plots of the measured strains on the repaired column FC13's steel jacket. Strain gage SG20 and SG21 were installed on the east side of column FC13 at 12 inches and 4 inches from the bottom of the splice. The plots in Figures 6.48 and 6.49 reveal that the measured strains in the steel jacket at the mid-height of the splice are almost

half the strains at 4 inches from the bottom of the splice. Similar results were revealed by the strain gage data on the strengthened column FC16's steel jacket, as shown in Figures 6.50 and 6.51.

## **6.6 MOMENT - CURVATURE AND LOAD - ROTATION DIAGRAMS**

The average values of the column curvature were measured over a length of 8, 10 and 20 inches from the bottom of the column (fixed end). The average curvatures measured in the 8 inches region, at the bottom of the column, include the fixed end rotation due to slippage of the longitudinal bars in the footing. This additional rotation could not be measured, but is believed to be very small. No attempt was made to correct the reported curvature for this effect.

Figures 6.52 through 6.56 show the moment-curvature diagrams for columns FC4, FC9, FC11, FC12 and FC13, respectively. The reported curvature values represent an average curvature over the lower 8 inches of the column. The moment-curvature plots show wide variation in the curvature distribution among the test specimens. This variation is attributed to the presence of the steel jacket and different patterns of adhesive anchor bolts and concrete strengths. Similarly, Figure 6.57 through 6.60 show the moment-curvature diagrams for column FC14, FC16, FC15 and FC17, respectively.

Differential rotation over 20 inches were measured between levels at 18 inches and 38 inches from the bottom of the column. This 20 inches distance spans over the top of the splice section and the top of the steel

jacket. Figure 6.61 through 6.69 show the lateral load versus the measured differential rotation. Since the measured rotation was over 20 inches, the plots are presented in load versus rotation instead of moment versus curvature. Column FC12 exhibited better ductility and higher energy dissipation. The plots of the load - differential rotation diagrams shown in Figures 6.63 and 6.64 reveal that column FC11 (with a short steel jacket) exhibited larger differential rotations than column FC12 (with a long steel jacket). Column FC12 showed smaller differential rotations because its steel jacket spans over a major critical section, the top of the splice. This reduces the amount of rotation that may be caused by the opening of the major flexural crack at the top of the splice.

## 6.7 SUMMARY

In this chapter comparison and further discussion of the flexural columns with inadequate lap splices were presented. All columns investigated were detailed according to the provisions of the ACI 318-56 and 318-83 codes. The following is a list of key observations of what were presented:

1. Unretrofitted reinforced concrete columns with inadequate lap splices were vulnerable to lateral loads. For columns having concrete strength  $\leq 3000$  psi, splice failure occurred before the development of the yielding flexural capacity of the column.
2. Rectangular steel jackets were very effective in strengthening of columns with inadequate lap splices. However, in addition to steel

jackets, adhesive anchor bolts were needed for effectively strengthening wide columns.

3. For 36 inch wide columns and smaller, having concrete strength  $\geq$  4900 psi plain steel jackets were adequate for strengthening reinforced concrete columns with inadequate lap splices.
4. For columns wider than 18 inches, having concrete strength below 4900 psi anchor bolts were required with the steel jacket for strengthening columns with inadequate lap splices.
5. The presence of anchor bolts forces the steel jacket to deform with the wide concrete columns in the splice regions, which may result in better confinement of the spliced bars than without anchor bolts.
6. Steel jackets were terminated at least 1.0" from the face of the footing or beam-column joint to prevent any possible bearing of the steel jacket against the footing or the beam-column joint.
7. It was found that the steel jackets loose their effectiveness in confining the column splice at a dilation strain of 770 micro strain.
8. Both unretrofitted and retrofitted columns investigated in this study showed very rapid lateral stiffness degradation, however, the stiffness degradation of the retrofitted columns was at lower rate.



9. The retrofitted columns exhibited much higher ductility and energy dissipation than the basic unretrofitted columns.
10. The retrofitted columns showed flexural capacity higher than the theoretical nominal flexural capacity of the basic unretrofitted columns.
11. For post-earthquake repair of columns with inadequate lap splices, steel jackets with through found to be more adequate than steel jackets with anchor bolts. Threaded rods provided at the bottom of the splice exhibited higher force increase than the rods located at higher levels.
12. Columns retrofitted with steel jackets of height equivalent to 1.5 times the splice length performed better than those retrofitted with steel jackets of height equivalent to 1.2 times the splice length.

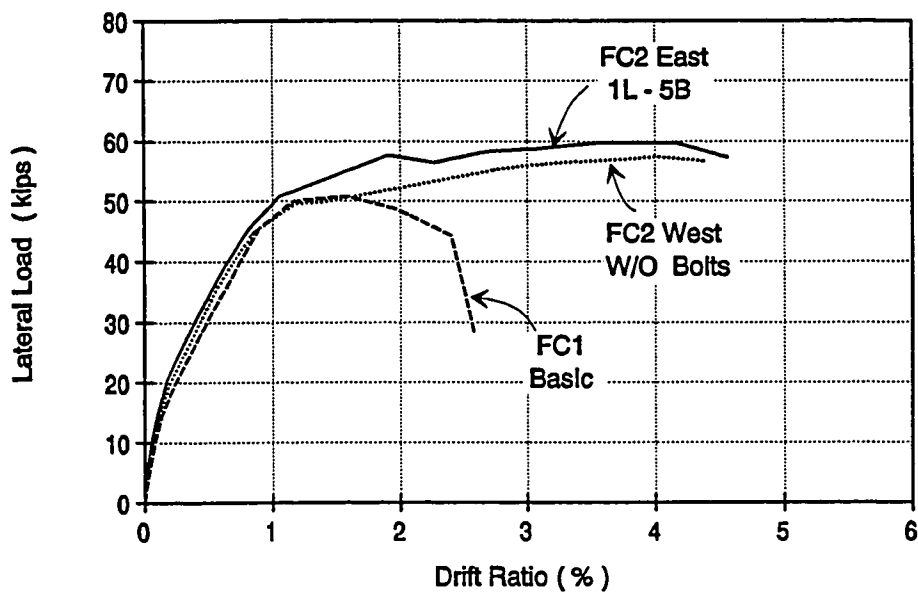


Figure 6.1 Envelopes of the Cyclic Response of the Flexural Columns FC1 & FC2 ( Pre-EQ-S )

L = Vertical Line(s) of Adhesive Anchor Bolts

B = Adhesive Anchor Bolts.

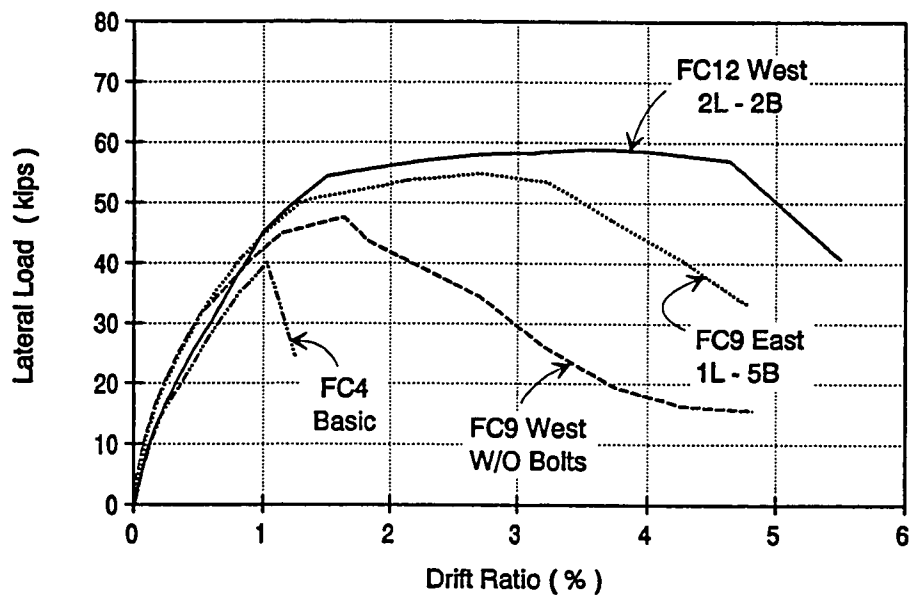


Figure 6.2 Envelopes of the Cyclic Response of the Flexural Columns FC4, FC9 & FC12 ( Pre-EQ-S )

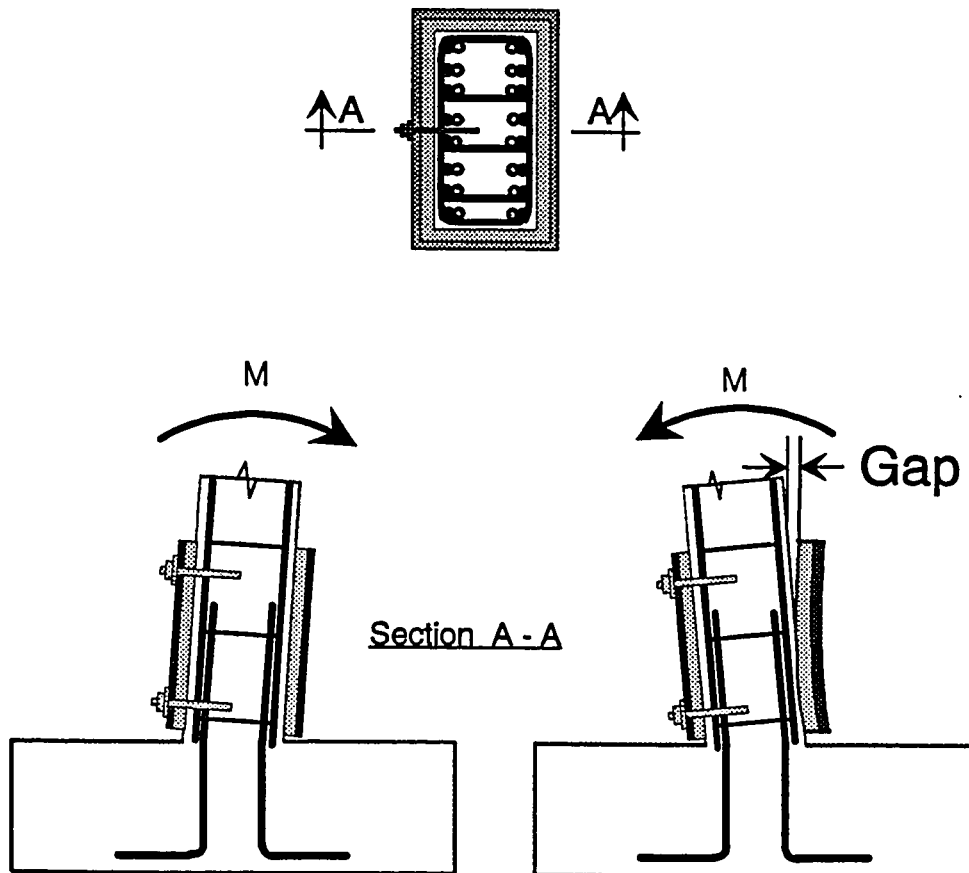


Figure 6.3 Behavior of Rectangular Steel Jackets  
With and Without Anchor Bolts

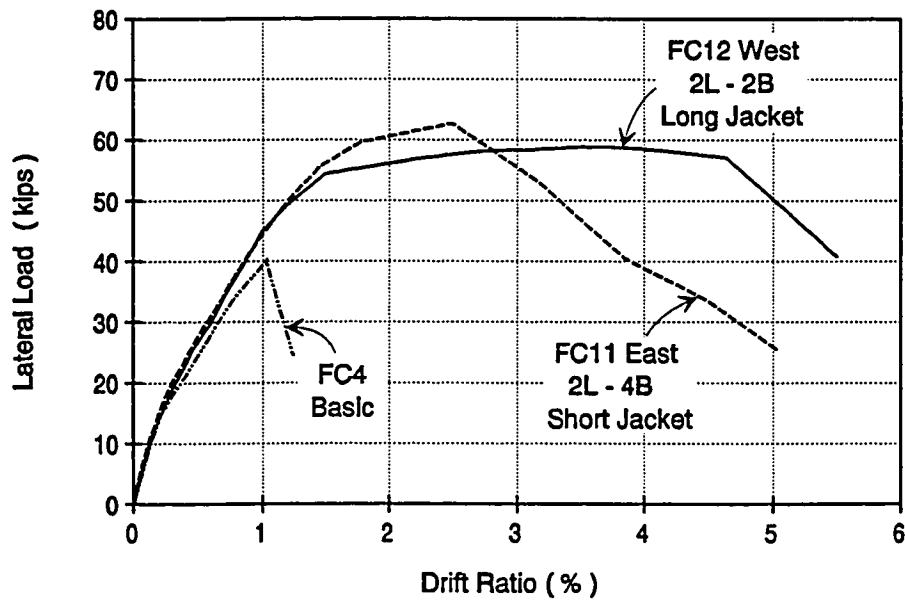


Figure 6.4 Envelopes of the Cyclic Response of the Flexural Columns FC4, FC11 & FC12 ( Pre-EQ-S )

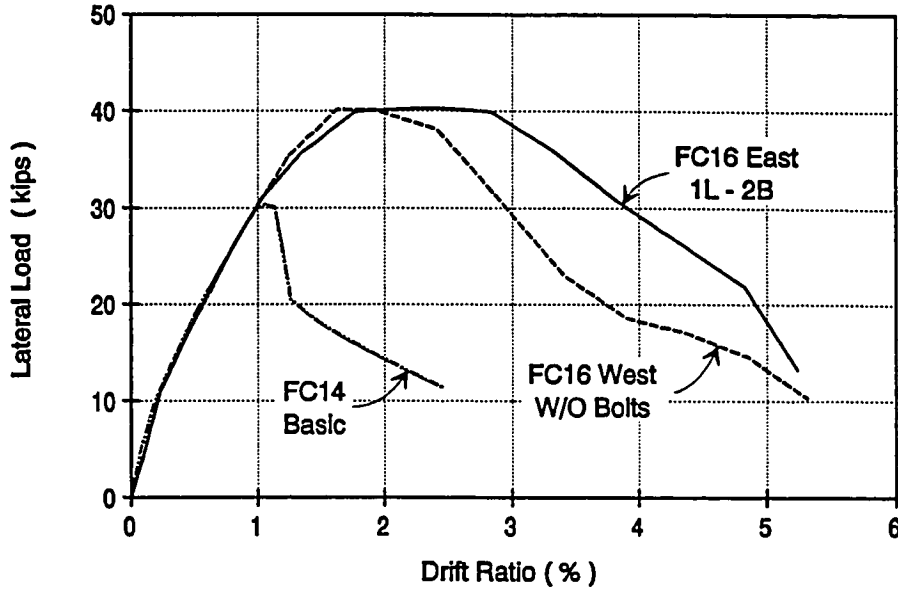


Figure 6.5 Envelopes of the Cyclic Response of the Flexural Columns FC14 & FC16 ( Pre\_EQ-S )

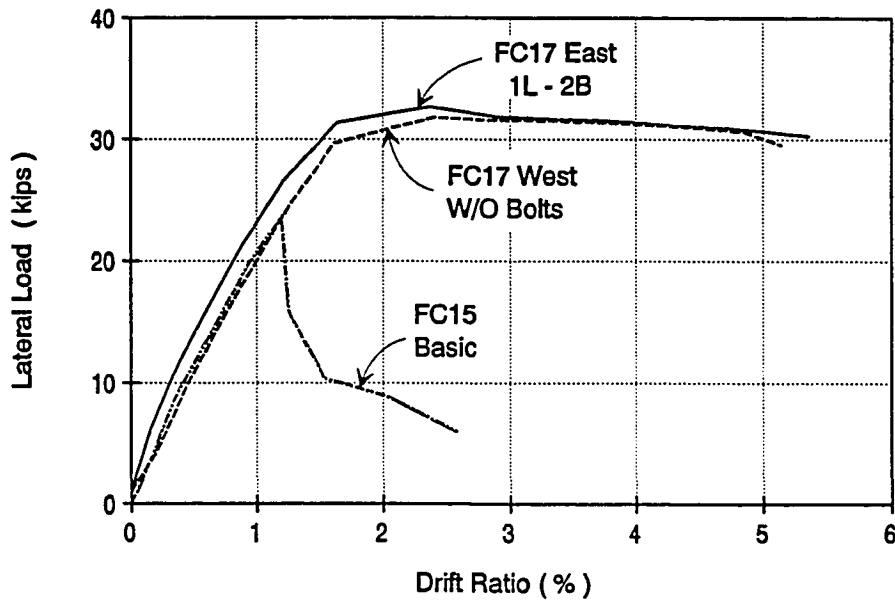


Figure 6.6 Envelopes of the Cyclic Response of the Flexural Columns FC15 & FC17 ( Pre-EQ-S )

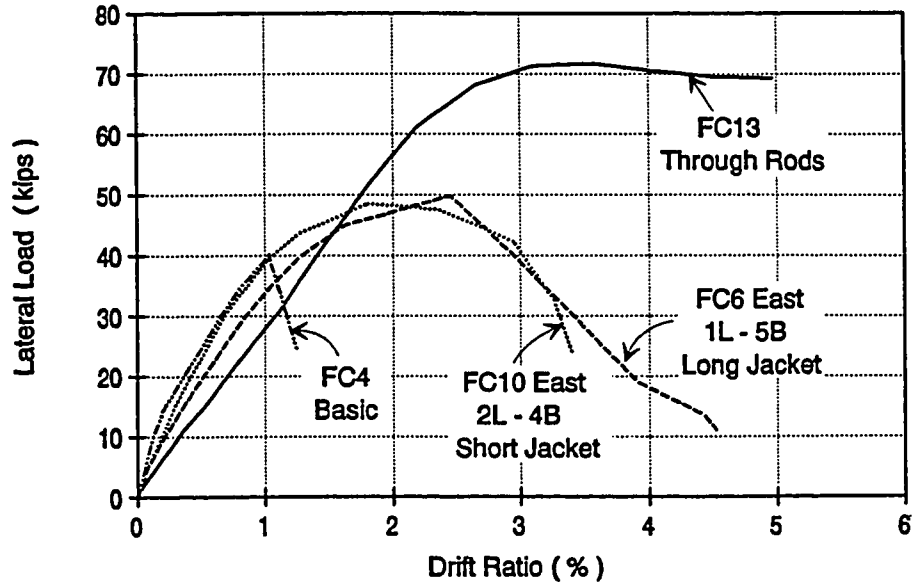


Figure 6.7 Envelopes of the Cyclic Response of the Flexural Columns FC4, FC6, FC10 & FC13 ( Post-EQ-R )

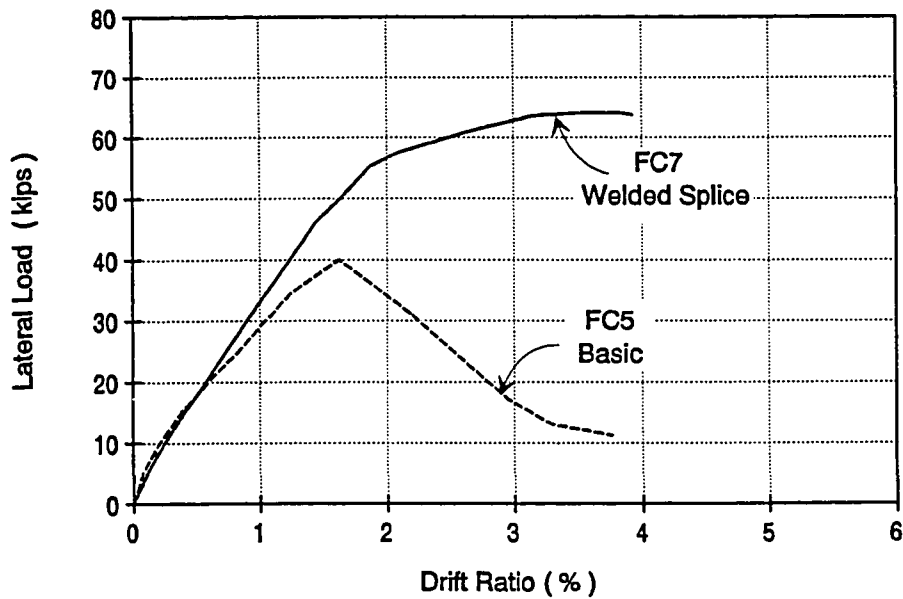


Figure 6.8 Envelopes of the Cyclic Response of the Flexural Columns FC5 & FC7 ( Post-EQ-R )

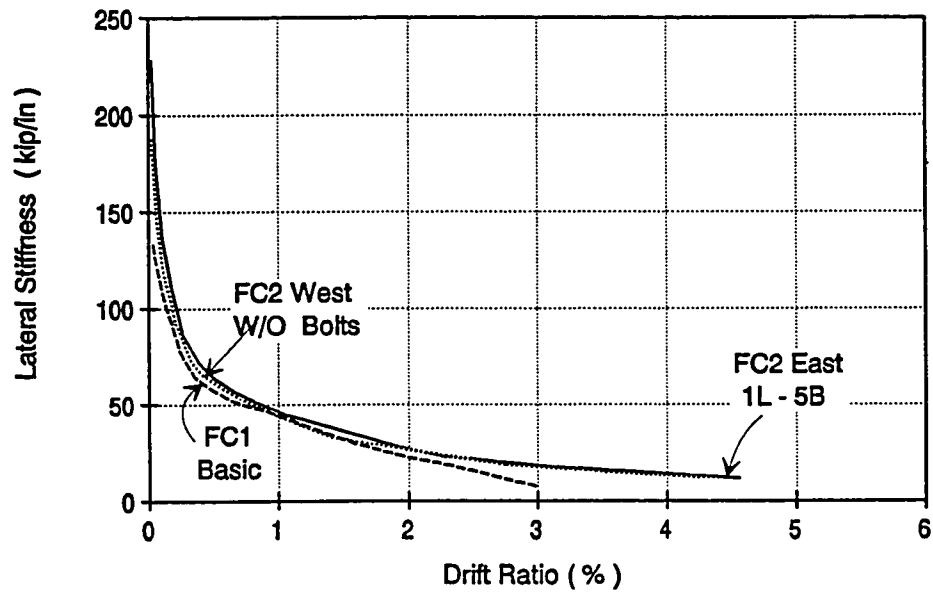


Figure 6.9 Envelopes of the Lateral Stiffness vs. Drift Ratio for the Flexural Columns FC1 & FC2 ( Pre-EQ-S )



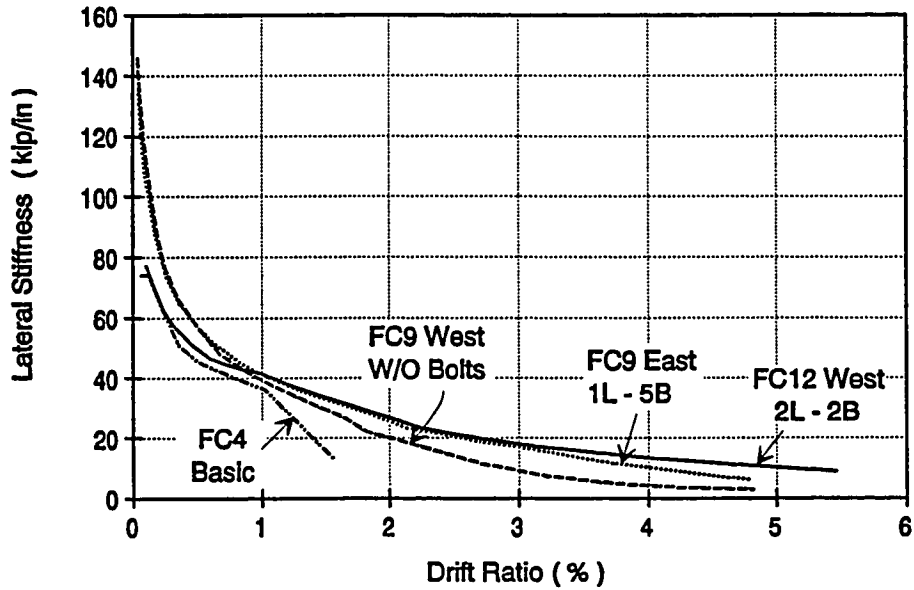


Figure 6.10 Envelopes of the Lateral Stiffness vs. Drift Ratio for the Flexural Columns FC4, FC9 & FC12 (Pre-EQ-S)

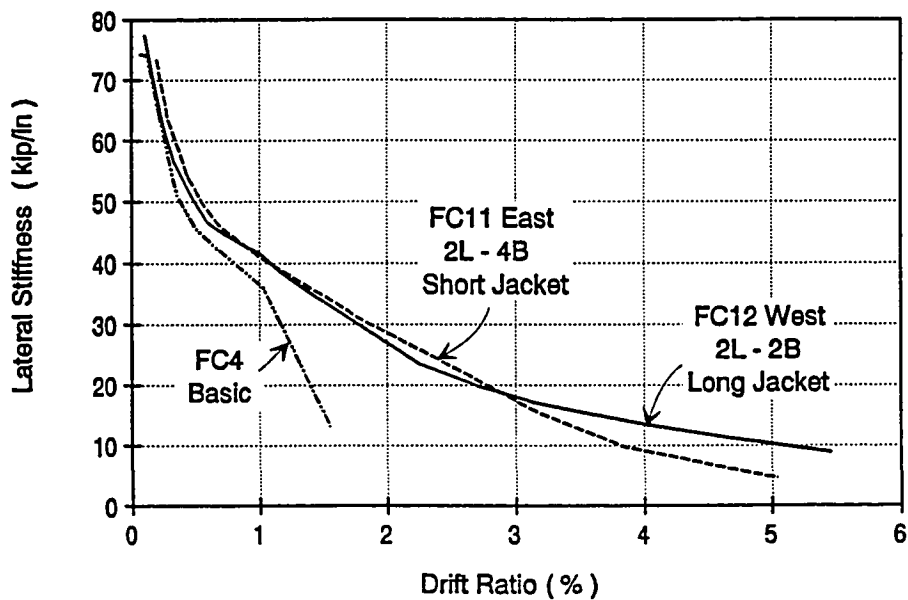


Figure 6.11 Envelopes of the Lateral Stiffness vs. Drift Ratio for the Flexural Columns FC4, FC11 & FC12 (Pre-EQ-S)

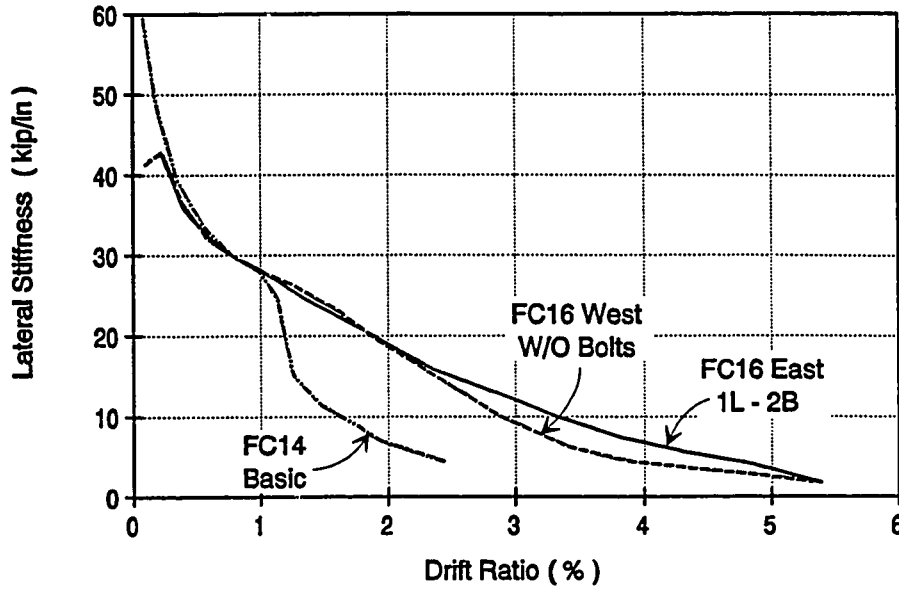


Figure 6.12 Envelopes of the Lateral Stiffness vs. Drift Ratio for the Flexural Columns FC14 & FC16 ( Pre-EQ-S )

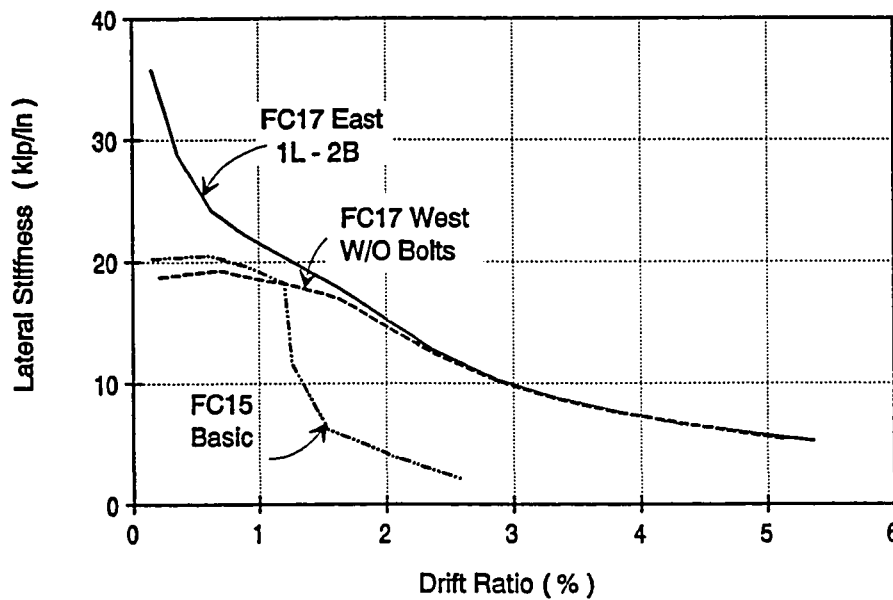


Figure 6.13 Envelopes of the Lateral Stiffness vs. Drift Ratio for the Flexural Columns FC15 & FC17 ( Pre-EQ-S )

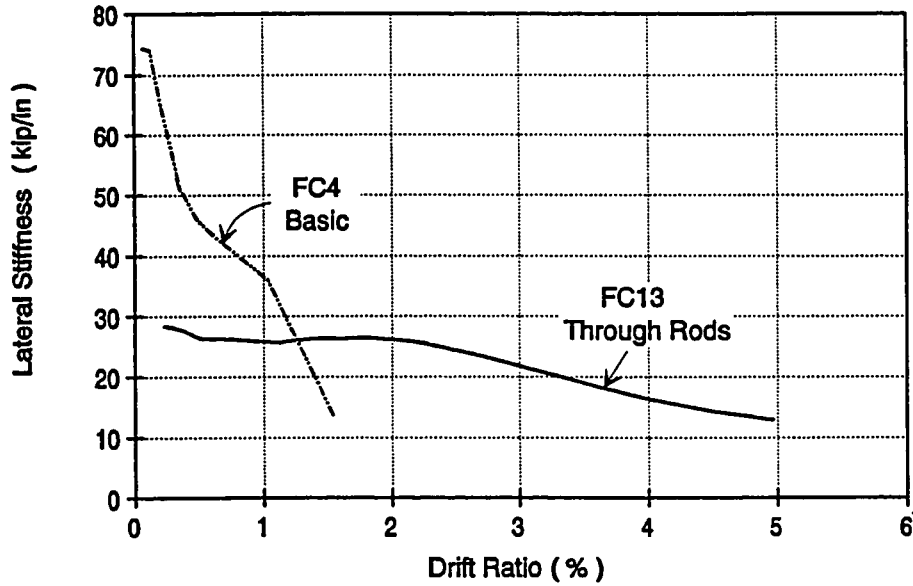


Figure 6.14 Envelopes of the Lateral Stiffness vs. Drift Ratio for the Flexural Columns FC4 & FC13 ( Post-EQ-R )

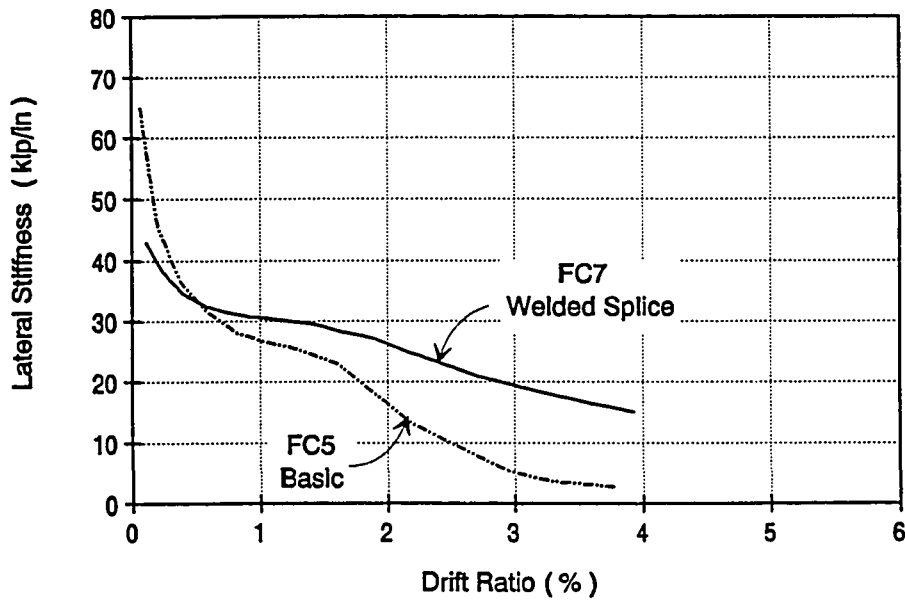


Figure 6.15 Envelopes of the Lateral Stiffness vs. Drift Ratio for the Flexural Columns FC5 & FC7 ( Post-EQ-R )

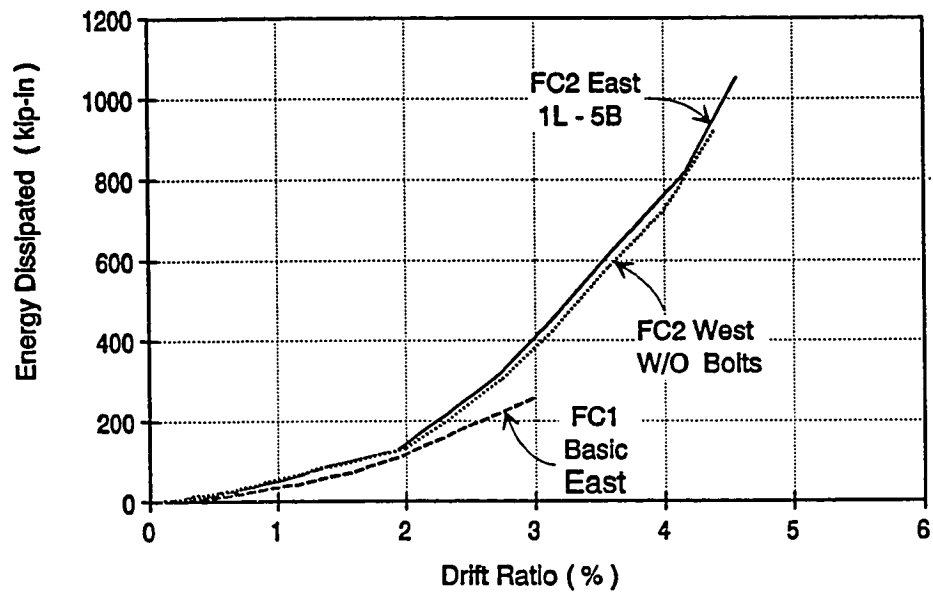


Figure 6.16 Envelopes of the Cumulative Energy Dissipated by the Flexural Columns FC1 & FC2 ( Pre-EQ-S )

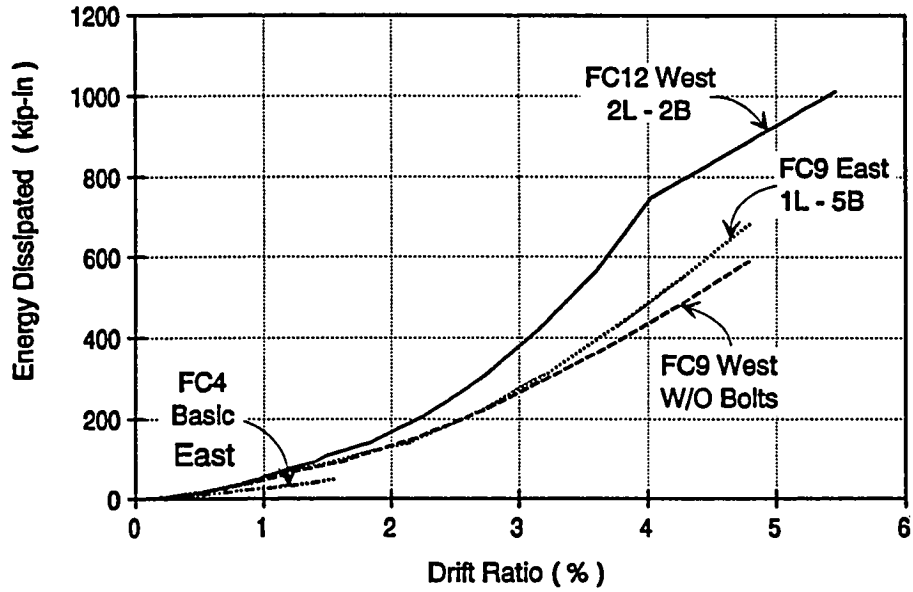


Figure 6.17 Envelopes of the Cumulative Energy Dissipated by the Flexural Columns FC4, FC9 & FC12 ( Pre-EQ-S )

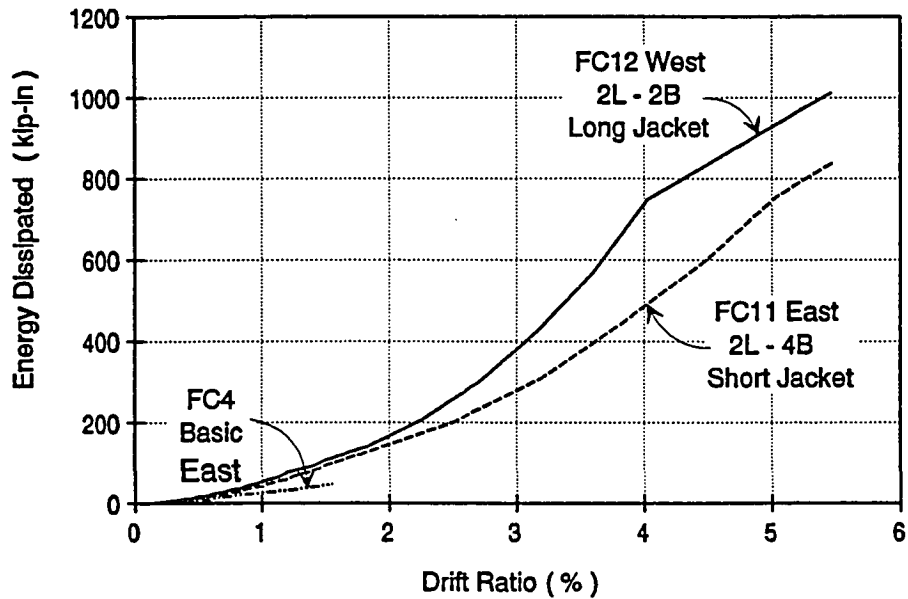


Figure 6.18 Envelopes of the Cumulative Energy Dissipated by the Flexural Columns FC4, FC11 & FC12 ( Pre-EQ-S )

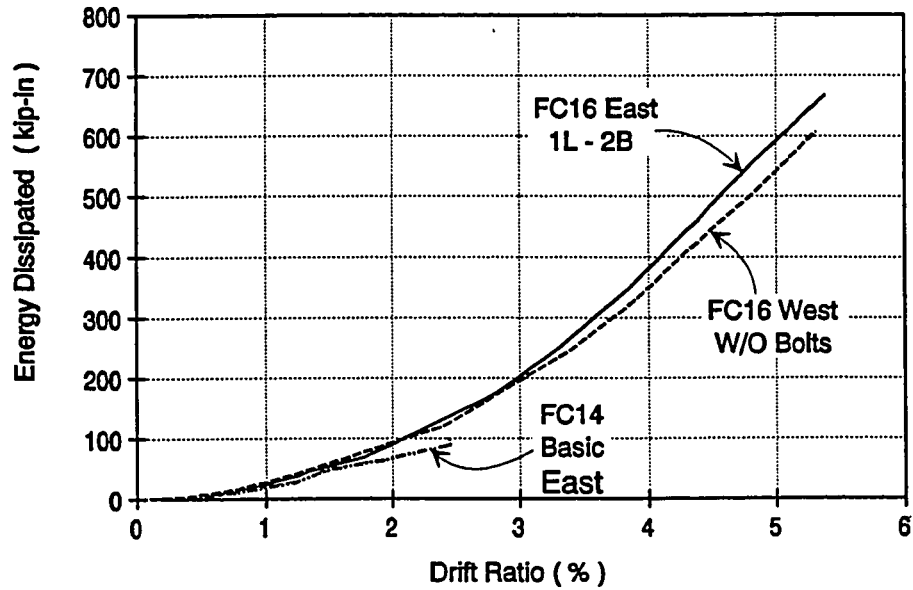


Figure 6.19 Envelopes of the Cumulative Energy Dissipated by the Flexural Columns FC14 & FC16 (Pre-EQ-S)

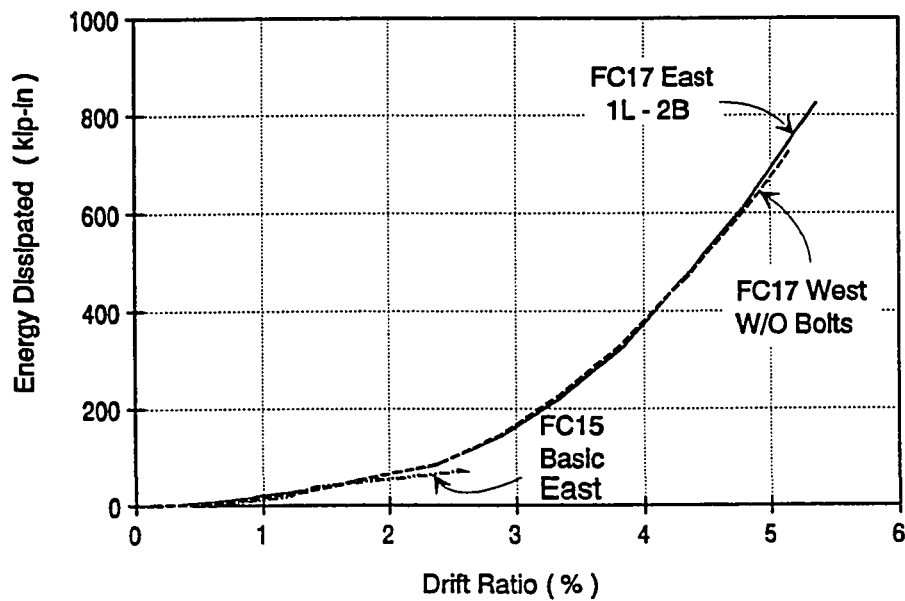


Figure 6.20 Envelopes of the Cumulative Energy Dissipated by the Flexural Columns FC15 & FC17 (Pre-EQ-S)

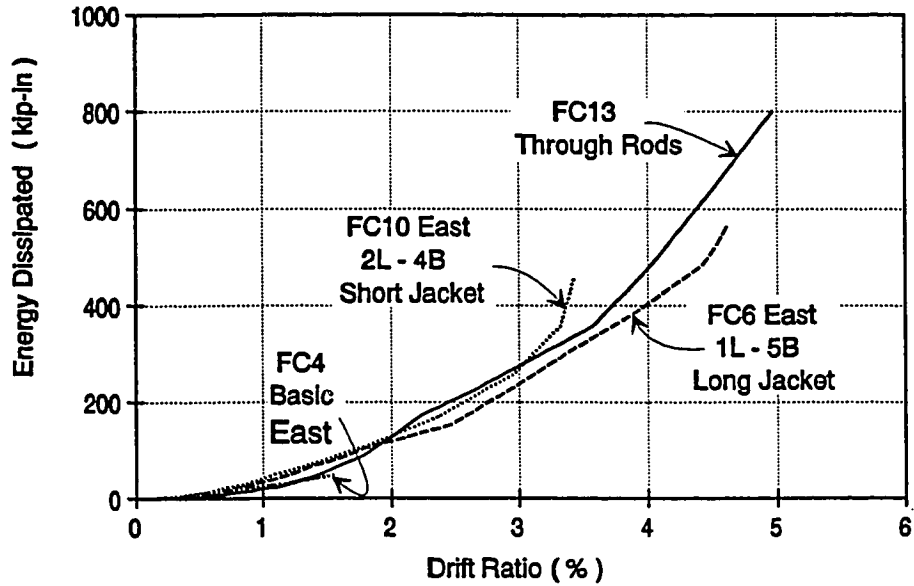


Figure 6.21 Envelopes of the Cumulative Energy Dissipated by the Flexural Columns FC4, FC6, FC10 & FC13 ( Post-EQ-R )

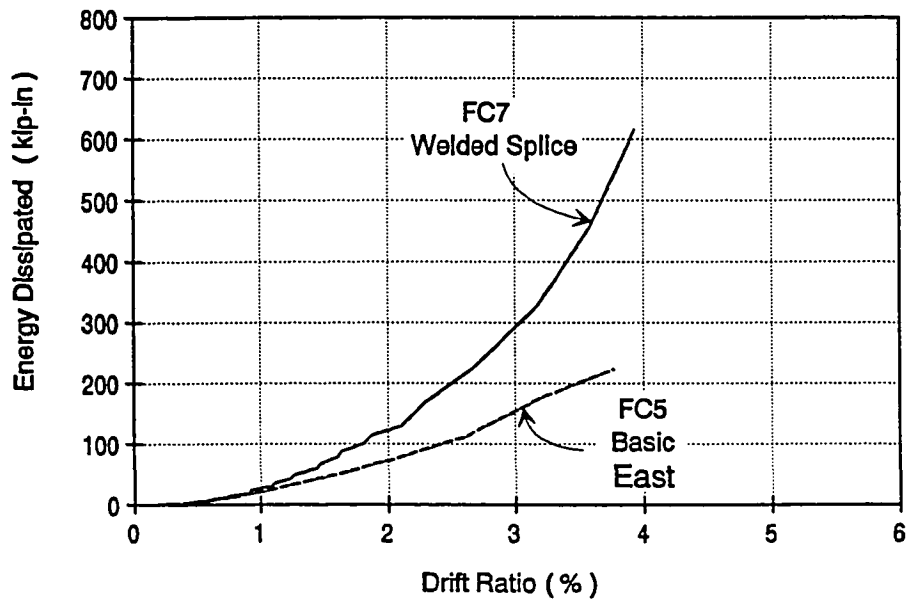
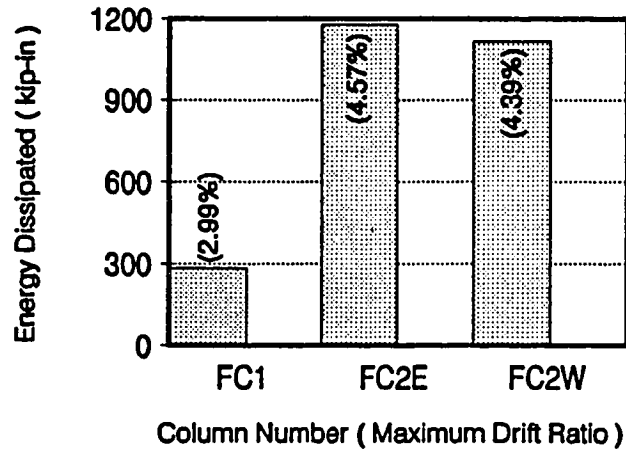
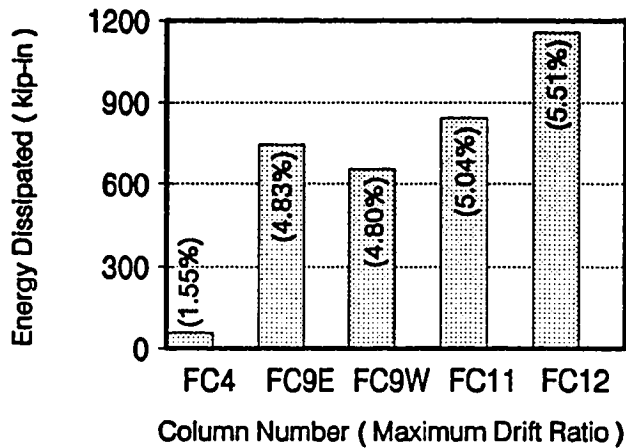


Figure 6.22 Envelopes of the Cumulative Energy Dissipated by the Flexural Columns FC5 & FC7 ( Post-EQ-R )



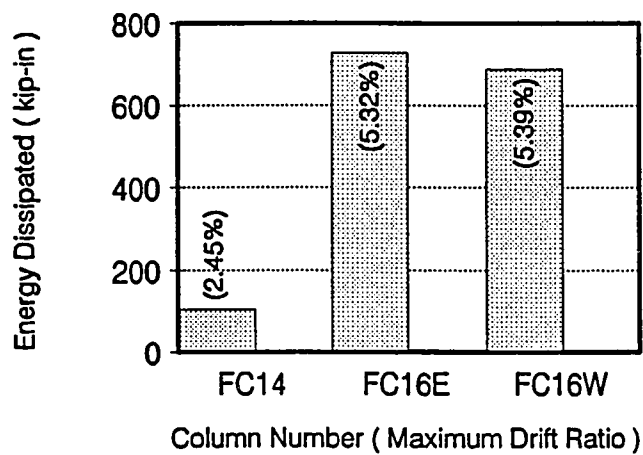
(a) Flexural Columns with X-tie at every Longitudinal Bar and High Concrete Strength



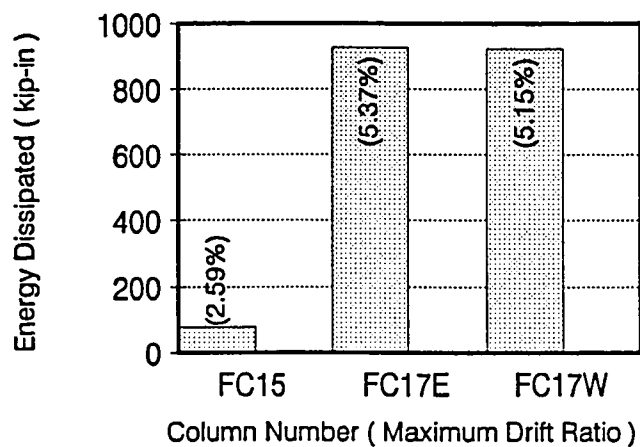
(b) Flexural Columns with X-tie at every other Longitudinal Bar and Low Concrete Strength

Figure 6.23 Cumulative Energy Dissipated by Flexural Columns ( PRE-EQ-S )



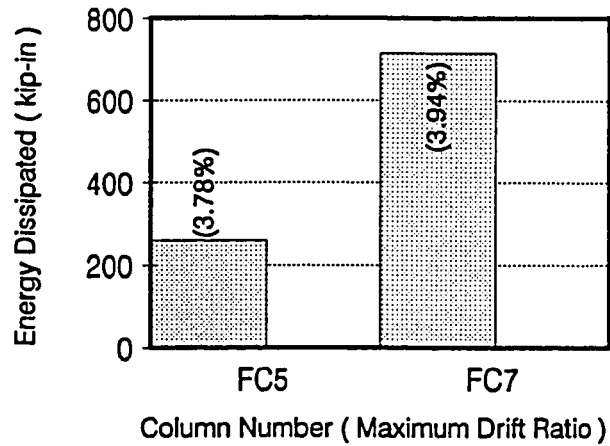


(a) 27 inch wide columns

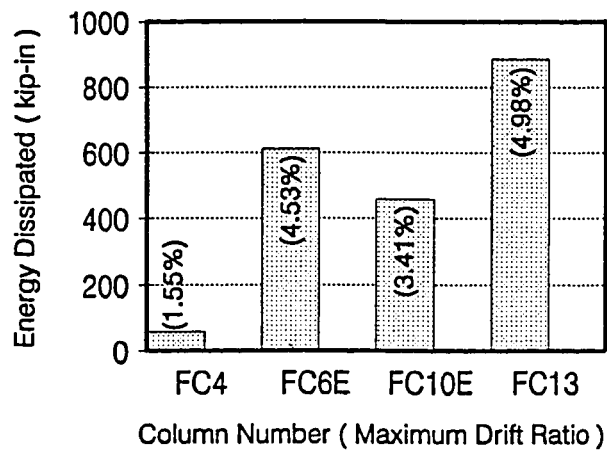


(b) 18 inch wide columns

Figure 6.24 Cumulative Energy Dissipated by Flexural Columns ( PRE-EQ-S )



(a) Flexural Columns with X-tie at every Longitudinal Bar



(b) Flexural Columns with X-tie at every other Longitudinal Bar

Figure 6.25 Cumulative Energy Dissipated by Flexural Columns ( POST-EQ-R )

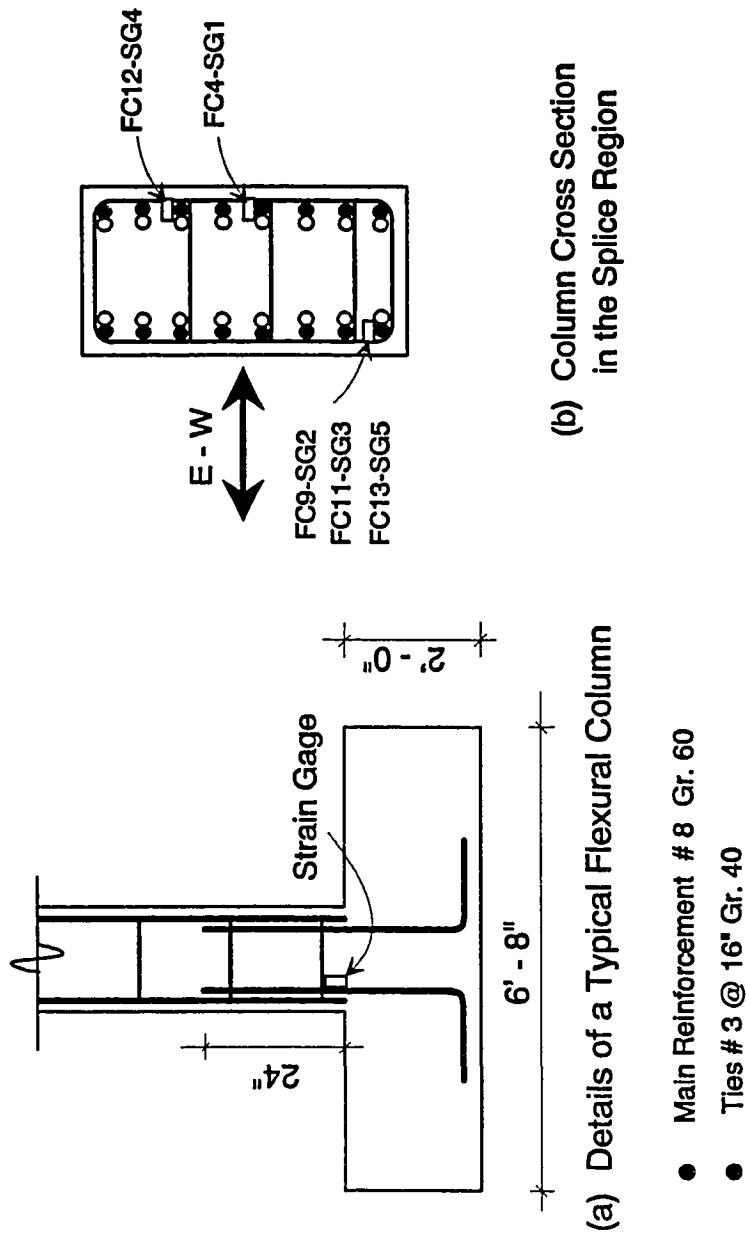


Figure 6.26 Locations of the Strain Gages on the Longitudinal Bars of the Flexural Columns

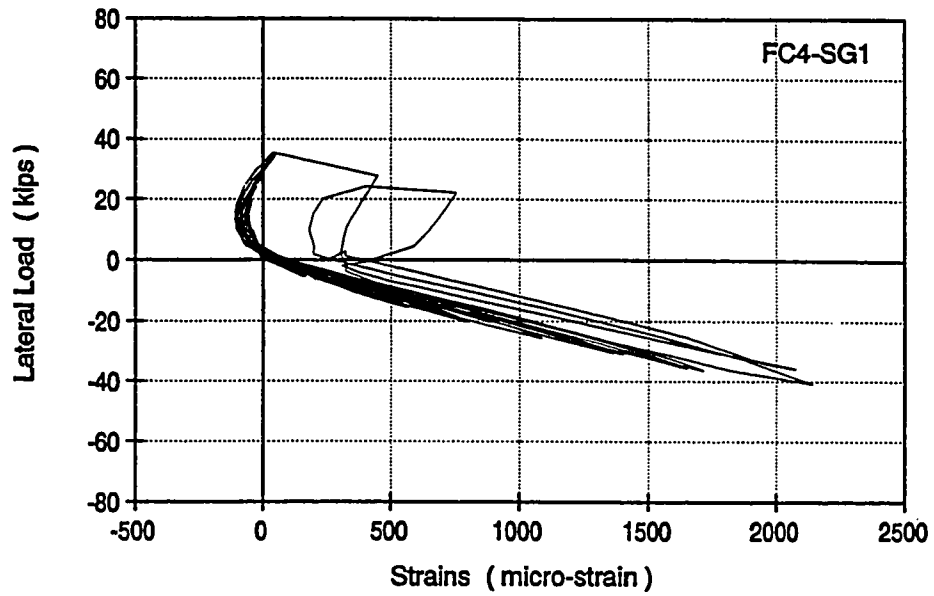


Figure 6.27 Strains in Gage # SG1

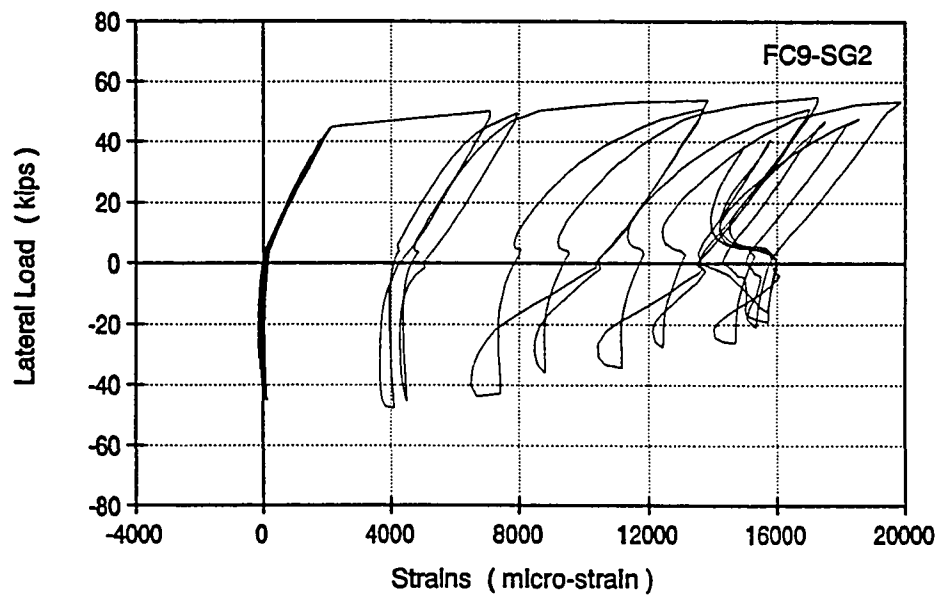


Figure 6.28 Strains in Gage # SG2

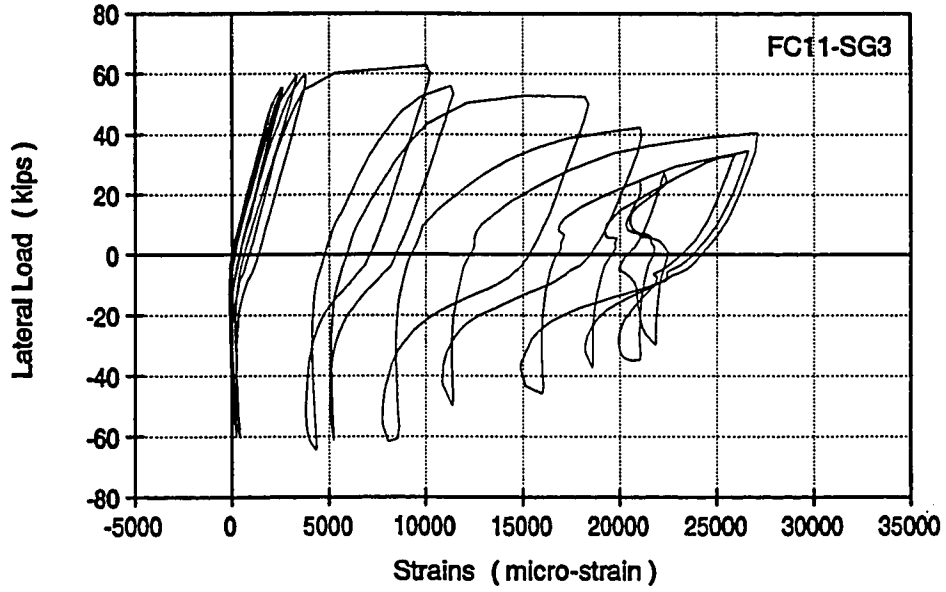


Figure 6.29 Strains in Gage # SG3

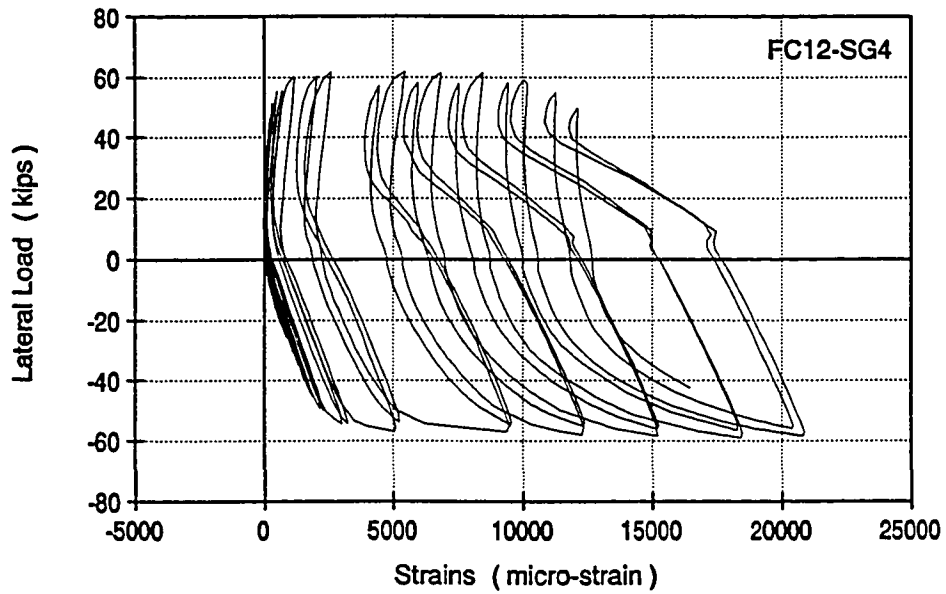


Figure 6.30 Strains in Gage # SG4

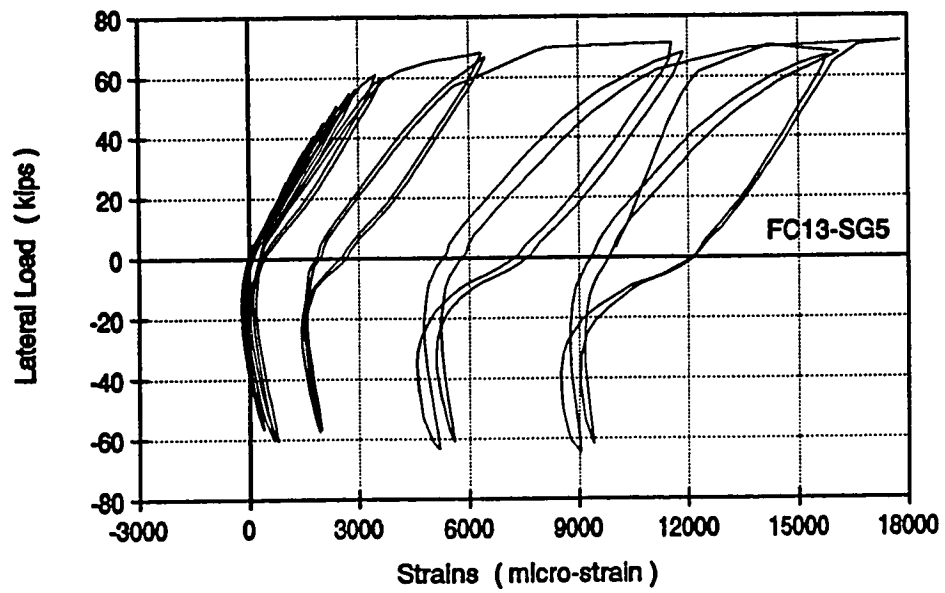


Figure 6.31 Strains in Gage # SG5

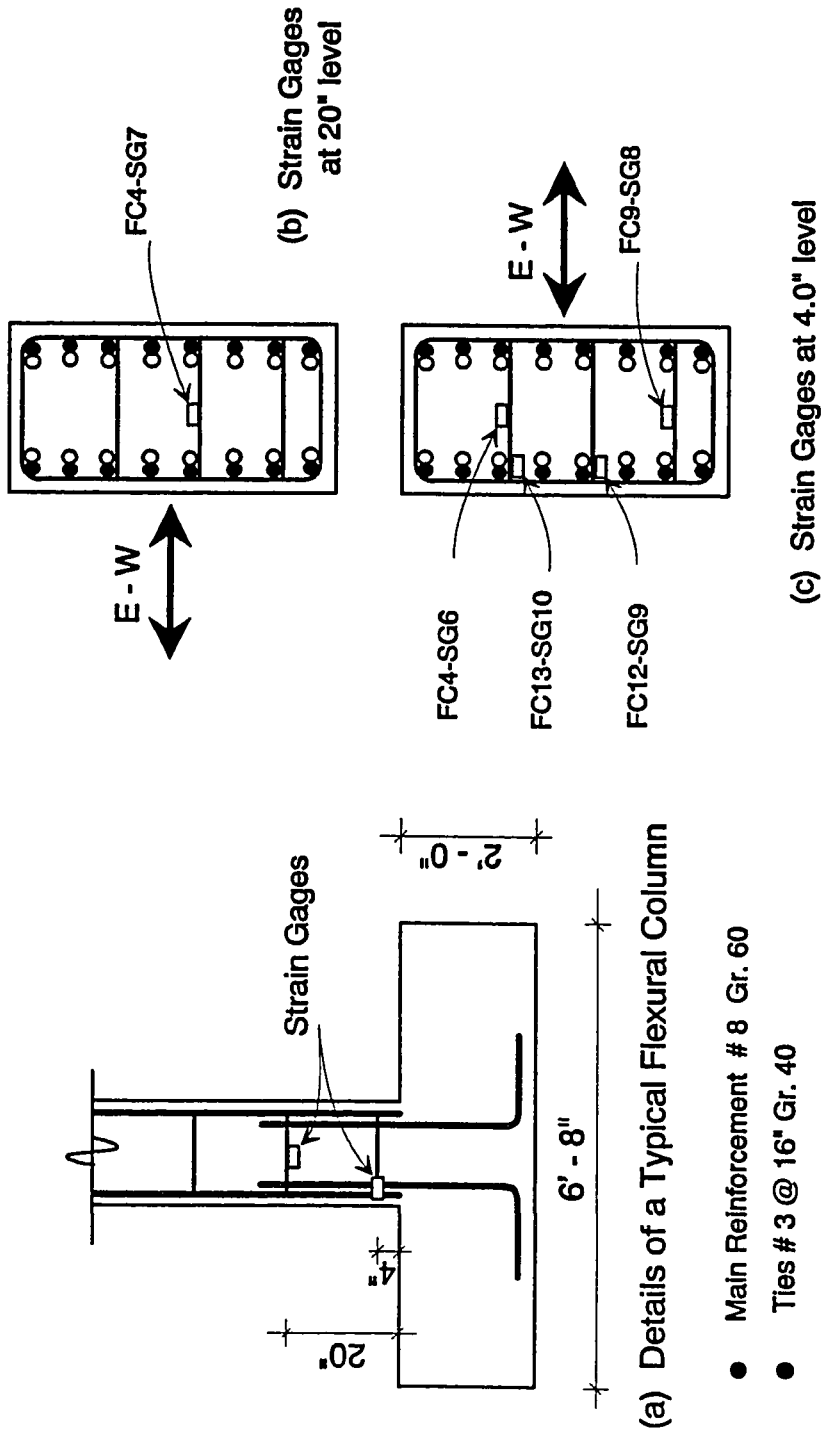


Figure 6.32 Locations of the Strain Gages on the Cross Ties of the Flexural Columns

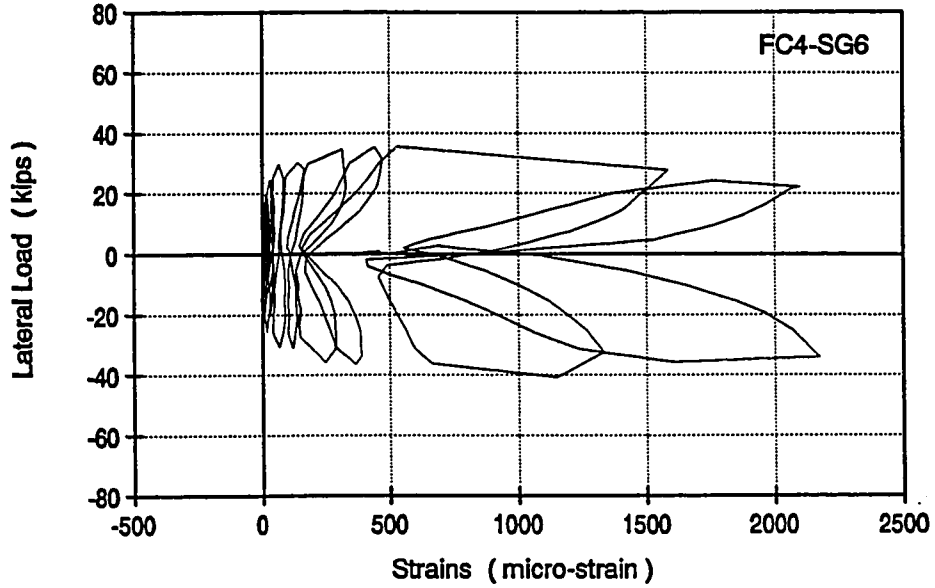


Figure 6.33 Strains in Gage # SG6

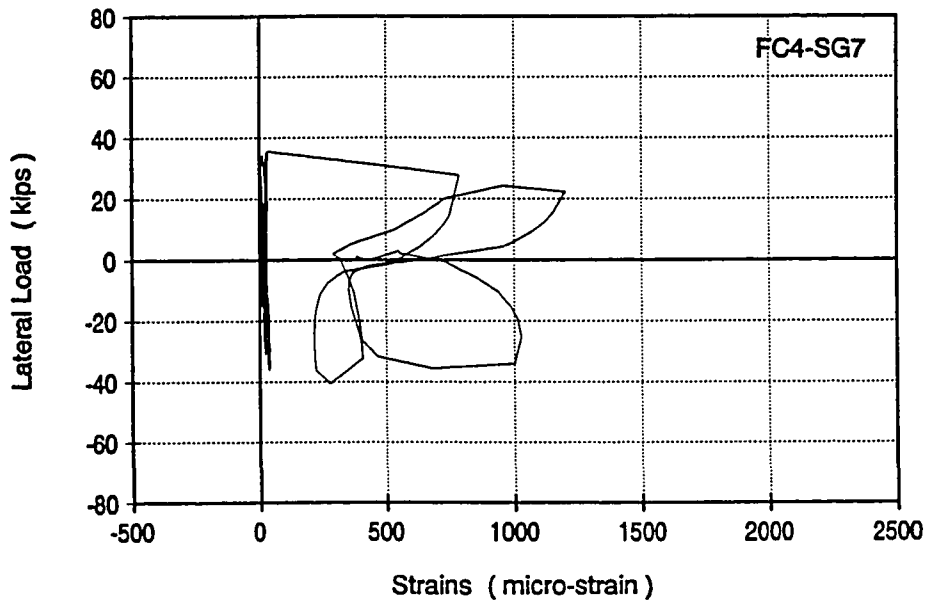


Figure 6.34 Strains in Gage # SG7



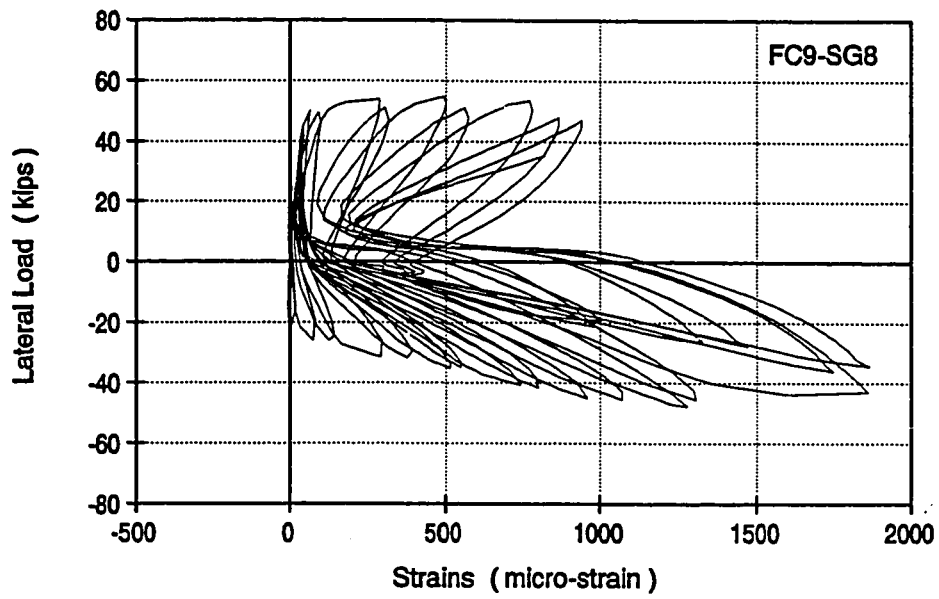


Figure 6.35 Strains in Gage # SG8

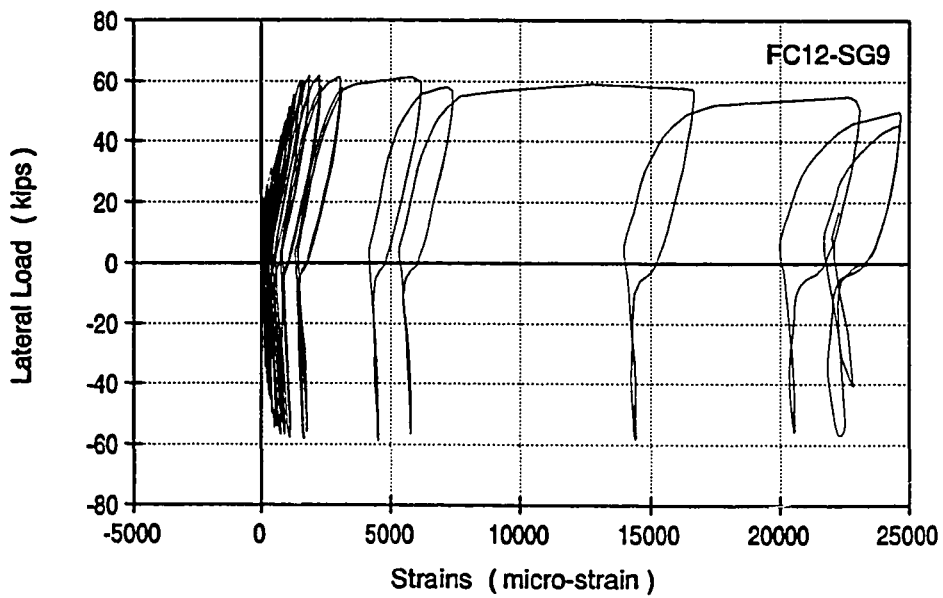


Figure 6.36 Strains in Gage # SG9

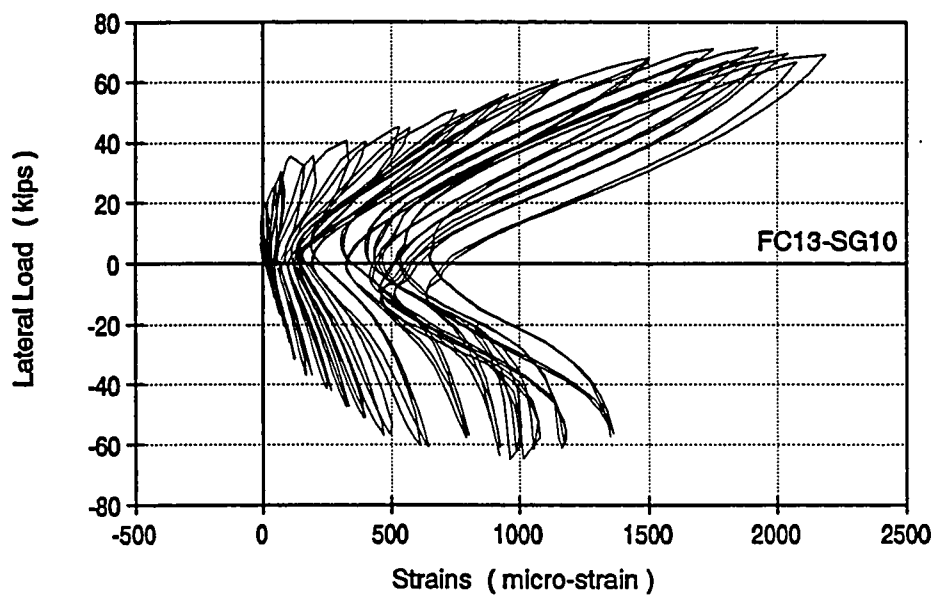


Figure 6.37 Strains in Gage # SG10

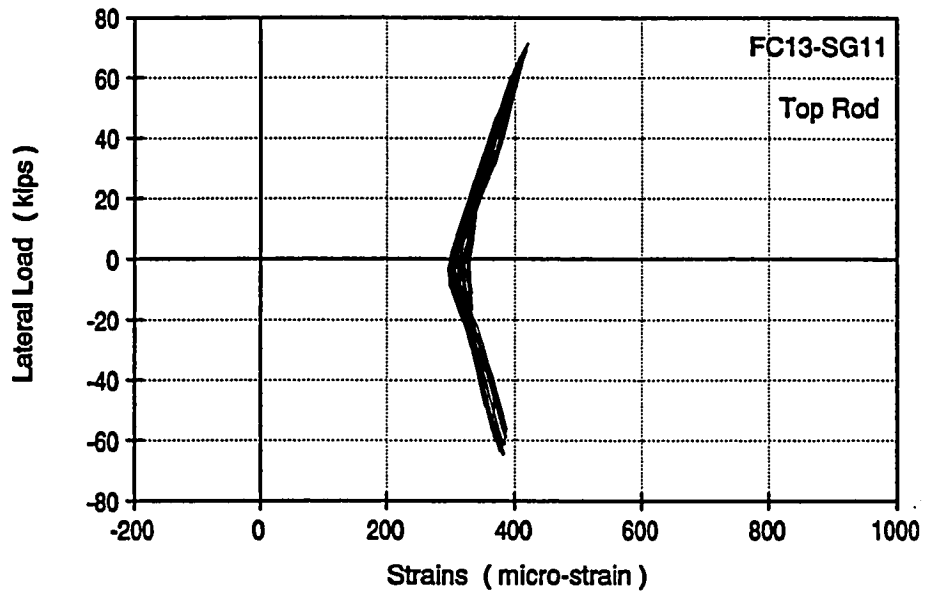


Figure 6.38 Strains in Gage # SG11

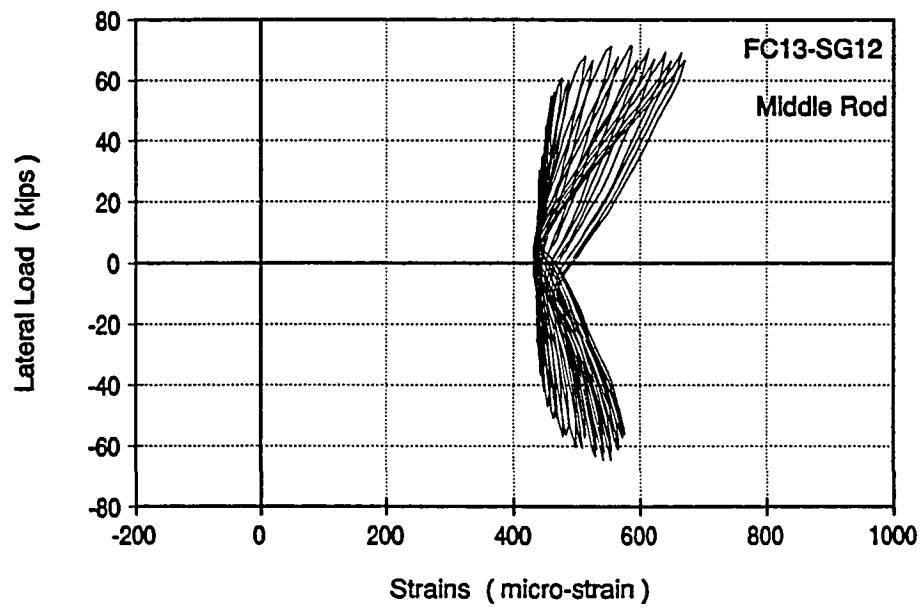


Figure 6.39 Strains in Gage # SG12

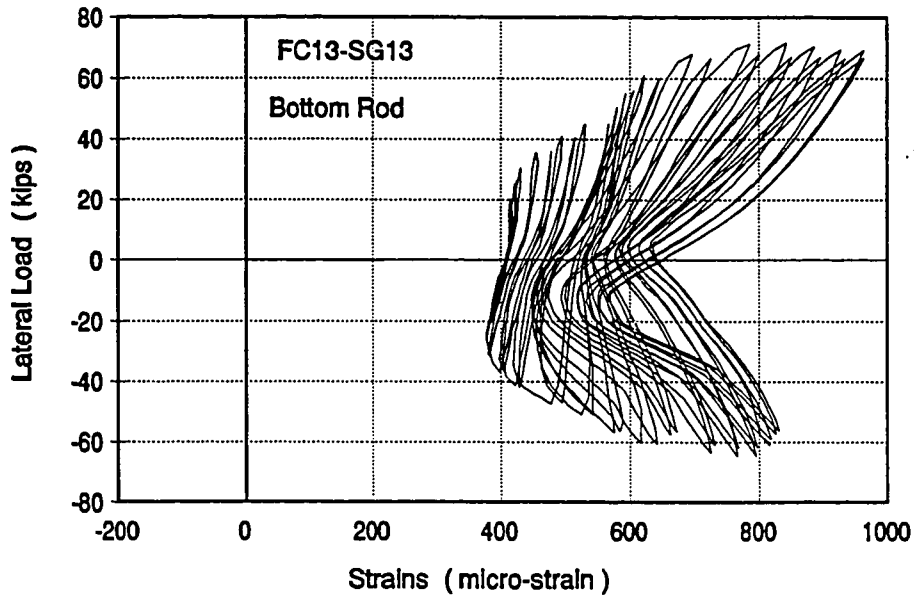


Figure 6.40 Strains in Gage # SG13

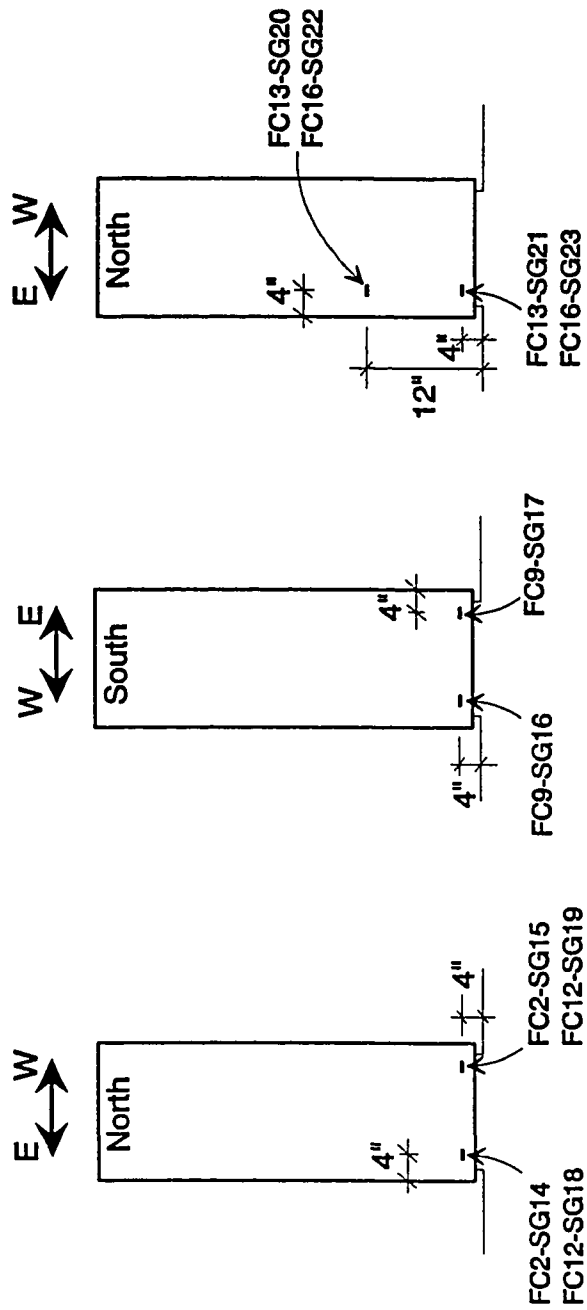


Figure 6.41 Locations of the Strain Gages on the Steel Jackets of the Flexural Columns

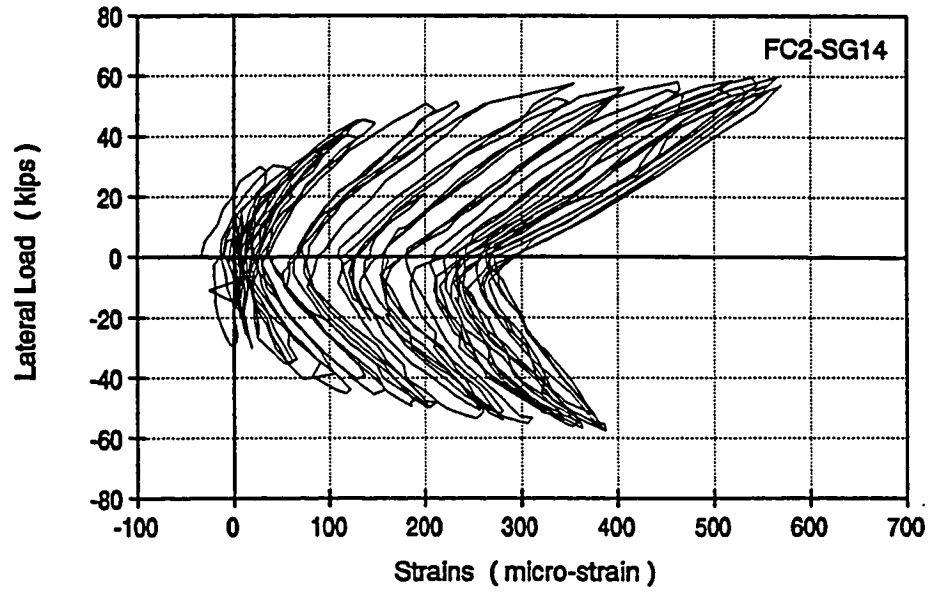


Figure 6.42 Strains in Gage # SG14

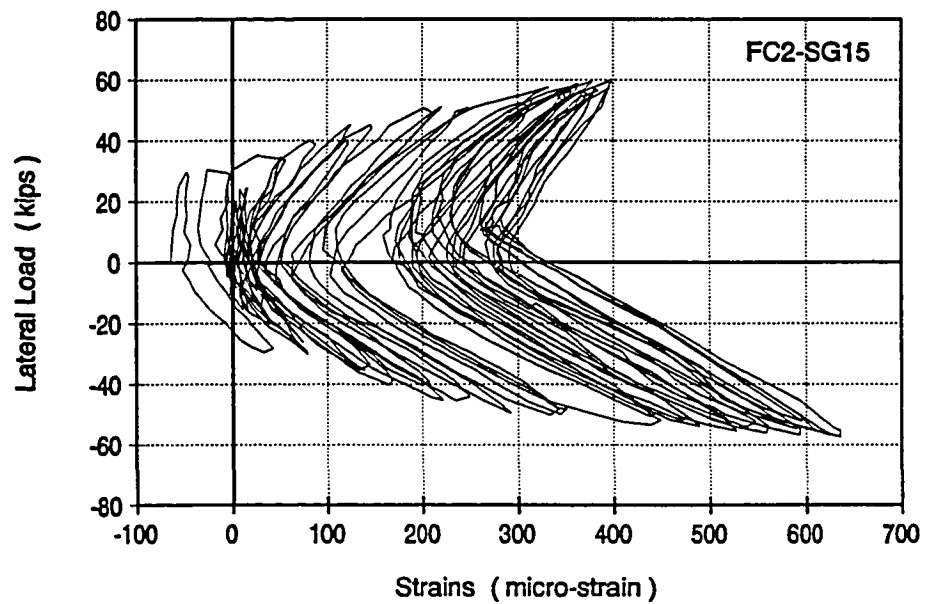


Figure 6.43 Strains in Gage # SG15

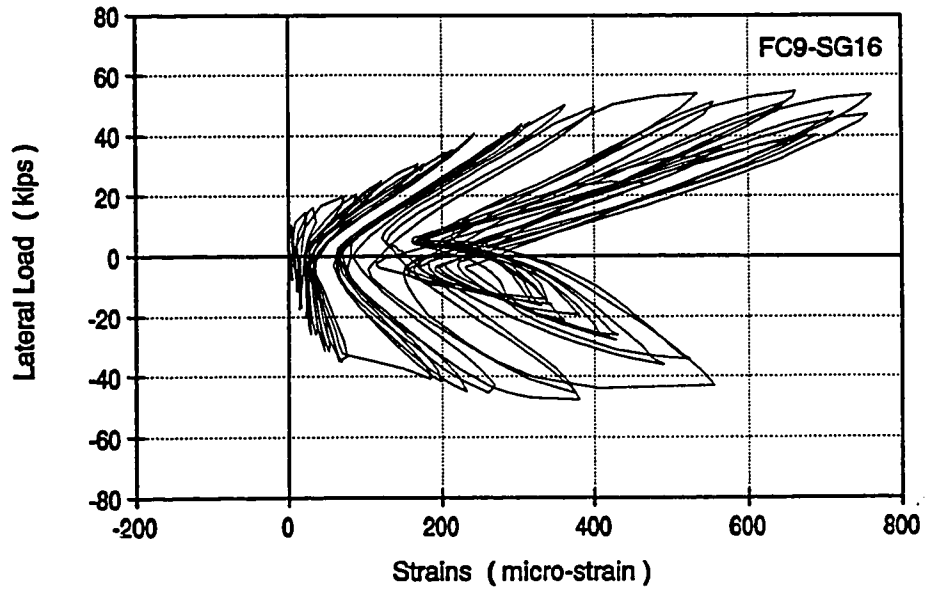


Figure 6.44 Strains in Gage # SG16

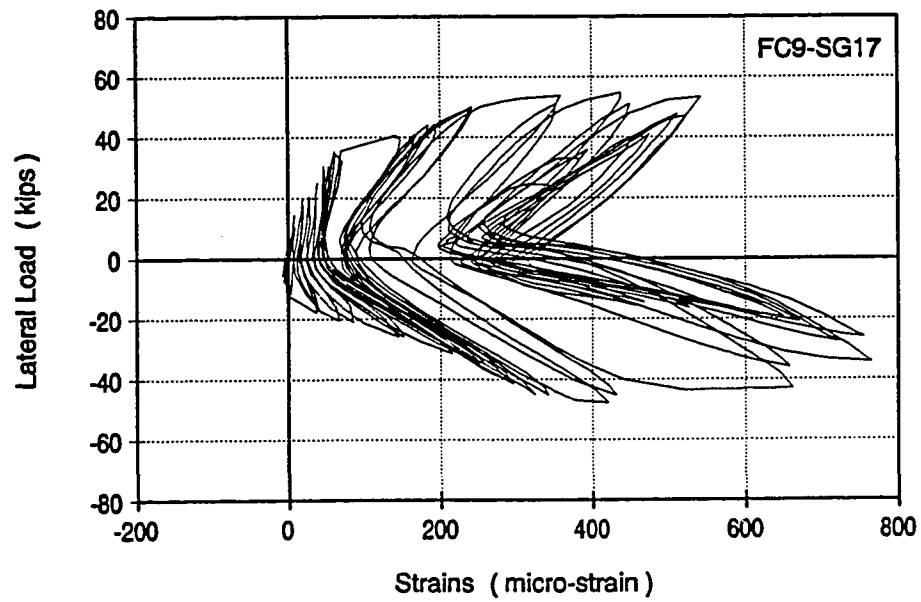


Figure 6.45 Strains in Gage # SG17

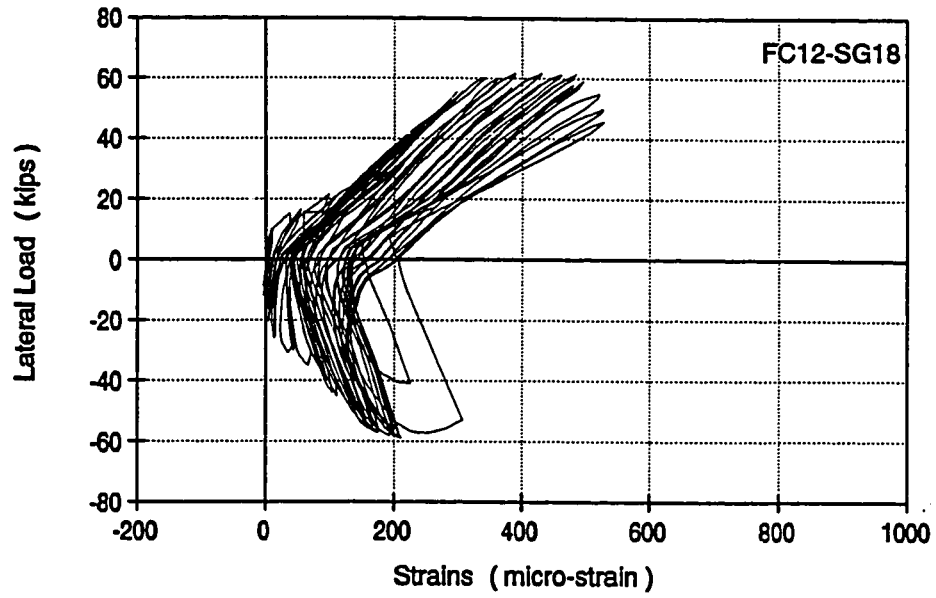


Figure 6.46 Strains in Gage # SG18

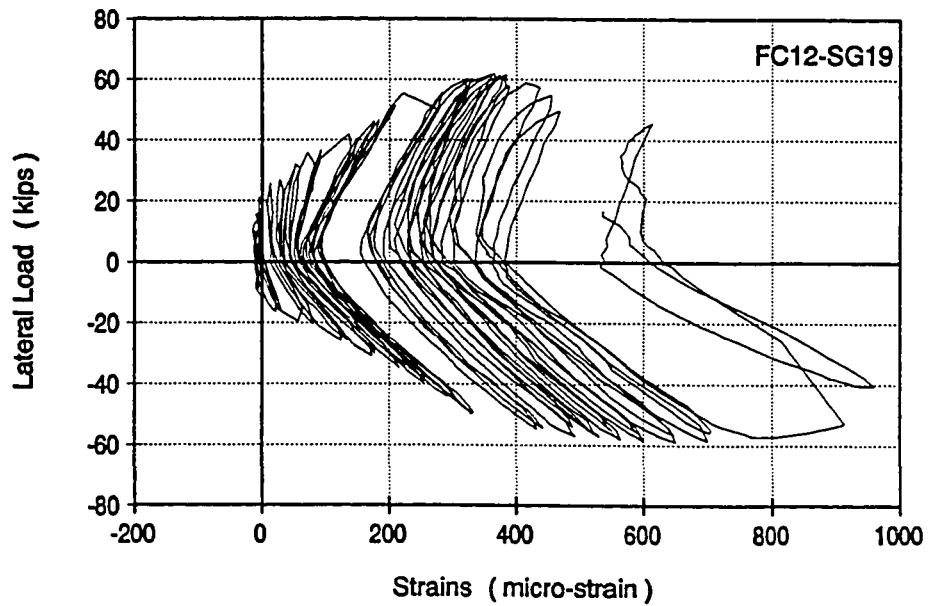


Figure 6.47 Strains in Gage # SG19



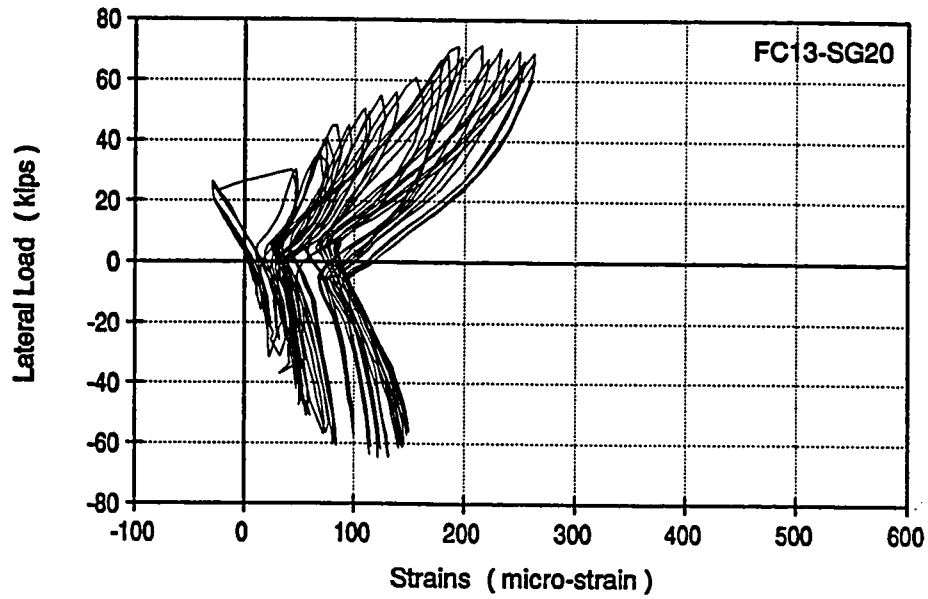


Figure 6.48 Strains in Gage # SG20

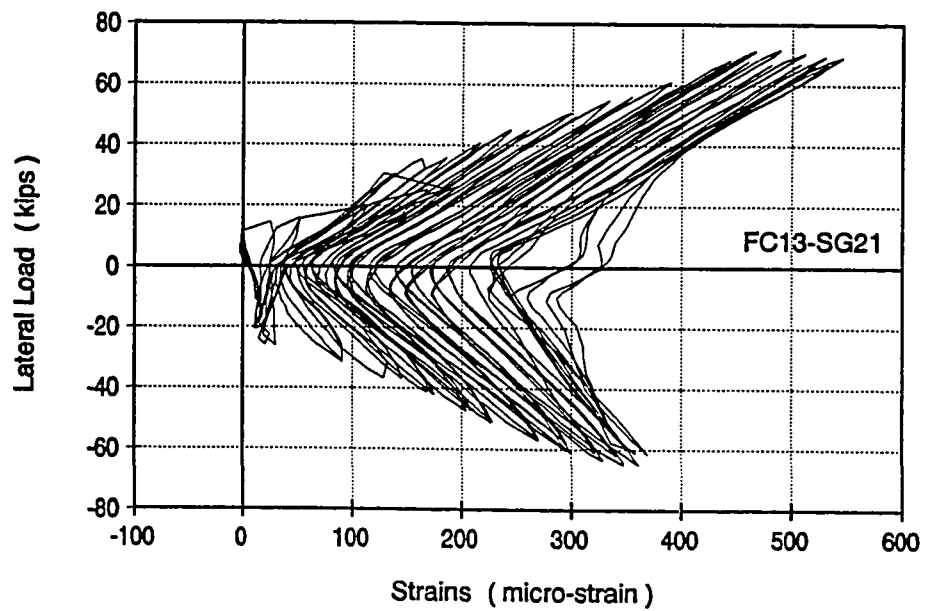


Figure 6.49 Strains in Gage # SG21

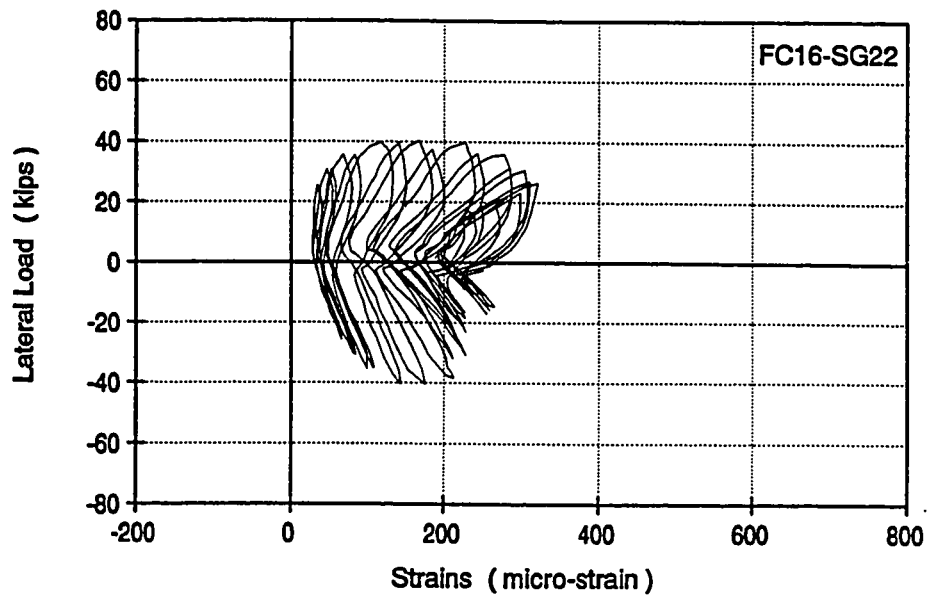


Figure 6.50 Strains in Gage # SG22

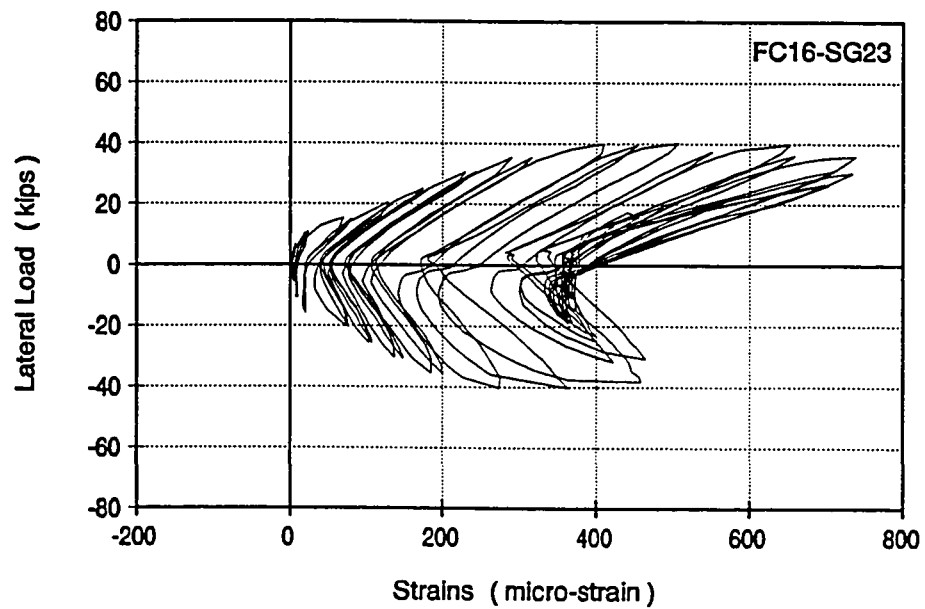


Figure 6.51 Strains in Gage # SG23

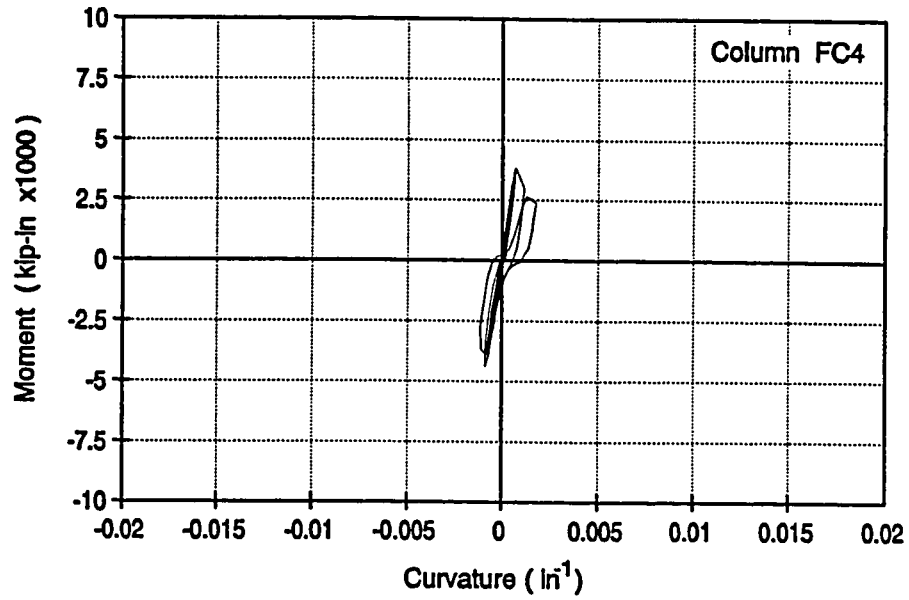


Figure 6.52 Column FC4 - Moment vs. Average Curvature

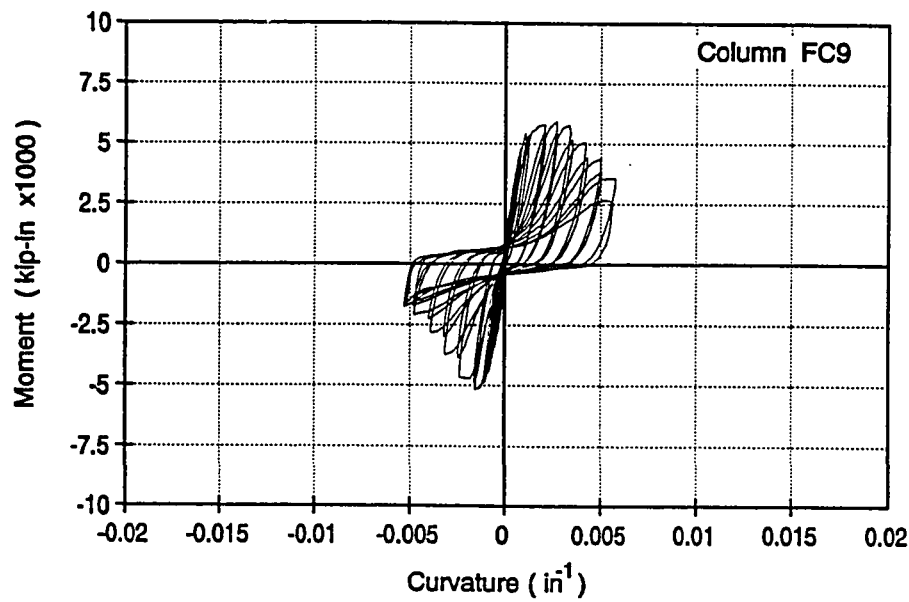


Figure 6.53 Column FC9 - Moment vs. Average Curvature

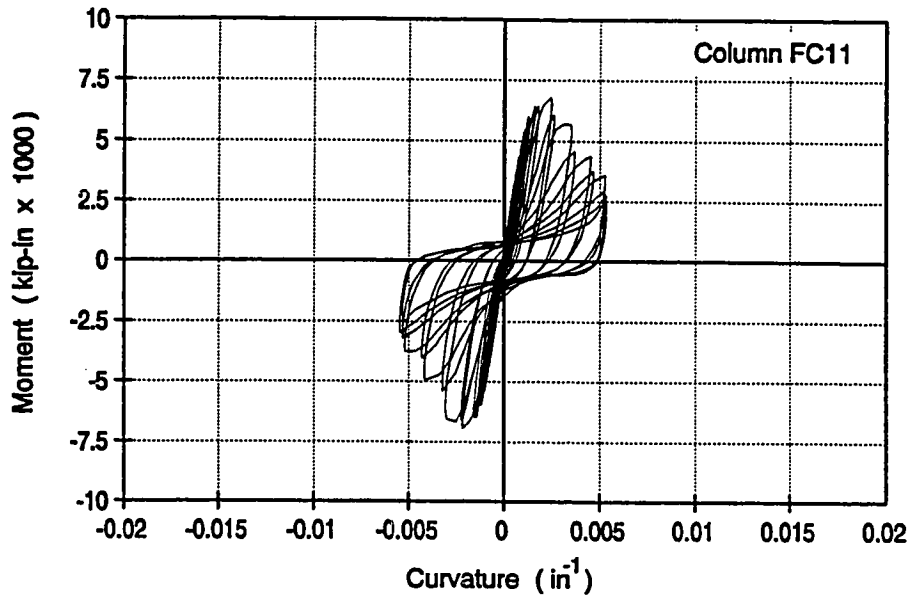


Figure 6.54 Column FC11 - Moment vs. Average Curvature

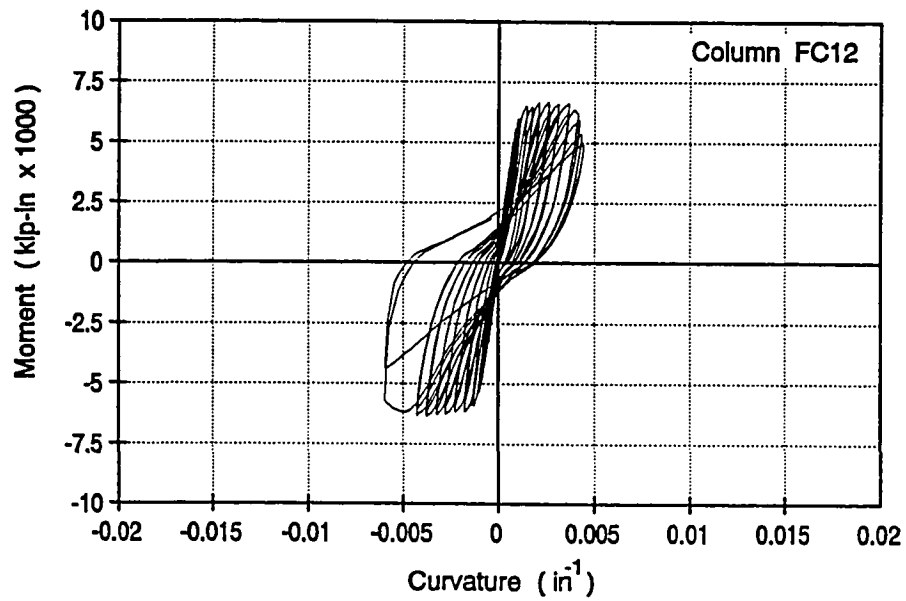


Figure 6.55 Column FC12 - Moment vs. Average Curvature

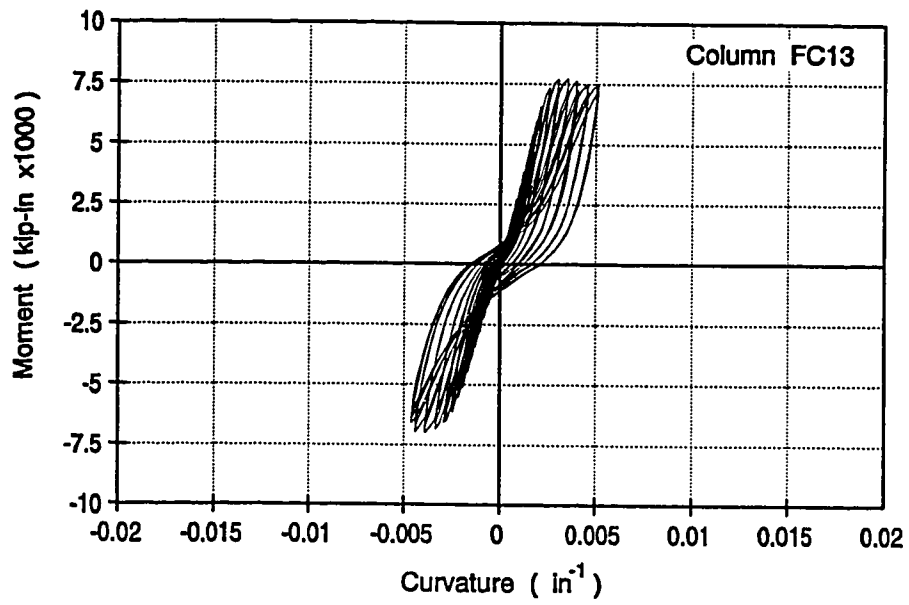


Figure 6.56 Column FC13 - Moment vs. Average Curvature

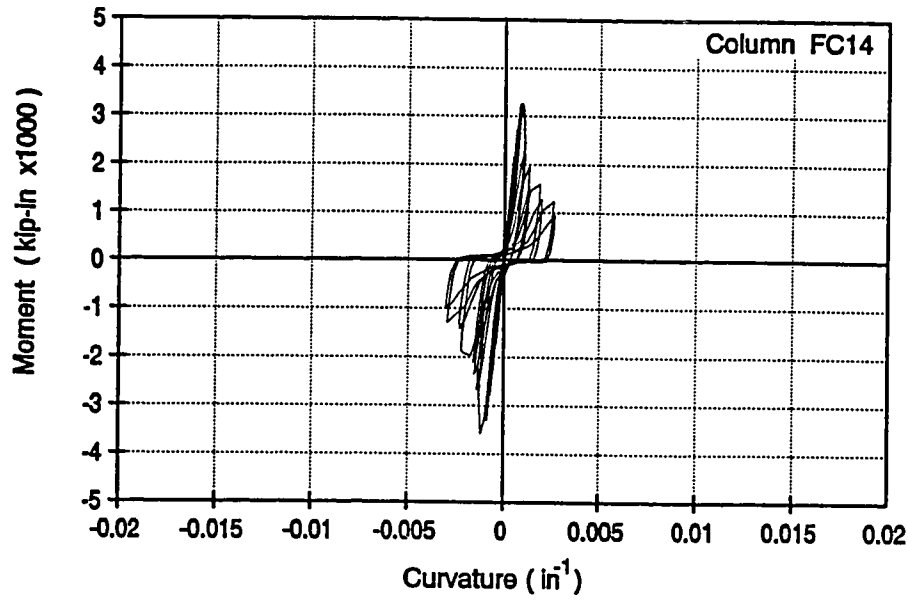


Figure 6.57 Column FC14 - Moment vs. Average Curvature

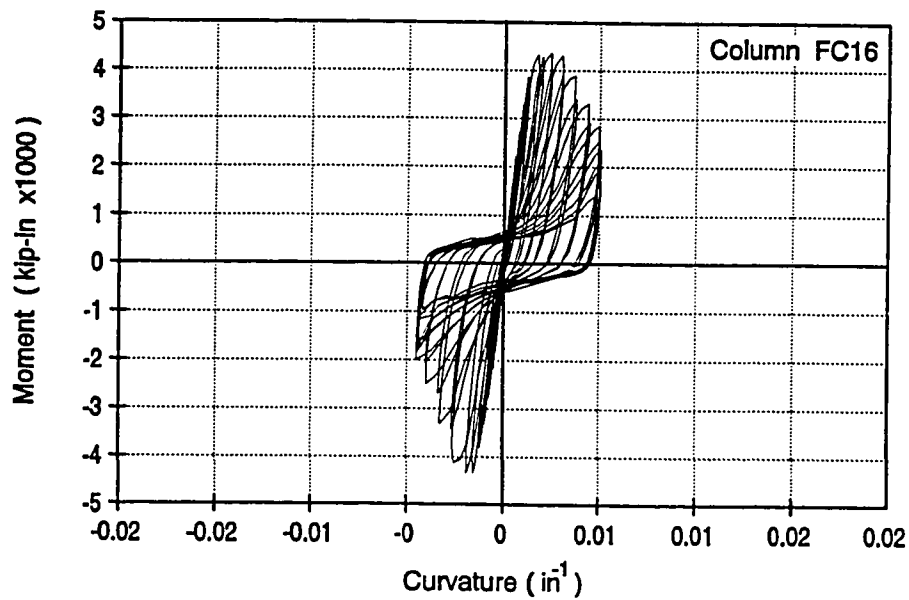


Figure 6.58 Column FC16 - Moment vs. Average Curvature

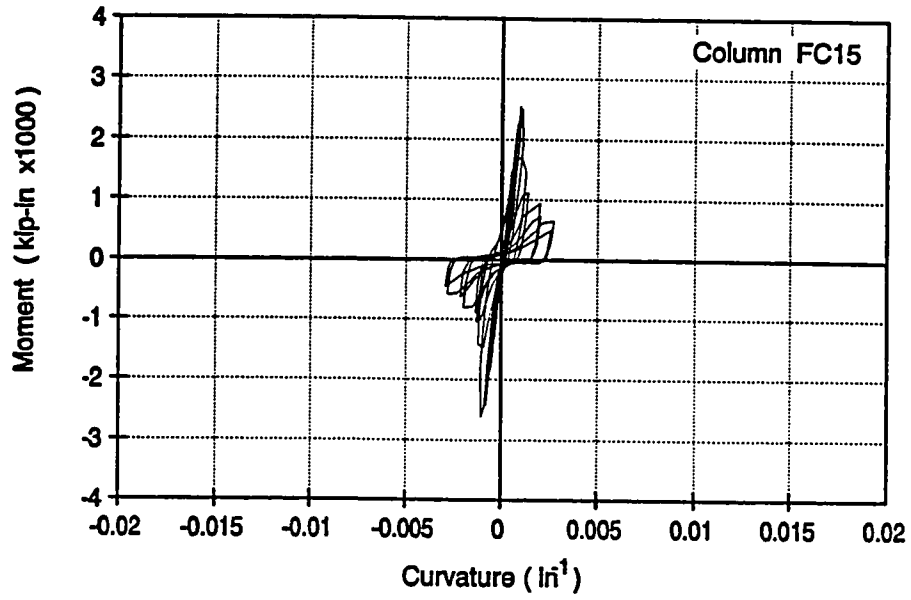


Figure 6.59 Column FC15 - Moment vs. Average Curvature

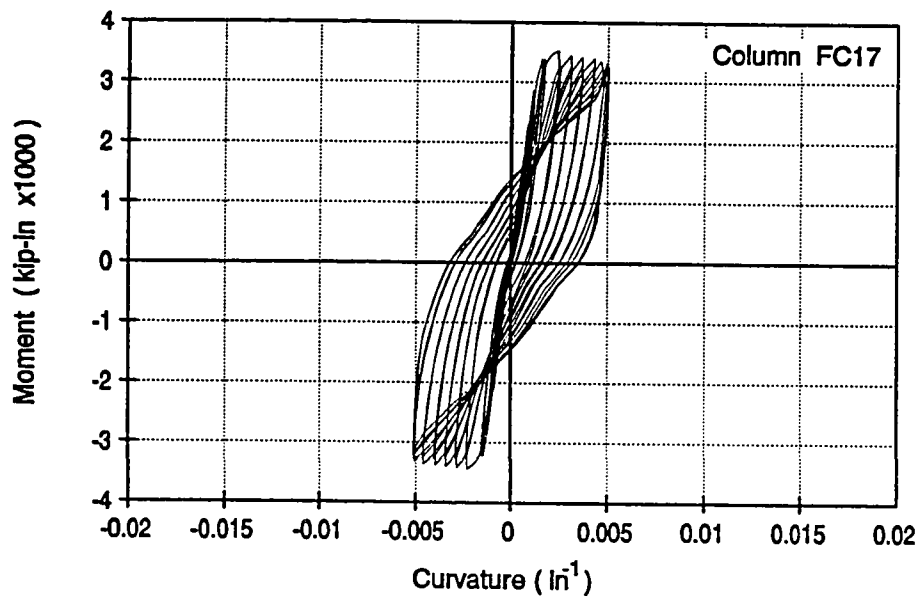


Figure 6.60 Column FC17 - Moment vs. Average Curvature

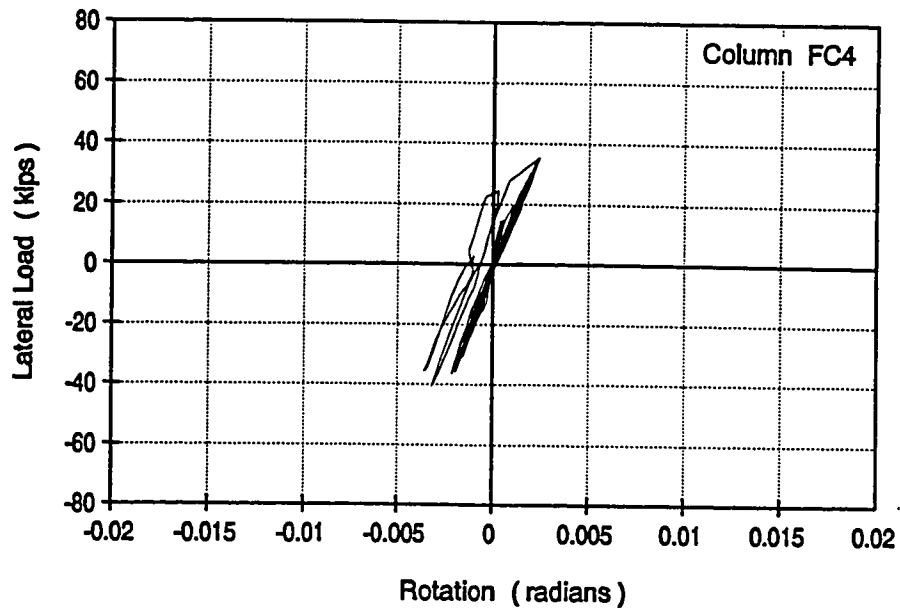


Figure 6.61 Column FC4 - Lateral Load vs. Differential Rotation between levels 18" and 38"

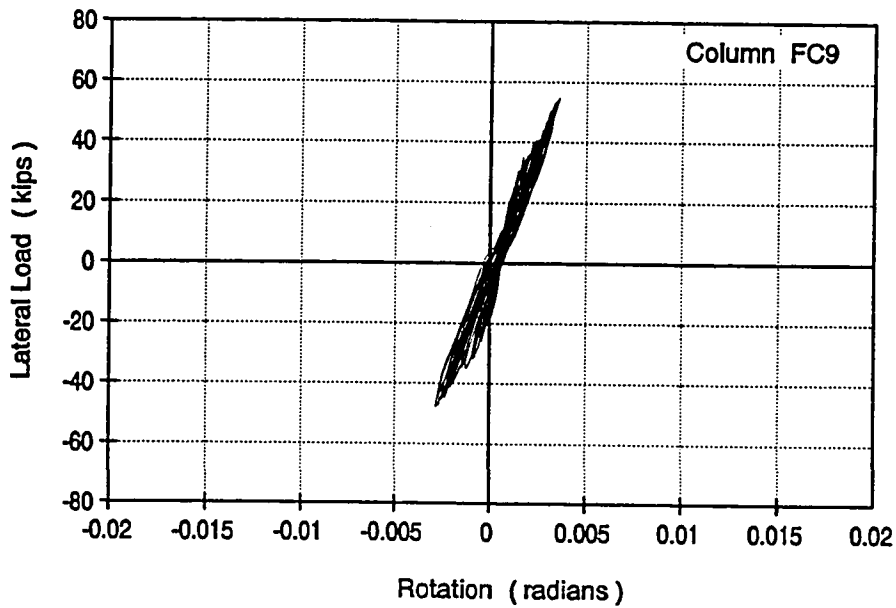


Figure 6.62 Column FC9 - Lateral Load vs. Differential Rotation between levels 18" and 38"



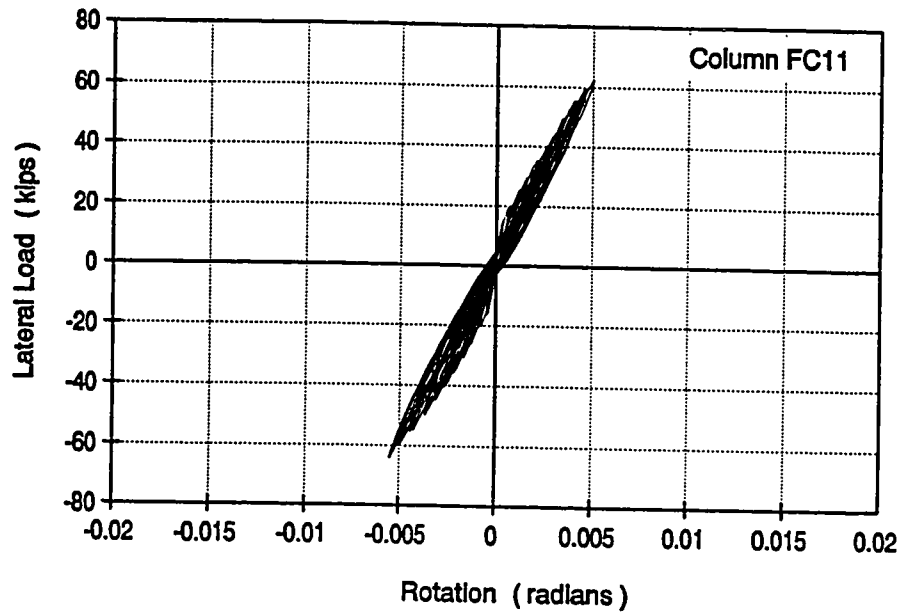


Figure 6.63 Column FC11 - Lateral Load vs. Differential Rotation between levels 18" and 38"

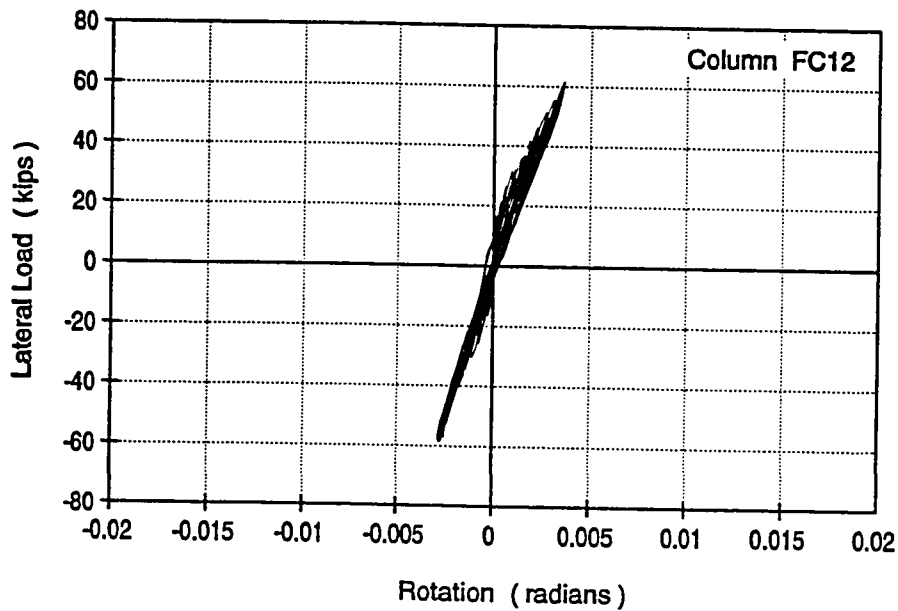


Figure 6.64 Column FC12 - Lateral Load vs. Differential Rotation between levels 18" and 38"

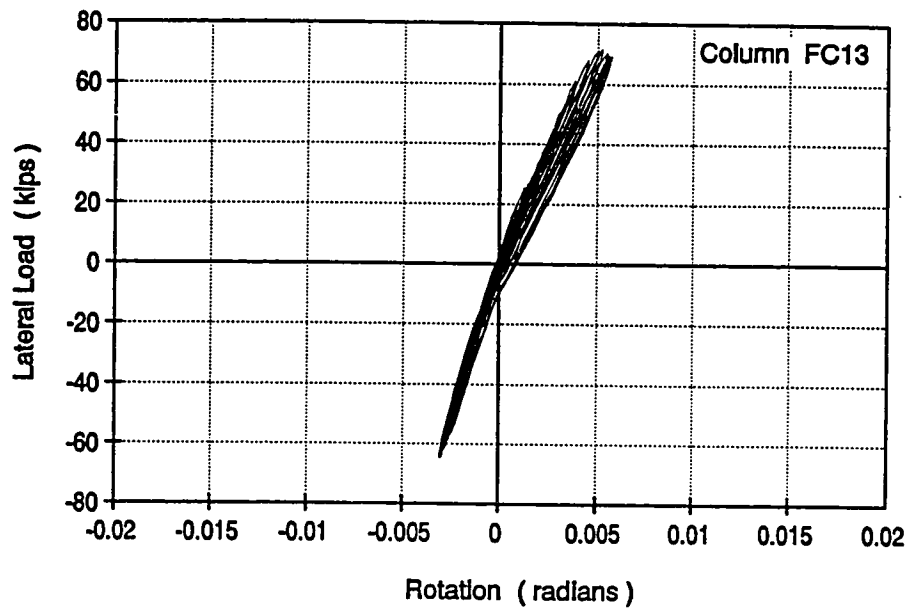


Figure 6.65 Column FC13 - Lateral Load vs. Differential Rotation between levels 18" and 38"

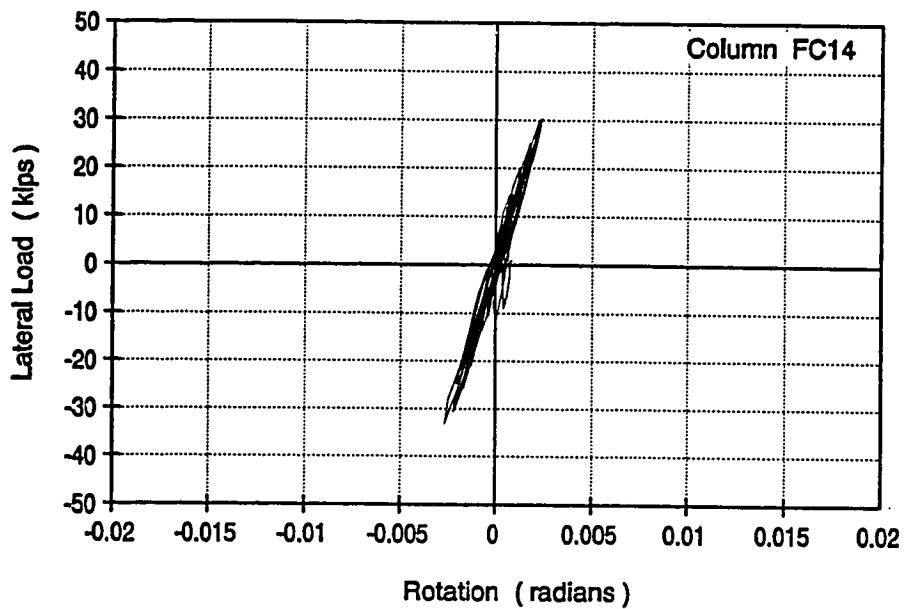


Figure 6.66 Column FC14 - Lateral Load vs. Differential Rotation between levels 18" and 38"

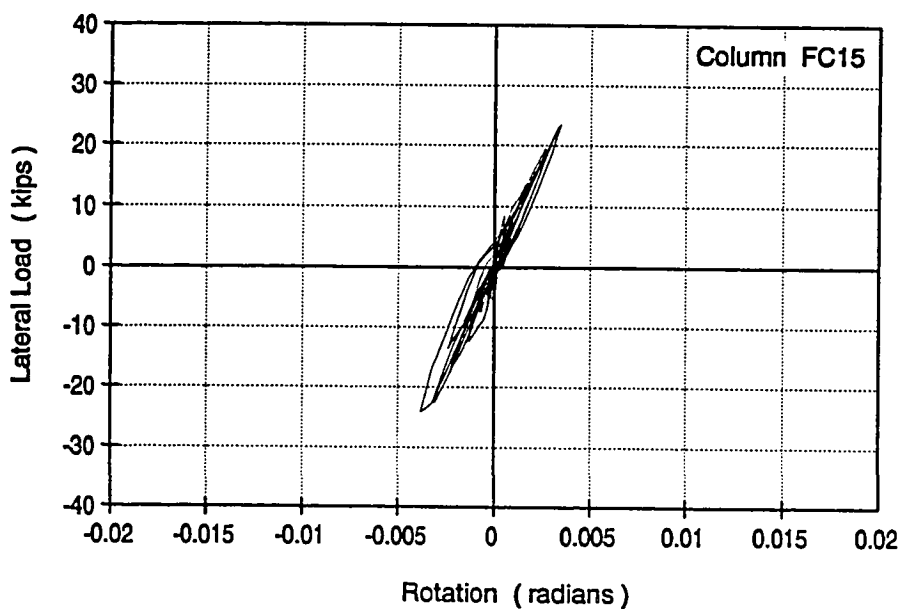


Figure 6.67 Column FC15 - Lateral Load vs. Differential Rotation between levels 18" and 38"

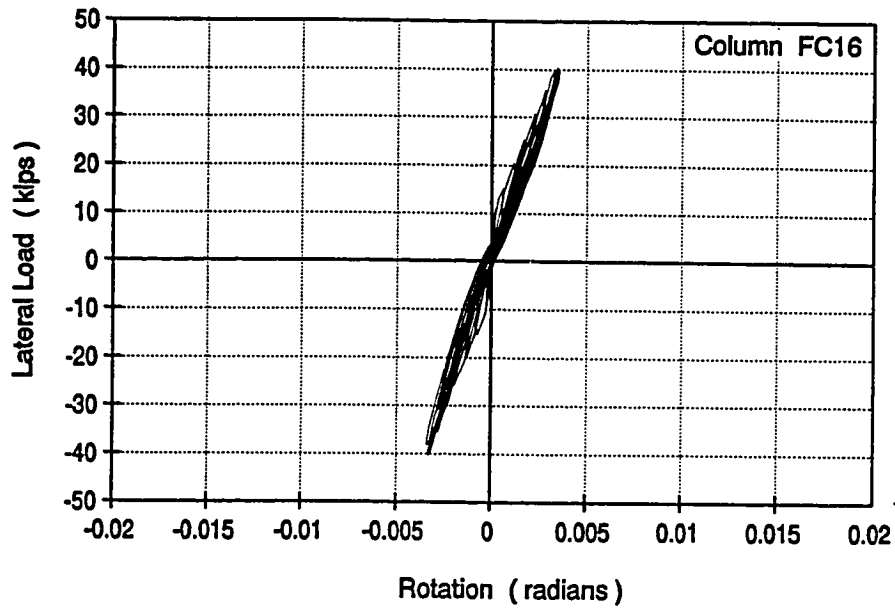


Figure 6.68 Column FC16 - Lateral Load vs. Differential Rotation between levels 18" and 38"

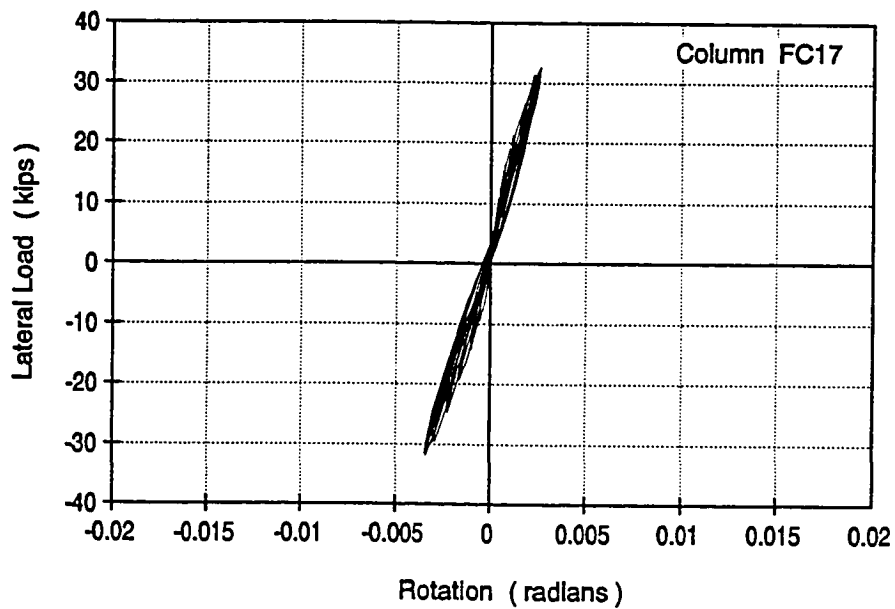


Figure 6.69 Column FC17 - Lateral Load vs. Differential Rotation between levels 18" and 38"

## **CHAPTER 7**

### **ADDITIONAL EXPERIMENTAL DATA - COLUMNS WITH INADEQUATE SHEAR STRENGTH**

#### **7.1 INTRODUCTION**

This chapter presents comparison and further discussion of the test results for columns with inadequate shear strength. Selected strain gage data measured on the longitudinal reinforcing bars, transverse reinforcement and steel jacket are also presented. Envelopes of the load-drift ratio, energy dissipation, column stiffness and column rotations are described. The effectiveness of partial and full steel jackets in strengthening columns with inadequate shear strength is evaluated. The influence of different variables is discussed. These variables include:

- direction of loading
- different types of steel jackets

Further discussion and analysis of the results are also provided in Chapter 8.

## 7.2 ENVELOPES OF THE CYCLIC RESPONSE

In this section, the response of the shear columns with inadequate shear strength is presented. The envelopes for the push cycles of the load-drift ratio curves are plotted on one quarter of the chart to facilitate comparisons.

Figure 7.1 shows the envelopes of the cyclic response of the shear columns SC1 and SC2. The concrete strength of columns SC1 and SC2 were higher than planned. Consequently, the basic unretrofitted column SC1 did not show a very dramatic shear failure. The use of steel collars slightly improved the ductility, but, severe degradation was observed during the test at large displacements.

Figure 7.2 shows the envelopes of the cyclic response of the shear columns SC3, SC5, SC6, SC7 and SC8. These columns were loaded in the weak direction. While the basic unretrofitted column SC3 did not develop the nominal flexural capacity, which is equivalent to a lateral load of 110 kips, the retrofitted shear columns with steel jackets exceeded the flexural yield capacity and exhibited large ductility and high energy dissipation. Column SC6 showed lateral strength higher than columns SC7 and SC8 because the longitudinal bars were strain hardened during a previous test (column SC4 test). The response of column SC7 better represents the actual response of a retrofitted shear column with inadequate shear strength, since the longitudinal bars were not previously strain hardened. Again, the plot reveals that the steel collar system was not as effective as the solid steel jacket

system.

Figure 7.3 shows the envelopes of the cyclic response of the shear columns SC9, SC10 and SC11. These columns were loaded in the strong direction. As shown in Figure 7.3, the basic unretrofitted column SC9 exhibited very dramatic shear failure. However, the retrofitted column SC10 exhibited much higher strength, ductility and energy dissipation. Column SC10 developed its ultimate flexural capacity by the fracture of one longitudinal bar on the tension side during the push cycle to 4.0 % drift ratio. However, if the main longitudinal bars of column SC10 were not strain hardened during previous tests, the fracture of the longitudinal bar may have occurred at higher drift ratio.

The envelopes of the cyclic response of the shear columns clearly demonstrate that thin rectangular steel jackets can considerably improve the strength, ductility and energy dissipation of rectangular columns with inadequate shear strength.

### **7.3 LATERAL STIFFNESS OF COLUMNS**

Stiffness degradation of short columns is usually attributed to decrease in the modulus of elasticity of the cracked concrete, bond deterioration between steel and the surrounding concrete, and alternate opening and closing of residual cracks. Comparison of the stiffness degradation of the shear columns is presented in this section, secant stiffness values were computed, as described in section 6.3.

Figures 7.4 through 7.6 show the envelopes of the lateral stiffness versus drift ratio for the shear columns SC1, SC2, SC3, SC6, SC9 and SC10. The plots reveal very rapid stiffness degradation for almost all the columns. However, the stiffness degradation of the retrofitted columns SC6 and SC10 was at lower rate. On the other hand, the rate of stiffness degradation of column SC2 was almost the same as that of the basic column SC1. This indicated that the steel collars did not improve the stiffness of columns with inadequate shear strength in this case.

#### **7.4 ENERGY DISSIPATION**

The energy dissipated during the tests was computed as the area within the hysteretic loops from the lateral load-displacement relation. Figure 7.7 through 7.9 show the envelopes of the cumulative energy dissipated by the basic unretrofitted and strengthened columns with inadequate shear strength. The actual energy values reported in these plots are half the total dissipated energy, to be consistent with the energy dissipation plots in Chapter 6.

As shown in Figures 7.7 through 7.9, the retrofitted shear columns are capable of dissipating large amounts of energy as compared to the basic unretrofitted columns, with the exception of column SC11. Figure 7.8 shows that columns retrofitted by the use of full solid steel jackets are capable of dissipating more energy than columns retrofitted by the use of partial steel jackets, or steel collars.

The total energy dissipated by each shear column was computed for



the push direction of the column. Figure 7.10 shows the cumulative energy dissipated by the shear columns. The numbers in parentheses represent the maximum drift ratio to which each column was loaded.

## **7.5 STRAIN GAGE DATA**

In this section, selected strain gage data, helpful in understanding the behavior of the unretrofitted and retrofitted columns is presented. Strain gages were used to monitor the strains in the transverse reinforcement and on the steel jackets. The properties of the steel bars and jackets are presented in Table 3.5. The strain gage data is presented as the lateral load applied on the column versus the strains in the steel bars or the steel jackets.

A large number of strain gages were used. However, only selected results are presented which represent typical strain gage data and which are most useful in understanding the behavior of the test specimens.

### **7.5.1 Strains in the Transverse Reinforcement**

The strains in the transverse reinforcement were measured at the mid-length of the cross ties or the periphery ties. The spacing between the layers of the transverse reinforcement was 16 inches. Shear columns had two transverse reinforcement layers at 8 inches and at 24 inches from the bottom of the column. The details of the transverse reinforcement were identical to those used in the flexural columns.

Figure 7.11 shows the locations of the strain gages. Strain gage SSG1 and SSG2 were installed on cross ties of column SC6, at 8 inches and 24 inches from the bottom of the column, respectively. For column SC7, strain gages SSG3 and SSG4 were installed on cross ties located at 8 inches and 24 inches from the bottom of the column, respectively. Figures 7.12 through 7.15 show the strain gage data for the strain gages SSG1 through SSG4, respectively. The plots show the strains in the transverse reinforcement at the 24 inch level are higher than those at 8 inches. The transverse reinforcement layer at 24 inches is very close to the intersection of the two theoretical major diagonal shear cracks. Also, the plots reveal that the transverse reinforcement at 24 inches yielded, which indicates that even in the presence of a steel jacket the existing transverse reinforcement contributes to the shear resistance of column. This is due to the passive confinement of the steel jacket.

Figures 7.16 and 7.17 show the plots of load versus strain in strain gages SSG5 and SSG6 for the basic unretrofitted column SC9 and the strengthened column SC10, respectively. Both strain gages were installed on mid-length of the peripheral tie located at 24 inches from the bottom of the column. Columns SC9 and SC10 were loaded in the strong direction. While strain gage SSG5 exhibited very high strains, column SC9 did not develop its yielding flexural capacity, but rather experienced very dramatic shear failure. On the other hand, the maximum strain measured by the strain gage SSG6 was below 1400 micro-strain. This maximum strain was low because of the presence of the steel jacket which did not allow the major diagonal shear cracks to open up, even at large lateral displacements of the column.

### 7.5.2 Strains in the Steel Jackets

Rectangular strain rosette gages and uniaxial strain gages were used to measure the strains in the steel jackets. Figure 7.18 shows the locations of the strain gages.

Strain gages SSG7 and SSG8 were installed on the west side of columns SC6's and SC10's steel jackets. The west side of the column is orthogonal to the direction of loading. Strain gages SSG7 and SSG8 were located at 8 inches from the bottom of the column, at the same level as the first layer of transverse reinforcement. Figures 7.19 and 7.20 show the strains in gage SSG7 and SSG8 during the test. The plots show that the outside face of the steel jacket experienced tensile strains in the transverse direction. These strains may be caused by the concrete lateral pressure on the compression side, which may develop bending strains in the steel jacket. But, since the strains on the outside face the steel jacket are tensile strains during the push as well as the pull cycles, it is believed that these strains are due to bearing of the concrete column on the sides of the steel jacket. Figure 7.21 illustrates the kind of deformations that developed in the steel jackets under lateral shear load.

Figures 7.22 through 7.27 show the strains in the rectangular strain rosette gages SRG1 and SRG2. Strain rosette gage SRG1 was installed on the north side of column SC6's steel jacket. It was located at 26 inches from the bottom of the column. Strain rosette gage SRG2 was installed on the north side of column SC10. It was located at 20 inches from the bottom of

the column. Figure 7.18 shows the locations of the strain gage SRG1 and SRG2.

Figure 7.22 through 7.24 show the strains in the strain gage SRG1 at angles of  $\Theta = 0^\circ, 45^\circ$  and  $90^\circ$ , respectively. Figures 7.25 through 7.27 show the strains in the strain gage SRG2 at angles  $\Theta = 45^\circ, 135^\circ$  and  $90^\circ$ , respectively. Column SC10 was loaded in the strong direction. It exhibited very satisfactory performance over the basic unretrofitted column SC9. However, major diagonal shear cracks formed on both columns SC9 and SC10 during the cycles to 110 kips. The steel jacket picked up shear forces at a much higher rate at loads above 110 kips, as shown in Figures 7.25 and 7.27.

## 7.6 MOMENT - CURVATURE DIAGRAMS

The average values of the column curvature were measured over a length of 7 inches from the bottom of the column (fixed end). The rotation at the fixed end due to slippage of the longitudinal bars in the footing was ignored. Figures 7.28 through 7.31 show the moment curvature diagrams at the bottom of columns SC3, SC6, SC9 and SC10, respectively. The plots show a large improvement in the curvature ductility of the columns when retrofitted with steel jackets.

## 7.7 SUMMARY

In this chapter comparison and further discussion of the shear columns

with inadequate shear strength were presented. All columns investigated in this study were detailed according to the provisions of the ACI 318-56 and 318-63 codes. The following is a list of key observations of what were presented:-

1. Thin rectangular steel jackets were very effective in strengthening of reinforced concrete columns with inadequate shear strength.
2. Columns strengthened with full rectangular steel jackets exhibited higher flexural capacity, ductility and energy dissipation than the basic unretrofitted columns.
3. Although steel jackets were very effective in enhancing the strength and ductility of columns of inadequate shear strength, they are considered passive systems. They start working effectively after the concrete column has developed major diagonal shear cracks.
4. Measured strains on the steel jackets were fairly low, never exceeding half the yielding strain of the steel jacket.

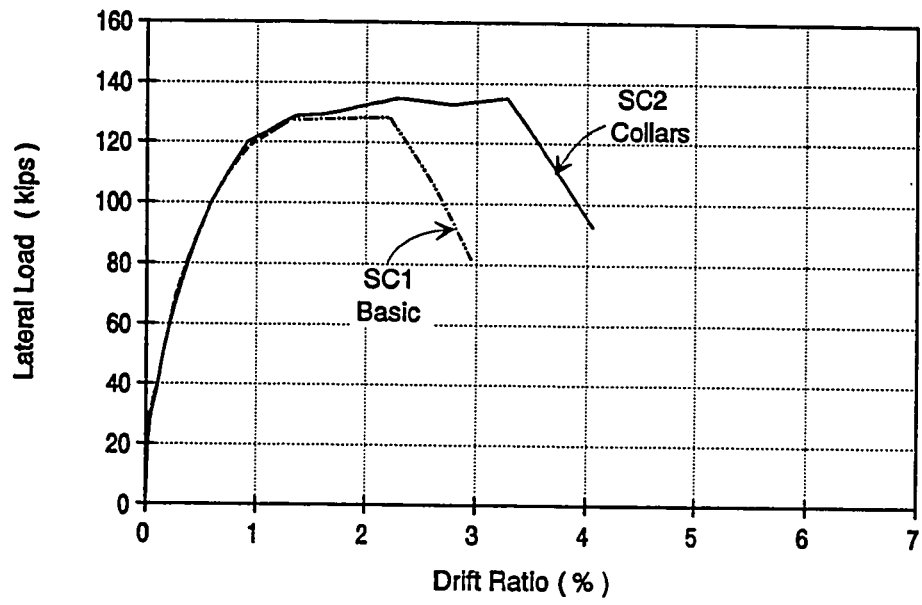


Figure 7.1 Envelopes of the Cyclic Response of the Shear Columns SC1 & SC2 (Weak Direction)

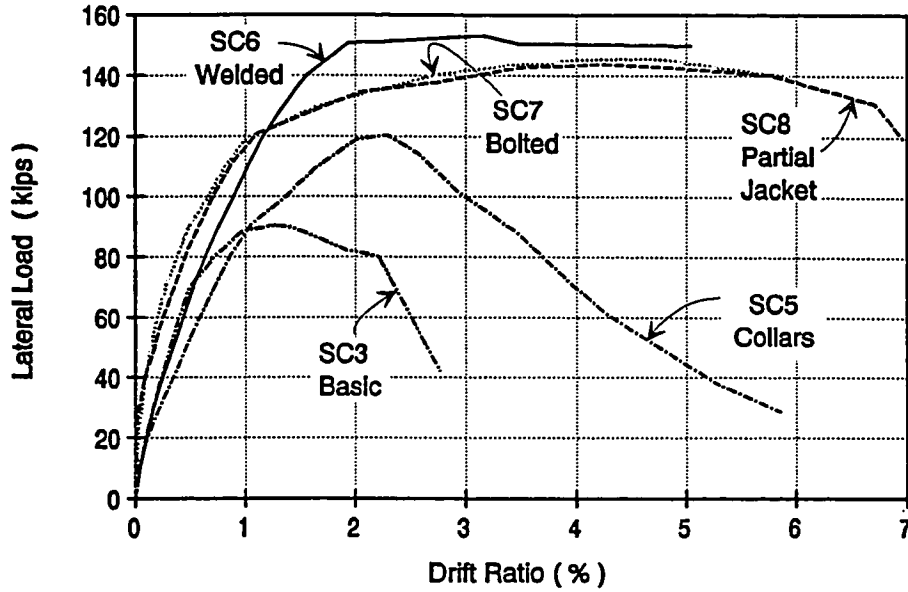


Figure 7.2 Envelopes of the Cyclic Response of the Shear Columns SC3, SC5, SC6, SC7 & SC8( Weak Direction )

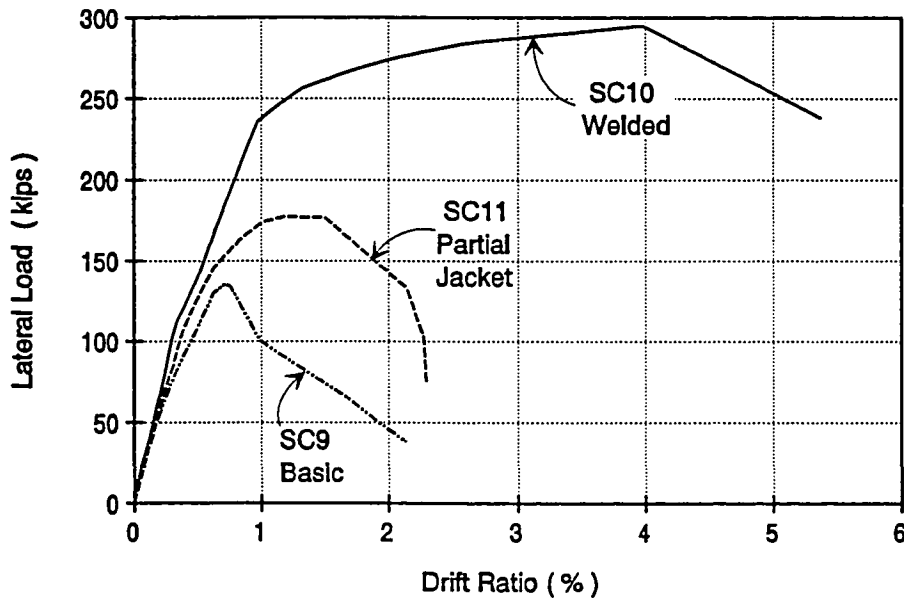


Figure 7.3 Envelopes of the Cyclic Response of the Shear Columns SC9, SC10 & SC11 ( Strong Direction )

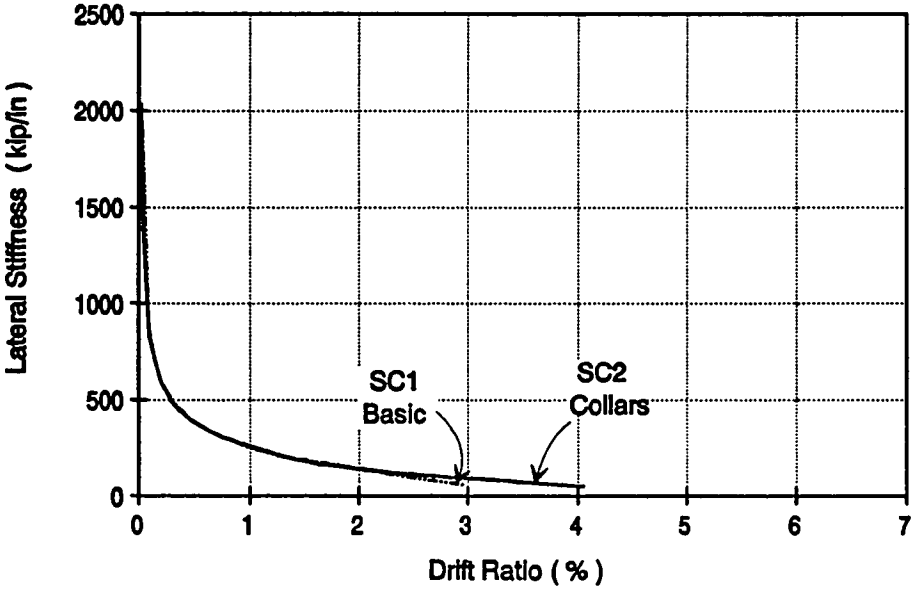


Figure 7.4 Envelopes of the Lateral Stiffness vs. Drift Ratio for the Shear Columns SC1 & SC2 (Weak Direction)



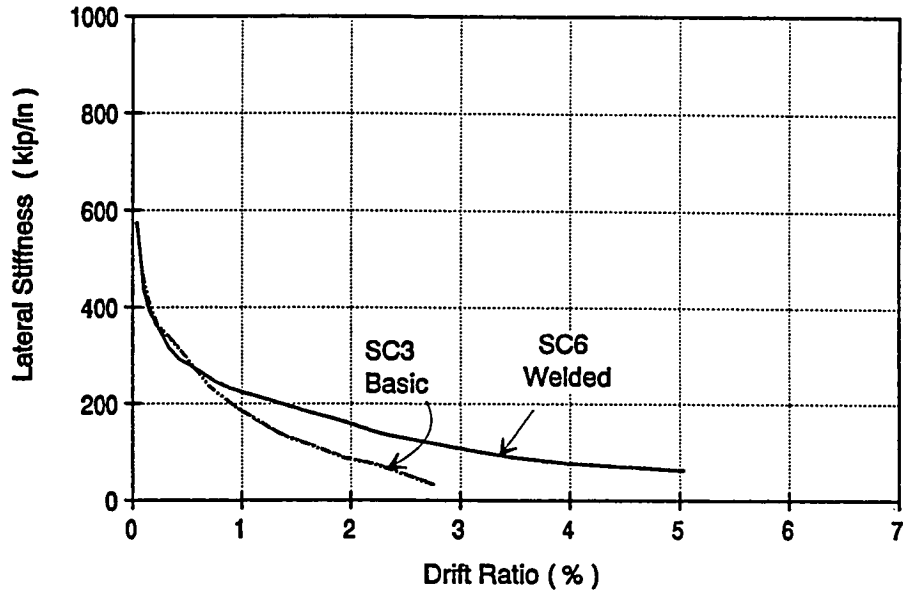


Figure 7.5 Envelopes of the Lateral Stiffness vs. Drift Ratio for the Shear Columns SC3 & SC6 ( Weak Direction )

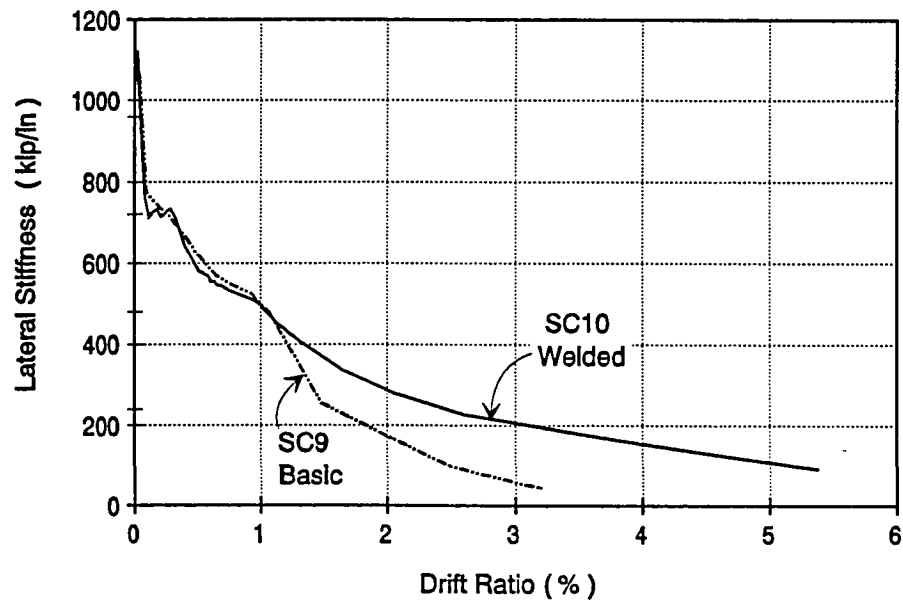


Figure 7.6 Envelopes of the Lateral Stiffness vs. Drift Ratio for the Shear Columns SC9 & SC10 ( Strong Direction )

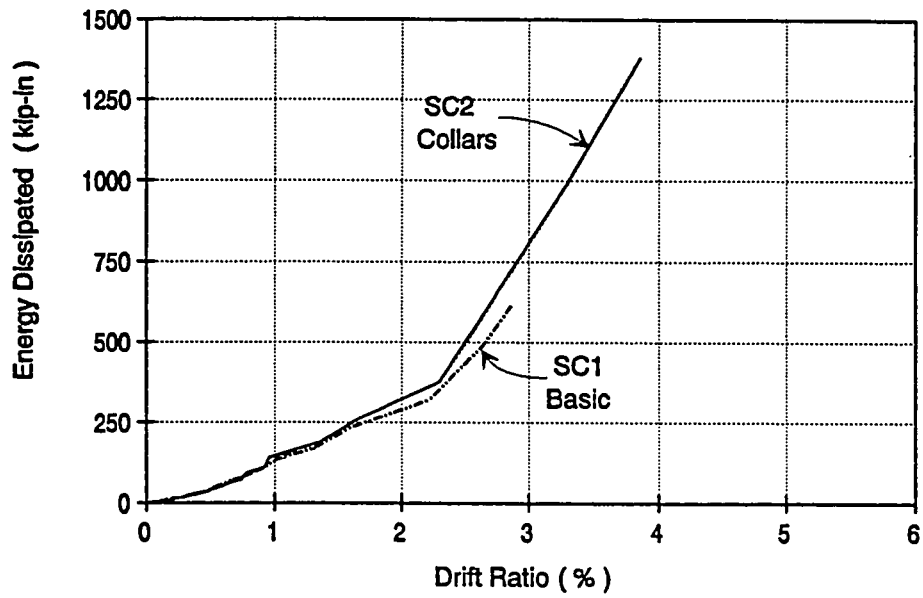


Figure 7.7 Envelopes of Cumulative Energy Dissipated for the Shear Columns SC1 & SC2 ( Weak Direction )

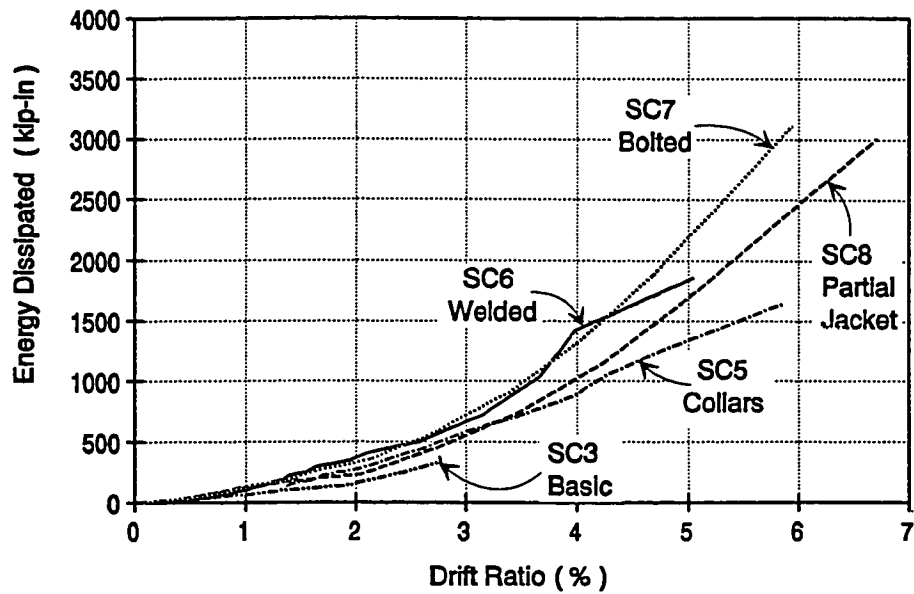


Figure 7.8 Envelopes of Cumulative Energy Dissipated for the Shear Columns SC3, SC5, SC6, SC7 & SC8 ( Weak Direction )

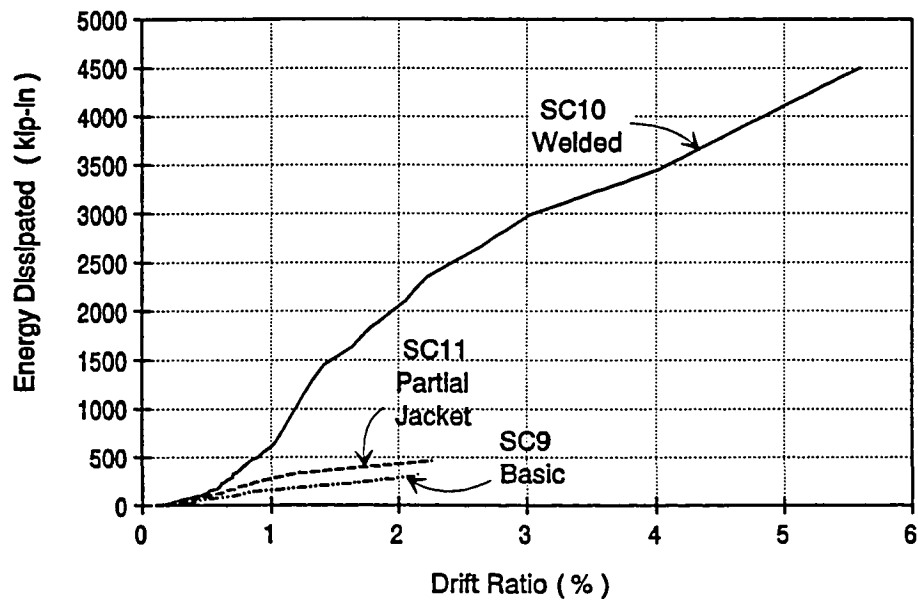
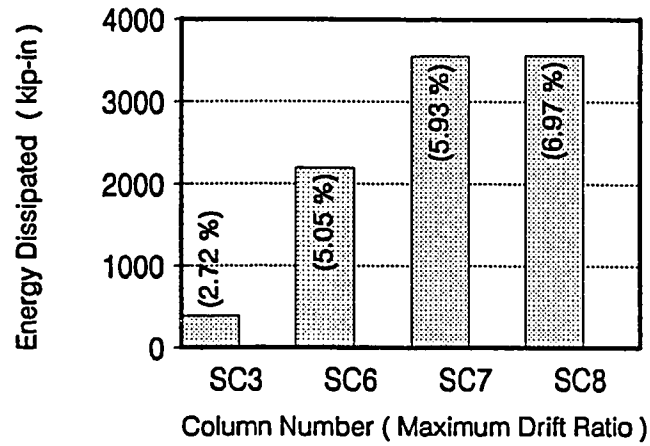
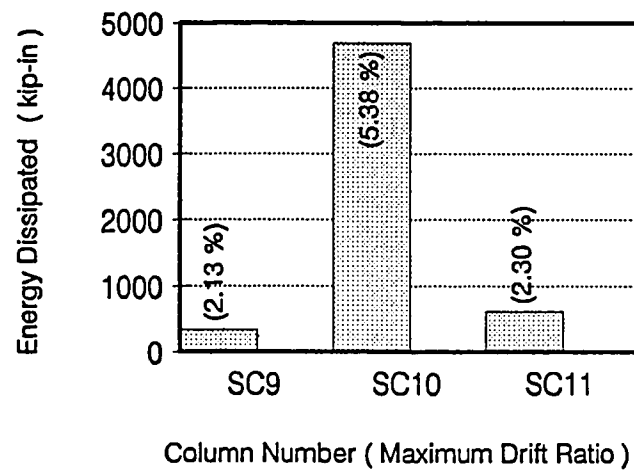


Figure 7.9 Envelopes of Cumulative Energy Dissipated for the Shear Columns SC9, SC10 & SC11 ( Strong Direction )



(a) Shear Columns Loaded in the Weak Direction



(b) Shear Columns Loaded in the Strong Direction

Figure 7.10 Cumulative Energy Dissipated by the Shear Columns

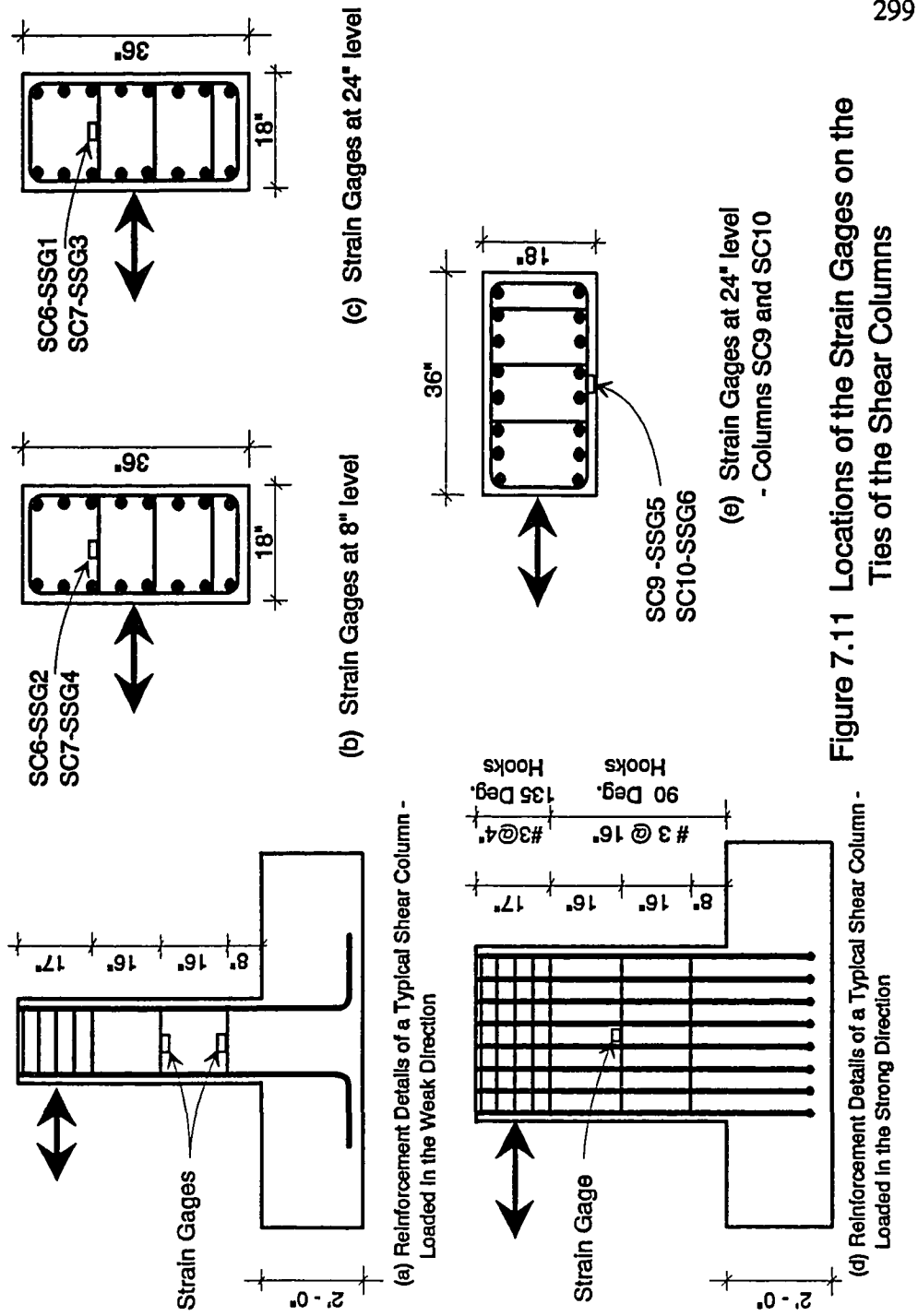


Figure 7.11 Locations of the Strain Gages on the Ties of the Shear Columns

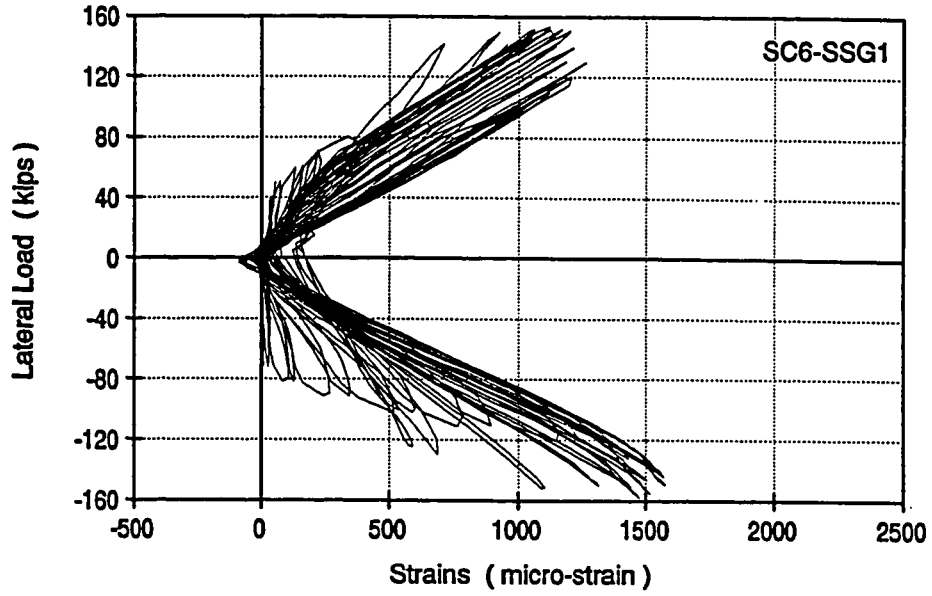


Figure 7.12 Strains in Strain Gage # SSG1

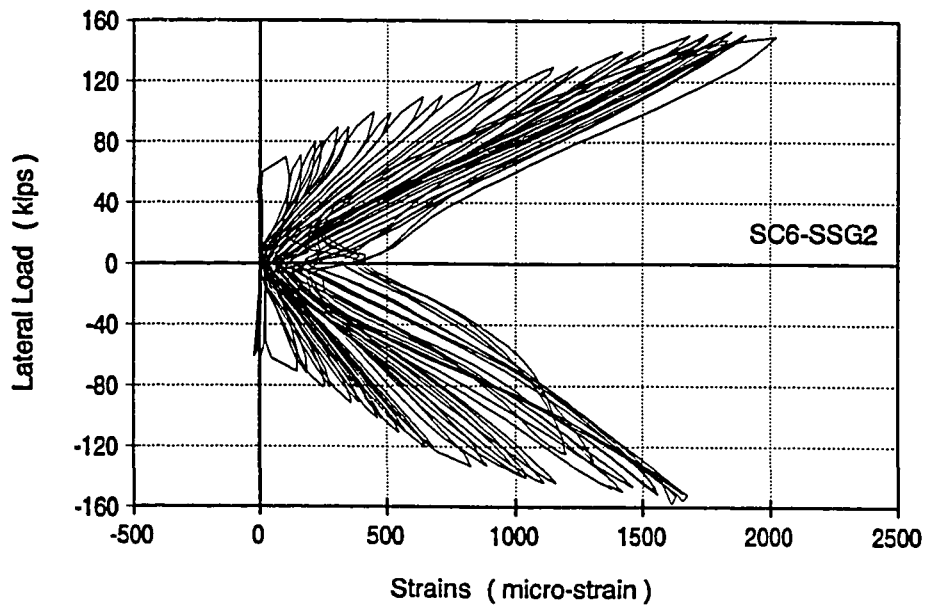


Figure 7.13 Strains in Strain Gage # SSG2

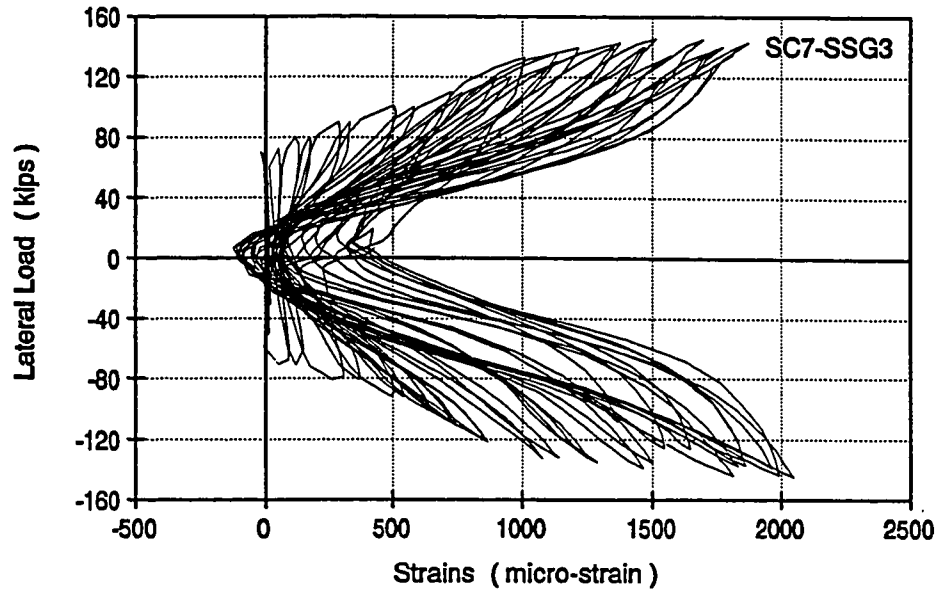


Figure 7.14 Strains in Strain Gage # SSG3

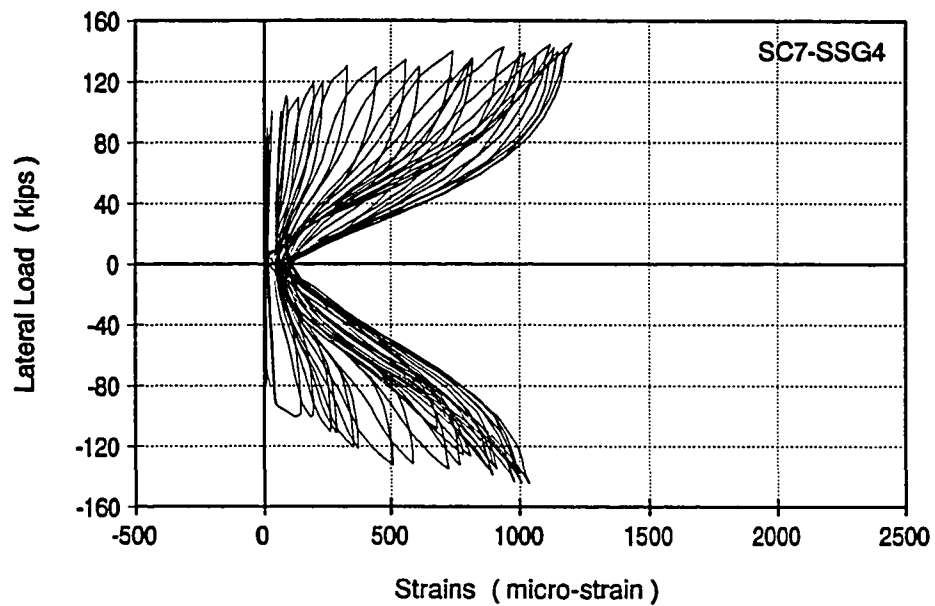


Figure 7.15 Strains in Strain Gage # SSG4

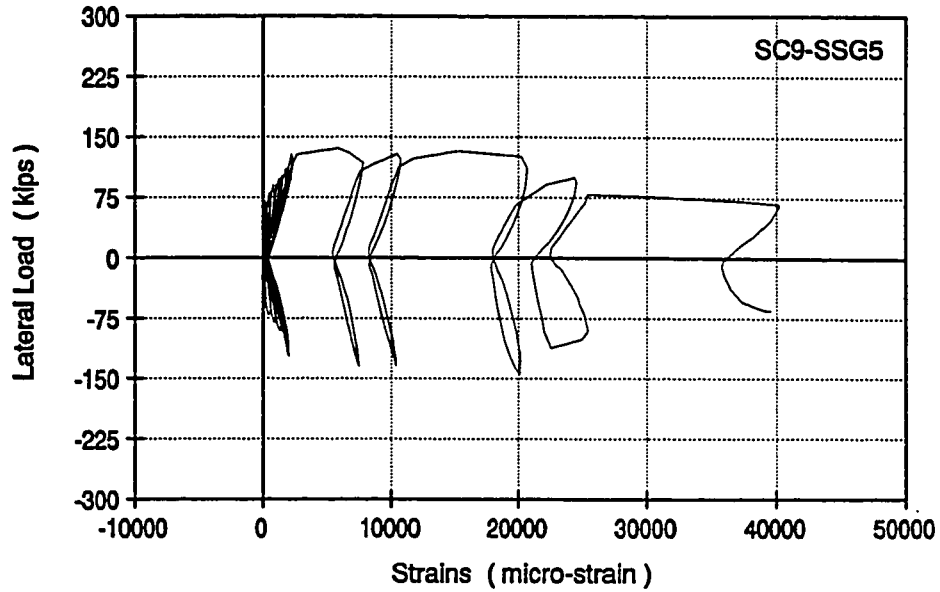


Figure 7.16 Strains in Strain Gage # SSG5

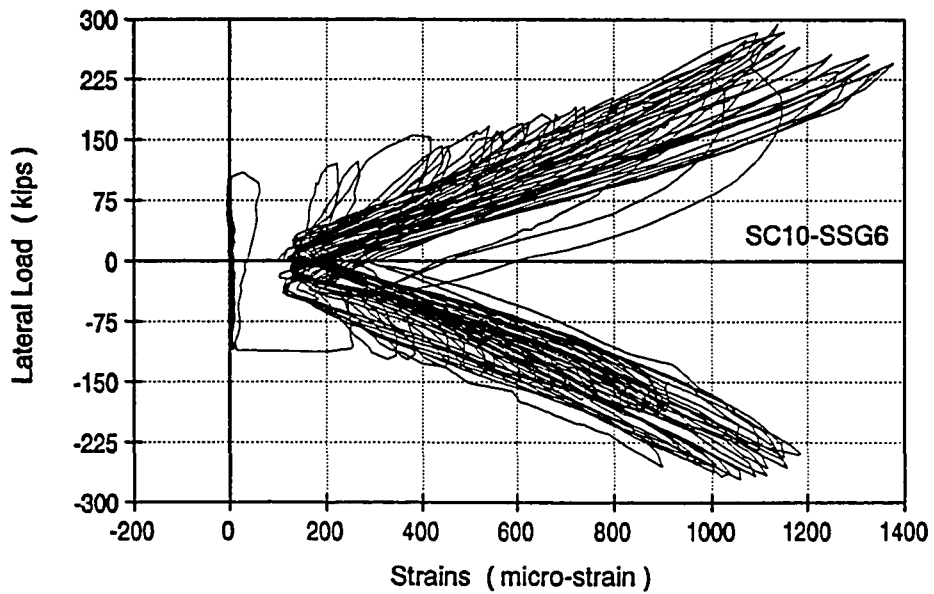


Figure 7.17 Strains in Strain Gage # SSG6



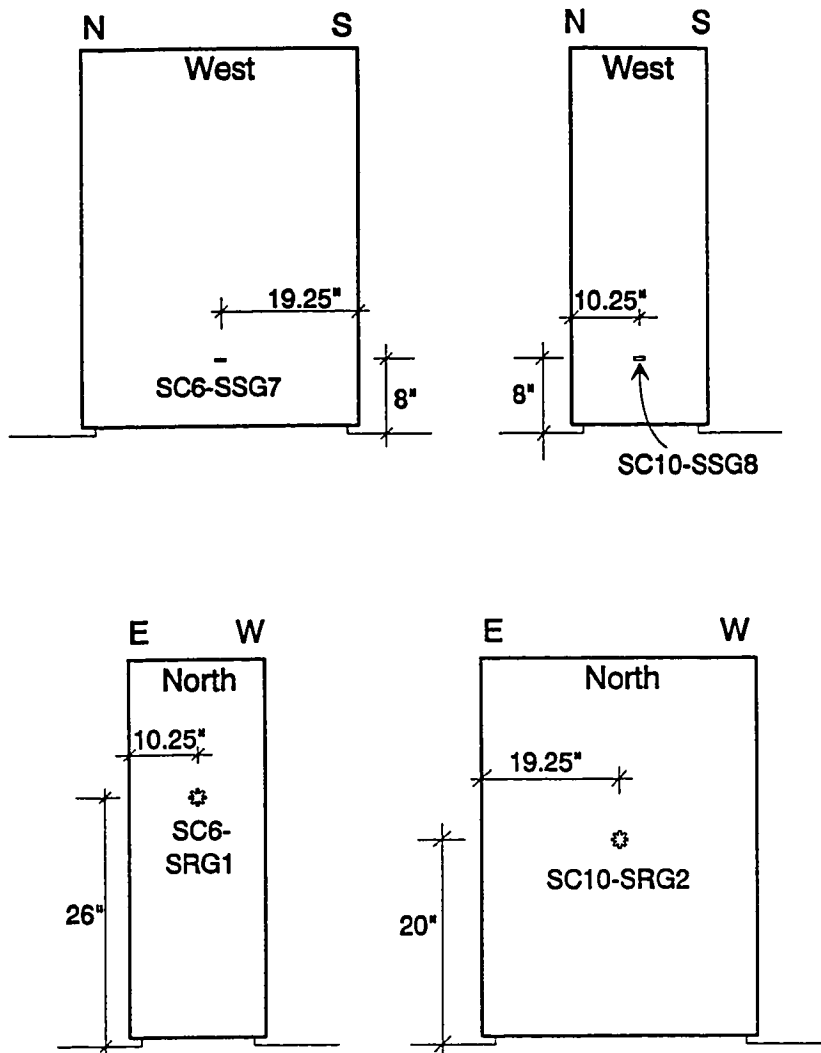


Figure 7.18 Locations of the Strain Gages on the Steel Jackets of the Shear Columns

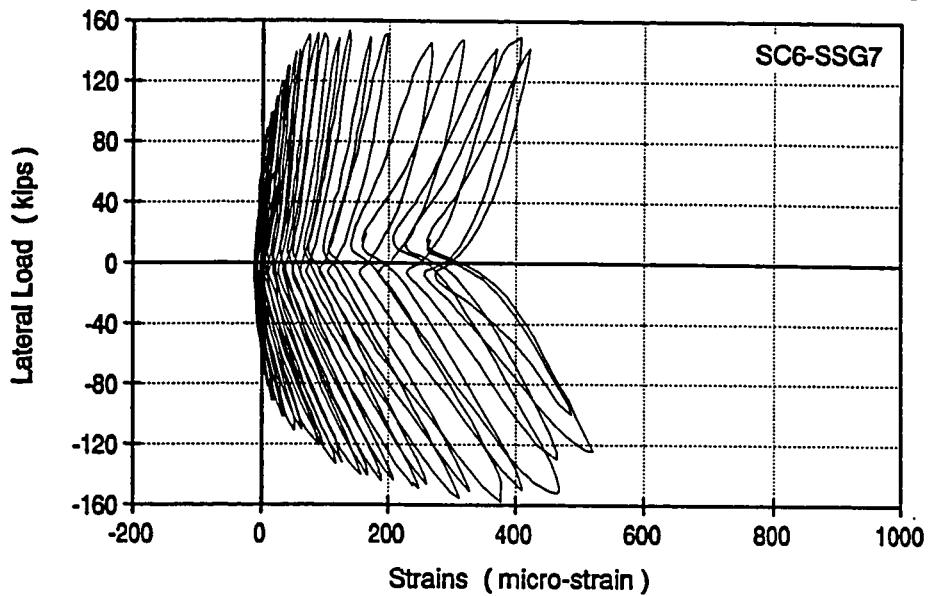


Figure 7.19 Strains in Strain Gage # SSG7

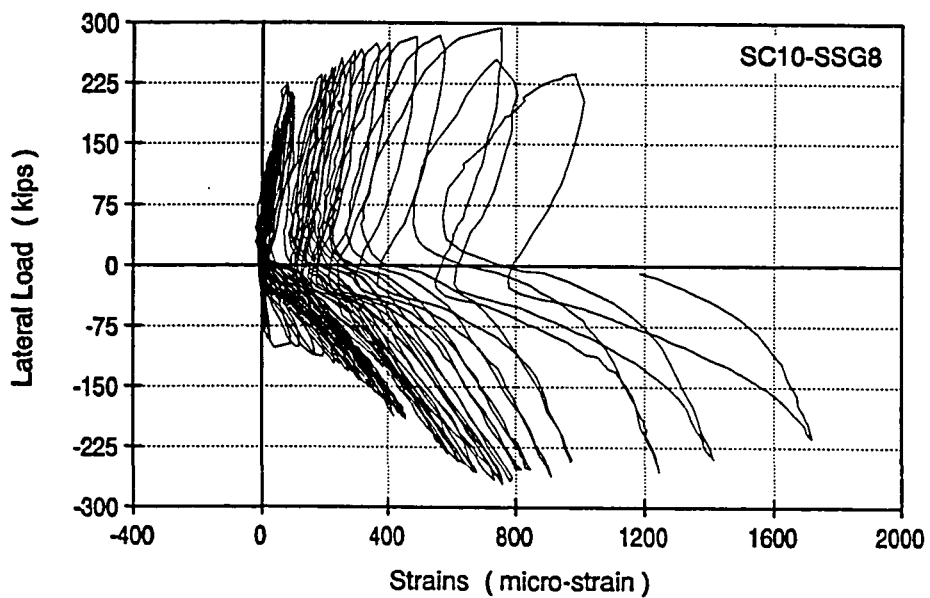
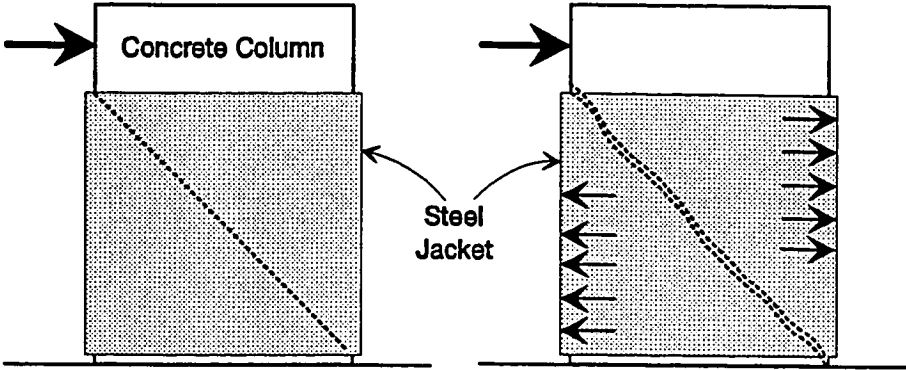
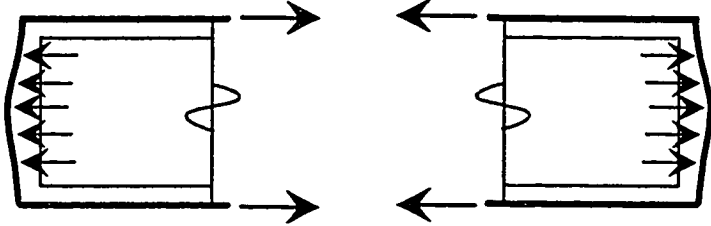


Figure 7.20 Strains in Strain Gage # SSG8



(a) Pressure on Steel Jacket caused by Column with Inadequate Shear Strength under Lateral Load



(b) Deformed Shape of the Steel Jacket

Figure 7.21 Deformed Shape of Steel Jackets under lateral Shear Loads

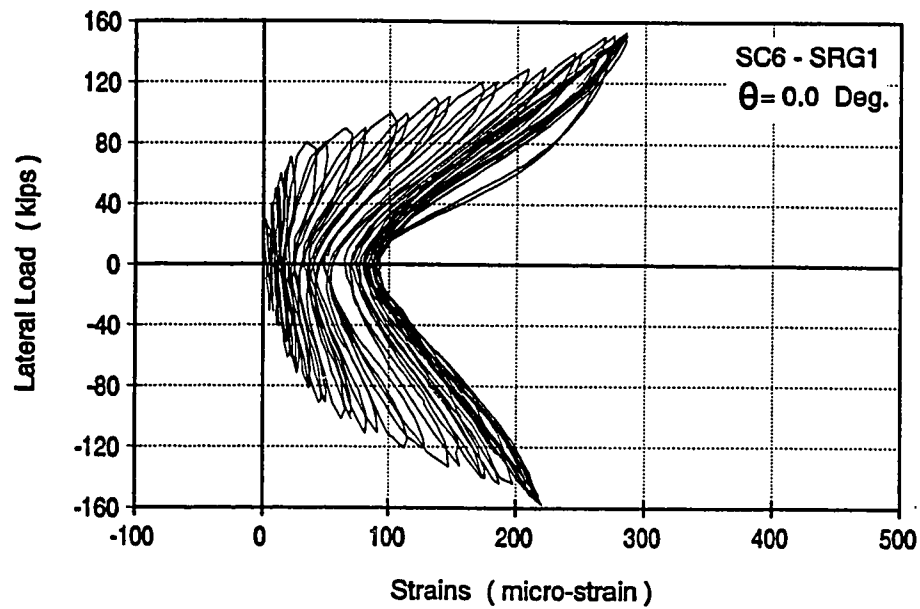


Figure 7.22 Strains in Strain Gage # SRG1 ( $\theta = 0.0$  Deg. )

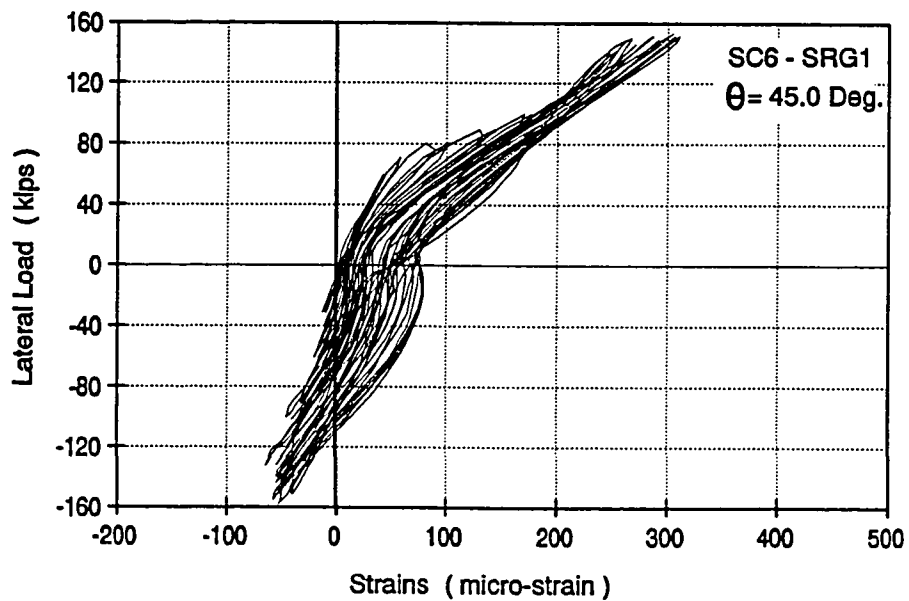


Figure 7.23 Strains in Strain Gage # SRG1 ( $\theta = 45.0$  Deg. )

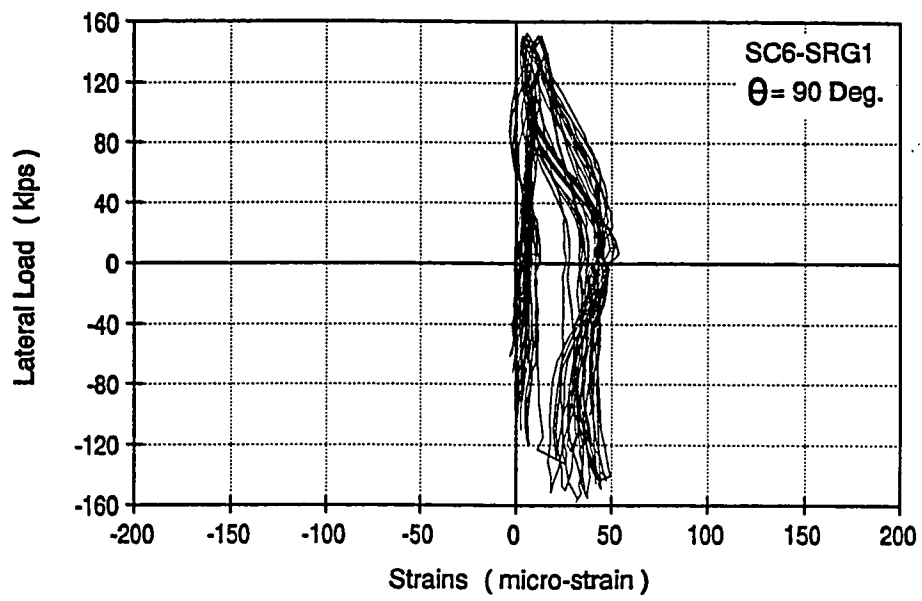


Figure 7.24 Strains in Strain Gage # SRG1 ( $\theta = 90$  Deg. )

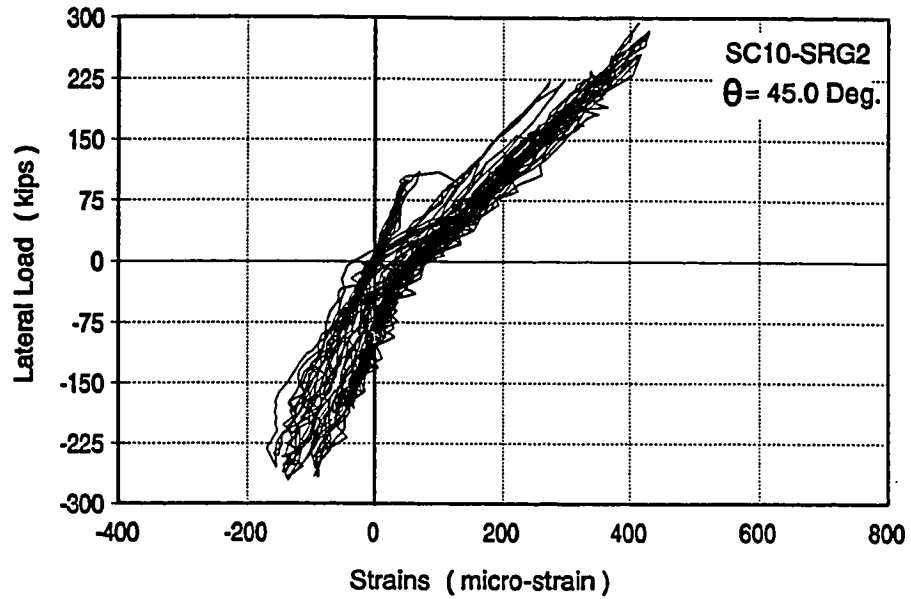


Figure 7.25 Strains in Strain Gage # SRG2 ( $\theta = 45.0$  Deg.)

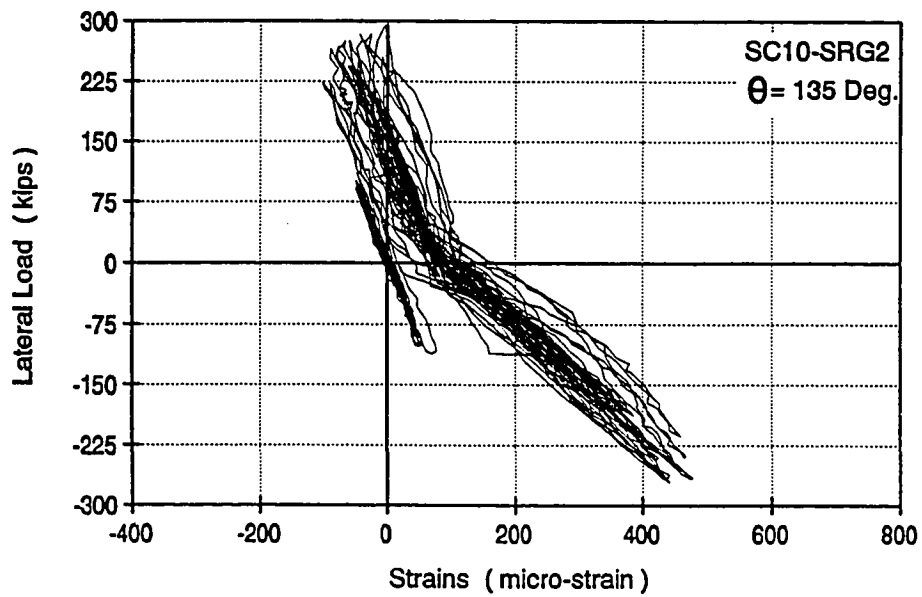


Figure 7.26 Strains in Strain Gage # SRG2 ( $\theta = 135$  Deg.)

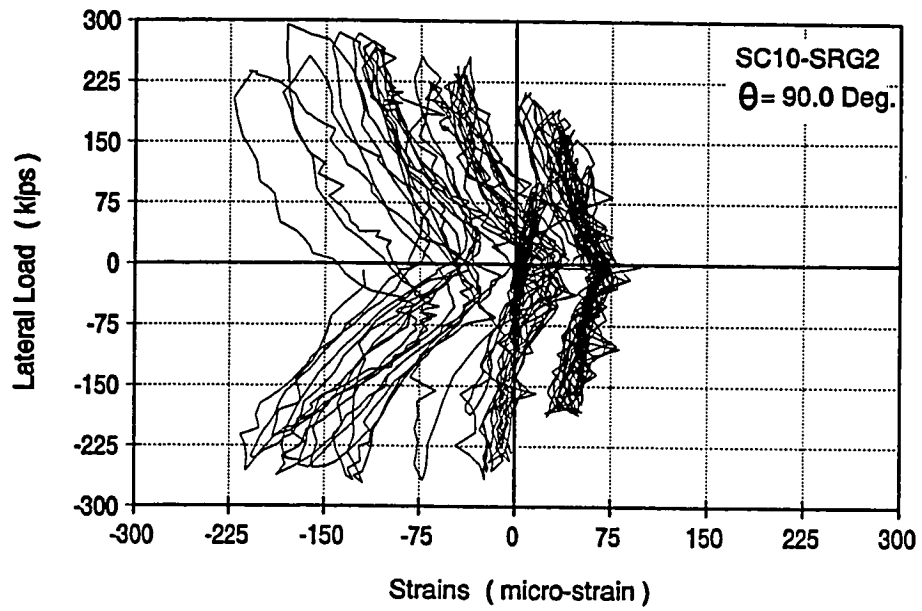


Figure 7.27 Strains in Strain Gage # SRG2 ( $\theta = 90.0$  Deg.)

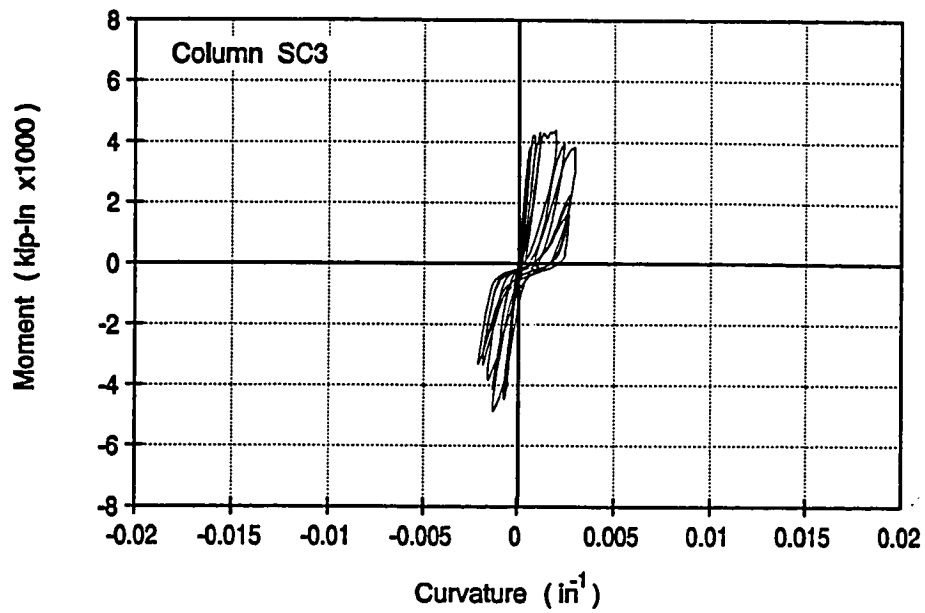


Figure 7.28 Column SC3 - Moment vs. Average Curvature

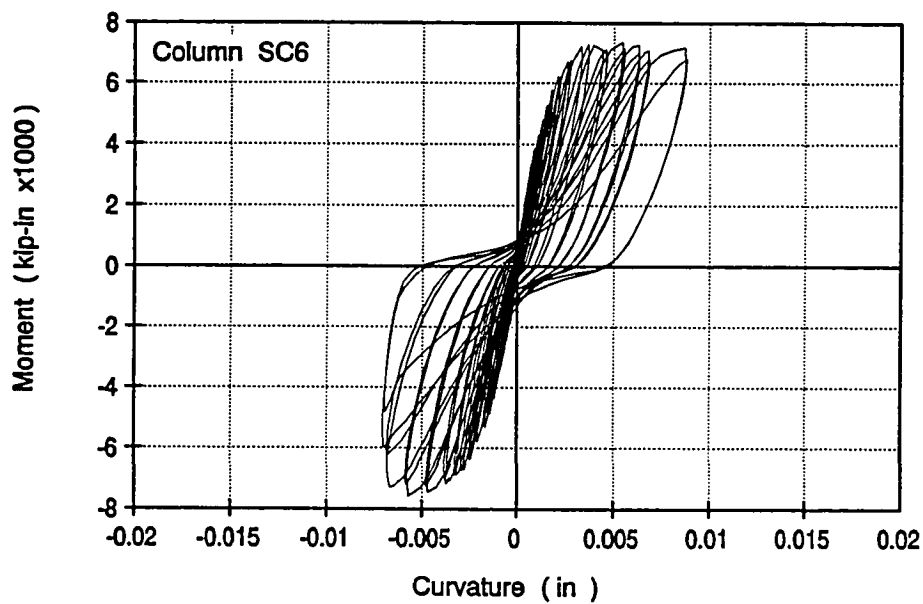


Figure 7.29 Column SC6 - Moment vs. Average Curvature



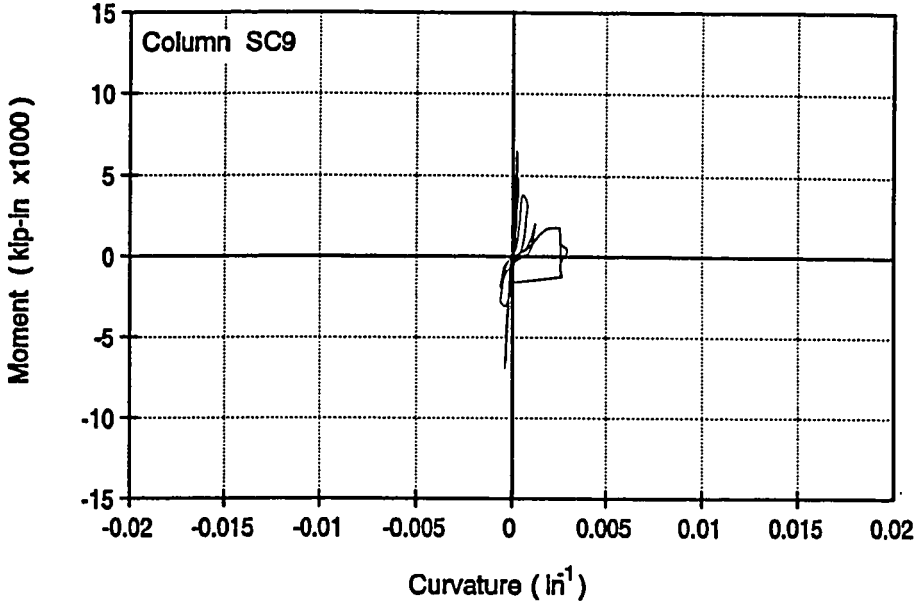


Figure 7.30 Column SC9 - Moment vs. Average Curvature

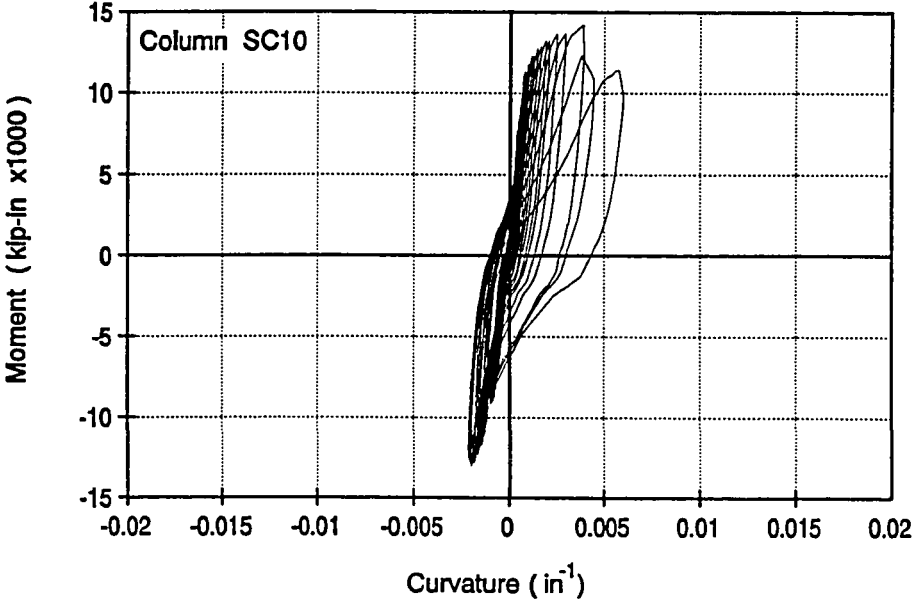


Figure7.31 Column SC10 - Moment vs. Average Curvature

## **CHAPTER 8**

### **EVALUATION AND DESIGN OF STEEL JACKETED COLUMNS**

#### **8.1 INTRODUCTION**

In this chapter, the effect of different variables on the performance of the test specimens is evaluated and discussed. Approaches for the design of steel jackets for retrofit of columns with an inadequate lap splice or inadequate shear strength are also discussed. Based on the results of the tests conducted in this study, preliminary design guidelines for the use of steel jackets for seismic retrofit of non-ductile reinforced concrete columns are presented. Analytical models for the design of seismic retrofit of columns with inadequate lap splices using rectangular steel jackets with and without anchor bolts are presented in sections 8.4 and 8.5. A simple model for the design of seismic shear retrofit of columns with inadequate shear strength is presented in section 8.12. A numerical example is presented in appendix "C".

#### **8.2 SHORTEST REPAIRABLE LAP SPLICE**

Columns investigated in this study were detailed according to the provisions of the American Concrete Institute codes ACI 318-56 and ACI 318-63. Some of the flexural columns with inadequate lap splices had an unintended concrete strength below 3000 psi. The splice length for these columns was only 75% of the splice length required by these older ACI code provisions for columns with concrete strength less than 3000 psi. However, the proposed steel jackets were effective in strengthening those columns. In general, however, using the results of this study for seismic strengthening of columns that do not meet

the requirements of the older ACI code provisions should be approached with caution.

The steel jackets tested were effective in strengthening columns with inadequate lap splices. However the length of the splice to be strengthened should not be less than  $L_{s(\min)}$ , below which bond failure would occur regardless of the passive confining stress provided by the steel jacket, anchor bolts and transverse reinforcement. If the splice length is shorter than  $L_{s(\min)}$  bond failure may occur by shearing-off a cylinder of concrete of a diameter slightly larger than that of the deformation of the reinforcing steel. This type of failure has been observed in beam steel passing through beam-column joints. Results from such tests indicate [37] that the effective bond stress corresponding to this failure is :

$$U_b = 16 \sqrt{f_c} \quad ( 8-1 )$$

Thus, the minimum required splice length to develop a stress of  $1.25 F_y$  in the bar is :

$$L_{s(\min)} = \frac{1.25 A_b F_y}{\pi d_b U_b} \approx \frac{0.020 d_b F_y}{\sqrt{f_c}} \quad ( 8-2 )$$

If the length of the column lap splice is below  $L_{s(\min)}$  as given in equation 8-2, steel jackets or other kinds of passive confinement might not be effective. In this case an active confining system such as externally prestressed stirrups or steel jackets with through rods may be more effective.

### 8.3 SHEAR FRICTION MECHANISM OF LAP SPLICES

For columns with inadequate lap splices, it was assumed that the main role of the steel jackets was to develop a passive clamping force across the splice splitting crack. Thus, the steel jacket should enable a shear friction mechanism to be used in transferring forces from one spliced bar to its counterpart. An equivalent friction factor of  $\mu = 1.0$  as for construction joints, appears to be appropriate for columns retrofitted with 1/4" thick steel jackets. Also, a friction factor of  $\mu = 1.40$  as for concrete placed monolithically, appears to be appropriate for columns retrofitted with 1/4" thick steel jackets and adhesive anchor bolts or through rods. The presence of anchor bolts would influence the deformation of the splice fracture surface, which may result in an increase in the confining pressure. However, for simplicity, the increase in the confining pressure is reflected as an increase in the shear friction factor. Numerical examples supporting the validity of the shear friction factors are presented later in this section.

The equivalent model of load transfer [30], using a 45 degree concrete compression field is shown in Figure 8.1 (a) & (b). Based on these assumptions the clamping force  $V_{sj}$  should be equal to the tension force  $T$  to be transmitted over the splice length  $L_s$ . Hence, the required thickness of the steel jacket can be estimated from equation 8-3.

$$V'_{sj} = T_b \quad \Rightarrow \quad 2 (t_{sj} * L_s) f_{sj} = A_s * (1.25 F_y)$$

$$t_{sj} \geq \frac{A_s * 1.25 F_y}{2L_s f_{sj}} \quad (8-3)$$

where

$V'_{sj}$  = confining force by the steel jacket (kips)

$T_b$  = tensile force in the longitudinal bars (kips)

$t_{sj}$  = thickness of the steel jacket (in)

- $L_s$  = length of the lap splice (in.)  
 $f_j$  = effective stress in the steel jacket (ksi)  
 $F_y$  = yield strength of the longitudinal bars (ksi)

Equation (8-3) does not take into account the contribution of the transverse reinforcement and the out-of-plane flexural stiffness of the steel jacket. As this study showed, anchor bolts may be needed to increase the stiffness of the steel jacket. More detailed methods for estimating the thickness of the steel jacket are presented in sections 8.4 and 8.5.

Like the clamping force  $V_{sj}$ , the shear friction force  $V_{sf}$  should be equal or greater than the yield strength of the longitudinal bars to ensure the development of the longitudinal bar's capacity before any splice failure. As shown in Figure 8.1 (c), the effective width of the crack surface, over which frictional shear stresses must be transferred, may be assumed to be the smaller of  $2C_s$  and  $3d_s$ , as suggested by Paulay [30], where  $C_s$  is equal to half the clear spacing between pairs of spliced bars. Following the provisions of the current ACI 318-89 code, shear stress at the development of the shear friction mechanism should not exceed  $0.2 f'_c$  or 800 psi. This is a safeguard against premature crushing of the concrete due to diagonal compression. These design criteria will seldom be critical unless the clear distance between pairs of spliced bars in a layer is very small.

The following is an example illustrating the procedure for checking the adequacy of column lap splices using the shear friction concept. Assume a 36" x 18" concrete column as the specimens tested in this study. The concrete strength is 3000 psi and the tensile yield strength of steel is 60 ksi.

$$v_{sf} = 0.2 f'_c \leq 800 \text{ psi} \quad (8-4)$$

where  $v_{sf}$  is the shear stress at the development of shear friction mechanism.

$$v_{sf} = 0.2 ( 3000 ) = 600 \text{ psi} < 800 \text{ psi} \quad \text{O.K.} \quad \therefore v_{sf} = 600 \text{ psi.}$$

The effective width of the shear crack surface  $W_{ss}$  is equal to the smaller of  $2C_s$  and  $3d_b$

$$\begin{aligned} W_{ss} &= 2C_s = 3.46 \text{ "} \\ &= 3d_b = 3.0 \text{ "} \quad \therefore W_{ss} = 3.0 \text{ "} \end{aligned}$$

The area of the shear surface  $A_{sf} = W_{ss} * L_s = 3.0 \text{ "} * 24 \text{ "} = 72 \text{ in}^2$

Maximum shear force ( $V_{sf}$ ) associated with the development of shear friction mechanism at the splice

$$V_{sf} = v_{sf} * A_{sf} = 600 \text{ psi} ( 72 \text{ in}^2 ) = 43,200 \text{ lbs.} = \underline{\underline{43.2 \text{ kips.}}}$$

Tensile yield capacity of longitudinal bar  $T_{by}$

$$T_{by} = A_s * F_y = 0.79 \text{ in}^2 ( 63 \text{ ksi} ) = 49.77 \text{ kips} \approx \underline{\underline{50 \text{ kips.}}}$$

$V_{sf} < T_{by}$   $\therefore$  the splice will fail before the tensile yield capacity of the longitudinal spliced bars is reached.

Check the same for column FC1,  $f_c = 4700 \text{ psi}$ ,

$$v_{sf} = 0.2 ( 4700 ) = 980 \text{ psi} > 800 \text{ psi} \quad \therefore \text{ use } v_{sf} = 800 \text{ psi.}$$

$$V_{sf} = v_{sf} * A_{sf} = 800 \text{ psi} * 72 \text{ in}^2 = 57600 \text{ lbs.} = \underline{\underline{57.6 \text{ kips.}}}$$

$V_{sf} > T_{by}$   $\therefore$  the spliced bars will develop tensile yield capacity before a shear friction failure occurs.

In the previous example the shear friction factor was considered equal to 1.0. The next example will present the application of the shear friction concept on the retrofitted columns with plain steel jackets without anchor bolts. The west side of columns FC2 and FC9 will be examined. As cited earlier that the equivalent shear friction factor  $\mu = 1.0$  appeared to be appropriate for columns retrofitted with plain steel jackets (without anchor bolts).

$$\begin{aligned} \text{Column FC2 ( West )} \quad f_c &= 4900 \text{ psi}, & \therefore v_{sf} &= 800 \text{ psi.} \\ V_{sf} &= 1.0 * ( 72 * 800 ) = 57600 \text{ lbs.} = \mathbf{57.6 \text{ kips}} > T_{by} \\ \text{Column FC9 ( West )} \quad f_c &= 2905 \text{ psi}, & \therefore v_{sf} &= 581 \text{ psi.} \\ V_{sf} &= 1.0 * ( 72 * 581 ) = 41832 \text{ lbs.} = \mathbf{41.8 \text{ kips}} < T_{by} \end{aligned}$$

Therefore, a plain steel jacket without adhesive anchor bolts would be able to strengthen column FC2, but it would not be able to strengthen column FC9. However, a steel jacket with anchor bolts would be adequate for retrofitting column FC9, since the presence of adhesive anchor bolts would increase the effective shear friction factor to 1.40. The next example presents the application of the shear friction concept on columns with inadequate lap splices retrofitted with steel jackets and anchor bolts. The East side of columns FC9 and FC12 will be examined.

$$\begin{aligned} \text{Column FC9 ( East )} \quad f_c &= 2905 \text{ psi}, & \therefore v_{sf} &= 581 \text{ psi.} \\ V_{sf} &= 1.40 * ( 72 * 581 ) = 58,565 \text{ lbs.} = \mathbf{58.6 \text{ kips}} > T_{by} \\ \text{Column FC12 ( West )} \quad f_c &= 3265 \text{ psi}, & \therefore v_{sf} &= 653 \text{ psi.} \\ V_{sf} &= 1.40 * ( 72 * 653 ) = 65,822 \text{ lbs.} = \mathbf{65.8 \text{ kips}} > T_{by} \end{aligned}$$

This indicates that the equivalent shear friction factor  $\mu = 1.40$  is appropriate for columns, with inadequate lap splices, retrofitted by the use of 1/4" thick steel jackets and adhesive anchor bolts. The experimental results of these two columns are in agreement with this observation.

#### 8.4 DESIGN OF STEEL JACKETS WITHOUT ANCHOR BOLTS

After studying the shear friction mechanism of any particular column with inadequate lap splice, the need for adhesive anchor bolts become apparent. The design of plain steel jackets without anchor bolts is presented in this section. The design approach considers the contribution of the transverse reinforcement in confining the lap splice.

In order to find the thickness of the steel jacket, the shear friction at the splice should be first estimated. The design shear friction should be the one associated with the development of  $1.25 F_y$ , the tensile yield strength of the longitudinal bars. The factor 1.25 accounts for the strain hardening of the steel bars. Assuming a 45 degree compression field at the splice, the equilibrium equation becomes

$$T_b = V_{sf} \quad (8-5)$$

where

$$T_b = A_s * 1.25 F_y \quad \text{and} \quad V_{sf} = \mu * v_{sf} * A_{sf}$$

$T_b$  = force in the longitudinal bar (kips)

$A_s$  = cross section area of the longitudinal bars ( $\text{in}^2$ )

$F_y$  = tensile yield capacity of longitudinal steel bars (ksi)

$V_{sf}$  = shear friction force on the shear surface (the plane of the spliced bars) at the development of shear friction mechanism (kips)

$\mu$  = shear friction factor equal to 1.0 for steel jackets without anchor bolts and 1.40 for steel jackets with anchor bolts.

$v_{sf}$  = shear stress on the shear surface (ksi)

$A_{sf}$  = effective shear surface area, equal to the smaller of  $3d_b * L_s$  and  $2C_s * L_s$  ( $\text{in}^2$ )



$d_b$  = nominal diameter of the longitudinal bar (in.)

$L_s$  = length of the lap splice (in.)

$C_s$  = half the clear spacing between longitudinal bars (in.)

For columns where  $2C_s$  is smaller than  $3d_b$ , the splitting crack may develop along the full width of the column. Equation (8-5) becomes

$$A_s * 1.25 F_y = \mu * v_{sf} * A_{sf}$$

$$v_{sf} = \frac{A_s * 1.25 * F_y}{\mu * A_{sf}} < 0.2 * f_c \leq 800 \text{ p.s.i.} \quad (8-6)$$

From Figure 8.2 the shear friction equilibrium equation is :

$$V_{sj} + V_{st} = V_{sf}$$

$$2 (t_{sj}) (s) f_{sj} * \frac{18}{h} + A_{st} F_{yt} = v_{sf} * b * s \quad (8-7)$$

where

$V_{sj}$  = confining force by the steel jacket per spacing  $s$  (kips)

$V_{st}$  = confining force by the transverse reinforcement (kips)

$b$  = width of the column (in.)

$s$  = spacing between layers of transverse reinforcement (in.)

$t_{sj}$  = thickness of the steel jacket (in.)

$f_{sj}$  = effective stress in steel jacket equivalent to the critical dilation strain (ksi)

$18 / h$  = factor reflecting the effect of column depth

$A_{st}$  = area of one layer of transverse reinforcement (in<sup>2</sup>)

$F_{yt}$  = tensile yield capacity of transverse ties (ksi)  $\leq 60$  ksi

$v_{sf}$  = shear friction stress (ksi)

Steel jackets lose their effectiveness in confining column splices at a critical dilation strain near the bottom of the splice. Experimentally, it was found that the critical dilation strain was 770 micro strain, which was equivalent to approximately 22 ksi. The total depth of all the flexural columns investigated in this study was 18 inches. Deeper column sections require a thicker steel jacket to be as effective as the steel jackets of the 18 inch deep columns. For the same steel thickness, a steel jacket for a deeper column section reaches its maximum effectiveness at strains lower than the dilation strain of 18 inch deep columns. Equation (8-7) can be rewritten as follows

$$t_{sj} \geq (v_{sf} * b * s - A_{sr} * F_{yr}) \frac{h}{36 * s * f_{sj}} \quad (8-8)$$

The following example illustrates the use of equation (8-8). For the 36 inch wide columns examined in this study, assuming the shear friction failure would occur over the full width of the column and along the full height of the spliced bars, the stress on the shear surface would be

$$v_{sf} = \frac{8 * (0.79) * (1.25 * 63)}{1.0 * (36 * 24)} = 0.576 \text{ ksi} \leq 0.2 * f_c$$

**Column FC9 ( 36" x 18")**

$$t_{sj} \geq [ 0.576 * 36 * 16 - 5 ( 0.11 ) 58 ] * \frac{18}{36 ( 16 ) 22}$$

$$\therefore t_{sj} \geq 0.426 "$$

**Column FC16 ( 27" x 18" )**

$$t_{sj} \geq [ 0.576 * 27 * 16 - 4 ( 0.11 ) 58 ] * \frac{18}{36 ( 16 ) 22}$$

$$\therefore t_{sj} \geq 0.317"$$

**Column FC17 ( 18" x 18" )**

$$t_{sj} \geq [ 0.576 * 18 * 16 - 2 ( 0.11 ) 58 ] * \frac{18}{36 ( 16 ) 22}$$

$$\therefore t_{sj} \geq 0.218"$$

The previous example showed that a 1/4" thick steel jacket without anchor bolts is effective for strengthening (18" x 18") columns, but not as effective for strengthening columns wider than or deeper than 18 inches. The results of Equation (8-8) are in good agreement with the experimental observation of columns FC9, FC16 and FC17.

## 8.5 DESIGN OF STEEL JACKETS WITH ANCHOR BOLTS

The design of steel jackets with anchor bolts is very similar to those without anchor bolts. As illustrated in Figure 8.3, anchor bolts force the steel jacket to deform with the concrete column and improve the confinement of the splice. Most of this improved performance is due to increase in the equivalent shear friction factor over the potential splitting crack on the plane of the spliced bars. Both the top and bottom anchor bolts contribute to deforming the steel jacket. Also, the bottom anchor bolts, installed within the splice length provide direct confinement to the spliced bars. However, this direct confinement is small due to the short embedment length of the anchor bolts beyond the splice plane.

An equivalent shear friction factor of 1.40 was found to be appropriate for columns retrofitted with steel jackets and anchor bolts.

Figure 8.4 shows a detail of an adhesive anchor bolt in the splice region. Bond failure between the anchor bolt and the surrounding concrete is considered the primary limit state. Thus, the maximum force that can be carried by an anchor bolt is

$$T_{ab} = u_b * \pi d_{ab} L_{ab} \quad (8-9)$$

where

$u_b$  = bond stress between anchor bolt and concrete (ksi), a value of  $16 \sqrt{f_c}$  is recommended. Please see section 8.8 for more details.

$d_{ab}$  = nominal diameter of anchor bolt, although the actual diameter of the fracture surface is slightly larger (in)

$L_{ab}$  = actual embedment length of anchor bolt, measured from the center of the spliced bars into the core of the concrete column (in.).

The shear friction stress estimated using equation (8-6) is also valid for columns retrofitted with steel jackets and anchor bolts. However, the shear friction factor  $\mu = 1.4$  should be used. It is believed that the 40 % increase in the shear friction force is resisted by the deformation of the steel jacket in the vertical direction, which causes an increase in the shear friction resistance. Figure 8.5 shows a cross section of a column retrofitted with a steel jacket and anchor bolts. The equilibrium equation of forces acting on the splice plane is

$$V_{sf} = V_{sj} + V_{st} + V_{ab} \quad (8-10)$$

where

$V_{ab}$  = confining force by the anchor bolt(s) (kips)

By substitution and rearrangement, equation (8-10) can be rewritten as follows

$$2 (t_{sj}) s * f_{sj} * 18/h = (v_{sf} . b . s) - [ u_b \pi d_{ab} L_{ab} (s / L_s) ] n_{ab} - (A_{st} * F_{yt})$$

where

$n_{ab}$  = number of anchor bolts within the splice region, must be located at a distance  $\geq 6.0$  inches below the top of the splice.

from which the thickness of the steel jacket can be estimated as follows

$$t_{sj} \geq [ (v_{sf} * b * s) - ( u_b \pi d_{ab} L_{ab} \frac{s}{L_s} ) n_{ab} - (A_{st} * F_{yt}) ] * \frac{h}{36 * s * f_{sj}} \quad (8-11)$$

Based on the test results of this study, it is recommended to limit the anchor bolt term in Equation (8-11) to 10-15% of the maximum shear friction force. The following examples demonstrates the application of equation (8-11).

#### Column FC12 ( 36" x18" )

The west side of column FC12 was retrofitted with a steel jacket and two vertical lines of two anchor bolts each. It had only two anchor bolts within the splice length. Therefore the required thickness of the steel jacket would be

$$v_{sf} = \frac{8 * (0.79) * (1.25 * 63)}{1.40 * (36 * 24)} = 0.411 \text{ ksi} < 0.2 * f_c \leq 800 \text{ p.s.i.}$$

$\therefore t_{sj} \geq 0.263$  " use 1/4" thick steel jacket.

$$t_j \geq [ ( 0.411 \cdot 36 \cdot 16 ) - ( 16 \cdot \frac{\sqrt{3265}}{1000} \cdot \pi \cdot 1.0 \cdot 5.125 \cdot \frac{16}{24} )^2 - 5(0.11)58 ] \cdot \frac{18}{36 (16) 22}$$

### Column FC16 ( 27" x 18" )

The east side of column FC16 was retrofitted with a steel jacket and one vertical line of two anchor bolts. It had only one anchor bolt within the splice length. Therefore the thickness of the steel jacket should be

$$t_j \geq [ ( 0.411 \cdot 27 \cdot 16 ) - ( 18 \cdot \frac{\sqrt{2565}}{1000} \cdot \pi \cdot 1.0 \cdot 5.125 \cdot \frac{16}{24} )^2 - 5(0.11)58 ] \cdot \frac{18}{36 (16) 22}$$

$\therefore t_{j1} \geq 0.203" > 3/16" \quad \therefore$  use the next thicker, a 1/4" thick steel jacket.

The performance of the east side of column FC16 was considered satisfactory with a 1/4" thick steel jacket. The concrete strength of column FC16 was only 2565 psi. For such low strength concrete, the lap splice length should have been 32 times the diameter of the longitudinal bar per ACI 318-63, the actual splice length of column FC16 was only 24  $d_b$ . If the actual splice length of column FC16 was exactly according to the provisions of ACI code 318-63, a 0.203" thick steel jacket with anchor bolts would be adequate for seismic strengthening of column FC16 according to Equation (8-11).

## 8.6 ULTIMATE FLEXURAL CAPACITY

It was observed that both the basic unretrofitted flexural and shear column specimens did not develop their nominal yield flexural capacity, with the exception of columns FC1 and SC1. On the other hand, all the retrofitted columns developed flexural resistance higher than the theoretical flexural capacity of the unretrofitted columns. This increase in the flexural resistance is primarily due to the following two reasons:

1. increase in the confinement of the concrete compression zones by the steel jacket,
2. strain hardening of the longitudinal reinforcing bars on the tension sides of the columns.

Concrete compression strength increases with the presence of lateral confinement. Well detailed longitudinal and transverse reinforcing bars provide good confinement for the concrete core but not for the concrete cover. Unlike ordinary reinforcing bars, steel jackets provide lateral confinement for the whole concrete section, including the concrete cover. Concrete in the compression zone exhibits higher useful stresses and strains when confined by steel jackets, which result in an increase in the flexural capacity as illustrated in Figure 8.6. This increase in the flexural capacity is primarily due to an increase in the moment arm between the resultant of the compression forces "C" and the resultant of the tensile forces "T". At large curvatures at the critical section, the longitudinal reinforcing bars experience stresses higher than the yield stress. Combined with the increase in the moment arm ( $d - a_c/2$ ), strain hardening of the longitudinal bars causes an additional increase in the flexural resistance of the concrete column as shown in Figure 8.7.

The observed experimental flexural capacity of the retrofitted columns was 30 - 35 % higher than the theoretical nominal flexural capacity of an unretrofitted reinforced concrete column with an inadequate splice. In order to estimate the ultimate flexural capacity of a steel jacketed column, the maximum compressive strength  $f'_{cc}$  of confined concrete under lateral pressure needs to be evaluated. Confined concrete strength is greatly influenced by the amount of the transverse reinforcement. For steel jacketed columns, the steel jacket provides sufficient confinement to the column concrete, prevents buckling of the longitudinal bars, and prevents shear failure. However, the steel jackets become ineffective in confining the splice region of concrete columns with inadequate lap splices at strains above some maximum useful strain. It was experimentally

found that the maximum useful strain (dilation strain) did not exceed 770 micro strain, which is equivalent to a stress of approximately 22 ksi. The dilation strain has a low value because the steel jacket is unbonded to the concrete column.

Figure 8.8 shows a cross section of a column retrofitted with a steel jacket. The confining pressure  $f_l$  can be estimated by writing the equilibrium equation

$$V_{st} + V_{sj} = f_l * b * s$$

$$(A_{st} * F_{yt}) + 2 (t_{sj}) s * f_{sj} * (18/h) = f_l * b * s$$

$$f_l = [ (A_{st} * F_{yt}) + 2 * (t_{sj}) * s * f_{sj} * \frac{18}{h} ] * \left( \frac{1}{b * s} \right) \quad (8-12)$$

Knowing the maximum useful stress in the steel jacket, the equivalent lateral pressure can be estimated using equation (8-12). Figure 8.9 presents a chart which can be used to estimate the compressive strength of confined concrete. The chart, adopted from reference [11], was developed by Mander et al, and is based on work conducted by Mander as well as other researchers [38,39,40].

To calculate the longitudinal compressive strain of confined concrete at failure  $\epsilon_{cc}$ , a simple equation suggested by Richart et al [41] was adopted.

$$\epsilon_{cc} = \epsilon_{co} [ 1 + 5 ( f'_{cc} / f'_{co} - 1 ) ] \quad (8-13)$$

where

$\epsilon_{cc}$  = concrete strain associated with the maximum confined concrete compressive strength  $f'_{cc}$



$\epsilon_{co}$  = concrete strain associated with the maximum unconfined compressive strength  $f'_{cc}$  (generally assumed 0.002).

Mander et al [11] developed a more refined method to estimate the confined concrete strain at the maximum concrete stress  $f'_{cc}$ . This method is based on an energy balance concept. It predicts the longitudinal compressive strain in concrete corresponding to first fracture of the transverse reinforcement by equating the strain energy capacity of the transverse reinforcement to the strain energy stored in the concrete as a result of the confinement. A similar approach can be used for steel jacketed columns. The only major difference is that the maximum compressive strain in the concrete should be that corresponding to the limiting dilation strain in the steel jacket, not the first fracture of the transverse reinforcement.

Knowing  $f_t$ ,  $f'_{cc}$  and  $\epsilon_{cc}$  the ultimate flexural capacity of a steel jacketed concrete column can be evaluated. Appendix "C" presents a numerical example for estimating the flexural capacity of a steel jacketed column.

## 8.7 HEIGHT OF THE STEEL JACKET

For columns with inadequate lap splices, the height of the steel jackets was either 1.2 or 1.5 times the length of the lap splice. Figure 8.10 shows two retrofitted columns with short and long steel jackets. Based on the results of column FC11, it was found that extending the steel jacket 4.5" above the top of the splice did not ensure good confinement of the splice by the steel jacket at large drift ratios. However, based on the results of column FC12, it was found that extending the steel jacket 12" above the top of the splice was considerably more effective in improving the ductility of columns with inadequate lap splices. The longer steel jacket has the advantage of being anchored to the concrete column at approximately 6 inches above the top of the splice. This allows anchoring the steel jacket to the concrete column away from the top of the

splice. In addition, it forces the steel jacket to deform better with the concrete column and help confine the splice region. It is recommended to use steel jackets of height equal to the larger of 1.5 times the length of the splice and  $(L_s + 12")$ .

For columns with inadequate lap splices, the steel jackets were terminated 1.5" from the face of the footing. This termination was made to avoid any possible bearing of the steel jacket against the footing, which may increase the flexural capacity of the column and cause local damage of the steel jacket at the bottom of the splice.

For columns with inadequate shear strength, the height of the steel jackets was equal to the full height of the column less by two inches, one inch at the top and one inch at the bottom.

## **8.8 CONCRETE COMPRESSIVE STRENGTH**

Force transmission between spliced bars relies on bond between bars and the surrounding concrete. In certain regions, particularly where inelastic and reversible strains occur, heavy demand may be imposed on stress transfer by bond.

Experimental results of the retrofitted column FC2 indicated that if the column concrete strength is higher than or equal to 4900 psi, a plain steel jacket without adhesive anchor bolts was adequate for strengthening 36 inch wide columns with inadequate lap splices. On the other hand, test results of the retrofitted column FC9 indicated that if the column concrete strength is lower than or equal to 2900 psi, a plain steel jacket without adhesive anchor bolts was inadequate for strengthening 36 inch wide columns with inadequate lap splices.

For columns with inadequate shear strength, test results indicated that rectangular steel jackets are very effective in enhancing shear strength and ductility of these columns. Columns with concrete strength as low as 2250 psi were successfully retrofitted with 1/4" thick rectangular steel jackets.

### **8.9 NON-SHRINK GROUT**

The unconfined compressive strength of 2 inch cubes of the non-shrink grout used in this study ranged between 4300 psi and 7490 psi. It was observed that the compressive strength of the non-shrink grout did not have major influence on the performance of the retrofitted columns. This is probably due to the confinement of the non-shrink grout between the steel jacket and the concrete column.

In this study, the thickness of the non-shrink grout was one inch. It is believed that the thickness of the grout could have been smaller without any significant change in the performance of the retrofitted columns. The one inch thickness was selected for ease of casting the grout.

### **8.10 ADHESIVE ANCHOR BOLTS**

As presented in the previous sections, when adhesive anchor bolts were required, they were provided at least at two levels, above the top of the splice and within the bottom half of the splice length. In plan, it was found that providing the anchor bolts at 12 inch intervals was adequate to confine the splice. Figure 8.11 shows a detail of an adhesive anchor bolt at a column lap splice. As shown in the figure, a 4" x 4" x 1/2" thick steel washer was used with every anchor bolt to distribute the bolt force over a larger area. If it were assumed that the effective confined zone is bounded by 45 degree lines radiating from the edge of the 4" washer, the width of the confined zone at the splice location would be approximately 12 inches. This may explain why a 12 inch

spacing between anchor bolts worked very well for the retrofitted columns with an inadequate lap splice.

Bolts used in this experimental research were 1.0 inch in diameter. Appendix "B" presents more details about the adhesive anchor bolts used in this study. The total length of the bolt was 12 inches, and it was embedded 8 inches into the concrete column. The bolt was embedded approximately 5 inches beyond the plane of the spliced bars. This distance is referred to later as  $L_{ab}$ . The total surface area of the embedded portion of the bolt beyond the plane of the spliced bars is equal to

$$A_{ab} = \pi * d_{ab} * L_{ab} \quad (8-14)$$

where

$A_{ab}$  = surface area of anchor bolt over embedment length  $L_{ab}$  (in<sup>2</sup>)

$d_{ab}$  = nominal diameter of anchor bolt (in.)

$L_{ab}$  = embedment length of anchor bolt beyond the plane of the spliced bar (in.).

As bond failure between the anchor bolt and the surrounding concrete is considered the primary limit state, it is very important to keep the level of bond stresses sufficiently low to prevent this limit state. A bond stress of  $16\sqrt{f_c}$  is considered appropriate for anchor bolts embedded in concrete, since for this particular case bond failure may occur by shearing-off a cylinder of concrete of a diameter slightly larger than the outside diameter of the anchor bolt. The actual bond failure would occur at the bolt adhesive-concrete interface, and the actual fracture surface would be located slightly into the concrete material. Some variables, such as  $d_{ab}$ ,  $L_{ab}$  and the horizontal spacing between bolts, were not thoroughly investigated in this study, but it is believed that some limitations are needed to ensure acceptable performance by retrofitted columns. These limitations are as follows:

1. horizontal spacing between bolts =  $12 - [24 (1.0 - d_{ab})] \leq 12"$
2. minimum embedment length =  $0.4 (d_{ab}^2) F_y \geq 5.0"$
3. minimum diameter of bolt =  $3/4"$ .

Surface preparation is the most important item when adhesive materials are involved. The pre-drilled hole for the anchor bolt should be cleaned very well before the installation of anchor bolts. Otherwise, bond failure may occur at early stages of loading.

For seismic retrofitting, adhesive anchor bolts are preferred over expansion anchors since they have higher stiffness and distribute the load to the concrete column over the whole embedment length  $L_{ab}$ . Figures 8.12 and 8.13 summarize the recommendations for strengthening and repair of columns with inadequate lap splices, by the use of rectangular steel jackets.

### 8.11 BEHAVIOR OF JACKETED COLUMNS FAILING IN SHEAR

Before the development of the major diagonal shear cracks, the response of the retrofitted columns with full steel jackets was almost identical to that of the basic unretrofitted columns, with the exception the retrofitted columns had a slightly higher stiffness. During the tests, the major diagonal shear cracks developed on both the unretrofitted and retrofitted columns at almost the same lateral loads. This suggests that the steel jackets were passive and did not provide significant shear resistance until the concrete column had deformed and developed major diagonal shear cracks.

Prior to major diagonal shear cracking, the strain in the steel jackets was very small, much smaller than the corresponding strain of the concrete. After the development of the major diagonal shear cracks, the steel jacket carried shear forces at higher rates. Thus, the steel jacket did not prevent the development of the shear cracks, but it prevented widening of the major

diagonal shear cracks. The development of the major diagonal shear cracks was associated with very high strains in the transverse reinforcement, well beyond its yielding strain.

The response of the transverse reinforcement to cyclic straining imposed by lateral forces does not involve significant cyclic degradation, provided that the reinforcement remains in the elastic range. Also, it is believed that the response of steel jackets to cyclic straining does not involve significant cyclic strength and stiffness degradation, provided that the steel jacket remains in the elastic range. Therefore, it is important that the steel jacket remains elastic to prevent any widening of the major diagonal shear cracks and consequently major loss of the column lateral strength and stiffness.

Since the steel jacket is unbonded to the concrete column, the diagonal shear cracks have to open widely in order to develop the yielding strain of the steel jacket. At that stage, shear transferred by the concrete may drop dramatically, due to loss of aggregate interlock across the crack.

## **8.12 SHEAR ANALYSIS OF STEEL JACKETS**

If the steel jacket is permitted to yield, significant shear deformations will result. The closure of wide diagonal cracks upon force reversal is associated with insignificant shear and hence seismic resistance. As a consequence, marked reduction of energy dissipation will also occur during cyclic lateral loading. For these reasons, the prevention of yielding of the steel jacket during an earthquake is one of the aims of the proposed simple model.

The shear strength enhancement provided by the rectangular steel jackets can be conservatively estimated by considering the jacket to act as a series of independent square ties of thickness and spacing  $t_{sj}$ , where  $t_{sj}$  is the steel jacket thickness. Conservatively, the shear stresses in the steel jacket between the

assumed square ties are ignored. The shear force carried by the steel jacket  $V_{sj}$  would be

$$V_{sj} = A_{sj} * F_{sj} * \frac{d_{sj}}{s_{sj}} \quad (8-15)$$

where

$$\begin{aligned} A_{sj} &= \text{area of the assumed square tie (in}^2\text{)} \\ &= (t_{sj})^2 \end{aligned}$$

$F_{sj}$  = stress in the steel jacket; recommended value is equal to half the actual yielding stress of the steel jacket (ksi)

$d_{sj}$  = total depth of the steel jacket (in)

$s_{sj}$  = spacing between the square ties, equal  $t_{sj}$  (in).

Equation (8-15) assumes that the diagonal strut inclination for the retrofitted columns is at an angle  $\theta = 45$  degrees. It can be rewritten as follows

$$V_{sj} = A_{sj} * (0.5 * F_y)_{sj} * \frac{d_{sj}}{s_{sj}} \quad (8-16)$$

The maximum column width that was investigated in this study was 36 inches. It was found that 1/4" thick rectangular steel jackets could provide adequate shear strength for reinforced concrete columns as wide as 36 inches. However, confinement of the compression zone may become a limit state. For columns wider than 36", thicker steel jackets should be used.

The nominal shear capacity of a retrofitted reinforced concrete column with inadequate shear strength by the use of rectangular steel jackets would be:

$$V_n = V_c + V_{st} + V_{sj} \quad (8-17)$$

where

$V_n$  = nominal shear force at section (kips)

$V_c$  = nominal shear force provided by concrete (kips)  
equal  $2.0 \sqrt{f_c} b_w d$ .

$V_{st}$  = nominal shear force provided by transverse ties (kips)  
equal  $A_{st} * F_{yt} * (d / s)$

$V_{sj}$  = nominal shear force provided by the steel jacket (kips)  
equal  $A_{sj} * F_{sj} * (d_{sj} / s_{sj})$ .

### 8.13 INFLUENCE OF AXIAL LOAD

In this study, columns were all tested under lateral cyclic loading, but without axial load. This section discusses the influence of axial load on the design of retrofitted columns with steel jackets.

Building columns are subjected to gravity axial compressive forces. During an earthquake, column axial load may increase or decrease depending on the structural system of the building and its response to ground motion. An increase in the axial compressive load will increase the shear capacity of the column, but will not necessarily increase column ductility, which is needed in seismic zones. Compressive axial load will require a larger concrete compressive force and compression zone. The contribution of the concrete compression zone in resisting shear is usually larger. But, after reaching its peak lateral load, an ordinary reinforced concrete column with axial compressive load will exhibit lower ductility and a higher rate of strength and stiffness degradation, as compared to columns without axial load.

For designing retrofitted shear columns subject to shear and axial compressive load, the new flexural capacity should be first estimated for the concrete column. The entire column cross section should be considered as a well confined concrete section. Jacketed columns under small axial load exhibit higher flexural capacity than a basic unretrofitted column without axial load.



The increase in the flexural capacity is due to two main reasons: presence of the compressive axial load and confinement of the whole concrete section provided by the steel jacket. After estimating the flexural capacity of the jacketed column, the retrofitted column should be designed for a shear force at least equal to that associated with the development of that new flexural capacity. It is believed that rectangular steel jackets should work well for columns with inadequate shear strength under axial compressive loads, as long as the steel jacket remains in the elastic range. Shear strength and stiffness degradation occur only after wide opening of the major diagonal shear cracks. Wide opening of the major diagonal shear cracks does not happen for a column retrofitted with a full steel jacket that remains elastic during an earthquake.

It is believed that if the steel jacket were allowed to yield, a major drop in strength and stiffness might occur after reaching the peak load. A sudden drop in strength may occur due to the possibility of loss of the shear resistance provided by the aggregate interlock. This drop in strength would be more dramatic in the presence of axial load.

For columns with inadequate lap splices, the presence of axial compressive load reduces the amount of tensile force transmitted by the splice, which may help the splice. However, in the presence of axial tension load, the spliced bars may have to transmit high tensile forces before the development of any significant rotations in the splice region to force the steel jacket to confine the splice.

#### **8.14 SUMMARY**

In this chapter, general evaluation of the performance of the test specimens and the effect of different variables were presented. In addition, a simple analytical model for the design of rectangular steel jackets was presented. The proposed model for the design of steel jackets for strengthening of columns

with inadequate lap splices was based on a shear friction mechanism of concrete in the plane of the spliced bars. The steel jackets may contain adhesive anchor bolts. The effectiveness of the steel jackets is considered limited by the critical dilation strain, which was determined experimentally.

For columns with inadequate shear strength, the proposed model for the design of steel jackets is based on equilibrium of shear forces. To avoid any possible dramatic loss of strength and stiffness at large displacements, stresses in the steel jacket were limited to half the yield strain of the steel jacket. A simple model was proposed to estimate the flexural capacity of jacketed columns. The model considers the increase of concrete strength due to lateral confinement provided by the steel jacket. A numerical example is presented in Appendix "C".

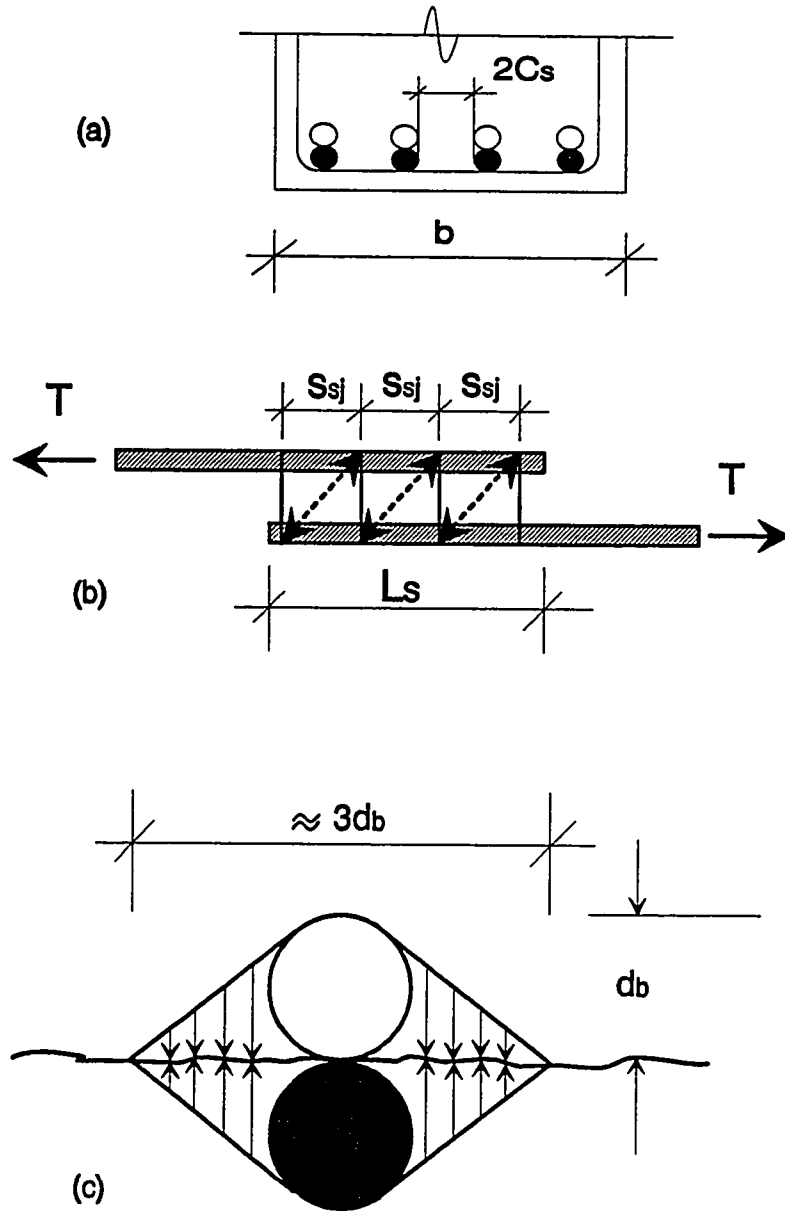


Figure 8.1 Compression Field Across Two Spliced Bars Developed by Steel Jacket

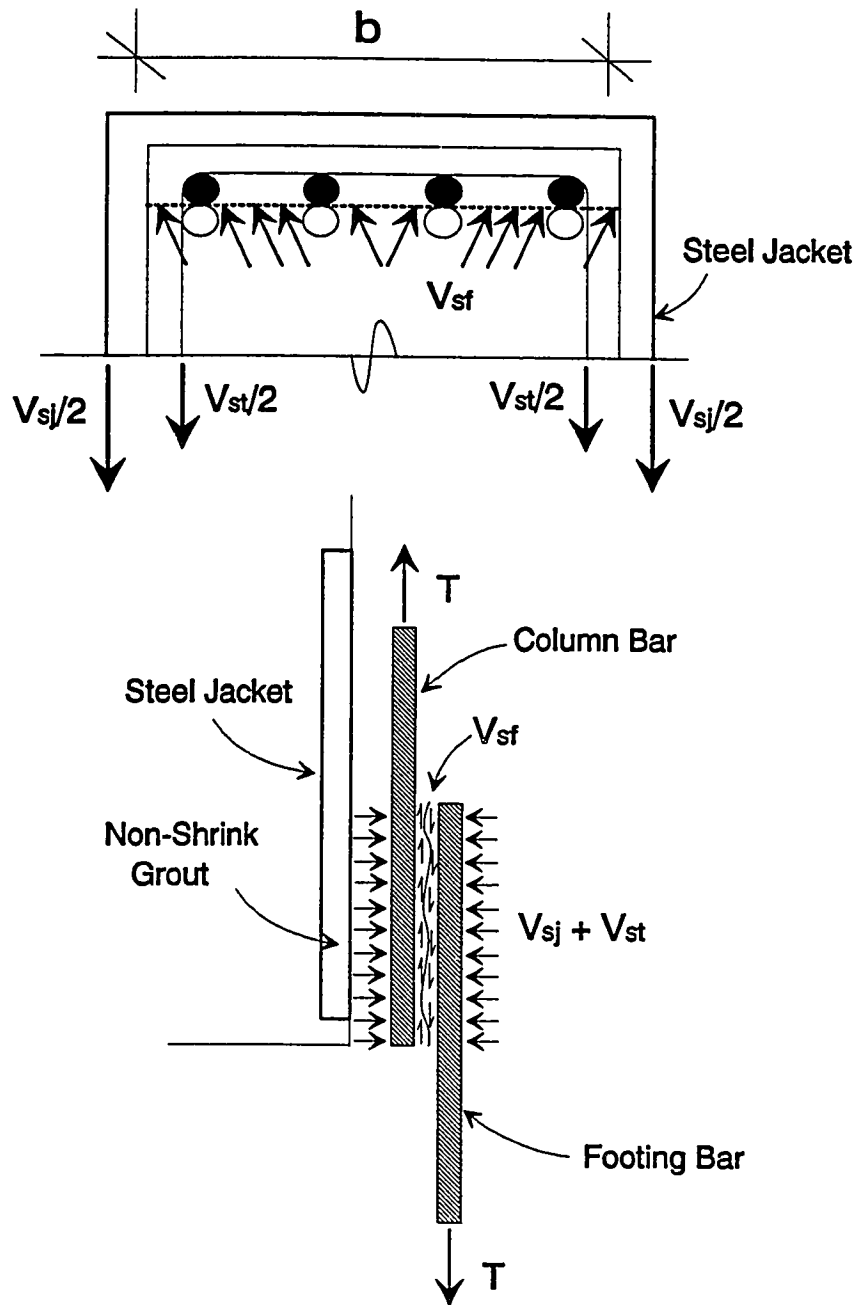


Figure 8.2 Shear Friction Mechanism at Spliced Bars of a Retrofitted Column With Steel Jacket

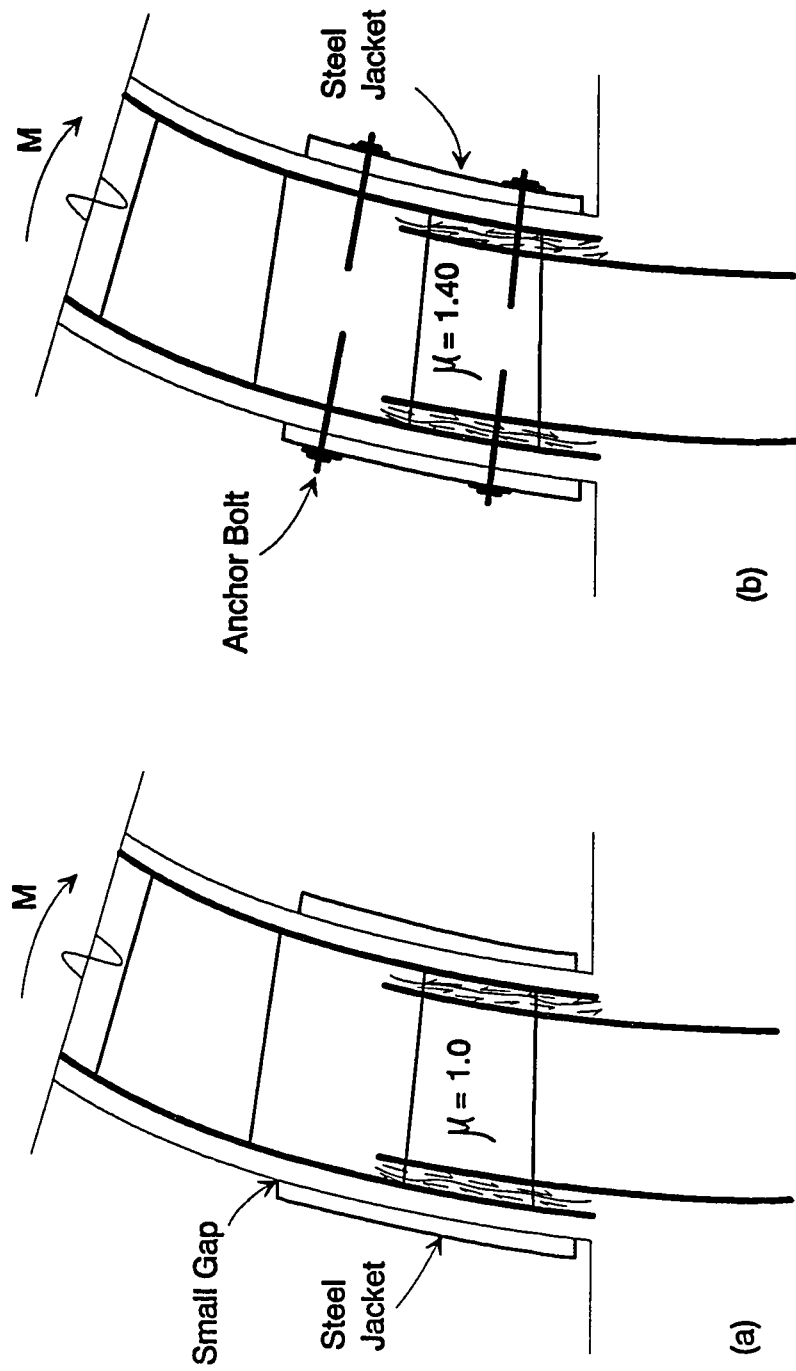


Figure 8.3 Splice Region of Retrofitted Flexural Columns by the use of :  
 (a) Plain Steel Jacket (b) Steel Jacket with Anchor Bolts

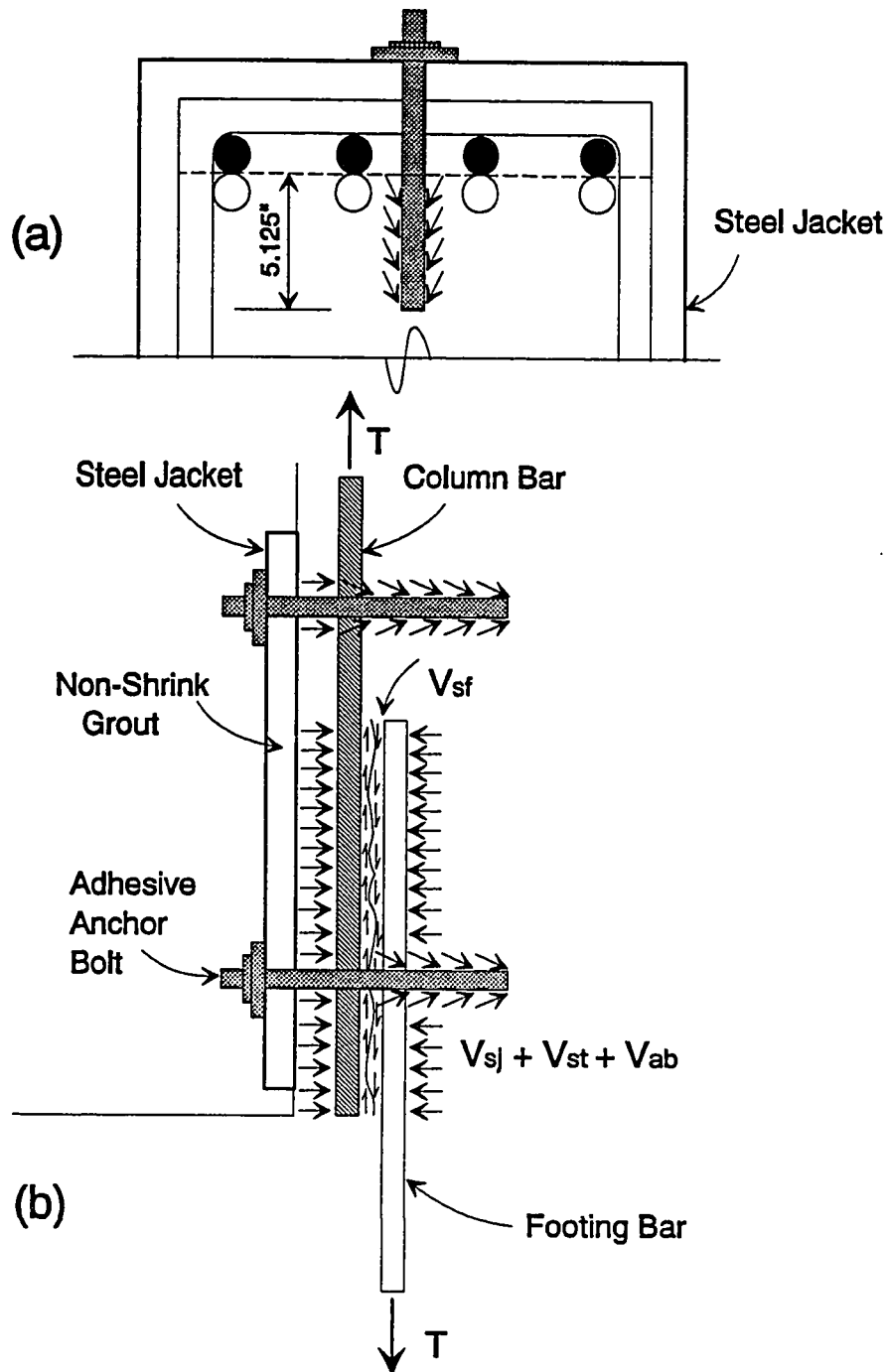


Figure 8.4 Detail of Adhesive Anchor Bolt in the Splice Region : (a) Plan (b) Side View

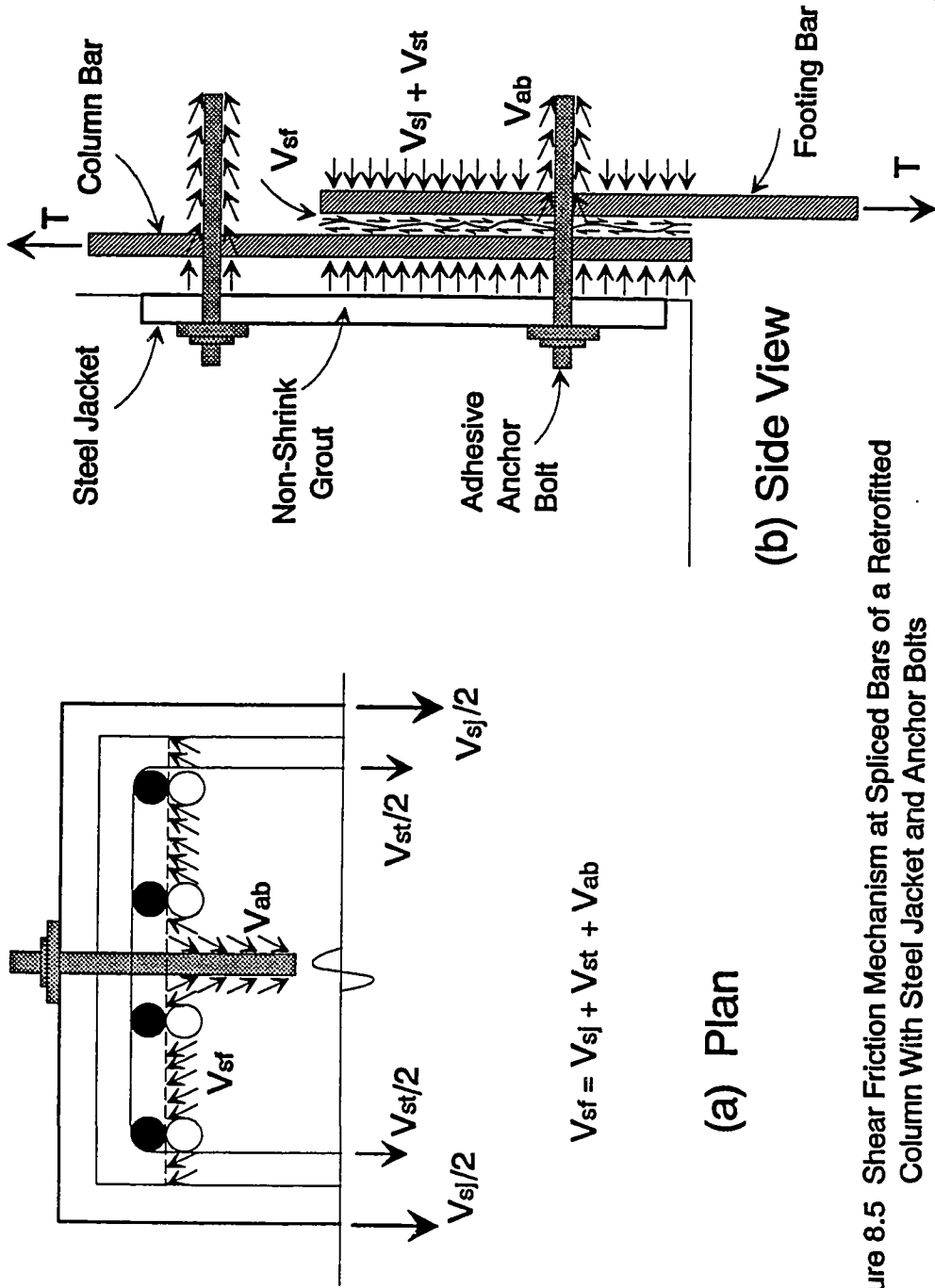
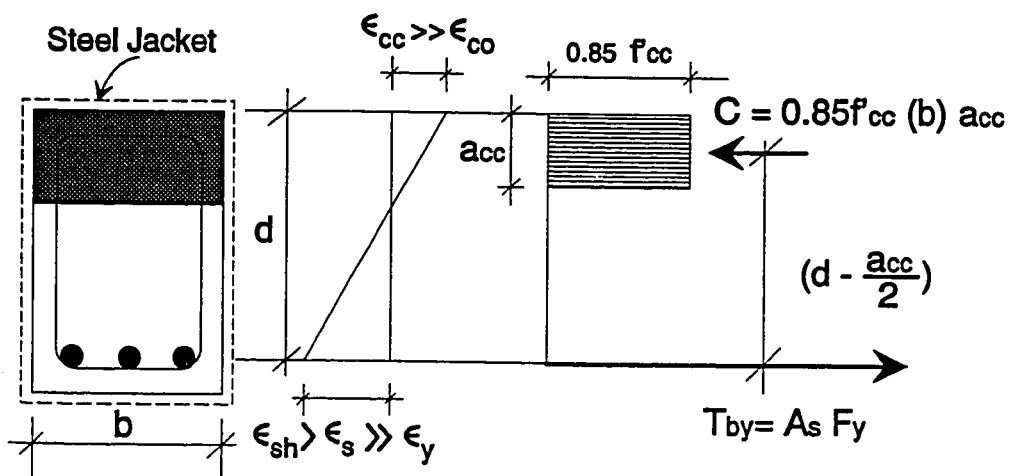
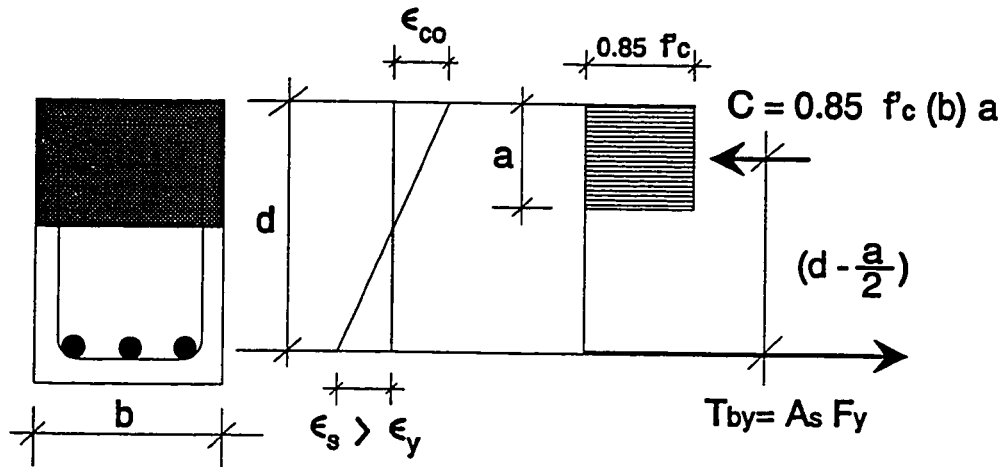


Figure 8.5 Shear Friction Mechanism at Spliced Bars of a Retrofitted Column With Steel Jacket and Anchor Bolts

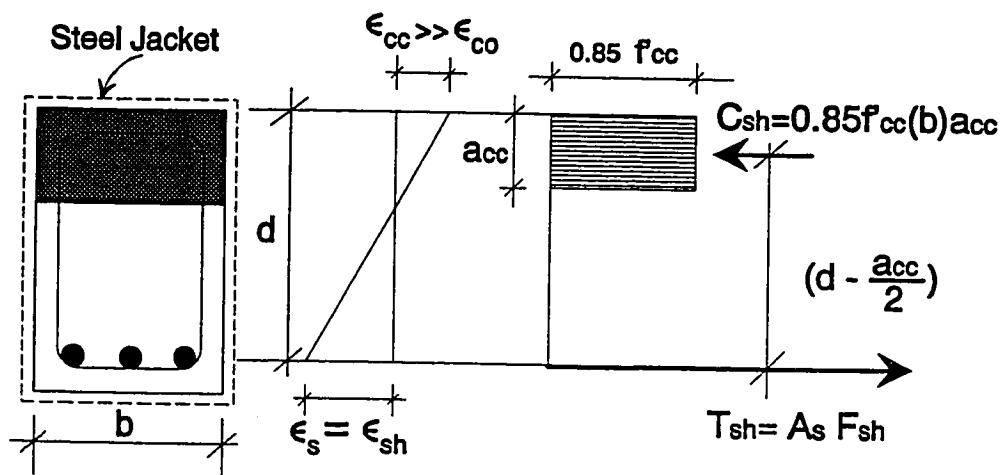
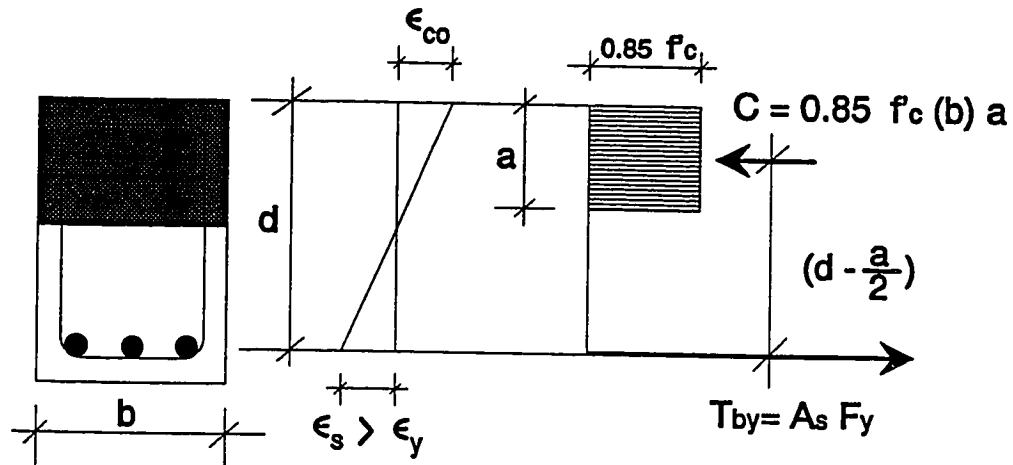


$$\begin{matrix} f_{cc} > f_c \\ T = C \end{matrix} \rightarrow a_{cc} < a \rightarrow \left(d - \frac{a_{cc}}{2}\right) > \left(d - \frac{a}{2}\right)$$

$M_{sj(y)} > M_n$

Figure 8.6 Flexural Capacity of R/C Sections  
 (a) Ordinary (b) Steel Jacketed





$$\begin{aligned} f_{cc} &> f_c \\ T_{sh} &= C_{sh} \end{aligned} \rightarrow$$

$$M_{sj(sh)} > M_{sj(y)} > M_n$$

Figure 8.7 Flexural Capacity of R/C Sections (a) Ordinary (b) Steel Jacketed, including Strain Hardening of the Main Bars

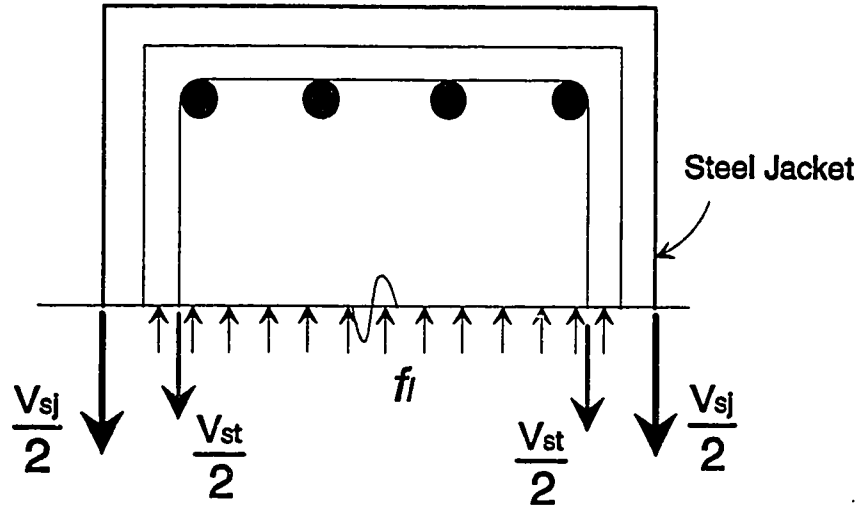


Figure 8.8 Lateral Confining Pressure  $f_l$

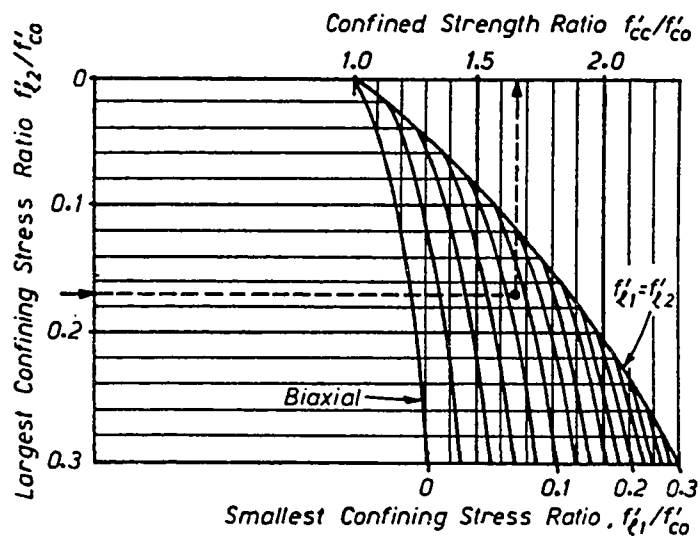


Figure 8.9 Confined Strength Determination from Lateral Confining Stresses for Rectangular Sections, Ref. [11].

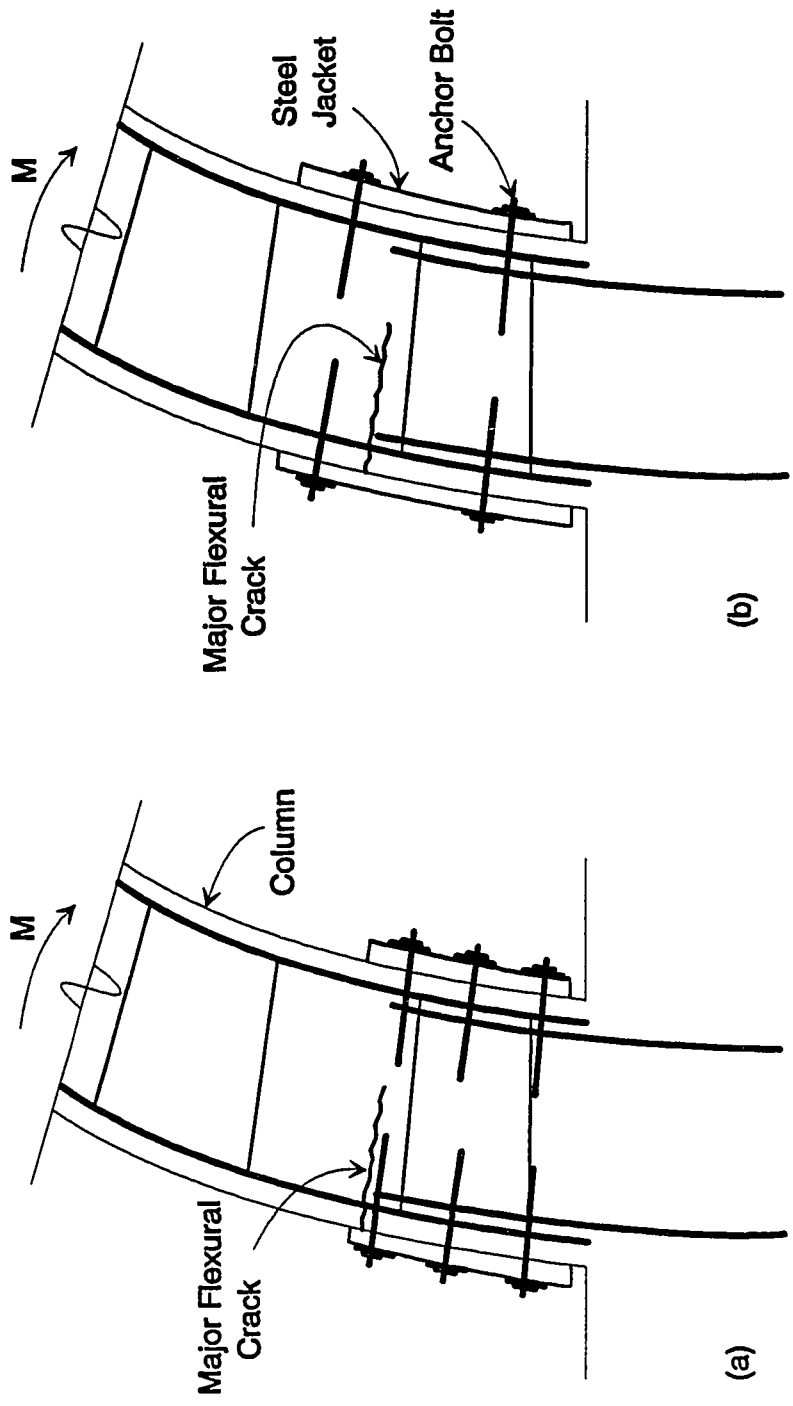
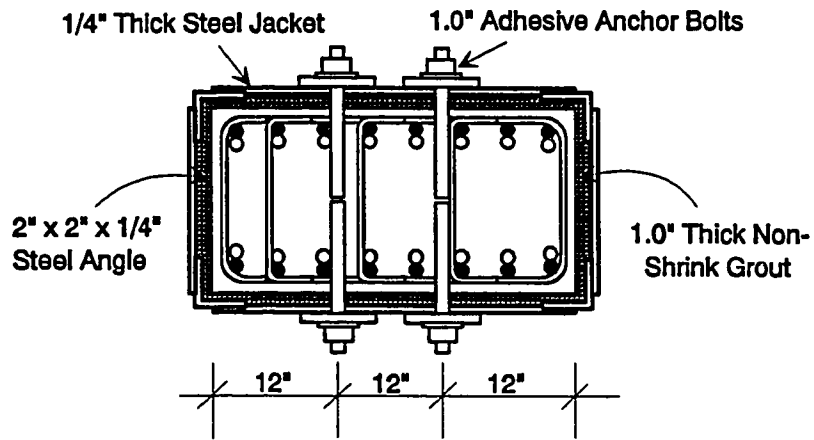
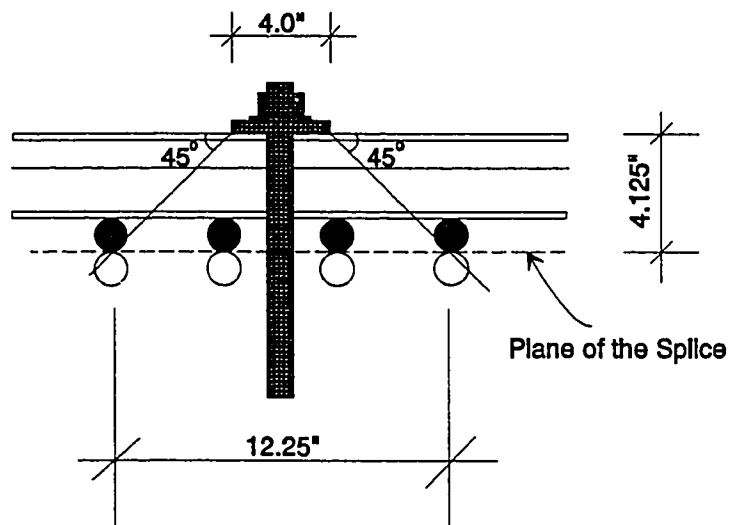


Figure 8.10 Splice Region of Retrofitted Flexural Columns by the use of :  
 (a) Short Steel Jacket (b) Long Steel Jacket

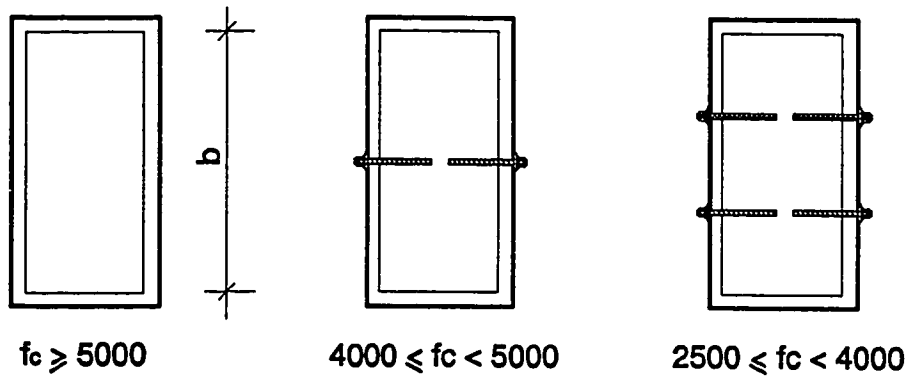


(a) Details of Steel Jacket with Anchor Bolts

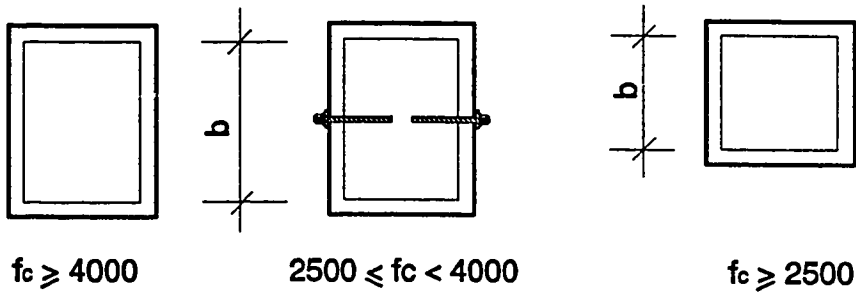


(b) Width of Confined Zone by Anchor Bolt at the Potential Crack Plane ( Plane of the Splice )

Figure 8.11 Width of Confined Zone by a Single Anchor Bolt



(a)  $27" < \text{Column Width "b"} \leq 36"$



(b)  $18" < \text{Column Width "b"} \leq 27"$

(c)  $\text{Column Width "b"} \leq 18"$

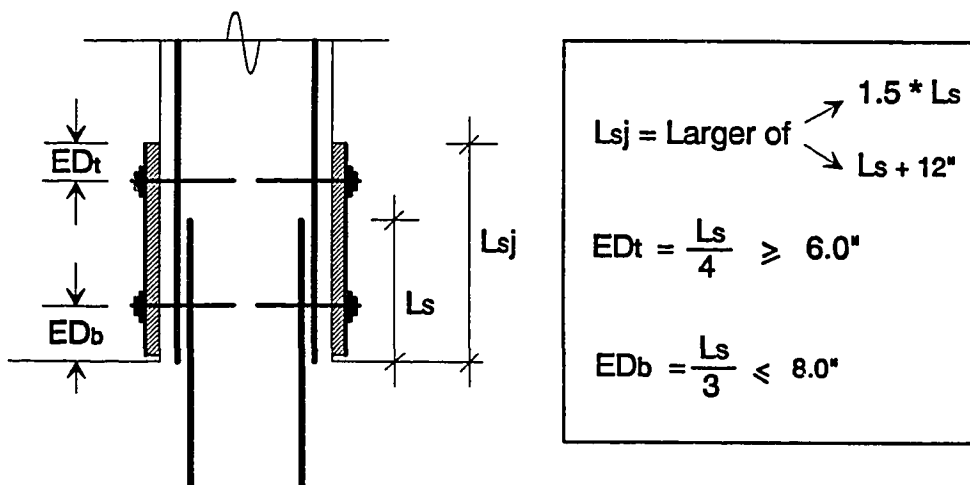


Figure 8.12 Summary of Recommendations for Pre-Earthquake Strengthening of Columns With Inadequate Lap Splices.

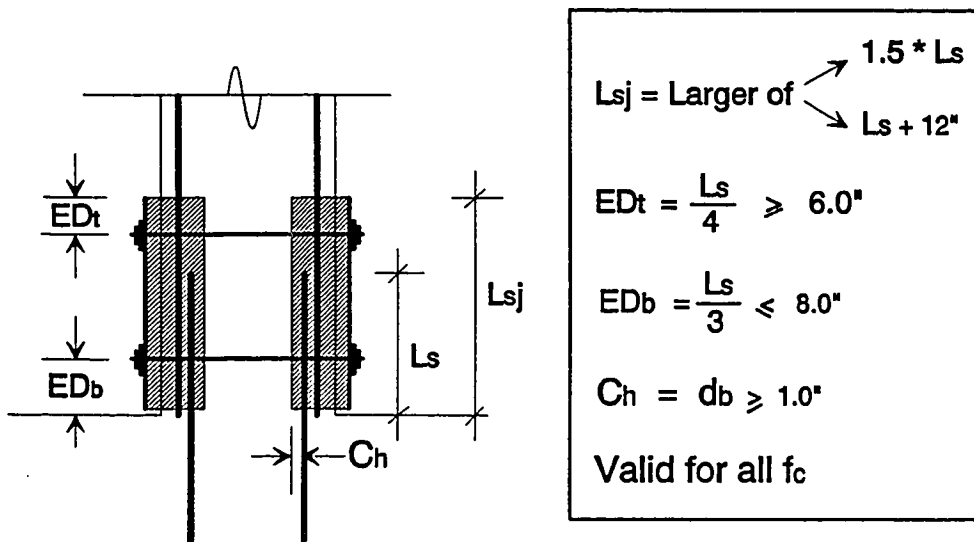
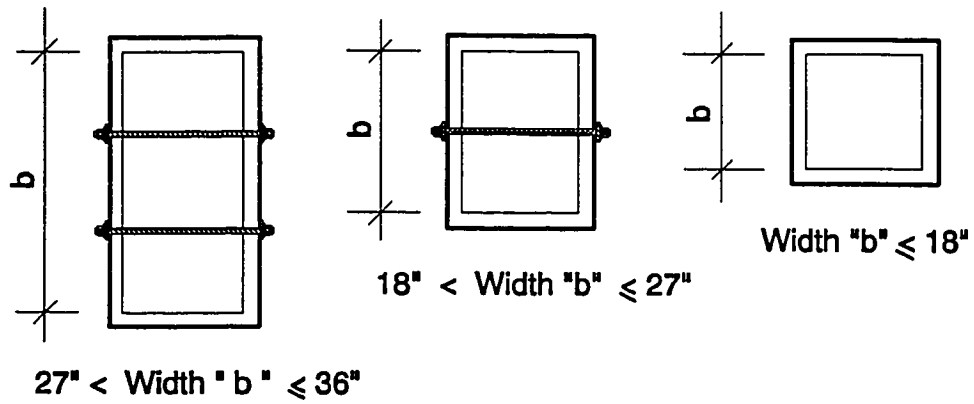


Figure 8.13 Summary of Recommendations for Post-Earthquake Repair of Columns With Inadequate Lap Splices.

## CHAPTER 9

### SUMMARY AND CONCLUSION

#### 9.1 SUMMARY

The use of thin rectangular steel jackets for seismic retrofit of non-ductile reinforced concrete columns was examined. Experiments were conducted on large scale columns with inadequate lap splices or inadequate shear strength. All the columns investigated in this research were detailed according to the provisions of the ACI 318-56 and ACI 318-63 codes. Design guidelines presented here are applicable to non-ductile reinforced concrete columns that meet the requirements of the older ACI code provisions.

Seventeen large scale columns with inadequate lap splices were tested under static cyclic loading. These columns were investigated for pre-earthquake strengthening and post-earthquake repair. Eleven large scale columns with inadequate shear strength were tested under static cyclic loading in both the weak and the strong direction of the column. The shear columns were investigated for pre-earthquake strengthening.

Simplified analytical models for the design of the rectangular steel jackets for seismic retrofit of reinforced concrete columns were presented. In addition, a simple model was presented for evaluation of the flexural capacity of a steel jacketed reinforced concrete column section.

## 9.2 CONCLUSIONS

The study was divided into two major parts: flexural columns with inadequate lap splices in the longitudinal reinforcement, and shear columns with inadequate shear strength. The flexural columns were divided into two groups representing pre-earthquake strengthening and post-earthquake repair. The shear columns were divided into two groups: columns loaded in the weak direction and columns loaded in the strong direction. Following are the major conclusions of this study:

### 9.2.1 Pre-Earthquake Strengthening of Flexural Columns

1. Thin rectangular steel jackets were very effective in strengthening of columns with inadequate lap splices detailed according to the older ACI code provisions. Sections 8.4 and 8.5 present a simple model for the design of steel jackets with and without anchor bolts.
2. Rectangular steel jackets without anchor bolts were adequate for strengthening of 36 inch wide columns and smaller, having concrete strength  $\geq 4900$  psi.
3. Rectangular steel jackets without anchor bolts were adequate for strengthening of 18 inch wide columns and smaller, having concrete strength higher than 2500 psi.
4. Rectangular steel jackets with anchor bolts were adequate for



strengthening of columns wider than 18 inches up to 36 inches, having concrete strength lower than 4900 psi but higher than 2500 psi.

5. The steel jackets should be terminated away from the of the footing to avoid any bearing of the steel jacket against the footing. In this study, the steel jacket was terminated 1.0" from the top of the footing.
6. The strengthened columns exhibited flexural capacity higher than the theoretical flexural strength of unretrofitted columns. Section 8.6 presents a simple model to estimate the flexural capacity of retrofitted columns.
7. The strengthened columns showed much higher ductility and energy dissipation than the basic unretrofitted columns.

### **9.2.2 Post-Earthquake Repair of Flexural Columns**

1. Thin rectangular steel jackets with through rods were very effective in seismic repair of damaged reinforced concrete columns with inadequate lap splices.
2. Rectangular steel jackets with anchor bolts are not as effective for post- earthquake repair as they are for pre-earthquake strengthening.
3. The column in which the damaged splice was repaired by welding showed very good performance. Welding should be conducted for such

columns according to the American Welding Society recommendations AWS D1.4-79.

4. Although it might not be severely damaged and loose, removal of the concrete in the vicinity of the spliced starter bars may be needed. In this study, the thickness of the removed concrete was 1.0 inch.
5. The repaired columns exhibited flexural capacity higher than the theoretical flexural strength of unretrofitted columns. Section 8.6 presents a simple model to estimate the flexural capacity of retrofitted columns.
6. The repaired columns showed much higher ductility and energy dissipation than the basic unretrofitted columns.

### **9.2.3 Strengthening of Shear Columns**

1. Thin rectangular steel jackets were very effective in strengthening of reinforced concrete columns with inadequate shear strength. Section 8.12 presents a simple analytical model for the design of steel jackets for shear strengthening.
2. Columns strengthened with full rectangular steel jackets exhibited higher flexural capacity, ductility and energy dissipation than the basic unretrofitted columns.

3. Rectangular steel jackets should be installed over the full height of the column, but terminated one inch from the top and one inch from the bottom of the column.
4. Although steel jackets are very effective in enhancing the strength and ductility of columns with inadequate shear strength, they are considered passive systems. They start working effectively after the concrete column has developed major diagonal shear cracks.

### **9.3 RECOMMENDED FUTURE RESEARCH**

The experimental test results and the analytical models of this study provide a better understanding of the use and design of rectangular steel jackets for seismic strengthening and repair of non-ductile reinforced concrete columns. Based on the results of this study alone, complete design recommendations cannot be developed due to the large number of variables.

In order to develop comprehensive design criteria for the use of rectangular steel jackets for seismic retrofit of reinforced concrete columns further research should be conducted:-

1. Investigation of retrofitted columns under axial and lateral loads.
2. Investigation columns with inadequate lap splices loaded in the strong direction.
3. The use of different types of anchor bolts, e.g. expansion bolts.
4. Research on steel jackets with various thicknesses.

## **APPENDIX A**

### **CONSTRUCTION OF BASIC COLUMNS**

Test specimens were constructed in two stages. The footings were cast in the first stage and the columns in a second stage. This resulted in a cold construction joint between the column and the footing. Figures A.1 through A.4 show the construction sequence of four test columns. The two front columns are flexural columns with an inadequate lap splice at the base of the column. The rear columns are shear columns with inadequate shear strength. The construction sequence can be summarized as follows:-

1. Assembling of footing steel cages, and erection of footing formwork.
2. Tying shear column longitudinal bars and flexural column starter bars to the footing reinforcement.
3. Casting of footing concrete.
4. Splicing flexural column main bars with the footing starter bars.
5. Tying transverse reinforcement.
6. Erection of column formwork.
7. Casting of column concrete.
8. Removal of column formwork.

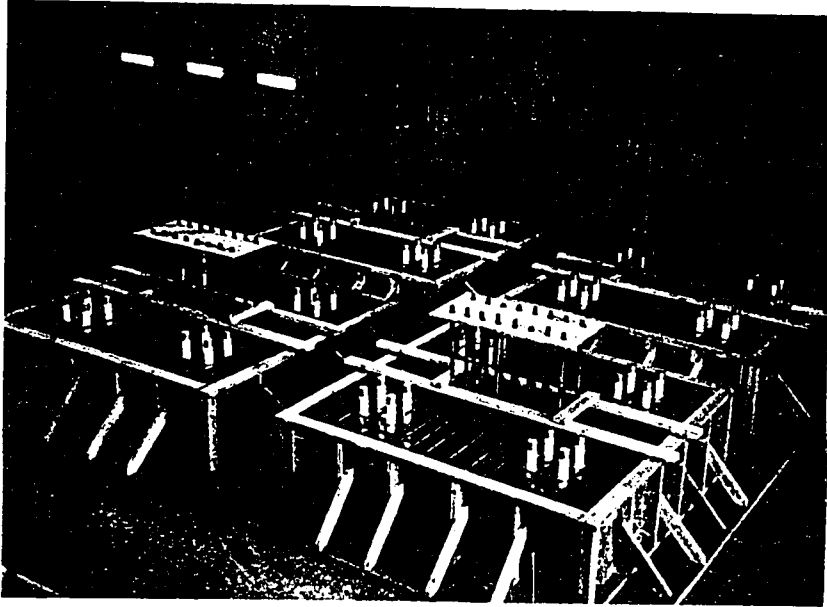


Figure A.1 Four footings prior to casting of concrete. Front footings are for flexural columns.

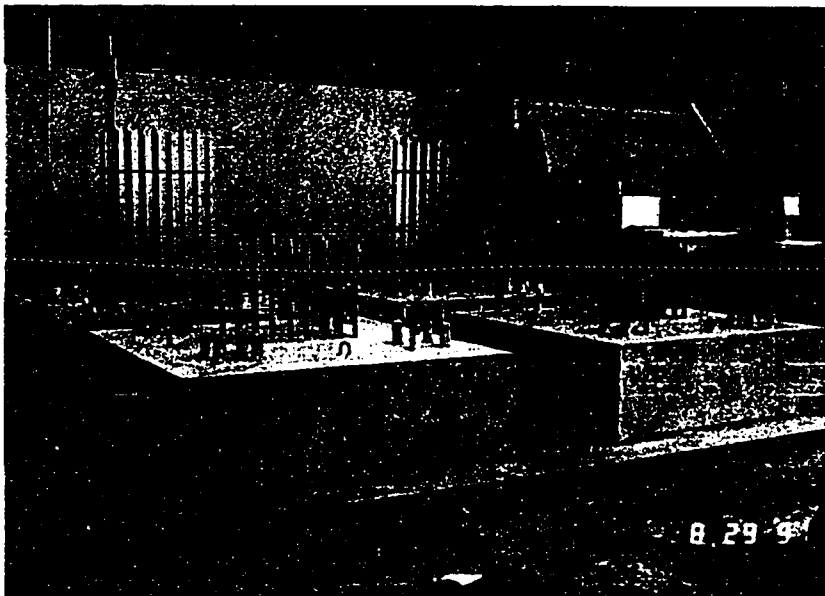


Figure A.2 The four footings after casting of the concrete.

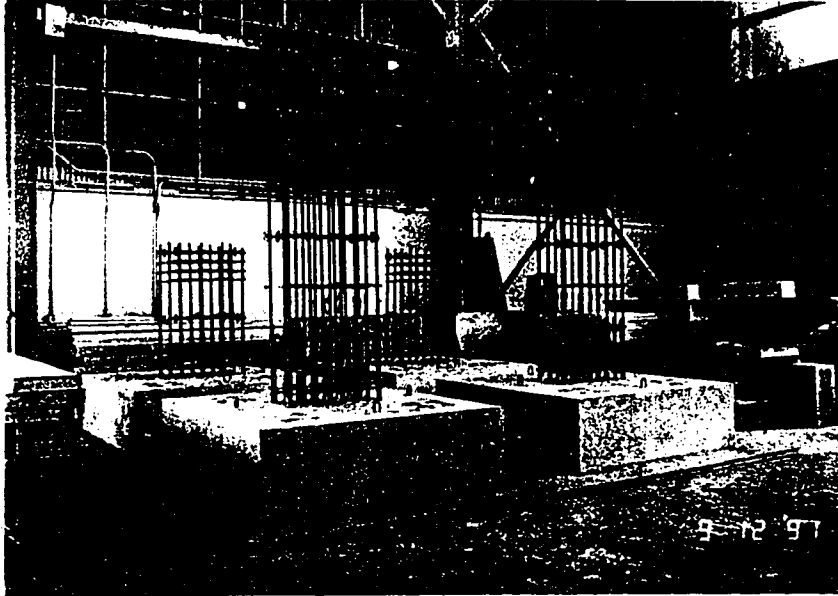


Figure A.3 Column reinforcement prior to the erection of formwork.

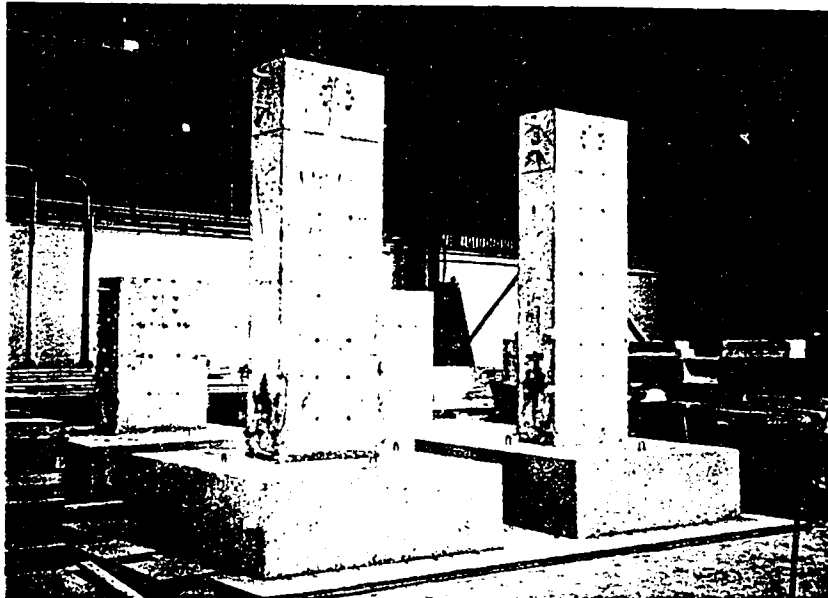


Figure A.4 Four basic columns. The front columns are the flexural columns and the rear columns are the shear columns.

## APPENDIX B

### INSTALLATION OF ANCHOR BOLTS

The anchor bolt system used in this study was the Hilti HVA adhesive Anchor System. It consisted of HAS anchor rod and HEA adhesive capsule. The HAS anchor was a 1.0 inch diameter threaded rod supplied with washer and nut. The HEA adhesive capsule consisted of a pre-measured amount of vinyl ester resin with a dibenzoyl peroxide hardener in a glass capsule. Figure B.1 shows the HAS anchor bolt and HEA adhesive capsule. The installation of the anchor bolts was conducted according to the manufacturer instructions, but the holes were not flushed with water nor blown out by compressed air. The holes were thoroughly brushed and dry vacuumed. Figure B.2 shows the installation instructions of the anchor bolts according to the manufacturer instructions.

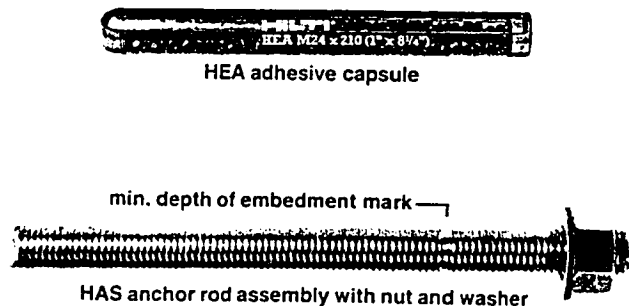
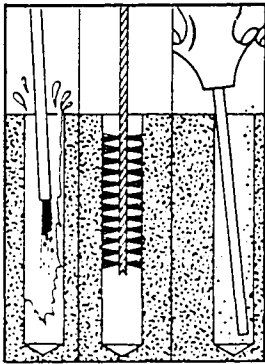
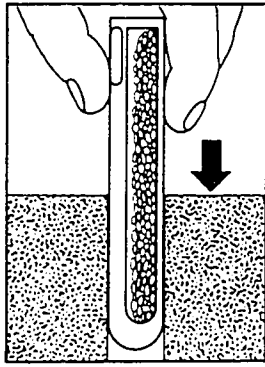


Figure B.1 HAS anchor rod and HEA adhesive capsule, Ref.[36].

## Installation Instructions — HAS Rod and HFA Insert



1. Set the drill depth gauge and hammer drill the hole to the required hole depth. **IMPORTANT:** Clear out dust and fragments; preferably using a jet of water or compressed air and a wire brush. The hole may be damp, but the standing water should be blown out.

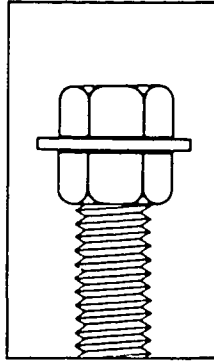


2. Insert appropriate diameter HEA adhesive capsule into pre-drilled hole in base material.

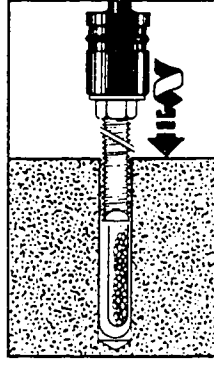
Curing Time	Base Material Temperature
3/8-1" $\phi$	1 1/4" $\phi$
20 Min.	40 Min.
30 Min.	1 Hr.
1 Hr.	2 Hr.
5 Hr.	5 Hr.
	23°F to 32°F
	50°F to 68°F
	32°F to 50°F
	23°F to 32°F

Below 23°F, consult your Hillr Engineer.

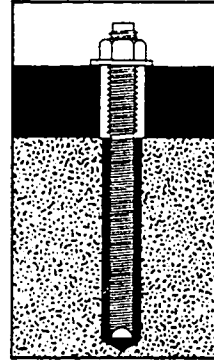
### HAS Rod (Option #1)



3. HAS (Option #1)  
Thread a nut on the HAS rod. Place a washer on top of the first nut and then thread a second nut down on top of the washer. Tighten the two nuts together "locking" the washer between them. The top nut should be flush with the top of the rod.



4. HAS (Option #1)  
Insert square drive shaft into hammer drill. Attach proper impact socket. At the rotary hammer drill setting engage the top nut of the HAS rod assembly with the socket and drive the rod in to the embedment mark.



5. HAS (Option #1)  
The set anchor rod may not be disturbed or loaded before the specified curing time.

Figure B.2 The installation of the Anchor Bolts according to the manufacturer instructions, Ref. [36].



## APPENDIX C

### DESIGN OF A RETROFITTED FLEXURAL COLUMN

In this appendix, an example for the design of retrofitted column with inadequate lap splice is presented. The details of the column are similar to those of column FC12, however, the strength of concrete is 3000 psi and the yield strength of steel is 60 ksi.

#### Solution:

- C.1** Check the actual length of the splice, minimum  $L_s$ , according to Equation (8-2) and the splice length  $L_s$ , according to ACI 318-63.

Actual  $L_s = 24$  inches.

$$L_{s(\min)} = \frac{1.25A_s F_y}{\pi d U_b} \approx \frac{0.020 d_b F_y}{\sqrt{f_c}} \approx \frac{0.02 (1.0'') 60,000 \text{ ksi}}{\sqrt{3000 \text{ p.s.i.}}} = 21.91''$$

$$(\text{ACI 318-63}) L_s = 24 (d_b) = 24 (1.0'') = 24.0''$$

The actual splice length meets the ACI 318-63 requirements and longer than  $L_{s(\min)}$ . Therefore, the splice is repairable with rectangular steel jacket.

- C.2** Check if anchor bolts are required.  
*calculate shear friction stress*

$$v_{sf} = 0.2 f'_c \leq 800 \text{ psi}$$

$$= 0.2 ( 3000 \text{ psi} ) = 600 \text{ psi} \leq 800 \text{ psi} \quad \therefore v_{sf} = 600 \text{ psi.}$$

*calculate the width of the shear friction surface*

$$W_{ss} = 2C_s = 3.46''$$

$$= 3 ( d_b ) = 3 ( 1.0'' ) = 3.0'' \quad \therefore W_{ss} = 3.0''$$

*calculate the shear friction force at the development of shear friction mechanism*

$$V_{sf} = v_{sf} * A_{sf} = v_{sf} ( W_{ss} * L_s ) = 600 \text{ psi} ( 3.0'' \times 24'' )$$

$$= 43,200 \text{ lbs.} = 43.2 \text{ kips.} \quad \therefore V_{sf} = 43.2 \text{ kips.}$$

*check the yield force in the longitudinal bar*

$$T_{by} = A_s * F_y = 0.79 \text{ in}^2 ( 60 \text{ ksi} ) = 47.4 \text{ kips.}$$

$V_{sf} < T_{by}$ , Shear Friction Mechanism will occur before the development of the yield capacity of the longitudinal reinforcing bars.

$\therefore$  Anchor bolts are required.

### C.3 Design of steel Jacket

*Estimate the actual shear friction stress, considering  $\mu = 1.40$ .*

$$2C_s = 3.46'' \Rightarrow C_s = 1.73'', C_c = 1.5 + 0.375 = 1.875''$$

∴ splitting over the entire width of the column may occur

$$v_{sf} = \frac{A_s * 1.25 * F_y}{\mu * A_{sf}} = \frac{8(0.79)(1.25 * 60000)}{1.40(36 * 24)} \approx 392 \text{ p.s.i.} < 0.2 * f_c$$

$$t_{sj} \geq [ (v_{sf} * b * s) - (u_b \pi d_{ab} L_{ab} \frac{s}{L_s}) n_{ab} - (A_{st} * F_{yt}) ] * \frac{h}{36 * s * f_{sj}} \quad (8-11)$$

$$v_{sf} * b * s = 0.392 (36) 16 = 226 \text{ kips.}$$

$$u_b = 16 \sqrt{f_c} = 16 \sqrt{3000} = 876 \text{ psi.} = 0.876 \text{ ksi.}$$

Width of Column = 36", ∴ use 2 anchor bolts dividing the width of the column into three 12 inch segments.

$$L_{ab} = 8.0" - 1.5 - 0.375 - 1.0 = 5.125"$$

$$u_b \pi d_{ab} L_{ab} (s/L_s) n_{ab} = 0.876 \pi (1.0) 5.125 (16/24) 2 = (9.40) 2 = 18.8 \text{ kips}$$

$$(18.8 / 226) 100 = 8.3 \% \text{ OK.}$$

$$A_{st} * F_{yt} = 5 (0.11) * 60 = 33.0 \text{ kips.}$$

$$f_{sj} = 22 \text{ ksi.}$$

$$t_{sj} \geq [ (226) - 18.8 - (33) ] * \frac{18}{36 * 16 * 22} = 0.247''$$

∴ Use 1/4" thick steel jacket with two vertical lines of two anchor bolts each.

#### C.4 Check the Ultimate Flexural Capacity of the Jacketed Column

Calculate the confining lateral pressure in the weak and the strong directions using Equation ( 8 - 12 ).

$$f_l = [ (A_{st} * F_{yt}) + 2 * (t_{sj}) * s * f_{sj} * \frac{18}{h} ] * ( \frac{1}{b * s} ) \quad (8-12)$$

confining pressure in the weak direction

$$f_{lw} = [ (5(0.11)60 + 2 (1/4) 16 * 22 * \frac{18}{20} ] * ( \frac{1}{36*16} ) = 0.332 \text{ ksi}$$

confining pressure in the strong direction

$$f_{ls} = [ (2(0.11)60 + 2 (1/4) 16 * 22 * \frac{18}{38} ] * ( \frac{1}{18*16} ) = 0.335 \text{ ksi}$$

$$\frac{f_{lw}}{f_{co}} = \frac{0.332}{3.0} = 0.110 \quad , \quad \frac{f_{ls}}{f_{co}} = \frac{0.335}{3.0} = 0.111$$

Use the chart in Figure 8.9 to find the strength magnification factor. The magnification factor = 1.65.

$$f'_{ce} = 1.65 ( 3000 ) = 4950 \text{ psi} = 4.95 \text{ ksi.}$$

*estimate the concrete strain that is associated with the maximum confined concrete compressive strength  $f'_{cc}$*

$$\varepsilon_{cc} = \varepsilon_{co} [ 1 + 5 ( f'_{cc} / f'_{co} - 1 ) ] \quad (8-13)$$

$$\varepsilon_{cc} = 0.002 [ 1 + 5 ( 4.95 / 3.0 - 1 ) ] = 0.0085$$

see Figure C.1,

$$\text{assume } a_{cc} = 3.13", \quad c = a_{cc} / 0.85 = 3.13 / 0.85 = 3.682"$$

$$\varepsilon_s \approx 0, \quad f_s = 0.$$

$$C_c = 0.85 ( 4.95 ) 36 ( 3.13 ) = 474 \text{ kips.}$$

$$C = 474 \text{ kips.}$$

$$T = 8 ( 0.79 ) \{ 1.25 * 60 \} = 474 \text{ kips.} \quad T \approx C \quad \text{OK.}$$

$$\begin{aligned} M_{sj} &= 474 ( 9 - 3.13/2 ) + 474 ( 9 - 3.375 ) \\ &= 3524 + 2666 = 6190 \text{ kip-in} = 515.8 \text{ kip-ft} \end{aligned}$$

compare with the test columns,

$$H = M / \text{height of column} = 515.8 / 9 = 57.3 \text{ kips} \quad \text{OK.}$$

**C.5 Check the Shear Capacity of the Jacketed Section**

$$V_{sj} = A_{sj} * (0.5 * F_y)_{sj} * \frac{d_{sj}}{s_{sj}} \quad (8-16)$$

$$V_{sj} = (0.25" \times 0.25") * (0.50 \times 36 \text{ ksi}) * (20" / 0.25") = 90 \text{ kips}$$

$$V_c = 2 \sqrt{f_c} b d = 2 \sqrt{3000} 36 (15.625) = 61618.78 \text{ lbs} \approx 61.6 \text{ kips}$$

$$V_{st} = A_{st} * F_{yt} = 5 (0.11) 60 = 33.0 \text{ kips.}$$

$$V_n = V_c + V_{st} + V_{sj} = 61.6 + 33.0 + 90 = 184.6 \text{ kips}$$

## APPENDIX D

### NOTATIONS

- $a$  = depth of the compression stress block for unconfined concrete (in)  
 $a_{cc}$  = depth of the compression stress block for confined concrete (in)  
 $A_{ab}$  = area of anchor bolt ( $\text{in}^2$ )  
 $A_b$  = area of reinforcing bar ( $\text{in}^2$ )  
 $A_s$  = area of longitudinal reinforcing bar(s) ( $\text{in}^2$ )  
 $A_{sab}$  = surface area of anchor bolt over the embedment length ( $\text{in}^2$ )  
 $A_{sf}$  = area of shear surface ( $\text{in}^2$ )  
 $A_{sj}$  = area of steel jacket ( $\text{in}^2$ )  
 $A_{\alpha}$  = area of transverse reinforcement ( $\text{in}^2$ )  
 $b$  = width of column (in)  
 $C$  = resultant of compressive forces (kips)  
 $C_c$  = thickness of the clear concrete cover to the main bars (in)  
 $C_h$  = minimum thickness of new concrete behind the spliced bars (in)  
 $C_s$  = half the clear spacing between two adjacent longitudinal bars (in)  
 $d$  = distance from the centroid of tension steel to extreme compression fiber of concrete (in)  
 $d_{ab}$  = nominal diameter of anchor bolt (in)  
 $d_b$  = nominal diameter of reinforcing bar (in)  
 $d_{sj}$  = total depth of the steel jacket (in)  
 $ED_b$  = bottom edge distance of a bolted steel jacket (in)  
 $ED_t$  = top edge distance of a bolted steel jacket (in)  
 $f_c$  = concrete compressive strength at the day of testing (psi)  
 $f'_c$  = uniaxial compressive strength of a 6.0" diameter concrete cylinder at 28 days (psi)

- $f'_{cc}$  = confined concrete compressive strength (psi, or ksi)  
 $f'_{co}$  = unconfined concrete compressive strength (psi, or ksi)  
 $f_l$  = lateral confining pressure in a concrete section (psi, or ksi)  
 $f_{ls}$  = lateral confining pressure in the strong direction (psi, or ksi)  
 $f_{lw}$  = lateral confining pressure in the weak direction (psi, or ksi)  
 $f_{sj}$  = effective stress in steel jacket (ksi)  
 $F_y$  = tensile yield strength of steel (ksi)  
 $F_{yt}$  = tensile yield strength of transverse reinforcement (ksi)  
 $h$  = total depth of column (in)  
 $L_{ab}$  = actual embedment length of anchor bolt (in)  
 $L_s$  = length of the lap splice (in)  
 $L_{sj}$  = height of steel jacket (in)  
 $M_n$  = nominal flexural capacity of ordinary reinforced concrete section (kip-in)  
 $M_{sj}$  = nominal flexural capacity of steel jacketed reinforced concrete section (kip-in)  
 $M_{sj(sb)}$  = nominal flexural capacity of steel jacketed reinforced concrete section at steel stress  $1.25 F_y$  (kip-in)  
 $n_{ab}$  = number of anchor bolts within the splice length (see section 8.5 for more details)  
 $s$  = spacing between layers of transverse reinforcement (in)  
 $s_{sj}$  = spacing between the imaginary square ties of the steel jacket (in)  
 $t_{sj}$  = thickness of the steel jacket (in)  
 $T_{ab}$  = force in anchor bolt (kips)  
 $T_b$  = tensile force in the longitudinal bars (kips)  
 $T_{by}$  = tensile yield force in the longitudinal bars (kips)  
 $u_b$  = bond stress between anchor bolt and concrete (ksi)  
 $U_b$  = effective bond stress corresponding to concrete "cylinder shear-off" failure (psi)  
 $v_{af}$  = shear stress at the development of shear friction mechanism



(psi, or ksi)

- $V_{ab}$  = confining force by the anchor bolts (kips)
- $V_c$  = nominal shear force carried by concrete (kips)
- $V_n$  = nominal shear force at section (kips)
- $V_{sf}$  = shear force at the development of shear friction mechanism (kips)
- $V_{sj}$  = nominal shear force carried by steel jacket (kips)
- $V'_{sj}$  = confining force by steel jacket (kips)
- $V_{st}$  = confining force by the transverse reinforcement (kips) or,
- $V_{st}$  = nominal shear force carried by transverse reinforcement (kips)
- $W_{sf}$  = width of shear friction surface (in)
- $\epsilon_s$  = steel strain
- $\epsilon_y$  = steel yield strain
- $\epsilon_{sh}$  = steel "strain hardening" strain
- $\epsilon_{cc}$  = concrete strain associated with the maximum confined concrete compressive strength  $f'_{cc}$
- $\epsilon_{co}$  = concrete strain associated with the maximum unconfined compressive strength  $f'_{co}$  (generally assumed 0.002)
- $\mu$  = shear friction factor

## BIBLIOGRAPHY

1. National Institute of Standards and Technology, "Performance of Structures During the Loma Prieta Earthquake of October 17,1989," NIST Publication 778, January 1990.
2. Chai,Y.H.; Priestley,M.J. and Seible,F., "Retrofit of Bridge Columns for Enhanced Seismic Performance," Proceedings of the U.S.-Japan Workshop on Seismic Retrofit of Bridges, Tsukuba, Japan, December 1990.
3. Yoshimura,K.; Kikuchi,K. and Kuroki,M. "Seismic Shear Strengthening Method for Existing Reinforced Concrete Short Columns," Proceedings of the ACI International Conference on Evaluation and Rehabilitation of Concrete Structures and Innovations in Design, SP 128-66,Hong Kong, 1991, pp 1065-1079.
4. Fung,G.G.; Lebeau,R.J.; Klein,E.D.; Belvedere,J. and Goldschmidt,A.F. "Field Investigation of Bridge Damage in the San Fernando Earthquake," Technical Report, Bridge Department, Division of Highways, California Department of Transportation, Sacracmento, 1971, 209 pp.
5. ACI Committee 318, "Building Code Requirements for Reinforced Concrete ( ACI 318-56),"American Concrete institute, Detroit, Michigan, 1956.
6. ACI Committee 318, "Building Code Requirements for Reinforced Concrete ( ACI 318-63),"American Concrete institute, Detroit, Michigan, 1963.

7. Kent,D.C. and Park,R. "Flexural Members with confined Concrete," *Journal of the Structural Division, Proceedings of the American Society of Civil Engineers*, Vol. 97, No. ST7, July, 1971, pp 1969-1989.
8. Kaar,P.H.; Fiorato,A.E.; Carpenter,J.E. and Corley,W.G., "Limiting Strains of Concrete Confined by Rectangular Hoops," *PCA Research and Development Bulletin*, 1978.
9. Sheikh,S.A. and Uzumeri,S.M., "Strength and Ductility of Tied Concrete Columns," *Journal of the Structural Division, Proceedings of the American Society of Civil Engineers*, Vol. 106, No. ST5, May, 1980, pp 1079-1102.
10. Sheikh,S.A. and Uzumeri,S.M., "Analytical Model for Concrete Confinement in Tied Columns," *Journal of the Structural Division, Proceedings of the American Society of Civil Engineers*, Vol. 108, No. ST12, December, 1982, pp 2703-2722.
11. Mander,J.B.; Priestley,M.J. and Park,R., "Theoretical Stress-Strain Model for Confined Concrete," *Journal of Structural Engineering*, Vol. 114, No. 8, August, 1988, pp 1804-1826.
12. Mander,J.B.; Priestley,M.J. and Park,R., "Observed Stress-Strain behavior of Confined Concrete," *Journal of Structural Engineering*, Vol. 114, No. 8, August, 1988, pp 1827-1849.
13. Pessiki,S.P.; Conley,C.H.; Gergely,P. and White,R.N., "Seismic Behavior of Lightly-reinforced Concrete Column and Beam-Column Joint Details," *Technical Report NCEER-90-0014*, National Center For Earthquake Engineering Research, Red Jacket Quadrangle, Buffalo, NY 14261.

14. Bertero, V.V. and Shadh, H., "El-Asnam, Algeria Earthquake, October 10, 1980," Earthquake Engineering Research Institute, Oakland, California, January, 1983, 190 pp.
15. Federal Highway Administration, "Seismic Retrofitting Guidelines for Highway Bridges," Report No. FHWA/RD-83/007, December, 1983.
16. Federal Emergency Management Agency, "Techniques for Seismically Rehabilitating Existing Buildings-Preliminary," Earthquake Hazards Reduction Series 49, FEMA-172/ May, 1989.
17. Gaynor, P.J., "The Effect of Openings on the Cyclic Behavior of Reinforced Concrete Infilled Shear Walls," Master of Science Thesis, The University of Texas at Austin, August 1988, 245 pp.
18. Jimenez, L., "Strengthening of Reinforced Concrete Frame Using an Eccentric Shear Wall," Master of Science Thesis, The University of Texas at Austin, May, 1989, 67 pp.
19. Alcocer, S.M. and Jirsa, J.O. "Reinforced Concrete Frame connections Rehabilitated by Jacketing," PMFSEL Report 91-1, Department of Civil Engineering, The University of Texas at Austin, July 1991, 219 pp.
20. Estrada, J.I. "Use of Steel Elements to Strengthen a Reinforced Concrete Building," Master Thesis, Department of Civil Engineering, The University of Texas at Austin, December 1990, 66 pp.
21. Pincheira, J.A. "Seismic Strengthening of Reinforced Concrete Frame Using Post-tensioned Bracing Systems," PhD. Dissertation, Department of Civil Engineering, The University of Texas at Austin, August 1992, 329 pp.

22. Bouadi,A.; Engelhardt,M.D.; Jirsa,J.O. and Kreger,M.E. "Use of Eccentric Steel Bracing for Strengthening of R/C Frames," Proceeding of the Structures Congress '93,The American Society of Civil Engineers, Irvine,CA, April 1993, pp 307-312.
23. Valluvan,R. "Issues Involved in Seismic Retrofit of Reinforced Concrete Frames Using infilled Walls," PhD. Dissertation, Department of Civil Engineering, The University of Texas at Austin, December 1993, 300 pp.
24. Unjoh,S. and Kawashima,K. "Seismic Inspection and Seismic Strengthening of Reinforced Concrete Bridge Piers," Proceedings of the Tenth World Conference on Earthquake Engineering, International Association For Earthquake Engineering, Vol.9, Madrid, Spain, July 1992, pp 5279-5284.
25. Bett,B.J; Klingner,R.E. and Jirsa,J.O. "Lateral Load Response of Strengthened and Repaired Reinforced Concrete Columns," ACI Structural Journal, American Concrete Institute, Sept.-Oct. 1988, pp 499-508.
26. Sugano,S. "Seismic Strengthening of Existing reinforced Concrete Buildings in Japan," Bulletin of the New Zealand National Society for Earthquake Engineering, Vol.14, December 1981, pp 209-222.
27. Orangun,C.O.; Jirsa,J.O.; and Breen,J.E. "Reevaluation of Test Data on Development Length and Splices," ACI Journal, American Concrete Institute, Vol.74, No.3, March 1977, pp 114-122.
28. Eligehausen,R.; Bertero,V.; and Popov,E. "Local Bond Stress-Slip Relationships of Deformed Bars under Generalized Excitations," EERC, Report UCB/EERC 83-23, University of California, Berkeley, 1983.

29. Lukose,K.; Gergely,P.;and White,R.N., "Behavior of Reinforced Concrete Lapped Splices under Inelastic Cyclic Loading," ACI Journal, American Concrete Institute, Vol.79, No.5, Sept.-Oct. 1982, pp 355-365.
30. Paulay,T., "Lapped Splices in Earthquake-Resisting Columns," ACI Journal, American Concrete Institute, Vol.79, No.6, Nov.-Dec. 1982, pp 458-469.
31. Panahshahi,N.; White,R.N., and Gergely,P., "Reinforced Concrete Compression Lap Splices under Inelastic Cyclic Loading," ACI Journal, American Concrete Institute, Vol.89,No.2, March-April 1992, pp 164-175.
32. Wakabayashi,M., "Design of Earthquake-Resistant Buildings," McGraw Hill Book Company, New York, 1986, 309 pp.
33. American Welding Society, "Structural Welding Code - Reinforcing Steel," AWS D1.4-79, Miami, Florida, September, 1979, 35 pp.
34. Priestley,M.J.N., "Flexural Test of High Strength Fiber Retrofitted Column," SEQAD Consulting Engineers, Report #90-06, Job #90-8, Solana Beach, California, November, 1990.
35. Priestley,M.J.N., "Shear Column Test No.1," SEQAD Consulting Engineers, Report #91-05, Job #90-8, Solana Beach, California, May, 1991.
36. Hilti, "Fastening Technical Guide," Publication # H-437D-6/92, Tulsa, Oklahoma. June, 1992, 117 pp.

37. Paulay, T. and Priestley, M.J.N., "Seismic Design of Reinforced Concrete and Masonry Buildings," A Wiley Interscience Publication, New York, 1992, 744 pp.
38. William, K.J. and Warnk, E.P., "Constitutive Model for the Triaxial Behavior of Concrete," Proceedings of the International Association For Bridge and Structural Engineering, Vol. 19, 1975, pp 1-30.
39. Popovics, S., "A Numerical Approach to the Complete Stress-Strain Curves for Concrete," Cement and Concrete Research, Vol. 3(5), May, 1973, pp 583-599.
40. Elwi, A., A. and Murray, D. W., "A 3D Hypoelastic Concrete Constitutive Relationship," Journal of Engineering Mechanics Division, ASCE, Vol. 105(4), April, 1979, pp. 623-641.
41. Richart, F. E., Brandtzaeg, A. and Brown, R.L., "A Study of the Failure of Concrete Under Combined Compressive Stresses," Bulletin 185, Univ. of Illinois, Engineering Experimental Station, Champaign, Illinois, 1928.

## VITA

Riyad Aboutaha was born in Beirut, Lebanon, on August 30, 1957, the son of Said Taher Aboutaha and Zehra Mohammad Aboutaha. After completing his work at Omer Ben Al-Kattab Secondary School (Al-Makassed), Beirut, in August 1976, he attended Beirut Arab University, Beirut, Lebanon. He received the degree of Bachelor of Engineering, Major: Civil Engineering from Beirut Arab University on September 1981.

In April 1982 he was employed by U.A.E. Corps of Engineers, Abu Dhabi, United Arab Emirates. In April 1989 he resigned his position from U.A.E. Corps of Engineers to continue his education. In September 1989 he entered the Graduate School of The University of Texas at Austin, where he was awarded the degree of Master of Science in Civil Engineering in December, 1990. In January 1991 he started working on his Ph.D. at The University of Texas at Austin.

He is a member of the American Society of Civil Engineers, American Concrete Institute, Precast/Prestressed Concrete Institute, Earthquake Engineering Research Institute, Tau Beta Pi, Chi Epsilon and Beta Alpha Phi.

Permanent Address:            Georgia Institute of Technology  
   School of Civil Engineering  
   Atlanta, Georgia 30332-0355

This dissertation was typed by the author.